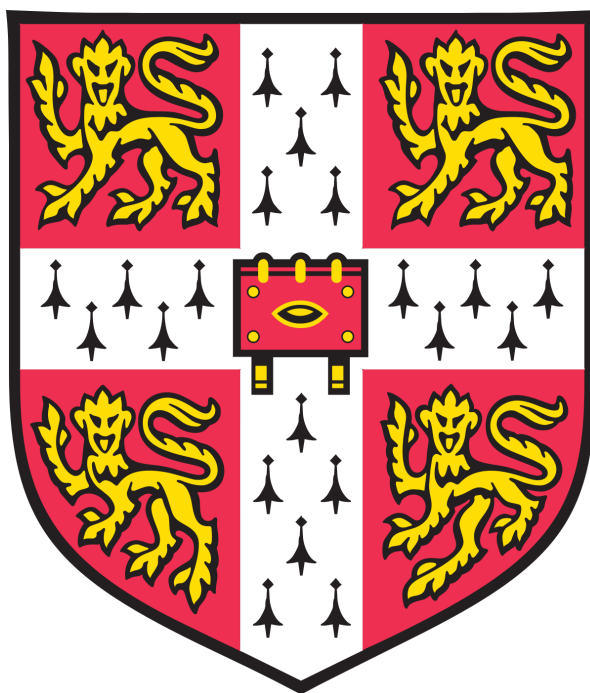


**Modulation of cyclic adenosine monophosphate
(cAMP) signalling and its therapeutic potential:
pharmacological characterisation of PDE inhibitors**



Dewi Safitri

Department of Pharmacology
University of Cambridge

This dissertation is submitted for the degree of Doctor of Philosophy

Hughes Hall

April 2021

PREFACE

I hereby declare that this thesis is the results of my own work and includes nothing which is the outcome of work done in collaboration except as declared in the Preface and specified in the text. It is not substantially the same as any that I have submitted or is being concurrently submitted for a degree or diploma or other qualification at the University of Cambridge, or any other university or similar institution except as declared in the Preface and/or specified in the text. I further state that no substantial part of my thesis has already been submitted for any such degree, diploma, or other qualification at the University of Cambridge or any other university or similar institution except as declared in the Preface and specified in the text. This thesis does not exceed the prescribed word limit of 60,000 excluding appendices, bibliography, footnotes, tables, and equations.

ACKNOWLEDGEMENTS

The work in this thesis would not have been possible without the help of many people. In this opportunity, I would like to express the sincerest gratitude to my supervisor, Dr. Graham Ladds, for his guidance through each process during my PhD. This thesis would have not been possible without his constant encouragement, guidance, and inspiration throughout my study. He has been teaching me to be an independent scientist, showing perseverance to pursue academic career, and motivating me to become a better person.

My gratitude also goes to LPDP (endowment fund for education) from the Ministry of Finance of Republic of Indonesia that has been providing academic and non-academic support for the work.

I am grateful that during my PhD I obtain opportunity to collaborate with Dr. Taufiq Rahman and Dr. Matthew Harper (Department of Pharmacology, University of Cambridge) for finishing the PDE project. I would like to thank my dearest friends who always provide continuous supports both personally and professionally Dr. Matthew Harris and Lidia Betcheva; Dr. Kerry Barkan and Dr. Ashley Clark who teach me techniques that were useful to finish my thesis. Despite not being able to see each other, thank you for being there giving me support while I was away from home: Camilla Ascanelli and Grup Masak Ambi. To Miss Helen Lin-Qin Jia who contributed during PAR4 experiments should be sincerely acknowledged. Members in the lab during my PhD: Sabrina Carvalho, Abi Pearce and Anna Suchankova, thank you for making the lab an enjoyable place to work. I would like also to thank Dr. Laurentya Olga and Rangga Dachlan for believing in me when I doubted myself. My sincerest gratitude would be addressed to Dr. Sampurna Chakrabarty and Dr. Winnie Yeung, who become wonderful companions since the first day I joined the department and together spent long hours inside and outside the laboratories.

I would like to extend my gratitude to Ladds' family: Grand Dad, Graham, Karine and adorable boys - Matt and Chris, with whom I have an opportunity to feel like a family. I believe thank is not enough for kindness, warmth, and compassion provided all the time which I owe for the entire of my life.

Lastly, but definitely not the least, my deepest gratitude and love to my parents and my sisters for their care, support, and resilience to inspire and shape me the way I am. Thank you for allowing me pursuing my dream. I dedicate this work to them.

DECLARATION OF AUTHORSHIP

Some of the data within this thesis is a part of collaborative work and the contributions are as listed as the following:

Additional repeats on determination of cAMP levels on both intracellular and extracellular compartment were performed together with Dr. Ho Yan Yeung (University of Cambridge) (Figure 3.17)

Table 5.2 and Table 5.3, Appendix 1 (Figure 1, 3, 4) were the summary from the previous study performed by Dr. Ian Winfield (University of Cambridge).

Helen Lin Jia-Qi (University of Cambridge) performed the β -arrestin recruitment on PAR4-T120 variants (Figure 6.8)

Appendix 1 Figure 2 was performed by Sabrina Carvalho (University of Cambridge).

Part of the work has been published (or is in pre-print) as follows:

Safitri, D., *et al.* 2020. Elevated intracellular cAMP concentration mediates growth suppression in glioma cells, *Biochemical Pharmacology*, 174

Kalash, L., *et al.* 2021. Structure-based identification of dual ligands at the A2AR and PDE10A with anti-proliferative effects in lung cancer cell lines. *Journal of Cheminformatics*, 13(1), p. 17

Clark, A.J., *et al.* 2021. CGRP-receptor family reveals endogenous GPCR agonist bias and its significance in primary human cardiovascular cells. *bioRxiv*, p. 2020

This thesis adheres to the word limit of 60,000 as determined by the Degree Committee of the Faculty Biology, not including references.

Word count: 50,000

ABSTRACT

The alteration of intracellular cyclic adenosine monophosphate (cAMP) levels plays important regulatory roles in both physiological and pathological conditions, such as cancer. As the most aggressive form of brain tumour, glioblastoma is currently incurable due to limited treatment modalities. Low level of intracellular cAMP levels has been reported to be a feature of brain tumours. Thus, it is hypothesised that increasing cAMP concentrations by targeting regulatory proteins involved in the cAMP signalling pathways may offer advantages in preventing or treating glioblastoma. The overarching goal of this study therefore is to determine the dynamic effects of cAMP modulation on glioblastoma cell proliferation.

The efficacies of compounds targeting various proteins involved in cAMP pathways were first investigated. The mechanisms explored were elevation of cAMP level through phosphodiesterases (PDEs) inhibition, adenylyl cyclase (AC) activation, as well as modulation via β -adrenoceptor (β -AR) and G proteins. A series of compounds were evaluated applying various assaying techniques and pharmacological tools using cAMP accumulation assays, cell proliferation, caspase-3/7 activation, and flow cytometry to determine cell cycle. It was demonstrated that increasing cAMP levels by multiple PDE inhibition or AC stimulation resulted in cell growth suppression on both rat and human glioblastoma models. The study was also extended to identify the role of possible crosstalk between calcium through SOCE (store-operated calcium entry) and cAMP pathways, which both were found to contribute to cell growth modulation.

The effect of the elevation of intracellular cAMP on cell proliferation was further explored through the direct activation of adenosine A_{2A} receptor ($A_{2A}R$) and inhibition of cAMP degradation via PDE10A. Previous computational studies revealed that the triazoloquinazoline-based compounds (compound 1-6), initially known as PDE10A inhibitors, are bound at the orthosteric site of $A_{2A}R$. To validate the computational results, these compounds were characterised using NanoBRET-based ligand binding studies with HEK293T expressing Nluc- $A_{2A}R$ and functional assays in lung cancer cell lines and glioma/glioblastoma cell models, which both cell models expressed endogenous levels of PDE10A and $A_{2A}R$. The study highlighted that compounds 1 and 5 were dual-target ligands to $A_{2A}R$ and PDE10A, whereas compound 3 appeared to be a pan-agonist of adenosine receptors (ARs), and compound 4 was more potent when $A_{2B}R$ was expressed. Compound 2 seems to possess toxic effects that may be independent of action to $A_{2A}R$ or PDE10A.

Lastly, preliminary studies were conducted to investigate the possibility of biased signalling by RAMPs on protease-activated receptor 4 (PAR4) and calcitonin-like receptor (CLR). Using PAR4 transiently transfected HEK293T cells, both cognate ligand and agonist peptide were used to profile PAR4 signalling including RAMPs-trafficking to the plasma membrane, promoting intracellular calcium release and recruiting β -arrestins. The effects of RAMPs were also investigated in HUVECs and cardiomyocytes focusing on the effect of endogenous ligands on cell growth. Whilst RAMPs altered PAR4 initial signalling events in promoting β -arrestin recruitment, the study on heterodimer complex of RAMPs and CLR on cell growth further corroborated that signalling bias can be translated into physiological responses in HUVECs and cardiomyocytes.

To conclude, these studies provided evidence on how the alterations of intracellular cAMP levels affected cell proliferation in numerous cancer models, and that the cAMP-mediated anti-proliferative effect was cell-line dependent. Targeting multiple PDEs suppressed cell growth in cancer-derived cells, therefore providing a viable target to reduce tumour progression. Given the critical role of PAR4 in platelet aggregation and pro-proliferative of

calcitonin peptide family, this research may have important implications for the role of RAMPs in cardiovascular pathologies.

TABLE OF CONTENT

| | |
|---|-------------|
| Acknowledgement | i |
| Declaration of authorship | ii |
| Abstract | iii |
| Table of content | iv |
| List of Figures | xi |
| List of Tables | xv |
| List of Abbreviations | xvii |
| Chapter 1 Introduction | 1 |
| 1.1 Cellular signalling | 1 |
| 1.2 Overview of signal transduction through G protein-coupled receptors (GPCRs)..... | 1 |
| 1.2.1 G protein-mediated signalling..... | 4 |
| 1.2.1.1 The $G\alpha_s$ family | 5 |
| 1.2.1.2 The $G\alpha_{i/o}$ family | 5 |
| 1.2.1.3 The $G\alpha_{q/11}$ family | 6 |
| 1.2.1.4 The $G\alpha_{12/13}$ family..... | 7 |
| 1.2.1.5 The $G\beta$ subunit | 7 |
| 1.2.1.6 The $G\gamma$ subunit | 8 |
| 1.2.2 Non-canonical GPCR signalling | 8 |
| 1.2.2.1 The role of G protein receptor kinases (GRKs) | 9 |
| 1.2.2.2 The arrestin family | 11 |
| 1.2.2.3 Other regulatory proteins that promote non-canonical GPCR signalling | 12 |
| 1.2.3 Modulatory action of RAMP in regulating GPCR signalling. | 12 |
| 1.2.4 Hallmark of cancer | 16 |
| 1.2.5 Overview of several GPCRs to be explored in this study.... | 18 |
| 1.2.6 Adenosine A_{2A} receptor ($A_{2A}R$)..... | 18 |
| 1.2.6.1 The role of $A_{2A}R$ signalling in cancer | 20 |
| 1.2.6.2 Triazoloquinazolines' dual action on $A_{2A}R$ and PDE10A..... | 22 |
| 1.2.7 Protease-activated receptor 4 (PAR4) | 22 |
| 1.2.7.1 An overview of PAR4 | 22 |
| 1.2.7.2 A novel strategy to manipulate PAR4 pharmacology | 24 |
| 1.2.8 The calcitonin receptor-like receptor | 25 |
| 1.2.8.1 An overview of CLR..... | 25 |
| 1.2.8.2 Physiological consequences of CLR-RAMP complex formation on cell growth: studies in human glioblastoma model and cardiovascular cells | 26 |
| 1.3 Signal transduction through second messenger | 26 |

| | | |
|------------------|---|-----------|
| 1.4 | cAMP, a key regulator second messenger | 27 |
| 1.4.1 | Homeostasis of cAMP concentration | 27 |
| 1.4.2 | Overview of PDE structure and function | 28 |
| 1.4.2.1 | PDE1 | 32 |
| 1.4.2.2 | PDE2 | 32 |
| 1.4.2.3 | PDE3 | 33 |
| 1.4.2.4 | PDE4 | 33 |
| 1.4.2.5 | PDE5 | 35 |
| 1.4.2.6 | PDE6 | 35 |
| 1.4.2.7 | PDE7 | 35 |
| 1.4.2.8 | PDE8 | 36 |
| 1.4.2.9 | PDE9 | 36 |
| 1.4.2.10 | PDE10 | 36 |
| 1.4.2.11 | PDE11 | 37 |
| 1.4.2.12 | Small molecule PDE inhibitors | 37 |
| 1.4.3 | Cyclic nucleotide extrusion | 39 |
| 1.4.4 | Downstream effectors of cAMP | 40 |
| 1.4.4.1 | Protein Kinase A (PKA) | 40 |
| 1.4.4.2 | Exchange protein activated by cAMP (EPAC) | 41 |
| 1.4.4.3 | Cyclic nucleotide gated channels (CNGCs) | 43 |
| 1.4.4.4 | The popeye domain containing protein (POPDC) and cyclic nucleotide receptor involved in sperm function (CRIS) | 43 |
| 1.4.5 | Interconnection with other second messenger pathways | 45 |
| 1.4.5.1 | cGMP signalling | 45 |
| 1.4.5.2 | Calcium (Ca ²⁺) signalling | 46 |
| 1.5 | Multimodal function of cAMP pathways | 48 |
| 1.6 | Glioma/glioblastoma and alteration on cAMP signalling | 48 |
| 1.7 | Aims | 52 |
| Chapter 2 | Material and Methods | 54 |
| 2.1 | Materials | 54 |
| 2.1.1 | General reagents | 54 |
| 2.1.2 | Compounds | 54 |
| 2.1.3 | Growth media | 55 |
| 2.1.4 | DNA expression constructs | 56 |
| 2.2 | Methods | 56 |
| 2.2.1 | Cell lines | 56 |
| 2.2.2 | Long-term storage and recovery | 57 |
| 2.2.3 | <i>E. coli</i> transformation | 58 |
| 2.2.4 | Plasmid DNA purification | 58 |
| 2.2.5 | RNA extraction, quality determination, and reverse transcriptase polymerase chain reaction (RT-PCR) | 59 |
| 2.2.6 | Mutagenesis of PAR4-A120 | 66 |
| 2.2.7 | Cloning of Nanoluciferase (NLuc)-tagged PAR4 | 67 |
| 2.2.8 | Transient transfection of HEK-293S/HEK-293T cells | 70 |

| | | |
|------------------|--|-----------|
| 2.2.8.1 | Fugene method | 70 |
| 2.2.8.2 | PEI method 1..... | 70 |
| 2.2.8.3 | PEI method 2..... | 71 |
| 2.2.9 | cAMP accumulation assay | 71 |
| 2.2.10 | Quantification of intracellular and extracellular cAMP concentrations | 73 |
| 2.2.11 | cGMP accumulation assay..... | 73 |
| 2.2.12 | Quantifying the extent of cell proliferation | 74 |
| 2.2.13 | Quantifying Caspase-3/-7 activity..... | 77 |
| 2.2.14 | Cell cycle analysis..... | 78 |
| 2.2.15 | Quantification of ligand binding affinity through BRET-based ligand binding assay..... | 79 |
| 2.2.16 | Quantification of RAMP cell surface expression using FACS..... | 80 |
| 2.2.17 | Quantification of intracellular calcium signalling..... | 81 |
| 2.2.18 | Quantification of ligand-mediated β -arrestin recruitment through bioluminescent resonance energy transfer (BRET)-based assay | 82 |
| 2.2.19 | Data analysis..... | 83 |
| Chapter 3 | Phosphodiesterase inhibition as a therapeutic target: study in a model of glioma..... | 85 |
| 3.1 | Introduction | 85 |
| 3.2 | Elevation of cAMP through β -adrenoceptor, G protein, and adenylyl cyclase exhibit differential range of anti-proliferative effects in C6 glioma cells | 87 |
| 3.3 | Determination of PDE expression profile in glioma cells..... | 90 |
| 3.4 | Pharmacological characterization of PDE inhibitors on modulating cAMP concentration | 91 |
| 3.4.1 | Development of a screening method to profile the efficacy of small molecule PDE inhibitors in modulating cAMP signalling..... | 92 |
| 3.4.2 | Elevation of intracellular cAMP positively correlates with cell growth suppression | 96 |
| 3.5 | Combinatorial effect of individual PDE2, PDE3, and PDE7 inhibitor was similar to that of, a multitarget PDE inhibitor trequinsin | 112 |
| 3.6 | Targeting both adenylyl cyclase and phosphodiesterase enhances anti-proliferative effect..... | 115 |
| 3.7 | Blockade of cAMP export enhances the anti-proliferative effect of forskolin, trequinsin, and the PDE inhibitor cocktail | 117 |
| 3.8 | Anti-proliferative effects of forskolin and PDE inhibitors are predominantly mediated through the cAMP/PKA signalling pathway | 122 |
| 3.9 | Trequinsin, but not forskolin or the PDE inhibitor cocktail, has cAMP-independent actions leading to apoptosis | 126 |
| 3.10 | Elevated intracellular cAMP induces growth arrest at the G2/M phase of the cell cycle..... | 127 |

| | | |
|--------|--|-----|
| 3.11 | Discussion | 129 |
| 3.11.1 | C6 cells as a suitable model to investigate role of PDE isoenzymes in glioblastoma | 130 |
| 3.11.2 | Elevation of intracellular cAMP through PDE inhibition or AC stimulation elicited a more potent anti-proliferative effect compared to modulating at GPCR levels or G proteins | 130 |
| 3.11.3 | The efficacy of PDE inhibitors demonstrates reliance on PDE expression profile | 131 |
| 3.11.4 | Trequinsin as multiple PDE inhibitor may have the potential effect that is independent of cAMP/PKA and can be counteracted by combining individual PDE2, PDE3, and PDE7 inhibitor..... | 131 |
| 3.11.5 | Forskolin and PDE inhibitor induces cell growth arrest..... | 133 |
| 3.11.6 | Modulation to increase cAMP concentration leads to negative regulation on cell growth | 133 |
| 3.11.7 | Conclusion | 134 |
| 3.12 | Summary | 134 |

Chapter 4 Investigating the role of second messengers in human

| | | |
|-------|---|------------|
| | glioblastoma cells | 136 |
| 4.1 | Introduction..... | 136 |
| 4.2 | Pharmacological characterisation of PDEs in model glioblastoma cells | 137 |
| 4.2.1 | Human glioblastoma cells express various PDEs at mRNA levels | 137 |
| 4.2.2 | Development of a method to characterise the role of PDEs in accumulating cAMP signalling | 139 |
| 4.2.3 | Pharmacological role of PDEs in cAMP and cell proliferation | 142 |
| 4.3 | Elevation of cAMP by targeting PDEs positively correlated with cell growth suppression | 159 |
| 4.4 | The combinatorial effect of PDE2, PDE3, and PDE7 inhibitors mimicks the effect of trequinsin | 162 |
| 4.5 | Concomitant targeting AC and PDEs only affects short-term cAMP production, but is insufficient to modulate cell proliferation in human glioblastoma cells | 168 |
| 4.6 | The pharmacological effect of cAMP efflux transporter in glioblastoma: MRP4 | 170 |
| 4.7 | Modulation of calcium signalling through SOCE mechanism exhibited negative effect on glioma/glioblastoma cell proliferation... .. | 171 |
| 4.8 | Discussion | 175 |
| 4.8.1 | Human glioblastoma cell lines are more aggressive model compared to rat C6 glioma cells | 175 |
| 4.8.2 | Differential responses towards PDE inhibitors: U87 vs T98 cells | 175 |

| | | |
|--|---|------------|
| 4.8.3 | Elevation of cAMP by PDE inhibitor cocktail and concomitant targeting..... | 177 |
| 4.8.4 | Inhibiting MRP4 efflux transporter improves forskolin- and trequinsin-mediated antiproliferative effect..... | 178 |
| 4.8.5 | Inhibiting SOCE as another approach to inhibiting human glioblastoma cell growth: is it a feasible target? | 180 |
| 4.9 | Summary | 180 |
| Chapter 5 Identifying dual action ligands agonising A_{2A}R and inhibiting PDE10A | | |
| | PDE10A | 182 |
| 5.1 | Introduction | 182 |
| 5.2 | Triazoloquinazolines displayed differential binding affinities at A _{2A} R | 188 |
| 5.3 | Non-small lung cancer cell lines as the appropriate model to validate multi-target ligand against A _{2A} R/PDE10A..... | 193 |
| 5.4 | Synergistic activities of dual mechanism of PDE10A inhibition and A _{2A} R agonism on ligand-mediated cAMP accumulation leading to cell growth suppression in human lung cancer cell lines | 195 |
| 5.4.1 | Triazoloquinazolines promoted cAMP production in human NSCLC cells | 195 |
| 5.4.2 | Triazoloquinazolines mediated anti-proliferative effects on human NSCLC cell lines..... | 198 |
| 5.5 | Multi-target ligands simultaneously displayed better efficacy across human lung cancer cell lines corresponding to cumulative expression of A _{2A} R and PDE10A | 200 |
| 5.6 | Targeting A _{2A} R/PDE10A elevated cAMP levels but did not optimally Expression profile of A _{2A} R and PDE10A in glioma/glioblastoma cell models..... | 204 |
| 5.6.1 | Expression profile of A _{2A} R and PDE10A in glioma/glioblastoma cell models..... | 204 |
| 5.6.2 | Triazoloquinazolines mediated cAMP accumulation in glioma and glioblastoma cells..... | 205 |
| 5.6.3 | Multi-target ligands suppressed cell proliferation on C6 cells but elicited differential responses across human glioblastoma cells | 208 |
| 5.7 | Elevation of cAMP levels by triazoloquinazolines failed to be translated into cell proliferation in glioma and glioblastoma cells..... | 211 |
| 5.8 | Discussion..... | 215 |
| 5.8.1 | Validation using functional assays proving triazoloquinazolines as dual-target ligands working on A _{2A} R and PDE10A..... | 215 |
| 5.8.2 | Differential effects of triazoloquinazolines in various cancer models | 216 |
| 5.9 | Summary | 219 |
| Chapter 6 Receptor activity modifying protein (RAMP) modulation of protease-activated receptor 4 (PAR4) and calcitonin-like receptor (CLR) signalling | | |
| | | 221 |

| | | |
|------------------|--|------------|
| 6.1 | Introduction..... | 221 |
| 6.2 | PAR4 is coupled to G α_q to promote intracellular calcium release | 223 |
| 6.3 | PAR4 recruits β -arrestin | 225 |
| 6.4 | RAMPs are promoted to plasma membrane in the presence of PAR4-A120 and PAR4-T120..... | 227 |
| 6.5 | RAMPs alter thrombin-mediated intracellular calcium mobilisation.. | 229 |
| 6.6 | RAMP alters β -arrestin recruitment to PAR4..... | 231 |
| 6.7 | Quantification of signalling bias at PAR4 in the presence of RAMPs | 235 |
| 6.8 | Stimulation by CGRP-based peptide agonists elevated cAMP concentration and promoted glioblastoma U87 cell growth..... | 236 |
| 6.9 | RAMP regulate cellular signalling and cell growth of HUVECs and hCMs | 238 |
| 6.10 | Discussion | 239 |
| | 6.10.1 The novel interaction of PAR4 with RAMPs changes β - arrestin1/2 recruitment..... | 239 |
| | 6.10.2 RAMP regulate CLR pharmacology: the study on cell growth | 242 |
| 6.11 | Summary | 245 |
| Chapter 7 | General discussion and future directions..... | 246 |
| 7.1 | Discussion | 246 |
| | 7.1.1 Targeting cAMP pathway and its therapeutic benefits in cancer | 246 |
| | 7.1.1.1 Different signalling profile between GPCR ligand- mediated and AC-/ PDE- mediated cAMP responses..... | 247 |
| | 7.1.1.2 Short-term vs prolonged exposure of cAMP and factors that may influence cell growth..... | 248 |
| | A. Spatiotemporal control by PDEs and association with other proteins within specific subcellular domain..... | 249 |
| | B. Multiple proteins activated by cAMP are cell-type dependent | 250 |
| | C. Crosstalk with MAPK signalling | 251 |
| | 7.1.1.3 Physiochemical properties of tested compounds.... | 252 |
| | 7.1.1.4 Resistance cells were not responsive towards Forskolin and PDE inhibitor..... | 253 |
| | 7.1.1.5 Drug combination vs multi-target ligands | 254 |
| | 7.1.1.6 Potential use of cAMP elevating agent and further consideration for targeting cAMP pathway..... | 256 |
| | 7.1.2 Modulatory action of RAMPs in dictating PAR4 and CLR pharmacology | 256 |
| 7.2 | Future Directions | 258 |
| Chapter 8 | Bibliography..... | 260 |

| | |
|---|------------|
| Appendix 1. Additional Figures | 316 |
| Appendix 2. Safitri, <i>et al.</i> 2020..... | 320 |
| Appendix 3. Kalash, <i>et al.</i> 2021 | 336 |
| Appendix 4. Clark, <i>et al.</i> 2021 | 354 |

LIST OF FIGURES

| | | |
|-------------|--|-----|
| Figure 1.1 | GPCR signalling cycle | 3 |
| Figure 1.2 | Schematic illustration of GRK family proteins | 10 |
| Figure 1.3 | The hallmark of cancer | 17 |
| Figure 1.4 | The exemplary structure of adenosine A _{2A} receptor | 19 |
| Figure 1.5 | Structure of PAR4 | 23 |
| Figure 1.6 | Exemplary of PDE catalytic domain from apo-PDE5A structure .. | 30 |
| Figure 1.7 | The schematic representation of 11 subfamilies of PDEs..... | 31 |
| Figure 1.8 | The schematic illustration of PDE4 isoenzymes | 34 |
| Figure 1.9 | The summary of cyclic nucleotide signalling network..... | 45 |
| Figure 1.10 | The summary of calcium signalling pathways | 47 |
| Figure 1.11 | The summary of overall PDE expressions on GBM database | 51 |
| Figure 1.12 | The illustration of the framework between glioma/ glioblastoma and cellular network in regulating cAMP concentration..... | 52 |
| Figure 2.1 | Principle of LANCE ® cAMP assay kit | 72 |
| Figure 2.2 | Principle of Cisbio Bioassays' cGMP assay kit | 74 |
| Figure 2.3 | Principle of CCK-8 (cell counting kit-8) assay | 74 |
| Figure 2.4 | The effect of un-supplemented and complete growth media upon U87 cell growth..... | 75 |
| Figure 2.5 | Influence of cell density and treatment period on U87 cell growth | 76 |
| Figure 2.6 | Cell proliferation assay in several cell lines..... | 76 |
| Figure 2.7 | Principle of CellEvent™ Caspase-3/7 assay kit | 78 |
| Figure 2.8 | Representative figures of cytogram for cell cycle analysis..... | 79 |
| Figure 2.9 | Principle of BRET-based ligand binding assay | 80 |
| Figure 2.10 | Principle of BRET-based β-arrestin recruitment assay | 83 |
| Figure 3.1 | Illustration of regulation process of intracellular level of cAMP | 86 |
| Figure 3.2 | Elevation of cAMP, but not cGMP, mediates cell growth Suppression | 88 |
| Figure 3.3 | Forskolin stimulation has a greater effect on suppression of C6 cell growth than activation of β-adrenoceptor or Gα G protein subunits | 89 |
| Figure 3.4 | Expression profile of PDE isoenzymes in C6 and ST14A cells.... | 91 |
| Figure 3.5 | Comparison in using pEC20 and pEC50 of forskolin to provide sufficient window of observation for developing screening method | 92 |
| Figure 3.6 | PDE inhibitors increased the concentration of cAMP in the presence of forskolin in C6 and ST14A cells..... | 94 |
| Figure 3.7 | Effect of a panel of established PDE inhibitors on forskolin- mediated cAMP production in C6 cells..... | 99 |
| Figure 3.8 | Effect of a panel of established PDE inhibitors on forskolin- mediated cAMP production in ST14A cells. | 101 |
| Figure 3.9 | Effect of a panel of established PDE inhibitors, forskolin, and cisplatin on modulating C6 cell growth | 105 |

| | | |
|-------------|--|-----|
| Figure 3.10 | Effect of a panel of established PDE inhibitors, forskolin, and cisplatin on modulating ST14A cell growth..... | 107 |
| Figure 3.11 | Elevation of intracellular cAMP is positively correlated with cell growth suppression..... | 109 |
| Figure 3.12 | Illustration of how selection criteria are calculated..... | 110 |
| Figure 3.13 | Selection criteria of each PDE inhibitor including forskolin and Cisplatin | 111 |
| Figure 3.14 | Trequinsin may have potential toxic effect compared to forskolin at the same concentration..... | 112 |
| Figure 3.15 | The effect of trequinsin on cAMP production and cell proliferation can be mimicked by combining PDE2, 3, and 7 inhibitors..... | 113 |
| Figure 3.16 | Forskolin and trequinsin act synergistically to increase cAMP accumulation and suppress cell growth..... | 116 |
| Figure 3.17 | Inhibiting MRP4 transporter elevates intracellular levels of cAMP in C6 cells..... | 119 |
| Figure 3.18 | Elevation of intracellular cAMP by inhibiting its efflux is correlated with cell growth suppression in C6 cells | 121 |
| Figure 3.19 | Forskolin, trequinsin, or PDE inhibitor cocktail-mediated anti-proliferative effect was partially rescued by PKA inhibitor, but not EPAC or PKG inhibitor..... | 122 |
| Figure 3.20 | The effect of downstream effectors of cAMP and cGMP on forskolin and trequinsin-mediated cell growth suppression of C6 cells | 125 |
| Figure 3.21 | Representative figure of C6 cells after 72 h treatment and were subsequently loaded with 2 μ M CellEvent TM caspase-3/-7 | 126 |
| Figure 3.22 | Population of dead cells and activity of caspase-3/7 in C6 cells after 72 h treatment..... | 127 |
| Figure 3.23 | Cell cycle analysis by flow cytometry after PI staining..... | 129 |
| Figure 4.1 | Illustration of calcium signalling and possible interplay between store operated calcium entry (SOCE) mechanism and the cyclic nucleotide pathway. | 137 |
| Figure 4.2 | Expression profile of PDEs in human glioblastoma cell lines (U87 and T98) in comparison to HEK293S cells | 138 |
| Figure 4.3 | PDE inhibition increased the concentration of cAMP in the presence of forskolin across glioblastoma cell lines | 140 |
| Figure 4.4 | Effect of a panel of established PDE inhibitors on forskolin-mediated cAMP production in U87 cells..... | 146 |
| Figure 4.5 | Effect of a panel of established PDE inhibitors on forskolin-mediated cAMP production in T98 cells | 148 |
| Figure 4.6 | Effect of a panel of established PDE inhibitors on forskolin-mediated cAMP production in HEK293S cells | 150 |
| Figure 4.7 | Effect of a panel of established PDE inhibitors, forskolin, and cisplatin on modulating U87 cell growth..... | 154 |
| Figure 4.8 | Effect of a panel of established PDE inhibitors, forskolin, and cisplatin on modulating T98 cell growth..... | 156 |

| | | |
|-------------|---|-----|
| Figure 4.9 | Effect of a panel of established PDE inhibitors, forskolin, and cisplatin on modulating HEK293S cell growth..... | 158 |
| Figure 4.10 | Elevation of intracellular cAMP positively correlates with cell Growth in U87 cells, T98 cells, and HEK293S cells..... | 160 |
| Figure 4.11 | Selection criteria of PDE inhibitor in U87, T98, and HEK293S cells | 161 |
| Figure 4.12 | The combinatorial effect of PDE2, PDE3, and PDE7 inhibitor was similar to that of trequinsin in modulating cAMP production . | 163 |
| Figure 4.13 | Anti-proliferative effect of trequinsin can be mimicked by combining individual PDE2, PDE3, and PDE7 inhibitor | 165 |
| Figure 4.14 | Co-treatment of forskolin and trequinsin mediated elevation of cAMP levels but showed marginal effect in cell proliferation across human glioblastoma cell lines..... | 169 |
| Figure 4.15 | PU23, an MRP4 inhibitor, potentiate anti-proliferative effect of forskolin on human glioblastoma U87 and T98 cells..... | 171 |
| Figure 4.16 | Some compounds that inhibit SOCE displayed anti-proliferative action in glioma and glioblastoma cell lines | 172 |
| Figure 5.1 | Representative traces of BRET signal in ligand binding Saturation assay of CA200645 in the absence or presence of ZM241385 | 189 |
| Figure 5.2 | Determination of dissociation constant of CA200645 using BRET-based kinetic binding studies..... | 190 |
| Figure 5.3 | BRET signal traces from competition binding assays of reference compounds at A _{2A} R..... | 191 |
| Figure 5.4 | Triazoloquinazolines were confirmed to bind at the A _{2A} R | 192 |
| Figure 5.5 | Non-small lung carcinoma (NSCLC) cell lines differentially expressed different levels of adenosine receptors and PDE10A..... | 195 |
| Figure 5.6 | Multitarget ligand mediated cAMP accumulation on NSCLC cell lines..... | 197 |
| Figure 5.7 | Differential anti-proliferative effect in NSCLC cell lines after triazoloquinazolines treatment..... | 199 |
| Figure 5.8 | Multi-target ligands simultaneously displayed better efficacies across cell lines corresponding to the cumulative expression of A _{2A} R and PDE10A..... | 201 |
| Figure 5.9 | Glioma and glioblastoma cell lines differentially expressed all subtypes of adenosine receptors and PDE10A | 205 |
| Figure 5.10 | Different effects of multi-target ligands on cAMP accumulation in glioma and glioblastoma cell lines | 207 |
| Figure 5.11 | Multi-target ligands did not show any particular pattern in inhibiting cell proliferation across cell lines tested..... | 210 |
| Figure 5.12 | There is no correlation between the elevation of cAMP level and cell growth upon stimulation with triazoloquinazolines on rat and human glioblastoma cells..... | 212 |
| Figure 6.1 | Representative figures of intracellular calcium release on HEK293T cells expressing PAR4-A120 upon stimulation with | |

| | | |
|-------------|--|-----|
| | thrombin | 224 |
| Figure 6.2 | Both thrombin and PAR4-agonist peptide promote intracellular calcium release | 225 |
| Figure 6.3 | The representative of BRET signal on β -arrestin recruitment Assay | 226 |
| Figure 6.4 | PAR4 both variants differentially recruited β -arrestin upon stimulation with AYPGKF-NH ₂ | 227 |
| Figure 6.5 | The presence of PAR4 influence RAMPs cell surface expression..... | 229 |
| Figure 6.6 | The presence of RAMPs modulate intracellular calcium mobilisation at PAR4 upon stimulation with thrombin..... | 230 |
| Figure 6.7 | PAR4 agonist peptide-mediated calcium release remain unaffected in RAMPs co-expressed with PAR4 in HEK293T cells..... | 231 |
| Figure 6.8 | RAMPs differentially modulate β -arrestin recruitment on both PAR4 polymorphisms upon stimulation with PAR4-agonist Peptide..... | 233 |
| Figure 6.9 | Quantification of biased signalling at PAR4 both variants by the presence of RAMPs | 236 |
| Figure 6.10 | Elevation on cAMP concentration by peptide ligands induced cell proliferation on U87 cells | 237 |
| Figure 6.11 | Stimulation by CGRP family peptides induced cell proliferation to different extents on HUVECs and hCMs..... | 239 |
| Figure 6.12 | CGRP and AM, but not AM2, mediate biphasic responses on cAMP production in U87 cells..... | 244 |

LIST OF TABLES

| | | |
|------------|--|-----|
| Table 1.1 | RAMP interacting GPCR partners..... | 13 |
| Table 1.2 | Characteristic of PDE isoenzyme families and their Km value for both cyclic nucleotides | 28 |
| Table 1.3 | The summary of small molecules that selectively inhibit each PDE subfamily protein..... | 38 |
| Table 2.1 | List of chemical compounds and protein used for this study..... | 54 |
| Table 2.2 | Plasmid/construct used in this study | 56 |
| Table 2.3 | Oligonucleotides used to amplify gene of interests within this study..... | 59 |
| Table 2.4 | Thermocycler set up for amplification..... | 66 |
| Table 2.5 | Oligonucleotides that were designed to generate PAR4 variant that express alanine at position 120..... | 67 |
| Table 2.6 | Summary of component reaction for mutagenesis..... | 67 |
| Table 2.7 | Oligonucleotides that were designed to introduce restriction sites on PAR4 constructs..... | 68 |
| Table 2.8 | List of components used for PCR amplification..... | 68 |
| Table 2.9 | Thermocycler set up for molecular cloning..... | 68 |
| Table 2.10 | Component for PCR colonies..... | 69 |
| Table 2.11 | Thermocycler set up for PCR colonies..... | 70 |
| Table 2.12 | Components used for FuGENE®HD transfection method | 71 |
| Table 2.13 | Components used for PEI transfection method in several different formats | 71 |
| Table 3.1 | The response of C6 and ST14A when were stimulated with forskolin and selected PDE inhibitors corresponding to pEC ₂₀ forskolin | 93 |
| Table 3.2 | Pharmacological parameters of forskolin in the presence of different PDE inhibitors in C6 cells | 95 |
| Table 3.3 | Pharmacological parameters of forskolin in the presence of different PDE inhibitors in ST14A cells | 95 |
| Table 3.4 | Established <i>in vitro</i> pIC ₅₀ values of each PDE inhibitors used in this study | 96 |
| Table 3.5 | Potency values for cAMP production (pEC ₅₀) and for cell growth inhibition (pIC ₅₀) of each PDE inhibitor in C6 and ST14A cells.... | 102 |
| Table 3.6 | Summary of the pharmacological effects of each PDE inhibitor on cAMP production and cell proliferation..... | 108 |
| Table 3.7 | C6- proliferation assay-combinatorial effect of PDE2, 3, 7 inhibitors | 114 |
| Table 3.8 | Concentration of intra- and extra-cellular of cAMP in cells treated with forskolin, trequinsin, or PDE inhibitor cocktail in the absence or in the presence of PU23, an MRP4 inhibitor | 119 |
| Table 3.9 | Pharmacological parameter of forskolin, trequinsin, PDE inhibitor cocktail on modulating cell proliferation... .. | 121 |
| Table 3.10 | Pharmacological parameters of forskolin, trequinsin, and PDE inhibitor cocktail in the absence and presence inhibitors | |

| | | |
|-----------|--|-----|
| | targeting downstream effectors of cAMP and cGMP signalling ... | 123 |
| Table 4.1 | Pharmacological parameters of forskolin in the presence of selected PDE inhibitors..... | 141 |
| Table 4.2 | Percentage response of each cell line in the presence of PDE inhibitors at the pEC ₂₀ concentration of forskolin alone | 142 |
| Table 4.3 | Potency values for cAMP production (pEC ₅₀) and span of each PDE inhibitor in U87, T98, and HEK-293S cells | 144 |
| Table 4.4 | Potency values for cell growth inhibition (pIC ₅₀) and span of each PDE inhibitor in U87, T98, and HEK-293S cells | 151 |
| Table 4.5 | Summary of the pharmacological effects of each PDE inhibitor on cAMP production and cell proliferation | 159 |
| Table 4.6 | Combinatorial effect of individual PDE2, PDE3, and PDE7 inhibitor in glioblastoma cell lines U87 and T98 cells in comparison to HEK293S cells | 166 |
| Table 4.7 | The summary of pharmacological parameters of SOCE inhibitors in modulating cell growth | 174 |
| Table 5.1 | The reference of triazoloquinazolines used in this study | 184 |
| Table 5.2 | Potency (pEC ₅₀) and E _{max} values for NECA, CGS 21680 and trizaoloquinazoline stimulation of adenosine A ₁ , A _{2A} and A _{2B} receptors in yeast expressing GPA1/Gα _{i1/2} or GPA1/Gα _s and CHO-K1-A ₃ Rcells..... | 186 |
| Table 5.3 | Potency (pEC ₅₀) and range of responses for cAMP production upon CGS21680 and triazoloquinazoline stimulated cAMP accumulation in CHO-K1-A _{2A} R and CHO-K1 cells..... | 187 |
| Table 5.4 | The summary of triazoloquinazolines-based compound according to previous characterisation on yeast and heterologous overexpression system | 188 |
| Table 5.5 | Binding affinities of triazoloquinazolines at the human A _{2A} R using fluorescent probes CA200645 | 193 |
| Table 5.6 | Summary of pharmacological activities of triazoloquinazolines across human NSCLC cells | 202 |
| Table 5.7 | Summary of pharmacological activities of triazoloquinazolines across glioma and glioblastoma cells | 213 |
| Table 6.1 | Pharmacological parameters of thrombin and PAR4-AP on PAR4-A120 and PAR4-T120 variants..... | 225 |
| Table 6.2 | The potency (pEC ₅₀) and E _{max} value of PAR-agonist peptide on both PAR4 variants in recruiting β-arrestins | 227 |
| Table 6.3 | Pharmacological parameters of PAR4-agonist peptide on PAR4-A120 and PAR4-T120 variants in the absence and presence of RAMPs | 234 |
| Table 6.4 | The value of potency (pEC ₅₀) and maximum responses (E _{max}) of agonist peptide on cAMP production and cell growth in U87 cells..... | 238 |
| Table 6.5 | The value of potency (pEC ₅₀) and maximum responses (E _{max}) of agonist peptides on cell growth in HUVECs and CMs..... | 239 |
| Table 6.6 | The value of potency and E _{max} of CGRP and AM after stimulation in U87 cells in cAMP accumulation assay | 244 |

LIST OF ABBREVIATIONS

| | |
|-------------------|---|
| 5-AMP | 5-adenosine monophosphate |
| 5-GMP | 5-guanosine monophosphate |
| A _{2A} R | adenosine A _{2A} receptor |
| ABC | ATP binding cassette |
| AC | adenylyl cyclase |
| ACKR | atypical chemokine receptor |
| ADGRF5 | adhesion G protein-coupled receptor F5 |
| AGC | protein kinases group of PKA, PKG, and PKC |
| AGS | activator of G protein signalling |
| AKAP | A-kinase anchoring protein |
| AM | adrenomedulin |
| AM2 | adrenomedulin 2 |
| AMY | amylin |
| ARs | adenosine receptors |
| ATF1 | activating transcription factor 1 |
| ATM | ataxia telangiectasia mutated |
| ATP | adenosine triphosphate |
| BAD | BCL2 associated agonist of cell death |
| BBB | blood-brain barrier |
| BIM | BCL2-interacting mediator of cell death |
| bp | base pair |
| BRCA1 | breast cancer type 1 susceptibility protein |
| BRET | bioluminescence resonance energy transfer |
| BSA | bovine serum albumin |
| C-terminus | carboxyl terminus |
| CaM | calmodulin |
| CaMK | calmodulin-dependent protein kinase |
| cAMP | cyclic adenosine monophosphate |
| CaSR | calcium-sensing receptor |
| CaV | Ca ²⁺ voltage-gated ion channel |
| CCR | chemokine receptor |
| CDK | cyclin dependent kinase |
| cDNA | complementary DNA |

| | |
|------------------|---|
| cGMP | cyclic guanosine monophosphate |
| CGRP | calcitonin-gene related polypeptide |
| CHK2 | checkpoint kinase 2 |
| CHO-K1 | chinese hamster ovary K1 |
| CLR | calcitonin receptor-like receptor |
| CMs | cardiomyocytes |
| CNB | cyclic nucleotide binding |
| CNGC | cyclic nucleotide gated channel |
| CNS | central nervous system |
| COS | cells being CV-1 (simian) in Origin and carrying the SV40 genetic material |
| CREB | cAMP response element binding |
| CREM | cAMP-responsive element modulator |
| CRIS | cyclic nucleotide receptor involved in sperm function |
| CTR | calcitonin receptor |
| CTx | cholera toxin |
| CXCR | CXC chemokine receptor |
| D ₂ R | dopamine D ₂ receptor |
| DAG | diacyl glycerol |
| DARPP-32 | dopamine- and cAMP-regulated phosphoprotein-32 |
| DEP | Dishevelled/EG1-10/pleckstrin |
| DHODH | dihydroorotate dehydrogenase |
| DMEM | Dulbecco's modified Eagle's medium |
| DMSO | dimethyl sulphoxide |
| DNA | deoxyribose nucleic acid |
| <i>E. coli</i> | Escherichia coli |
| E3KARP | NHE3 kinase A regulatory protein |
| ebBRET | enhanced bystander bioluminescence resonance energy transfer |
| EBP50 | ezrin-radixin-moesin (ERM)-binding phosphoprotein 50 |
| ECD | extracellular domain |
| EHNA | erythro-9-(2-hydroxy-3-nonyl)-adenine |
| E _{max} | maximum level of response |
| ENPP1 | ectonucleotide pyrophosphatase/ phosphodiesterase 1 |
| EPAC | exchange protein activated by cAMP |
| ER | endoplasmic reticulum |

| | |
|-----------|--|
| ERK1/2 | extracellular signal-regulated kinase 1/2 |
| FACS | fluorescence activated cell sorting |
| FBS | fetal bovine serum |
| FRET | fluorescence resonance energy transfer |
| FRET | Forster-resonance energy transfer |
| G protein | guanine nucleotide-binding proteins |
| GABA | γ -aminobutyric acid |
| GAF | cGMP-specific phosphodiesterases, adenylyl cyclases and FhIA |
| GAPs | GTPase activating proteins |
| GC | guanylyl cyclase |
| GCGR | glucagon receptor |
| GDI | guanine nucleotide dissociation inhibitor |
| GDP | guanosine diphosphate |
| GEPR | G protein estrogen receptor 1 |
| GPCR | G protein-coupled receptor |
| GRK | G protein receptor kinase |
| GTP | guanosine triphosphate |
| H2AX | histon family member X |
| HBSS | Hank's balanced salt solution |
| hCMs | human cardiomyocytes |
| HCN | hyperpolarization-activated cyclic nucleotide-gated |
| HEK | human embryonic kidney |
| hPSCs | human pluripotent stem cells |
| HUVECs | human umbilical vein endothelial cells |
| IBMX | 3-isobutyl-1-methylxanthine |
| ICL | intracellular loop |
| I_{max} | maximum inhibition of response |
| IP3 | inositol triphosphate |
| JNK | c-Jun N-terminal kinase 3 |
| KTR | kinase translocation reporters |
| LANCE | Lanthanide Chelate Excite |
| LARG | leukemia associated RhoGEF |
| LUAD | lung adenocarcinoma |
| LUSC | lung squamous cell carcinoma |
| MAPK | mitogen-activated protein kinase |

| | |
|-------------------|--|
| MAPKK | mitogen-activated protein kinase kinase |
| MAPKKK | mitogen-activated protein kinase kinase kinase |
| MCS | multi-cloning site |
| MEM | minimal essential medium |
| MRP | multidrug resistant protein |
| mTOR | mammalian target of rapamycin |
| NBS1 | nibrin |
| NHERF | Na ⁺ /H ⁺ exchanger regulatory factor or NHERF-1 |
| Nluc | nanoluciferase |
| NMDA | N-methyl-D-aspartate |
| NO | nitric oxide |
| NSCLC | non-small cell lung cancer |
| PAC1R | pituitary adenylate cyclase-activating peptide receptor |
| PAFR | platelet activating receptor |
| PAR | protease-activated receptor |
| PAS | Per-Arnt-Sim |
| PCR | polymerase chain reaction |
| PDE | phosphodiesterase |
| PDZ | postsynaptic density 95, PSD-95; Disc large, Dlg; Zonula occluden-1, ZO-1 |
| pEC ₅₀ | negative logarithm of concentration of agonist required to produce a half-maximal response |
| PH | pleckstrin homology |
| PI3K | phosphatidylinositol-3 kinase |
| pIC ₅₀ | negative logarithm of concentration of inhibitor required to produce a half-maximal response |
| PKA | protein kinase A |
| PKB | protein kinase B |
| PKC | protein kinase C |
| PKG | protein kinase G |
| PLC | phospholipase C |
| PLL | poly-L-lysine |
| POPDC | the popeye domain-containing proteins |
| pRB | retinoblastoma pathway |
| PTEN | phosphatase and tensin |

| | |
|-------------------|--|
| PTHr | parathyroid hormone receptor |
| PTx | pertussis toxin |
| RAMP | receptor activity-modifying protein |
| RGC | receptor guanylyl cyclase |
| RGS | regulator of G protein signalling |
| RH | RGS homology |
| Rluc | <i>Renilla</i> luciferase |
| RNA | ribonucleic acid |
| RTK | receptor tyrosine kinase |
| RYR | ryanodine receptors |
| sAC | soluble adenylyl cyclase |
| SEM | standard error of the mean |
| sGC | soluble guanylyl cyclase |
| SOcAMP | store operated cAMP entry |
| SOCE | store operated calcium entry |
| STAT3 | signal transducer and activator of transcription 3 |
| STIM | stromal interaction molecule 1 |
| T2DM | type 2 diabetes mellitus |
| TM | transmembrane |
| TMD | transmembrane domain |
| TME | tumour microenvironment |
| TRPC | transient receptor potential cation channels |
| TTFields | tumour-treating fields |
| UCR | upstream conserved region |
| V ₂ R | vasopressin V ₂ receptor |
| VPACR | vasoactive intestinal peptide receptor |
| WD-40 | tryptophan-aspartate, 40 repeats |
| ZIP4 | zinc transporter 4 |
| β ₂ AR | β ₂ -adrenergic receptor |

CHAPTER 1

INTRODUCTION

1.1 Cellular signalling

As the smallest unit of a living organism, cells can sense changes in their environment, leading to an adjustment of their function. Stimuli or signals come in a range of forms including chemicals, light and pressure. Whilst a cell can recognise these changes, it also can produce signalling molecules that induce different cells to respond – so forming a cellular communication network (Lodish; *et al.*, 2016). Significantly, signalling molecules synthesised by these cells are not only limited to affect neighbouring cells but also function intracellularly, controlling fundamental processes, including gene transcription, cell growth, and metabolism.

In order to recognise extracellular signalling molecules, cells possess integral proteins embedded in the plasma membrane, known as cell-surface receptors. These receptors bind molecules on the extracellular side of the cell and transmitting the signal intracellularly to cytoplasmic proteins or other effectors, including enzymes or transcription factors. This hypothesis was first introduced in the mid-19th century when Langley used the term “receptive substance” as the first concept of receptors (Rang, 2006). Cell surface receptors generally consist of 3 regions: an extracellular ligand-binding domain, a plasma-membrane-spanning domain, and an intracellular domain. A number of receptors have been identified and can be classified into two main families: intracellular receptors (nuclear receptor) and transmembrane receptors. The latter can be categorised into receptor tyrosine kinases (RTKs), G protein-coupled receptor (GPCRs), ion channels, and cytokine receptors (Arey, 2014). The following sections will focus upon GPCR-mediated signalling cascade.

1.2 Overview of signal transduction through G protein-coupled receptor (GPCRs)

GPCRs, are seven-transmembrane (TM) proteins, and account for approximately 4% of proteins encoded in the human genome (Matthews and Sunde, 2012). The family is one of the most numerous proteins that have been identified, of the 826 approximately 400 are non-sensory GPCRs with the remaining being olfactory receptors (Yang *et al.*, 2021). As one of the most identifiable targets for treating various diseases, GPCRs have contributed to more than 40% of drugs which are currently

available in the market (Hauser *et al.*, 2017). GPCRs have various endogenous ligands, including odour, light, hormones, neurotransmitters, chemokines, carbohydrates, lipids, amines, peptides, and proteins. The physiological roles of GPCRs are numerous and consequently they have been implicated in many diseases, including type 2 diabetes mellitus (T2DM), obesity, cancer, Huntington's disease, Alzheimer's disease, and others (Rosenbaum, Rasmussen and Kobilka, 2009; Sebastiani *et al.*, 2018).

GPCRs mediate their signalling through activation of a heterotrimeric G protein complex that consists of a $G\alpha$ subunit bound to a $G\beta\gamma$ dimer. In the resting state, the $G\alpha$ subunit is bound to GDP which facilitates tight binding to the $G\beta\gamma$ heterodimer. Not only does this interaction help to anchor $G\alpha$ subunit to the plasma membrane, but it also serves as a guanine nucleotide dissociation inhibitor (GDI) by slowing the rate of GDP release from the $G\alpha$ (Brandt and Ross, 1985; Higashijima, Ferguson and Sternweis, 1987). Upon conformational changes after an agonist binds to the GPCR, it becomes a guanine nucleotide exchange factor, promoting the exchange of guanosine diphosphate (GDP) to guanosine triphosphate (GTP) at $G\alpha$ subunit, and resulting in dissociation of $G\alpha$ -GTP from the $G\beta\gamma$ subunits (McCudden *et al.*, 2005). Subsequently, both GTP-bound $G\alpha$ and $G\beta\gamma$ can activate an array of downstream signalling events. Conformational changes of $G\alpha$ subunit are tightly regulated by nucleotide-binding and have been implicated in signal transduction (Goricanec *et al.*, 2016). However, a recent study on vasopressin V_2 receptor (V_2R) demonstrated that formation of V_2R - $G\alpha_{12}$ complexes generate unproductive signalling which is independent of guanine nucleotide binding (Okashah *et al.*, 2020). The signal from the $G\alpha$ is terminated by the enzymatic activity of intrinsic GTPase of $G\alpha$, hydrolysing GTP into GDP, which allows re-association with the $G\beta\gamma$ dimer. The schematic illustration of this process is depicted in Figure 1.1. Apart from its intrinsic enzymatic activity, proteins called Regulator of G protein signalling (RGS) serve as GTPase activating proteins (GAPs) for specific $G\alpha$ subunits. GPCRs have been shown to activate diverse downstream signalling pathways through canonical G protein mediated signalling or non-canonical β -arrestin pathways.

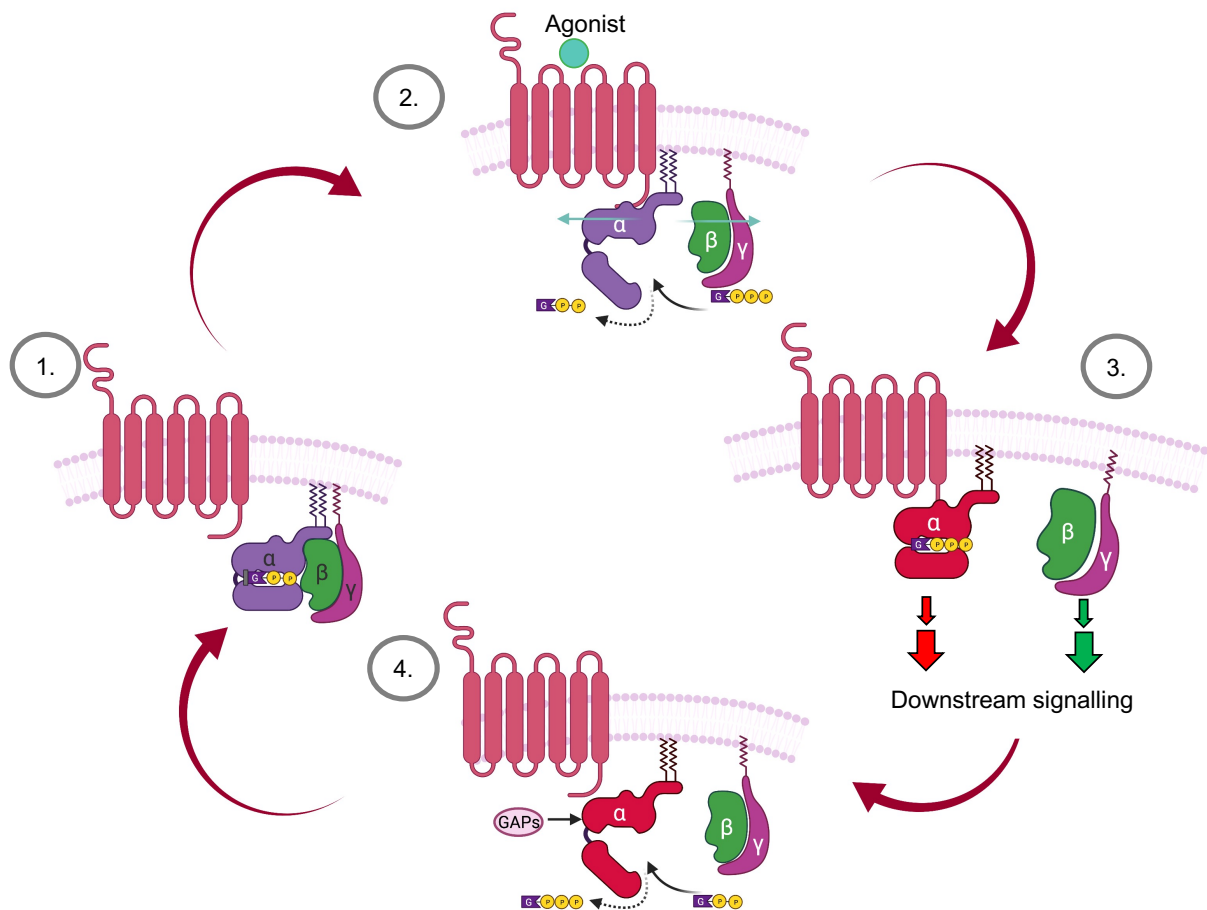


Figure 1.1 GPCR signalling cycle. It is postulated that in resting state, $G\alpha$ is bound to GDP and forming heterotrimeric complex with $G\beta\gamma$ subunits (1). Upon agonist binding, it promotes conformational changes of the receptor into the active states. This process induces recruitment of heterotrimeric $G\alpha\beta\gamma$ protein, which is followed by the exchange of GDP for GTP in the $G\alpha$ subunit protein (2). GTP-bound $G\alpha$ protein stabilises the active form of receptor and further induce $G\alpha$ and $G\beta\gamma$ dissociation. This process allows both $G\alpha$ and $G\beta\gamma$ proteins to activate their respective effectors (3). Signal transduction is terminated by the intrinsic GTPase activity of $G\alpha$ subunit, accelerated by RGS proteins (4). The hydrolysis of GTP to GDP returns to the $G\alpha$ resting state, allowing it to re-associate with $G\beta\gamma$ heterodimer. The figure was created with BioRender.com

Based on the phylogenetic tree, GPCRs can be classified into five classes which are commonly known as GRAFS systems: glutamate, rhodopsin, adhesion, frizzled, and secretin class (Fredriksson *et al.*, 2003). Another more common nomenclature classifies GPCRs into class A-F. It consists of class A (rhodopsin), class B (secretin), class C (glutamate), class D (fungal mating pheromone receptors), class E (cAMP receptors), and class F (frizzled/smoothened). This classical A-F systems was determined based on sequence homology and functional similarity (Attwood and Findlay, 1994; Kooistra *et al.*, 2021).

GPCRs have been studied for almost 40 years and it is widely accepted that GPCR activation allows physical association with a heterotrimeric G protein (De Lean, Stadel and Lefkowitz, 1980; Limbird, Gill and Lefkowitz, 1980; Gether and Kobilka, 1998). Although the study of GPCRs has expanded, the understanding of receptor and G protein dynamic is not without debate. Currently, at least two different models have been suggested. The first concept, that has been widely accepted, postulates that the G protein and the GPCR only interact following agonist binding to the receptor - the so call collision coupling model. In contrast, the second model conjectures that GPCR and G proteins exist in pre-coupled complexes prior to agonist-binding (Hein and Bünemann, 2009; Ayoub, Al-Senaidy and Pin, 2012; Lohse, Nuber and Hoffmann, 2012).

Whatever the mechanism both models lead to G protein activation as described above initiating post-GPCR signal transduction. Typically, this will involve second messengers, enabling signal amplification. These second messengers comprise four classes: cyclic nucleotides (cyclic adenosine 3',5' monophosphate (cAMP) and cyclic guanosine 3',5' monophosphate (cGMP)) and other soluble molecules, lipid messengers, ions, and gases-free radicals (Newton, Bootman and Scott, 2016). The particular section about cAMP and cGMP will be introduced later.

1.2.1 G protein-mediated signalling

Heterotrimeric G proteins consist of α , β , and γ subunits. In humans, there are 16 G α genes encoding 23 G α proteins; 5 genes encoding 5 G β , and 12 genes encoding G γ subunits (Downes and Gautam, 1999). G α subunits are varied in range of 39-45 kDa with many, but not all, being post-translationally modified to contain myristate/palmitate at their N-terminal, which aids membrane localisation (Peitzsch and McLaughlin, 1993; Nürnberg, Gudermann and Schultz, 1995; Wedegaertner, Wilson and Bourne, 1995). G α proteins, fall into 4 subclasses based on structure similarities: G α_s that stimulates adenylyl cyclase (AC) generating cAMP, G α_i that inhibits AC therefore reduces cAMP production, G α_q that stimulates phospholipase C- β (PLC- β) thus mediating intracellular Ca²⁺ release from endoplasmic reticulum (ER), and G_{12/13} that triggers small Rho-GTPase (Simon, Strathmann and Gautam, 1991). The following sections provides a general description of each G protein sub-family.

1.2.1.1. The $G\alpha_s$ family

The activation of this $G\alpha$ subunit mediates AC-activation that leads to an increase in cAMP synthesis. $G\alpha_{olf}$ also belongs to this protein family but is mainly expressed in olfactory sensory neurons (Jones and Reed, 1989). Aside from stimulating AC, the $G\alpha_s$ subunit has also been shown to regulate Ca^{2+} channels, through direct and indirect mechanisms (Yatani and Brown, 1989). Currently, 3 different isoforms of the $G\alpha_s$ subunit have been identified, consisting of $Gs_{(s)}$, $Gs_{(L)}$, $Gs_{(XL)}$. Their activities have been suggested to differ with $Gs_{(XL)}$ being reported to be involved in brachydactyly, trauma-related bleeding, and various neurological problems (Milligan and Kostenis, 2006) while activation of $Gs_{(L)}$ has shown to activate the Src kinase family – so called non-tyrosine kinases (Romero, 2014).

In order to dissect the role of $G\alpha_s$ -mediated responses, cholera toxin (CTx) can be utilised as a pharmacological tool. CTx mediates ADP-ribosylation on the $G\alpha_s$ subunit by targeting a specific arginine residue (Arg²⁰¹) which significantly decreases the intrinsic GTPase activity of $G\alpha$ subunit, leaving $G\alpha_s$ permanently activated. As a result, the production of cAMP is continuously increased. In addition, the use of selective inhibitors has become an invaluable approach to investigating the involvement of G proteins in mediating cellular responses. NF449 and NF503 have both been demonstrated to inhibit $G\alpha_s$ coupling to the β -adrenoceptors (β -ARs), although subsequently they have been shown to also influence on $G\alpha_i/G\alpha_o$ - and $G\alpha_q$ -coupled receptor signal transduction (adenosine A₁ receptor (A₁R) and angiotensin II receptor, respectively) (Hohenegger *et al.*, 1998).

1.2.1.2. The $G\alpha_{i/o}$ family of G proteins

$G\alpha_{i/o}$ has been reported to be the most diverse $G\alpha$ subtypes. This family consists of $G\alpha_{i1}$, $G\alpha_{i2}$, $G\alpha_{i3}$, $G\alpha_o$ (which has 2 splice variants), $G\alpha_{t-rod}$, $G\alpha_{t-con}$ (transducin), $G\alpha_{gust}$ (gustucin) and $G\alpha_z$ (McCudden *et al.*, 2005). $G\alpha_t$ is involved in photoreception in the eyes, whereas $G\alpha_{gust}$ is commonly known as the taste specific G protein, highly expressed in the taste buds. Both $G\alpha_t$ and $G\alpha_{gust}$ are involved in the activation of cGMP-specific phosphodiesterases (PDEs) (Rarick, Artemyev and Hamm, no date; Yan *et al.*, 2001).

All $G\alpha_{i/o}$ family members are myristoylated at their N-terminus, except for $G\alpha_t$ which contains a palmitate that is reversibly attached near the N-terminus. Unlike $G\alpha_s$, this family inhibits the activity of AC, except $G\alpha_o$, thereby reducing the production of cAMP. $G\alpha_o$ has been demonstrated to increase phosphoinositide release (Birnbaumer

et al., 1990). Although $G\alpha_z$ displays a resemblance to this subfamily, its GTPase activity is significantly lower compared to other $G\alpha_{i/o}$ family members (Simon, Strathmann and Gautam, 1991).

All member of the $G\alpha_{i/o}$ class (with the exception of $G\alpha_z$) possess a cysteine residue 4 amino acids sites from their C-terminus that is susceptible to modification by pertussis toxin (PTx). PTx is a toxin produced by *Bordetella pertussis* in an inactive form and catalyses ADP-ribosylation on a cysteine residue at C-terminal of $G\alpha_{i/o}$ (Mangmool and Kurose, 2011). This modification causes G protein – GPCR uncoupling and blocks its signal transduction because of steric hindrance between both proteins (Campbell and Smrcka, 2018) so preventing further interaction with AC (Hsia *et al.*, 1984; Burns, 1988). Inhibition of $G\alpha_{i/o}$ activity by PTx is usually slow onset. Although PTx has been widely used to determine $G\alpha_{i/o}$ signalling, a recent finding identified that PTx has a $G\alpha_{i/o}$ -independent effect with other proteins by binding B-oligomer with cell surface-specific proteins (Mangmool and Kurose, 2011). BIM-46174 and BIM-46187 have been demonstrated to target all $G\alpha$ subtype families (Prévost *et al.*, 2006).

1.2.1.3. The $G\alpha_{q/11}$ family

This subfamily comprises of $G\alpha_q$, $G\alpha_{11}$, $G\alpha_{14}$, $G\alpha_{15}$, and $G\alpha_{16}$ subunits. Of all G proteins, this family shares the most sequence homology, with $G\alpha_q$, $G\alpha_{11}$, $G\alpha_{14}$, $G\alpha_{15/16}$ displayed 90, 80, and 57% similarities (Kamoto *et al.*, 2015). The $G\alpha_{q/11}$ family does not have cysteine residue four amino acids from the C-terminus, mediating its resistant towards PTx (Simon, Strathmann and Gautam, 1991). All $G\alpha_{q/11}$ members have shown to activate PLC- β , leading to the mobilisation of Ca^{2+} from the ER into the cytoplasm via inositol 1,4,5-trisphosphate (IP_3) production. Besides activating PLC- β , $G\alpha_{q/11}$ also has been reported to interact with p63RhoGEF, activating Rho through the action of RhoGTPase (Campbell and Smrcka, 2018). This interaction appears to be cell-type dependent. $G\alpha_{15}$ and $G\alpha_{16}$, on the other hand, can couple to a wide variety of GPCRs. For instance, these two $G\alpha$ proteins mediate the production of IP_3 through β_2 -adrenoceptor (β_2 -AR) and M_2 -muscarinic receptors leading to elevation of intracellular Ca^{2+} in COS-7 cells (COS cells are fibroblast like cells derived from monkey kidney tissue, COS refers to cells being CV-1 (simian) in Origin and carrying the SV40 genetic material) (Gluzman, 1981; Offermanns and Simon, 1995).

The most common $G\alpha_{q/11}$ inhibitor that has been widely used is YM-254890, a cyclic depsipeptide that inhibits the GDP to GTP exchange on the α subunit of $G\alpha_{q/11}$ complex. However, recent findings argued the compound's selectivity properties as it

also inhibited $G\alpha_s$ and exhibited biased inhibition on $G\alpha_{i/o}$ (Peng *et al.*, 2021). In addition, U73122 has also been identified to inhibit the activity of $G\alpha_{q/11}$ by blocking PLC- β (Wu, Pei and Fan, 1998). Whilst BIM-46187 has been reported to be a pan- $G\alpha$ inhibitor and depending on the cellular context, it elicits selectivity towards $G\alpha_{q/11}$ over the remaining $G\alpha$ protein subfamily (Schmitz *et al.*, 2014). However, no known $G\alpha$ inhibitor are available for $G\alpha_{14}$, $G\alpha_{15}$, and $G\alpha_{16}$. Therefore, a genetic approach of knocking down the genes encoding G proteins may be required, but this strategy is not without challenges.

1.2.1.4. The $G\alpha_{12/13}$ subfamily

Analogous to the $G\alpha_{q/11}$ family, $G\alpha_{12/13}$ also lacks a cysteine residue at its C-terminal and is insensitive towards PTx (Simon, Strathmann and Gautam, 1991). Both $G\alpha_{12}$ and $G\alpha_{13}$ are ubiquitously expressed in many tissues and are currently known to interact with p115RhoGTPase proteins, PDZ-RhoGEF (PDZ for postsynaptic density 95, PSD-95; Discs large, Dlg; Zonula occludens-1, ZO-1; GEF for guanine nucleotide exchange factor), and leukaemia associated RhoGEF (LARG) (Suzuki *et al.*, 2003). $G\alpha_{12}$ activates the small monomeric G protein (Rho) through its RhoGTPase mediating catalysis of Rho-GDP for Rho-GTP. Besides interacting with RhoGEF family proteins, $G\alpha_{12/13}$ family also activates PLC ϵ and PLC δ , phosphatase 5, and A-kinase anchoring proteins 110 (AKAP110) (Milligan and Kostenis, 2006). $G\alpha_{12/13}$ are also known as *gcp* proto-oncogenes and serves as prognostic tools for cancer patients (Y. M. Yang *et al.*, 2020). These family members have also demonstrated their role as regulators in energy metabolism and immune-mediated responses (Healy *et al.*, 2016; Y. M. Yang *et al.*, 2020).

1.2.1.5. The $G\beta$ subunit

To date, at least 5 $G\beta$ subunits have been identified in the human genome (Downes and Gautam, 1999). The $G\beta$ subunit comprises of N-terminal α -helix and seven bladed β -propeller sheets. Each blade is composed of four antiparallel strands containing multiple tryptophan/aspartate (WD-40) motifs (Simon, Strathmann and Gautam, 1991). These motifs are specifically responsible for the structure of the $G\beta$ subunit generating a so-called propeller shape and are implicated as the region where $G\beta$ and $G\gamma$ may interact. Of the five different $G\beta$ subunits, β_5 is not homologous compared to the other four subunits and is believed to have different roles. Unlike other $G\beta$ subunits, β_5 dissociates from $G\gamma$ and is known to be able to interact with RGS proteins that contain

a G protein- γ -like domain, C-A-A-X motif (Milligan and Kostenis, 2006). G β 3 has been suggested to be involved in atherosclerosis, hypertension, and metabolic syndrome (Milligan and Kostenis, 2006).

1.2.1.6. The G γ subunit

The G γ subunit protein is only stable in the form of dimer with G β subunits. There are currently 12G γ identified. Each G γ subunit undergoes post-translational modification, either a 15-carbon farnesyl or 20-carbon geranylgeranylisoprenoid, that is attached to the cysteine residue of C-A-A-X motif (Simon, Strathmann and Gautam, 1991), all of which leads to membrane targeting. The presence of G γ is necessary for correct folding of G β subunit protein. G β and G γ form a heterodimer and are not found as individual units in the natural settings. (Schmidt *et al.*, 1992; Higgins and Casey, 1994).

Most cells express multiple types of G β and G γ subtypes. Since G β and G γ are commonly found in dimers, little is known about the functions of each subunit. Upon dissociation with G α , G $\beta\gamma$ complex transduces to their downstream effectors. G protein coupled-gated inwardly rectifying potassium channel (GIRK) are opened through direct binding with the G $\beta\gamma$ heterodimer after stimulation of muscarinic acetylcholine receptors, γ -aminobutyric acid (GABA) receptors, dopamine receptors, and opioid receptors (Lüscher and Slesinger, 2010). In addition, voltage-dependent inhibition of N-type Ca²⁺ channels was also mediated through G $\beta\gamma$ activation (Ikeda, 1996). Activators of G protein signalling 3 (AGS3) is a non-receptor protein activated by G $\beta\gamma$ subunits. Silencing AGS3 protein has been implicated to disruption of apical-basal cellular division through its control in spindle orientation (Sanada and Tsai, 2005).

Small molecule G $\beta\gamma$ inhibitors have been developed to selectively block their interactions with their effectors, this includes M119 and its analogue, gallein (Lehmann, Seneviratne and Smrcka, 2008). Later, Blattermann also discovered Gue1645 a compound that selectively prevents G $\beta\gamma$ -mediated signalling without having any effect on G α (Blättermann *et al.*, 2012).

1.2.2 Non-canonical GPCR signalling

Although it was first thought that GPCR signalling was solely dependent on G proteins, currently, the paradigm has shifted, demonstrating multidimensional signalling of GPCRs. This notion has been implicated in biased signalling, formation of oligomers with other receptors, and sustained signalling from intracellular compartments (Shchepinova *et al.*, 2020).

1.2.2.1. The role of G protein receptor kinase (GRKs)

G protein receptor kinase (GRKs) are known to interact with GPCRs upon their activation. Upon agonist-binding, GPCRs typically engaged to the G proteins, undergo phosphorylation by GRKs, and bind with β -arrestin to mediate desensitisation or internalisation. β -arrestins can bind to active GPCRs and phosphorylated GPCRs and promote receptor internalisation via clathrin-coated pits (Paccauds *et al.*, 1993). Together with β -arrestin, GRKs are key modulators in controlling the rate and desensitisation of GPCRs. To promote receptor desensitisation, the receptor intracellular loop 3 (ICL3) and the C-terminal tail have been reported to be the interaction sites with GRKs (Komolov and Benovic, 2018).

The first GRKs originally called the “opsin/rhodopsin kinase” was found in 1972 but has subsequently been renamed to GRK1. It was shown to mediate phosphorylation of rhodopsin, a prototypical GPCR (Kühn and Dreyer, 1972). GRK1s main function was first thought to mediate rhodopsin deactivation, however, later GRK1 was found to be associated with a broader range of receptors. Although GRKs are classified in the AGC kinase super family (the AGC protein group is a family of serine/threonine protein kinases that is closely related to protein kinase **A** (PKA), protein kinase **G** (PKG), and protein kinase **C** (PKC) (Manning *et al.*, 2002)), the presence of the RGS homology (RH) domain in GRKs makes them different from any of the other kinases in the family (Gurevich *et al.*, 2012). There are 7 members of the GRKs (GRK1-7), with only four classes that are thought to be involved in recognising active GPCRs: GRK1, GRK2, GRK3, and GRK7 (Gurevich and Gurevich, 2019).

All GRKs share the N-terminal domain, catalytic kinase domain, RH domain and a C-terminal domain (Figure 1.2). A pleckstrin homology (PH) domain, is also present in GRK2 and GRK3, as part of their C-terminal domain (Touhara *et al.*, 1994). However, it is reported that the RH domain is only functional in GRK2/3 to regulate phosphorylation-independent GPCR desensitisation, whereas the PH domain is responsible for the binding to the G $\beta\gamma$ dimer (Gurevich and Gurevich, 2017; Sun and Kim, 2021). GRK2, in particular, has shown to have kinase activity to non-GPCR desensitisation that is important to maintain a balance between receptors and signal transduction (Han *et al.*, 2016). GRK2 has also been suggested to be involved in a negative feedback regulatory mechanism that influences extracellular signal-regulated kinase (ERK) signalling, as demonstrated in human embryonic kidney 293 (HEK293) cells (Pitcher *et al.*, 1999).

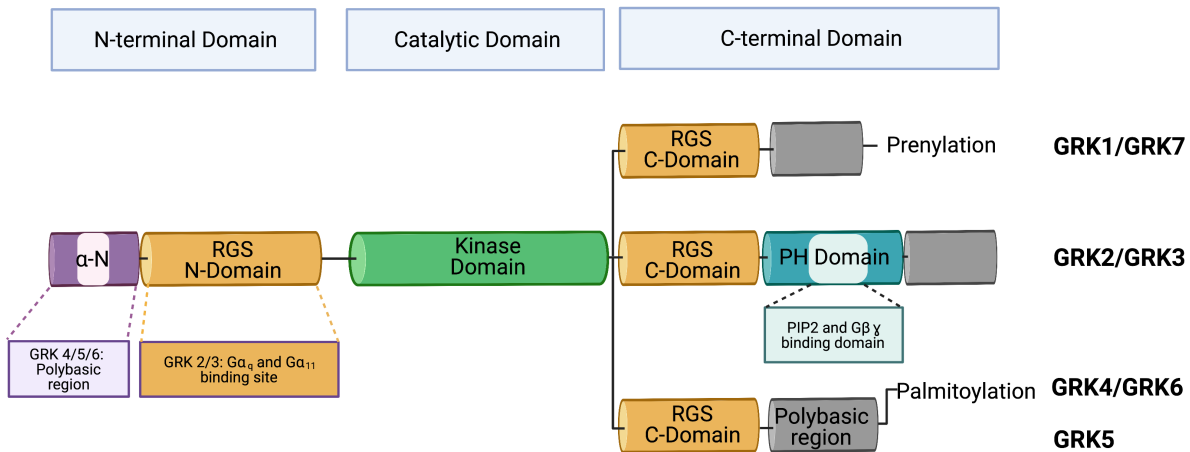


Figure 1.2 Schematic illustration of GRK family proteins. All GRK family members shares three domains consisting of N-terminal domain, catalytic domain, and C-terminal domain that is vary amongst member of GRK family. Figure was adapted from (Sun and Kim, 2021) and created with BioRender.com

Although GRK2 and GRK3 are homologous proteins, they only share 39% similarities (Pitcher, Freedman and Lefkowitz, 1998). Within the PH domain (residue 553-656), a 19 amino acid motif is involved in G $\beta\gamma$ dimer binding. In *in vitro* studies, the PH domain has also been demonstrated to display specific binding to phosphatidylinositol 4,5-bisphosphate (PIP₂) so suggesting multiple sites for phosphorylation. Several other molecules have been identified as ligands of the PH domain, these include receptor for C activated kinase 1 (RACK1), PKC, $G\alpha_{12}$, and F-actin (Yang *et al.*, 2003). The PH domain is not only present in GRK2/3 but also in other proteins including some serine/threonine kinase proteins, tyrosine-specific kinase, all known mammalian PLCs, RGS proteins, and a number of cytoskeletal proteins (Pitcher, Freedman and Lefkowitz, 1998).

GRK4 and GRK6 are associated with the plasma membrane due to the presence of palmitoylation on their C-terminal and N-terminal lipid-binding region (Figure 1.2) (Gurevich *et al.*, 2012). However, the molecular mechanism on GRK4 and GRK6 cellular localisation remains to be established. GRK5 is also a membrane-bound kinase anchored through PIP₂ binding domain near its N-terminal (Stoffel, Pitcher and Lefkowitz, 1997) and amphipathic helix membrane-binding domain at its C-terminal (Gurevich *et al.*, 2012).

1.2.2.2 The arrestin subfamily

Arrestins are small family of cytosolic proteins that regulate GPCR signalling. Due to their preferential binding to an active receptor, the recruitment of this protein family prevents the coupling of phosphorylated receptors to their respective G proteins. In mammalian cells, there are at least four arrestin paralogs that can be classified into 2 major classes: visual arrestins and β -arrestins. Visual arrestins comprised of arr-1 and arr-4 are expressed mainly in the retina, whereas β -arrestins consist of β -arrestin1 and 2 (or also known as arr-2 and arr-3) play crucial roles to recognise GPCRs in most human cells (Indrischek *et al.*, 2017; Aydin and Coin, 2021). Arrestins inhibit GPCR coupling mainly by two mechanisms: i) preventing GPCR activation (desensitisation) by binding to the receptor C-terminal so blocking G protein activation and ii) serving as scaffolds for protein kinases and mediators for receptor internalisation. Furthermore, it has been suggested that both β -arrestins, when bound to an agonist-coupled GPCR may also elicit distinct signalling capabilities (Gurevich and Gurevich, 2020). GPCR- β -arrestin complexes can promote activation of ERK1/2 and mitogen-activated protein kinase (MAPK) signalling cascade through direct and indirect mechanisms (Luttrell *et al.*, 2001; Song *et al.*, 2009; Gurevich and Gurevich, 2019). The indirect mechanism is provided by RTK transactivation by β -arrestin (Wetzker and Böhmer, 2003; Shah and Catt, 2004; Werry, Sexton and Christopoulos, 2005). Interestingly, some reports also indicated that β -arrestins can interact directly to the ERK1/2 and c-Jun N-terminal kinase 3 (JNK3) that belong to MAPK family (DeFea *et al.*, 2000; McDonald, 2000). The N-terminus of β -arrestin2 peptide (T1A) also acts as a scaffold for ASK1/MKK4/7-JNK3 that activate JNK3 to control apoptosis, cell division, and synaptic changes in neurons (Zhan *et al.*, 2016).

Signalling through β -arrestin is thought to be separable from G protein-mediated signalling given the fact that β -arrestins “arrest” GPCR activation by interfering with G protein binding. However, recent evidence has shown that the $G\alpha_i$ family, but not other $G\alpha$ proteins, form a complex with β -arrestin at the plasma membrane upon stimulation with V_2R agonist. This interaction generates a productive ERK1/2 signalling and cell migration (Smith *et al.*, 2021).

1.2.2.3 Other regulatory proteins that promote non-canonical GPCR signalling

The EBP50 (for ezrin-radixin-moesin (ERM)-binding phosphoprotein-50) phosphoprotein is known to be able to bind to the C-terminus of the β 2-AR through its PDZ domains (Reczek, Berryman and Bretscher, 1997; Cao *et al.*, 1999). Other proteins that contain a PDZ motif, such as Na⁺/H⁺ exchange regulatory factor-1 (NHERF) and NHE3 kinase A regulatory protein (E3KARP), bind to the cytoplasmic side of the β 2-AR promoting/activating particular pathways (Hall *et al.*, 1998). EBP50 is also reported to involve platelet activating receptor (PAFR) internalisation (Dupré, Rola-Pleszczynski and Stankova, 2012) and promote receptor recycling in δ -opioid receptors (Lauffer *et al.*, 2009). Another protein, AGS3-6 has been reported to compete with G $\beta\gamma$ to bind the G α promoting G $\beta\gamma$ to activate its downstream signalling and has been shown to modulate immune systems (Boullaran and Kehrl, 2014). In some cases, transactivation of RTKs by GPCRs leads to the recruitment of scaffold proteins, such as Shc, Grb2, and Sos, which together activates MAPK signalling (Natarajan and Berk, 2006)

1.2.3 Modulatory action of receptor activity-modifying proteins (RAMPs) in regulating GPCR signalling

RAMPs are single transmembrane proteins that were first studied to interact with calcitonin receptor-like receptor (CLR) (McLatchie *et al.*, 1998). Initially it was thought that RAMPs solely acted as chaperones for CLR. However, RAMPs are now known to play important roles in altering many GPCRs pharmacology. The Human genome encodes for three RAMP isoforms (RAMP1, RAMP2 and RAMP3) (McLatchie *et al.*, 1998; Klein, Matson and Caron, 2016). RAMPs share ~30% sequence homology, with RAMP2 being slightly larger (175 amino acid residues) compared to RAMP1 and RAMP3 (140 amino acid) (McLatchie *et al.*, 1998). All RAMPs share three domains which include an extracellular domain (ECD), a single transmembrane domain (TMD), and a short C-terminal domain that comprises about 10 residues. The N-terminal has been shown to be responsible for determining ligand specificity, whereas the C-terminus is important to alter downstream signalling (Udawela *et al.*, 2006).

RAMPs have been reported to allosterically alter CLR signalling and provide a point for direct binding that further modulates G protein-coupling, changes ligand binding, affects receptor trafficking, receptor internalisation and signalling capabilities (Simms *et al.*, 2009; Klein, Matson and Caron, 2016; Weston *et al.*, 2016; Woolley *et al.*, 2017; Garelja *et al.*, 2018). The best characterised site of interaction between

RAMPs and CLR has been suggested to be the ECD (Hay *et al.*, 2016). However, other reports have highlighted other possibilities of RAMP-CLR interaction regions. Through molecular dynamics (MD) simulation, Weston and colleagues demonstrated the interaction occurs on the RAMP transmembrane (TM) helix and CLR TM6/TM7 (Weston *et al.*, 2016). The study also highlighted Helix 8 (H8) involvement with $G\alpha_s$ suggesting RAMP may contribute to bias in G protein-coupling by the CLR (Weston *et al.*, 2016). Notably, the C-terminal domain of the RAMPs may also be involved in interaction with GPCRs, although this requires further elucidations (Bomberger, Spielman, *et al.*, 2005; Udawela *et al.*, 2006).

Aside from CLR, recent findings by Harris and colleagues further dissect the mechanism of RAMP in regulating signalling bias and internalisation of gastric inhibitory polypeptide receptor/ glucose-dependent insulinotropic polypeptide receptor (GIPR) (Harris *et al.*, 2021). RAMPs have been demonstrated to modulate G protein activations and influence cell surface expressions. The alteration of GIPR signalling at the molecular level has been implicated both for acute and prolonged responses, as demonstrated in overexpression surrogate systems and *in vivo* studies.

RAMP-GPCR interaction has been well studied, especially with class B GPCRs (secretin family). Interestingly, the interaction is not limited to the class B but also has been shown to form heteromers with class A and C GPCRs (Poyner *et al.*, 2002; Hay *et al.*, 2016; Barbash *et al.*, 2017; Mackie *et al.*, 2019). Current RAMPs interacting partners are summarised in Table 1.1

Table 1.1
RAMP interacting GPCR partners

| Receptor Family | GPCR | Associating RAMPs | References |
|-----------------|---------------------|---------------------|--------------------------------|
| A | GPR30/GPER | RAMP3 | (Lenhart <i>et al.</i> , 2013) |
| A | Chemerin receptor 1 | RAMP2, RAMP3 | (Mackie <i>et al.</i> , 2019) |
| A | CCR1 | RAMP1, RAMP2, RAMP3 | (Mackie <i>et al.</i> , 2019) |
| A | CCR2 | RAMP1, RAMP2, RAMP3 | (Mackie <i>et al.</i> , 2019) |
| A | CCR3 | RAMP1, RAMP2, RAMP3 | (Mackie <i>et al.</i> , 2019) |

| Receptor Family | GPCR | Associating RAMPs | References |
|------------------------|-------------|---------------------------|--|
| A | CCR4 | RAMP1, RAMP2, RAMP3 | (Mackie <i>et al.</i> , 2019) |
| A | CCR5 | RAMP1, RAMP2, RAMP3 | (Mackie <i>et al.</i> , 2019) |
| A | CCR6 | RAMP1, RAMP2, RAMP3 | (Mackie <i>et al.</i> , 2019) |
| A | CCR7 | RAMP1, RAMP2, RAMP3 | (Mackie <i>et al.</i> , 2019) |
| A | CCR8 | RAMP1, RAMP2, RAMP3 | (Mackie <i>et al.</i> , 2019) |
| A | CCR9 | RAMP1, RAMP2, RAMP3 | (Mackie <i>et al.</i> , 2019) |
| A | CCR10 | RAMP1, RAMP2, RAMP3 | (Mackie <i>et al.</i> , 2019) |
| A | CXCR1 | RAMP1, RAMP2, RAMP3 | (Mackie <i>et al.</i> , 2019) |
| A | CXCR2 | RAMP2, RAMP3 | (Mackie <i>et al.</i> , 2019) |
| A | CXCR3 | RAMP2, RAMP3 | (Mackie <i>et al.</i> , 2019), (Lorenzen <i>et al.</i> , 2019a) |
| A | CXCR4 | RAMP1, RAMP3 | (Mackie <i>et al.</i> , 2019) |
| A | CXCR5 | RAMP3 | (Mackie <i>et al.</i> , 2019) |
| A | CXCR6 | RAMP3 | (Mackie <i>et al.</i> , 2019) |
| A | CX3CR1 | RAMP1, RAMP2, RAMP3 | (Mackie <i>et al.</i> , 2019) |
| A | XCR1 | RAMP1, RAMP2, RAMP3 | (Mackie <i>et al.</i> , 2019) |
| A | ACKR1 | RAMP1, RAMP2, RAMP3 | (Mackie <i>et al.</i> , 2019) |

| Receptor Family | GPCR | Associating RAMPs | References |
|-----------------|-------------------|---------------------------|--|
| A | ACKR2 | RAMP1, RAMP2, RAMP3 | (Mackie <i>et al.</i> , 2019) |
| A | ACKR3 | RAMP1, RAMP2, RAMP3 | (Mackie <i>et al.</i> , 2019), (Lorenzen <i>et al.</i> , 2019a) |
| A | ACKR4 | RAMP2, RAMP3 | (Mackie <i>et al.</i> , 2019) |
| A | ACKR5 | RAMP2, RAMP3 | (Mackie <i>et al.</i> , 2019) |
| A | GPR4 | RAMP1, RAMP2, RAMP3 | (Lorenzen <i>et al.</i> , 2019a) |
| A | GPR182 | RAMP1, RAMP2, RAMP3 | (Lorenzen <i>et al.</i> , 2019a) |
| B | CLR | RAMP1 RAMP2 RAMP3 | (McLatchie <i>et al.</i> , 1998) |
| B | CTR | RAMP1 RAMP2 RAMP3 | (Christopoulos <i>et al.</i> , 1999) |
| B | CRF1R | RAMP2 | (D Wootten <i>et al.</i> , 2013) |
| B | CRF2R | RAMP3 | (Lorenzen <i>et al.</i> , 2019a) |
| B | GCGR | RAMP2 | (Christopoulos <i>et al.</i> , 2003; Cegla <i>et al.</i> , 2017) |
| B | GLP-1R | RAMP1 RAMP2 RAMP3 | (Lorenzen <i>et al.</i> , 2019a) |
| B | GLP-2R | RAMP1 RAMP2 RAMP3 | (Lorenzen <i>et al.</i> , 2019a) |
| B | GIPR | RAMP1 RAMP2 RAMP3 | (Lorenzen <i>et al.</i> , 2019a), (Harris <i>et al.</i> , 2021) |
| B | PTH1R | RAMP2 | (Christopoulos <i>et al.</i> , 2003) |
| B | PTH2R | RAMP3 | (Christopoulos <i>et al.</i> , 2003) |
| B | GHRHR | RAMP2 RAMP3 | (Lorenzen <i>et al.</i> , 2019a) |
| B | Secretin Receptor | RAMP3 | (Harikumar <i>et al.</i> , 2009) |

| Receptor Family | GPCR | Associating RAMPs | References |
|-----------------|--------|-------------------------|--------------------------------------|
| B | VPAC1R | RAMP1 RAMP2 RAMP3 | (Christopoulos <i>et al.</i> , 2003) |
| B | VPAC2R | RAMP1 RAMP2 RAMP3 | (D. Wootten <i>et al.</i> , 2013) |
| B | PAC1R | RAMP1 RAMP2 RAMP3 | (Lorenzen <i>et al.</i> , 2019a) |
| C | CaSR | RAMP1 RAMP3 | (Bouschet, Martin and Henley, 2005) |
| Adhesion family | ADGRF5 | RAMP1 RAMP2 RAMP3 | (Lorenzen <i>et al.</i> , 2019a) |

GPCR, G protein oestrogen receptor 1; CCR, chemokine receptor; CXCR, CXC chemokine receptor; ACKR, atypical chemokine receptor; CLR, calcitonin-receptor like receptor; CTR, calcitonin receptor; CRFR, corticotropin releasing factor receptor; GCGR, glucagon receptor; GLP(1/2)R, glucagon-like receptor (1/2); GIPR, gastric inhibitory polypeptide receptor/ glucose-dependent insulinotropic polypeptide receptor; PTHR, parathyroid hormone receptor; PAC1R, pituitary adenylate cyclase-activating peptide receptor; VPACR, vasoactive intestinal peptide receptor; CaSR, calcium-sensing receptor; ADGRF5, adhesion G protein-coupled receptor F5

The study of RAMP interactions has been intensively studied in CLR. Neither CLR nor RAMP1/2 are able to traffic to the plasma membrane (Pioszak and Hay, 2020). RAMP3 does appear to display some plasma membrane localisation independent of GPCR interaction. RAMP1 has demonstrated $G\alpha_s$ -mediated responses of calcitonin gene related peptide receptor (CGRP-R) and $G\alpha_i$ coupling of adrenomedullin (AM1-) and adrenomedullin 2 (AM2-) receptor (Weston *et al.*, 2016; Pioszak and Hay, 2020). Furthermore, recent studies emphasised that physical engagement of RAMP to CLR in human umbilical vein endothelial cells (HUVECs) and human cardiomyocytes (hCMs) acted as a “signalling barcode” selectively activating particular cascades (Clark *et al.*, 2021).

1.2.4. The hallmark of cancer

More than 367,000 new cancer cases were reported in the UK between 2015 and 2017

¹. The incidence rate was envisaged to increase by 2% between 2014 and 2035.

¹ <https://www.cancerresearchuk.org/health-professional/cancer-statistics/incidence#heading-Zero> (accessed 5 September 2021)

Worldwide, the mortality rate is between 100 to 350 per 100,000 people per year. As one of the most complicated pathological conditions, it is due to cellular regulation loss to control cell growth and proliferation. Cell proliferation alone may not be causing cancer, however, sustained growth in an environment in the presence of inflammatory cells, growth factors, DNA damaging agents, as well as activated stroma increases the risk of neoplasticism (Coussens and Werb, 2002).

Hanahan and Weinberg proposed in their review that at least there are eight biological capabilities of cells in tumour development (Hanahan and Weinberg, 2011), which genetic predispositions become the underlying issue. The hallmark of cancers includes (Figure 1.3): (i) cancer cells can maintain chronic proliferation, somatic mutations may be involved to activate growth factor-mediated signalling pathways, to disrupt negative feedback loop in order to sustain pro-proliferative actions, and to overexpress genes and signals that trigger cells to enter senescence, (ii) the ability to circumvent suppressor of proliferation, disruptions of TGF- β signalling that results in malignancy, and attenuation of apoptosis, (iii) activating invasion and metastasis, (iv) enabling replicative immortality, (v) promoting angiogenesis, (vi) resisting cell death, (vii) reprogramming of energy metabolism, and (viii) evading immune destruction (Hanahan and Weinberg, 2011).

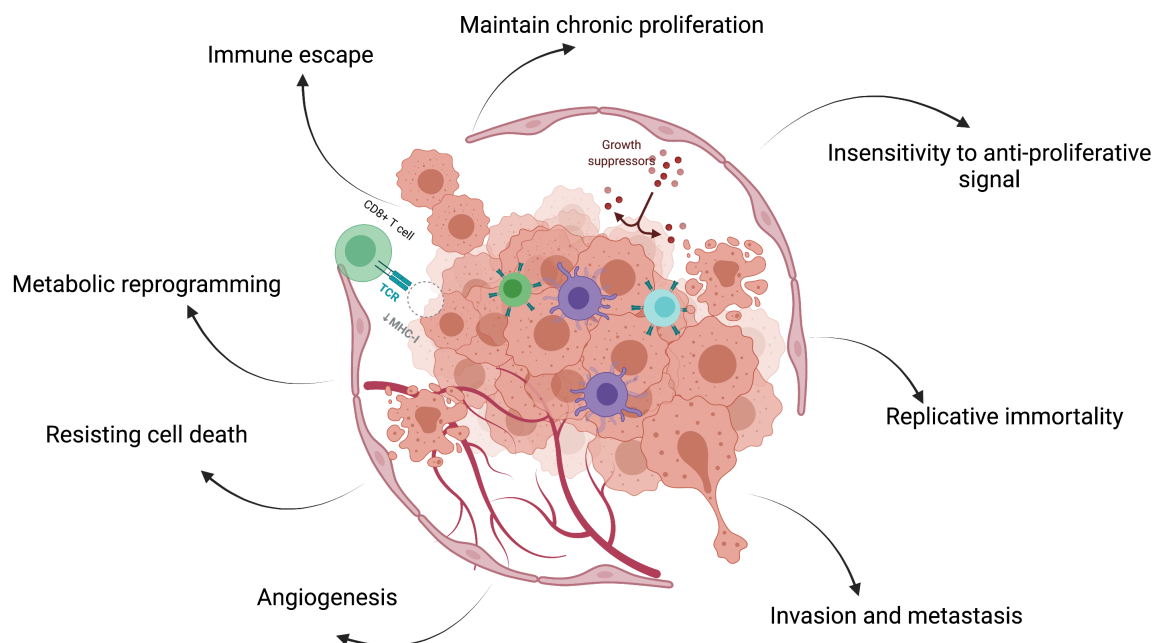


Figure 1.3. The hallmark of cancer. During tumourigenesis, there are eight biological capabilities that are present in cancer cells. While some of these changes exist, it may

result in less destructive phenotypes. The figure was adapted from (Hanahan, 2011) and created with BioRender.com.

In tumourigenesis, genetic predisposition and the interaction between host and cancer cells in the tumour microenvironment play crucial roles. The protection by the natural immune defence against cancer development was debatable in the early '80s, however, the concept gained more recognition leading to the notion of cancer immunosurveillance. Later the concept develops to the broader process called cancer immunoediting as an evolutionary pressure enabling cancer cells to be adaptable against the host's immune system. While it serves as a protective mechanism, it also has dual actions to sculpt the tumour microenvironment (Gavin P. Dunn, Old and Schreiber, 2004; Vinay *et al.*, 2015). Due to the critical roles of immune cells in tumour development, immunotherapy has emerged to aid host immune systems in eliminating cancer. An extensive review has been published to cover the process of immunoediting during tumour development that involves elimination, equilibrium, and escape processes or commonly known as "three E's of immunoediting (Gavin P Dunn, Old and Schreiber, 2004). The immunotherapies below have been used in clinical settings to treat cancer, and these include the use of immune checkpoint inhibitors that target PD-1/PDL-1, CTL-4; T-cell transfer therapy, monoclonal antibody, vaccines, and immunomodulatory agents².

1.2.5 Overview of relevant GPCRs in this study

A number of the GPCRs that have been studied in this thesis will be described in more detail in the following sections. These GPCRs included: adenosine A_{2A} receptor (A_{2A}R), protease-activated receptor 4 (PAR4), and CLR. The study on A_{2A}R is part of the work in Chapter 5 exploring the multi-target ligands and their implication on cell growth. Whereas PAR4 and CLR were studied in Chapter 6 as interacting partners of RAMP. Here the impact of RAMP interactions on downstream signalling for PAR4 and the functional consequences of CLR on cell growth were examined.

1.2.6 Adenosine A_{2A} receptor (A_{2A}R)

The adenosine A_{2A} receptor (A_{2A}R) is a class A GPCR that, together with the other 3 subtypes, A₁R, A_{2B}R, and A₃R, comprise the adenosine receptor family (ARs). All ARs are activated by the endogenous agonist adenosine although they display different

² <https://www.cancer.gov/about-cancer/treatment/types/immunotherapy>

affinities. Many ARs are related to vital organ functions in the cardiovascular and nervous system, also being involved in inflammatory responses (Sebastiao and tiberiro 2009, Headrick 2013, Sachdeva and Gupta 2013). A_{2A}R was first isolated in 1976 (Hejtmancik and Comstock, 1976) as depicted in Figure 1.4 and since then, it has become one of the most studied receptors. Yet, the mechanism of action if A_{2A}R being internalised remains poorly understood.

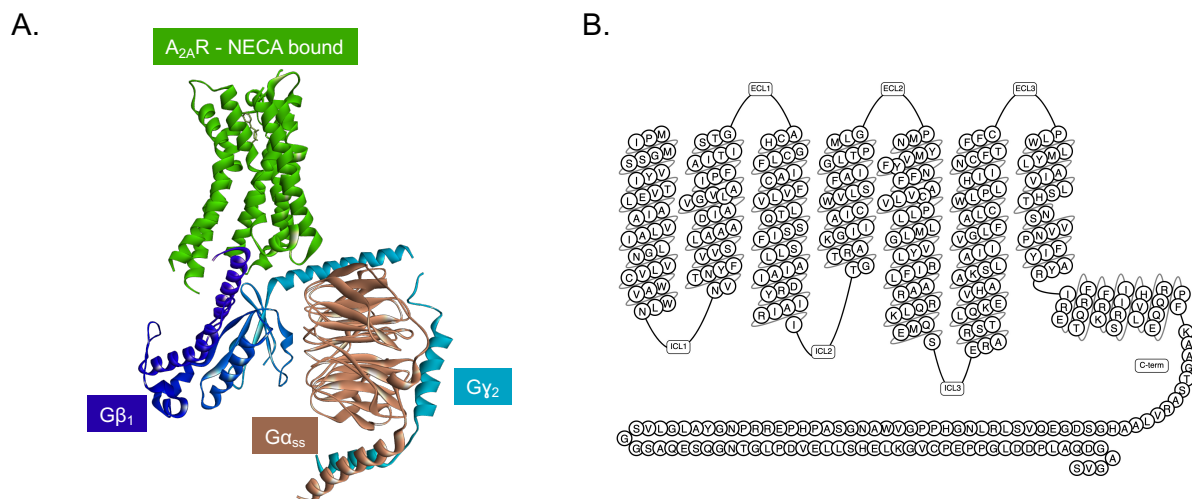


Figure 1.4. The exemplary structure of adenosine A_{2A} receptor. (A) The A_{2A}R model bound with G protein heterotrimeric (PDB 6GDG). (B) Snake structure of A_{2A}R, the figure was taken from gpcrdb.com.

The A_{2A}R is predominantly coupled to Gα_s and its activation promotes the elevation of intracellular cAMP via AC stimulation. A_{2A}R has been reported to couple to Gα_s in the peripheral system but is engaged to Gα_{oif} in the striatum (Kull, Svenningsson and Fredholm, 2000). The A_{2A}R contains a long intracellular C-terminus (122 amino acids), that is thought to provide sites for phosphorylation. This region has been proposed to be involved in receptor desensitisation and internalisation mechanisms (Borea *et al.*, 2018). Notably, Klaasse highlighted that A_{2A}R does not undergo palmitoylation at its C-terminus (Klaasse *et al.*, 2008). Although some studies remarked prolonged exposure with CG21680 triggered A_{2A}R desensitisation, indicated by loss of AC activity and reduction of Gα_s levels, however, no change in A_{2A}R expression was observed (Ramkumar *et al.*, 1991; Chern *et al.*, 1993; Mundell, Benovic and Kelly, 1997; Mundell and Kelly, 1998). In contrast, Carvalho and colleagues reported that there was no A_{2A}R internalisation observed upon stimulation by NECA and adenosine (Carvalho *et al.*,

2020). Currently, desensitisation and/or internalisation of the A_{2A}R remains inconclusive, therefore this notion needs to be addressed further.

The A_{2A}R binds to the endogenous ligand, adenosine, which is also a cognate ligand for all ARs subtypes. A₁R, A_{2A}R, and A₃R displayed high affinity to adenosine, whereas A_{2B}R has a weaker binding. A_{2A}R-mediated production of cAMP results in activation of PKA. Several reports also suggested A_{2A}R to be involved in the modulation of MAPK (Merighi *et al.*, 2002). The cAMP/PKA pathway activated by A_{2A}R, induces phosphorylation of cAMP responsive element binding protein (CREB), PDEs, and dopamine- and cAMP-regulated phosphoprotein (DARPP-32) (Prete *et al.*, 2015). Activation of aforementioned transcription factors further phosphorylate a wide range of proteins leading to various cellular responses such as regulating hormones, stimulating bone growth, regulating blood pressure, responding to olfactory stimuli and regulating blood glucose levels (Conti *et al.*, 1991, 1995; Ahlstrom *et al.*, 2005).

CGS21680 is a moderately A_{2A}R-selective agonist that is commonly used as a pharmacological tool. Currently, new compounds including ATL-146e and PSB-077777 have shown higher affinity at the A_{2A}R than CGS21680 (El-Tayeb *et al.*, 2011). ZM241385 and SCH 58261 are highly potent A_{2A}R antagonists (Baraldi *et al.*, 1998; Jacobson and Gao, 2006), even though ZM241385 also shows a weak affinity towards A₁R and A_{2B}R (Baraldi *et al.*, 1998; Jacobson and Gao, 2006).

A_{2A}R has been reported to form heteromers, either with other ARs subtypes and other GPCRs. The best characterised examples of heterodimers containing the A_{2A}R are with the A₁R or the dopamine D₂ receptor (D₂R). In the brain, A_{2A}R colocalises with D₂R and together they control motor functions (Borea *et al.*, 2018). A_{2A}R activation decreased the binding affinity of D₂R for its agonist; therefore, the use of antagonists was firstly developed from this concept to treat Parkinson's disease (Ferre *et al.*, 1991). A_{2A}R has also been found to have a protective effect caused by immunosuppressive actions leading to inflammatory processes (Melani *et al.*, 2014). Beyond neurodegenerative diseases, A_{2A}R also has potential as a target to treat cardiovascular disease and cancer (De Lera Ruiz, Lim and Zheng, 2014; Antonioli *et al.*, 2021).

1.2.5.1 The role of A_{2A}R signalling in cancer

It has been suggested that the A_{2A}R plays a significant role in cancer progression. It is now widely accepted that tumour progression involves various aspects of the tumour microenvironment (TME). The complexity is not only limited to the cell proliferation in affected areas but also in the surrounding environment enriched with inflammatory

cells, growth factors, harmful substances to promote DNA damage, all of which promote cancer cells progression.

Some reports highlighted the involvement of $A_{2A}R$ activation in reducing cancer cell viability through apoptotic signalling mediated by PKC and MAPK pathways (Merighi *et al.*, 2002; Trincavelli *et al.*, 2003). Cancer sometimes occurs when some tissues suffer from prolonged inflammation (Coussens and Werb, 2002). The presence of inflammation may exacerbate cancer. Therefore, anti-inflammatory agents may decrease cancer proliferation, alter cellular signalling, circumvent cell migration or induce cell death. In agreement with this, activation of $A_{2A}R$ has demonstrated anti-inflammatory effects following acute lung injury (Friebe *et al.*, 2014; Borea *et al.*, 2018). Since pro-tumour inflammation occurs in cancers, it can promote cancer survival, growth, and metastasis (Grivennikov, Greten and Karin, 2010; Greten and Grivennikov, 2019). Therefore, drugs that can interfere with prolonged inflammatory process maybe beneficial. Activation of $A_{2A}R$ decreases lung T helper cell number and expanded T_{reg} during allergen exposure, suggesting that $A_{2A}R$ agonists can improve immunotherapies for inflammatory-related pathologies (Pei and Linden, 2016; Borea *et al.*, 2018).

Due to limited number of cancer treatments as well as chemoresistance, the evolutionary pressure that enable cancer cells to evade immune system adds another layer of complexity to tackle this disease (Allard *et al.*, 2016). The latter has been reported to occur due to high adenosine levels produced by ectonucleotidases CD39 and CD73 (R. Yang *et al.*, 2020). Both enzymes mediate the conversion of ATP into adenosine. $A_{2A}R$, in particular, is highly expressed in immune cells, especially T cells. $A_{2A}R$ signalling can inhibit T-cell activation, proliferation, and production of inflammatory mediators, particularly in the central nervous system (CNS) (Jacobson and Gao, 2006), thereby providing an opportunity for cancer cells to escape from the natural immune system to eliminate cancerous cells (Beavis *et al.*, 2013; Steingold and Hatfield, 2020).

It is apparent that activation of $A_{2A}R$ may have contradictory actions by inducing anti-inflammatory actions and being immunosuppressive. However, there has been growing evidence demonstrating that blocking $A_{2A}R$ signalling may improve the ability of immune cells (dendritic cells, NK cells, T cells, etc) to recognise and eliminate cancer cells. As a result, many compounds have been developed to antagonise/inhibit $A_{2A}R$ signalling. Currently, therapies have been focused on antagonising $A_{2A}R$ to reverse

adenosine-mediated immune suppression. Therefore, A_{2A}R antagonist may enhance the efficacy of immune checkpoint inhibitors (Leone *et al.*, 2018; Fong *et al.*, 2020).

1.2.5.2 Triazoloquinazolines' dual action on A_{2A}R and PDE inhibitors

Triazoloquinazoline are a tricyclic heteroaromatic moiety that have been shown to bind to the ARs. The triazoloquinazoline-based compound, CGS15943, was first synthesised in the late 1980s to be a non-xanthine adenosine antagonist (Ghai *et al.*, 1987; Williams *et al.*, 1987). Since then, substitutions on this backbone structure have been developed to block ARs, such as MRS1220, an A₃R antagonist (Jacobson *et al.*, 1997). Interestingly, a series of compounds with a triazoloquinazoline-based structure have also been established as inhibitors of PDE10 (Kehler *et al.*, 2011). Starting from this viewpoint, and as part of a collaborative work programme with Dr. Kalash (University of Cambridge), we explore the possibility of triazoloquinazoline-based compounds to act as dual-action ligands of the A_{2A}R and PDE10A. An in-depth analysis of this approach is presented in Chapter 5.

1.2.7 Protease-activated receptor 4 (PAR4)

1.2.7.1 An overview of PAR4

Protease-activated receptor 4 (PAR4) comprises 385 amino acids. Together with other PAR isotypes (PAR1-3), they are classified as class A GPCRs and are expressed in numerous tissues such as adipose, breast, and lung³. The expression of PAR4 is especially enriched in platelets and endothelial cells, suggesting a role in cardiovascular physiology (Coughlin, 1999). PAR4 is activated by the endogenous serine protease thrombin with a putative cleavage site at R47/G48 revealing tethered ligand GYPGQV (Figure 1.5).

³ <https://www.proteinatlas.org/ENSG00000127533-F2RL3>

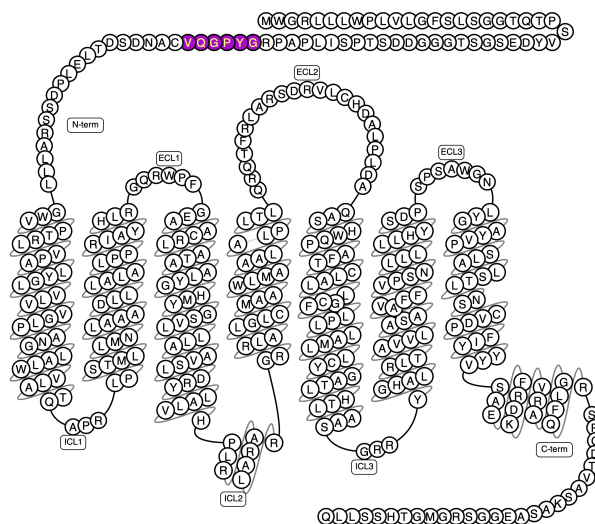


Figure 1.5. Structure of PAR4. The tethered ligand (highlighted in purple) is exposed after proteolysis by thrombin leading to conformational changes and activation of PAR4. Picture was taken from www.gpcrdb.org

Thrombin and trypsin cleave at the same specific sites at the N-terminal of the receptor (Heuberger and Schuepbach, 2019). Unlike the other PARs that are digested preferentially by thrombin or trypsin, PAR4 shows similar sensitivity towards both enzymes (French and Hamilton, 2016). This occurs due to the thrombin binding site that is absent in PAR4. Activation of PAR4 by different agonists may activate different signalling cascades and are reported to influence receptor trafficking (Zhao, Metcalf and Bunnett, 2014).

Since the 1990s, there has been a concerted effort to develop PAR modulators related to their role in thrombus formation (Coughlin, 1999). The discovery of vorapaxar, a PAR1 antagonist, has shown efficacy as an antiplatelet drug. However, its propensity to cause severe bleeding has limited its use in the clinic (Cunningham *et al.*, 2012). On the other hand, PAR4 is another thrombin receptor that shows slower kinetics than PAR1 (Xu *et al.*, 1998; Shapiro *et al.*, 2000). The lack of a thrombin binding domain on the PAR4 structure was believed to be responsible for this action (Faruqi *et al.*, 2000; French and Hamilton, 2016). In human, PAR1 and PAR4 are the primary thrombin receptors, whilst in mice PAR3 and PAR4 play as the primary receptor systems (Kahn *et al.*, 1998). Interestingly, although PAR4 is also involved in platelet aggregation, inhibition on PAR4 does not induce bleeding like PAR1. This evidence has demonstrated the potential of targeting PAR4 in preventing cardiovascular events.

Peptide agonists for PAR4 are currently limited and the low potency synthetic peptide AYPGKF-NH₂ has been widely used as an agonist to activate PAR4 without

proteolysis (Faruqi *et al.*, 2000; Hollenberg and Saifeddine, 2001). Recent modifications based on the AYPGKF-NH₂ backbone have been published using compound libraries so providing a toolkit to investigate PAR4 signalling (Thibeault *et al.*, 2019). Whereas ML354, BMS-986120, and YD-3 are usually used to inhibit PAR4 activation (Wu *et al.*, 2000; Moschonas *et al.*, 2017; Lin *et al.*, 2019).

1.2.7.2 A novel strategy to manipulate PAR4 pharmacology

PAR4, together with PAR1, is expressed in human platelets. Both receptors play essential roles in platelet activation, thereby blocking their signalling has been suggested to be beneficial in preventing thrombus formation and cardiovascular events. Since vorapaxar has shown excessive bleeding, PAR4 maybe an alternative target.

Despite many strategies available, biased signalling has become an attractive approach to modify receptor pharmacology. A few approaches have been developed, these include the use of peptidomimetics, small molecules, pepducins, and parmodulins (Heuberger and Schuepbach, 2019). Although these strategies are applicable for PAR1 and PAR2, this has not been validated in PAR4. To date, the most depicted biased agonism comes from synthetic drugs.

With the concept of the two-state receptor model, receptors were thought to have two distinct states: two states and extended ternary complex. However, recent development showed that receptors are conformationally flexible, generating a multitude of conformations by different ligands. Biased agonism can only be applied in the ternary complex model where the receptor can act as an allosteric microprocessor with pluridimensional efficacy (Smith, Lefkowitz and Rajagopal, 2018). Thus, they may adopt a specific conformational state and stabilised by particular ligands to promote signal transduction for different pathways.

The plasticity of GPCR has demonstrated that GPCR can engage in multiple active states mediating both short-term signalling and long-term regulatory mechanism that specific ligands can achieve. Biased agonism is believed to associate with the different ligand's ability to differentially or selectively activate signalling cascades, including mediating alteration in receptor trafficking and the fate of receptors. The formation of different protein complexes upon ligand bind to the receptor, including G proteins, arrestins, GRKs, and kinases, triggers different signalling events. To date, the most depicted biased agonism comes from synthetic drugs.

Interestingly, there has been growing evidence that RAMPs can also modulate a number of GPCRs, as mentioned earlier. Numerous receptors have demonstrated the advantages of biased signalling, for instance, activation of μ -opioid receptor mediated analgesia, but β -arrestin signalling induced causes respiratory depression (Bohn *et al.*, 1999; Bohn, Lefkowitz and Caron, 2002). An additional example is, carvedilol, a β -blocker, that has been shown to increase the survival rate from patients with heart failure, by antagonising G protein activation but still enabling β -arrestin recruitment (Wisler *et al.*, 2007).

Given that RAMPs are expressed in the platelets but without known GPCR interacting partners (Rowley *et al.*, 2011), it is of great interest to investigate whether PAR4 interacts with RAMP. The study in Chapter 6 focused upon determining if PAR4 and RAMP show interactions and investigating the consequences of the interaction on receptor signalling profile.

1.2.8 The calcitonin receptor-like receptor (CLR)

1.2.8.1 An overview of CLR

CLR is class B1 GPCR that has been shown to interact with RAMPs (McLatchie *et al.*, 1998) to generate new complexes with differential affinities towards peptide CGRP, AM, and AM2. Like other class B1 GPCRs, CLR has a large N-terminal ECD that serves essential roles for peptide binding. According to the crystal structure of the CLR and RAMP, they form heterodimers with a stoichiometry ratio of 1:1 (ter Haar *et al.*, 2010). However, later Heroux and colleagues demonstrated that complexes consist of two CLR and a single RAMP1 (H eroux *et al.*, 2007a). Although the stoichiometry has not been fully elucidated, other possibilities that CLR and RAMP may interact with a higher degree of stoichiometry should be taken into account (H eroux *et al.*, 2007b; Sexton *et al.*, 2009).

It has been reported that the ECD and TMD of the RAMP are key determinant of ligand selectivity, however, the possibility of other regions cannot be ruled out (Pioszak and Hay, 2020). Mutagenesis studies have implicated that the C-terminus of each peptides and RAMP1 W84, RAMP2 E101, and RAMP3 E74 are fundamental as a points of interaction for the peptide and receptor (Liang *et al.*, 2018). Regardless of these finding, the major question of how RAMPs modulate CLR pharmacology remains unanswered and requires further elucidation.

CLR does not translocate alone to the cell surface without association with one of RAMP1/2/3 (McLatchie *et al.*, 1998). These heteromers formation produced new

receptors: CGRP-R, AM1-R, and AM2-R, which elicited differential affinities towards the following peptides: CGRP, AM, and AM2. CGRP (α and β) are potent neuropeptides that elicit vasodilation and cardioprotective actions and are mainly expressed in trigeminal neurons (Edvinsson *et al.*, 2018). Both AM and AM2 also play essential roles in cardiovascular functions in adults, including vasodilators, cardioprotective, and being involved in the heart development (Pioszak and Hay, 2020). Currently, CGRP-based targeted therapies have been developed to treat migraine, either as CGRP antagonists (such as ubrogepant) or monoclonal antibody therapies against CGRP (eptinezumab, fremanezumab, galcanezumab) or CGRP-R (erenumab) (Edvinsson *et al.*, 2018; Serafin *et al.*, 2020; Bhakta *et al.*, 2021).

1.2.8.2 Physiological consequences of CLR-RAMP complex formation on cell growth: studies in human glioblastoma model and cardiovascular cells

RAMPs have been extensively studied, mainly with CLR. Many studies have been performed to dissect the interaction between CLR and RAMP by using the heterologous overexpression systems. Currently, CLR-RAMP complexes have been a target to treat migraines and suggested to play an essential role in cardiovascular systems. Several reports also highlighted the upregulation of CTR families in numerous cancers (Ostrovskaya *et al.*, 2016, 2019; Y. Zhang *et al.*, 2020). Although the correlation between the CTR family expression and cancer is not clearly elucidated, it would be of interest to explore if the interaction of RAMP and CLR, in particular, maybe the target with therapeutic benefits in the field of cancer. As part of a collaborative study with Dr. Ashley Clark (University of Cambridge), we investigated the downstream signalling properties of CLR-based agonists to promote cell proliferation in cardiovascular-derived cell lines. We extended the study to explore the potential targeting of RAMP-CLR complexes in human glioblastoma models.

1.3 Signal transduction through second messenger

Upon receptor activation by the “first message”, the signals are converted and transduced into an intracellular process. The process of relaying the signal is mainly mediated by second messengers, in the form of small molecules or ions, as well as other proteins. The physicochemical properties of second messengers allow them to transduce signals within membranes, cytosol, or between the membrane and the cytosol (e.g. gases and free radicals) (Newton, Bootman and Scott, 2016). As previously mentioned, there are four types of second messengers: cyclic nucleotides

(cAMP and cGMP) and other soluble molecules, lipid messengers, ions, and gas-free radicals (Newton, Bootman and Scott, 2016). The main topic in this thesis relates to cAMP signalling, the proteins involved in maintaining the intracellular concentration of cAMP and how this may impact upon cell growth and proliferation.

1.4 cAMP, a key regulator second messenger

The second messenger concept was first introduced by Sutherland and colleagues (1958), implying its function to transduce signals after stimuli were received by a plasma membrane receptor (Rall and Sutherland, 1958; Sutherland and Rall, 1958). As a ubiquitous second messenger, cAMP is synthesised from adenosine triphosphate (ATP) within the cells by the membrane-bound enzyme called adenylyl cyclase (AC). Together with cAMP, other second messengers, including cGMP, IP₃ and diacylglycerol (DAG), are produced upon activation at the receptor level, to modulate various cellular effector system. cAMP, in particular, is an essential component for signalling cascades within the cells, influencing various effector proteins, which will be discussed later.

1.4.1 Homeostasis of cAMP concentration

The intracellular concentrations of cAMP are maintained through the balance of its synthesis and degradation. AC generates cAMP in response to its direct activation or through GPCRs which are themselves activated through stimulation by drugs, hormones, and neurotransmitter.

AC is a heptahelical enzyme predominantly bound to the plasma membrane. In mammals, there are currently ten types of AC isoforms: types 1-9 are embedded in the plasma membrane, whereas type 10 also known as soluble AC (sAC), is present in the cytoplasm (Khannpnavar *et al.*, 2020). All AC isoforms generally contain between 1064 and 1610 amino acid residues. AC isoforms appear to be widely distributed in most tissues (Taussig, 2013).

As previously explained, GPCRs can engage with different G proteins. Of all G protein classes, G α_s and G α_i , in particular, directly modulate AC activity. Whilst G α_s stimulates AC to promote cAMP production, activation of G α_i results in reduced cAMP levels. Aside from GPCRs, activation on RTKs has also been reported to influence the activity of some particular types of AC isoforms (Tan *et al.*, 2001). However, the mechanism is poorly understood.

In order to characterise the activity of AC, many pharmacological tools have been developed. Of all tools, forskolin, a labdane diterpene that is an active substance from *Coleus forskohlii* sp, has been the most widely used experimentally. Forskolin is a pan-AC activator, thereby stimulating the production on cAMP (Singh and Tandon, 1982). Other pharmacological tools that inhibit AC activity are currently available, for instance, SQ 22536 (non-competitive antagonist) (Haslam, Davidson and Desjardins, 1978), NKY80 (Klotz and Kachler, 2016). Interestingly, KH7 is a selective activator of sAC (Stessin *et al.*, 2006).

1.4.2 Overview of PDEs structure and function

Following synthesis cAMP diffuses within cells and is hydrolysed to 5'-adenosine monophosphate (5'AMP) by PDEs. PDEs are a subfamily of ectonucleotidases consisting of 11 isoforms (PDE1–11) in mammals and are encoded by 21 different genes (Beavo, 1995). PDEs are distributed in many types of tissue (Soderling and Beavo, 2000). Each isoenzyme possesses different: i) affinities for cAMP and/or cGMP, ii) kinetic characteristics, iii) allosteric regulation by cAMP/cGMP, iv) phosphorylative control by various protein kinases, and v) cellular location. All these properties dictates their response to a stimulus (Menniti, Faraci and Schmidt, 2006; K Omori and Kotera, 2007a). To date, there are three classes of PDEs subdivided according to their substrate specificities: cAMP-specific PDEs (PDE4, PDE7 and PDE8), cGMP-specific PDEs (PDE5, PDE6 and PDE9), and dual-substrate PDEs (PDE1, PDE2, PDE3, PDE10 and PDE11) (Francis, Blount and Corbin, 2011). Through metabolising both cAMP and cGMP, PDEs generate intracellular gradients and microdomains for these second messengers to regulate their spatio-temporal signalling (Conti, Mika and Richter, 2014). PDEs prevent non-specific activations, enabling both specificity and selectivity toward intracellular targets (Ladilov and Appukuttan, 2014). The summary of preference of each PDEs to cAMP and cGMP are summarised in Table 1.2.

Table 1.2

Characteristic of PDE isozyme families and their K_m^* value for both cyclic nucleotides

| Family (N) | Characteristics | K_m (μ M) cAMP/cGMP |
|---------------|---|----------------------------|
| PDE1 (3) | Ca ²⁺ /calmodulin-stimulated | 0.3–124/0.6–6 |
| PDE2 (1) | cGMP-stimulated | 15/15 |

| Family (N) | Characteristics | Km (μ M) cAMP/cGMP |
|------------|--|-------------------------|
| PDE3 (2) | cAMP-selective, cGMP-inhibited | 0.2/0.1 |
| PDE4 (4) | cAMP-specific, cGMP-insensitive | 2/>300 |
| PDE5 (1) | cGMP-specific | 150/1 |
| PDE6 (6) | cGMP-specific, transducin activated | 2000/60 |
| PDE7 (2) | cAMP-specific, high-affinity rolipram-insensitive | 0.2/>1000 |
| PDE8 (2) | cAMP-selective, IBMX insensitive rolipram-insensitive | 0.06/NA |
| PDE9 (1) | cGMP-specific, IBMX insensitive | NA/0.07–0.17 |
| PDE10 (1) | cGMP-sensitive, cAMP-selective | 0.02–1/13 |
| PDE 11 (1) | cGMP-sensitive, dual specificity | 0.5–2/0.3–1 |

(N) = gene numbers. The summary of PDE activities was adapted from (T Keravis and Lugnier, 2012) and updated accordingly. NA – not applicable

*Km is the concentration of substrate where the enzyme achieves half of V_{max}

V_{max} is the maximum rate of enzymatic activity when it is fully saturated by the substrate

Currently there are ten crystal structure of PDEs available in the databases. These are, PDE1B (Zhang *et al.*, 2004), PDE2A (Iffland *et al.*, 2005), PDE3B (Scapin *et al.*, 2004), PDE4B (Xu *et al.*, 2000; Card *et al.*, 2004), PDE4D (Lee *et al.*, 2002; Huai, Colicelli and Ke, 2003; Huai, Liu, *et al.*, 2004), PDE5A (Sung *et al.*, 2003; Card *et al.*, 2004; Huai, Liu, *et al.*, 2004; Zhang *et al.*, 2004), PDE7A (Wang *et al.*, 2005), PDE8A (Wang *et al.*, 2008), PDE9A (Huai, Wang, *et al.*, 2004), and PDE10A (Yoshikawa *et al.*, 2016). However, to date, there are no structures of any PDE holoenzymes available. In general, PDEs contain three regions consisting of a catalytic domain, which is shared within all PDE isoenzymes, an N-terminal regulatory domain and a C-terminal domain, whose length depends on the specific PDE subfamilies (Figure 1.6). The regulatory domain is close to the N-terminal, whilst highly conserved catalytic subunit are located near the C-terminal of the enzymes. For enzymes that belong to the same gene family, approximately 80% similarity has been reported compared to different PDE family, which only account for ~25% - 40% (Cheng and Grande, 2007).

The catalytic domain for all PDEs have similar motifs: H(X)₃H(X)₂₅₋₃₅D/E, where the active site pocket contains 11 of the 17 conserved residues (Jin, Swinnen and Conti, 1992). The catalytic domain can be further classified into three helical subdomains, which include an N-terminal cyclin-fold region, a linker region, and a C-

terminal helical region, as depicted in Figure 1.6. At the subdomain interface, a deep hydrophobic pocket is formed consisting of four sites, where the M site is served for metal binding, the Q site as core pocket, the hydrophobic H pocket, and the lid L region (Y H Jeon *et al.*, 2005).

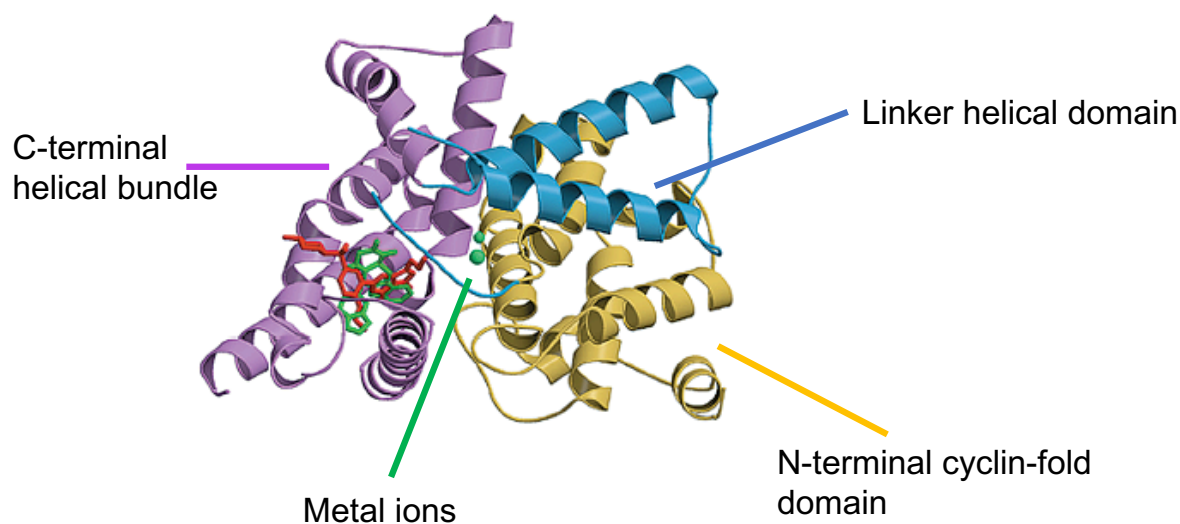


Figure 1.6 Exemplary of PDE catalytic domain from apo-PDE5A structure. The catalytic domain displays the interaction regions with sildenafil (compound in green) and tadalafil (red). The catalytic domain contains: N-terminal cyclin-fold domain, linker helical domain, and C-terminal helical bundle. There are two metal ions represented as green spheres in the centre of the catalytic domain structure. The picture was taken from (Y. H. Jeon *et al.*, 2005) from original structure with the accession code 1T9S published by (Zhang *et al.*, 2004).

There is a glutamine residue within the Q pocket which is postulated to be a descriptor for enzyme selectivity towards cAMP, cGMP, or both cyclic nucleotides. The notion is known as a "glutamine switch". Zhang suggested that the side chain's orientation on glutamine residues dictated the substrate specificity by forming two hydrogen bonds with either cAMP or cGMP (Zhang *et al.*, 2004). While the glutamine switch mechanism was observed in PDE4B, PDE5A, and PDE1B structures, several lines of evidence were reported against the glutamine switch concept (Iffland *et al.*, 2005; Zoraghi, Corbin and Francis, 2006; Wang *et al.*, 2007). The mechanism of selectivity of PDEs remains unsolved.

Within the PDE catalytic domain, it was observed that at the end of its cleft, there was a bound ion, Zn^{2+} or Mg^{2+} , which plays a crucial function for catalysis. The latter has a weaker affinity to the catalytic pocket (Xu *et al.*, 2000; Ke, 2004; Wang *et al.*, 2005). The regulatory domains function are essential for cAMP/cGMP binding, oligomerisation, and kinase recognition/phosphorylation (M Conti and Beavo, 2007).

The presence of the cGMP-specific PDEs, ACs and FhIA (GAF) domain in particular PDEs serve to enable cyclic nucleotide recognition. For instance, cGMP acts as an allosteric modulator of PDE2 and occupies GAF-B domain switching the kinetics for the cyclic nucleotide hydrolysis resulting in increased activity at lower substrate concentrations. This regulatory action, where cGMP can negatively modulate cAMP, makes PDE2 known as a cGMP-stimulated PDE (M Conti and Beavo, 2007). A distinct regulatory domain is unique for each PDEs. While some PDEs contain the GAF domain in their N-terminal, some particular PDEs have distinct motifs. For example, PDE1 has a calmodulin-binding domain, providing a crosstalk point with Ca^{2+} signalling. The upstream conserved region (UCR) and Per-Arnt-Sim (PAS) domain are only observed in PDE4 and PDE8, respectively. On the contrary, PDE9 does not contain a specific regulatory domain at its N-terminal (Figure 1.7). Different from the remaining PDEs, the PDE3 catalytic domain contains an additional 44-amino acid insert (Perry, biology and 1998, no date; Degerman, Belfrage and Manganiello, 1997; Torphy, 1998; Dousa, 1999; Cheng and Grande, 2007). Hung and colleagues reported that this insert maybe involved in substrate binding and PDE3 conformational changes (Hung *et al.*, 2006).

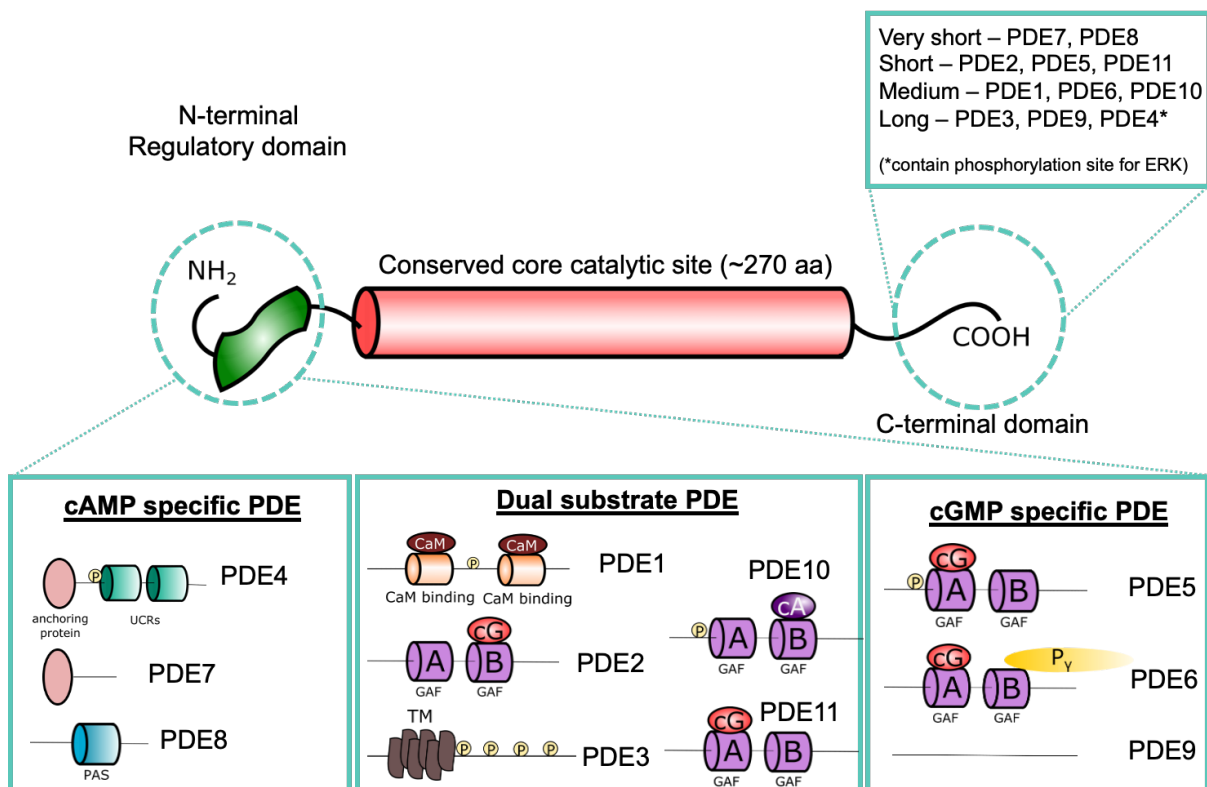


Figure 1.7 The schematic representation of 11 subfamilies of PDEs. In general, all PDE family has the conserved catalytic domain, located near C-terminal domain. Phosphorylation sites are depicted as P symbol. Abbreviations: UCRs, upstream

conserved regions; PAS, period, aryl-hydrocarbon receptor nuclear translocator (ARNT), and single minded; CaM, calmodulin; cG, cGMP; cA, cAMP; GAF, cGMP-activated PDEs, adenylyl cyclase, and Fh1A; TM, transmembrane domain of PDE3; $\text{P}\gamma$, PDE γ subunit. Figure was adapted from (M Conti and Beavo, 2007) and modified accordingly.

Their structure, function, and spatial heterogeneity enables PDEs to have modulatory roles, both temporally and spatially, upon secondary messenger signalling (Menniti, Faraci and Schmidt, 2006). Intracellular cAMP levels are tightly regulated and balanced between formation, degradation, and modulation of other pathways. Cyclic nucleotides, cAMP and cGMP, are metabolised into 5-AMP and 5-GMP, respectively, allowing the cellular signal to be terminated (M Conti and Beavo, 2007; Moorthy, Gao and Anand, 2011). It has been revealed that PDEs are involved in signalling, creating micro-domains and cyclic nucleotide gradients within cells (Menniti, Faraci and Schmidt, 2006). Due to this gradient, cells can transmit the signal into specific areas within cells and activate particular pathways, exhibiting biological responses.

1.4.2.1 PDE1

PDE1 was previously known as calmodulin-stimulated PDE (CaM-PDE) due to the presence of CaM binding site at the N-terminal regulatory domain (Bender and Beavo, 2006). PDE1 is encoded by three different genes - PDE1A, PDE1B, and PDE1C. Whilst PDE1A and PDE1B preferably hydrolyse cGMP, PDE1C exhibits similar affinity for both cAMP and cGMP (Thérèse Keravis and Lugnier, 2012b). This PDE family is expressed in many tissues, including brain, olfactory epithelium, heart, vascular smooth muscle, testis, and liver (Bender and Beavo, 2006; Menniti, Faraci and Schmidt, 2006). Its responsivity to modulate cyclic nucleotides based on Ca^{2+} levels is believed to be a point for cross-talking with the Ca^{2+} signalling cascade. It has been demonstrated that PDE1 was involved in the smooth muscle contractile responses that were mediated by noradrenaline (Noguera *et al.*, 2001).

1.4.2.2 PDE2

PDE2 exists as a homodimer comprised of approximately 105kDa and is encoded by the PDE2A gene that has three different variants: PDE2A1, PDE2A2, and PDE2A3. PDE2A1 variant is cytosolic whereas the remaining are membrane-bound (Thérèse Keravis and Lugnier, 2012b). The N-terminal domain of PDE2 consists of GAF-A and GAF-B as cGMP-binding domain. Aside from facilitating binding to cGMP, GAF-A is

reported to mediate PDE2 dimerisation. GAF-B mediates cAMP hydrolysis due to allosteric modulation by cGMP (Marco Conti and Beavo, 2007). PDE2 is widely distributed in adrenal gland, heart, lung, liver, platelets, endothelial cells (Thérèse Keravis and Lugnier, 2012b).

1.4.2.3 PDE3

Similar to PDE1 and PDE2, PDE3 is also a dual-substrate PDE hydrolysing both cyclic nucleotides. The PDE3 family is encoded by two genes: PDE3A and PDE3B. The V_{\max} (the maximum rate of activity when enzyme is fully saturated with the substrate) of cAMP hydrolysis is 10-fold faster than that of cGMP, yet the substrate affinity for cGMP is higher than cAMP. Given this action, cGMP acts as a competitive inhibitor for cAMP hydrolysis. Therefore, PDE3 is also known as a cGMP-inhibited PDE. It has been reported that upon PKA activation by cAMP, PKA also activates PDE3 to give negative feedback regulation in maintaining intracellular cAMP levels. Besides PKA, PDE3 may also be activated by the action of protein kinase B (PKB) and PKC. PDE3B in particular, is involved as a protein scaffold with phosphatidylinositol 3' kinase (PI₃K) (Wilson *et al.*, 2011).

The structure of the catalytic domain of PDE3B is the only structure available for this PDE family. It contains three subdomains, consisting of 16 α -helices, similar to the remaining established PDE structures (Scapin *et al.*, 2004). Between helices 6 and 7, there is an insert of 44 amino acid residue (Arg⁷⁵⁵ – Ser⁷⁹⁸), a typical motif that PDE3 family possess.

PDE3 is highly expressed in the heart and found in other tissues including smooth muscle, lung, liver, platelets, adipocytes, immunocytes (Thérèse Keravis and Lugnier, 2012b). PDE3B plays a role in potentiating cAMP-enhancement of glucose-stimulated insulin release from pancreatic β -cells (Härndahl *et al.*, 2002). Inhibition of PDE3 by amrinone and milrinone in the heart has been shown to improve inotropy and lusitropy, which is also supported by the vasodilation effects making it a potential treatment for patient with heart failure (Silver, 1989; Wynands, 1994). PDE3 inhibitors have been also shown to increase lipolysis in adipocytes (Degerman *et al.*, 2011).

1.4.2.4 PDE4

PDE4 is known as a cAMP-specific PDE and has four isoforms. These include, PDE4A, PDE4B, PDE4C and PDE4D. All of them possess different promoters and they are alternatively spliced with Bolger and colleagues discovering 25 splice variants

from PDE4 gene (Bolger, Conti and Houslay, 2019). PDE4 is the only family that consists of a signature motif at the N-terminal called the upstream conserved sequences (UCR). Notably, the various isoforms encoded by each PDE gene can be classified further into long, short, and super-short forms (Figure 1.8). Long forms comprise both UCR1 and UCR2, whereas short forms only contain UCR2, and the super-short forms contain half of UCR2. Both UCRs do not play a direct role in catalysis. Instead, they are known to be authentic protein domains for PDE4. Their action is equivalent to other protein domains, such as SH2 and SH3 domains, while having the ability to undergo self-folding (Pawson and Scott, 1997).

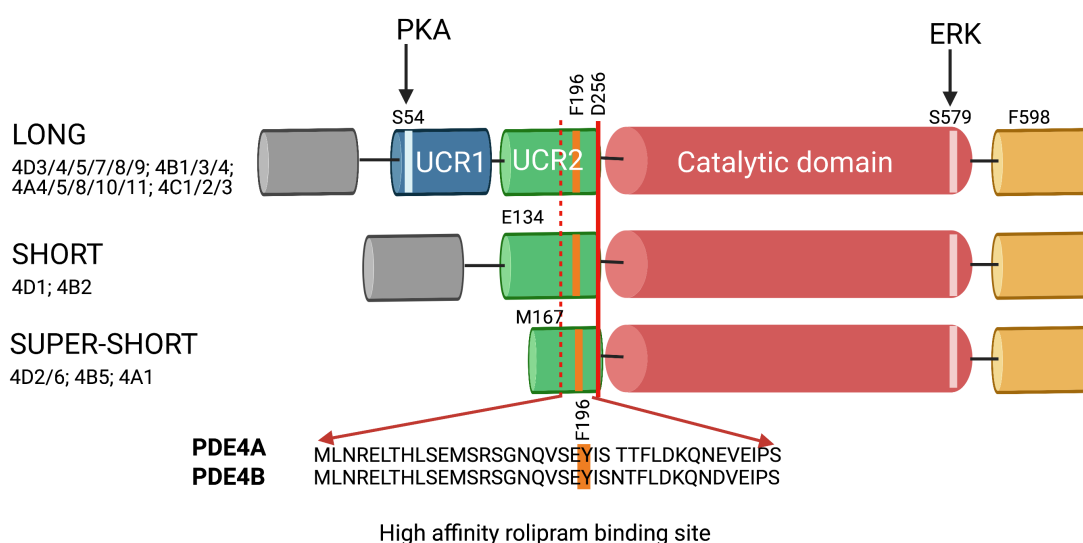


Figure 1.8. The schematic illustration of PDE4 isoenzymes. Long forms contain UCR1 and UCR2, whilst short forms only have UCR2. The truncated N-terminal of UCR2 only presents in the super-short forms of PDE4. Sites for phosphorylation by PKA and ERK are displayed at residue S54 and S579, respectively. The high affinity binding rolipram site is located close to the C-terminal of UCR2, as indicated. The illustration was adapted and modified accordingly (Gurney *et al.*, 2011). Figure was created with BioRender.com

Many studies reported that PDE4 forms a signalosome with other proteins. Dodge-Kafka *et al* revealed that this PDE family formed an ERK5-PDE4D3-EPAC1-mAKAP complex (EPAC for exchange protein activated by cAMP; mAKAP for muscle A kinase anchoring protein), although the function remains unclear (Dodge-Kafka *et al.*, 2005). Similarly, the formation of a PDE4D5- β -arrestin- β 2-AR complex in cardiac myocytes has been suggested to be involved in cardiac remodelling and stress-induced cardiac hypertrophy (Shi *et al.*, 2017).

1.4.2.5 PDE5

PDE5 is one of the PDEs that specifically hydrolyses cGMP. PDE5 is allosterically activated by cGMP. Similar to PDE2, PDE5 also contains two GAF domains: GAF-A and GAF-B. While GAF-A is responsible for allosteric cGMP binding, GAF-B contributes to PDE5 dimerisation. The binding of cGMP at GAF-A domain triggers phosphorylation of PDE5 leading to activation of catalytic activity to enhance cGMP binding affinity further. This sequence of processes stabilises an active form of PDE5. This enzyme is highly expressed in male reproductive organs, lung, platelets, smooth muscle, heart, endothelial cells, and brain (Thérèse Keravis and Lugnier, 2012b). Of all PDE inhibitor, sildenafil - under the brand name Viagra, has been known to treat erectile dysfunction and pulmonary arterial hypertension.

1.4.2.6 PDE6

PDE6 plays an essential role in phototransduction. It has been long known as photoreceptor PDE and its expression is mainly restricted to the eyes and pineal glands (Thérèse Keravis and Lugnier, 2012b). Beyond the eyes, PDE6 subtypes have been found in HEK293 cells (Wan *et al.*, 2001) and mouse lung (Tate, Arshavsky and Pyne, 2002). PDE6 is encoded by a number of PDE6 genes: PDE6A-D, G and H, that together contribute to produce each component for PDE6 holoenzymes ($\alpha\beta\gamma_2$). In terms of structure, PDE6 has 2 large catalytic subunits (PDE6 $\alpha\beta$ heterodimer) and 2 small inhibitory (PDE6 γ) subunits (Lugnier, 2006). To relay the signal, upon activation of rhodopsin (a GPCR) by light, it triggers the activation of PDE6 and lead to reduction of cGMP levels (Baehr, Devlin and Applebury, 1979). These steps induce the closure of a cyclic nucleotide gated channel (CNGCs), (CNGCs will be introduced in the section 1.4.4.3) leading to hyperpolarisation, thereby converting a light signal into an electrical signal.

1.4.2.7 PDE7

Although classified as a cAMP-specific PDE, there is no known regulatory domain at its N-terminal (as depicted in Figure 1.5). PDE7 is commonly known as a bifunctional protein. Besides its activity to hydrolyse cAMP, the N-terminal interacts with the catalytic (C) subunit of PKA (discussed later) directly leading to kinase activity blockage (Thérèse Keravis and Lugnier, 2012b). Due to its expression in the brain, PDE7 elicits an important role in neurotransmission (Nozal *et al.*, 2021). The expression of this family is also described in peripheral blood cells and T cells, which

may indicate PDE7 involvement in T cell function (Szczypka, 2020). However, the precise role of this PDE family remains to be established.

1.4.2.8 PDE8

PDE8 shows the highest affinity to cAMP and is insensitive to the non-selective PDE inhibitor 3-isobutyl-1-methylxanthine (IBMX) (Vasta, Shimizu-Albergine and Beavo, 2006). The regulatory domain contains the N-terminal receiver (REC) and PAS domain, yet its function remains to be established. PDE8 has been reported to have numerous variant splices: PDE8A1-A5, A2, B1-B4, all of which are diverse regarding the presence of REC and PAS domain (Wang *et al.*, 2001; Hayashi *et al.*, 2002; Gamanuma *et al.*, 2003). In addition, three putative phosphorylation sites are available located between the PAS domain and the catalytic domain. This enzyme family is widely distributed in testes, eye, liver, skeletal muscle, heart, kidney, ovary, brain, T lymphocytes, and thyroid (Thérèse Keravis and Lugnier, 2012b).

1.4.2.9 PDE9

Amongst all cGMP specific PDEs, PDE9 has been demonstrated to display the highest affinity towards cGMP. Similar to PDE8, this PDE family is also insensitive to IBMX. About twenty-one variants of PDE9 N-terminal have been identified, but little is known about the characterisation of this enzyme family. No known regulatory sequence has been discovered in the N-terminal domain and no phosphorylation sites are known in the PDE9 protein family (Bender and Beavo, 2006; Kenji Omori and Kotera, 2007). This family is highly expressed in kidney, liver, lung, brain (Thérèse Keravis and Lugnier, 2012b).

1.4.2.10 PDE10

PDE10 is known as a dual-substrate PDE. PDE10A contains two GAF domains at the N-terminal. Unlike other GAF domains in other PDEs that are responsible for cGMP binding, GAF-A in PDE10 is essential for cAMP binding. Opposite to the action of PDE3, PDE10 is known as a cAMP-inhibited cGMP PDE. PDE10 subfamily only has one member, PDE10A, which is found in brain, testes, and thyroid (Thérèse Keravis and Lugnier, 2012b). Due to its prominent expression in the central nervous system, PDE10A has become the target for numerous neurological disorders. Several studies have shown that inhibition of PDE10 improves striatal and cortical pathology in Huntington's disease model (Niccolini *et al.*, 2015; Deb, Frank and Testa, 2017),

Parkinson's disease (Lee *et al.*, 2019), and psychiatric disease (Farmer *et al.*, 2020). A very potent and specific PDE10 inhibitor, TP-10, was investigated preclinically for schizophrenia treatment (Schmidt *et al.*, 2008).

1.4.2.11 PDE11

PDE11 is classified as a dual-substrate PDE. However, it resembles PDE5 more closely than PDE10A. To date, there are four N-terminal variants of the PDE11A genes producing PDE11A1-4, all of which vary in the number of GAF domains in their N-terminal. Whilst PDE11A2 and PDE11A3 have one complete and one incomplete GAF domain (Kenji Omori and Kotera, 2007), there are two GAF domains at N-terminal of the PDE11A4 (Yuasa *et al.*, 2001). However, the function of the GAF domain in PDE11A has not been fully elucidated. PDE11 is expressed in various tissues including skeletal muscle, prostate, pituitary gland, liver, and heart (Thérèse Keravis and Lugnier, 2012b).

1.4.2.12 Small molecule PDE inhibitors

Selective PDE inhibitors have been developed either as pharmacological tools to dissect the involvement of PDE in cellular signalling or as therapeutic agents. A number of PDE inhibitors available are summarised in Table 1.3, some of which were used for the studies presented in Chapter 3 and 4. Aside from compounds that selectively inhibit specific PDEs, compounds including caffeine, IBMX, theophylline (weak activity), dipyridamole, zaprinast, trequinsin, and zardaverine display non-selective actions. Whilst caffeine inhibits all PDEs (Soderling, Bayuga and Beavo, 1999), dipyridamole acts as PDE5/6/8/10/11 inhibitor (Meester *et al.*, 1998; Fujishige *et al.*, 1999; Soderling, Bayuga and Beavo, 1999), zaprinast inhibits PDE5/6/9/11 and activates GPR35 (Lugnier, 2006; Taniguchi, Tonai-Kachi and Shinjo, 2006), while zardaverine acts as dual-selective inhibitor of PDE3 and PDE4 (Galvan and Schudt, 1990). Interestingly, none of compound that selectively targeting PDE6 are available without eliciting actions towards other PDEs. Some of these inhibitors are also used in clinical setting, such as amrinone and milrinone for congestive heart failure through their action to improve inotropy, lusitropy, and vasodilation (Levy, Ramsay and Bailey, 1990). Rolipram, a prototypic PDE4 inhibitor, was firstly used as an antidepressant in

the early 1990 but discontinued due to narrow therapeutic index. Rolipram is currently in clinical trial for multiple sclerosis as immunomodulatory therapy⁴.

Table 1.3

The summary of small molecule that selectively inhibit each PDE subfamily protein

| Family (N) | Inhibitor |
|------------|--|
| PDE1 (3) | MMPX, vinpocetine, IC86340, IC295, dioclein, nimodipin |
| PDE2 (1) | EHNA, PF 05180999, BAY60-7550, ND7001 |
| PDE3 (2) | Anagrelide hydrochloride, cilostamide, cilostazol, enoximone, amrinone, milrinone, trequinsin, motapizone |
| PDE4 (4) | Rolipram, CDP840 HCl, CGH2466 HCl, CP 80633, eggmanone, etazolate HCl, ibudilast, roflumilast, piclamilast, RO 20-1724 |
| PDE5 (1) | Gysadenafil besylate, sildenafil, tadalafil, T 0156 |
| PDE6 (6) | No selective PDE6 inhibitor is available |
| PDE7 (2) | TC3.6, BRL-50481, IC242, ASB 16165 |
| PDE8 (2) | BC 11-38 |
| PDE9 (1) | (S)-C33, PF 04449613 |
| PDE10 (1) | TC0E 5005, PF 2545920 |
| PDE 11 (1) | PH 04671536 |

MMPX, 8-Methoxymethyl-3-isobutyl-1-methylxanthine; EHNA, erythro-9-(2-hydroxy-3-nonyl) adenine.

Despite their complexity, PDEs regulate many fundamental physiological processes in various pathophysiological states such as cardiovascular diseases, neurodegenerative diseases, and asthma (Torphy and Udem, 1991; Menniti, Faraci and Schmidt, 2006; Knight and Yan, 2013). Differential expression and localisation of PDEs have been found throughout the brain (Menniti, Faraci and Schmidt, 2006) and act in a very complex manner. Also, abnormalities in PDEs expression, that can lead to disruption of cellular signalling have reportedly been associated with changes in pathophysiology (for example in cancers and some neurological disorders).

In many types of diseases, especially in cancer, PDE's divergent expression has been linked with malignancy (Savai *et al.*, 2010a) although the complete picture is complicated by the cross-talk between cAMP and cGMP signalling systems. The

⁴ <https://clinicaltrials.gov/ct2/show/NCT00011375>

recent discovery of a range of particular PDE inhibitors promises to clarify this situation (DeNinno, 2012), providing the tools to manipulate the two cyclic nucleotides intracellular concentrations.

1.4.3 Cyclic nucleotide extrusion

Aside from formation and degradation, the intracellular concentration of cAMP is also controlled by the ability of cells to extrude cAMP extracellularly. This extrusion mechanism has been reported to involve an efflux transporter called multidrug-resistant protein (MRP), a member of the ATP-binding cassette (ABC) superfamily of efflux transporters.

Almost all species express ABC protein families. They are found in bacteria, yeast, plants, and mammals (Davidson *et al.*, 2008; Moussatova *et al.*, 2008; Eitinger *et al.*, 2011; Teichmann *et al.*, 2017; Feng *et al.*, 2020). In the latter, ABC transporters are responsible for transporting anticancer drugs (Borst and Oude Elferink, 2002). These proteins use the energy from ATP hydrolysis to transport drugs across the plasma membrane. MRPs share similar homology with members of ABC family including multiple TMDs and a nucleotide binding (CNB) domain for ATP binding and hydrolysis. MRP4, together with MRP5, are known as “short MRPs” since their TMD8 and TMD9’s lacks an additional N-terminal TMD0. Not only do MRPs extrude xenobiotics, but these proteins also pump endogenous substances, including cAMP, into the extracellular space.

Wang and colleagues summarised in their review that at least 4 MRP classes were found to be responsible for transporting cyclic nucleotides out of cells, including MRP1, MRP4 (ABCC4), MRP5 (ABCC5), and MRP8 (ABCC11) (Kruh and Belinsky, 2003; Wang *et al.*, 2021). MRP4 also plays an important role for cellular protection by exporting exogenous compounds and harmful substances (Bloise *et al.*, 2016; Kochel *et al.*, 2017; Khoury *et al.*, 2018). In cardiomyocytes (CMs), MRP4 has been suggested to increase cAMP concentrations, so modulating cardiac muscle contraction and hypertrophy. It has also been reported that β -AR are colocalised with MRP4 and are internalised together in caveolin pits (Sassi *et al.*, 2008; Sellers *et al.*, 2012). Both MRP1 and MRP4 have been demonstrated to be overexpressed in various cancers (glioma, breast cancer, pancreatic ductal carcinoma), leading to significant suppression on cAMP levels (Calatuzzolo *et al.*, 2005; Andric, Kostic and Stojilkovic, 2006; Decleves *et al.*, 2008; Carozzo *et al.*, 2019). In comparison, MRP5 up-regulation may associate with cisplatin resistance in patients with non-small lung cancer (NSCLC)

(Masetto *et al.*, 2020). In the male reproductive organ system, the role of MRP5 was highlighted to regulate cGMP levels in smooth muscle to modulate erectile function (Gupta, Singh-Gupta and Sabbah, 2019).

1.4.4 Downstream effecters of cAMP

1.4.4.1 Protein kinase A (PKA)

It has been long known that protein kinase A (PKA) is the major effector of cAMP. Activated PKA phosphorylates serine and threonine residues on substrate proteins. In the inactive form, PKA is a holo-tetramer consisting of 2 regulatory (R) and two catalytic (C) subunits. Two isoforms of R have been identified, type I and II, and further classified into two different subtypes: α and β (Hofmann *et al.*, 1975). In mammals, three different isoforms of C subunits have been identified: C α , C β , and C γ (Uhler, Chrvia and McKnight, 1986; Beebe *et al.*, 1990). Each R subunit has a CNB domain that allows this enzyme to bind four cAMP molecules. Upon binding, the C subunit will dissociate due to conformational changes of PKA (Murray, 2008). Whilst the catalytic monomer binds to ATP, this subunit becomes active and is able to phosphorylate serine and threonine residues on their respective protein substrate. AKAPs are also expressed within the cell to ensure PKA phosphorylates the correct regulatory proteins (Wong and Scott, 2004). This mechanism ensures local subcellular action of PKA is attributed to specific signalling events. A few examples of downstream substrates that PKA mainly phosphorylates are the transcription factors CREB, cAMP-responsive element modulator (CREM), and activating transcription factor 1 (ATF1) (Sassone-Corsi, 2012). In addition, PKA can also phosphorylate the Ras superfamily of small GTPases Rap1 at its C-terminal to facilitate cAMP-mediated ERK activation (Y. Li *et al.*, 2016).

PKA is reported to form macromolecular interactomes that involve GPCRs, GTPases, protein phosphatase, PDEs, and other protein kinases (Newton, Bootman and Scott, 2016). For instance, the PDE4 isoform PDE4D and PDE4C has been reported to form a complex with the PKA subunit PKA-RII in COS1 cells. The study also indicates that this complex is tethered via AKAP450 to the perinuclear space (McCahill *et al.*, 2005). In addition, PDE4D5 specifically interacts with β -arrestins and suppresses PKA activity in phosphorylating β 2-AR (Lynch *et al.*, 2005). By forming a signalosome that comprises AKAP, PKA, and PDE; PKA may activate PDEs that reduced cAMP levels so localising the signal (Sunahara, Dessauer and Gilman, 1996; Boullaran and Gales, 2015).

Since its discovery, PKA has been implicated in various cellular processes including the modulation of other kinases, calcium, and transcription factors (Murray, 2008). PKA inhibitors have been predominantly used as the primary tool to characterise downstream cAMP signalling. A few compounds have been widely applied to inhibit PKA activity, including H89, KT 5720, and Rp-8-Br-cAMPS. The latter has been reported to be a potent and specific inhibitor for PKA. These compounds, however, have a distinct mechanism to block PKA activity. While H89 (isoquinolone backbone) and KT5720 (firstly isolated from fungus *Nocardioopsis sp*) competitively bind to the ATP binding site in catalytic subunit (Kase *et al.*, 1987; Engh *et al.*, 1996), Rp-8-Br-cAMPS acts as a competitive antagonist to the CNB domain at the R unit, preventing the release of C subunits. Another PKA inhibitor class, the protein kinase inhibitors (PKIs), are also available to bind to free catalytic subunits and prevent further phosphorylation of PKA substrate (Dalton and Dewey, 2006).

Currently, a number of reporters to determine PKA activities have been developed, of which the best-in-class Förster-resonance energy transfer (FRET)-based reporters include: tAKAR α (Ma *et al.*, 2018), AKAR3-EV (Komatsu *et al.*, 2011), and AKAR4 (Depry, Allen and Zhang, 2011). The AKAR3 sensor consists of four regions: a donor fluorophore (CFP), a phosphopeptide binding domain (FHA1), a PKA specific phosphorylatable sequence, and an acceptor (Venus or other YFP). Upon phosphorylation by PKA, the substrate of PKA binds to the FHA1 domain leading to an increase of FRET signal. Chen and colleagues further modified the AKAR3 biosensor to be compatible with 2 photon microscopy therefore is applicable to quantify PKA activity in tissue, namely FLIM-AKAR3 (Yao Chen *et al.*, 2014). The newest fluorescent protein-based PKA biosensors, ExRai-AKAR2 (based on excitation-ratio metric PKA activity reporter) has been developed and is reported to show an enhanced dynamic range compared to other reporters (Zhang *et al.*, 2021).

1.4.4.2 Exchange protein activated by cAMP (EPAC)

Although EPAC is a relatively newly identified effector of cAMP, this protein family, similar to PKA, have high affinity for cAMP. Structurally similar to PKA, EPAC possess a CNB domain that binds cAMP and an analogous R subunit. In mammalian cells, two isoforms have been identified, EPAC1 and EPAC2. Upon binding to cAMP, EPACs serve as guanine nucleotide exchange proteins for the Ras GTPase homologous, Rap1 and Rap2, mediating conversion from inactive GDP- to active GTP-bound forms

(Bos, 2003). EPAC1 and EPAC2 differentially bind to both types of Rap (Cheng *et al.*, 2008)

While EPAC1 is ubiquitously expressed, EPAC2 expression is limited to specific tissues including brain, neuroendocrine and endocrine tissues such as pancreatic cells (de Rooij *et al.*, 1998; Kawasaki *et al.*, 1998). Similar to other enzymes, both EPACs contain an N-terminal regulatory unit and a C-terminal catalytic region. The difference between both EPACs lies in the structure of the N-terminal domain. Whilst EPAC1 and EPAC2 contain the Dishevelled/EG1-10/pleckstrin (DEP) domain which is followed by the CNB domain, EPAC2 has an additional CNB domain CBD-A, that binds cAMP with low affinity (De Rooij *et al.*, 2000).

A number of small molecules EPAC inhibitors have been developed and used as pharmacological tools in many studies. ESI-05 is a specific inhibitor of EPAC2 and has been shown to have no effect on EPAC1 nor PKA (Tsalkova *et al.*, 2012). In comparison, ESI-09 elicits non-selective activity over both EPAC isoforms (Almahariq *et al.*, 2013). Another compound identified in 2012, CE3F4, inhibits EPAC1 without affecting PKA (Courilleau *et al.*, 2013). Finally, HJC 0350 has been reported to be a specific antagonist of EPAC2 (Chen *et al.*, 2013).

The discovery of EPAC adds to the complexity of cAMP-mediated signalling. EPAC elicited cAMP-mediated responses independent of PKA to modulate cell growth, cell adhesion, cell-cell-junction, cell differentiation, apoptosis, and neurotransmission. In CMs, EPAC is responsible for gap junction formation, where ion channels present, and therefore indirectly it regulates cardiac contractions (Somekawa *et al.*, 2005). EPAC has also been shown to enhance intracellular Ca^{2+} release through the activation of both calcium-calmodulin-dependent protein kinase II (Pereira *et al.*, 2007) and phospholipase C ϵ (Oestreich *et al.*, 2007).

Both PKA and EPAC are known to be acceptors of cAMP and therefore provide precise and integrated controlling mechanism of cAMP signalling cascades. Intriguingly, EPAC has been reported to show contradictory outcomes with that of PKA-mediated signalling. The mechanism between PKA and EPAC has added more layers of complexity to cAMP regulation and raised further questions of whether the responses on cells are generated through the net effect of PKA and EPAC individually or all together. In another study, both EPAC and PKA antagonistically controlled insulin-stimulated PKB and cell proliferation (Omar *et al.*, 2009). In contrast, some authors have reported that EPAC and PKA could also have synergistic effects on downstream signalling of neurotensin secretion and attenuation of cAMP signalling

through phosphodiesterase (Li *et al.*, 2007; Cheng *et al.*, 2008). However, how these two cAMP acceptors elicit antagonistic effects requires further elucidation.

1.4.4.3 Cyclic nucleotide gated channels (CNGCs)

CNGCs are non-selective cation channels that specifically bind to cyclic nucleotides. These channels have been reported to play a pivotal role in the olfactory and visual systems, and are highly expressed in sensory neurons but can be found in other tissues such as heart, brain, testis, and kidney (Murray, 2008; Biel, 2013). In general, CNGC comprises two subtypes of channels, including cyclic nucleotide-gated (CNG) channels and the hyperpolarisation-activated cyclic nucleotide-gated (HCN) channels. Both channels are the six transmembrane superfamily and contain a CNB domain at the C-terminal. CNGC is heterotrimeric complex of subunits identified as A-type and B-type. There are four types of A subunits (further categorised as CNGA1-4), whereas the B subunits consist of CNGB1 and CNGB3 in mammals (Bradley *et al.*, 2001). To be activated, the CNGC requires binding of either cAMP or cGMP, which promotes ion gating. CNG channels are voltage-gated ion channels that share high homology with voltage-gated K⁺ channels (Flynn, Johnson and Zagotta, 2001). While CNG allows the transport of Na⁺/K⁺ and preferentially binds cGMP compared to cAMP (Podda, 2013), HCN channels open upon hyperpolarization with cAMP enhancing their activity by enabling activation at more positive voltages (Scicchitano *et al.*, 2012).

1.4.4.4 The popeye domain containing protein (POPDC) and cyclic nucleotide receptor involved in sperm function (CRIS)

The Popeye domain-containing proteins (POPDC) are a new member of cAMP effector family alongside PKA, EPAC, and CNCG. Although this protein was firstly identified decades ago, POPDC function remains poorly understood. POPDC is highly expressed in heart and skeletal muscle (Swan *et al.*, 2019) and contains conserved intracellular POPEYE domain that elicits high binding affinity to cAMP (Froese *et al.*, 2012; Brand and Schindler, 2017; Brand, 2018; Tibbo *et al.*, 2020). Brand and colleagues reported that POPDC1 acted as an anchoring protein, similar to AKAP, that together with PDE4 formed a macromolecule complexes regulating cAMP signalling (Brand and Schindler, 2017).

POPDC consists of 3 protein subtypes which include POPDC1, POPDC2 and POPDC3. It has two invariant sequence motifs (FL/ID~~S~~PEW/F) and (FQVT/SL/I) in the cAMP-binding pocket (Brand and Schindler, 2017). In general, it has a binding affinity

comparable to that of PKA (IC_{50} 120 nM vs 100nM, respectively) (Froese *et al.*, 2012). POPDC displays weaker binding affinity for cGMP with a reported IC_{50} of approximately 5 μ M obtained using a radioligand binding competition assay. This has also been corroborated using a FRET sensor (Froese *et al.*, 2012). The C-terminal domain of POPDC is subjected to different splicing and seems to be responsible for phosphorylation mediated by β 1-adrenoceptor (β 1-AR). The POPDC protein family all appear to be phosphorylated upon stimulation with adrenergic agonists. POPDC1 has nine phosphorylation sites, POPDC2 and POPDC3 contains four sites and single residue for phosphorylation, respectively (Lundby *et al.*, 2013).

Recent findings suggested an association of POPDC1 with cancer, where it acts as a tumour suppressor (Tucker and Zorn, 2021). Downregulation of POPDC1 or POPDC3 has been correlated with poor clinical prognosis in numerous cancers: gastric cancer, lung cancer, hepatocellular carcinoma, and colorectal cancer (Kim *et al.*, 2010; Williams *et al.*, 2011; Luo *et al.*, 2012; Han *et al.*, 2014). Although there are potential therapeutic benefits by targeting the POPDC protein family, the concurrence between low expression of POPDC and cancer requires further elucidations. To date, there are no inhibitors of POPDC that can be used as pharmacological tools to dissect their activities, thus the use of small interfering RNA technology may be the only approach to manipulate POPDC-mediated responses.

Finally, the cyclic nucleotide receptor involved in sperm function (CRIS) is another family protein that possesses a highly conserved CNB domain (Krähling *et al.*, 2013). CRIS has been identified in all published mammalian genomes. CRIS is highly expressed in spermatocytes and round spermatids playing a fundamental physiological function during spermatogenesis (Krähling *et al.*, 2013). To summarise the homeostasis of intracellular cAMP levels and its effectors, the illustration is depicted in Figure 1.9.

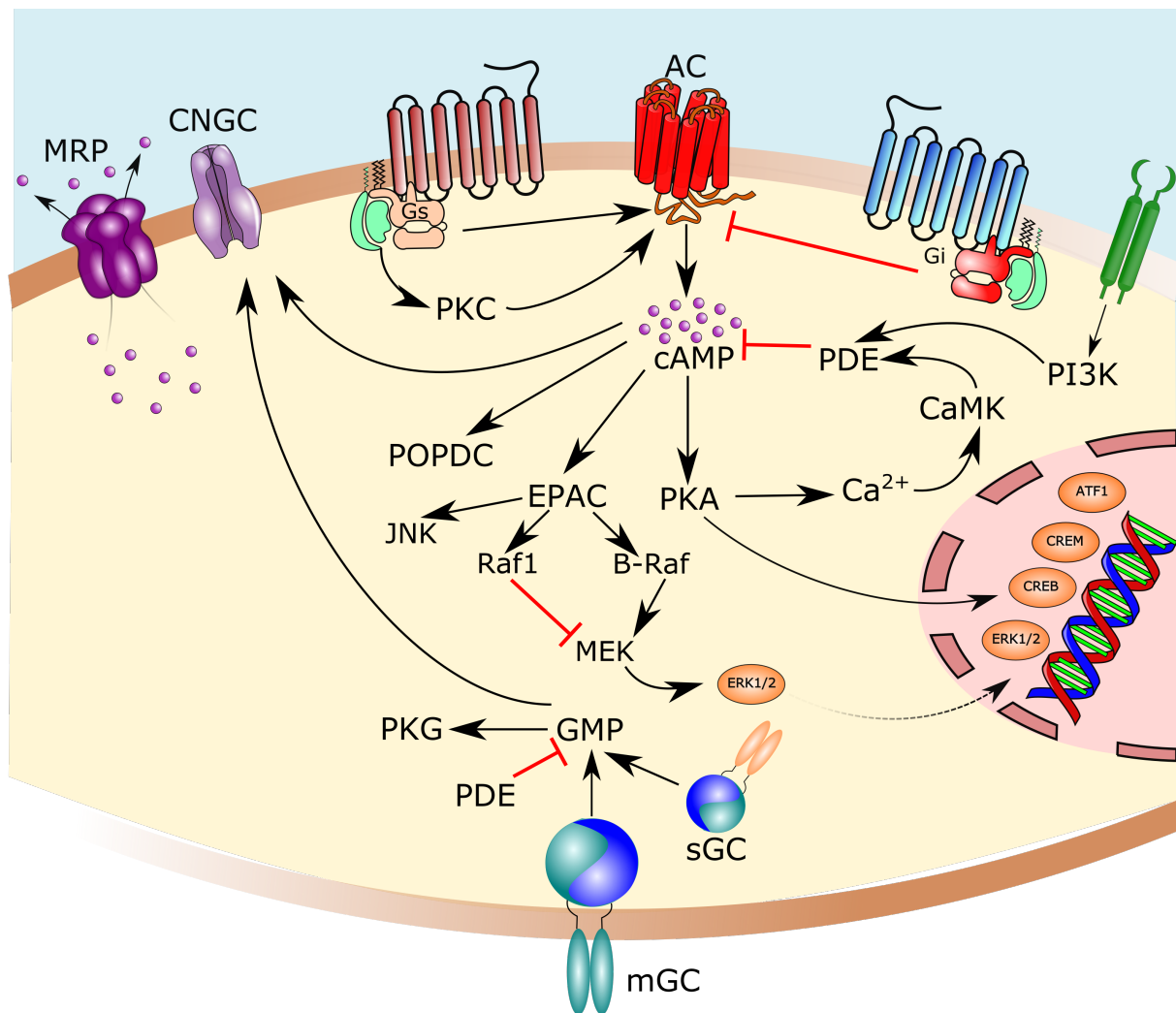


Figure 1.9 The summary of cyclic nucleotide signalling network. cAMP: cGMP, AC: adenylyl cyclase, PDE, CNGC: cyclic nucleotide gated channel, MRP: multidrug resistant protein, PKA: protein kinase A, PKC: protein kinase C, PKG: protein kinase G, EPAC: exchange protein directly activated by cAMP, POPDC: POPEYE-domain containing protein, MEK: , ERK: extracellular signal-regulated kinase, CREB: cAMP response element binding protein, CREM: cAMP response element modulator, ATF1: activating transcription factor-1, PI3K: phosphatidylinositol 3' kinase; JNK, c-Jun N-terminal kinases.

1.4.5 Interconnection with other second messenger pathways

1.4.5.1 cGMP signalling

cGMP is another second messenger that, together with cAMP, often works in balance to maintain cellular functions. cGMP is synthesised by two types of guanylyl cyclase (GCs): receptor GC (RGC) and soluble GC (sGC). sGC resembles AC in terms of its structure. Upon production, similar to that of cAMP, cGMP will bind to several effectors including protein kinase G (PKG), ion channels and Ras guanine nucleotide exchange factors (CNRasGEF), and HCNs, all of which contain CNB domains (Pham *et al.*,

2000). PKG was firstly characterised by (Kuo and Greengard, 1969) as the major effector of cGMP.

Elevated cGMP levels occur upon stimulation of sGC by nitric oxide (NO) and natriuretic peptides at RGCs (Takimoto, 2012). cGMP signalling appears to modulate specific functions in maintaining cardiac contractility and cardio-protection, transducing signals in olfactory and sensory neurons, and it has been associated with intestinal epithelial injury and neoplasia (Meyer *et al.*, 2000; Takimoto, 2012; Rappaport and Waldman, 2018). Although cAMP and cGMP play an essential role in cellular physiology, these cyclic nucleotides often exert opposing effects. In addition, the presence of dual-substrate PDEs serves the interconnection between cAMP and cGMP so adding more complexity to cAMP regulation.

1.4.5.2 Calcium (Ca²⁺) signalling

Ca²⁺ ions are a versatile small molecule that controls a myriad of physiological roles. Ca²⁺ has been demonstrated to control muscle contraction, NO production, fertilisation, cell growth, neurogenesis, synaptic plasticity, and secretion of saliva (Whitaker, 2006; Ambudkar, 2016; Berridge, 2016; Toth, Shum and Prakriya, 2016). While resting cells maintain Ca²⁺ gradients between intra- and extracellular space (~100 nM vs 1-2 mM range, respectively), high levels of cytoplasmic Ca²⁺ has been reported to trigger apoptosis (Rizzuto *et al.*, 2003; Clapham, 2007). Ca²⁺ is mainly generated after activation of GPCRs and RTKs, which in turn activate PLCβ1, hydrolysing PIP₂ in the plasma membrane to IP₃ and DAG (Berridge, 2012). ER-bound IP₃ receptors (IP₃Rs) recognises IP₃ molecules and acts as a Ca²⁺-channel, together with the ryanodine receptor (RYR), allowing Ca²⁺ release from the ER. The process is initially thought to be one-directional; however, in the past decade, it has been highlighted that control of Ca²⁺ is more complex and modulated through several regulatory proteins. These include the classical transient receptor potential channel (TRPC), store-operated Ca²⁺ entry (SOCE), and Ca²⁺ voltage-gated (CaV) ion channel (Clapham, 2007; Rahman, 2020).

Cytosolic Ca²⁺ interacts with many proteins, two of which are PKC and calmodulin (CaM) (Clapham, 2007). PKC is one of the Ca²⁺ sensors that, upon binding, will activate the Ras/Raf protein complex. This signalling cascade has been established to activate ERK1/2 through MEK1/2 phosphorylation. ERK1/2 has been implicated to be responsible for controlling cell cycle, cell proliferation and cell differentiation (Meloche and Pouysse´gur, 2007; Mebratu and Tesfaigzi, 2009).

Besides Ras, PKC can also directly activate transcription factor p50 and p65, which are fundamental in gene expression and intracellular signalling in the nucleus. In addition, CaM recognises the elevation of Ca^{2+} levels and further phosphorylates CREB through Ca^{2+} /calmodulin-dependent protein kinase type IV (CaMKIV). A summary of Ca^{2+} signalling is illustrated in Figure 1.10.

The concept of interconnection between second messengers, especially cAMP and Ca^{2+} signalling has been suggested, but the mechanisms require further characterisation. Willoughby highlighted the possibility of crosstalk through cAMP-mediated SOCE activation (Willoughby *et al.*, 2012). As an alternative, the interconnection between two pathways has been reported to occur through store-operated cAMP (SOcAMP) mechanism (Lefkimmiatis *et al.*, 2009; Maiellaro *et al.*, 2012). Whilst SOCE requires the changes in cytosolic Ca^{2+} to be activated, SOcAMP occurs independently of Ca^{2+} dynamics but acquires the stromal interaction molecule1 (STIM1) to be interconnected to cAMP signalling (Nichols *et al.*, 2015). In addition, the activity of PDE1 that is also regulated by calmodulin provides another aspect that is required to be considered when discussing for the crosstalk between Ca^{2+} and cAMP signalling.

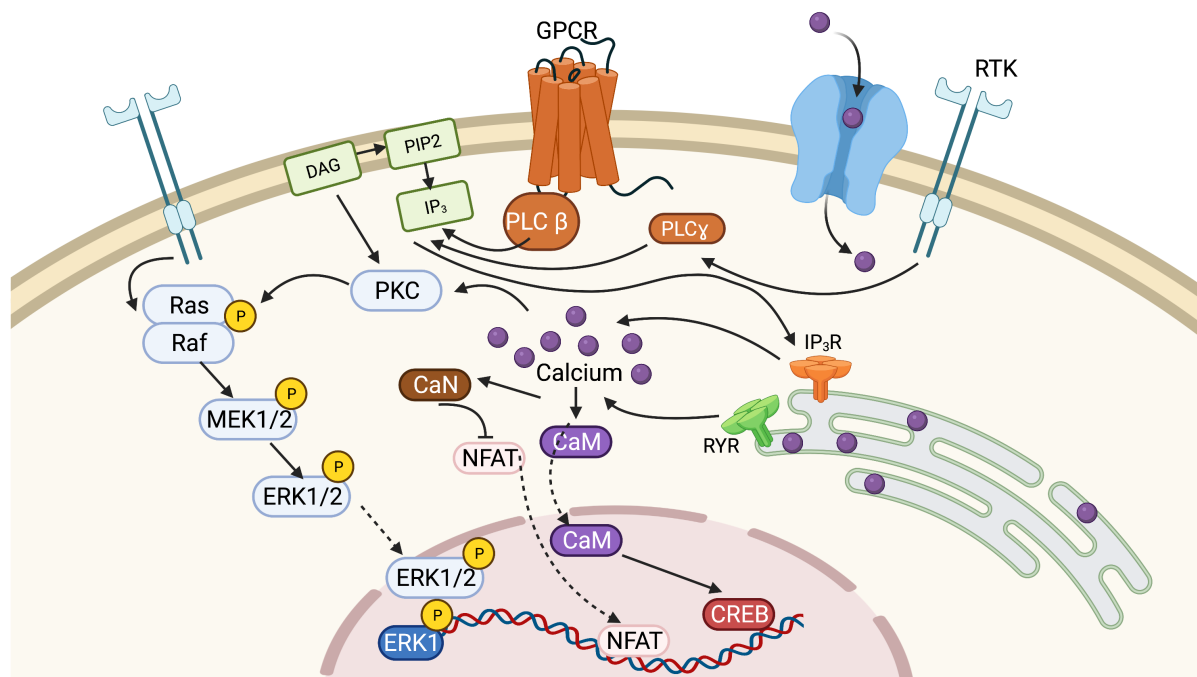


Figure 1.10. The summary of calcium signalling pathways. Ca^{2+} is generated through the activation of either GPCRs or RTKs, as well as regulatory transport within the cell mediated by IP_3R and RYR. Subsequently, calcium activates PKC or bind to

CaM to modulate further signalling cascades. GPCR, G protein-coupled receptor; RTK, receptor tyrosine kinase; PLC, phospholipase C; PKC, protein kinase C; PIP₂, phosphatidylinositol biphosphate; IP₃, inositol triphosphate; DAG, diacyl glycerol; MEK, mitogen activated protein; ERK, extracellular signal-regulated kinase; CaM, calmodulin; CaN, calcineurin; NFAT, Nuclear factor of activated T-cells; IP₃R, IP₃ receptor; RYR, ryanodine receptor. Picture was adapted from (<https://www.creative-diagnostics.com/calcium-signaling-pathway.htm>). The figure was created with BioRender.com.

1.5 Multimodal function of cAMP pathways

Depending on the cell type, cAMP may play a role in either promoting or suppressing cell proliferation. This incongruity can be explained by two theories related to the cAMP signalling cascade. The first theory proposes that elevation of intracellular cAMP is beneficial for suppressing cell proliferation in most mesenchymal and epithelial cell lines, such as glioblastoma (Kang *et al.*, 2014), thyroid cells (Sawa *et al.*, 2017), ovarian granulosa cells (Zwain and Amato, 2001), fibroblasts (Huston *et al.*, 2006), and primary cardiomyocytes (Ding *et al.*, 2005). In contrast, the second theory proposes that cAMP promotes cell survival, which has been observed in myeloid cells, pancreatic β -cells, hepatocytes, gastric and intestinal cells, spinal motor, superior cervical ganglion sympathetic, dorsal root ganglion, dopaminergic neurons, cerebral granule and septal cholinergic neurons (Lerner and Epstein, 2006). These two divergent roles of cAMP may be crucial in both physiological maintenance and pathological conditions, but whether these signalling cascades are interconnected remains unclear.

Since there were several reports highlighting the potential role of cAMP in inhibiting tumour progression, the work presented in this thesis focused efforts to elevate intracellular concentration of cAMP, mainly through PDE inhibition. Given that the production of cAMP is also regulated via G protein-dependent mechanisms, the study also explored upstream signalling at the receptor levels, that included β -ARs and A_{2A}R.

1.6 Glioma/glioblastoma and alteration on cAMP signalling

Glioblastoma is the most high-grade form of brain tumour in adults and originates from astrocytes. Glioblastoma belongs to a group of brain tumours known as glioma and is considered grade IV cancer by World Health Organisation (WHO) due to its invasiveness. Whilst glioblastoma only represents 15% of brain tumour cases, it shows high recurrence reaching 85% and 5-year survival rate less than 5%. Poorly

reproducible diagnoses and the resistance to chemotherapy regimens have contributed to insufficient outcomes of glioblastoma therapy (Lombardi and Assem, 2017).

Glioma, a type of brain tumour that is developed from glial cells, can be classified into several classes according to the type of glial cell it originates from: astrocytoma (originates from astrocytes), ependymoma (from ependymal cells), oligodendroglioma (from oligodendrocytes), and mixed type (normally a mixture of astrocytes and oligodendrocytes). Glioma can be graded from low to high and it may progressively lead to death if not treated early (Mamelak and Jacoby, 2007; Harris *et al.*, 2018). Meanwhile glioblastoma, the most common type of glioma, has been reported to be the deadliest, with a 5-year survival rate of only 5% (Schwartzbaum *et al.*, 2006; Delgado-López and Corrales-García, 2016).

Regardless of advanced diagnosis modality, current treatments do not improve progression-free survival and/or overall survival. Conventional radiotherapy alone or in combination with temozolomide – an alkylating agent- have been established as standard therapies for glioma, however, there is little progress made for this disease (Stupp *et al.*, 2017). Despite its ability to be able to penetrate into brain tissue, patients still experience many adverse effects from temozolomide treatment including fatigue, haematological and thromboembolic events, and increased rate of infection (HartMG, 2016). In addition, platinum-based treatments may increase the risk of cardiovascular incidents and hypersensitivity (Herradón *et al.*, 2017; Ruggiero *et al.*, 2017) leading to poor quality of life. All of these symptoms are correlated with the lack of selective properties of anti-neoplastic agents.

Current treatment modalities are limited to the surgery and radiotherapy with/without temozolomide chemotherapy. Another treatment that has shown promising results is the addition of tumour-treating fields (TTFields) to maintain temozolomide therapy. Concurrent application of TTFields with temozolomide significantly improves progression-free survival and overall survival (Stupp *et al.*, 2017). Despite advancement in innovation in both diagnosis and new therapies, it has been a challenge to successfully cure glioblastoma. Understanding more about targeting cellular signalling that is disrupted at the cellular levels would be beneficial for finding better therapies.

Many signalling pathways have been reported to be altered in association with glioblastoma pathogenesis. These include, those involved in oncogenic pathways, intra-tumour heterogeneity, and even transition from epithelial to mesenchymal

phenotypes. Oncogenic pathways involve activation/overexpression of RTKs or mutations on the receptor that causes increased in constitutive activity of RTKs, Ras pathway, retinoblastoma (pRB) pathway, the phosphatidylinositol-4,5-bisphosphate 3-kinase/phosphatase and tensin homolog/serine threonine kinase Akt (PI3K/PTEN/Akt) pathway, and cAMP signalling cascade.

Alteration in cyclic nucleotide signalling has been also reported to occur in glioma resulting in suppression of intracellular cAMP levels. Whilst normal brain tissue contained cAMP approximately 98.8 pmole/mg protein, the concentration of cAMP was suppressed up to 4-fold (Furman and Shulman, 1977). It is postulated that many regulatory proteins involved in cAMP regulation may become potential targets to reverse the abnormalities in cell growth.

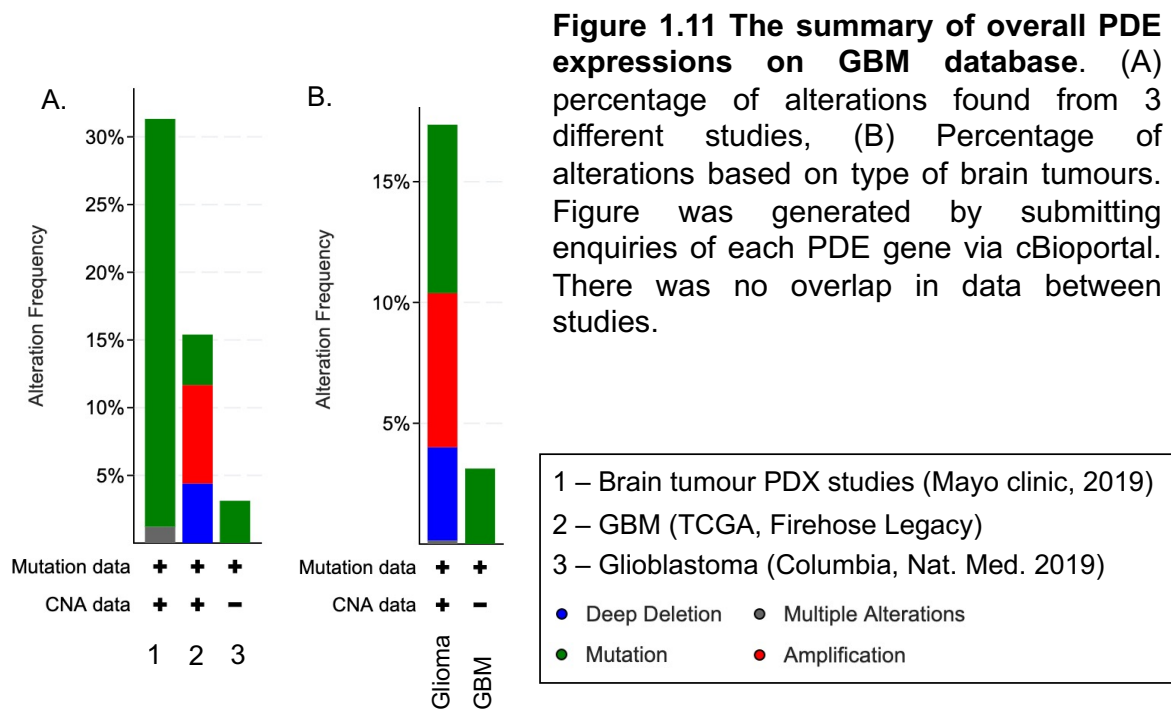
Abnormal expression of PDEs has been linked with malignancy (Savai et al., 2010), although the complete picture is made complicated by the crosstalk between cAMP and cGMP signalling systems. Relevance with the clinical settings, about 6% of samples collected, all PDE genes were upregulated in glioma patients (Figure 1.9). The recent discovery of a range of highly specific PDE inhibitors promises to clarify this situation (DeNinno, 2012), providing the tools to manipulate intracellular concentrations of the two cyclic nucleotides, particularly with cAMP. Moon and colleagues reported that applying PDE inhibitors, IBMX and rolipram, reduced the survival percentage of U87 glioblastoma cells (Moon *et al.*, 2012). It has been proposed that cell death on glioblastoma could be associated with PKA and EPAC1/Rap1-mediated pathways (Moon *et al.*, 2012), which is activated by cAMP.

The following data, that were composed from 731 samples collected from 724 patients with glioblastoma, have shown the cumulative percentage of alteration for all PDE isoforms (accessed from cBioportal). These studies were selected to be not overlapping with each other. In brain tumours patient-derived xenograft (PDX) studies, about 30% PDEs have been mutated, whereas 7.26% of PDEs have been reported to be amplified with 5.74% genes were found to be mutated in TCGA studies. About 3.13% PDEs gene were reported to be mutated found from Columbia studies (Figure 1.11)⁵. This suggested that proportion of altered PDE genes may contribute to the

5

http://www.cbioportal.org/results/cancerTypesSummary?Action=Submit&RPPA_SCORE_THRESHOLD=2.0&Z_SCORE_THRESHOLD=2.0&cancer_study_list=gbm_mayo_pdx_sarkaria_2019%2Cgbm_columbia_2019%2Cgbm_tcga_pan_can_atlas_2018&case_set_id=all&data_priority=0&gene_list=PDE1A%250APDE1B%250APDE1C%250APDE2A%250APDE3A%250APDE3B%250APDE4A%250APDE4B%250APDE4C%250APDE4D%250APDE5A%250APDE6A%250APDE6B%250APDE6C%250APDE6D%250APDE6G%250APDE6H%250APDE7A%250APDE7B%250APDE8A%250APDE8B%250APDE9A%250APDE10A%250APDE11A&geneset_list=%20&profileFilter=0&tab_index=tab_visualize (accessed in 30 July 2020)

pathogenesis of glioma/glioblastoma. Therefore, targeting PDEs may offer therapeutic benefits in cancer therapy.



Given that suppression of cAMP has been associated with malignancy, the work presented in this thesis focused on efforts to enhance the concentration of intracellular cAMP. It is postulated that elevation of cAMP level may restore cellular function to control cell growth. The study mainly focused on phosphodiesterase given that PDE genes were generally up-regulated the clinical settings that might contribute to the lower level of cAMP intracellularly. This work was not only limited to PDEs, but also some other investigation on proteins at downstream levels (Figure 1.12)

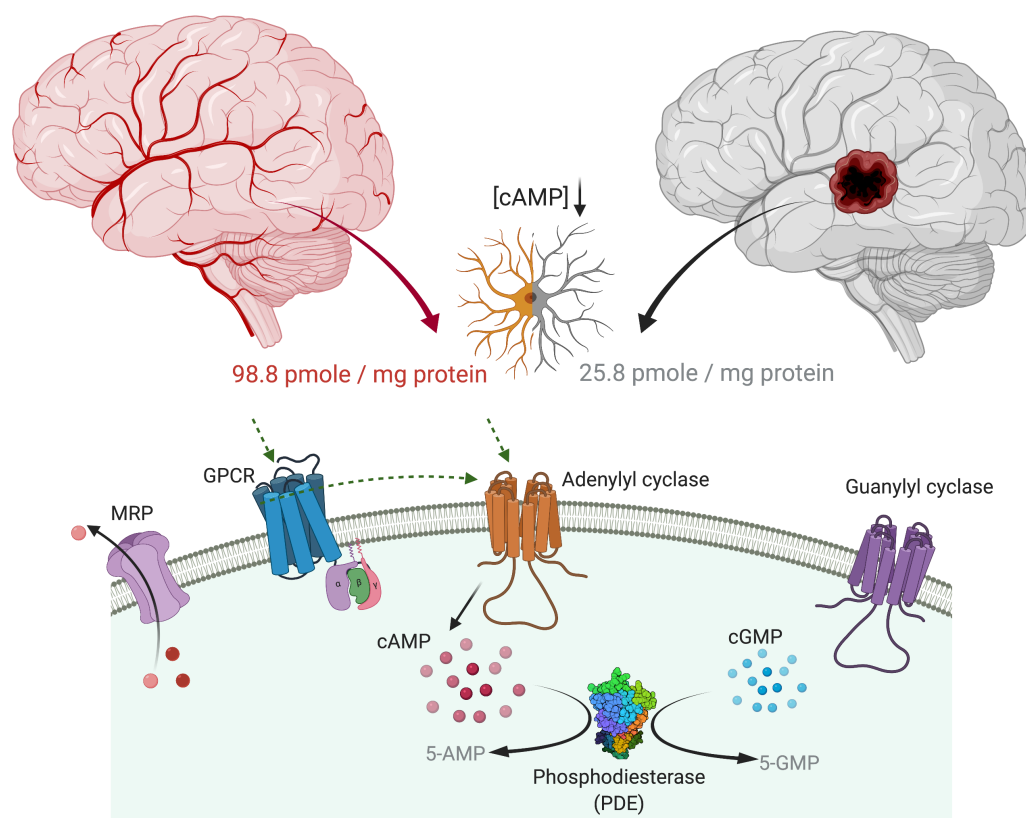


Figure 1.12. The illustration of the framework between glioma/glioblastoma and cellular network in regulating cAMP concentration. Since there may be an association between lower level of cAMP and malignancy, the main focus of this thesis would be to reinstate balance of cAMP through modulation on various proteins. These include the activation at AC, PDE inhibition, GPCR stimulations, and the blockade of MRP4 efflux transporter. The figure was created with BioRender.com

1.7 Aims

Given the possible therapeutic benefits of modulating cAMP pathways in cancer, the primary objective of this study was to investigate the potential of targeting crucial proteins involved in cAMP pathways, and its impact upon cell growth in numerous cancer models. The specific aims are as follows:

- Evaluate the potential of PDE inhibitors to modulate cell proliferation in a rat glioma cell model
- Dissect the mechanism of action of cAMP-mediated inhibition of cell proliferation in glioma cells.
- Investigate if concomitant targeting of PDE with other proteins, is a feasible approach to potentiate cell growth suppression. This particular point would be expanded to observe combinatorial effect of PDE and AC; and synergistic action of inhibiting PDE and agonising $A_{2A}R$ through multi-target ligand design.
- Determine the role of PDEs in human glioblastoma models

As a second section of this thesis, I also sought to explore the following aims related to RAMP interactions with GPCRs. The specific aims were:

- Investigate the role of RAMP and PAR4 as a novel interacting partners of RAMP and how this interaction influence PAR4 signalling, especially in affecting intracellular calcium mobilisation and β -arrestin
- Characterise the impact of CLR and RAMP interactions on cell growth in two different models: human glioblastoma cell lines and primary cardiovascular cells

CHAPTER 2

MATERIALS AND METHODS

2.1 Materials

2.1.1 General reagents

All reagents used in this study were analytical grade and unless specifically stated, were obtained from Sigma Aldrich (UK).

2.1.2 Compounds

The compounds used in this study was summarised in Table 2.1. Unless stated, the compounds used in this study were pro-analytic grade with >99% purity.

Table 2.1

List of chemical compounds and protein used for this study

| Compounds | Source | Stock concentration |
|--------------------------|---------------------------------|---------------------|
| Amb236403 | Ambinter, France | 10 mM in DMSO |
| Amb212236 | Ambinter, France | 10 mM in DMSO |
| Amb9792412 | Ambinter, France | 10 mM in DMSO |
| Amb4051701 | Ambinter, France | 10 mM in DMSO |
| Amrinone | Sigma-Aldrich, UK | 100 mM in DMSO |
| AYPGKF-NH ₂ | Cambridge Bioscience, UK | 10 mM in PBS |
| BAY 41-8543 | Tocris, UK | 100 mM in DMSO |
| BAY 73-6691 | Sigma-Aldrich, UK | 100 mM in DMSO |
| BC 11-38 | Tocris, UK | 100 mM in DMSO |
| Brequinar Na | Tocris, UK | 10 mM in DMSO |
| BRL-50481 | Sigma-Aldrich, UK | 100 mM in DMSO |
| Caffeine | Sigma-Aldrich, UK | 100 mM in DMSO |
| CA200645 | HelloBio, UK | 100 mM in DMSO |
| CE3F4 | Sigma-Aldrich, UK | 10 mM in DMSO |
| Cholera Toxin (CTX) | Sigma-Aldrich, UK | 35 µg/ml in water |
| Cilostamide | Sigma-Aldrich, UK | 10 mM in DMSO |
| Cisplatin | Cambridge Bioscience, UK | 3 mM in PBS |
| EHNA | Sigma-Aldrich, UK | 100 mM in DMSO |
| ESI-09 | Sigma-Aldrich, UK | 10 mM in DMSO |
| Forskolin | Sigma-Aldrich, UK | 100 mM DMSO |
| HJC0350 | Sigma-Aldrich, UK | 10 mM in DMSO |
| Hoechst 33342 | VWR International, UK | 17.79 mM in water |
| Human α -Thrombin | Thermo Fisher Scientific, UK | 0.2 mM in water |
| IBMX | Sigma-Aldrich, UK | 100 mM in DMSO |
| Ibudilast | Sigma-Aldrich, UK | 100 mM in DMSO |

| | | |
|----------------------------|---------------------------|----------------------------|
| Ionomycin | Cambridge Bioscience, UK | 100 mM in ethanol absolute |
| Isoprenaline hydrochloride | Sigma-Aldrich, UK | 10 mM in water |
| KT5720 | Insight Biotechnology, UK | 100 mM in DMSO |
| KT5823 | Insight Biotechnology, UK | 1 mM in DMSO |
| Milrinone | Sigma-Aldrich, UK | 100 mM in DMSO |
| MK571 | Tocris, UK | 50 mM in DMSO |
| Pertussis Toxin (PTX) | Sigma-Aldrich, UK | 100 µg/ml in water |
| PF 04671536 | Tocris, UK | 100 mM in DMSO |
| PF-04449613 | Sigma-Aldrich, UK | 100 mM in DMSO |
| PF-2545920 | Sigma-Aldrich, UK | 100 mM in DMSO |
| Piclamilast | Sigma-Aldrich, UK | 100 mM in DMSO |
| Propidium Iodide | Sigma Aldrich, UK | 1.5 mM in water |
| PU23 | Tocris, UK | 50 mM in DMSO |
| Pyr6 | SelleckChem, UK | 35 mM in DMSO |
| Roflumilast | Sigma-Aldrich, UK | 100 mM in DMSO |
| Rolipram | Sigma-Aldrich, UK | 100 mM in DMSO |
| Sildenafil | Sigma-Aldrich, UK | 100 mM in DMSO |
| Staurosporine | Tocris, UK | 100 mM in DMSO |
| SQ22536 | Sigma-Aldrich, UK | 100 mM in DMSO |
| Tadalafil | Sigma-Aldrich, UK | 100 mM in DMSO |
| Teriflunomide | Tocris, UK | 100 mM in DMSO |
| TC3.6 | Sigma-Aldrich, UK | 100 mM in DMSO |
| Trequinsin | Sigma-Aldrich, UK | 50 mM in DMSO |
| Trypsin | Sigma-Aldrich, UK | 0.2 mM in NaCl |
| Vinpocetine | Sigma-Aldrich, UK | 100 mM in DMSO |
| Vidoflunimus | SelleckChem, UK | 10 mM in DMSO |
| YC-1 | Tocris, UK | 100 mM in DMSO |
| Zaprinast | Sigma-Aldrich, UK | 100 mM in DMSO |
| ZM241354 | Tocris, UK | 10 mM in DMSO |

2.1.3 Growth media

Sterile LB (Luria-Bertani) medium, either as solution or agar plate, was used for *Escherischia coli* cultivation for cloning and plasmid DNA propagation.

The following media were used for mammalian cell culture including Gibco® Minimum Essential Medium (MEM, Thermo Fisher Scientific, UK), Gibco® Dulbecco's modified Eagle's Medium (DMEM)/F12 1:1 (1X) – Glutamax™ (Thermo Fisher Scientific, UK), MEM (Sigma, UK), Gibco® RPMI 1640 (Thermo Fisher Scientific, UK), and in Gibco® DMEM high glucose with Glutamax™ (Thermo Fisher Scientific, UK). Unless specified, growth media was supplemented with 10% v/v Foetal Bovine Serum (FBS, Sigma-Aldrich, UK), 1% v/v antibiotic/antimycotic (Sigma, UK). Growth media for each cell lines in this study was explained in detail in section 2.2.1.

2.1.4 DNA expression constructs

The plasmid and DNA expression constructs used in this study were obtained from sources listed in Table 2.2.

Table 2.2
Plasmid/construct used in this study

| Construct | Source |
|---|----------------------------------|
| pcDNA3.1-PAR4-T120 (PAR4 mutant variant having threonine residue at position 120) | Dr. Margaret Cunningham |
| pcDNA3.1-PAR4-A120 | Generated in this study |
| pcDNA3.1-PAR4-T120-Nluc | Generated in this study |
| pcDNA3.1-PAR4-A120-Nluc | Generated in this study |
| pcDNA3.1-FLAG-RAMP1 | (D Wootten <i>et al.</i> , 2013) |
| pcDNA3.1-FLAG-RAMP2 | (D Wootten <i>et al.</i> , 2013) |
| pcDNA3.1-FLAG-RAMP3 | (D Wootten <i>et al.</i> , 2013) |
| pcDNA3.1-HA-CLR | Harriet Watkins |
| pcDNA3.1-A _{2A} R | Prof. David Poyner |
| pcDNA3.1-Nluc-A _{2A} R | Dr. Steve Briddon |
| pEYFPN1 β -arrestin1 | Dr. Kathleen Caron |
| pEYFPN1 β -arrestin 2 | Dr. Kathleen Caron |
| GIPR-Nluc in pcDNA3.1 | Generated by Matthew Harris |
| pBK(A)mGRK5 | Dr. Kathleen Caron |
| pCDNA3.1(-)-Zeo | Invitrogen |
| MCS-Nluc in pcDNA3.1(-)-zeo | Modified by Abigail Pearce |

2.2 Methods

2.2.1 Cell lines

Procedures relating to cell culture were conducted using proper aseptic technique in a flow laminar tissue culture hood in accordance with safe laboratory practices and standard microbiological procedures. All solutions and equipment that come into contact with cells were sterile and growth medium was prewarmed in a water bath 37°C prior use. Unless otherwise stated, all cells were maintained in growth complete medium at 37°C in humidified 95% air and 5% CO₂.

C6 glioma cells (a gift from Prof. Colin Taylor, University of Cambridge) were cultured in Gibco® MEM (Thermo Fisher Scientific, UK) supplemented with 10% FBS, 2 mM L-glutamine (Sigma-Aldrich, UK), and 1% antibiotic/antimycotic.

Human embryonic kidney 293S (HEK-293S) cells were a gift from Astra Zeneca, HEK-293T and CV-1 in origin and carrying the SV40 genetic material (COS-7) cells were gifts from Prof. David Poyner. U87 glioblastoma cells were purchased from Sigma-Aldrich (UK). These cells were grown in Gibco® DMEM/F12 1:1 (1X) – Glutamax™ (Thermo Fisher Scientific, UK), supplemented with 10% FBS and 1% antibiotic/antimycotic.

T98 glioblastoma cells were purchased from American Type Culture Collection (ATCC) and were grown in MEM (Sigma, UK) containing 2 mM L-glutamine, 1 mM sodium pyruvate (Thermo Fisher Scientific, UK), 10% FBS, and 1% antibiotic/antimycotic.

LK2 and H1792 cells (LUAD, lung adenocarcinoma), and H520 and H1563 cells (LUSC, lung squamous carcinoma) were all provided by Dr. Walid Khaled (Department of Pharmacology, University of Cambridge, UK). All cells were grown in Gibco® RPMI 1640 supplemented by L-Glutamine, 10% FBS, and 1% antibiotic/antimycotic.

ST14A cells (rat-derived striatal cells (Tissue and Cell Biotechnologies, Italy) were grown in Gibco® DMEM/F12 1:1 (1X) – Glutamax™ (Thermo Fisher Scientific, UK), supplemented with 10% FBS and 1% antibiotic/antimycotic. ST14A cells were grown at 33°C in humidified 95% air and 5% CO₂ because propagation of ST14A cells at 37°C has been shown to induce differentiation into glial cells (Ehrlich *et al.*, 2001)

In general, cell lines were propagated in T25 or T75 flasks (Corning, UK) and were subcultured before they reached confluency. For harvesting or subculturing purposes, culture medium was discarded, and phosphate buffer saline (PBS) was added to wash the cells. Briefly, trypsin/ethylenediaminetetraacetic acid (EDTA) solution was used to detach monolayer cells for 1 to 3 minutes, meanwhile cell dissociation buffer was added when working with cell expressing PARs. Prewarmed complete medium was added to deactivate trypsin before collecting all cells and centrifuging at 1400 rpm for 4 minutes. Subsequently, supernatant was withdrawn, and the cell pellet was resuspended to the appropriate seeding concentration.

2.2.2 Long-term storage and recovery

Cells were grown to ~90% confluency in appropriate complete media in a culture vessel (T25 or T75 flask). Cells were detached using trypsin/EDTA or cell dissociation

buffer. All cells were harvested and centrifuged before resuspending cells in freezing medium and aliquoted into cryogenic storage vials. Freezing medium consisted of 90% of complete medium and 10% dimethyl sulfoxide DMSO (v/v). Cells were frozen gradually in an insulated box in -70 to -80°C freezer before transferring to liquid nitrogen storage or -140°C cryo-freezer.

To recover, cells from long-term storage were thawed as rapidly as possible by gently swirling the vial in 37°C water bath to minimize intracellular ice crystal growth during the warming process. The cell suspension was then diluted slowly after thawing process using prewarmed complete medium. Cell suspension was centrifuged at 1400 rpm for 4 minutes and subsequently, supernatant was decanted without disturbing the cell pellet. Cells were then resuspended in complete growth medium and transferred into appropriate culture vessel.

2.2.3 *E. coli* transformation

Competent *E. coli* DH5 α cells (Stratagene, San Diego, California, US) were used to amplify plasmids in this study. *E. coli* were propagated using standard methods as described (Glover, 1991).

Before use, competent cells were slowly defrosted on ice. Approximately 100 ng of plasmid was added into 100 μ l *E. coli* suspension and the mixture was incubated on ice for 5 minutes. Heat shock was performed at 42 °C for 1.5 to 2 minutes on water bath. The cell suspension was then returned to ice and further incubated for 5 minutes. Bacterial culture was propagated in LB media with constant shaking at 180 rpm or on LB agar plates containing either ampicillin (final concentration of 100 μ g/ml) or kanamycin (final concentration 50 μ g/ml), as appropriate, and incubated overnight at 37°C.

2.2.4 Plasmid DNA purification

Plasmid purification was performed using QIAprep Spin Miniprep Kit (Qiagen, UK) following the manufacturer's instruction. Overnight bacterial culture was centrifuged at 3200 rpm for 5 minutes to collect the cell pellet. Briefly, bacterial pellet was lysed under alkaline conditions using buffer P1, subsequently neutralized using buffer P2, and adjusted to high-salt binding solution using buffer N3. After high-speed centrifugation (13000 rpm for 10 minutes), the supernatant was then purified on QIAprep silica membrane (QIAprep minispin column), washed with ethanol-based buffer PE, and eluted in 30 μ l of warm water. Yield of purification was determined using NanoDrop™

Lite spectrophotometer (Thermo Scientific, UK). Samples that have yield value minimum of 100 ng/ μ l and $A_{260/280} > 1.8$ were used for further experiment.

2.2.5 RNA extraction, quality determination, and reverse transcriptase polymerase chain reaction (RT-PCR)

RNA was extracted from cells using RNAqueous®-4PCR Total RNA Isolation Kit (Life Technologies, UK) according to manufacturer's instructions. In order to remove any contaminating genomic DNA, all RNA samples were treated with DNase I included in the kit. The purity of RNA samples was quantified using a NanoDrop™ Lite spectrophotometer and only samples that had a minimum yield of 100 ng/ μ L and $A_{260/280} > 1.9$ were used in the experiments. Complementary DNA was synthesized using a QuantiTect reverse transcription kit (Qiagen, UK), as per the manufacturer's instructions.

The oligonucleotides (Sigma, UK) used for polymerase chain reaction (PCR) were designed specifically either for human or rat, which were listed in Table 2.3

Table 2.3

Oligonucleotides used to amplify gene of interests within this study

| Gene of interest | Sequence (5' → 3') | Amplicon size (bp) | Source or PrimerBank ID |
|-------------------|-----------------------------------|--------------------|---------------------------------|
| Rats | | | |
| GAPDH | Forward - TCCCTCAAGATTGTCAGCAA | 300 | (Lee <i>et al.</i> , 2009) |
| | Reverse - AGATCCACAACGGATACATT | | |
| A ₁ R | Forward: CTCCATTCTGGCTCTGCTCG | 207 | (Dixon <i>et al.</i> , 1996) |
| | Reverse: ACACTGCCGTTGGCTCTCC | | |
| A _{2A} R | Forward: CCATGCTGGGCTGGAACA | 150 | (Dixon <i>et al.</i> , 1996) |
| | Reverse: GAAGGGGCAGTAACACGAACG | | |
| A _{2B} R | Forward: TGGCGCTGGAGCTGGTTA | 160 | (Dixon <i>et al.</i> , 1996) |

| Gene of interest | Sequence (5' → 3') | Amplicon size (bp) | Source or PrimerBank ID |
|------------------|-------------------------------------|--------------------|--|
| A ₃ R | Reverse: GCAAAGGGGATGGCGAAG | 665 | (Dixon <i>et al.</i> , 1996) |
| | Forward: AGAAGCTAGGTCCACTGGC | | |
| PDE1A | Reverse: GCACATGACAACCAGGGGGATGA | 211 | (Giorgi <i>et al.</i> , 2002) |
| | Forward: CGCCTGAAAGGAATACTAAGA | | |
| PDE1B | Reverse: TAGAAGCCAACCAGTCCCGGA | 309 | (Giorgi <i>et al.</i> , 2002) |
| | Forward: CTGTCACCCCGCAGTCCTCCG | | |
| PDE1C | Reverse: GAAGGTGGAGGCCAGCCAGTC | 237 | (Giorgi <i>et al.</i> , 2002) |
| | Forward: CGCGGGCTGAGGAAATATAAG | | |
| PDE2A | Reverse: GAAGGTGGAGGCCAGCCAGTC | 86 | (Ellinghaus, Peter; Wilmen, Andreas; Hendrix, Martin; Tersteegen, 2006) |
| | Forward: CCAATCAGGGACCTCATATTCC | | |
| PDE3A | Reverse: GGTGTCCCACAAGTTCACCAT | 123 | (Tian <i>et al.</i> , 2011) |
| | Forward: CACAAGCCCAGAGTGAACC | | |
| PDE3B | Reverse: TGGAGGCAAACCTTCTTCTCAG | 103 | (Tian <i>et al.</i> , 2011) |
| | Forward: GTCGTTGCCTTGTATTTCTCG | | |
| | Reverse: | | |

| Gene of interest | Sequence (5' → 3') | Amplicon size (bp) | Source or PrimerBank ID |
|------------------|---|--------------------|-------------------------------|
| PDE4A | AACTCCATTTCCACCTCCAGA | 73 | (Tian <i>et al.</i> , 2011) |
| | Forward: CGACAAGCACACAGCCTCT | | |
| PDE 4B | Reverse: CTCCCACAATGGATGAACAAT | 787 | (Kostic <i>et al.</i> , 1997) |
| | Forward: CAGCTCATGACCCAGATAAGTGG | | |
| PDE 4C | Reverse: GTCTGCACA(AG)TGTACCATGTT GCG | 582 | (Kostic <i>et al.</i> , 1997) |
| | Forward: ATGGCCCAGATCACTGGGCTGCGG | | |
| PDE 4D | Reverse: GCTGAGGTTCTGGAAGATGTCGCAG | 262 | (Kostic <i>et al.</i> , 1997) |
| | Forward: CCCTCTTGACTGTTATCATGCACACC | | |
| PDE 5A | Reverse: GATCCTACATCATGTATTGCACTGGC | 193 | (Kostic <i>et al.</i> , 1997) |
| | Forward: CCCTGGCCTATTCAACAACGG | | |
| PDE 7A | Reverse: ACGTGGGTCAGGGCCTCATA | 85 | (Tian <i>et al.</i> , 2011) |
| | Forward: GAAGAGGTTCCCACCCGTA | | |
| PDE 7B | Reverse: CTGATGTTTCTGGCGGAGA | 99 | (Tian <i>et al.</i> , 2011) |
| | Forward: GGCTCCTTGCTCATTTGC | | |
| PDE 8A | Reverse: GGAACTCATTCTGTCTGTTGATG | 97 | (Tian <i>et al.</i> , 2011) |
| | Forward: TGGCAGCAATAAGGTTGAGA | | |
| | Reverse: | | |

| Gene of interest | Sequence (5' → 3') | Amplicon size (bp) | Source or PrimerBank ID |
|-------------------|------------------------------------|--------------------|---|
| PDE 8B | CGAATGTTTCCTCCTGTCTTT | 147 | (Tian <i>et al.</i> , 2011) |
| | Forward: CTCGGTCCTTCCTCTTCTCC | | |
| PDE 9A | Reverse: AACTTCCCCGTGTTCTATTTGA | 107 | (Tian <i>et al.</i> , 2011) |
| | Forward: GTGGGTGGACTGTTTACTGGA | | |
| PDE 10A | Reverse: TCGCTTTGGTCACTTTGTCTC | 115 | (Tian <i>et al.</i> , 2011) |
| | Forward: GACTTGATTGGCATCCTTGAA | | |
| PDE 11A | Reverse: CCTGGTGTATTGCTACGGAAG | 87 | (Tian <i>et al.</i> , 2011) |
| | Forward: CCCAGGCGATAAATAAGGTTTC | | |
| Human | Reverse: TGCCACAGAATGGAAGATACA | 87 | (McCurdy, McGrath and Mackay-Sim, 2008) |
| | Forward: TGCACCACCAACTGCTTAGC | | |
| A ₁ R | Reverse: GGCATGGACTGTGGTCATGAG | 128 | 115305570c1 |
| | Forward: CCACAGACCTACTTCCACACC | | |
| A _{2A} R | Reverse: TACCGGAGAGGGATCTTGACC | 109 | 156142194c1 |
| | Forward: CGCTCCGGTACAATGGCTT | | |
| A _{2B} R | Reverse: TTGTTCCAACCTAGCATGGGA | 147 | 22907046c1 |

| Gene of interest | Sequence (5' → 3') | Amplicon size (bp) | Source or PrimerBank ID | |
|------------------|------------------------------------|-------------------------------------|-------------------------|-------------|
| A ₃ R | TGCACTGACTTCTACGGCTG | | | |
| | Reverse: GGTCCCCGTGACCAA ACTT | | | |
| | Forward: GGCCAATGTTACCTACATCACC | 140 | 4501953a1 | |
| | Reverse: CCAGGGCTAGAGAGACAATGAA | | | |
| PDE1A | Forward: ATGGGGTCTAGTGCCACAGAG | 187 | 51102298c1 | |
| | Reverse: GCACAGATGCCGCATATTCAAT | | | |
| | PDE1B | Forward: CTGCGCTACATGGTGAAGCA | 123 | 260436978c1 |
| | | Reverse: CAAGATTTGCCGTGTCTCATCTA | | |
| PDE1C | | Forward: GATGTGGACAAGTGGTCCTTTG | 123 | 300796870c1 |
| | | Reverse: GGGGATCTTGAAACGGCTGA | | |
| | PDE2A | Forward: GAAAGTCCGGGAGGCTATCAT | 121 | 344925850c1 |
| | | Reverse: CACTTGGGTATCAGGAGCCA | | |
| PDE3A | | Forward: CTGCACCAGTACGGAGAGAC | 213 | 347658968c3 |
| | | Reverse: AGGGCGATGAAAGAGGTGAAA | | |
| | PDE3B | Forward: ATTCAGGAGACCGTCGTTGC | 154 | 219879808c2 |
| | | Reverse: TGACACCATATTGCGAGCCTC | | |
| PDE4A | | Forward: GAACGAGAAAAACAGCAAGCG | 150 | 341572546c2 |

| Gene of interest | Sequence (5' → 3') | Amplicon size (bp) | Source or PrimerBank ID |
|------------------|-------------------------------------|--------------------|-------------------------|
| PDE4B | Reverse: CCCAAATCGGGGAATGTTAGAGT | 110 | 82799485c1 |
| | Forward: AACGCTGGAGGAATTAGACTGG | | |
| PDE4C | Reverse: GCTCCCGGTTTCAGCATTCT | 243 | 341604763c1 |
| | Forward: CAAGGCCATGTCTCGGAACTC | | |
| PDE4D | Reverse: AGCTCGTCTAGCGTCTCCAA | 187 | 308387383c1 |
| | Forward: GACCAATGTCTCAGATCAGTGG | | |
| PDE5A | Reverse: GTCAAGGGCCGGTTACCAG | 239 | 61744429c2 |
| | Forward: CGGCCTCTTAGACCCATTGTT | | |
| PDE6A | Reverse: AGGGAATAGCGGTCAGCAGAT | 111 | 170650673c1 |
| | Forward: CCTGCGGGACTTTCAGGAG | | |
| PDE6B | Reverse: GTCCGGTACATGAACAGGCTC | 111 | 223718033c1 |
| | Forward: GACGTGTGGTCTGTGCTGAT | | |
| PDE6C | Reverse: CTTGCCGTGGAGGATGTAGTC | 187 | 157364938c2 |
| | Forward: ATGGACAAGCAAACCTGGGTATG | | |
| PDE6D | Reverse: TGGTGTGATGAAGCCTTAGGAT | 134 | 56676309c3 |
| | Forward: TTCAAAGGGCAATGCCTAGAAG | | |
| | Reverse: | | |

| Gene of interest | Sequence (5' → 3') | Amplicon size (bp) | Source or PrimerBank ID |
|------------------|-------------------------------------|--------------------|---------------------------------|
| PDE6G | TTCCCAGTTAAGACGCTTGCT | 250 | (Nikolova <i>et al.</i> , 2010) |
| | Forward: TTTAAGCAGCGACAGACCAG | | |
| PDE6H | Reverse: ATATTGGGCCAGCTCGTG | 90 | 291045288c1 |
| | Forward: GCAGACTCGCCAATTCAAGAG | | |
| PDE7A | Reverse: TCTGTTCCCTAGCCCCTCCATT | 201 | 341823662c1 |
| | Forward: CGTATGCTAGGAGATGTACGTGT | | |
| PDE7B | Reverse: TGAAACCGCAGTACCACGAAA | 120 | 57242789c3 |
| | Forward: TTGACTTCCGCCTACTTAACAGT | | |
| PDE8A | Reverse: TAATTCCACGAAGCAGCCTTG | 116 | 341823697c2 |
| | Forward: TCCAGCCAGAGACGACACT | | |
| PDE8B | Reverse: ACAGGCATGGGACTACTTTCC | 177 | 300244576c3 |
| | Forward: ACGCAGGCTTCAACAGGAG | | |
| PDE9A | Reverse: CGTGGTCATCGCTTGTTATTTCT | 222 | 48762733c1 |
| | Forward: GACTCCTCGACGCGATGTTC | | |
| PDE 10A | Reverse: TTTCTGTAGTTGTCGTGGACG | 240 | 359465520c1 |
| | Forward: GGACCTTCTAATAATGCGAGCTG | | |
| | Reverse: TCCCTGCATATTCGTATCTTGGT | | |

| Gene of interest | Sequence (5' → 3') | Amplicon size (bp) | Source or PrimerBank ID |
|------------------|--|--------------------|-------------------------|
| PDE 11A | Forward: TGATGACTTTTCTCTCGACGTTG Reverse: AAGCCACCTACACAGTGTCTC | 115 | 116536086c1 |

PCR amplification was performed using standard *Taq* polymerase (New England Biolab, UK) protocol as summarised in the Table 2.4.

Table 2.4
Thermocycler set up used for amplification

| Step | Temperature | Time |
|-------------------------|-------------|--------|
| Denaturation | 95°C | 5 min |
| Amplification–36 cycles | 95°C | 30 s |
| | 60°C | 60 s |
| | 72°C | 60 s |
| Final extension | 72°C | 10 min |
| Final step | 4°C | ∞ |

All PCR products were run on a 2% agarose gel. The gel was visualised in the presence of ethidium bromide and imaged using a G Box iChemi gel documentation system. Density of each band was analysed with GeneTools analysis software (Syngene, UK).

2.2.6 Mutagenesis of PAR4-A120

PAR4T120 in pcDNA3.1 served as a template for the point-mutation to switch the threonine to alanine residue at position 120. Single point mutagenesis was performed using QuikChange Lightning Site-Directed Mutagenesis Kit in accordance with the manufacturer's instruction. Table 2.5 and 2.6 display the oligonucleotides and the components used, respectively, for generating PAR4-A120 variant. Oligonucleotides for mutagenesis were designed using the online QuikChange Primer Design programme (<https://www.agilent.com/store/primerDesignProgram.jsp>).

Table 2.5

Oligonucleotides that were designed to generate PAR4 variant that express alanine at position 120

| Oligonucleotides | Sequence (5' → 3') |
|------------------|--|
| Forward | ³⁴⁴ TGATGAACCTCGCG(G)CTGCTGACCTCCTG ³⁷² |
| Reverse | ³⁷² CAGGAGGTCAGCAG(C)CGCGAGGTTTCATCA ³⁴⁴ |

The start and end nucleotide positions within PAR4 sequence that bind with oligonucleotide are indicated by superscript. Whereas points mutations are indicated by sequence in bracket.

Table 2.6

Summary of component reaction for mutagenesis

| Component | Volume |
|----------------------------------|--------------|
| 10x reaction buffer | 5 µl |
| DNA template (plasmid/construct) | 100 ng |
| Forward oligonucleotides (10 mM) | 1 µl |
| Reverse oligonucleotides (10 mM) | 1 µl |
| dNTP mix (10 mM) | 1 µl |
| QuikSolution reagent | 1.5 µl |
| ddH ₂ O | Add to 50 µl |
| QuikChange Lightning Enzyme | 1 µl |

Successful mutagenesis was determined by Sanger sequencing (Department of Biochemistry, University of Cambridge, UK).

2.2.7 Cloning of Nanoluciferase (NLuc)-tagged PAR4

PAR4 A120 and T120 variants served as the template for generating C-terminally Nano luciferase (NLuc) tagged receptors. Oligonucleotides were designed to introduce 5' and 3' *Xba*I and *Eco*RI restriction sites, respectively to the template. DNA fragments were ligated into MCS-NLuc in pcDNA3.1(-)-zeo plasmid.

Briefly, PAR4 templates were amplified by PCR using oligonucleotides that have been designed (Table 2.7). PCR was performed using Phusion DNA polymerase, as summarised in the Table 2.8, and thermocycler set up in Table 2.9.

Table 2.7

Oligonucleotides that were designed to introduce restriction sites on PAR4 constructs

| Oligonucleotide | Restriction enzyme | Sequence (5' → 3') |
|-----------------|--------------------|--|
| Forward | <i>Xba</i> I | GGGGT [↓] CTAGA ATG TGGGGGGGC ACTGC |
| Reverse | <i>Eco</i> RI | GGGGG [↓] AATTCCTGGAGCAAAG AGGAGTGGG |

Start codon was indicated by bold letter (ATG). Stop codon was omitted to be able put the construct in pcDNA3.1-Nluc construct

Table 2.8

List of components used for PCR amplification

| Component | 50 µl reaction | Final Concentration |
|-------------------------------|----------------|---------------------|
| Nuclease-free water | 30 µl | 1X |
| 5x Phusion HF buffer | 10 µl | 200 µM |
| 10 mM dNTPs | 1 µl | 0.5 µM |
| 10 µM forward oligonucleotide | 2.5 µl | 0.5 µM |
| 10 µM reverse oligonucleotide | 2.5 µl | < 250 ng |
| DNA template (1pg-10 ng) | 1 µl | |
| DMSO | 2.5 µl | 3% |
| Phusion DNA polymerase | 0.5 µl | 1.0 units/50 µl PCR |

Table 2.9

Thermocycler set up for molecular cloning

| Step | Temperature | Time |
|---------------------------|----------------|-------------|
| Denaturation | 98°C | 30 s |
| Amplification – 30 cycles | 98°C | 30 s |
| | 40°C/50°C/60°C | 30 s |
| | 72°C | 30 s per kb |
| | 72°C | 10 minutes |
| Final step | 4°C | ∞ |

The elongation cycle parameters were performed for 45 s for the insert PAR4 of 1158 kb. PCR amplicons were run on a 2% agarose gel for > 45 minutes at 120V. Appropriate bands were cut and extracted using QIAquick gel extraction kit (Qiagen, UK). The yield value of the samples was determined using a NanoDrop™ Lite spectrophotometer. Approximately 1µg of each vector and insert fragments were digested with *XbaI* and *EcoRI*. The mixture was incubated at 37°C for 1 hour. Afterwards, samples were electrophoresed on a 2% agarose gel for 45 minutes at 120V before correct band size was extracted.

DNA fragments were inserted into plasmid vector with 1:3 ratio (NEBioCalculator™) and ligated by T4 DNA ligase. The ligation mixture was incubated for at least 1 hour at room temperature. As a control, vector alone was used to verify that the vector was completely digested. The resulting recombinant plasmids were then transformed into competent *E. coli* on antibiotic selective LB agar plates.

Approximately 3 colonies from each plate showing bacterial growth were isolated and suspended in 10 µl sterile water. The cells were lysed by pipetting up and down and samples were amplified using for PCR (components were described in table 2.9) to verify the colonies contained an insert of the correct size.

The amplified fragment (using the set up described in Table 2.10 and the PCR set up in Table 2.4) was then run on a 2% agarose gel at 120V for about 30 minutes or until well separated. If a band of correct size was visualised, the remaining cell suspension was used for bacterial transformation. To determine if the sequence was correct, the purified plasmid was sent for Sanger sequencing.

Table 2.10
Component for PCR colonies

| Component | 10 µl Reaction |
|--------------------------------|-----------------------|
| Nuclease-free water | 7.5 µl |
| 10x Taq buffer | 1 µl |
| 10 mM dNTPs | 0.2 µl |
| 100 µM forward oligonucleotide | 0.1 µl |
| 100 µM reverse oligonucleotide | 0.1 µl |
| DNA template (1pg-10 ng) | 1 µl |
| Taq DNA polymerase | 0.1 µl |

2.2.8 Transient transfection of HEK-293S/ HEK-293T cells

Transient transfection of HEK-293S or HEK-293T cells, as appropriate, was performed 48 hours before assaying using either FuGENE®HD (Promega, UK) or polyethylenimine (PEI, with MW 25kDa, Polyscience Inc, UK). PEI was prepared into a stock of 1 mg/ml following the manufacturer's instruction. Approximately 100 mg of PEI was dissolved at 90 ml of water (to a concentration of 1.11 mg/ml) and pH of solution was adjusted to reach pH 2.0 by adding 12 M hydrochloric acid (HCl). The solution was mixed continuously for approximately 3 hours until the solution became clear prior to the addition of 10 M sodium hydroxide until reaching pH 7.0. PEI solution was then aliquoted in microcentrifuge tubes and stored at -20 °C. Detailed methods are as following.

2.2.8.1 Fugene method

Cells were grown 24 hours before transfection to reach ~60-70% confluency. DNA and FuGENE®HD were mixed in serum free DMEM/F12 at a 1:3 w/v ratio (Table 2.11) and incubated for 10 minutes before addition to cells:

Table 2.11
Components used for FuGENE®HD transfection method

| Format | Component | Volume (in µl) or amount (in µg) |
|---------------|------------------|---|
| 24 well plate | DNA | 0.25 µg |
| | FuGENE® HD | 0.75 µl |
| | Serum free media | Add to 25 µl |

2.2.8.2 PEI method 1

PEI is a stable cationic polymer that condenses DNA and generates a positive charge around the particle. DNA-PEI complexes are then endocytosed by cells. Unless described, transient transfection of HEK-293T or HEK-293-S cells in this study using PEI was performed using this method. The protocol outlined in this study uses a 1:6 of DNA to PEI (w/v) as described on table 2.12. DNA and PEI was diluted separately in NaCl 150 mM solution and incubated for 5 minutes at room temperature. Afterwards, PEI mixture was added into DNA solution, gently mixed by pipetting up and down, then were incubated for further 10 minutes. The overnight culture medium was replenished with fresh complete medium before adding DNA-PEI complexes slowly to the cells.

Table 2.12

Components used for PEI transfection method in several different formats

| Format | Mixture 1 | | Mixture 2 | |
|---------------|------------------|-------------------|------------------|-------------------|
| 96-well plate | DNA | 100 ng | PEI | 0.6 μ l |
| | NaCl 150 mM | Add to 4 μ l | NaCl 150 mM | Add to 4 μ l |
| 24-well plate | DNA | 250 ng | PEI | 1.5 μ l |
| | NaCl 150 mM | Add to 40 μ l | NaCl 150 mM | Add to 40 μ l |
| 6-well plate | DNA | 2 μ g | PEI | 12 μ l |
| | NaCl 150 mM | Add to 80 μ l | NaCl 150 mM | Add to 80 μ l |

2.2.8.3 PEI method 2

This method was utilized for transfection on COS-7 applying ratio of DNA to PEI 1:3 (w/v). The following format was used to describe PEI transfection protocol for each well in 24 well-plate. DNA and PEI solution were mixed into un-supplemented growth medium as described (in table 2.12 or 2.13) for 15 minutes at room temperature. The DNA-PEI solution was then added to the cells dropwise.

Table 2.13

Component used for transfection using PEI in 24 well plate

| Format | Component | Volume (in μl) or amount (in μg) |
|---------------|------------------|---|
| 24-well plate | DNA 1 | 0.25 μ g |
| | DNA 2 | 0.25 μ g |
| | PEI | 1.5 μ l |
| | Serum free media | Add to 25 μ l |

2.2.9 cAMP accumulation assay

Cells were grown to confluency in appropriate growth medium. Cells were then trypsinised for 1 minute, re-suspended in stimulation buffer (PBS with 0.1% bovine serum albumin (BSA)) and plated onto 384-well optiplates (Perkin Elmer, UK) at a density of 2000 cells/well (for C6 and ST14A cells) or 1500 cells/well (for U87 and HEK-293S cells). To determine the efficacy of individual PDE inhibitors, cells were co-stimulated, immediately after seeding, with three different concentrations of compounds (which spanned 100-fold either side of the individual IC_{50} value *in vitro*) and pEC_{20} values of forskolin (1.6 μ M for C6 cells, 50 nM for ST14A cells, 0.15 μ M for U87 cells, 0.2 μ M for T98 cells and 0.35 μ M for HEK-293S cells) for 30 minutes.

Stimulating cells with the pEC₂₀ of forskolin, enables a larger range to observe any effect of the PDE inhibitors on cAMP production.

To generate full dose response curves, compounds were added to cells in the range of 0.1 pM – 100 μM for 30 minutes. Detection of cAMP was assessed using LANCE cAMP detection kit (Perkin Elmer, UK) and end-point measurement was performed using a Mithras LB940 microplate reader (Berthold Technologies, Germany). The detection was applied based on time-resolved fluorescence resonance energy transfer (TR-FRET), using europium-streptavidin/biotin-cAMP to detect free cAMP from the cells. The principle of the assay is illustrated in Figure 2.1.

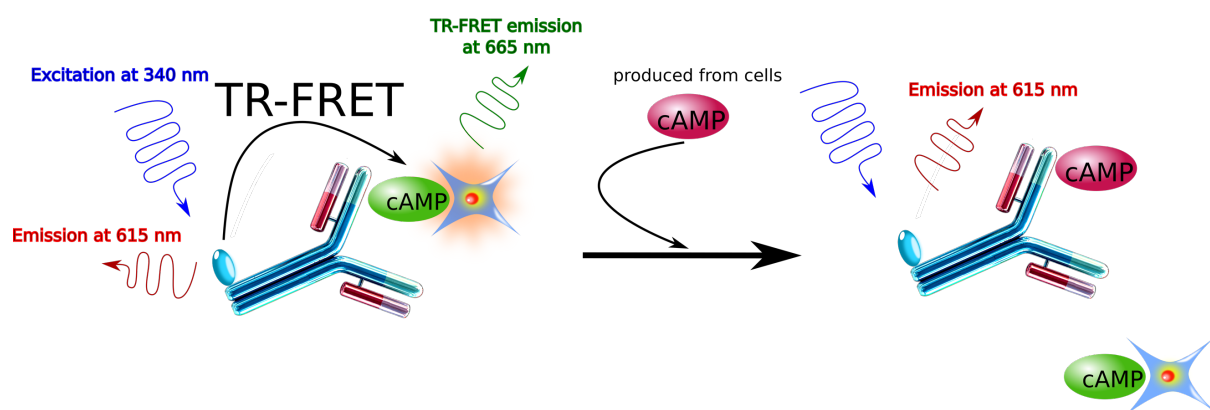


Figure 2.1 Principle of LANCE® cAMP assay kit. The assay is homogenous time-resolved fluorescence energy transfer (TR-FRET) immunoassay which is based on the competition between cAMP tracer complex (europium-labelled cAMP) with cAMP generated by the cells. Biotin-bound cAMP will form a tight complex with europium-streptavidin. If the tracer complex binds to AlexaFluor®647 conjugated-anti cAMP antibody, energy from the dye is transmitted to cAMP tracer resulting in emission at 665 nm. This binding will be replaced in the presence of produced cAMP from the cells, thereby reducing the FRET ratio.

To determine the role of individual of G proteins subtypes on cAMP production, C6 cells were grown in complete MEM medium in the presence of either pertussis toxin (PTx) or cholera toxin (CTx) for 16 hours (as a pre-treatment). Subsequently, cells were dissociated using trypsin for 1 minute after which, complete medium was added to inactivate trypsin. Cells were washed, resuspended in PBS containing 0.1% BSA, and plated onto 384-well optiplates at a density of 8000 cells/well. Total accumulation of cAMP was determined using the same protocol as described above. Data were either normalised to the maximal level of cAMP accumulation from cells in response to 100 μM forskolin stimulation or were interpolated to the cAMP standard curve and expressed as the concentration cAMP per 10⁶ cells.

2.2.10 Quantification of intracellular and extracellular cAMP concentrations

C6 cells were trypsinised and resuspended in PBS containing 0.1% BSA. 150,000 cells were then treated with various concentrations of PU23, a multidrug resistance protein-4 (MRP4) inhibitor (10 μ M, 3.16 μ M, and 1 μ M, diluted in PBS containing 0.1% BSA) for 30 minutes. After treatment, cells were washed with PBS containing 0.1% BSA and stimulated with the pEC₅₀ concentration of forskolin (3.16 μ M), trequinsin (4.7 μ M) or the PDE inhibitor cocktail (26 μ M) for 1 or 2 hours, in the presence or absence of each concentration of MRP inhibitors. After stimulation, cells were centrifuged at 5000 rpm for 4 minutes to separate supernatant and cell pellet. LANCE cAMP detection kit was used to determine extracellular cAMP levels (supernatant) and intracellular cAMP levels (cell pellet). The concentration of cAMP was determined by interpolating the TR-FRET values to the cAMP standard curve.

2.2.11 cGMP accumulation assay

Confluent C6 cells were trypsinised and resuspended in PBS containing 0.1% BSA. Cells were plated onto a 384-well plate at a density of 500,000 cells/well and immediately stimulated with compounds for 30 minutes. After stimulation, 5 μ l of cGMP-labelled with d2 reagent (d2-cGMP) analogue and 5 μ l of anti-cGMP antibody conjugated with europium cryptate (mAb-cryptate) were added to each well and incubated for 1 hour at room temperature as per the manufacturer's instruction (Cisbio, France). The principle of the assay is illustrated in Figure 2.2. The d2-cGMP fluorophore was excited at a wavelength of 337 nm and emission was detected at 665 nm and 620 nm. Fluorescence was measured using a Mithras LB940 microplate reader. Delta F% values were calculated using the 665 nm/620 nm ratio and all data were interpolated to a standard curve which covered a range cGMP concentration between 0.5 to 500 nM.

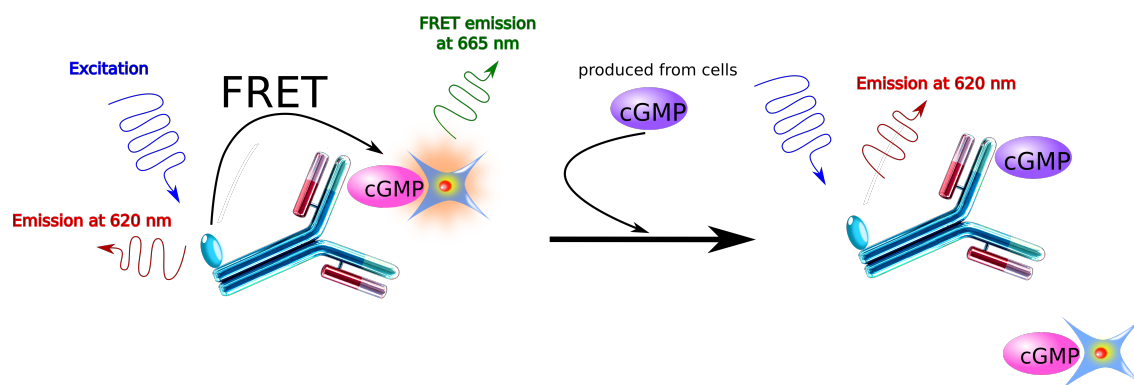


Figure 2.2 Principle of Cisbio Bioassays' cGMP assay kit. The assay is homogenous time-resolved fluorescence energy transfer (HT-FRET) immunoassay based on the competition between cGMP acceptor complex (d2-cGMP) with cGMP generated by the cells. If the tracer complex binds to anti-cGMP conjugated with europium cryptate antibody (as donor), energy from the dye is transmitted to cGMP acceptor resulting in emission at 665 nm. This binding will be replaced in the presence of produced cGMP from the cells, thereby reducing the FRET fluorescence intensity.

2.2.12 Quantifying the extent of cell proliferation

To determine compounds effect on cell growth, CCK-8 kit (cell counting kit-8) was utilised. The assay is based on the ability of alive cells to convert WST salt which is exist in the kit to WST-8 formazan dye. The amount of WST-8 formazan formed is directly proportional to the number of viable cells and can be detected by measuring the absorbance at 450 nm (Figure 2.3). Cell proliferation was calculated as a percentage of number of cells treated with vehicle alone.

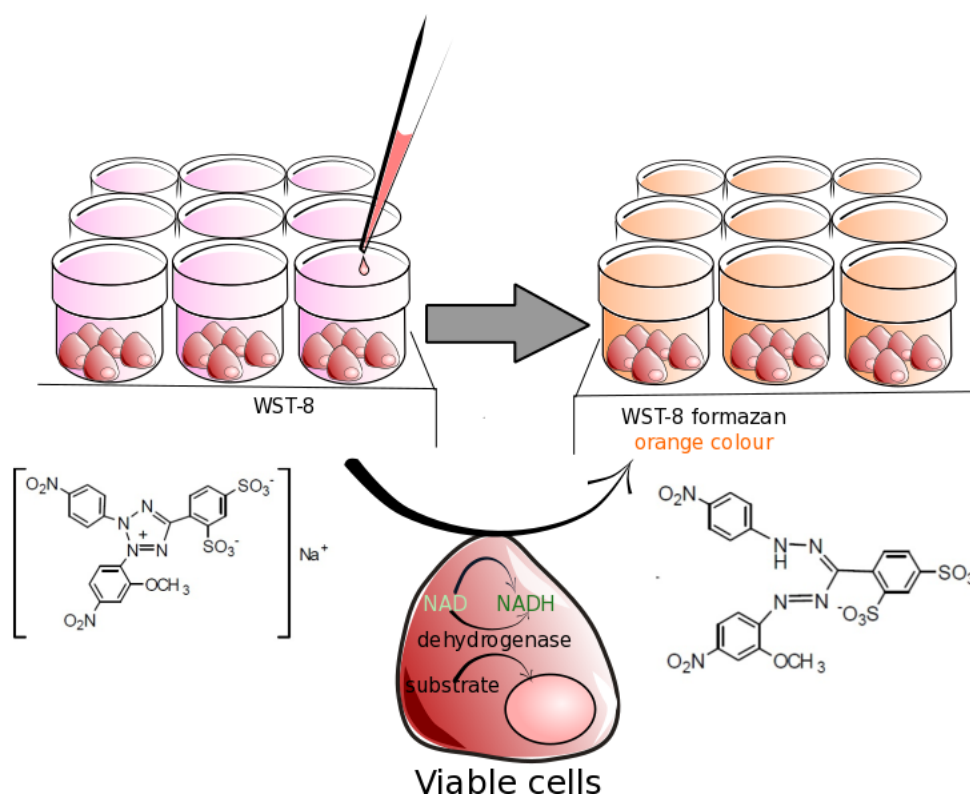


Figure 2.3 Principle of CCK-8 (cell counting kit-8) assay. Cell proliferation assay using CCK-8 is based on colorimetric method allowing determination of cell viability. WST-8, tetrazolium salt as the main component in CCK-8 kit, will be reduced by the activity of dehydrogenase in viable cells generating WST-8, which is soluble in tissue culture medium. The amount of formazan WST-8 dye is proportional to the number of viable cells and can be detected by measuring the absorbance at 450 nm.

All cells in this study were seeded at a density of 2,500 cells/well in a clear flat bottom 96-well plate (Corning). After 24 hours, cells were exposed to test compounds or vehicle, in appropriate growth medium supplemented with serum, and were incubated for 72 hours. The optimum conditions for this assay were determined and displayed in Figure 2.4 and 2.5. Initial optimisation was initially performed in U87 cells and similar conditions were further applied to a range of cell lines for validation (Figure 2.6).

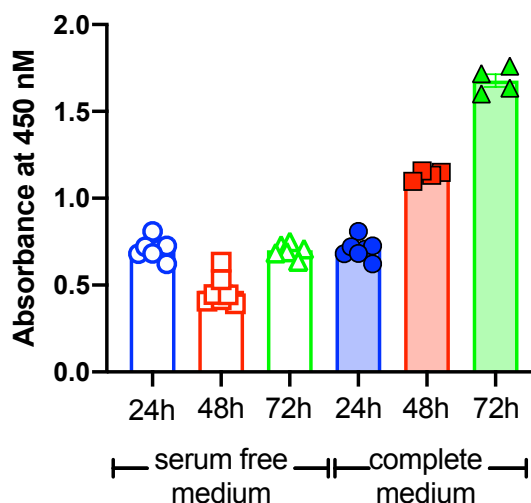


Figure 2.4 The effect of un-supplemented and complete growth media upon U87 cell growth. Proliferation of U87 cells after incubation in serum free media (open symbols) or complete growth medium (closed symbols) after 24, 48 or 72 hours. Cells were initially seeded at the same cell density of 10,000 cells/well. Data are expressed as the raw absorbance values measured at 450 nm, with intensity proportional to the number of cells/proliferating cells. Data are the mean \pm SEM of 4-6 individual repeats.

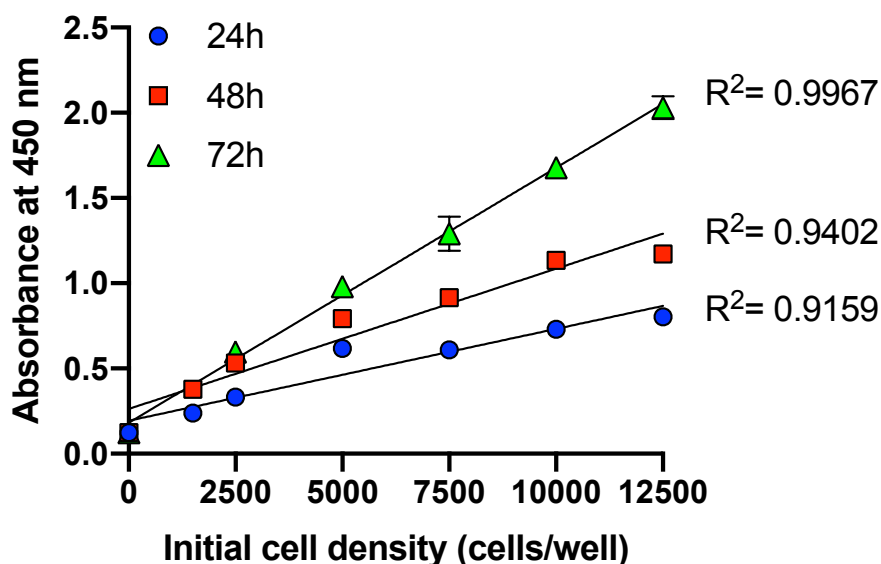


Figure 2.5 Influence of cell density and treatment period on U87 cell growth. Proliferation of U87 cells seeded at varying cell densities up to 12500 cells per well after 24-, 48- or 72-hour incubation in complete growth medium. Data are expressed as the raw absorbance values measured at 450 nm, with intensity proportional to the number of cells/proliferating cells. Simple linear regression was utilized to fit the curve and the goodness-of-fit was displayed as R^2 value. Data are the mean \pm SEM of 4-5 individual data

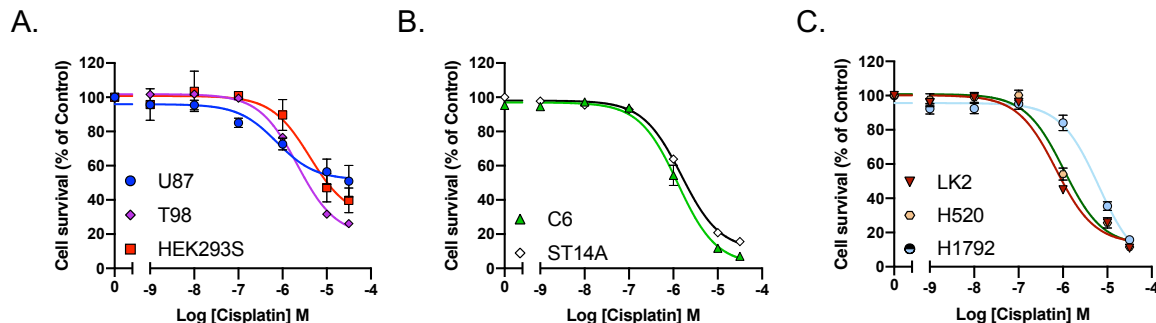


Figure 2.6 Cell proliferation assay in several of cell lines. Selected conditions that were determined on U87 cells were applicable for other cell lines. Cells were initially seeded at the density of 2500 cells/well and treated by cisplatin for 72 hours. Cisplatin, as a cytotoxic reference compound, displayed anti-proliferative effect in a dose-dependent manner in all cell lines: (A) U87, T98, and HEK293S; C6 and ST14A (B); LK2, H520, and H1792 (C) cells. Data are expressed as percentage of cell survival compared to vehicle-treated group (PBS 1%) in complete media. Data were fitted into non-linear regression of 6-14 individual data.

To further investigate whether downstream pathways of cAMP influenced cell proliferation, cells were cotreated with selective inhibitors that target cAMP/cGMP sensors including PKA, PKG, and Epac1/2. Cells were seeded as previously described and treated with either forskolin or trequinsin in the presence of the following inhibitors:

KT5720 to inhibit PKA, KT5823 to inhibit PKG, ESI-09 as non-selective Epac1/2 inhibitor, CE3F4 as a selective Epac1 inhibitor, and HJC0350 as a selective Epac2 inhibitor. In order to investigate the effect of blockade of cAMP export on cell proliferation, cells were treated with forskolin, trequinsin or PDE inhibitor cocktail in the presence, or absence, of various concentrations of PU23 (10 μ M, 3.16 μ M, and 1 μ M). After 72 hours incubation, 5 μ L of Cell Counting Kit – 8 (CCK-8, Sigma, UK) was added to each well and the cells were incubated for an additional 2-3 hours at 37°C in the dark. The absorbance of each well was measured using a Mithras LB940 microplate reader with an excitation of 450 nm.

2.2.13 Quantifying Caspase-3/-7 activity

C6 cells were seeded into clear bottom black 96-well plates (Corning) and treated with forskolin (1-100 μ M), trequinsin (1-100 μ M) or staurosporine (1 μ M, a pan caspase activator) in complete MEM media. 1% DMSO was used as vehicle control. Cells were exposed to test compounds for 72 hours, plates were treated with 2 μ M of the CellEvent™Caspase-3/7 green detection reagent (Life Technologies, UK) for 60 minutes at 37°C in the dark. Caspase activity was detected by cleavage of the tetrapeptide substrate DEVD (aspartic acid-glutamic acid-valine-aspartic acid), which is conjugated to a nucleic acid binding dye (illustrated in Figure 2.7). Intracellular caspase-3/7 activities were imaged using a BD Pathway 855 Bioimager (BD Biosciences, USA). To normalise the number of cells with caspase activated, cells were also labelled with Hoechst 33342 (Cambridge Bioscience, UK). Activated caspase-3/7 cleaves substrate and produce green fluorescence which was visualised using FITC/Alexa Fluor™ 488 filter setting. To determine the total number of cells Hoechst 33342 was added and measured on the was measured on the BD Pathway 855 using 350 nm excitation and 461 nm emission filters. The cell number was quantified automatically using Fiji (Schindelin *et al.*, 2012) by applying classic watershed plugin on the captured image.

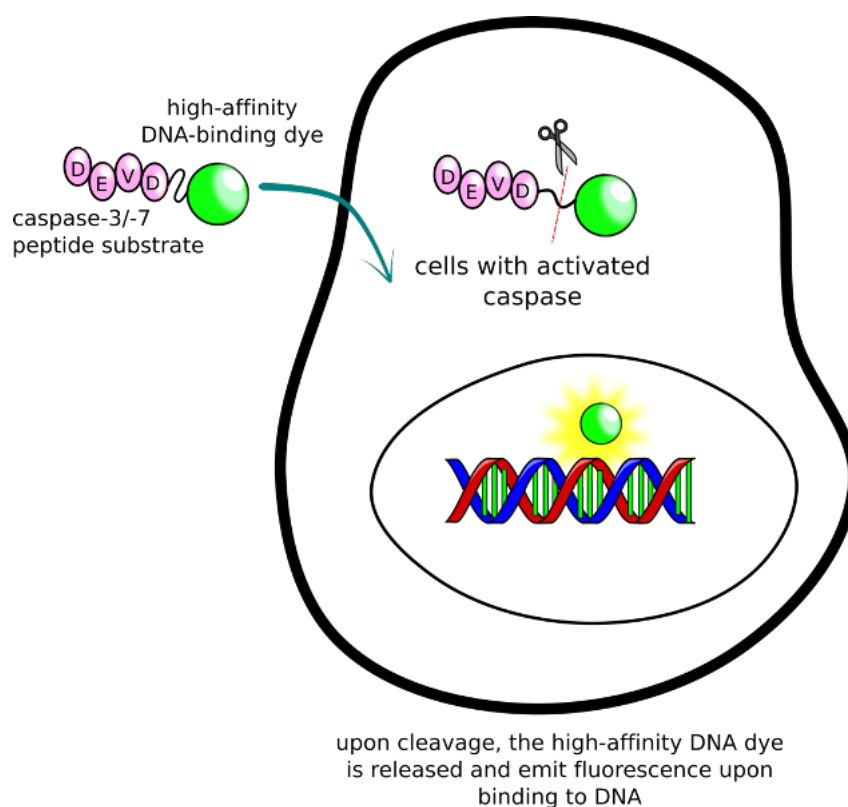


Figure 2.7 Principle of CellEvent™ Caspase-3/7 assay kit. The kit consists of 4 amino acid (DEVD) conjugated to a high-affinity nucleic acid binding dye. DEVD conjugated dye is non-fluorescent intrinsically. Cell with activated caspase-3/7 such as in apoptotic cells, will cleave DEVD peptide releasing DNA-binding dye and allowing dye to bind DNA. Upon binding with DNA, the dye will emit fluorescence light (~530 nm) that can be detected using appropriate filter.

2.2.14 Cell cycle analysis

Cell cycle analysis using fluorescence-activated cell sorting (FACS) provides information on the distribution of cells in interphase stages of the cell cycle (G_0/G_1 , S, and G_2/M). C6 cells were seeded in 24-well plates and cultured for 24 hours. Cells were exposed to selected treatments including forskolin, trequinsin, and a combination of individual PDE2,3,7 inhibitor for 72 hours. Subsequently, cells were harvested and resuspended in PBS containing 0.1% Triton X-100, 10 $\mu\text{g/ml}$ RNase A, and 5 $\mu\text{g/ml}$ propidium iodide (PI) before incubation at 37°C for 15 minutes. Samples were analysed using a BD Accuri C6 flow cytometer (BD Biosciences) and cell cycle analysis was performed using BD C6 software.

The samples will be plotted in a graph with forward scatter area (FCS-A) and side scatter area (SSC-A) as the axes. For analysis, gating on the single cell population to exclude debris and aggregates, as depicted in Figure 2.8A. The single cells have been gated and by combining with signal recorded from FL2-A (from channel 2),

histogram plot was shown (Figure 2.8B) for further analysis. Area M1, M2, and M3 (Figure 2.8B) represent each of cell cycle of G₀/G₁, S, and G₂/M phase, respectively.

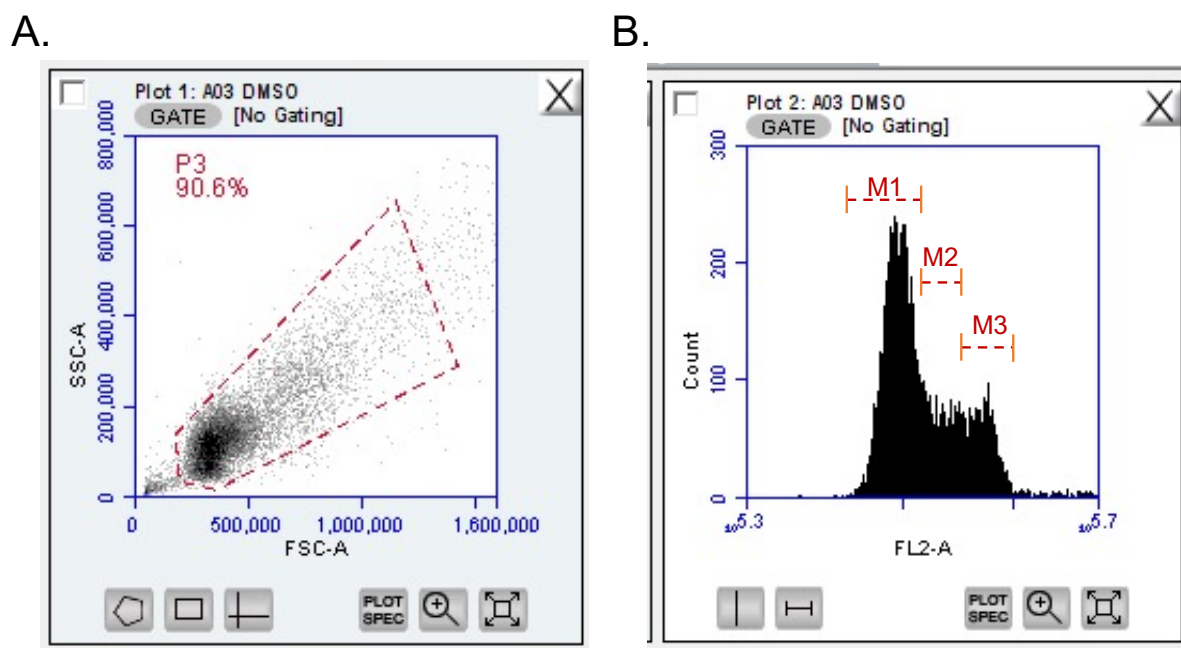


Figure 2.8. Representative figures of cytogram for cell cycle analysis. (A) Gating the alived cells and exclude debris or doublets. (B) Representative histogram of cell treated with vehicle control (DMSO 1%) from channel 2 (FL2-A). This filter channel records signal from propidium iodide. Each phase of cell cycle was counted based on M1 area (G₀/G₁ phase), M2 (S), and M3 (G₂/M).

2.2.15 Quantification of ligand affinity through BRET-based ligand binding assay

10⁶ cells/well of HEK293T cells were seeded into 6 well-plate for 24 h in DMEM/F12 medium supplemented with 10% FBS and 1% antibiotic/antimycotic at 37°C. Cells were then transfected with 1.5 µg Nluc-A_{2A}R construct (a gift from Dr. Stephen Briddon, and Professor Steven Hill, University of Nottingham, UK) per well using PEI method, with the ratio of DNA:PEI was 1:6 in 150 mM NaCl, as described in the method section. After 24h, cells were harvested and re-seeded into PLL-coated white 96-well plates (Greiner, UK) at a density of 50,000 cells/well. Cells were then cultured overnight. On the day of the assay, culture medium was replaced by 80 µl BRET buffer (PBS supplemented with 0.9 mM CaCl₂, 0.5 mM MgCl₂, and 1% BSA (w/v)). The assay was initiated by adding 10 µl of furimazine (Promega, UK) to a final concentration of 0.4 µM, diluted in BRET buffer. Furimazine is a substrate of Nanoluciferase (NLuc) and the principle of the assay is depicted in Figure 2.9. The plate was incubated at room temperature in the dark for 5 minutes.

In association-dissociation kinetic experiments, 40 nM of CA200645 was added following incubation with furimazine. After 19 minutes of association, CGS21680 was

injected to a final concentration of 10 μM to displace all bound CA200645. For competition association assays, following furimazine incubation, 300 nM CA200645 was added simultaneously in the presence of unlabelled “cold” ligand in a range of 10 pM to 100 μM . BRET signal was recorded for 50 minutes (for kinetic experiments) or 20 minutes (for competition assays), on a Mithras LB940 to allow signal from CA200645 and Nluc. The BRET ratio refers to the ratio of the emission from CA200645 using long pass filter (640-685 nm) over the Nluc fluorescence at 460 nm. ΔBRET ligand-induced was used to generate both association-dissociation kinetics and competition binding curves of unlabelled “cold” ligand. To generate dose-response relationship, the BRET ratio was subtracted by the signal from vehicle only group.

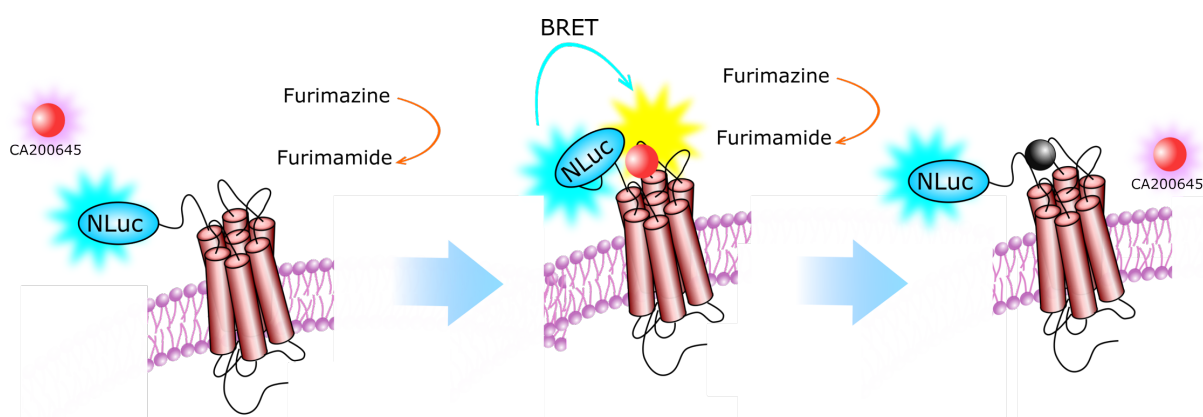


Figure 2.9 Principle of BRET-based ligand binding assay. The $A_{2A}R$ N-terminally tagged Nluc and a probe CA200645 (red circle) – an adenosine receptor antagonist, were utilised to quantify ligand binding at the $A_{2A}R$. BRET relies on the transfer of energy between a bioluminescent donor (Nluc) and a fluorescent ligand, CA200645, where the proximity between these substances is within $\sim 10\text{nm}$. Before the binding of fluorescent probe to the Nluc- $A_{2A}R$, there is no BRET signal detected. The binding of the probe to the Nluc- $A_{2A}R$ leads to production of BRET signal – representing the association phase. The presence of unlabelled “cold” ligand (black circle) displaces bound CA200645 which lead to the dissociation phase where the BRET signal is diminished.

2.2.16 Quantification of RAMP cell surface expression using FACS

COS-7 cells were seeded in 24-well plates and cultured for 24h in complete growth medium. For initial screening, FACS analysis were performed in COS-7 expressing different GPCRs (PAR4A120, or PAR4T120) and FLAG tagged RAMP at the same ratio of 1:1 (section 2.2.8, Table 2.13). FLAG is polypeptide protein tag served as epitope in recombinant technology that consist of 8 amino acids: DYKDDDDK.

Cells were grown for further 48 hours before being harvested using cell dissociation buffer. Subsequently, cells were washed once with PBS followed by 3

washes in FACS buffer (PBS with 1% BSA and 0.03% sodium azide) and resuspended in 50 μ l FACS buffer containing allophycocyanin (APC)-conjugated anti-FLAG antibody (BioLegend 1:80 dilution). Cells were incubated in the dark at room temperature on rotating mixer for 1h. Before being analysed, cells were washed twice in FACS buffer and resuspended in 50 μ l FACS buffer. Samples were analysed using a BD Accuri C6 flow cytometer. The percentage of events with an increased APC intensity was normalised to that of vector as 0% and HA-CLR RAMP2 co-expressed cells as 100%. APC antibody is cell-impermeable thus the signals that were recorded come from the antibody attached to cell surface.

2.2.17 Quantification of intracellular calcium signaling

HEK-293T cells were seeded in a 6-well plate at a density of 10^6 cells/well. 24 hours later, cells were transiently transfected with PAR4 (A120 or T120) and co-expressed with RAMP/vector with the ratio of 1:1 (PAR4:RAMP) using PEI (section 2.2.8, table 2.12). After a further 24 hours, cells were harvested and seeded onto poly-L-lysine (PLL) coated black, clear bottomed, 96-well plates, at a density of 10^5 cells/well, and were grown overnight. On the day of the assay, cells were washed with calcium containing Hank's Balance Salt Solution (HBSS) and incubated with 10 μ M Fluo-4 AM Direct™ calcium assay kits (Invitrogen), for 1 hour in the dark at room temperature. Fluo-4 AM is an indicator that exhibits increase in fluorescence upon binding to Ca^{2+} . Fluo-4 bound calcium will emit green fluorescence light that can be detected using appropriate filter in flow cytometer or microscope. Afterwards, cells were washed twice using HBSS containing calcium to remove residual dye. A dilution series of ligands including α -thrombin, trypsin, AYPGKF-NH₂ (PAR4 selective agonist peptide) were injected robotically using a BD Pathway 855 Bioimaging Systems. The excitation wavelength of the Ca^{2+} -bound fluo-4 was at 494 nm and emission wavelength at 516 nm. The intensity of fluorescence was determined immediately after injection of ligands and responses were recorded every second for 80 s. After correcting for background fluorescence using Fiji (Is Just) Image J, peak intensity was measured for generating dose-response curves. The results were normalized to the maximum intensity produced by 10 μ M ionomycin.

2.2.18 Quantification of ligand-mediated β -arrestin recruitment through bioluminescent resonance energy transfer (BRET)-based assay

HEK-293T cells were seeded in 6-well plates at density of 10^6 cells/well and grown overnight. Cells were transfected with the following components: PAR4T/A120-NLuc (0.167 μ g); RAMP (0.167 μ g); β -arrestin1-YFP (yellow fluorescent protein) or β -arrestin-2-YFP (0.83 μ g) and vector (6.67 μ g). The ratio of DNA:PEI used for this transfection was 1:6 in 150 mM NaCl. Cells that were transfected with Gastric Inhibitory Polypeptide Receptor (GIPR), β -arrestin-2-YFP, and G protein-coupled receptor kinase 5 (GRK5) were used as positive control. The amount of DNA for each transfection was maintained. Cells were grown overnight, harvested and seeded at a density of 10^5 cells/well into PLL-coated white 96-well plates (Greiner, UK) in MEM serum-reduced media (supplemented with 2% FBS (v/v), 1% antibiotic/antimycotic, 2mM L-glutamine) and cultured for a further 24h.

On the day of the assay, culture medium was discarded and replaced by 80 μ l BRET buffer which consist of PBS supplemented with CaCl_2 , MgCl_2 , and 1% BSA (w/v). For PAR4-Nluc expressed cells, the assay was started by adding 10 μ l of furimazine (Promega, UK) (diluted in PBS supplemented with CaCl_2 , MgCl_2 , and 1% BSA (w/v) to a final concentration of 4 μ M) and the plate was incubated in the dark at room temperature for 5 minutes before adding 10 μ l of ligand (AYPGKF-NH₂). The principle of the assay is illustrated in Figure 2.10.

Thrombin and trypsin were used as the non-selective ligand for PAR1 and PAR2, respectively, TFLLR-NH₂ as selective PAR1 agonist, and SLIGKV-NH₂ as selective PAR2 agonist. BRET signal was recorded for 20 minutes on a Mithras LB940 plate reader allowing sequential integration of signal detected from YFP and Nluc or Rluc, as appropriate. The BRET ratio corresponds to the ratio of light emission from acceptor (YFP, 530nm) over donor (Nluc 460 nm or Rluc 485 nm). Ligand-induced Δ BRET was used to construct the concentration response curve at 13 minutes time point for AYPGKF-NH₂,

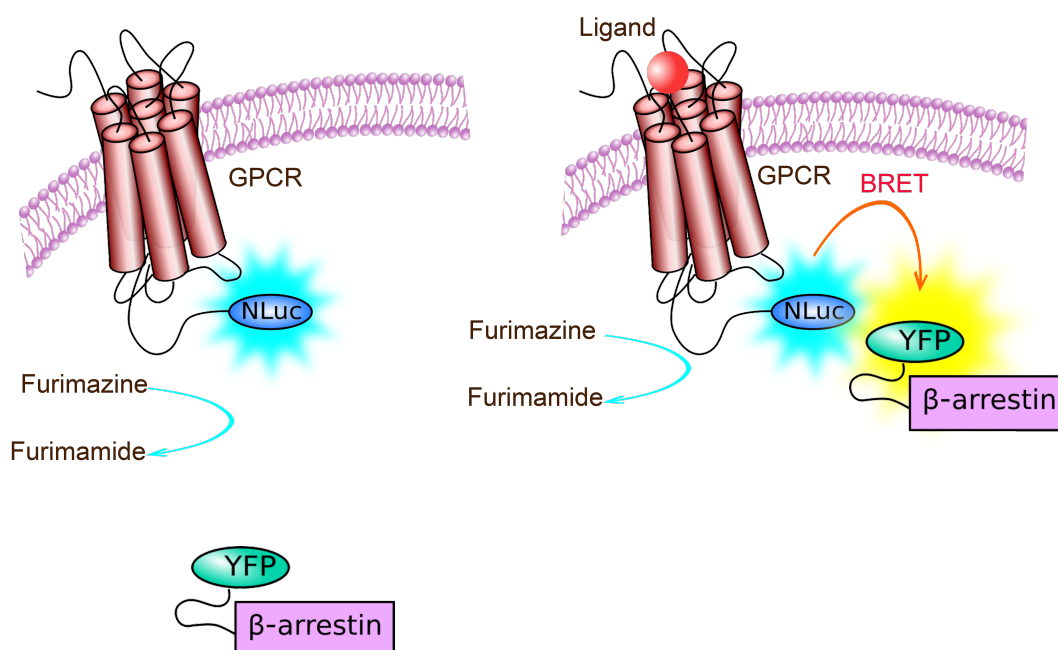


Figure 2.10 Principle of BRET-based β -arrestin recruitment assay. BRET relies on the transfer of energy between a bioluminescent donor (NLuc) and a fluorescent acceptor (YFP) where the proximity between these proteins is within ~ 10 nm. Light emission from acceptor, YFP, is detected at 520 nm, whereas bioluminescent transmitted energy is recorded at 460 nm.

2.2.19 Data Analysis

All data analysis was performed in GraphPad Prism 8.4 (San Diego, US). To quantify gene expression through RT-PCR, the densitometry results of each gene of interest were normalised to GAPDH signal.

For cAMP accumulation, cell proliferation assays, intracellular calcium mobilisation assay, and BRET-based β -arrestin recruitment assays, data were fitted to obtain concentration–response curves using the three-parameter logistic equation using GraphPad Prism 8 (GraphPad Software, San Diego) to obtain values of E_{\max} / I_{\max} , pEC_{50}/pIC_{50} , baseline, and span.

$$Y = Bottom + \frac{(Top - Bottom)}{(1 + 10^{(LogEC_{50} - X)})} \quad (1)$$

Where Y is pharmacological response; top (E_{\max}) and bottom (baseline) values are upper and lower plateau of sigmoidal dose-response curve. The equation (1) was also used to determine % response (Y) corresponds to effect of forskolin (at the concentration giving 20% of E_{\max} , pEC_{20}) in the presence of PDE inhibitor in optimisation experiment. Span is the range between E_{\max} and baseline values and is

expressed as %. X is concentration in logarithmic scale. By assuming Hill slope to be 1, $\log EC_{20}$ can be determined using the formula below:

$$\log EC_F = \log EC_{50} + \left(\frac{1}{Hill\ Slope} \right) \times \log \left(\frac{F}{100 - F} \right) \quad (2)$$

Statistical differences were analysed using one-way ANOVA followed by Dunnett's post-hoc (for comparisons amongst more than two groups) or independent Student's t-test (for comparison between two groups). To determine the correlation of cAMP levels and cell proliferation of each PDE inhibitor in all cell lines, Pearson's correlation coefficient (r) was calculated with 95% confidence interval. To compare the ability of compounds to suppress glioma/glioblastoma cell proliferation, a selection criterion was calculated, whereby the term for affinity (pIC_{50}) was multiplied by the term for efficacy (span). Error for this composite measure was propagated by applying the following equation.

$$Pooled\ SEM = \sqrt{\left(\frac{SEM_A}{\bar{x}_A} \right)^2 + \left(\frac{SEM_B}{\bar{x}_B} \right)^2} \times \bar{x}_{AB} \quad (3)$$

Where, SEM_A and SEM_B are the standard error of measurement A and B with mean of \bar{x}_A and \bar{x}_B , \bar{x}_{AB} is the composite mean and n is the number of repeats.

CHAPTER 3

PHOSPHODIESTERASE INHIBITION AS A THERAPEUTIC TARGET: STUDY IN A MODEL OF GLIOMA

3.1 Introduction

Glioma, a type of brain tumour that originates from astrocytes, has been a challenge due to its pathological progressiveness. Glioblastoma multiforme (GBM), the most common type of glioma, is reported to be the deadliest, with a 5-year survival rate of 5% (Schwartzbaum *et al.*, 2006; Delgado-López and Corrales-García, 2016).

Abnormalities in several signalling pathways have been reported to be involved in glioma-genesis, these include alterations to the following cascades: phosphatidylinositol-3 kinase/ phosphatase and tensin/ protein kinase B/ mammalian target of rapamycin (PI3K/PTEN/Akt/mTOR) cascade that often deletes or suppresses phosphatase and tensin (PTEN) suppressor gene (Rekers, Sminia and Peters, 2011; X. Li *et al.*, 2016) ; the retinoblastoma pathway (pRB) (Burns *et al.*, 1998), the Ras/ mitogen-activated protein kinase (RAS/MAPK) pathway (Rekers, Sminia and Peters, 2011); signal transducer and activator of transcription 3 (STAT3) (Jahani-As *et al.*, 2016); zinc transporter 4 (ZIP4) (Lin *et al.*, 2013; Kang *et al.*, 2015); and adenylyl cyclase (AC) pathway (Mao *et al.*, 2012). Aberrant signalling in the AC system results in cAMP suppression approximately 4-fold lower compared to normal healthy brain cells: 25.8 pmol/mg protein versus 98.8 pmol/mg protein (Furman and Shulman, 1977; Mao *et al.*, 2012).

Targeting cAMP using forskolin has been shown to beneficially impact in a broad range of relevant anti-cancer effects (Illiano *et al.*, 2018) which involve improving sensitivity towards chemotherapeutic agents, blocking cell motility and migration (Naviglio *et al.*, 2010; Quinn *et al.*, 2017), and suppressing cell growth (Sawa *et al.*, 2017). While cAMP-analogues such as 8-bromo-cAMP, 8-chloro-cAMP, monobutyl cAMP and dibutyl cAMP also showed promising results, the use of these compounds were not recommended due to toxicity (Hirsh *et al.*, 2004). Hence, there is an urgency to develop relatively safe and effective compounds that elevate cAMP levels.

As mentioned previously, PDEs hydrolyse cAMP into adenosine 5'-monophosphate (AMP) to control the functional level of cAMP (Figure 3.1) (K Omori and Kotera, 2007b). However, several PDEs including PDE1, PDE4, PDE5, and PDE7

have been found to be upregulated in a range of tumours to alter the basal level of cAMP. This evidence is supported by other reports that lower cAMP levels are associated with malignancy (Savai *et al.*, 2010b; Sengupta *et al.*, 2011; Brooks *et al.*, 2014; Cesarini *et al.*, 2017). Therefore, increasing the level of cAMP through PDE inhibition to compensate for overexpression of PDEs may be a viable approach for cancer therapy (Chen *et al.*, 2007).

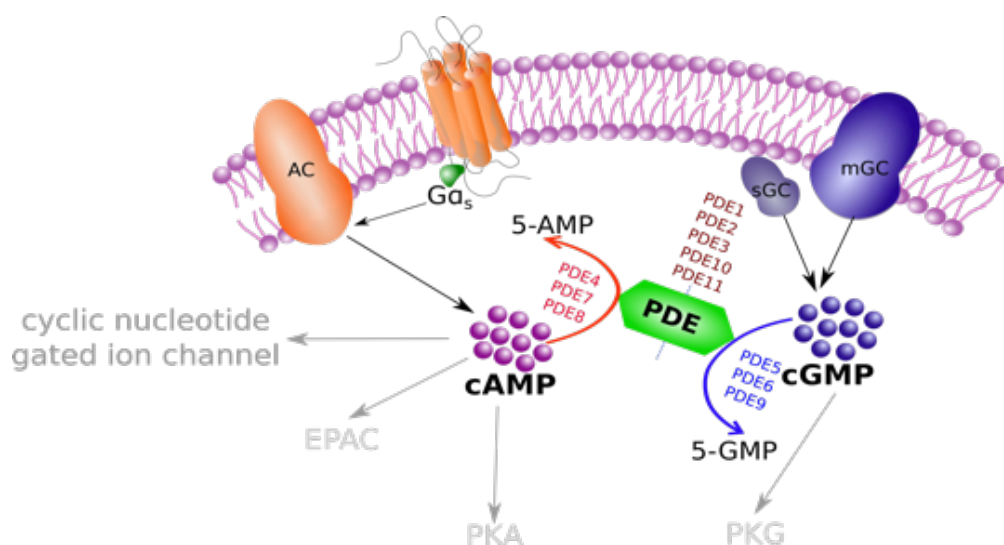


Figure 3.1. Illustration of regulation process of intracellular level of cAMP. Intracellular concentration of cAMP is tightly controlled by its production: through activation of GPCR or direct stimulation at adenylyl cyclase (AC); its degradation through phosphodiesterase (PDE) activities; as well as cGMP levels through dual-substrate PDEs.

In this study, C6 cells were used as model for glioma and as the tool to characterise pharmacological role of PDEs. C6 cells is glioma cells derived from rat origin that is continuously exposed to *N*-Nitroso-*N*-methylurea (Benda *et al.*, 1968). This cell line is reported to be genetically close to GBM and resembles numerous properties including morphological and development of tumor *in vivo*, and the angiogenesis during tumor development (Giakoumettis, Kritis and Foroglou, 2018). Indeed, the C6 rat glioma model is considered the most common model that has been studied to investigate growth, aggressiveness, and invasion of high-grade glioma (Auer, Maestro and Anderson, 1981; Nagano *et al.*, 1993; Giakoumettis, Kritis and Foroglou, 2018). For comparison, ST14A cells, a medium spiny neurons-like cell line derived from rat embryonic striatum, was used as a model of healthy neurons (Ehrlich *et al.*, 2001).

Considering that intracellular concentration of cAMP is not only controlled by its synthesis through AC, but also is influenced by other affecters including GPCR and G

proteins, PDEs, and cGMP which all of them contribute to regulating spatiotemporal action of this secondary messenger (Figure 3.1). Therefore, in this study, the role of each PDE isoenzymes through cAMP pathway were investigated as well as impact on cell growth. The study also would include upstream proteins that involve in cAMP production as well as another secondary messenger – cGMP.

3.2 Elevation of cAMP through β -adrenoceptor, G protein, and adenylyl cyclase exhibit differential range of anti-proliferative effects in C6 glioma cells

It has been suggested that elevation in cyclic nucleotides can lead to changes in cell growth. Using the rat C6 cells as a model for glioma, the role of intracellular cyclic nucleotides in modulating cell growth was investigated. Firstly, the ability of an AC activator (forskolin) and guanylyl cyclase (GC) activators (YC-1 and BAY 41-8543) to stimulate cAMP or cGMP production was assessed.

There was a dose-dependent elevation in cAMP levels in C6 cells upon stimulation with forskolin, YC-1, and BAY 41-8543 for 30 minutes (Figure 3.2A) with the rank order of potency (pEC_{50}): forskolin (5.75 ± 0.24) > BAY 41-8543 (5.38 ± 1.00) > YC-1 (5.11 ± 0.81). This time point was taken based on the routines in the laboratory and has been proven to be able providing sufficient window of observation for most of the compounds. Whilst very small amount of cAMP was detected in vehicle treated group (DMSO 1%), the maximal cAMP level in response to GC activators approximately 30-fold lower compared to that of forskolin ($p < 0.001$, Figure 3.2B).

Although there was an increase in cGMP accumulation upon stimulation with the nitric oxide donor, SNAP and GC activator ($p < 0.001$, Figure 3.2C), in general, cGMP production was ~1000-fold lower in C6 cells than cAMP production. Treatment with forskolin dose-dependently suppressed proliferation of C6 cells (pIC_{50} 5.34 ± 0.09), whilst YC-1 and BAY 41-8543 only reduced cell proliferation at 100 μ M (Figure 3.2D). These results suggest that cell growth is predominantly affected by cAMP signalling compared to cGMP. A previous report by Zaccolo and Movsesian (Zaccolo and Movsesian, 2007), details that crosstalk between cAMP and cGMP occurs through PDEs. Taking this into account, accumulation of cGMP levels may allosterically regulate dual-substrate PDEs modulating the concentration of cAMP and suppressing cell proliferation. This also may explain the findings that GC activator-mediated cAMP accumulation and cell growth suppression that has been mentioned previously.

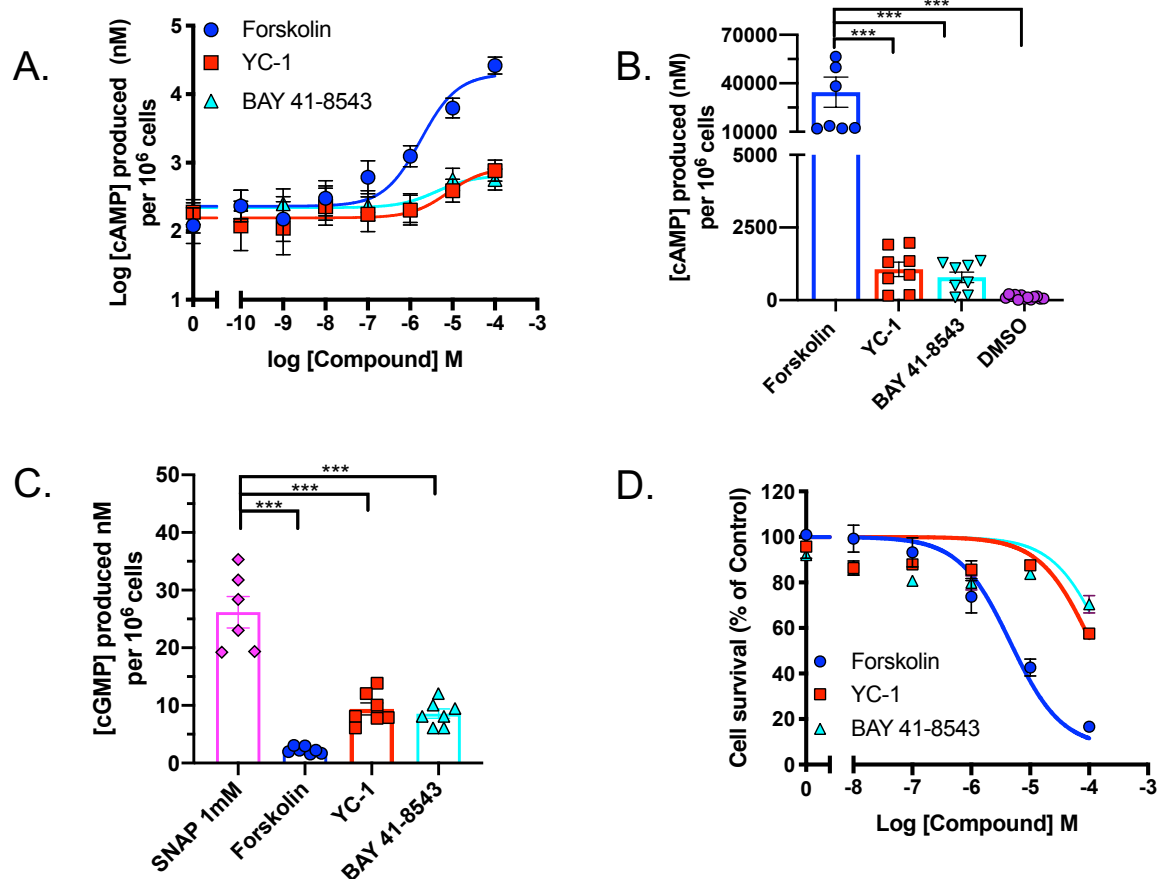


Figure 3.2 Elevation of cAMP, but not cGMP, mediates cell growth suppression.

A. cAMP levels following 30 minutes treatment with adenylyl cyclase activator (forskolin) or guanylyl cyclase activators (YC-1 and BAY 41-8543). cAMP levels following 30 minutes treatment with adenylyl cyclase activator (forskolin) or guanylyl cyclase activators (YC-1 and BAY 41-8543). B-C. Comparison of accumulation of cAMP and cGMP in C6 cells in response to forskolin (100 μ M), BAY 41-8543 (100 μ M), YC-1 (100 μ M), or SNAP (100 μ M). D. Survival of C6 cells following 72 hours treatment with forskolin, BAY 41-8543 or YC-1. Data are expressed as percentage survival relative to vehicle alone and are the mean \pm SEM of 6-9 individual experiments. Statistical significance was determined using a one-way analysis of variance followed by Dunnett's post hoc test (***, $p < 0.001$).

Since GPCRs can also stimulate the production of cAMP, here, we tested the effects of isoprenaline, a non-selective β -adrenoceptor agonist on cAMP production and cell proliferation. Although isoprenaline (pEC_{50} : 8.62 ± 0.13) was more potent compared to forskolin (pEC_{50} : 6.11 ± 0.12) in cAMP accumulation assay, the anti-proliferative effect was significantly lower than that of forskolin (pIC_{50} isoprenaline 4.55 ± 0.25 ; pIC_{50} forskolin 5.84 ± 0.13 , $p < 0.01$) (Figure 3.3A and B). Furthermore, direct targeting of G proteins using PTx (pertussis toxin) or CTx (cholera toxin), show that G protein-mediated cAMP elevation only moderately suppresses cell growth (~20%

suppression, Figure 3.3C and D), with the potency of each would be 0.14 ± 0.38 and 0.66 ± 0.15 ng/ml, for PTx and CTx, respectively.

It can be concluded that either transiently activation of GPCRs or directly modifying heterotrimeric G proteins display sub-optimally anti-proliferative effects compared to forskolin treatment. Taken together, these data suggest that elevation of cAMP, through direct AC activation, triggers cell growth suppression with a possible involvement of cGMP signalling.

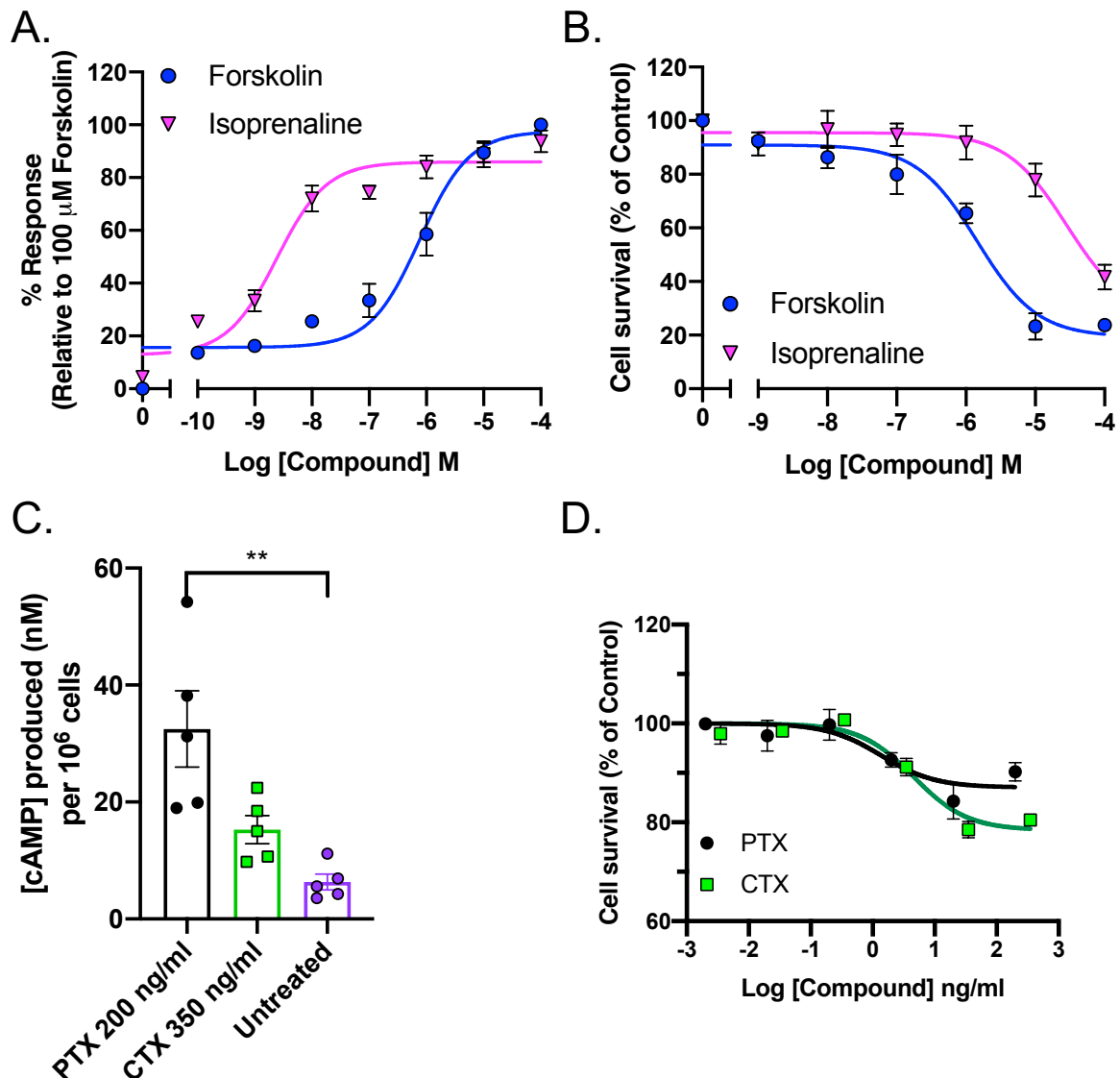


Figure 3.3 Forskolin stimulation has a greater effect on suppression of C6 cell growth than activation of β -adrenoceptor or $G\alpha$ G protein subunits. *A.* Comparison of accumulation of cAMP in C6 cells in response to forskolin and isoprenaline. *B.* Survival of C6 cells following 72 hours treatment with forskolin, isoprenaline. *C.* Concentration of cAMP in C6 cells after 16 hours pre-treatment with PTx or CTx in comparison to untreated cells. *D.* Survival of C6 cells after treatment with PTx and CTx. Data are expressed as percentage survival relative to vehicle alone and are the mean \pm SEM of 6-9 individual experiments. Statistical significance was

determined using a one-way analysis of variance followed by Dunnett's *post hoc* test (**, $p < 0.01$).

3.3 Determination of PDE expression profile in glioma cells

The concentration of intracellular cAMP is tightly regulated by the action of AC and PDEs. However, given the fact that AC is more abundantly expressed in various tissues leading to lack of selectivity, therefore, determination of AC roles was ruled out. It was next necessary to profile PDE expression in C6 cells as model for glioma, in comparison with ST14A cells.

To do this, reverse transcription polymerase chain reaction (rt-PCR) was conducted to identify expression levels of genes of interests. GAPDH, glyceraldehyde 3-phosphate dehydrogenase, is one of housekeeping gene that is commonly used as the reference to normalise other genes of interests (Karge, Schaefer and Ordovas, 1998). Despite the reports that GAPDH as housekeeping gene will be affected by the experimental setting (Barber *et al.*, 2005), using the same tissue GAPDH remains valid as denominator for gene expression studies. To validate there was no contamination from genomic DNA (gDNA), the similar PCR reaction was performed without including reverse transcriptase.

Since PDE6 isoenzymes are specifically expressed in the eyes, amplification of these isoforms was precluded. As shown in Figure 3.4, the overall expression of PDEs at the mRNA level was greater in C6 compared to ST14A cells. While expression of PDE1C, PDE4B, PDE4D, PDE7A, and PDE7B were statistically upregulated in C6 cells, discrepancy amongst remaining isoforms was minor. It is worth noting that amongst all PDEs, the highest expression was detected on PDE1C, PDE4B, and PDE4D in C6 cells.

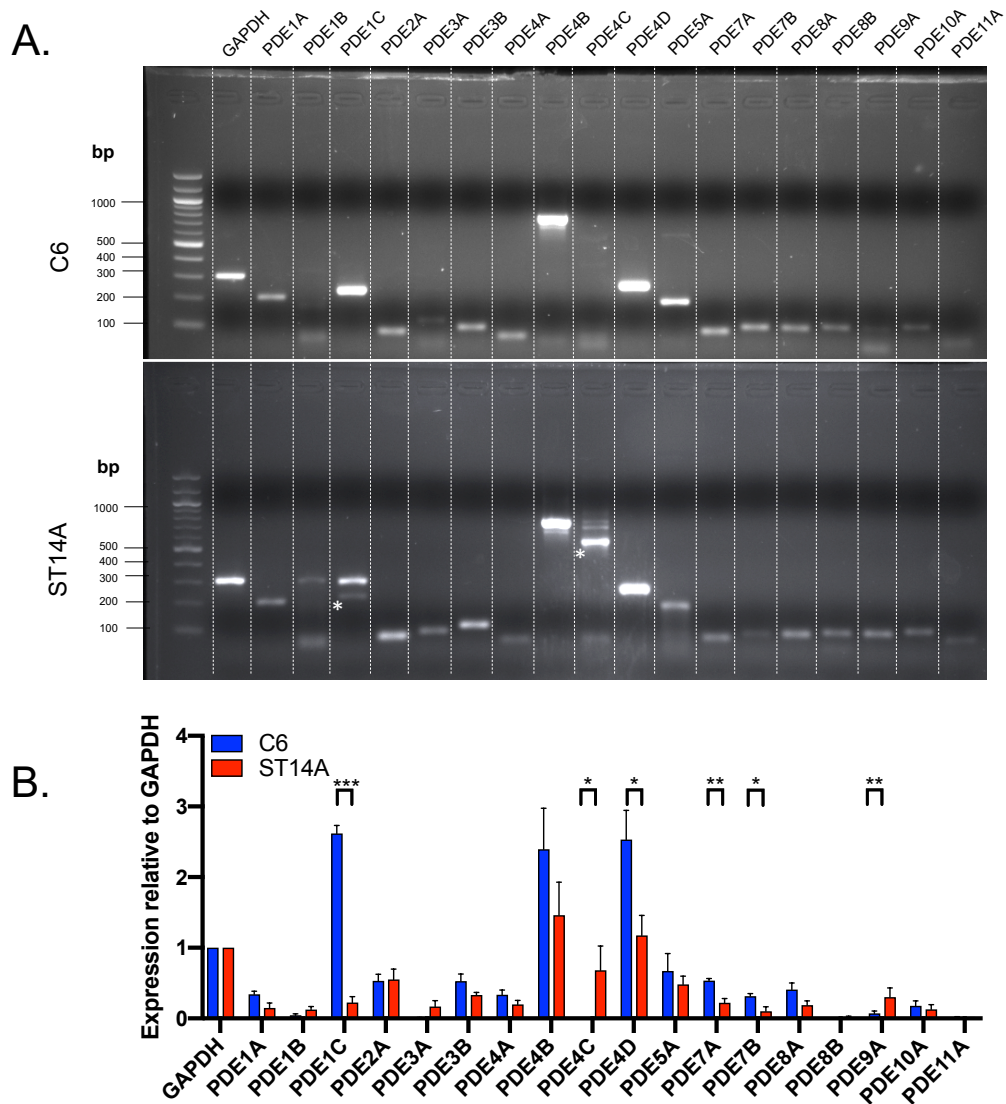


Figure 3.4 Expression profile of PDE isoenzymes in C6 and ST14A cells. *A.* Representative gel documentation showing amplified PDEs genes from C6 and ST14A cell line. (*) on the gel showed correct band size. *B.* Semi-quantitative mRNA levels in C6 cells and ST14A cells. Expression of each gene of interest was normalised relative to GAPDH. Data are expressed as the mean \pm SEM from 5-7 individual repeats. Data were determined as statistically different (*, $p < 0.05$; **, $p < 0.01$; ***, $p < 0.001$) compared to individual isoenzyme between both cell lines using Student's t-test analysis.

3.4 Pharmacological characterization of PDE inhibitors on modulating cAMP concentration

Since the expression profiles obtained from rt-PCR were only semi-quantitative, it was next required to determine the role of each PDE isoforms through functional assays. Small molecule selective PDE inhibitors were used to probe the involvement of each PDE isoenzymes in modulating intracellular concentration of cAMP and its impact on cell growth.

3.4.1 Development of a screening method to profile the efficacy of small molecule PDE inhibitors in modulating cAMP signalling

Before characterising the role of each PDE isoenzymes, preliminary studies were conducted to establish an appropriate rapid and high throughput but robust screening method to test the activity of each compound in modulating the total concentration of cAMP.

Illustrated in Figure 3.5, if cells were co-stimulated with a concentration equivalent to the pEC_{50} value of forskolin, the window of observation would be too narrow to detect elevation of cAMP because of reaching the plateau of the maximal response (Figure 3.5). Instead, using a concentration equivalent to the pEC_{20} provides a wider range of observation of elevated cAMP in the presence of different PDE inhibitor (Figure 3.5). The effect of PDE inhibitor treatment on the forskolin response was determined by comparing the response at the pEC_{20} concentration of forskolin in the absence of PDE inhibitor (Figure 3.5).

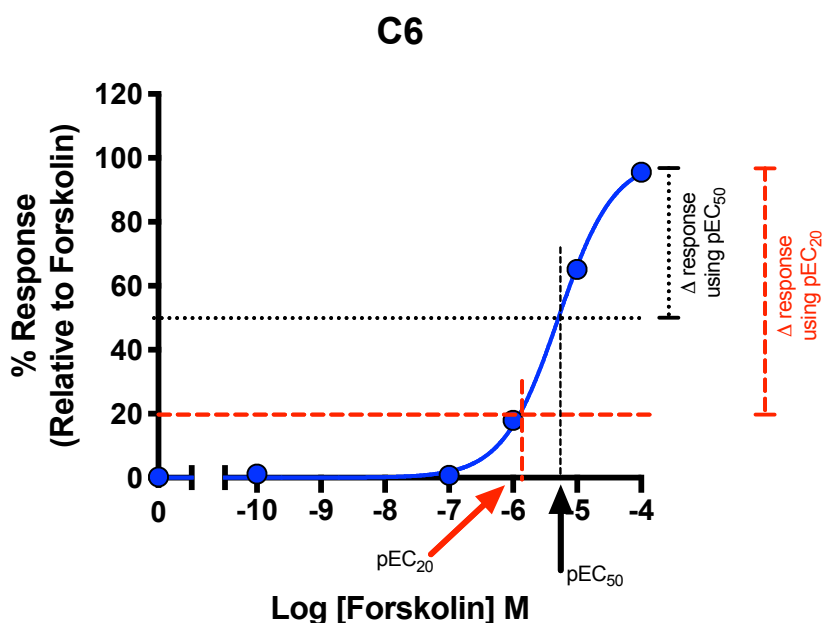


Figure 3.5 Comparison in using pEC_{20} and pEC_{50} of forskolin to provide sufficient window of observation for developing screening method. The graph represents the dose-response curve of forskolin without any PDE inhibitor upon stimulation for 30 minutes. This graph shows that if cells were co-stimulated with pEC_{20} forskolin and compounds that synergistically increase cAMP levels, the range of response will be wider compared to that of pEC_{50} forskolin.

To validate this approach, the following PDE inhibitors: rolipram (PDE4; was used at concentration of 25 μ M), IBMX (non-selective; 50 μ M), trequinsin (PDE2,3,7; 12.5 μ M), and RO20-1724 (PDE4; 10 μ M) were co-stimulated with forskolin for 30 minutes.

These PDE inhibitors were selected as the inhibitors that are commonly used in our laboratory. As mentioned previously, 30-minute time point was chosen based on similar protocols used to study GPCR-mediated cAMP production (Knight *et al.*, 2016a). The response of forskolin in the presence of PDE inhibitors was quantified (formula (1) in section 2.19) at corresponding pEC₂₀. Data are summarised in Figure 3.6 and Table 3.1. Meanwhile the pharmacological parameters for each dose-response curve are summarised in Table 3.2 and 3.3 for C6 and ST14A cells, respectively.

As displayed in Figure 3.6 and Table 3.1, co-stimulation with selected PDE inhibitors resulted in raising cAMP accumulation in correspondence with forskolin alone. Not only did PDE inhibitors increase the potency of forskolin, but they also elevated the baseline level especially in ST14A cells. Whilst IBMX and trequinsin elevated the basal cAMP >15% in C6 cells, (Table 3.2), the baseline was raised to 20-40% in ST14A cells in the presence of all PDE inhibitor with RO20-1724 increased only 8% (Table 3.3). In both cells, rolipram showed the highest efficacy (increased cAMP levels up to 78%), followed by IBMX/trequinsin (in a range of 70-76%), and RO20-1724 (~57%). By co-stimulating cells with small amount of forskolin, it is evident that this approach is a viable method to quantify the differential effects of each PDE inhibitor in accumulating cAMP. This method is beneficial to provide bigger range of observation and avoid misinterpretation due to reaching the plateau of maximal response of the system. Thus, the effect of each PDE isoenzymes using this approach was next determined. By applying formula (2) based on the dose-response curve of forskolin in each cell lines, pEC₂₀ of forskolin was calculated to be 5.83 ± 0.04 for C6 cells and 7.34 ± 0.09 for ST14A cells.

Table 3.1

The response of C6 and ST14A cells when were stimulated with forskolin and selected PDE inhibitors corresponding to pEC₂₀ forskolin.

| Group | % Response (relative to forskolin) | |
|------------------------|------------------------------------|-----------------|
| | C6 | ST14A |
| Forskolin | 20.09 ± 0.58 | 18.34 ± 0.90 |
| Forskolin + Rolipram | 78.49 ± 2.80*** | 78.70 ± 4.49*** |
| Forskolin + IBMX | 72.83 ± 2.90*** | 76.13 ± 3.37*** |
| Forskolin + trequinsin | 74.86 ± 3.76*** | 70.92 ± 2.67*** |
| Forskolin + RO20-1724 | 58.15 ± 1.50*** | 57.00 ± 1.27*** |

Percentage of response of each compound was equal to total cAMP levels. Values are expressed as mean ± SEM. Statistical significance was determined by comparing the

value of 6-8 data sets to that of forskolin by using one-way ANOVA followed by Dunnett's *post-hoc* analysis. (***, $p < 0.001$).

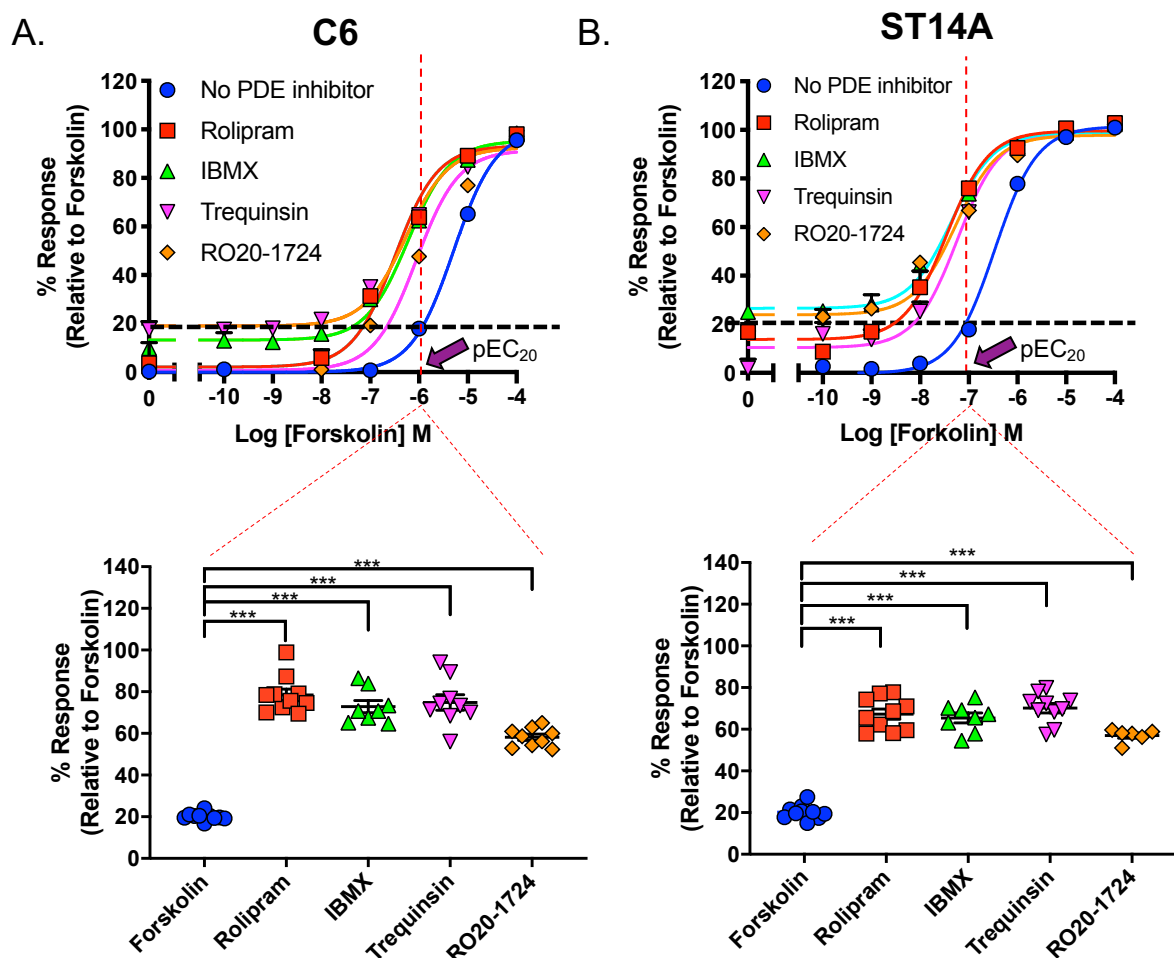


Figure 3.6 PDE inhibitors increased the concentration of cAMP in the presence of forskolin in C6 and ST14A cells. Representative dose-response curve of forskolin in the absence/presence of selected PDE inhibitors in C6 cells (A) and ST14A cells (B). Black and red lines are displayed to visualize interpolation of pEC₂₀. Scatter plot of individual data as a comparison to the corresponding pEC₂₀ of forskolin were displayed on the bottom panel for each cell line. Values are expressed as mean \pm SEM of 6-10 individual data set. Statistical significance was determined by comparing the value of n data sets to that of forskolin by using one-way ANOVA and Dunnett's *post-hoc* analysis (***, $p < 0.001$).

Table 3.2

Pharmacological parameters of forskolin in the presence of different PDE inhibitors in C6 cells

| Group | Basal (%) | E _{max} (%) | pEC ₅₀ | Span (%) |
|------------------------|-----------------|----------------------|-------------------|---------------|
| Forskolin | 0.04 ± 0.17 | 100.00 ± 0.90 | 5.23 ± 0.04 | 100.1 ± 0.9 |
| Forskolin + rolipram | 3.81 ± 1.40 | 101.70 ± 2.76 | 6.35 ± 0.06*** | 97.9 ± 2.3 |
| Forskolin + IBMX | 15.78 ± 3.55*** | 102.40 ± 2.63 | 6.15 ± 0.08*** | 86.7 ± 3.7*** |
| Forskolin + trequinsin | 18.61 ± 1.45*** | 100.10 ± 2.54 | 6.21 ± 0.09*** | 81.5 ± 2.4*** |
| Forskolin + RO20-1724 | 2.08 ± 1.38 | 94.21 ± 1.53 | 6.06 ± 0.07*** | 92.1 ± 1.7 |

The values are generated after curve fitting using three logistic equation by Prism 8.4. The response was normalised to 100 µM forskolin upon stimulation for 30 minutes. The values are represented as mean ± SEM of 9-10 individual data set. Statistical difference was determined using one-way ANOVA followed by Dunnett's *post-hoc* analysis (*, p<0.05; **, p<0.01; ***, p<0.001).

Table 3.3

Pharmacological parameters of forskolin in the presence of different PDE inhibitors in ST14A cells

| Group | Basal (%) | E _{max} (%) | pEC ₅₀ | Span (%) |
|------------------------|-----------------|----------------------|-------------------|---------------|
| Forskolin | -0.16 ± 0.71 | 99.97 ± 0.25 | 6.77 ± 0.08 | 100.1 ± 0.6 |
| Forskolin + rolipram | 20.92 ± 4.64*** | 99.46 ± 0.72 | 7.49 ± 0.10*** | 78.6 ± 4.3*** |
| Forskolin + IBMX | 31.79 ± 3.03*** | 99.67 ± 0.72 | 7.32 ± 0.07*** | 67.4 ± 2.7*** |
| Forskolin + trequinsin | 38.97 ± 4.31*** | 101.2 ± 1.46 | 7.33 ± 0.09*** | 62.3 ± 3.7*** |
| Forskolin + RO20-1724 | 8.61 ± 2.12 | 99.35 ± 0.66 | 7.26 ± 0.08** | 89.9 ± 1.7 |

The values are generated after curve fitting using three logistic equation by Prism 8.4. The response was normalised to 100 µM forskolin upon stimulation for 30 minutes. The values are represented as mean ± SEM of 9-10 individual data set. Statistical difference was determined using one-way ANOVA followed by Dunnett's *post-hoc* analysis (*, p<0.05; **, p<0.01; ***, p<0.001).

3.4.2 Elevation of intracellular cAMP positively correlates with cell growth suppression

Having established the screening method, selected small molecules that have been reported to inhibit PDE isoenzymes (provided by IOTA Pharmaceutical Ltd) were assayed to determine which PDEs are involved in cAMP signalling and cell proliferation. Selective PDE inhibitors against each isoform were initially blind-screened and subsequently decoded after data analysis. Four concentrations were used spanning 100-fold of the established *in vitro* estimates of the IC₅₀ concentration (Table 3.4).

Table 3.4

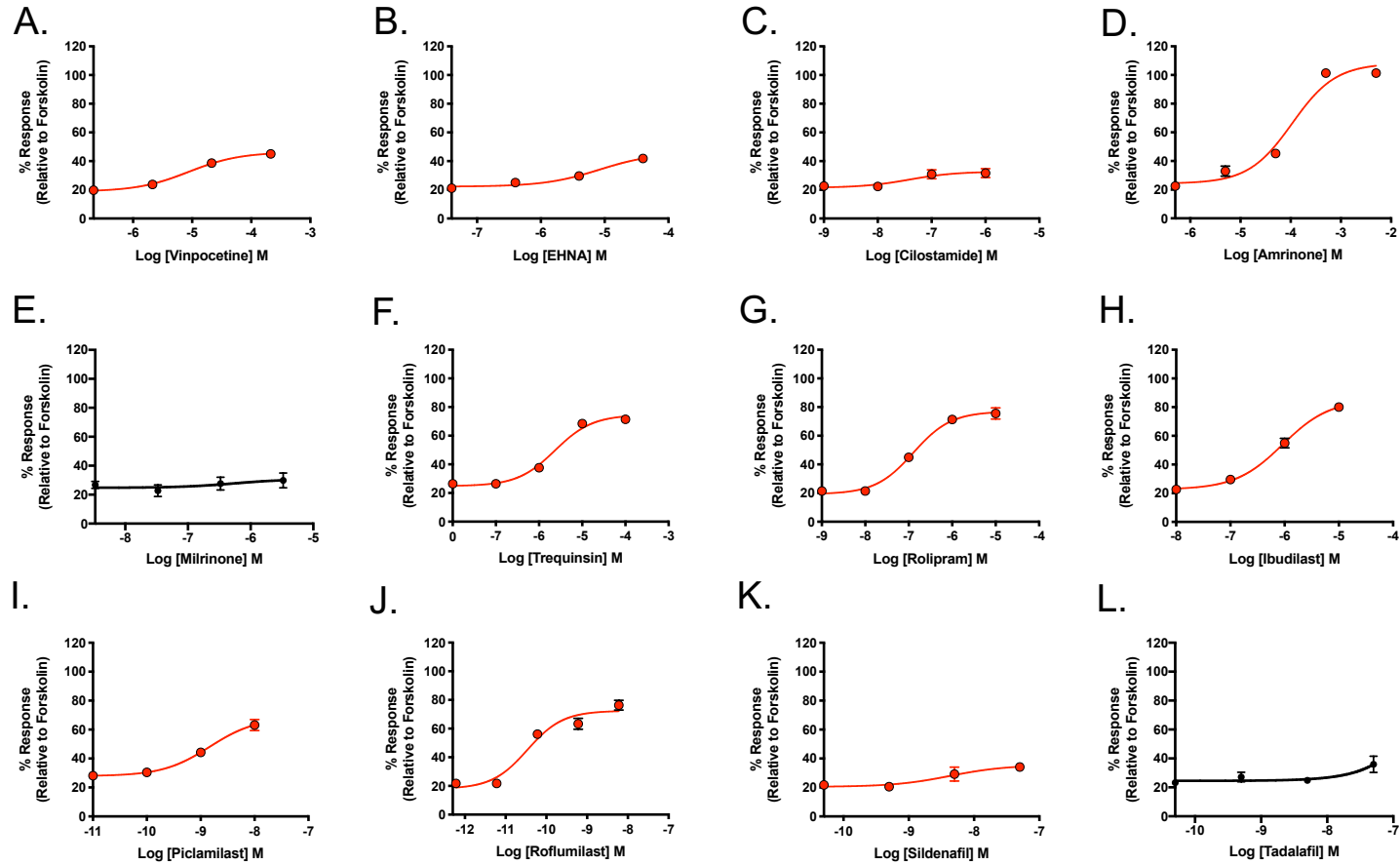
Established *in vitro* pIC₅₀ values of each PDE inhibitors used in this study

| Compounds | Target PDE(X) | <i>In vitro</i> pIC ₅₀ |
|-------------|---------------|---|
| Vinpocetine | 1 | 21 µM |
| EHNA | 2 | 4 µM |
| Cilostamide | 3 | 0.1 µM |
| Amrinone | 3 | 50 µM |
| Milrinone | 3 | 0.33 µM |
| Trequinsin | 2,3,7 | 250 pM (for PDE3) 5 µM (for PDE5) 12.5 µM |
| Rolipram | 4 | 1 µM |
| Ibudilast | 4 | 1 µM |
| Piclamilast | 4 | 1 nM |
| Roflumilast | 4 | 0.6 nM |
| Sildenafil | 5 | 5 nM |
| Tadalafil | 5 | 5 nM |
| Caffeine | 1,4,5 | 10 µM |
| Zaprinast | 5,6,9,11 | 2.6 µM |
| TC3.6 | 7 | 1 µM |
| BRL-50481 | 7 | 180 nM |
| BC 11-38 | 8 | 0.28 µM |
| BAY-736691 | 9 | 55 nM |
| PF-0449613 | 9 | 14 nM |
| PF 2545920 | 10A | 0.37 nM |
| PF 04671536 | 11 | 2 nM |
| IBMX | Non-selective | 20 µM |

Both cell lines were stimulated with the pEC₂₀ equivalent concentrations of forskolin as described previously (section 3.4.1). The individual dose-response curve in cAMP assays is displayed in Figure 3.7 and 3.8 for both cell lines. Whereas the

pharmacological results are shown in Table 3.5. From this series of experiments, some compounds were found to be able to elevate total cAMP concentration in a forskolin-mediated cAMP production in C6 cells: vinpocetine, EHNA, cilostamide, amrinone, trequinsin, rolipram, ibudilast, piclamilast, roflumilast, BRL-50481, and IBMX. While there was a marginal increase in cells stimulated with sildenafil, tadalafil, and zaprinast; the remaining PDE inhibitors did not show any effects. Fewer compounds elevated cAMP production in ST14A cells compared to C6 cells, those compounds include: amrinone, milrinone, trequinsin, rolipram, ibudilast, piclamilast, roflumilast, and IBMX. Interestingly, sildenafil, tadalafil, and PF0449613 suppressed the production of cAMP in ST14A cells, whilst forskolin-mediated cAMP production remains unaffected in the presence of the rest of the compounds.

Subsequently, the compounds were tested for their ability to modulate cell proliferation (Figure 3.9 to 3.10, Table 3.5). In general, compounds that elevate cAMP production were found to exhibit anti-proliferative effects, especially in C6 cells. However, these patterns were not entirely followed in ST14A cells (summarised in Table 3.6).



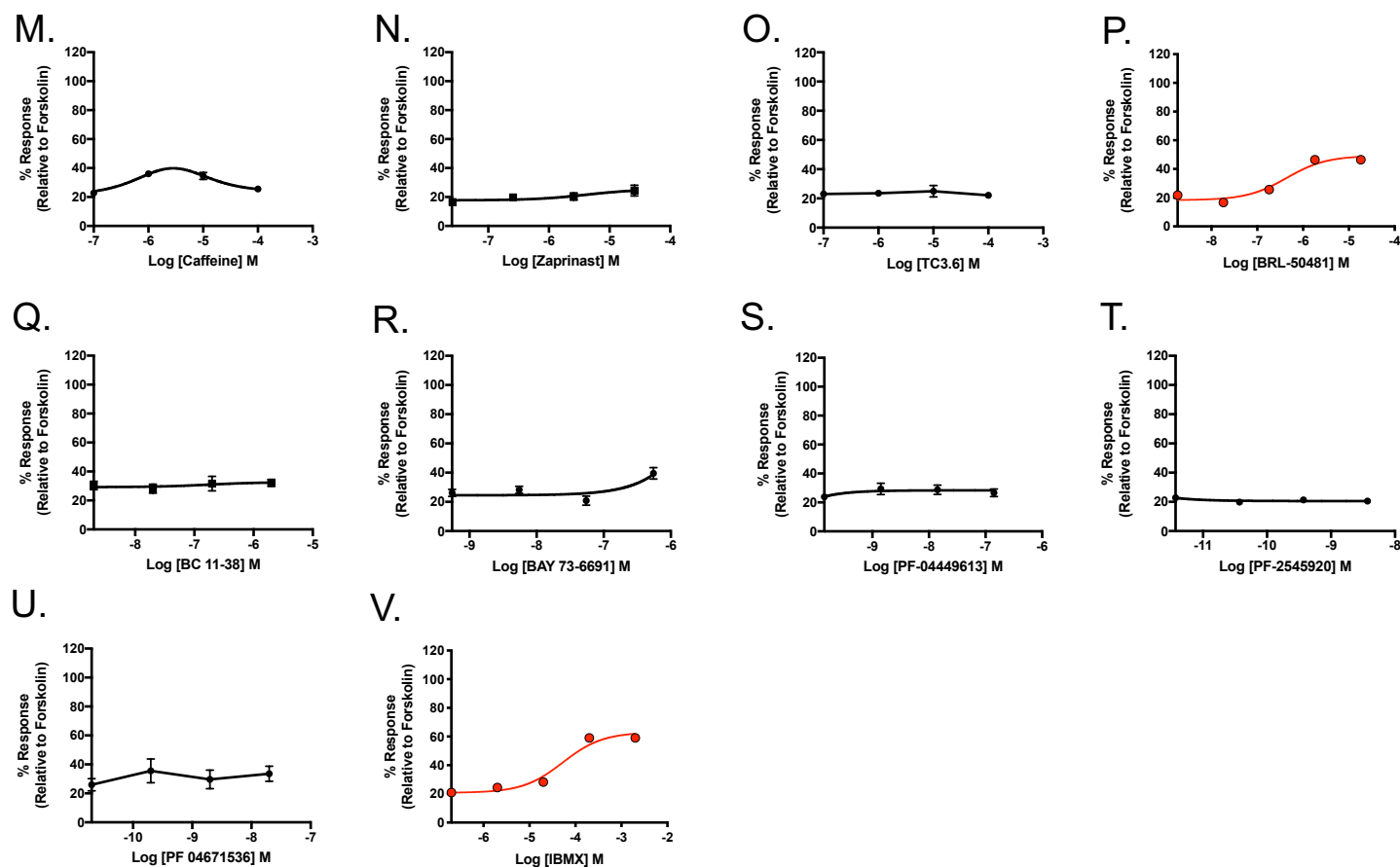
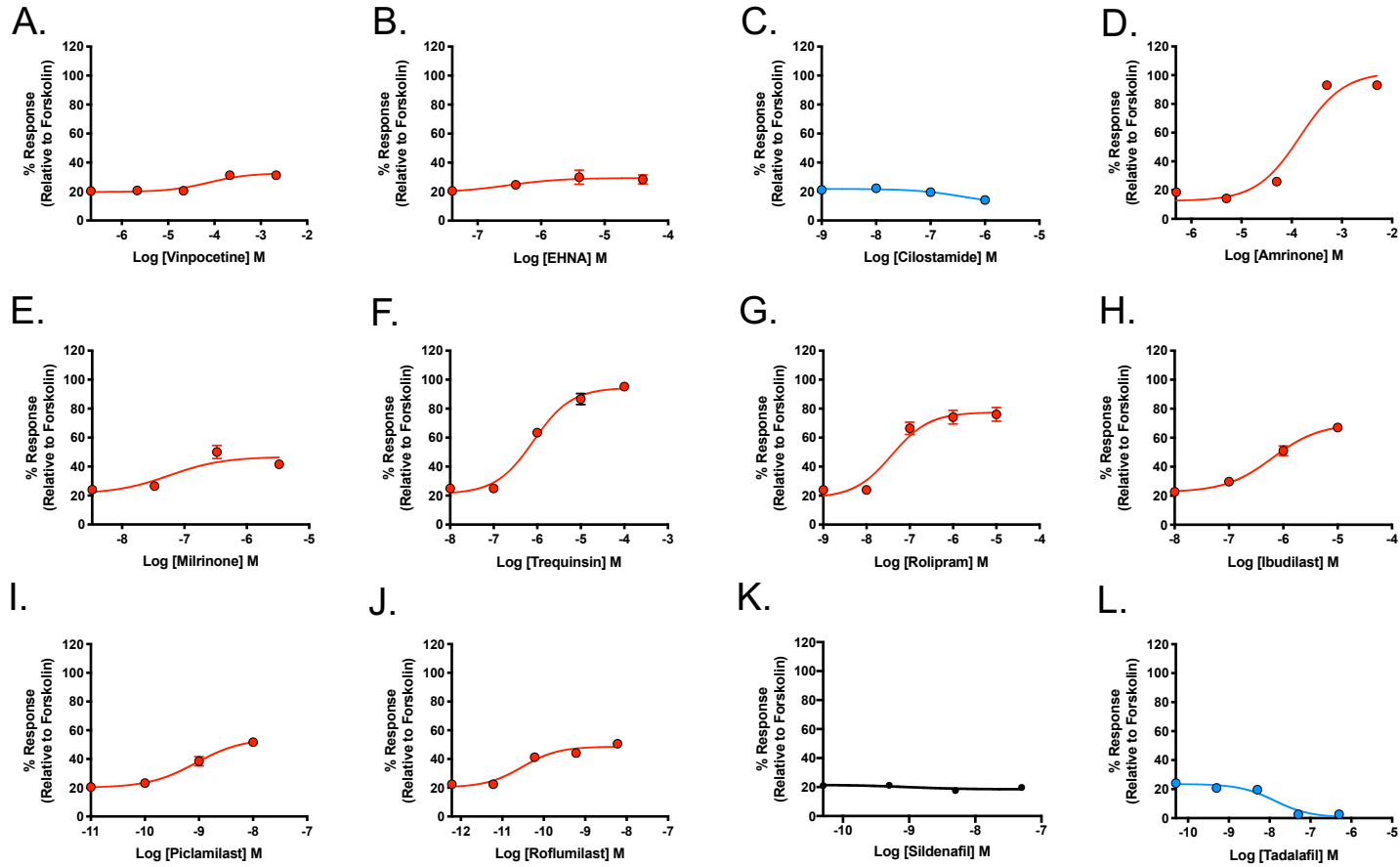


Figure 3.7 Effect of a panel of established PDE inhibitors on forskolin-mediated cAMP production in C6 cells. Dose-response curve of each PDE inhibitors in the presence of small amount of forskolin after 30 minutes stimulation. Responses were normalised to 100 μ M forskolin. Each data point is expressed as mean \pm SEM of 6-9 individual data set. Compounds that elevate cAMP concentration are red colour coded, whereas all of which suppress cAMP level are displayed in blue. Compounds that show no effect are shown as black curves.



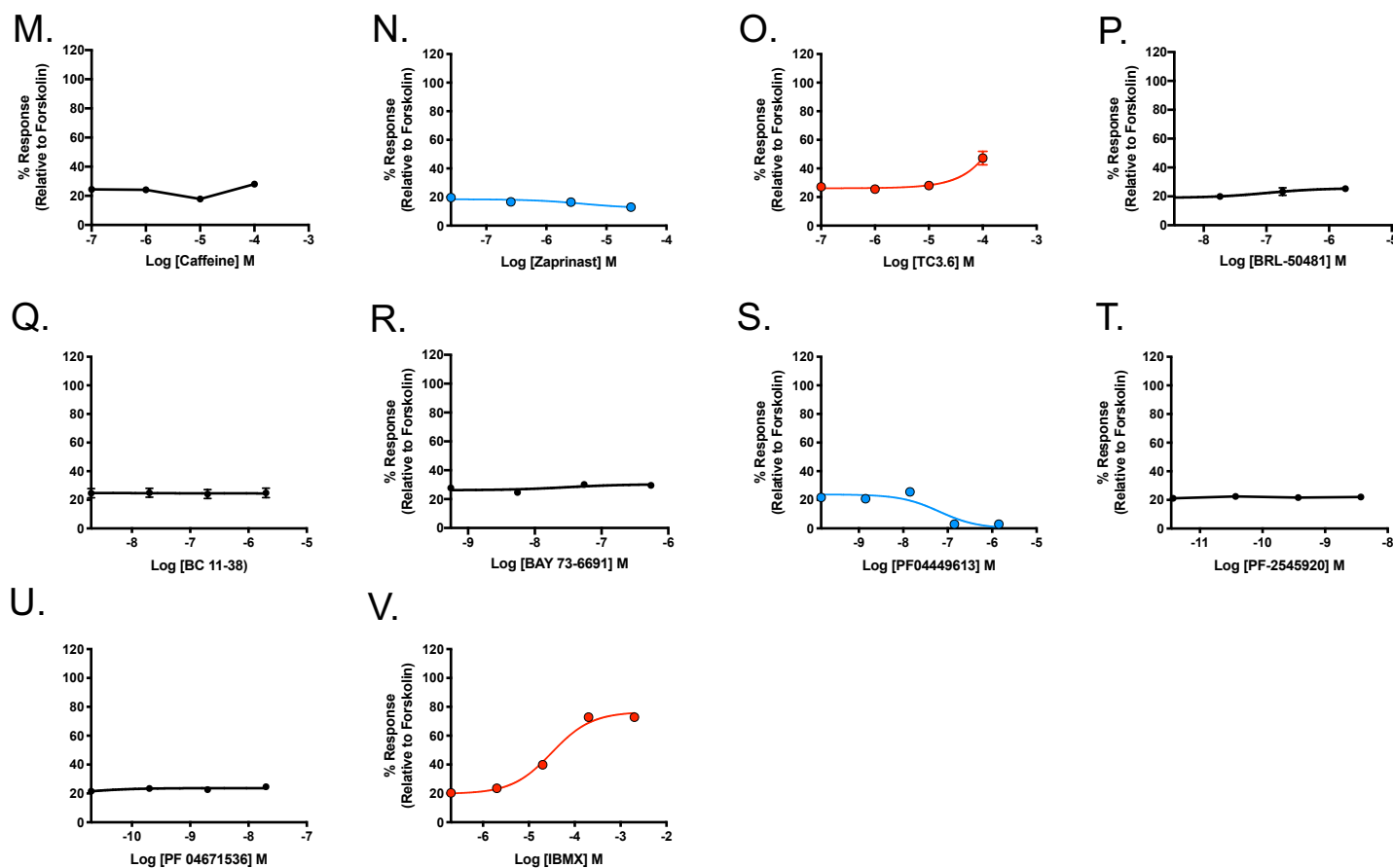


Figure 3.8 Effect of a panel of established PDE inhibitors on forskolin-mediated cAMP production in ST14A cells. Dose-response curve of each PDE inhibitors in the presence of small amount of forskolin after 30 minutes stimulation. Responses were normalised to 100 μ M forskolin. Each data point is expressed as mean \pm SEM of 6-9 individual data set. Compounds that elevate cAMP concentration are red colour coded, whereas all of which suppress cAMP level are displayed in blue. Compounds that show no effect are shown as black curves.

Table 3.5

Potency values for cAMP production (pEC₅₀) and for cell growth inhibition (pIC₅₀) of each PDE inhibitor in C6 and ST14A cells.

| Compounds | Target PDE(X) [∞] | C6 | | | | ST14A | | | |
|-------------|----------------------------|--------------------------------|------------------------------|--------------------------------|---------------------------------------|--------------------------------|------------------------------|--------------------------------|---------------------------------------|
| | | pEC ₅₀ ^a | Span (cAMP) ^b (%) | pIC ₅₀ ^c | Span (proliferation) ^d (%) | pEC ₅₀ ^a | Span (cAMP) ^b (%) | pIC ₅₀ ^c | Span (proliferation) ^d (%) |
| Vinpocetine | 1 | 5.10 ± 0.08 [*] | 27.9 ± 1.1 ^{***} | 5.83 ± 0.13 [*] | 45.3 ± 3.1 ^{***} | 4.16 ± 0.04 ^{***} | 13.2 ± 2.2 ^{***} | N/A | N/A |
| EHNA | 2 | 5.06 ± 0.07 [*] | 24.3 ± 1.8 ^{***} | 5.04 ± 0.25 | 36.3 ± 3.3 ^{***} | N/A | N/A | 6.57 ± 0.08 ^{***} | 20.9 ± 1.2 ^{***} |
| Cilostamide | 3 | 7.19 ± 0.09 ^{***} | 15.2 ± 1.4 ^{***} | N/A | N/A | N/A | N/A | 8.39 ± 0.15 ^{***} | 10.6 ± 1.9 |
| Amrinone | 3 | 3.68 ± 0.08 ^{***} | 108.9 ± 4.8 ^{***} | 4.11 ± 0.04 ^{***} | 86.4 ± 2.3 | 3.84 ± 0.02 ^{***} | 89.7 ± 1.1 ^{**} | 3.91 ± 0.11 ^{***} | 54.4 ± 6.2 ^{***} |
| Milrinone | 3 | N/A | N/A | 8.06 ± 0.13 ^{***} | 34.5 ± 4.7 ^{***} | 7.05 ± 0.18 ^{***} | 27.5 ± 2.4 | N/A | N/A |
| Trequinsin | 2,3,7 | 5.65 ± 0.08 | 50.6 ± 2.0 ^{***} | 4.87 ± 0.07 | 96.9 ± 0.9 | 6.21 ± 0.06 | 80.3 ± 1.9 | 4.62 ± 0.04 ^{***} | 75.8 ± 0.8 ^{***} |
| Rolipram | 4 | 6.96 ± 0.04 ^{***} | 60.5 ± 3.7 | 6.78 ± 0.20 ^{***} | 23.4 ± 2.9 ^{***} | 7.41 ± 0.04 ^{***} | 59.3 ± 4.1 ^{**} | 7.23 ± 0.05 ^{***} | 15.6 ± 1.3 ^{***} |
| Ibudilast | 4 | 6.03 ± 0.11 ^{***} | 64.2 ± 3.5 | 7.05 ± 0.17 ^{***} | 31.8 ± 1.3 ^{***} | 6.15 ± 0.12 | 48.6 ± 2.2 ^{***} | N/A | N/A |
| Piclamilast | 4 | 8.72 ± 0.04 ^{***} | 41.3 ± 2.9 ^{***} | N/A | N/A | 9.02 ± 0.14 ^{***} | 35.2 ± 1.9 ^{***} | N/A | N/A |
| Roflumilast | 4 | 10.47 ± 0.03 ^{***} | 54.6 ± 3.1 | 10.57 ± 0.22 ^{***} | 14.7 ± 1.7 ^{***} | 10.48 ± 0.08 ^{***} | 28.8 ± 0.8 ^{***} | 10.92 ± 0.09 ^{***} | 7.2 ± 1.6 ^{***} |
| Sildenafil | 5 | N/A | N/A | 8.56 ± 0.16 ^{***} | -6.8 ± 3.5 ^{***#} | 8.79 ± 0.20 ^{***} | -4.6 ± 0.9 ^{***#} | 9.67 ± 0.11 ^{***} | 12.7 ± 2.0 ^{***} |
| Tadalafil | 5 | N/A | N/A | N/A | N/A | 7.88 ± 0.04 ^{***} | -23.2 ± 1.4 ^{***#} | 8.81 ± 0.43 ^{***} | -2.7 ± 1.6 ^{***#} |
| Caffeine | 1,4,5 | N/A | N/A | N/A | N/A | N/A | N/A | 6.65 ± 0.06 ^{***} | 9.0 ± 1.0 ^{***} |
| Zaprinast | 5,6,9,11 | 5.61 ± 0.11 | 14.3 ± 1.1 ^{***} | 6.03 ± 0.30 ^{***} | 49.7 ± 4.6 ^{***} | N/A | N/A | 5.86 ± 0.09 ^{***} | 46.7 ± 1.5 ^{***} |
| TC3.6 | 7 | N/A | N/A | 7.53 ± 0.26 ^{***} | 15.3 ± 2.5 ^{***} | N/A | N/A | 5.69 ± 0.05 ^{***} | 21.2 ± 1.5 ^{***} |
| BRL-50481 | 7 | 6.41 ± 0.09 ^{***} | 31.3 ± 1.7 ^{***} | 6.70 ± 0.15 ^{***} | 33.1 ± 2.7 ^{***} | N/A | N/A | 7.73 ± 0.24 ^{***} | 4.5 ± 1.7 ^{***} |
| BC 11-38 | 8 | N/A | N/A | N/A | N/A | N/A | N/A | N/A | N/A |
| BAY-736691 | 9 | N/A | N/A | N/A | N/A | N/A | N/A | N/A | N/A |
| PF-0449613 | 9 | N/A | N/A | N/A | N/A | 7.55 ± 0.12 ^{***} | -23.5 ± 1.8 ^{***#} | 8.05 ± 0.08 ^{***} | 6.4 ± 0.7 |
| PF 2545920 | 10A | N/A | N/A | 9.46 ± 0.06 ^{***} | -8.9 ± 3.1 [#] | N/A | N/A | 10.78 ± 0.11 ^{***} | 11.9 ± 4.1 |
| PF 04671536 | 11 | N/A | N/A | N/A | N/A | N/A | N/A | N/A | N/A |
| IBMX | Non-selective | 4.30 ± 0.06 ^{***} | 42.8 ± 1.5 ^{***} | 6.12 ± 0.06 ^{***} | 54.2 ± 3.2 | 4.56 ± 0.06 ^{***} | 57.5 ± 3.5 | 4.20 ± 0.09 | 47.9 ± 2.7 |
| Forskolin | AC activator | 5.43 ± 0.08 | 64.9 ± 3.5 | 5.12 ± 0.06 | 84.7 ± 1.4 | 6.43 ± 0.12 | 74.1 ± 3.1 | 6.44 ± 0.02 | 45.1 ± 1.2 |
| Cisplatin | DNA crosslinker | N/A | N/A | 6.02 ± 0.09 ^{***} | 96.9 ± 2.6 | N/A | N/A | 5.92 ± 0.09 ^{***} | 86.5 ± 2.3 ^{***} |

Data are the mean \pm SEM of 6-9 individual data sets.

^a The negative logarithm of the agonist concentration required to produce a half-maximal response.

^b the range between basal and E_{max} on cAMP accumulation assay

^c The negative logarithm of the inhibitor concentration required to inhibit a half-maximal response

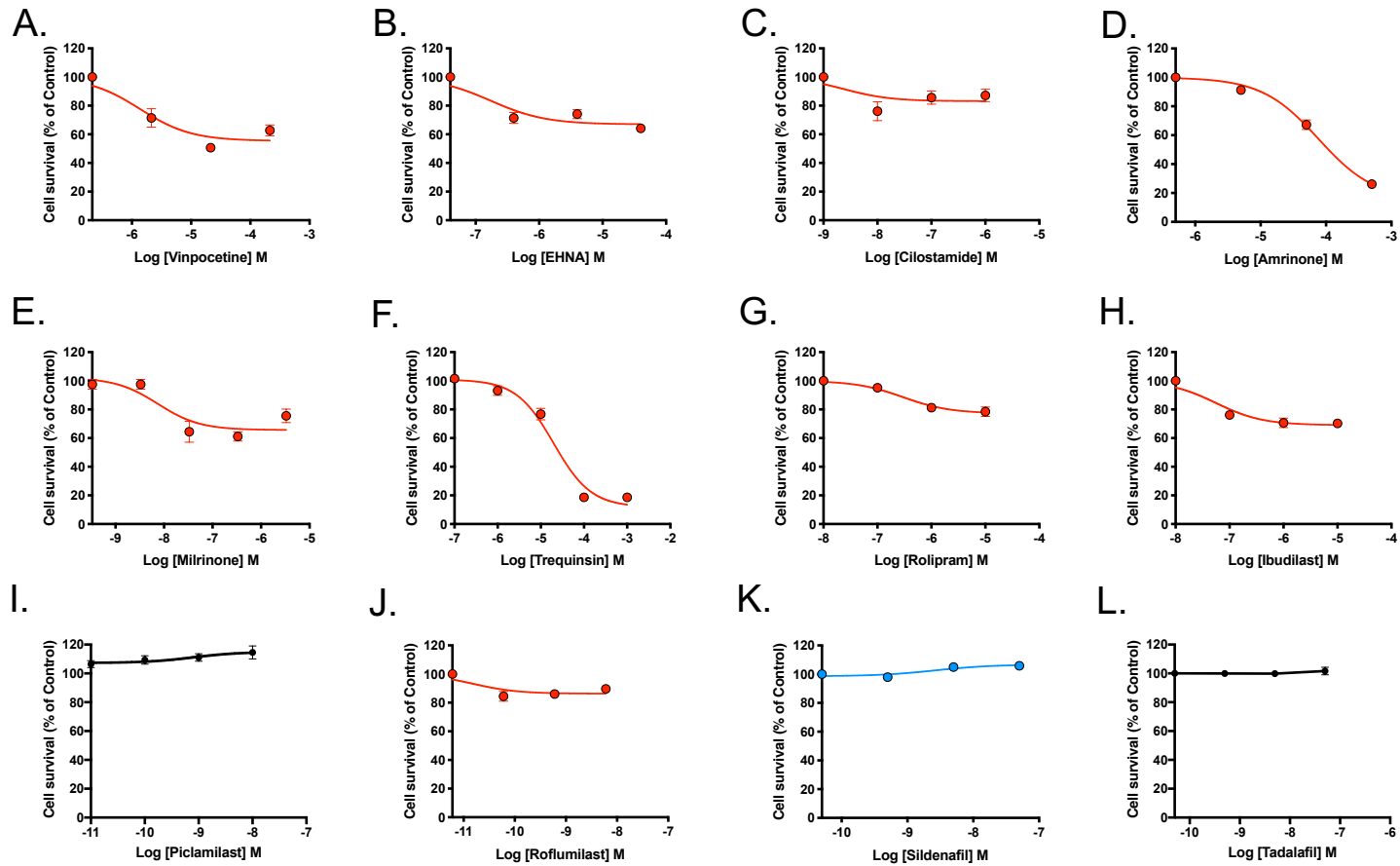
^d The range between survival in vehicle control and inhibitory maximal in cell proliferation assay

N/A – not applicable; compounds did not have any effect on cAMP production or cell growth inhibition.

∞ , unless mentioned, targets refer to particular PDE isoform.

[#], showing negative responses, either suppressing cAMP accumulation or being pro-proliferative.

Data were determined as statistically different (*, $p < 0.05$; ***, $p < 0.001$) compared to forskolin using one-way ANOVA followed by Dunnett's *post-hoc* analysis.



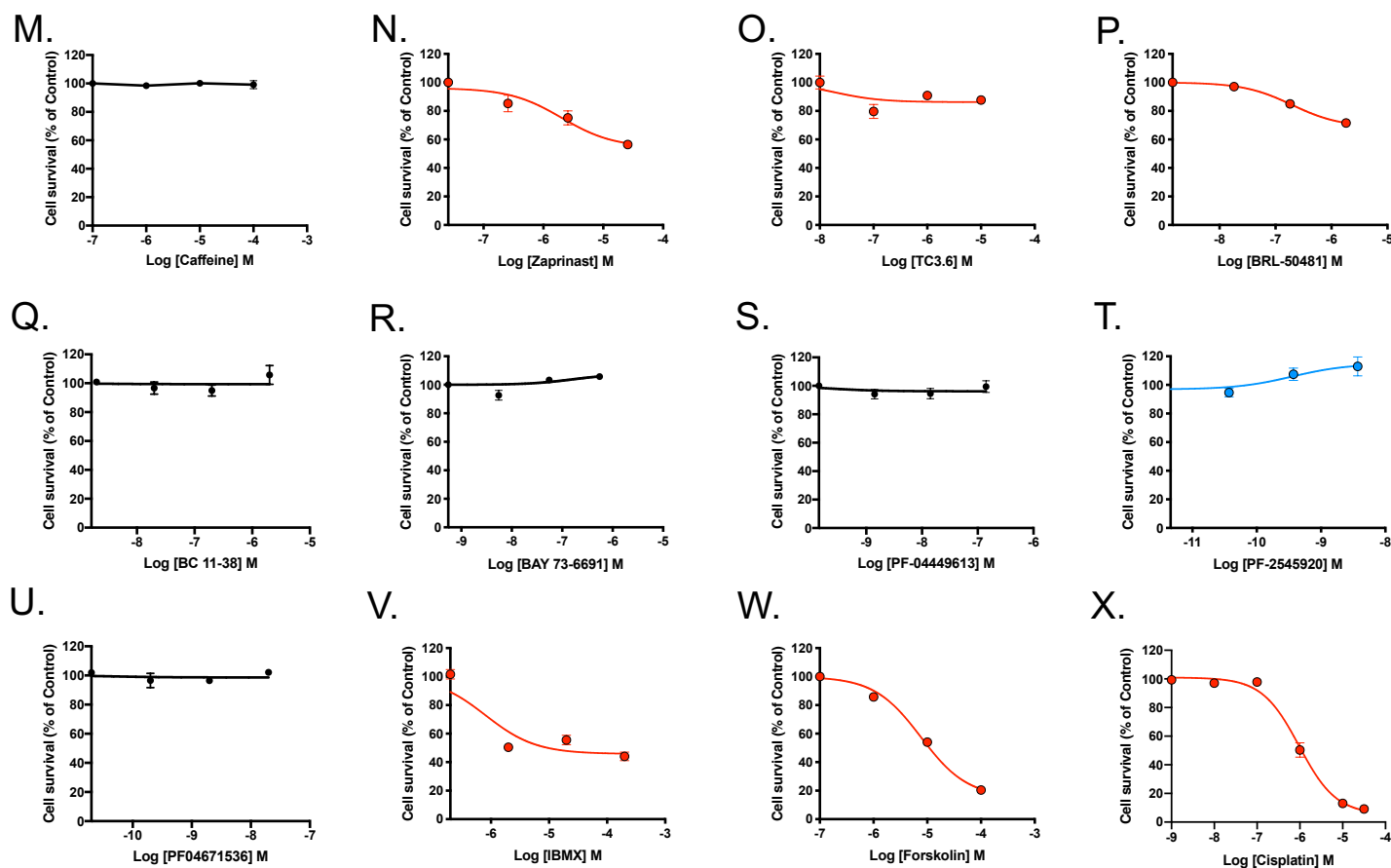
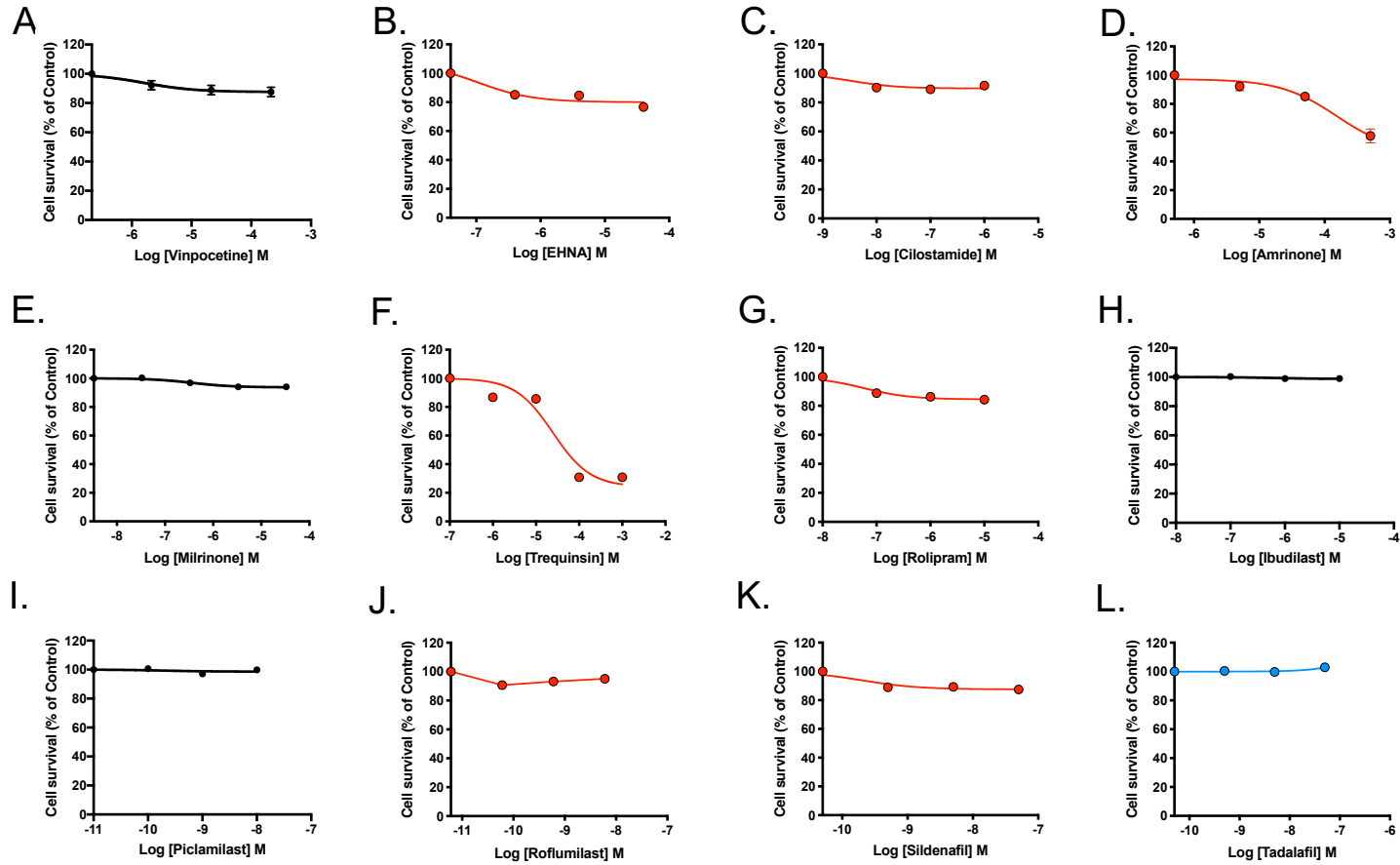


Figure 3.9 Effect of a panel of established PDE inhibitors, forskolin, and cisplatin on modulating C6 cell growth. Cell survival was determined in C6 cells following 72 hours incubation with each PDE inhibitor. Cisplatin was used as cytotoxic reference compound exhibiting anti-proliferative action. Data are expressed as percentage of cell proliferation relative to vehicle (complete medium containing 1% DMSO) from 6-9 data sets. Data are expressed as mean \pm SEM. Compounds that suppress cell growth are red colour coded, whereas all of which pro-proliferative are displayed in blue. Compounds that show no effect is shown as black curves.



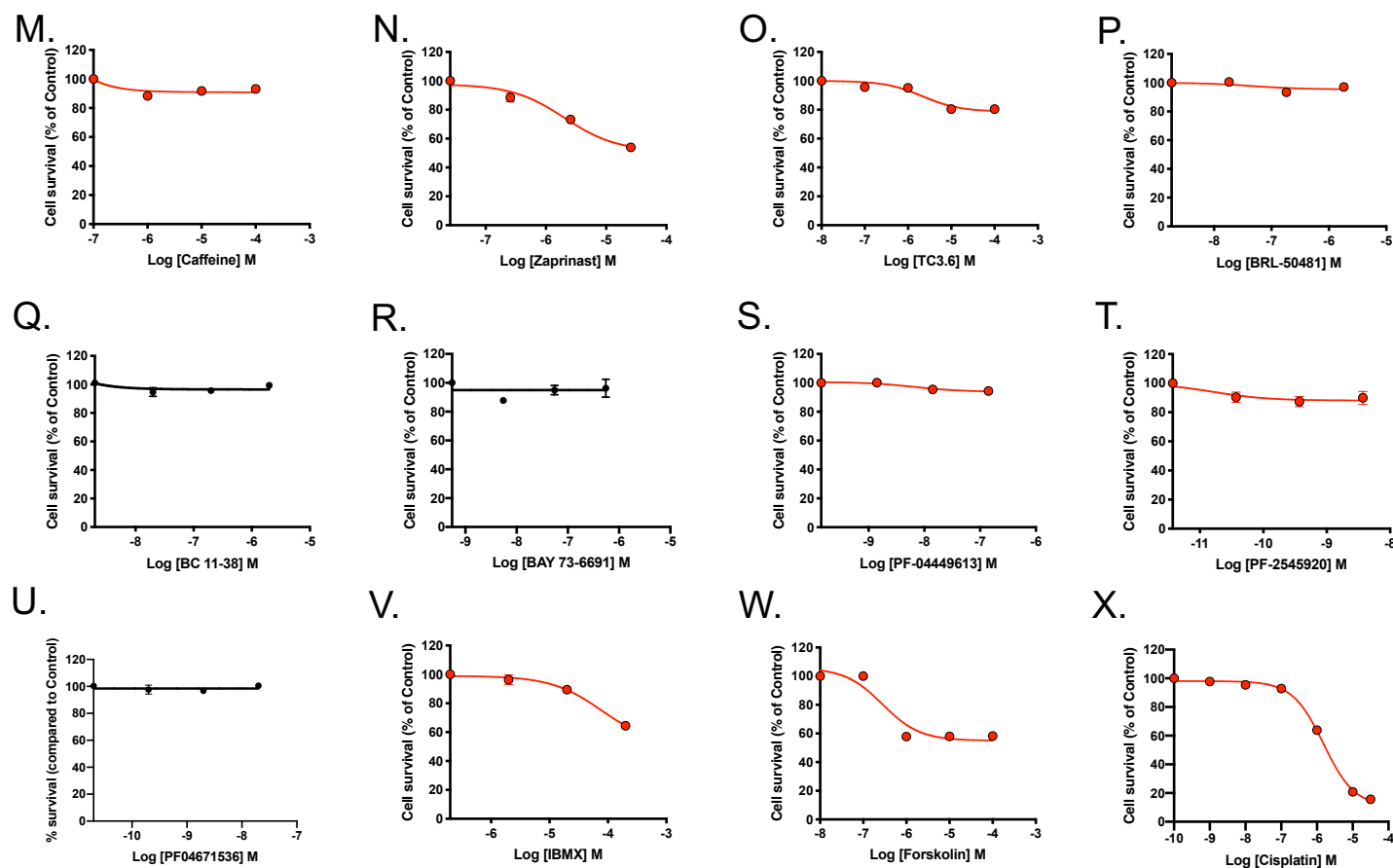


Figure 3.10 Effect of a panel of established PDE inhibitors, forskolin, and cisplatin on modulating ST14A cell growth. Cell survival was determined in C6 cells following 72 hours incubation with each PDE inhibitor. Cisplatin was used as cytotoxic reference compound exhibiting anti-proliferative action. Data are expressed as percentage of cell proliferation relative to vehicle (complete medium containing 1% DMSO) from 6-9 data sets. Data are expressed as mean \pm SEM. Compounds that suppress cell growth are red colour coded, whereas all of which pro-proliferative are displayed in blue. Compounds that show no effect is shown as black curves.

Table 3.6

Summary of the pharmacological effects of each PDE inhibitor on cAMP production and cell proliferation

| Compound | Target | C6 | | ST14A | |
|-------------|---------------|------------|---------------|-------|---------------|
| | | cAMP | Proliferation | cAMP | Proliferation |
| Vinpocetine | 1 | ↑ | ↓↓ | ↑ | - |
| EHNA | 2 | ↑ | ↓↓ | - | ↓ |
| Cilostamide | 3 | ↑ | - | - | ↓ |
| Amrinone | 3 | ↑↑↑ | ↓↓↓ | ↑↑↑ | ↓↓↓ |
| Milrinone | 3 | - | ↓↓ | ↑ | - |
| Trequinsin | 2,3,7 | ↑↑↑ | ↓↓↓ | ↑↑↑ | ↓↓↓ |
| Rolipram | 4 | ↑↑↑ | ↓ | ↑↑↑ | ↓ |
| Ibudilast | 4 | ↑↑↑ | ↓↓ | ↑↑ | - |
| Piclamilast | 4 | ↑↑ | - | ↑↑ | - |
| Roflumilast | 4 | ↑↑↑ | ↓ | ↑ | ↓ |
| Sildenafil | 5 | - | ↑ | ↓ | ↓ |
| Tadalafil | 5 | - | ↑ | ↓ | ↑ |
| Caffeine | 1,4,5 | Bell-shape | - | - | ↓ |
| Zaprinast | 5,6,9,11 | ↑ | ↓↓ | - | ↓↓ |
| TC3.6 | 7 | - | ↓ | - | ↓ |
| BRL-50481 | 7 | ↑↑ | ↓↓ | - | ↓ |
| BC 11-38 | 8 | - | - | - | - |
| BAY-736691 | 9 | - | - | - | - |
| PF-0449613 | 9 | - | - | ↓ | ↓ |
| PF 2545920 | 10A | - | ↑ | - | ↓ |
| PF 04671536 | 11 | - | - | - | - |
| IBMX | Non-selective | ↑↑ | ↓↓↓ | ↑ | ↓↓ |

↑ = increase 10-30%, ↑↑ = increase 31-50%, ↑↑↑ = increase >50%, ↓: suppress 10-30%, ↓↓: suppress 31-50%, ↓↓↓: suppress >50%

To determine whether there was any correlation between cAMP production and cell proliferation, the potency of each PDE inhibitor for cAMP production against the potency for the suppression of cell growth was plotted (Figure 3.11). Calculation of the Pearson's correlation indicated there was a significant association between elevation of cAMP and anti-proliferative effect in both C6 cells ($r = 0.83$ (95% confidence interval 0.46–0.95)) and ST14A cells ($r = 0.97$ (95% confidence interval (0.73–0.99))). Thus, these data suggest that increasing in intracellular concentration of cAMP prevents cell proliferation.

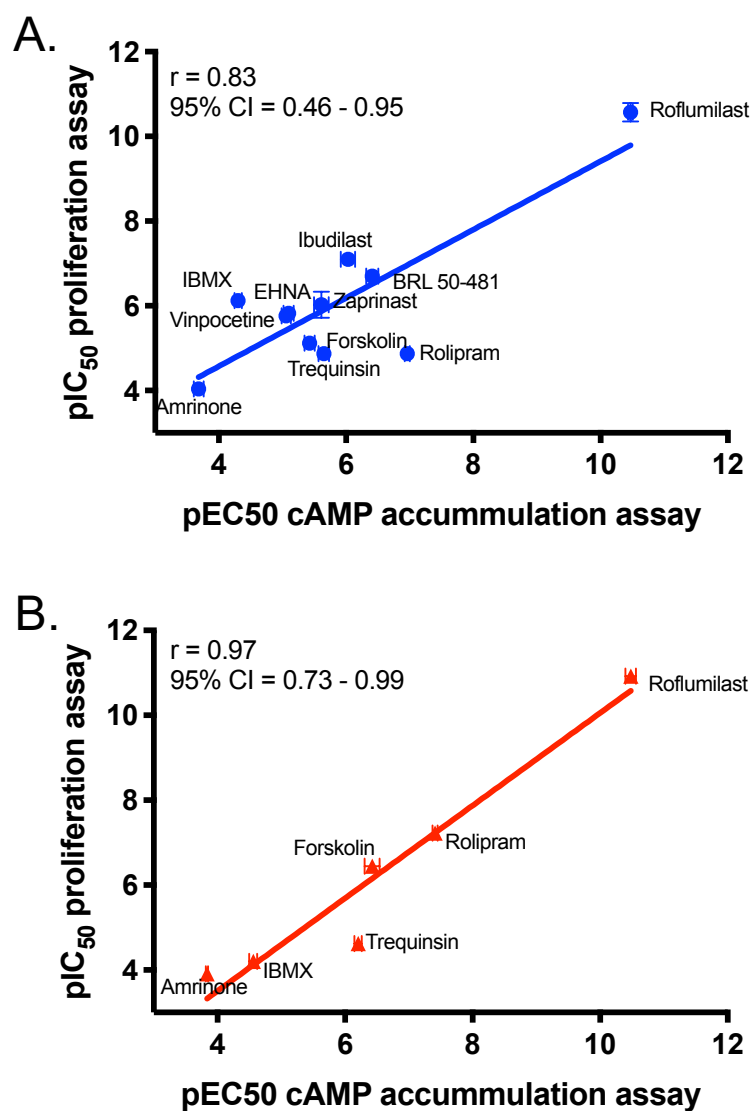


Figure 3.11 Elevation of intracellular cAMP is positively correlated with cell growth suppression. Correlation (with 95% confidence interval) of log potencies of each PDE inhibitor in C6 (A) and ST14A cells (B) was determined by calculating Pearson's correlation coefficient (r). Data are expressed as mean SEM of 4-8 individual repeats.

In addition, to easily compare the PDE inhibitors and determine which would be suitable for further investigation, "selection criteria" was calculated by multiplying the terms of efficacy (span) and affinity (potency) for each of the compounds.

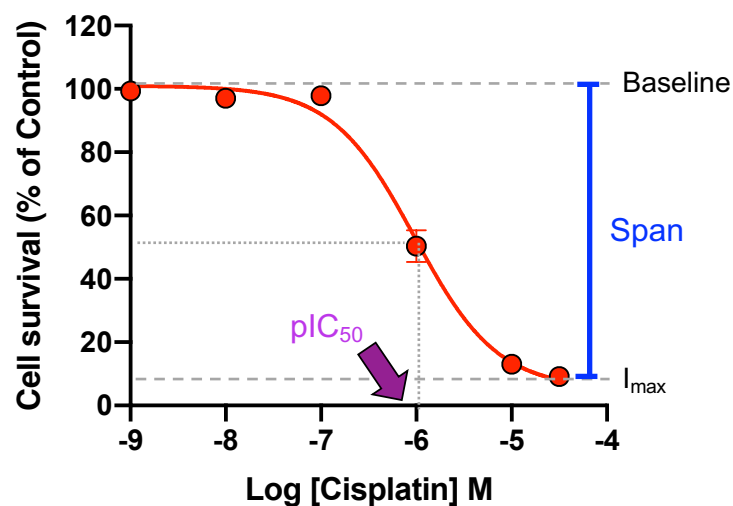


Figure 3.12 Illustration of how selection criteria are calculated. Displayed is cisplatin anti-proliferation curve on C6 cells, the selection criteria of cisplatin can be quantified by multiplying the terms of efficacy (span) and affinity (potency).

These criteria are expressed as arbitrary units with 200 set as the lower threshold. All compounds that exceeded this number were considered worthy of further study. In this calculation, cisplatin, a non-selective cytotoxic agent, was used as a reference compound to validate this approach. Cisplatin exhibited a potent anti-proliferative effect in both cell lines (Figure 3.13 and Table 3.5), displaying the highest selection criteria values (582.1 in C6 cells and 511.1 in ST14A cells). This proves that this calculation may be beneficial in determining how efficacious the compounds are at inhibiting cell growth.

According to selection criteria, the following compounds surpassed the threshold in C6 cells: vinpocetine (PDE1 inhibitor), amrinone, milrinone (both PDE3 inhibitors), ibudilast (PDE4 inhibitor), trequinsin, IBMX and zaprinast (multiple PDE isoform inhibitors), BRL50481 (PDE7 inhibitor) and forskolin. A comparison of the PDE isoenzymes targeted by these inhibitors with the mRNA expression levels in C6 cells showed a good correlation (Figure 3.4). Following on from this, we set a selection criteria value of 350 as more rigorous threshold. Some compounds including forskolin, trequinsin, amrinone, and IBMX also passed this more stringent threshold. With the exception of amrinone, the aforementioned compounds are suggested to target other components out of cAMP synthesis and degradation pathways, thereby explaining their superior potency and efficacy.

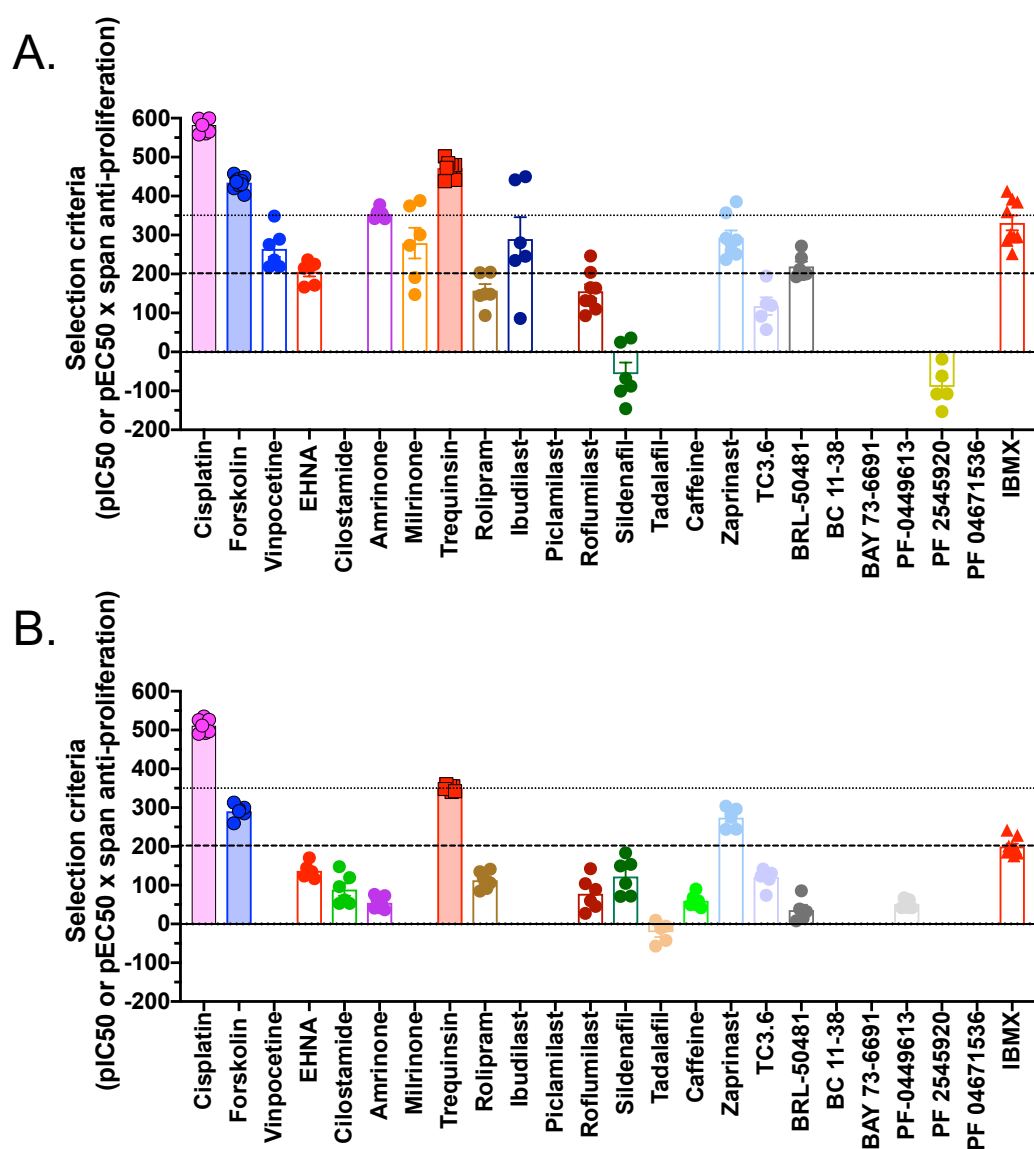


Figure 3.13 Selection criteria of each PDE inhibitor including forskolin and cisplatin. Compound selection criteria from C6 (A) and ST14A cells (B) was calculated based on potency and efficacy in proliferation assay. The dashed lines represent threshold value of 200 (less stringent criteria) and the dotted lines a higher criteria value of 350. Individual data point was obtained from Figures 3.9 – 3.10

While IBMX acts as non-selective PDE inhibitor, it also antagonises the action of the adenosine A1 receptor (Morgan, Murray and Challiss, 1993). Similarly, zaprinast - a non-selective PDE5,6,9,11 inhibitor, has also been reported to be a GPR35 agonist (Taniguchi, Tonai-Kachi and Shinjo, 2006). For this reason, IBMX and zaprinast were excluded from future investigations. In ST14A cells, all tested compounds showed lower selection criteria values, which was correlated well with the lower PDE expression compared to C6 cells (Figure 3.4). Taken together, compounds that are considerably efficacious in rat glioma models demonstrate reliance on the expression of each PDE isoenzymes.

3.5 Combinatorial effect of individual PDE2, PDE3, and PDE7 inhibitor was similar to that of, a multitarget PDE inhibitor trequinsin

Trequinsin has been showing to be the most potent compound at increasing cAMP levels and suppressing cell growth in C6 and ST14A cells. Upon 72 h treatment with forskolin, cell density was lower, but in terms of cell morphology, there was no significant difference to that of vehicle control (Figure 3.14). There was a substantial feature that was observed under the microscope. The remaining cells were considered metabolically active demonstrated by limited absorbance in cell proliferation assay, but cells underwent significant morphological changes compared to either vehicle control or forskolin. However, this effect was not observed in trequinsin with lower concentration nor PDE inhibitor cocktail.

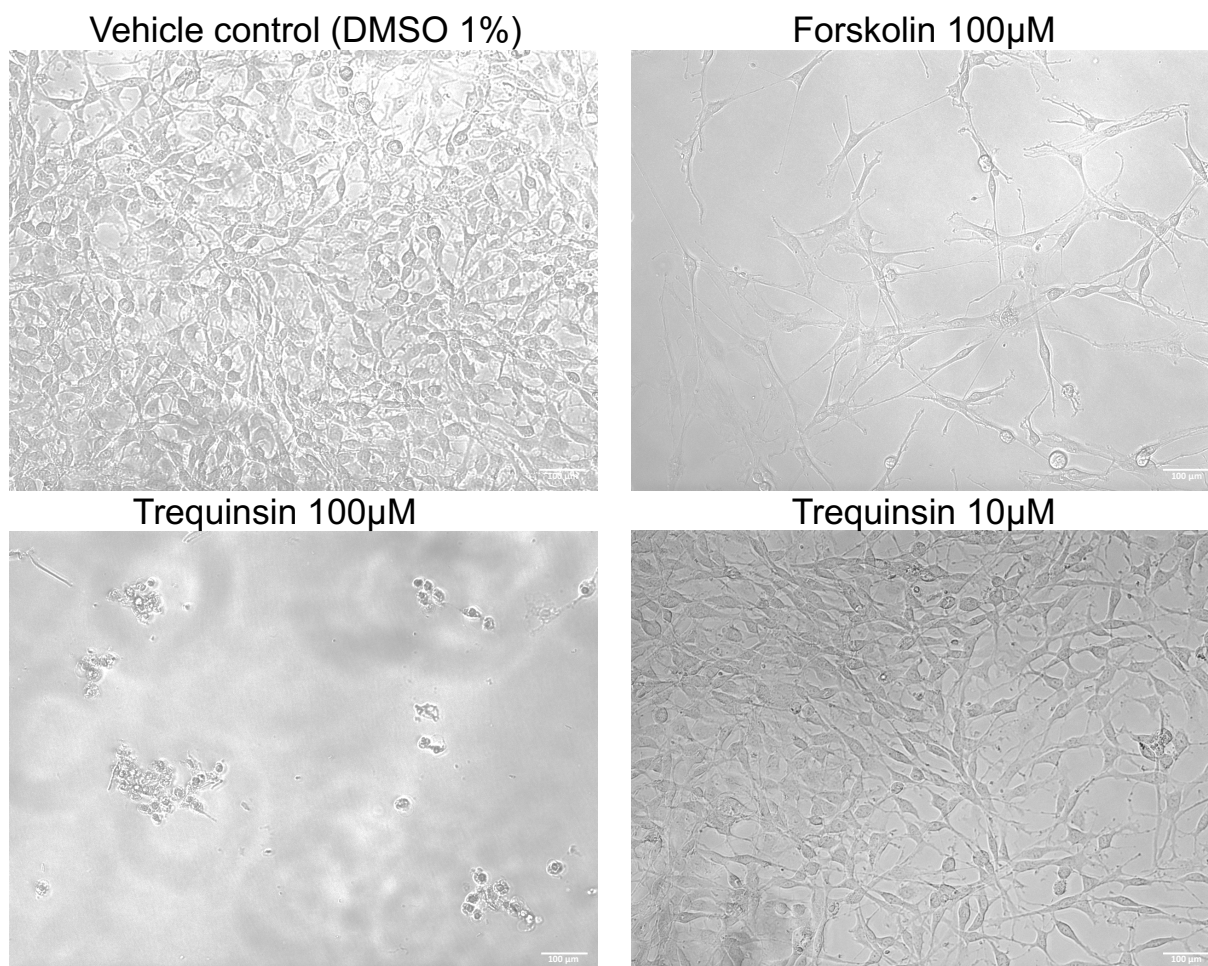


Figure 3.14 Trequinsin may have potential toxic effect compared to forskolin at the same concentration. The figures are representative of C6 cells upon 72 h treatment with DMSO 1% as vehicle control, forskolin 100 µM, trequinsin 100 µM, and trequinsin trequinsin. Whilst the cell density was suppressed in forskolin treated group,

morphological changes as well as cell condensation were observed in trequinsin 100 μM group but not in trequinsin lower concentration.

Although trequinsin is commonly known to inhibit mainly PDE3, another report suggests it also inhibits PDE2 and PDE 7 in hydrolysing cAMP (Rickles *et al.*, 2010). However, there has not been any comprehensive study probing the mechanism of action of trequinsin. Therefore, in this study, further investigation was performed to address this particular aspect by using individual PDE2, PDE3, and PDE7 inhibitors – EHNA, amrinone, and BRL-50481.

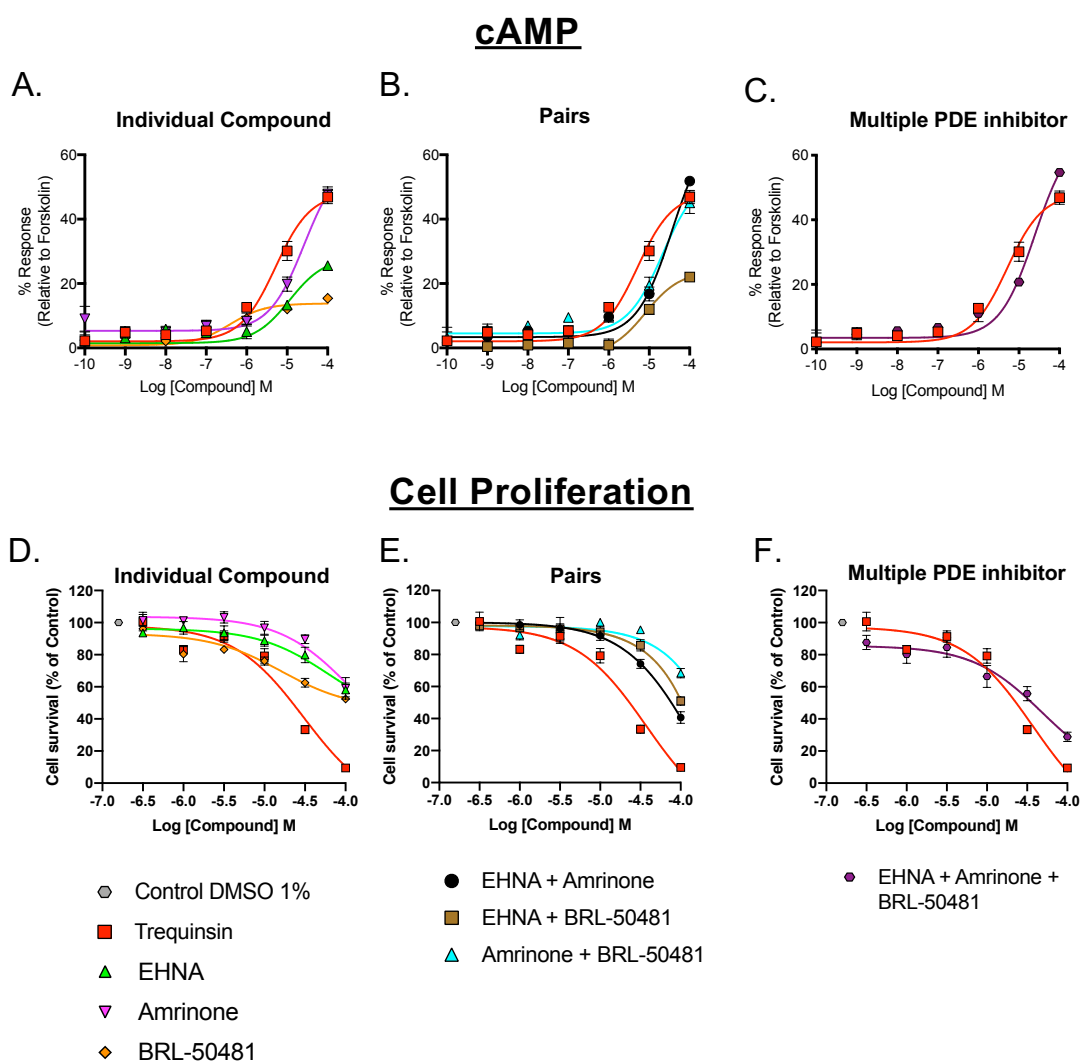


Figure 3.15 The effect of trequinsin on cAMP production and cell proliferation can be mimicked by combining PDE2, 3, and 7 inhibitors. cAMP accumulation was determined in C6 cells following 30-minute stimulation with EHNA, Amrinone, or BRL-50481 alone (A), in pairs (B), or in combination (C). Data are expressed relative to 100 μM forskolin. Cell survival was determined in C6 cells following 72 hours incubation with EHNA, Amrinone or BRL-50481 alone (D), in pairs (E), or combined (F). Data are expressed as percentage of cell proliferation relative to vehicle from 6-9 data sets. The

effect of trequinsin alone is displayed on each graph for comparison. All data are the mean \pm SEM of 6–9 individual repeats.

In this experiment, C6 cells were stimulated with PDE inhibitors alone, in pairs, and combination of all three (PDE inhibitor cocktail). It is evident that none of the individual treatments displayed better activity than trequinsin in both cAMP signalling and cell proliferation, with all showing reduced potency and/or efficacy (detailed in Table 3.7). Although BRL-50481 was more potent in ligand-mediated cAMP accumulation (pEC_{50} 6.20 ± 0.34), its span parameter was far less amongst the compound tested (13.86 ± 0.74 %). A similar pattern was also shown in cell proliferation. Despite having a similar maximal cAMP response to trequinsin, amrinone was only able to suppress cell proliferation by $\sim 50\%$ relative to trequinsin. Interestingly, although treatment in pairs did not equal the activity of trequinsin, the activity of compounds was improved compared to the individual treatments, indicated by a larger magnitude of cell growth suppression. When the individual PDE2, PDE3, and PDE7 inhibitors were used in combination, surprisingly, the effect was comparable to that of trequinsin (Figure 3.14). It is clearer to see the improvement of efficacy/potency by comparing the selection criteria values from each treatment (Table 3.7). While the combination in pairs showed larger numbers compared to individual compounds, the PDE inhibitor cocktail (containing all three blockers) displayed a similar value to that of trequinsin. Taken together, these indicate that activity of trequinsin can be mimicked by concomitant inhibition of PDE2, PDE3, and PDE7.

Table 3.7

C6- proliferation assay-combinatorial effect of PDE2, 3, 7 inhibitors

| Compound | cAMP accumulation assay | | Proliferation Assay | | Selection criteria* |
|-----------------------------|-------------------------|----------------|---------------------|------------------|---------------------|
| | pEC_{50} | Span (%) | pIC_{50} | Span (%) | |
| Trequinsin | 5.33 ± 0.11 | 46.3 ± 1.9 | 4.52 ± 0.11 | 91.21 ± 8.3 | 411.94 ± 38.52 |
| EHNA | 4.91 ± 0.10 | 26.2 ± 0.9 | 4.20 ± 0.21 | 57.21 ± 10.5 | 240.44 ± 45.57 |
| Amrinone | 4.58 ± 0.04 | 53.9 ± 1.6 | 3.94 ± 0.15 | 87.79 ± 13.6 | 346.01 ± 55.26 |
| BRL-50481 | 6.20 ± 0.34 | 13.9 ± 0.7 | 4.79 ± 0.17 | 47.02 ± 4.5 | 225.39 ± 22.73 |
| EHNA + amrinone | 4.58 ± 0.03 | 62.5 ± 2.2 | 4.19 ± 0.17 | 85.97 ± 12.3 | 361.56 ± 53.66 |
| EHNA + BRL-50481 | 5.05 ± 0.20 | 27.2 ± 1.4 | 4.07 ± 0.13 | 77.77 ± 9.7 | 316.34 ± 40.85 |
| Amrinone + BRL-50481 | 4.65 ± 0.07 | 49.7 ± 2.9 | 3.77 ± 0.17 | 66.75 ± 11.9 | 248.98 ± 45.30 |
| EHNA + amrinone + BRL-50481 | 4.58 ± 0.07 | 64.9 ± 1.8 | 4.52 ± 0.14 | 84.64 ± 8.7 | 382.12 ± 41.10 |

Data are expressed as mean \pm SEM from 7-10 individual data.

* Compound selection criteria was calculated based on potency and efficacy in proliferation assay (data obtained from Figure 3.14).

3.6 Targeting both adenylyl cyclase and phosphodiesterase enhances anti-proliferative effect

According to previous data, growth-inhibitory actions in C6 glioma cells were mediated by activation of AC that directly synthesises cAMP or through prevention of cAMP degradation by inhibition of PDEs. Therefore, this study was extended to investigate if concomitant targeting of AC and PDEs may synergistically suppress cell proliferation. To do this, cells were exposed simultaneously to forskolin and trequinsin. The combinatorial effect was evaluated through measurement of cAMP accumulation and cell proliferation.

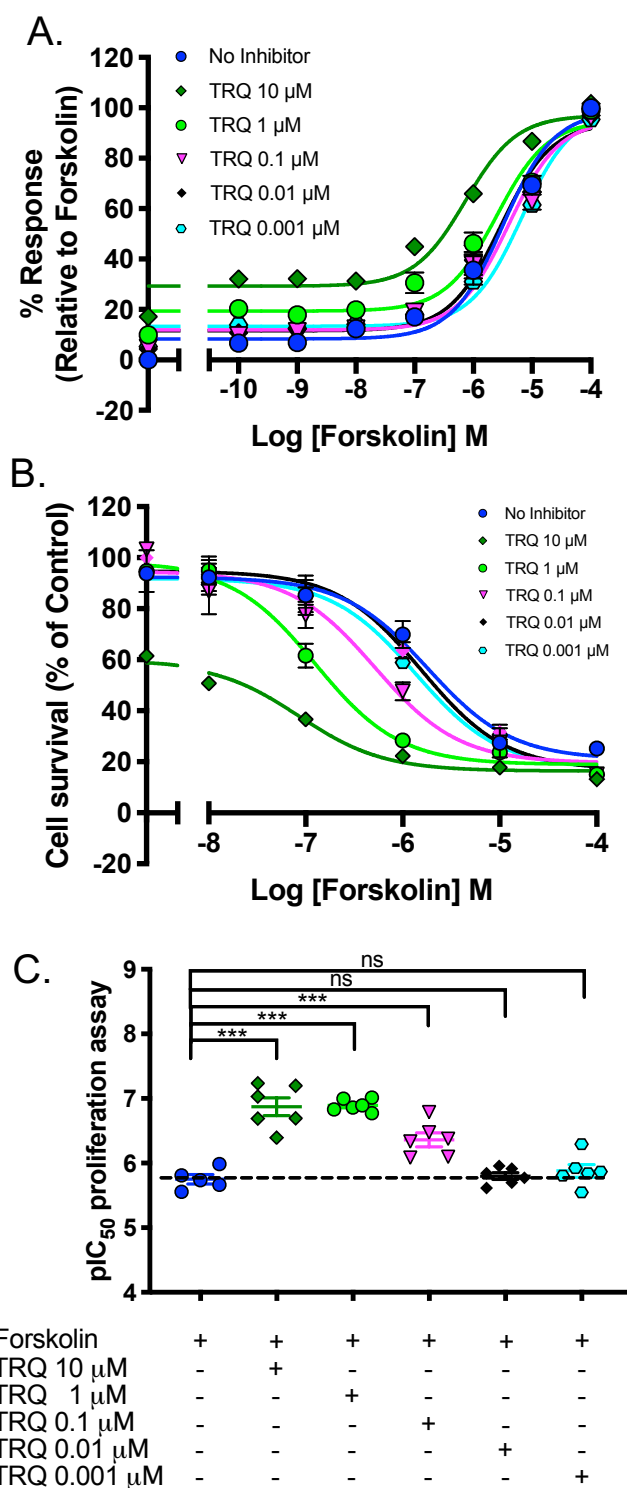


Figure 3.16 Forskolin and trequinsin act synergistically to increase cAMP accumulation and suppress cell growth. *A.* Concentration-dependent effect of trequinsin upon cAMP accumulation in C6 cells following 30 min stimulation with forskolin. Data are expressed relative to 100 μ M forskolin in the absence of trequinsin. *B.* Concentration-dependent inhibitory effect of trequinsin on C6 cell growth following 72-hour incubation with forskolin. Data are expressed as percentage cell survival relative to vehicle. *C.* pIC_{50} values for individual cell survival curves for each treatment condition. All data are the mean \pm SEM of 6-9 individual repeats. Data were determined

as statistically different (ns, not significant; ***, $p < 0.001$) compared to forskolin using one-way ANOVA followed by Dunnett's *post-hoc* analysis. TRQ – trequinsin.

In general, the effects of the co-treatment of forskolin and trequinsin was similarly on both cAMP assay and cell proliferation (Figure 3.16). Regarding cAMP accumulation assay, the baseline level was increased in a dose-dependent manner (Figure 3.16A). It is worth noting that the assay was conducted as end-point measurement. Therefore, an increase in basal levels may occurred due to accumulation of cAMP that was not degraded by trequinsin. Not only did combination elevate accumulation of cAMP levels (Figure 3.16A), it also dose-dependently increased the anti-proliferative effect (Figure 3.16B and C). The addition of trequinsin synergistically potentiated forskolin-mediated cell growth suppression, with the potency (IC_{50}) of forskolin with 10 μ M trequinsin was enhanced to 6.87 ± 0.13 compared to 5.75 ± 0.07 for forskolin only. Of note, co-treatment of forskolin with trequinsin also elevated baseline level in cAMP accumulation assay. Trequinsin as multiple PDE inhibitor prevents the breakdown of produced cAMP. As mentioned previously, this assay was performed as end-point experiment, so that the elevated basal level was most likely due to accumulation of cAMP over 30-minute stimulation. In addition, cell growth was also suppressed in the combination of forskolin and trequinsin 10 μ M. The observable effect at the lowest concentration of forskolin was possibly a result of trequinsin activity alone. Taken together, these data proved that targeting both AC and PDEs exhibiting synergistically increases cAMP signalling and enhances the magnitude of growth suppression.

3.7 Blockade of cAMP export enhances the anti-proliferative effect of forskolin, trequinsin, and the PDE inhibitor cocktail

The spatiotemporal signalling of cAMP is also controlled by an ATP-binding cassette (ABC) transporter, such as multidrug resistant protein 4 (MRP4). These proteins act as drug efflux transporters that are responsible for the transport of cAMP into the extracellular environment. As previously mentioned, brain tumour tissues have significantly lower concentration of cAMP (about 25%) compared to normal healthy brain tissue. Interestingly, C6 cells were reported to overexpress multidrug resistant protein 4 (MRP4), which may contribute to the lower content of cAMP. Thus, the study was extended to investigate if retaining cAMP within the intracellular compartment by pre-treating cells with PU23, an MRP4 inhibitor, will modulate cAMP levels and thus cell growth.

To determine the effect of cAMP efflux pump, the PDE inhibitor cocktail was also appended. Since there is potential toxic consequence by trequinsin, it was necessary to investigate if there are any differences between trequinsin and combination of PDE inhibitor on cAMP in extra- and intra-cellular regions.

The concentration of cAMP was monitored for 1h and 2h time-point in forskolin, whereas trequinsin and PDE inhibitor cocktail was evaluated for over 2h to increase window of observation. Upon 1h or 2h stimulation, pre-treatment with PU23 resulted in a dose-dependent reduction of extracellular cAMP levels compared to forskolin/ trequinsin/ PDE inhibitor cocktail alone (Table 3.8). Forskolin induced cAMP production up to 3 μ M, with less than 1 μ M of cAMP were detected extracellularly (Figure 3.17A). Without inhibiting cAMP efflux pump, cAMP was transported into extracellular compartment, whereas it was degraded intracellularly by the absence of PDE inhibitor (Figure 3.17B). The co-treatment of PU23 and forskolin marginally affected cAMP levels within the cells after 1h stimulation, interestingly, PU23 dose dependently reduced concentration of extracellular cAMP (Figure 3.17A). The clearer responses were observed over 2 h stimulation by forskolin where PU23 not only reduced the cAMP from being expelled, but also retained it in the intracellular compartment (Figure 3.17B). In general, intracellular levels of cAMP were slightly higher in PU23-treated cells in both trequinsin and PDE-inhibitor cocktail group (Figure 3.17 and Table 3.8).

When it comes to cell growth, co-treatment with PU23 also mediated dose-dependently anti-proliferative effect. These results suggest that in normal circumstances without PDE inhibitors, blockade of cAMP efflux transporter maintains higher levels of intracellular cAMP.

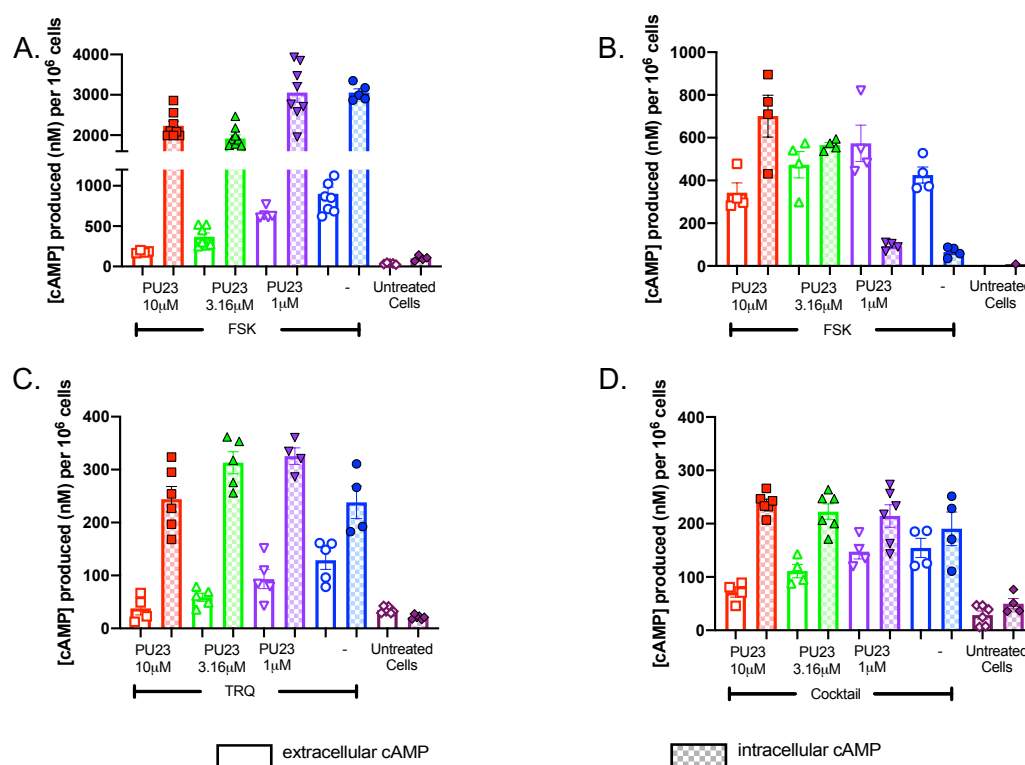


Figure 3.17 Inhibiting MRP4 transporter elevates intracellular levels of cAMP in C6 cells. Extracellular and intracellular cAMP levels from C6 cells following stimulation with; forskolin for 1h (A) and 2h (B); trequinsin for 2h (C); or PDE inhibitor cocktail for 2h (D), in the presence and absence of a range of concentrations of the MRP4 inhibitor, PU23. All data are the mean \pm SEM of 4-8 individual repeats. FSK – forskolin, TRQ – trequinsin. Additional repeats for this experiment were performed together with Dr. Ho Yang Yeung (University of Cambridge).

Table 3.8

Concentration of intra- and extra-cellular of cAMP in cells treated with forskolin, trequinsin, or PDE inhibitor cocktail in the absence or in the presence of PU23, an MRP4 inhibitor

| Group | cAMP concentration (nM per 10 ⁶ cells) | |
|-----------------------|---|--------------------|
| | Intracellular | Extracellular |
| Forskolin – 1h | | |
| Without inhibitor | 3058.00 \pm 90.49 | 900.50 \pm 84.75 |
| +PU23 10 μ M | 2232.00 \pm 112.40 | 181.70 \pm 8.08 |
| +PU23 3.16 μ M | 1918.00 \pm 89.75 | 368.40 \pm 46.61 |
| +PU23 1 μ M | 3057.00 \pm 240.60 | 648.50 \pm 30.88 |
| Untreated | 102.20 \pm 16.22 | 34.92 \pm 3.79 |
| Forskolin – 2h | | |
| Without inhibitor | 65.72 \pm 12.04 | 425.3 \pm 37.68 |
| +PU23 10 μ M | 701.20 \pm 97.98 | 343.30 \pm 45.37 |
| +PU23 3.16 μ M | 565.10 \pm 12.61 | 473.60 \pm 61.49 |
| +PU23 1 μ M | 93.30 \pm 9.45 | 573.50 \pm 84.97 |
| Untreated | 8.36 \pm 0.00 | N.R. |

| Group | cAMP concentration (nM per 10 ⁶ cells) | |
|------------------------------------|---|----------------|
| | Intracellular | Extracellular |
| Trequinsin – 2h | | |
| Without inhibitor | 238.20 ± 30.57 | 128.90 ± 17.35 |
| +PU23 10 µM | 244.10 ± 24.07 | 37.84 ± 12.40 |
| +PU23 3.16 µM | 313.10 ± 20.79 | 58.81 ± 7.56 |
| +PU23 1 µM | 325.50 ± 15.51 | 93.33 ± 18.02 |
| Untreated | 21.15 ± 1.58 | 34.45 ± 2.47 |
| PDE inhibitor cocktail – 2h | | |
| Without inhibitor | 190.40 ± 21.46 | 154.50 ± 18.11 |
| +PU23 10 µM | 237.90 ± 7.97 | 71.66 ± 9.39 |
| +PU23 3.16 µM | 222.60 ± 14.48 | 111.10 ± 12.50 |
| +PU23 1 µM | 214.40 ± 21.12 | 147.60 ± 13.72 |
| Untreated | 49.83 ± 9.59 | 28.42 ± 7.68 |

N.R. – no results because the values were undetectable

Data are expressed as mean ± SEM of 4-8 individual data. Concentration of cAMP in both extracellular and intracellular have been recalculated to the standard curve and is expressed in nM unit per 10⁶ cells.

Combination with forskolin, trequinsin, or the PDE inhibitor cocktail potentiated anti-proliferative effects compared to each compound alone (Figure 3.18). Forskolin, in the absence of PU23 dose-dependently suppressed cell growth displaying potency of 5.39 ± 0.88 . It was only PU23 10 µM that potentiated forskolin-mediated antiproliferative effect. While there was no significant effect on potency/span values while forskolin is combined with PU23 1 µM, the span of inhibitory effect is significantly reduced from 95.12 ± 3.55 % to 36.27 ± 1.43 % and 60.74 ± 3.83 % in combination with PU23 10µM and 3 µM, respectively (Table 3.8). The similar pattern was also observed in trequinsin- and PDE inhibitor cocktail- treated cells. While co-treatment with PU23 1 µM barely affected anti-proliferative effect of the compounds, the presence of MRP4 inhibitor both 10 µM and 3 µM increased potency of trequinsin and combination of PDE inhibitor (table 3.8). In conclusion, efforts to increase intracellular cAMP lead by inhibiting efflux transporter led to more potent cell growth suppression.

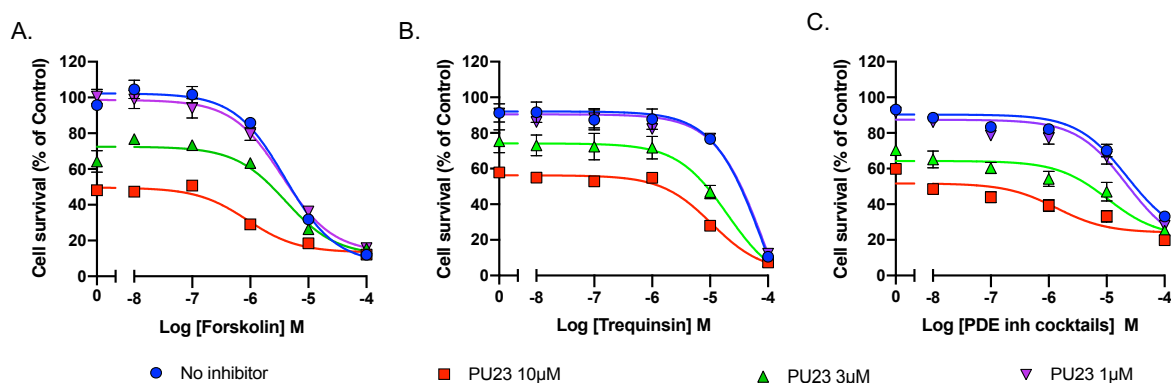


Figure 3.18 Elevation of intracellular cAMP by inhibiting its efflux is correlated with cell growth suppression in C6 cells. Survival of C6 cells following 72-hour treatment with forskolin (A), trequinsin (B), or PDE inhibitor cocktail (C) in the absence and presence of increasing concentrations of PU23, an MRP4 inhibitor. Data are expressed as percentage cell survival relative to vehicle. All data are the mean \pm SEM of 4-8 individual repeats. FSK – forskolin, TRQ – trequinsin.

Table 3.9

Pharmacological parameter of forskolin, trequinsin, PDE inhibitor cocktail on modulating cell proliferation

| Group | Bottom (%) | Top (%) | pIC ₅₀ | Span (%) | n |
|------------------------|------------------|-------------------|--------------------|-------------------|---|
| Forskolin | | | | | |
| No inhibitor | 7.18 \pm 3.38 | 102.30 \pm 1.63 | 5.40 \pm 0.08 | 95.1 \pm 3.6 | 8 |
| PU23 10 μ M | 13.33 \pm 0.97 | 49.60 \pm 1.15 | 6.05 \pm 0.07*** | 36.3 \pm 1.4*** | 7 |
| PU23 3 μ M | 11.75 \pm 3.63 | 72.49 \pm 1.88 | 5.39 \pm 0.13 | 60.7 \pm 3.8*** | 7 |
| PU23 1 μ M | 13.22 \pm 4.10 | 98.65 \pm 2.22 | 5.45 \pm 0.11 | 85.4 \pm 4.4 | 8 |
| Trequinsin | | | | | |
| No inhibitor | 10.60 \pm 1.05 | 89.4 \pm 2.01 | 4.07 \pm 0.30 | 89.4 \pm 1.0 | 3 |
| PU23 10 μ M | 7.35 \pm 1.56 | 50.54 \pm 2.21 | 4.97 \pm 0.10** | 50.5 \pm 1.2** | 6 |
| PU23 3 μ M | 7.80 \pm 1.67 | 67.51 \pm 6.49 | 4.70 \pm 0.29* | 67.5 \pm 8.1 | 7 |
| PU23 1 μ M | 12.21 \pm 0.86 | 78.67 \pm 2.62 | 4.03 \pm 0.36 | 78.7 \pm 1.4 | 3 |
| PDE inhibitor cocktail | | | | | |
| No inhibitor | 20.43 \pm 6.60 | 90.33 \pm 1.50 | 4.65 \pm 0.14 | 69.9 \pm 6.5 | 4 |
| PU23 10 μ M | 24.05 \pm 3.26 | 51.70 \pm 2.35 | 5.87 \pm 0.29* | 27.6 \pm 3.8*** | 4 |
| PU23 3 μ M | 21.56 \pm 5.60 | 64.29 \pm 2.10 | 4.98 \pm 0.28 | 42.7 \pm 5.7*** | 4 |
| PU23 1 μ M | 15.14 \pm 8.64 | 87.42 \pm 2.05 | 4.66 \pm 0.18 | 72.3 \pm 8.5 | 4 |

Data are expressed as the mean \pm SEM of n individual data

Data were determined as statistically different (*, $p < 0.05$; **, $p < 0.01$; ***, $p < 0.001$) compared to no inhibitor using one-way ANOVA followed by Dunnett's *post-hoc* analysis.

3.8 Anti-proliferative effects of forskolin and PDE inhibitors are predominantly mediated through the cAMP/PKA signalling pathway

To delineate which downstream pathways are involved in cAMP-mediated cell growth suppression, small molecule inhibitors of cAMP and cGMP downstream effectors was utilised, including inhibitors against PKA, Epac, GC activation and PKG. KT5720 was selected to inhibit PKA, ESI-09 to non-selectively block both Epac subtypes, CE3F4 for Epac1, HCJ0350 for Epac2, BAY 41-8543 as GC activator, and KT5823 to inhibit PKG.

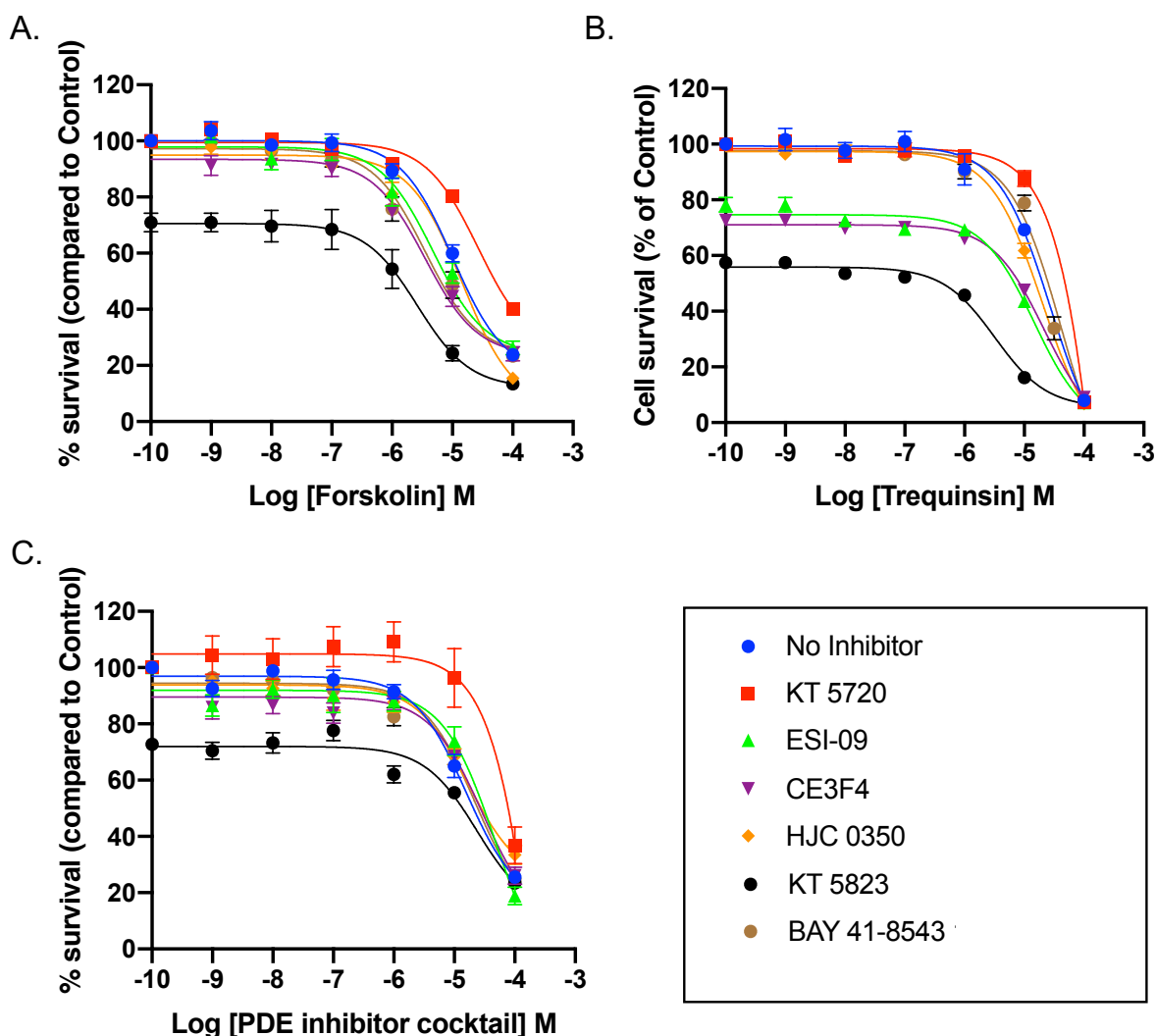


Figure 3.19 Forskolin, trequinsin, or PDE inhibitor cocktail-mediated anti-proliferative effect was partially rescued by PKA inhibitor, but not EPAC or PKG inhibitor. Cell survival was determined in C6 cells following 72 hours incubation with forskolin (A), trequinsin (B), or a combination of PDE2,3,7 inhibitors (C) in the presence of either KT5720 (10 μ M), ESI-09 (10 μ M), CE3F4 (10 μ M), HJC0350 (10 μ M), KT5823 (10 μ M), BAY41-8543 (10 μ M). Data are represented as dose response curve relative to control vehicle. KT5720 – PKA inhibitor, ESI-09 - non-selective Epac1/2 inhibitor,

CE3F4 – Epac1 inhibitor, HJC0350 - Epac2 inhibitor, KT5823 PKG inhibitor, BAY41-8543 – GC activator.

Individual dose-response curves for cell proliferation (Figure 3.19) showed that co-treatment with KT5720 attenuated the anti-proliferative effect of forskolin, indicated by reduction in potency from 4.95 ± 0.09 to 4.53 ± 0.08 (Table 3.9, $p < 0.01$). The similar pattern was also displayed in trequinsin- and PDE inhibitor cocktail- treated cells. Whilst the potency (pIC_{50}) of trequinsin was 4.80 ± 0.03 , co-treatment with KT5720 reduced trequinsin-mediated anti-proliferation potency to 4.60 ± 0.03 (Table 3.9, $p < 0.001$). The presence of PKA inhibitor also attenuated antiproliferative effect of the inhibitor cocktail to pIC_{50} : 4.49 ± 0.03 compared to the compound alone 4.74 ± 0.09 (Table 3.9, $p < 0.05$).

Dual or selective inhibition of Epac did not significantly affect the cell growth response, with the exception of when ESI-09 or CE3F4 with trequinsin (Figure 3.19B) indicated by smaller spans, although no difference was observed in its potency (Table 3.9 and Figure 3.20). Interestingly, concurrent treatment with KT5823, a PKG inhibitor enhanced cell growth suppression compared to all individual treatments indicated by smaller span, but no potentiation on pIC_{50} on forskolin and trequinsin-treated cells were observed (Table 3.9, $p < 0.01$ in forskolin group, $p < 0.001$ in both trequinsin and combination of PDE inhibitors). Whereas BAY 41-8543 increased potency in forskolin-treated cells ($p < 0.01$), but not other groups. The suppression of cell growth in combination with KT5823 suggest that it may not purely inhibit the activity of PKG. The effect of GC inhibition on the forskolin response indicates a possible involvement of GC/cGMP pathway in cell proliferation. All data suggest that suppression in cell growth is mainly mediated through the cAMP/PKA-dependent pathway.

Table 3.10

Pharmacological parameters of forskolin, trequinsin, and PDE inhibitor cocktail in the absence and presence inhibitors targeting downstream effectors of cAMP and cGMP signalling

| Group | pIC_{50} | Span (%) | n |
|-------------------------|-----------------------|---------------------|----|
| <i>Forskolin</i> | | | |
| No inhibitor | 4.95 ± 0.09 | 83.6 ± 3.3 | 16 |
| + KT5720 | $4.53 \pm 0.08^{**}$ | 75.4 ± 3.7 | 20 |
| + ESI-09 | 5.31 ± 0.12 | 74.1 ± 3.9 | 8 |
| + CE3F4 | $5.42 \pm 0.12^{**}$ | 70.0 ± 3.1 | 7 |
| + HJC0350 | 4.82 ± 0.06 | 90.4 ± 4.6 | 8 |
| + KT5823 | $5.66 \pm 0.12^{***}$ | $58.6 \pm 4.9^{**}$ | 7 |
| + BAY 41-8543 | $5.43 \pm 0.10^{**}$ | 74.9 ± 2.8 | 7 |

| Group | pIC ₅₀ | Span (%) | n |
|-------------------------------|-------------------|---------------|---|
| Trequinsin | | | |
| No inhibitor | 4.80 ± 0.03 | 101.3 ± 2.8 | 9 |
| + KT5720 | 4.60 ± 0.03*** | 103.0 ± 2.5 | 9 |
| + ESI-09 | 4.81 ± 0.02 | 76.9 ± 1.0*** | 7 |
| + CE3F4 | 4.89 ± 0.04 | 75.8 ± 2.6*** | 9 |
| + HJC0350 | 4.87 ± 0.04 | 96.9 ± 1.2 | 9 |
| + KT5823 | 5.48 ± 0.03*** | 50.2 ± 1.4*** | 9 |
| + BAY 41-8543 | 4.72 ± 0.03 | 90.0 ± 0.0 | 7 |
| PDE inhibitor cocktail | | | |
| No inhibitor | 4.74 ± 0.09 | 87.4 ± 2.7 | 9 |
| + KT5720 | 4.49 ± 0.03* | 73.4 ± 2.0* | 9 |
| + ESI-09 | 4.65 ± 0.04 | 80.8 ± 2.5 | 8 |
| + CE3F4 | 4.51 ± 0.05 | 83.3 ± 3.9 | 9 |
| + HJC0350 | 4.68 ± 0.10 | 75.0 ± 6.4 | 8 |
| + KT5823 | 4.82 ± 0.04 | 62.3 ± 2.9*** | 8 |
| + BAY 41-8543 | 4.66 ± 0.04 | 85.4 ± 3.3 | 6 |

Values are generated from n individual data after curve fitting from Figure. 3.21 and are expressed as mean ± SEM. Data were determined as statistically different (*, p < 0.05; **, p < 0.01; ***, p < 0.001) compared to in the absence of compounds using one-way ANOVA followed by Dunnett's *post-hoc* analysis.

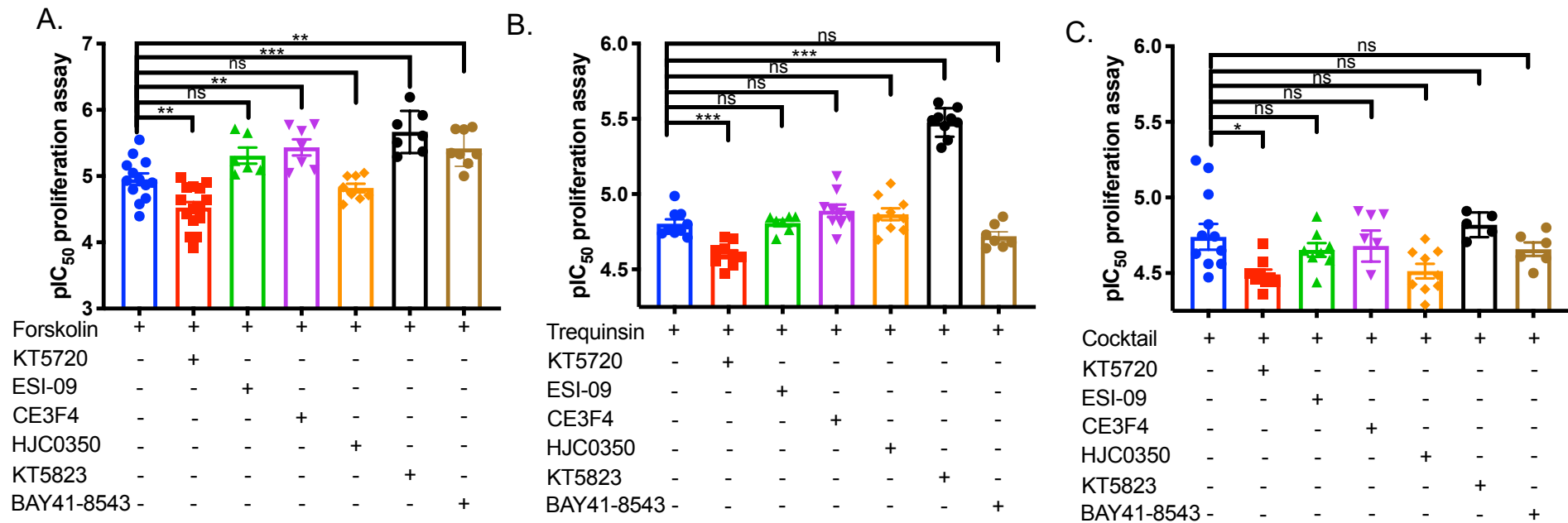


Figure 3.20 The effect of downstream effectors of cAMP and cGMP on forskolin and trequinsin-mediated cell growth suppression of C6 cells. Cell survival was determined in C6 cells following 72 hours incubation with forskolin (A), trequinsin (B), or a combination of PDE2,3,7 inhibitors (C) in the presence either KT5720 (10 μ M), ESI-09 (10 μ M), CE3F4 (10 μ M), HJC0350 (10 μ M), KT5823 (10 μ M), or BAY41-8543 (10 μ M). Data are represented as individual pIC_{50} values for anti-proliferation curves for each treatment condition (Fig. 3.20). Data were determined as statistically different (ns, not significant; *, $p < 0.05$; **, $p < 0.01$; ***, $p < 0.001$) compared to in the absence of compounds using one-way ANOVA followed by Dunnett's *post-hoc* analysis.

3.9 Trequinsin, but not forskolin or the PDE inhibitor cocktail, has cAMP-independent actions leading to apoptosis

Having confirmed strong association between cAMP signalling and anti-proliferative effect, we sought to determine the mechanism of how forskolin, trequinsin, and the PDE inhibitor cocktail inhibit cell growth. To do this, the effects of the compounds on apoptosis and cell death were explored.

Apoptosis is a cell death programme that is activated if there are any abnormalities within cells. Caspase activity, especially caspase-3 and -7, has been reported to be a biomarker to detect early apoptosis. To detect activation of caspase-3 and -7, treated cells were labelled with CellEvent™ Caspase-3/-7 and the number of cells that positively emitted fluorescence (green) was counted using the appropriate filter (Figure 3.21). Cells were also stained with nuclei-dye Hoechst 33342 to determine total cell number (cells in blue), and propidium iodide (PI) to label non-viable cells (in red) (Figure 3.21).

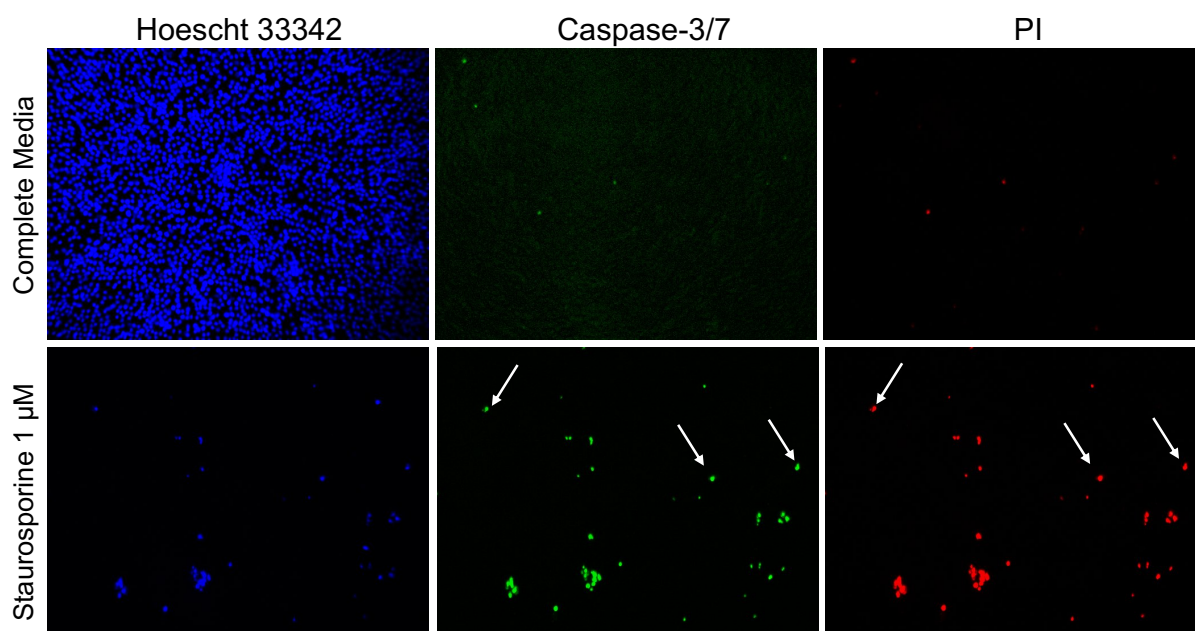


Figure 3.21 Representative figure of C6 cells after 72 hours treatment and were subsequently loaded with 2 μM CellEvent™ caspase-3/-7. Representative figures of C6 cells were displayed after being treated with Staurosporine 1 μM in comparison with complete media. Images were taken using BD Pathway 855 Biomiaging Systems utilising 3 different filters to visualise total cell number (using Hoescht filter), activated caspase-3/-7 (using FITC filter), and dead cells (using propidium iodide (PI) filter). Arrows pointed to cells that were labelled as positive caspase-3/7 (green) or non-viable cells (red). The number of activated caspase-3/-7 or dead cells were counted and subsequently normalised to total cell number. Percentage of cell population for each treatment was summarised in Figure 3.22 as the mean \pm SEM.

Staurosporine, a pan-caspase activator was used as the reference compound. As displayed in Figure 3.21, cells that were cultured in complete media showed many cells with a minimal number of dead cells and/or with activated caspase-3/-7. In contrast, cells that were treated with staurosporine were far less numerous, indicating cell death and significant caspase-3/-7 activation. This finding is also supported by PI staining showing that all cells with activated caspase-3/-7 were dead. Using the same method, the cell population with activated caspase-3/-7 and dead cells were quantified in similar method for all treated groups and the summary was in Figure 3.22. While treatment with forskolin or the PDE inhibitor cocktail resulted in <10% of the population with activated caspase, only trequinsin 100 μ M-treated cells showed a comparable response to that of staurosporine (Figure 3.22). These data indicate that trequinsin at a high dose may have non-specific actions leading to cell death, which is not observed for forskolin or the combination of PDE inhibitors.

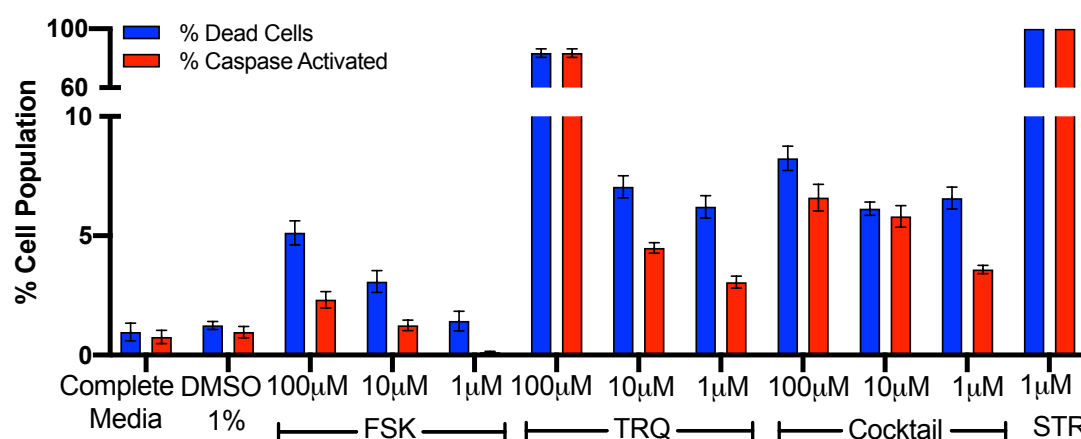


Figure 3.22 Population of dead cells and activity of caspase-3/7 in C6 cells after 72 h treatment. Percentage of dead cells determined by staining with propidium iodide and the percentage of cells with activated caspase-3/7, visualised by CellEvent™ caspase-3/7. All values are normalised to total cell number in each well. Staurosporine 1 μ M was used as a control for apoptotic cell death and cause 100% dead cells. All data are the mean \pm SEM of 4-5 individual data. FSK – forskolin, TRQ – trequinsin, STR – staurosporine.

3.10 Elevated intracellular cAMP induces growth arrest at the G₂/M phase of the cell cycle

In the previous section, it has been shown that elevation of cAMP by forskolin or PDE inhibitor cocktail did not lead to apoptosis, in contrast to trequinsin at a higher dose (100 μ M). We hypothesised that the different biological responses observed for

forskolin-, PDE inhibitor cocktail-, and trequinsin low dose- treated cells may relate to the compounds effect on the cell cycle.

In normal cell cycle, about 60% of cell population were distributed in G_0/G_1 phase, where approximately 35% were evenly distributed between G_2/M and S phase, and a very little amount of aneuploids. Interestingly, forskolin and PDE inhibitor cocktail altered cell cycle distribution thus cells were arrested at G_2/M phase up to ~70%. Whereas about 70% of cells became aneuploid in trequinsin-treated group. There was dose-dependent improvement on cell cycle distribution while lower concentration of compounds was used (Figure 3.23).

Further confirmation by FACS analysis, corroborated the findings from the previous section, whereby the dead cells population was dominantly observed in cells treated with 100 μ M trequinsin. The population of alive cells treated with trequinsin at a high dose were arrested in G_2/M phase and remaining cells were found to be in aneuploid. Cells were predominantly arrested in G_2/M phase, further suggesting non-apoptotic effect of forskolin and the PDE inhibitor cocktail. These results were also aligned with results in previous section (Figure 3.22). We concluded that both forskolin and the combination of PDE2, PDE3, and PDE7 inhibitor alter cell cycle by a similar mechanism. However, it is possible that the apoptotic effect of 100 μ M trequinsin is independently related to the cAMP pathway.

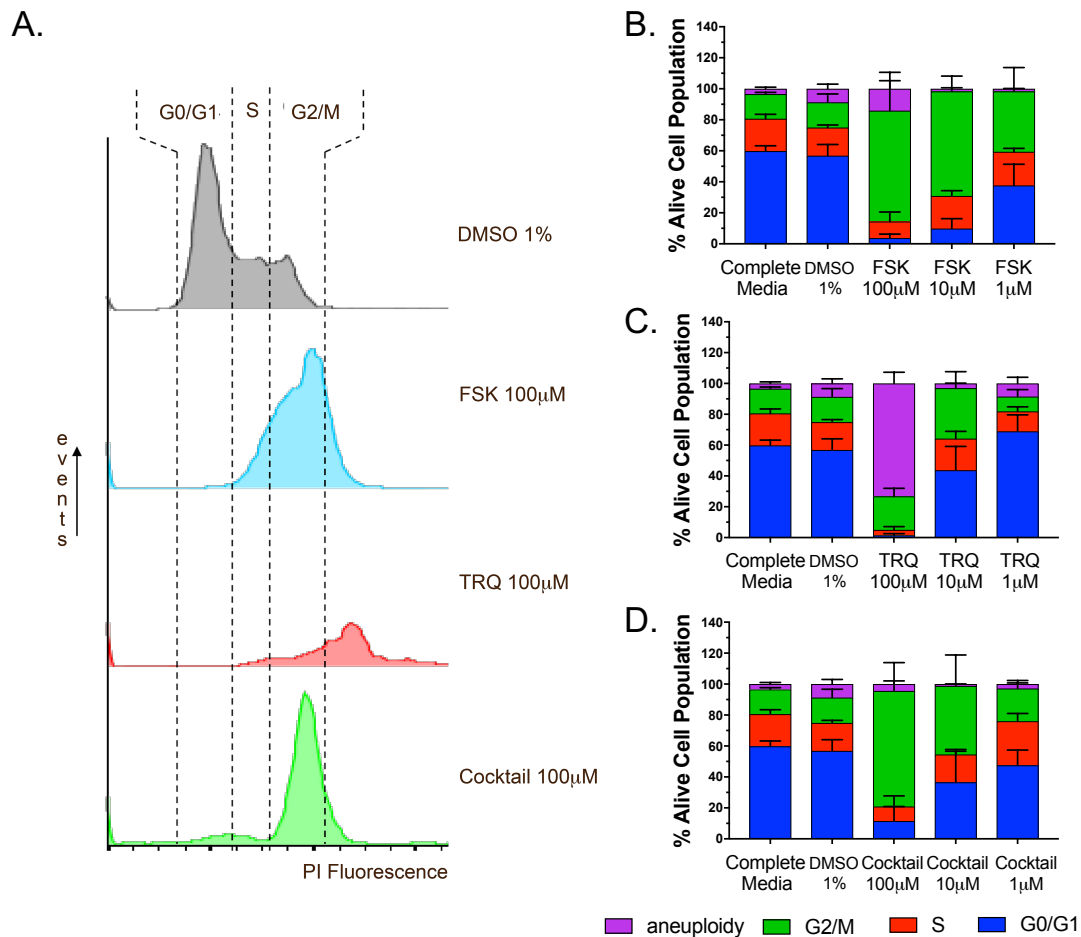


Figure 3.23 Cell cycle analysis by flow cytometry after PI staining. Representative histograms of cell cycle distribution of C6 cells were displayed with selected treatment (A). Histograms of cells following treatment with forskolin (B), trequinsin (C), or PDE2,3,7 inhibitor cocktail (D) for 72 h. The percentage of cell distribution for each treatment include G₁, S, G₂/M, and dead cell population (n= 4-8 individual data). All data are the mean \pm SEM. FSK – forskolin, TRQ – trequinsin, STR – staurosporine.

3.11 Discussion

As a secondary messenger, both cAMP and cGMP control a plethora of both physiological and pathological responses (Sutherland, 1972) which also include reparative processes and cell proliferation. However, the incongruity of cAMP effect on cell growth have been reported which seems to be depending on cell types and the machinery of the selected cells (Cullen *et al.*, 2004; Lerner and Epstein, 2006; Sawa *et al.*, 2017). External and internal factors including stimulus, intracellular effector of cAMP, and compartmentalizations appear to be the reason of divergent effect of cAMP (Insel *et al.*, 2012). As mentioned early on, cAMP concentration in brain tumors is 4-fold lower than that of healthy brain tissues (Furman and Shulman, 1977), it is

hypothesised that increasing intracellular concentration of cAMP may have beneficial effect in preventing cell growth.

3.11.1 C6 cells as a suitable model to investigate role of PDE isoenzymes in glioblastoma

Although C6 cells were originally derived from rats, their genotypic and phenotypic features resemble human glioblastoma (Grobben, De Deyn and Slegers, 2002). Therefore, most of the studies have used C6 cells to study tumour characteristic before moving forward to use human tissues. In terms of practicality to further investigate it in animal models, C6 cells have been widely explored as *in vivo* models to provide better resemblance with humans.

As previously mentioned, a reduction in cAMP concentration is found in brain tumour tissues. Besides, from the clinical studies collected from TCGA (details in chapter 1), PDE expression in brain tissues from glioblastoma patients was either upregulated or mutated. This data base may explain one factor that contributes to a lower level of cAMP in glioblastoma tissue. Having confirmed by rt-PCR (Figure 3.3), C6 cells showed higher expression of PDE at mRNA level than ST14A, rat medium spiny neurons as a comparison. This observation justifies that C6 cells can be used for further experimental validation to look over PDE roles in glioblastoma models.

3.11.2 Elevation of intracellular cAMP through PDE inhibition or AC stimulation elicited a more potent anti-proliferative effect compared to modulating at GPCR levels or G proteins

In this study, direct activation on AC or inhibition on PDE activity has been proven to exhibit to increase cAMP accumulation and suppress glioma cell proliferation. Other strategies to modulate G protein-mediated AC activation through. Although activation of Gs-coupled β -ARs by isoprenaline or modulation of G protein activity by PTx or CTx could elevate cAMP levels, none of them significantly demonstrated better efficacy in suppressing glioma cell growth. Targeting receptor or G proteins in this particular study seems to trigger transient activation of cAMP effectors, receptor desensitisation, or spatial localisation of cAMP within the cells that prevent further growth signalling. Not only does sustained stimulation using GPCR agonists cause receptor desensitisation, but it also may results in receptor downregulation because of changes in transcription levels (Hausdorff, Caron and Lefkowitz, 1990). It is also worth noting the chemical

instability of isoprenaline in aqueous solution may account for this effect; therefore, antioxidant addition may be beneficial to prevent degradation of isoprenaline.

3.11.3 The efficacy of PDE inhibitors demonstrates reliance on PDE expression profile

ST14A cells appeared to be more responsive than C6 cells by stimulation of forskolin indicated by smaller pEC₂₀ value (section 3.4.1). Since ST14A cells are considered normal and healthy cells, they have lower basal levels of cAMP; therefore, cells appear to be more responsive when stimulated by AC activator. Given that ST14A cells also expressed less PDE isoforms than C6 cells, ST14A cells may not possess sufficient tuning mechanism to control stimulation by cAMP. It is also worth noting there is a possibility that AC expression is higher in ST14A cells. However, this notion needs to be confirmed further.

This study is the first to dissect the pharmacological roles of PDEs in C6 glioma cells. As displayed in Figure 3.3, both C6 and ST14A expressed most PDE isoenzymes. As for PDE6, because these enzymes are specifically expressed in the eyes and involved in phototransduction (Zhang *et al.*, 2015), the role of PDE6 was excluded. However, specific inhibition on cAMP or cGMP PDEs showed minimal effects on cell proliferation, except ibudilast (cAMP-specific PDE4 inhibitor). While inhibition of PDE1, PDE2, PDE3, PDE4 and PDE7 increased cAMP accumulation in par with a more significant cell growth suppression. Apart from PDE4 and PDE7, PDEs mentioned earlier are known as dual-substrate PDE hydrolysing both cAMP and cGMP. This PDE category provides a function for crosstalk between both second messengers and possess distinct tuning mechanism (Surapisitchat *et al.*, 2007; Francis *et al.*, 2010).

3.11.4 Trequinsin as multiple PDE inhibitor may have the potential effect that is independent of cAMP/PKA and can be counteracted by combining individual PDE2, PDE3, and PDE7 inhibitor

Although trequinsin is firstly known as a PDE3 inhibitor, for the first time, this study has revealed the possible mechanism of action of trequinsin through multiple inhibitions of PDE2, PDE3, and PDE7. While there is a possibility of toxic effect by trequinsin, the combination of individual PDE2, PDE3, and PDE7 inhibitor exhibited similar affinity and efficacy in cAMP and cell proliferation assays to that of trequinsin. These effects, however, were less profound in either individual treatment or as in pair. Not only did

the PDE inhibitor cocktail showed similar efficacy, but also without significant toxic effect in C6 glioma cells. Trequinsin, especially at higher concentration, caused caspase activation leading to apoptosis. Although the cell number with activated caspase-3/7 in cocktail-treated cells is higher than that of forskolin, this effect was far less than trequinsin, the observable effect is likely due to available PDEs become caspase substrate (Lerner and Epstein, 2006)

Using several pharmacological tools, it appears that the observed effect of forskolin is mediated through cAMP/PKA pathways. This also applies to trequinsin and PDE inhibitor cocktails. cAMP has been known to preferentially bind to PKA over Epac1/2 with the affinity towards PKA to be 5 – 24.6 nM and 4 μ M/1.2 μ M towards Epac1/2 (Bubis, Saraswat and Taylor, 1988; Ringheim and Taylor, 1990; de Rooij *et al.*, 1998). Taken together, both stimulation at AC and inhibition of PDE induce the elevation of cAMP intracellularly, therefore PKA pathway may be prominently activated with the minor involvement of Epac1/2 leading to cell growth suppression. Anti-proliferative effect of cAMP also has been reported to involve complex mechanism between PKA, MAPK/ERK, and CDK2 (Vadiveloo *et al.*, 1997; Favot *et al.*, 2003). Cotreatment with PKG inhibitor, surprisingly, potentiated anti-proliferative effect of forskolin, trequinsin, and PDE inhibitor cocktail. Since some of PDEs act as dual substrate enzymes, it is possible that the effect was likely generated from cross-talk between secondary messengers.

Although PDE2 and PDE3 are known as dual substrate enzymes, the mechanism of regulation is distinct depending on cGMP concentration. Whilst hydrolysis rate of cAMP is allosterically modulated by cGMP at PDE2 (affinity 1-5 μ M), cGMP has a higher affinity to the catalytic site of PDE3 (180 nM) and elicited competitive binding at the same binding pocket of PDE3 with cAMP. (K Omori and Kotera, 2007b; T Keravis and Lugnier, 2012). Since C6 cells have weaker liability to produce cGMP, a moderate elevation on cGMP levels is likely to compete with cAMP to bind to the same catalytic sites, leading to slower degradation of cAMP by these particular PDEs. These events may predominantly activate PKA due to the net elevation of cAMP within the intracellular compartment. Subsequently, sustained elevation of intracellular cAMP through PDE inhibition may provide an adequate signal to promote anti-proliferative effect.

Whilst co-treatment using PKG inhibitor or GC activator enhances forskolin- and trequinsin-mediated cell growth suppression, no significant effect was observed in cocktail-treated cells. Despite there is a possibility that KT5823, a PKG inhibitor, does

not selectively inhibit PKG, the cellular compartmentalisation should be taken into account to explain the functional effect of PDE inhibitor cocktails. An increase in cGMP concentration may occur in particular regions leading to local activation of PKA, possibly via anchoring proteins (AKAP) that is specifically distributed into the different intracellular compartment (T Keravis and Lugnier, 2012). Indeed, this notion needs further investigation.

3.11.5 Forskolin and PDE inhibitor induces cell growth arrest

Whilst high doses of trequinsin caused caspase-3/7-dependent apoptosis, neither forskolin nor the PDE inhibitor cocktail showed substantial death upon 72 h treatment. In the case of trequinsin 100 μ M, it is possible that rapid and large elevation of cAMP causes cell failure to go through the normal cell cycle and unable to exit mitotic point. Although there have been no studies on the mechanism of trequinsin-mediated apoptosis and aneuploidy, it is suggested that PDE inhibitor may activate protein phosphatase 2A (PP2A) and Bim/BAD expression through phosphorylation of PKA which in the end activate caspase and promote apoptosis (Lerner and Epstein, 2006). Cells treated by forskolin and combination of PDE2, PDE3, and PDE7 were trapped prominently in G₂/M, demonstrating the possibility of failure to synthesise essential proteins for replication.

3.11.6 Modulation to increase cAMP concentration leads to negative regulation on cell growth

Although trequinsin may pose potential toxic effects, its ability to inhibit multiple PDEs is considerably better, displayed as the most potent PDE inhibitor to modulate both cAMP accumulation and cell growth suppression. To minimise the compound toxicity, the synergistic combination can be applied without compromising the efficacy and selectivity. In the previous section, it has been proven that the combination of forskolin and trequinsin can increase cAMP levels and display negative effect on cell proliferation. The combinatorial effect was shown to be better than forskolin alone, therefore the dose of each compound could be reduced.

Another effort to increase intracellular cAMP was conducted by targeting cAMP efflux transporter, namely MRP4. It is evident that this pump protein controls cAMP signalling and by blocking its activity, cAMP remains trapped within intracellular regions. The cAMP concentration was enhanced in all treated cells with forskolin,

trequinsin, and PDE inhibitor cocktail. The augmentation of cAMP has also potentiated the anti-proliferative action of each group.

3.11.7 Conclusion

This study has been conducted using pharmacological tools to explore potential roles of cAMP in inhibiting glioma cell growth. Forskolin elevated concentration of cAMP intracellularly which led to activation of PKA and altered cell cycle distribution. Whereas trequinsin as potent multiple PDE inhibitors not only elicited anti-proliferative effect through cAMP/PKA pathways, but also activated caspase-3/7 and induced cell death. Taken together, it is evident that trequinsin possess toxic effect that is independent from cAMP/PKA signaling. Combination of PDE2, PDE3, and PDE7 inhibitor has shown to be an alternative to trequinsin. The efficacy of PDE inhibitor cocktail is equipotent to that of trequinsin in glioma cells without having substantial toxic effect. In addition, synergistic mechanism is also found to potentiate cell growth suppression by concomitant targeting at AC and PDEs, therefore provides other strategies to minimise the adverse effect of trequinsin.

3.12 Summary

It has been reported that many signalling pathways are involved in malignancy leading to brain tumours. One of the abnormalities that was of interest on this study was the influence of the concentration of intracellular cAMP. Having reported to be associated with severity of malignancy, cancer cells have specific mechanism to maintain lower levels of cAMP. Here, we report findings to show that there is an association between increasing intracellular cAMP and suppression of cell proliferation.

Concentration of cAMP is tightly controlled by homeostasis between its synthesis and degradation. As a secondary messenger, cAMP also undergoes cross-talk mechanism with cGMP through sequestration of non-specific PDEs. Firstly, the investigation has been made covering direct activation on AC and activation on beta-adrenergic receptor and heterotrimeric G proteins. Secondly, we also look at the functionality of each PDE isoenzymes using small molecule inhibitors to tease out which PDEs are involved. This study also covered the possible mechanism between cAMP and cGMP in regulating cAMP levels as well as cell growth.

Although we have shown that GPCR or G protein-mediated cAMP elevation suppresses C6 cell growth, PDE inhibition and direct activation on AC demonstrate greater anti-proliferative effects. Forskolin suppresses cell growth in a PKA-dependent

manner by inducing cell arrest at G₂/M phase. In contrast, trequinsin (a non-selective PDE2, PDE3, and PDE7 inhibitor), not only inhibited cell growth via PKA, but also stimulated caspase-3/-7 independently of the cAMP/PKA pathway. Treatment with trequinsin was also shown to induce C6 cells to be aneuploidy phenotype. Interestingly, a cocktail of individual PDE2, PDE3, and PDE7 inhibitors suppressed cell growth in similar mechanism to forskolin. In addition, the PDE inhibitor cocktail activity is similar to that of trequinsin but without significant toxicity. Finally, we demonstrate that concomitant targeting of both AC and PDEs synergistically elevate intracellular concentration of cAMP and enhance anti-proliferative effects. In conclusion, targeting cAMP is a viable approach to suppress cell growth in glioma model.

CHAPTER 4

INVESTIGATING THE ROLE OF SECOND MESSENGERS IN HUMAN GLIOBLASTOMA CELLS

4.1 Introduction

Glioblastoma multiform (GBM) is the most common and fatal type of primary brain tumour that originates from astrocytes. Whilst its annual incidence is about 3.2 cases per 100,000 population (Cesarini *et al.*, 2017) or about 15% of all brain tumour cases, the recurrence rate is considerably high reaching 85%. In the UK, approximately 2200 cases of GBM are reported each year (Public Health England, 2014). Patients with glioblastoma have poor prognosis, with the overall median survival being 6 months. The major barrier to improving prognostic factors is the chemoresistance of these tumours. In addition, the understanding of the complexity of signal transduction in tumour cells, as well as interaction within tumour microenvironment remain limited, it has become a challenge to find potential targets to optimally halt tumour progression.

As has been mentioned in the previous chapter, targeting cyclic nucleotide pathways through PDE inhibition or activating AC may be beneficial to counter abnormality in cell growth, a common feature in cancer. Using human cell lines, this study was extended to determine if the findings can be translated to human cells. The importance of secondary messenger will be investigated further in this chapter.

It has been suggested that glioblastoma cells maintain lower cAMP concentrations (Daniel, Filiz and Mantamadiotis, 2016). In five types of cancer including glioblastoma, lung adenocarcinoma, bladder urothelial carcinoma, uterine endometrial carcinoma, as well as stomach and esophageal carcinoma, concentration of cAMP is suppressed highlighting its association with malignancy (Daniel, Filiz and Mantamadiotis, 2016). From 4 clinical studies, approximately 12% of all glioblastoma samples have been found to have PDEs upregulated at the mRNA level (cBioportal).

Due to the convoluted machinery cancer cells possess, it is also necessary to look at other potential targets/pathways. Dynamic signal transduction between calcium (Ca^{2+}) and cAMP was initially reported in 1970 (Rasmussen, 1970), but it was not until 2009 that the existence of store-operated cAMP signalling (SOcAMPS), was linked to store-depleted mechanism (store operated calcium entry, SOCE) of AC signalling that leads to elevation of intracellular cAMP (Lefkimmiatis *et al.*, 2009). The illustration of

this dynamic is depicted in Figure 4.1. Despite this evidence, the dynamic role between these two pathways has not been fully resolved. Dr. Rahman's previous work utilising computational methods to repurpose available drugs was used to investigate their action in modulating calcium signalling (Rahman, 2020). Here, the study was extended to validate the pharmacological role of compounds in cell proliferation that were previously characterised to influence SOCE mechanism.

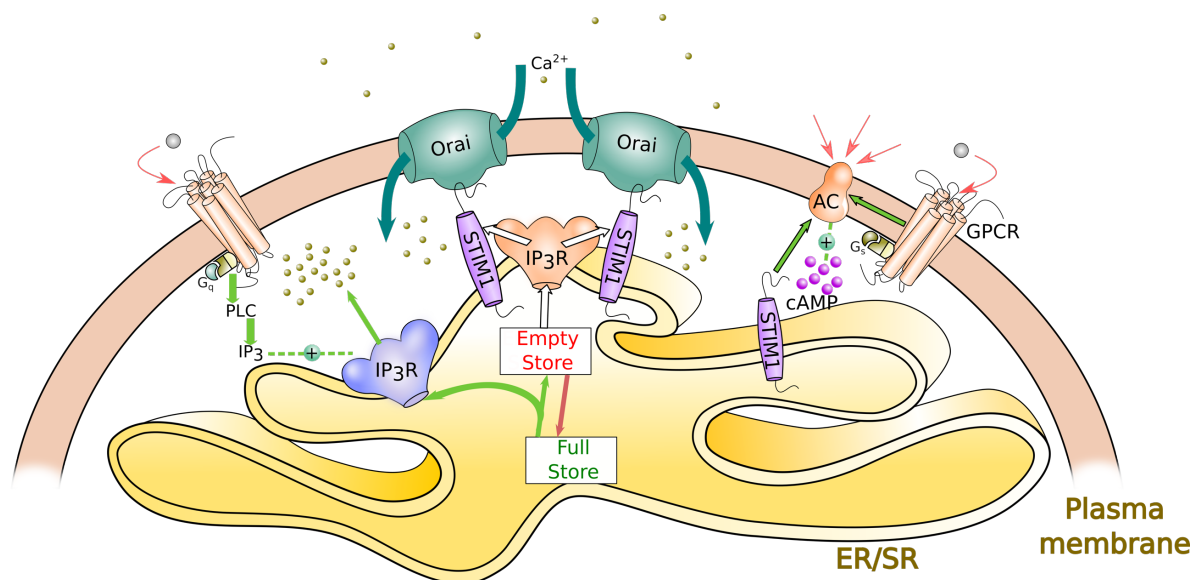


Figure 4.1. Illustration of calcium signalling and possible interplay between store operated calcium entry (SOCE) mechanism and the cyclic nucleotide pathway. SOCE is mediated through the formation of Orai-STIM1 macromolecular complex facilitating calcium influx. STIM1, but not Orai, is believed to be a modulator to influence AC activity leading to cAMP synthesis. Lefkimmatis indicated the possibility of SOcAMPS representing cross-talk between calcium and cAMP signalling event (Lefkimmatis *et al.*, 2009). IP₃R: inositol-1,4,5-trisphosphate receptor, STIM1: stromal interaction molecule 1, IP₃: inositol-1,4,5-triphosphate, PLC: phospholipase C, GPCR: G protein-coupled receptor, AC: adenylyl cyclase, ER: endoplasmic reticulum, SR: sarcoplasmic reticulum. (Figure was adapted from (Berridge, Lipp and Bootman, 2000; Putney, 2009), with some modification).

4.2 Pharmacological characterisation of PDEs in model glioblastoma cells

4.2.1 Human glioblastoma cells express various PDEs at mRNA levels

To characterise the role of PDEs in human glioblastoma models, U87 and T98 cells were used. Both cell lines were originally isolated from male glioblastoma patients⁶⁷. Before validating the functions of PDE isoenzymes in GBM cell model, the expression levels of each PDEs were quantified using rt-PCR. The gene expression was determined semi-quantitatively, at mRNA level, relative to the expression of the

⁶ https://www.sigmaaldrich.com/catalog/product/sigma/cb_92090213?lang=en®ion=GB

⁷ https://www.lgcstandards-atcc.org/products/all/HTB-14.aspx?geo_country=gb#generalinformation

housekeeping gene, GAPDH. Representative gel documentation is displayed in Figure 4.2 for U87 (A), T98 (B), and HEK293S (C) cells. With the exception of PDE1B, PDE1C, PDE5A, PDE8A, PDE9A, and PDE10A, there was no significant difference observed between glioblastoma cell lines (U87 and T98 cells) and control (HEK293S). PDE5A expression was distinctively higher in T98 cells compared to other cell lines. Despite expected tissue specificity of PDE6 which is expressed in the eye, low levels of most PDE6 isoforms were observed in HEK293S cells with PDE6B, PDE6D, and PDE6G also expressed T98 and U87 cells. Meanwhile, PDE6H was marginally expressed in human glioblastoma models but not detected in HEK293S cells.

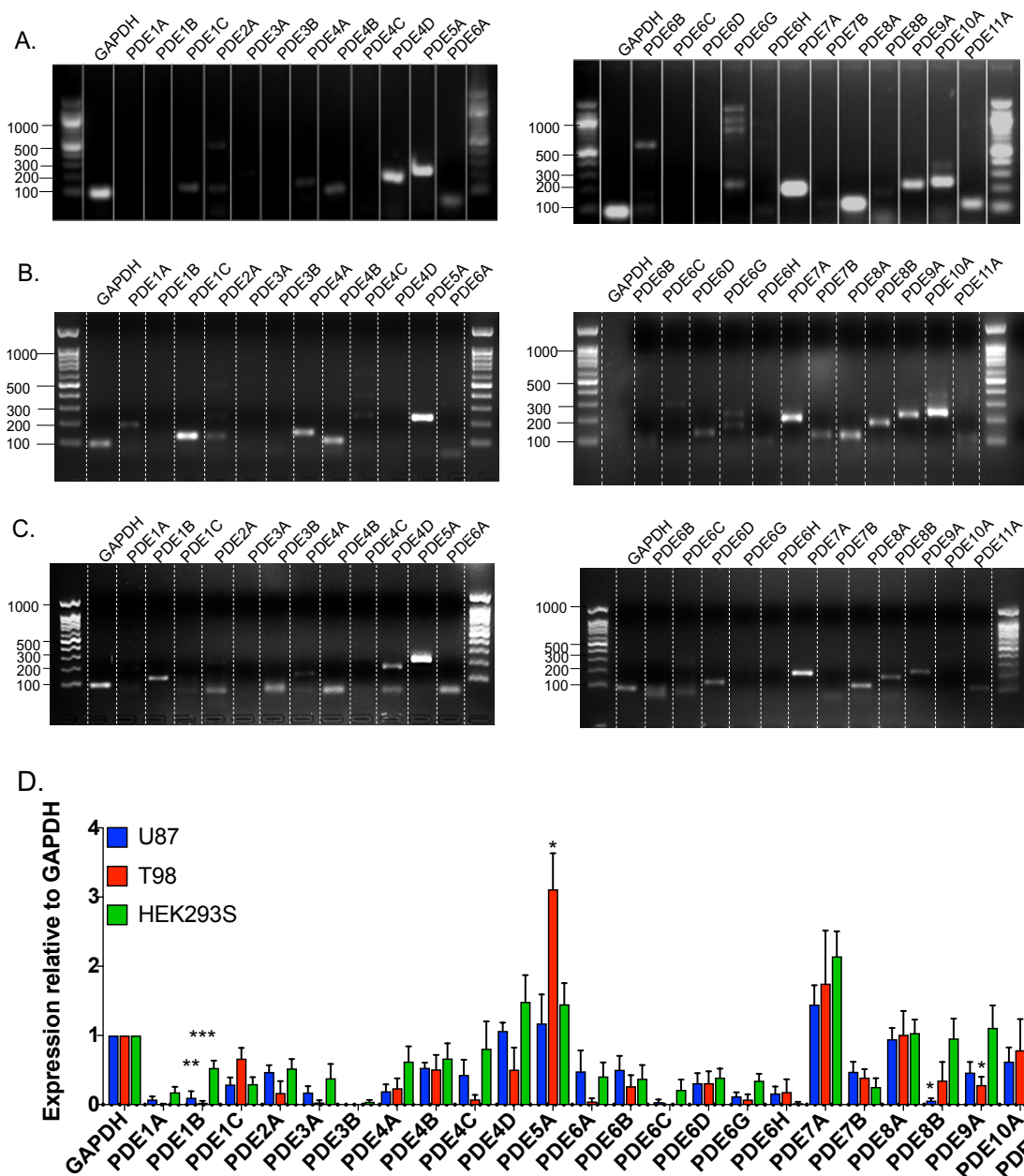


Figure 4.2 Expression profile of PDEs in human glioblastoma cell lines (U87 and T98) in comparison to HEK293S cells. Representative gel documentation showing

amplified PDE genes from U87 (A), T98 (B), and HEK293S (C) cell lines. Semi-quantitative expression profile of PDE isoenzymes in U87, T98, and HEK293S cells at mRNA levels (D). Expression of each gene of interest was normalised relative to GAPDH. Data are expressed as the mean \pm SEM from 4-6 individual repeats. Data were determined as statistically different (*, $p < 0.05$; **, $p < 0.01$; ***, $p < 0.001$) compared to individual isoenzyme among these cell lines using one-way ANOVA following by Dunnett's *post-hoc* analysis.

4.2.2 Development of a method to characterise the role of PDEs in accumulating cAMP signalling

Using human glioblastoma cells: U87 and T98 cells, further investigation was performed by utilising functional assays to probe the pharmacological role of PDE isoforms. Similar to the previous chapter using rat C6 glioma cells, it was necessary to validate if the findings can be translated to human cells. To do this, the study began by validating the activity of PDE inhibitors in modulating cAMP levels. The full dose-response curve of forskolin was determined in the absence and in the presence of PDE inhibitors. Initially, several, commonly used PDE inhibitors, which include rolipram, IBMX, trequinsin, and RO20-1724 were selected. Representative dose response curve of forskolin with/without PDE inhibitors are displayed in Figure 4.3 with the pharmacological values represented in Table 4.1.

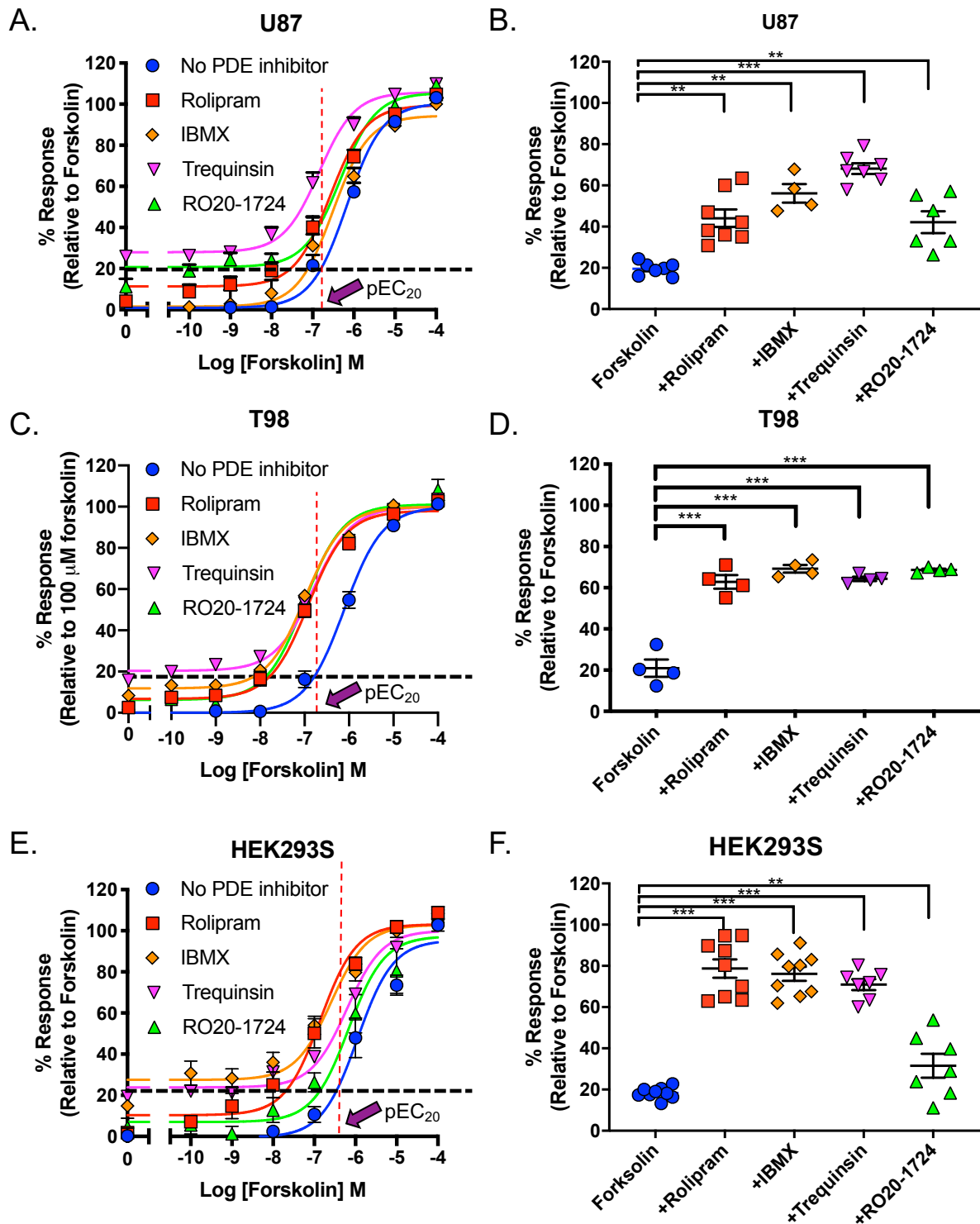


Figure 4.3. PDE inhibition increased the concentration of cAMP in the presence of forskolin across glioblastoma cell lines. Representative cAMP dose-response curves following 30 minutes stimulation with forskolin in the absence or presence of selected PDE inhibitors in U87 (A), T98 (C), and HEK293S (E) cells. Black and red dashed lines are displayed to visualize interpolation of pEC_{20} . Data are expressed relative to the maximal response produced by 100 μ M forskolin in the absence of PDE inhibitor. Individual data are displayed as a scatter plot as a comparison to the corresponding pEC_{20} of forskolin alone in U87 (B), T98 (D), and HEK293S (F) cells. Values are expressed as mean \pm SEM of 6-10 individual data sets. Statistical

significance was determined by comparing the value of n data sets to that of forskolin using a one-way ANOVA and Dunnett's *post-hoc* analysis. (**, $p < 0.01$; ***, $p < 0.001$).

Based upon the pharmacological parameters that are displayed in Table 4.1, co-stimulation of forskolin with selected PDE inhibitors not only improved the potency, but also in some groups increased the baseline level. The classical approach by looking at pEC_{50} and span may not be optimal for these experiments to screen of compounds since the window of observation is restricted. Instead, using pEC_{20} approach, it will be more practical to evaluate the compounds over a bigger range to understand if they are able to elevate cAMP level (as described in chapter 3).

Table 4.1

Pharmacological parameters of forskolin in the presence of selected PDE inhibitors

| Treatment | pEC_{50} | Span (%) | n |
|------------------------|-----------------------|----------------------|---|
| U87 | | | |
| Forskolin | 6.23 ± 0.13 | 100.1 ± 0.5 | 8 |
| Forskolin + rolipram | $6.60 \pm 0.08^*$ | 89.2 ± 2.9 | 8 |
| Forskolin + IBMX | 6.36 ± 0.06 | $84.4 \pm 5.3^{**}$ | 6 |
| Forskolin + trequinsin | $6.85 \pm 0.11^{***}$ | $79.0 \pm 3.4^{***}$ | 8 |
| Forskolin + RO20-1724 | 6.49 ± 0.08 | 92.8 ± 3.1 | 5 |
| T98 | | | |
| Forskolin | 6.11 ± 0.05 | 100.0 ± 2.2 | 4 |
| Forskolin + rolipram | 6.92 ± 0.06 | 91.2 ± 2.2 | 4 |
| Forskolin + IBMX | 6.99 ± 0.04 | 88.1 ± 1.6 | 4 |
| Forskolin + trequinsin | 6.80 ± 0.05 | 79.5 ± 1.6 | 4 |
| Forskolin + RO20-1724 | 7.00 ± 0.07 | 94.8 ± 2.9 | 4 |
| HEK293S | | | |
| Forskolin | 5.94 ± 0.19 | 100.6 ± 2.5 | 9 |
| Forskolin + rolipram | $7.03 \pm 0.19^{***}$ | 96.7 ± 3.7 | 9 |
| Forskolin + IBMX | $6.71 \pm 0.16^{**}$ | 76.2 ± 8.8 | 9 |
| Forskolin + trequinsin | 6.40 ± 0.14 | 87.8 ± 8.1 | 7 |
| Forskolin + RO20-1724 | 6.35 ± 0.12 | 99.1 ± 7.1 | 7 |

The values are expressed as mean \pm SEM from n individual data. Statistical significance was determined by comparing the value of n data sets to that of forskolin using a one-way ANOVA and Dunnett's *post-hoc* analysis. (*, $p < 0.1$; **, $p < 0.01$; ***, $p < 0.001$).

Using formula (1) that was explained in chapter 2, the cAMP accumulation can be quantified upon stimulation with forskolin in the presence of PDE inhibitor (Table 4.2). From the curve fitting, it was found that the pEC_{20} value of forskolin for the cell lines

were 6.84 ± 0.13 in U87 cells, 6.86 ± 0.13 in T98 cells, and 6.46 ± 0.26 in HEK293S cells.

As displayed in Table 4.2, all PDE inhibitors differentially increased total cAMP levels. In U87 cells, the highest potentiation was observed in cells co-treated with trequinsin, followed by IBMX, whereas rolipram efficacy was comparable to that of RO20-1724 (Figure 4.3.A,B). Both rolipram and RO20-1724 are selective PDE4 inhibitors even though they preferentially inhibited different PDE4 isoforms. Interestingly, all PDE inhibitors increased forskolin-mediated cAMP production to the same extent in T98 cells (C-D). In HEK293S cells, cAMP production increased to ~80% in the presence of rolipram, IBMX and trequinsin, whilst co-treatment with RO20-1724 only increased cAMP levels up to 30% (Figure 4.3. E-F). These data suggest that co-stimulating cells with a small amount of forskolin provides a suitable range for screening the ability of PDE inhibitors to modulate cAMP levels. T98 cells in particular, appeared to have less control to modulate cAMP concentration compared to the remaining cells. This seemed to be correlated with a few numbers of PDE isoenzymes that were expressed in T98 cells (Figure 4.2). Having established this method, further investigation was performed to explore the role of each isoform.

Table 4.2

Percentage response of each cell line in the presence of PDE inhibitors at the pEC₂₀ concentration of forskolin alone

| Group treatment | % Response (Relative to forskolin) | | |
|------------------------|------------------------------------|-----------------|-----------------|
| | U87 | T98 | HEK293S |
| Forskolin | 19.55 ± 1.20 | 20.96 ± 4.19 | 18.34 ± 0.90 |
| Forskolin + rolipram | 44.10 ± 4.22*** | 62.89 ± 3.29*** | 78.70 ± 4.49*** |
| Forskolin + IBMX | 56.15 ± 4.50*** | 69.23 ± 1.86*** | 76.13 ± 3.37*** |
| Forskolin + trequinsin | 68.16 ± 2.60*** | 64.31 ± 1.01*** | 70.92 ± 2.68*** |
| Forskolin + RO20-1724 | 42.14 ± 5.31*** | 68.67 ± 0.59*** | 31.54 ± 5.76 |

Statistical significance was determined by comparing the value of n data sets to that of forskolin using a one-way ANOVA and Dunnett's *post-hoc* analysis. (***, p<0.001).

4.2.3 Pharmacological role of PDEs in cAMP and cell proliferation

By applying the modified cAMP assay that has been mentioned in the previous section, activity of PDE inhibitors was assessed. A similar approach was carried out to that of performed in rat C6 cells in the chapter 3.

Aside from forskolin, some compounds were found to increase cAMP production in all three cell lines including amrinone, trequinsin, rolipram, ibudilast,

piclamilast, roflumilast, and IBMX (Figure 4.4 to 4.6). BRL-50481 and BAY 73-6691, on the other hand, appeared to be active in U87 and HEK293S cells only (Figure 4.5 and 4.6), whilst sildenafil increased forskolin-mediated cAMP accumulation in T98 and HEK293S cells (Figure 4.5 and 4.6). Surprisingly, sildenafil, a selective PDE5A (a cGMP specific PDE) inhibitor, was able to increase cAMP in T98 cells because the cells expressed higher levels of PDE5A (Figure 4.2D). EHNA, caffeine, and PF-04449613 were able to modulate cAMP levels in only U87 cells (Figure 4.4), whereas vinpocetine, milrinone, TC3.6, BC 11-38, PF-2545920, and PF 04671536 elevated total cAMP concentration in HEK293S cells (Figure 4.6).

Thereafter, PDE inhibitors were also tested for their ability to modulate cell proliferation (Figure 4.7 to 4.9). As expected, most of the compounds that elevated cAMP levels suppressed cell growth. Having displayed the characterisation of each PDE inhibitors from Figure 4.4 to 4.9 pharmacological parameters for the ability of the compounds to modulate both cAMP levels and cell growth are shown in Table 4.3 and 4.4. The summary of effects of each PDE inhibitor in both assays are displayed in Table 4.5

Table 4.3Potency values for cAMP production (pEC₅₀) and span of each PDE inhibitor in U87, T98, and HEK-293S cells.

| Compounds | Target PDE(X) ∞ | U87 | | T98 | | HEK-293S | |
|-------------|--------------------|--------------------------------|---------------------------------|--------------------------------|---------------------------------|--------------------------------|---------------------------------|
| | | pEC ₅₀ ^a | Span (cAMP) ^b (%) | pEC ₅₀ ^a | Span (cAMP) ^b (%) | pEC ₅₀ ^a | Span (cAMP) ^b (%) |
| | | Vinpocetine | 1 | N/A | N/A | N/A | N/A |
| EHNA | 2 | 6.15 ± 0.33 | 21.3 ± 5.3 | N/A | N/A | 4.73 ± 0.63 | 4.19 ± 1.31 |
| Cilostamide | 3 | N/A | N/A | N/A | N/A | N/A | N/A |
| Amrinone | 3 | 4.07 ± 0.09 | 69.1 ± 2.7 | 3.80 ± 0.15 | 77.8 ± 7.6 | 4.13 ± 0.11 | 62.73 ± 3.88 |
| Milrinone | 3 | N/A | N/A | N/A | N/A | 5.78 ± 0.25 | 26.16 ± 5.04 |
| Trequinsin | 2,3,7 | 5.20 ± 0.18 | 66.4 ± 6.2 | 5.78 ± 0.18 | 40.6 ± 3.8 | 4.77 ± 0.21 | 52.14 ± 6.34 |
| Rolipram | 4 | 5.75 ± 0.39 | 25.5 ± 5.9 | 7.53 ± 0.38 | 26.9 ± 4.8 | 5.47 ± 0.32 | 29.40 ± 6.18 |
| Ibudilast | 4 | 5.50 ± 0.31 | 12.9 ± 1.9 | 6.32 ± 0.29 | 38.6 ± 5.5 | 5.72 ± 0.41 | 11.07 ± 2.68 |
| Picamilast | 4 | 10.09 ± 0.91 | 13.0 ± 6.8 | 10.00 ± 0.71 | 22.0 ± 8.8 | 9.26 ± 0.25 | 16.17 ± 2.01 |
| Roflumilast | 4 | 10.98 ± 0.51 | 22.3 ± 9.4 | 10.66 ± 0.99 | 25.8 ± 17.3 | 8.53 ± 0.26 | 16.69 ± 2.19 |
| Sildenafil | 5 | 7.56 ± 0.56 | -12.7 ± 4.6 | 8.22 ± 0.84 | 10.6 ± 5.1 | 8.08 ± 0.25 | 31.08 ± 4.46 |
| Tadalafil | 5 | 9.92 ± 1.38 | 9.1 ± 9.0 | N/A | N/A | N/A | N/A |
| Caffeine | 1,4,5 | 5.91 ± 0.37 | 16.5 ± 3.4 | N/A | N/A | 6.61 ± 0.52 | 7.34 ± 1.83 |
| Zaprinast | 5,6,9,11 | N/A | N/A | N/A | N/A | 4.81 ± 0.68 | 3.77 ± 1.35 |
| TC3.6 | 7 | N/A | N/A | N/A | N/A | 5.38 ± 0.57 | 10.59 ± 2.92 |
| BRL-50481 | 7 | 5.89 ± 1.18 | 13.4 ± 14.7 | 6.09 ± 2.07 | -14.4 ± 21.4 | 6.52 ± 0.26 | 17.32 ± 2.57 |
| BC 11-38 | 8 | N/A | N/A | N/A | N/A | 7.47 ± 2.29 | 9.32 ± 11.21 |
| BAY-736691 | 9 | 6.91 ± 0.54 | 9.6 ± 3.1 | 9.06 ± 1.70 | 3.3 ± 3.0 | 7.15 ± 0.22 | 16.26 ± 2.09 |
| PF-0449613 | 9 | 7.86 ± 0.28 | 23.2 ± 3.7 | N/A | N/A | N/A | N/A |
| PF 2545920 | 10A | 8.78 ± 0.78 | -5.6 ± 5.7 | N/A | N/A | 8.42 ± 0.71 | 38.64 ± 31.26 |
| PF 04671536 | 11 | 9.67 ± 1.66 | -5.9 ± 5.3 | N/A | N/A | 9.35 ± 1.05 | 23.94 ± 11.25 |
| IBMX | Non-selective | 3.75 ± 0.59 | 7.3 ± 2.4 | 4.66 ± 0.24 | 28.5 ± 3.9 | 4.52 ± 0.24 | 12.14 ± 2.71 |
| Forskolin | AC activator | 5.40 ± 0.15 | 66.3 ± 5.6 | N/D | N/D | 4.73 ± 0.31 | 37.69 ± 7.72 |
| Cisplatin | DNA crosslinker | N/D | N/D | N/D | N/D | N/D | N/D |

Data are the mean ± SEM of 6-9 individual data sets.

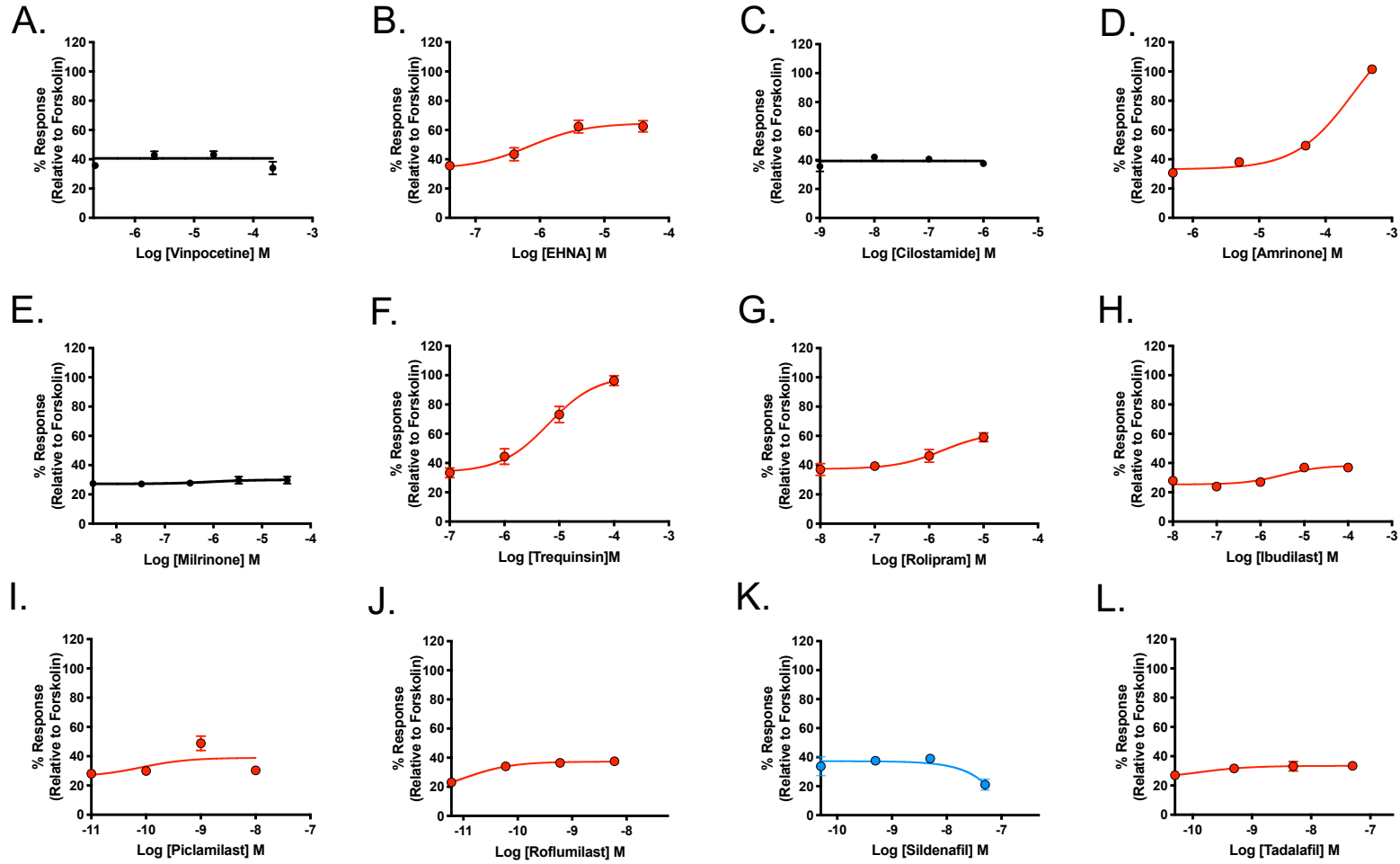
^a The negative logarithm of the agonist concentration required to produce a half-maximal response.^b The range between basal and E_{max} on cAMP accumulation assay.

N/A – not applicable; compounds did not have any effect on cAMP.

N/D – not determined.

∞, unless mentioned, targets refer to particular PDE isoform.

#, showing negative responses, either suppressing cAMP accumulation or being pro-proliferative.



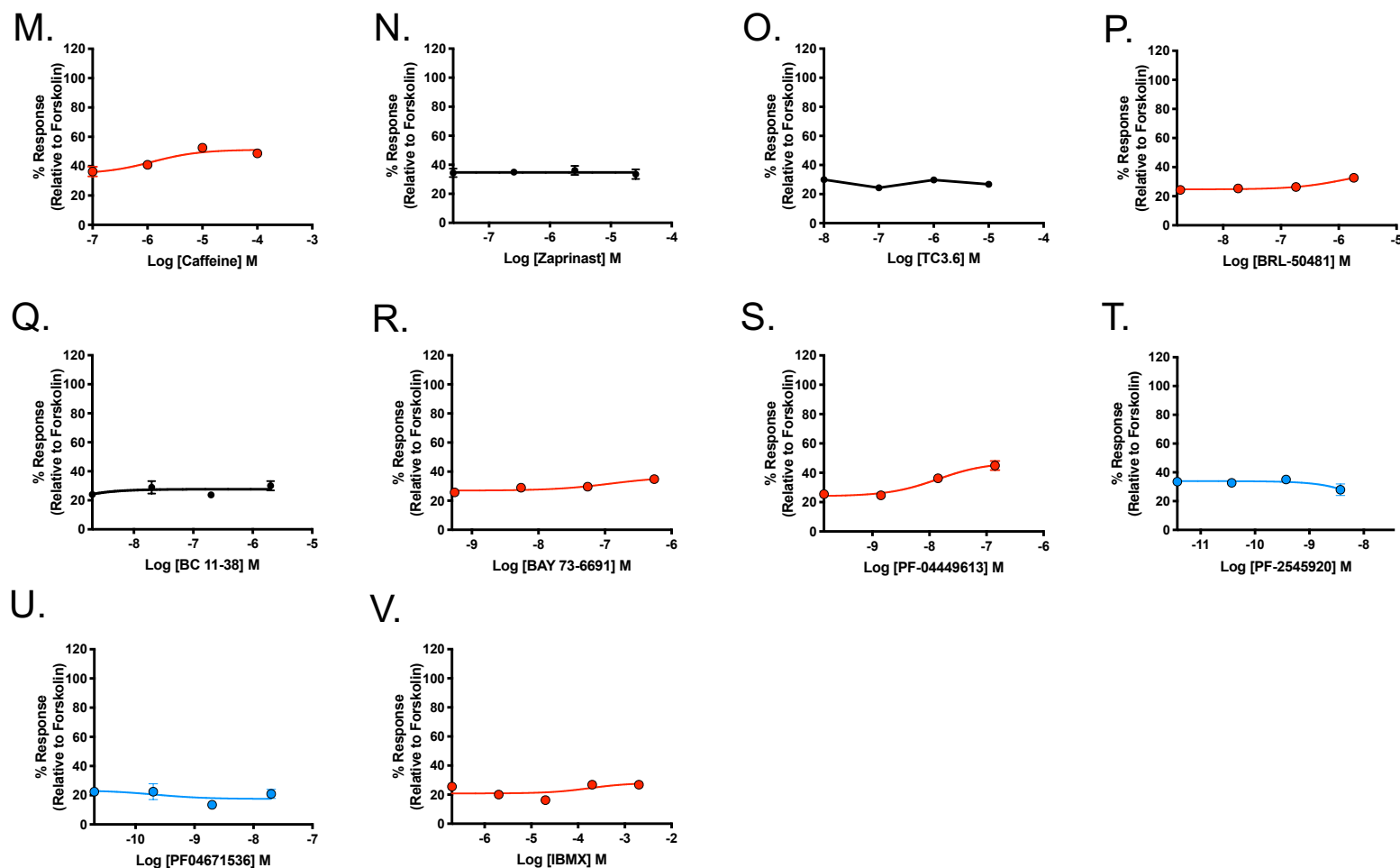
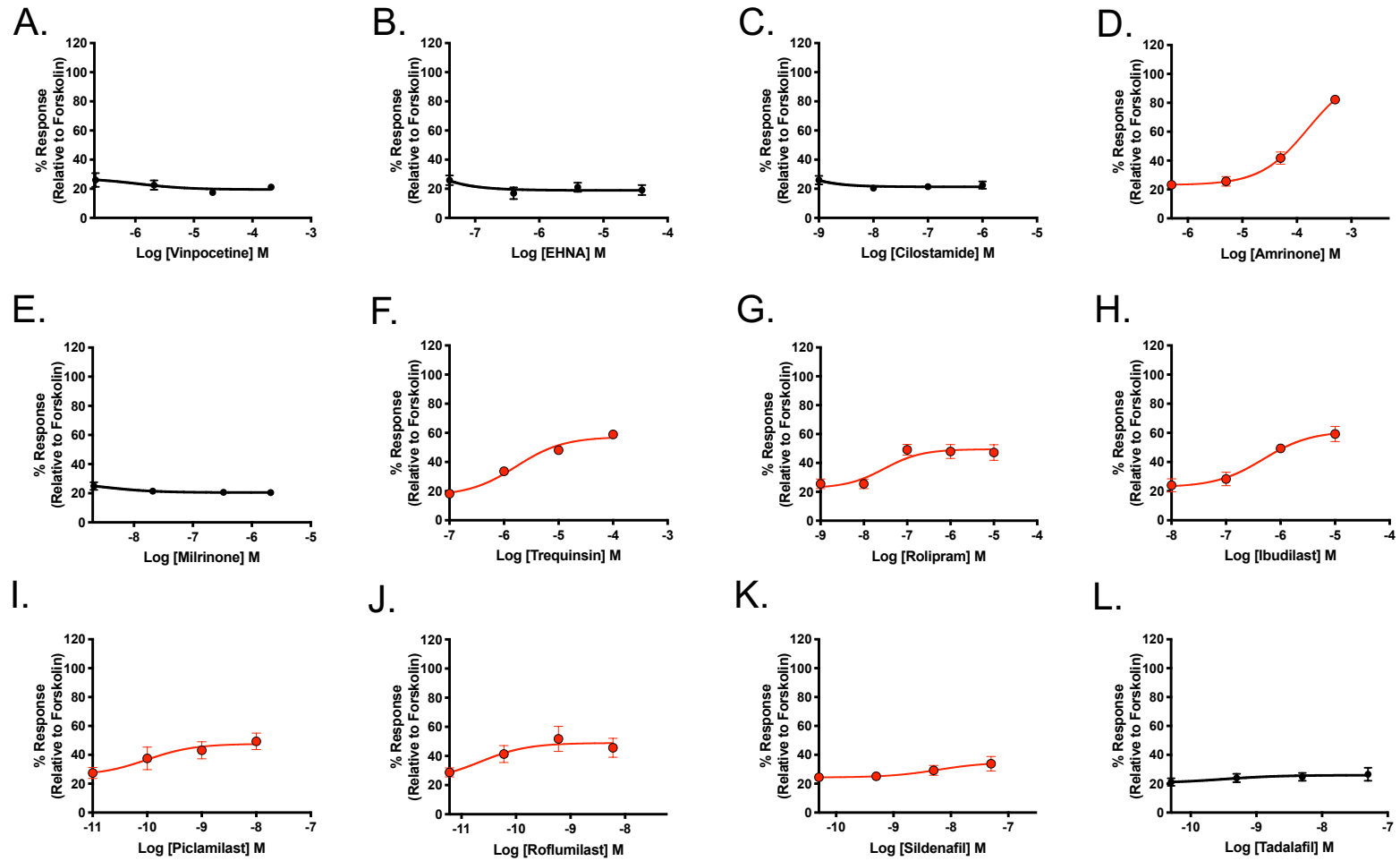


Figure 4.4 Effect of a panel of established PDE inhibitors on forskolin-mediated cAMP production in U87 cells. Dose-response curve of each PDE inhibitors in the presence of small amount of forskolin after 30 minutes stimulation. Responses were normalised to 100 μ M forskolin. Each data point is expressed as mean \pm SEM of 6-9 individual data set. Compounds that elevate cAMP concentration are red colour coded, whereas those suppress cAMP level are displayed in blue. Compounds that show no effect are shown as black curves.



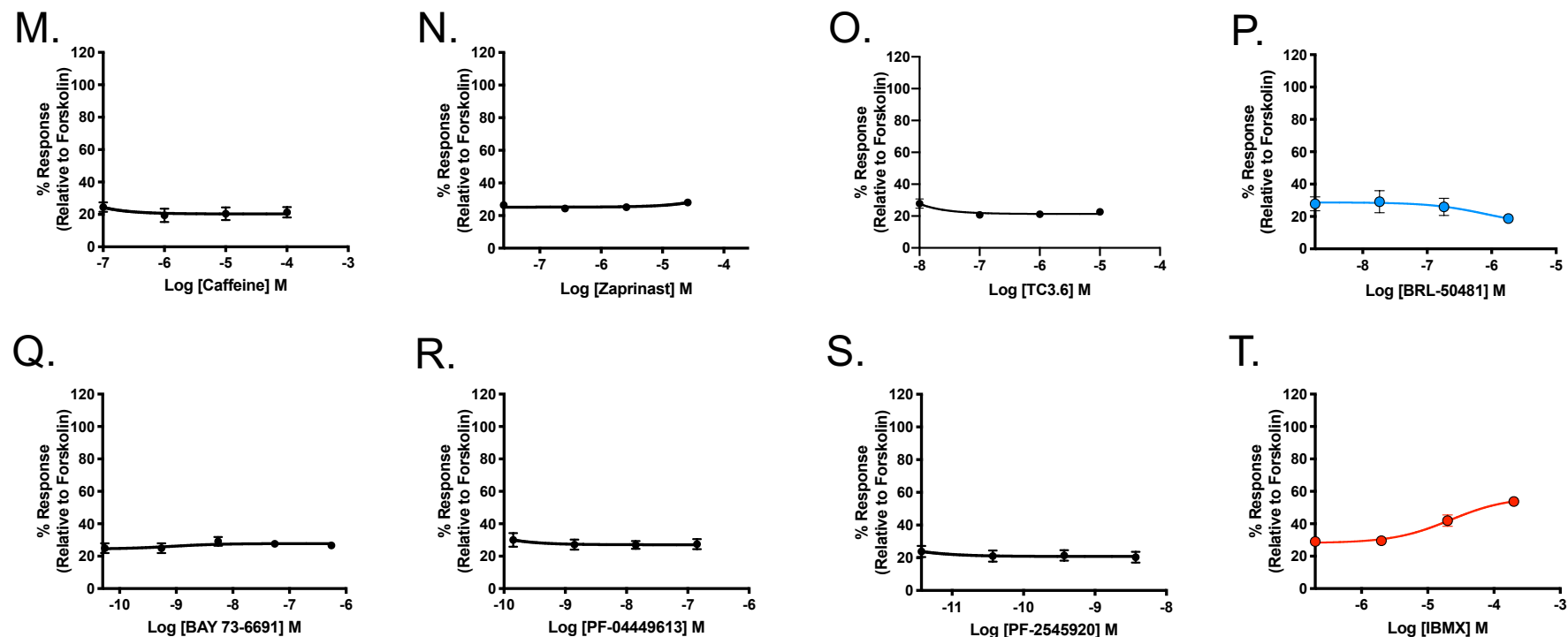
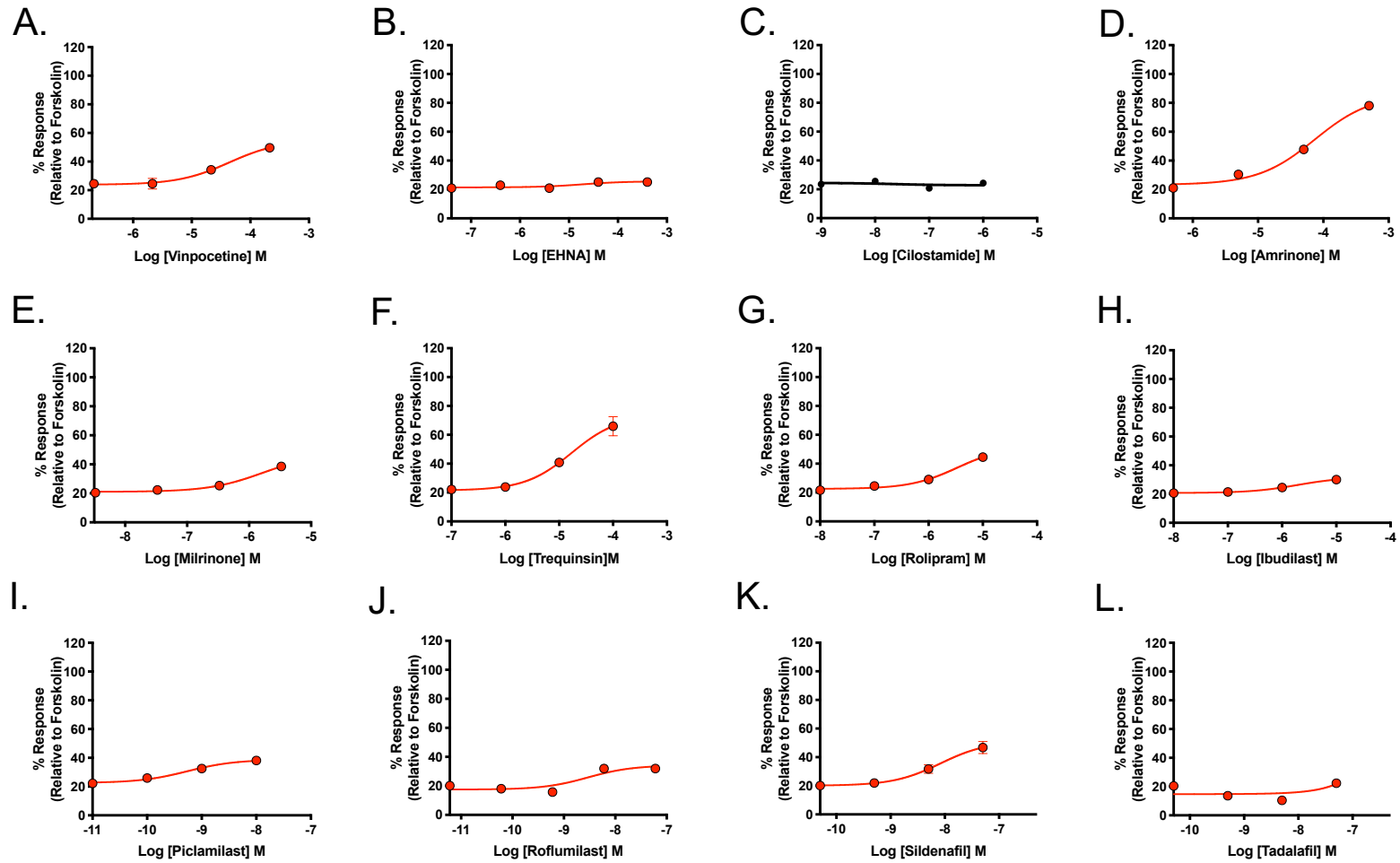


Figure 4.5 Effect of a panel of established PDE inhibitors on forskolin-mediated cAMP production in T98 cells. Dose-response curve of each PDE inhibitors in the presence of small amount of forskolin after 30 minutes stimulation. Responses were normalised to 100 μ M forskolin. Each data point is expressed as mean \pm SEM of 6-9 individual data set. Compounds that elevate cAMP concentration are red colour coded, whereas those suppress cAMP level are displayed in blue. Compounds that show no effect are shown as black curves. Note: the experiment to test BC 11-38 and PF04671536 cannot be accomplished due to covid-19 restriction.



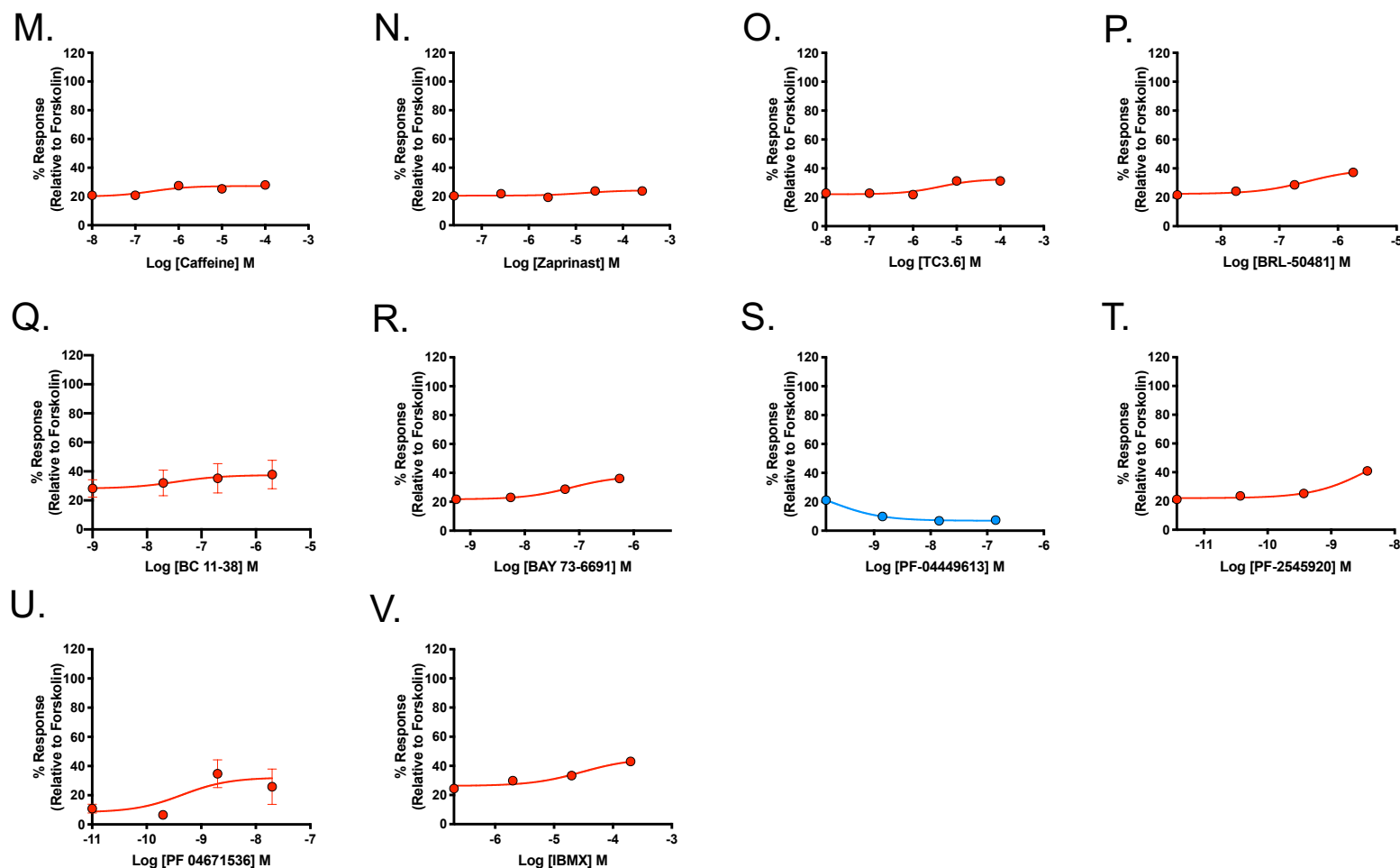


Figure 4.6 Effect of a panel of established PDE inhibitors on forskolin-mediated cAMP production in HEK293S cells. Dose-response curve of each PDE inhibitors in the presence of small amount of forskolin after 30 minutes stimulation. Responses were normalised to 100 μ M forskolin. Each data point is expressed as mean \pm SEM of 6-9 individual data set. Compounds that elevate cAMP concentration are red colour coded, whereas those suppress cAMP level are displayed in blue. Compounds that show no effect are shown as black curves.

Table 4.4Potency values for cell growth inhibition (pIC₅₀) and span of each PDE inhibitor in U87, T98, and HEK-293S cells

| Compounds | Target PDE(X) ∞ | U87 (%) | | T98 | | HEK-293S | |
|-------------|--------------------|--------------------------------|---|--------------------------------|---|--------------------------------|---|
| | | pIC ₅₀ ^a | Span (proliferation) ^b (%) | pIC ₅₀ ^a | Span (proliferation) ^b (%) | pIC ₅₀ ^a | Span (proliferation) ^b (%) |
| Vinpocetine | 1 | 4.70 ± 0.36 | 30.4 ± 6.2 | 6.00 ± 0.41 | 27.7 ± 6.7 | 4.10 ± 0.71 | 25.0 ± 11.7 |
| EHNA | 2 | 6.72 ± 0.31 | 25.5 ± 4.0 | 4.95 ± 0.22 | 33.3 ± 4.7 | 5.13 ± 0.22 | 57.4 ± 7.3 |
| Cilostamide | 3 | 8.23 ± 0.54 | 27.5 ± 7.6 | 6.41 ± 0.95 | 17.9 ± 11.6 | 7.02 ± 0.87 | -16.9 ± 8.3 |
| Amrinone | 3 | 4.36 ± 0.23 | 60.2 ± 7.6 | 4.13 ± 0.25 | 57.6 ± 8.5 | 3.90 ± 0.11 | 77.2 ± 0.9 |
| Milrinone | 3 | 8.06 ± 0.24 | 31.4 ± 3.6 | 8.00 ± 0.22 | 46.0 ± 4.8 | N/A | N/A |
| Trequinsin | 2,3,7 | 4.86 ± 0.14 | 84.6 ± 2.1 | 4.69 ± 0.13 | 77.8 ± 3.3 | 4.79 ± 0.06 | 84.4 ± 1.8 |
| Rolipram | 4 | 7.50 ± 0.39 | 26.8 ± 4.9 | 7.50 ± 0.42 | 57.9 ± 11.4 | 7.28 ± 0.93 | 9.9 ± 5.4 |
| Ibudilast | 4 | 7.55 ± 0.27 | 32.8 ± 4.1 | 7.57 ± 0.69 | 39.0 ± 18.1 | 6.16 ± 0.30 | 12.6 ± 2.0 |
| Picamilast | 4 | 10.30 ± 0.19 | 31.7 ± 3.9 | 10.43 ± 0.34 | 33.2 ± 5.3 | N/A | N/A |
| Roflumilast | 4 | 10.81 ± 0.21 | 26.1 ± 2.6 | 10.53 ± 0.31 | 27.2 ± 3.9 | N/A | N/A |
| Sildenafil | 5 | 9.28 ± 0.84 | 20.5 ± 9.6 | 9.58 ± 0.56 | 18.4 ± 8.4 | N/A | N/A |
| Tadalafil | 5 | 7.29 ± 2.56 | 29.2 ± 8.5 | N/A | N/A | 8.58 ± 0.68 | -15.8 ± 5.4 |
| Caffeine | 1,4,5 | 6.44 ± 0.13 | 38.9 ± 2.3 | N/A | N/A | 6.22 ± 0.37 | 15.9 ± 3.5 |
| Zaprinast | 5,6,9,11 | N/A | N/A | 5.24 ± 0.21 | 78.9 ± 8.4 | 4.64 ± 0.17 | 24.8 ± 5.7 |
| TC3.6 | 7 | N/A | N/A | 7.52 ± 0.45 | 22.7 ± 4.8 | N/A | N/A |
| BRL-50481 | 7 | 8.27 ± 0.49 | 12.9 ± 3.1 | 7.43 ± 0.36 | 22.9 ± 3.8 | N/A | N/A |
| BC 11-38 | 8 | 8.15 ± 0.72 | 15.2 ± 3.4 | N/A | N/A | 7.30 ± 0.62 | -18.2 ± 5.5 |
| BAY-736691 | 9 | 8.69 ± 0.13 | 43.1 ± 2.5 | 8.82 ± 0.25 | 36.8 ± 4.4 | 8.82 ± 0.57 | 24.8 ± 6.7 |
| PF-0449613 | 9 | 9.42 ± 0.27 | 30.8 ± 4.0 | 9.41 ± 0.32 | 27.9 ± 4.2 | 7.79 ± 0.56 | 11.6 ± 3.73 |
| PF 2545920 | 10A | N/A | N/A | N/A | N/A | 10.57 ± 0.38 | -22.2 ± 4.9 |
| PF 04671536 | 11 | 8.27 ± 1.47 | -19.6 ± 17.6 | N/A | N/A | 10.15 ± 0.72 | -24.1 ± 10.6 |
| IBMX | Non-selective | N/A | N/A | 4.14 ± 0.45 | 30.9 ± 9.1 | N/A | N/A |
| Forskolin | AC activator | N/A | N/A | 6.42 ± 0.25 | 23.6 ± 2.7 | N/A | N/A |
| Cisplatin | DNA crosslinker | 5.73 ± 0.29 | 44.1 ± 5.9 | 5.52 ± 0.33 | 41.3 ± 6.5 | 5.38 ± 0.32 | 71.2 ± 11.9 |

Data are the mean ± SEM of 6-9 individual data sets.

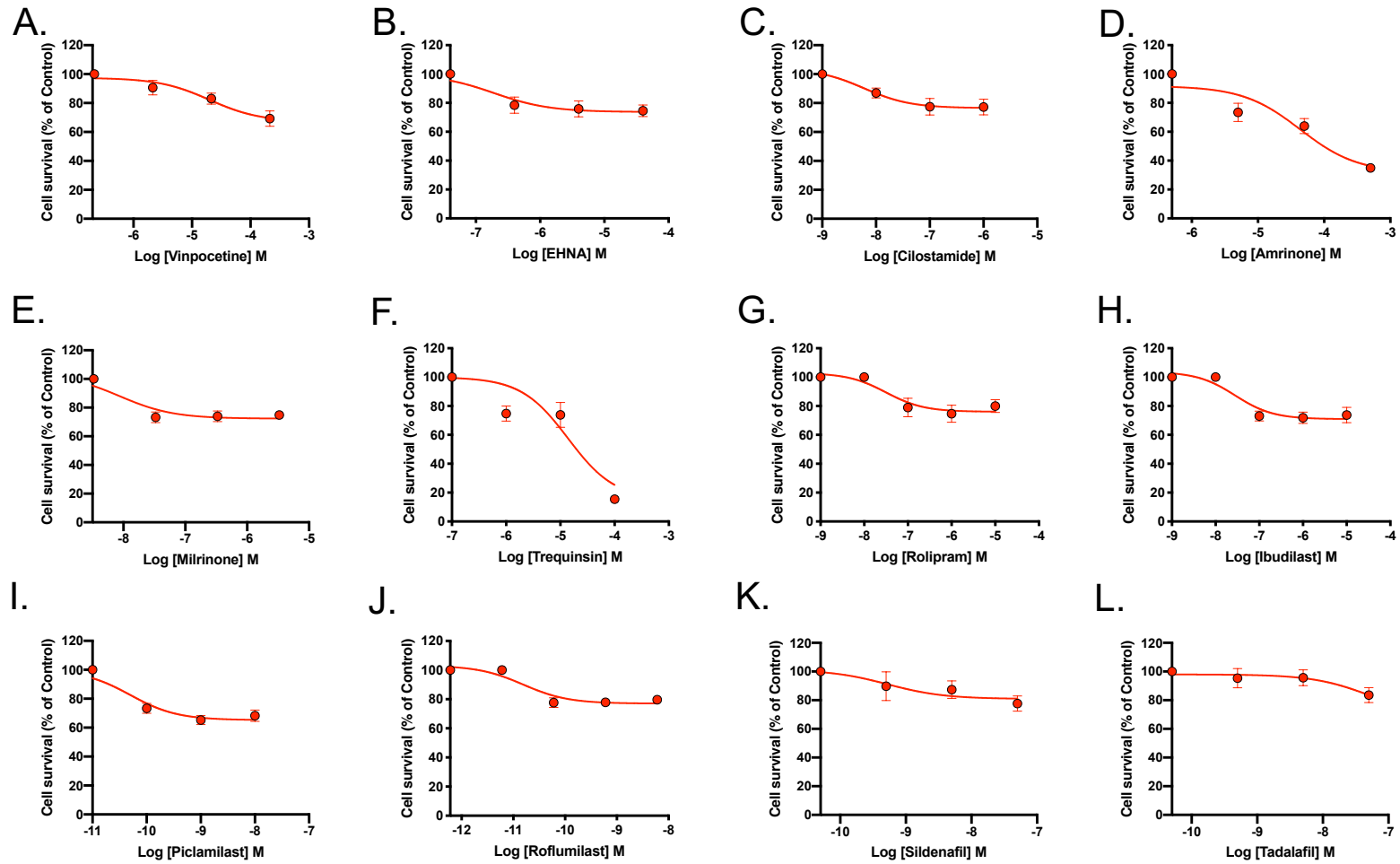
^a The negative logarithm of the inhibitor concentration required to inhibit a half-maximal response^b The range between survival in vehicle control and inhibitory maximal in cell proliferation assay

N/A – not applicable; compounds did not have any effect on cAMP production or cell growth inhibition.

∞, unless mentioned, targets refer to particular PDE isoform.

#, showing negative responses, either suppressing cAMP accumulation or being pro-proliferative.

Data were determined as statistically different (*, $p < 0.05$; ***, $p < 0.001$) compared to forskolin using one-way ANOVA followed by Dunnett's *post-hoc* analysis.



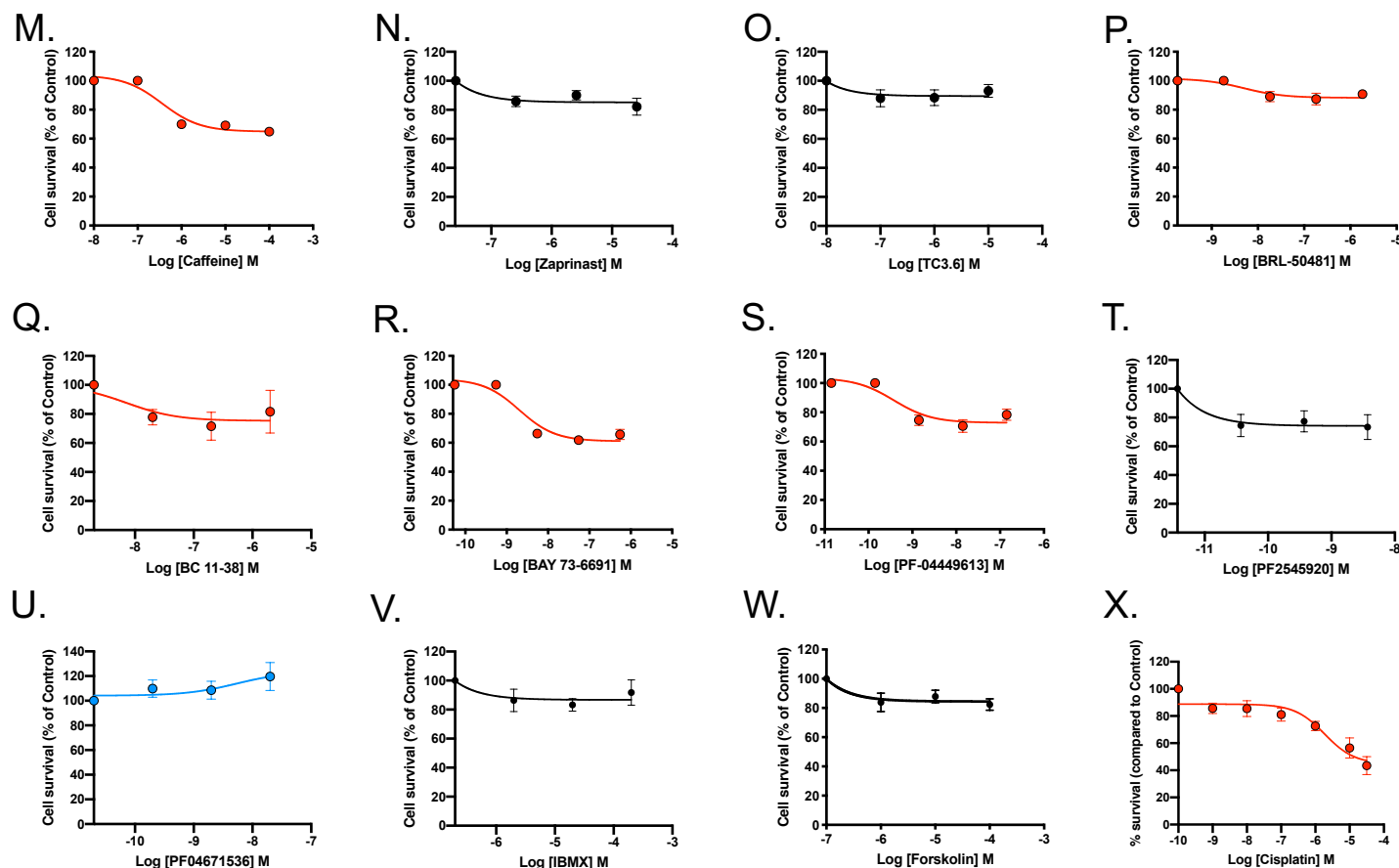
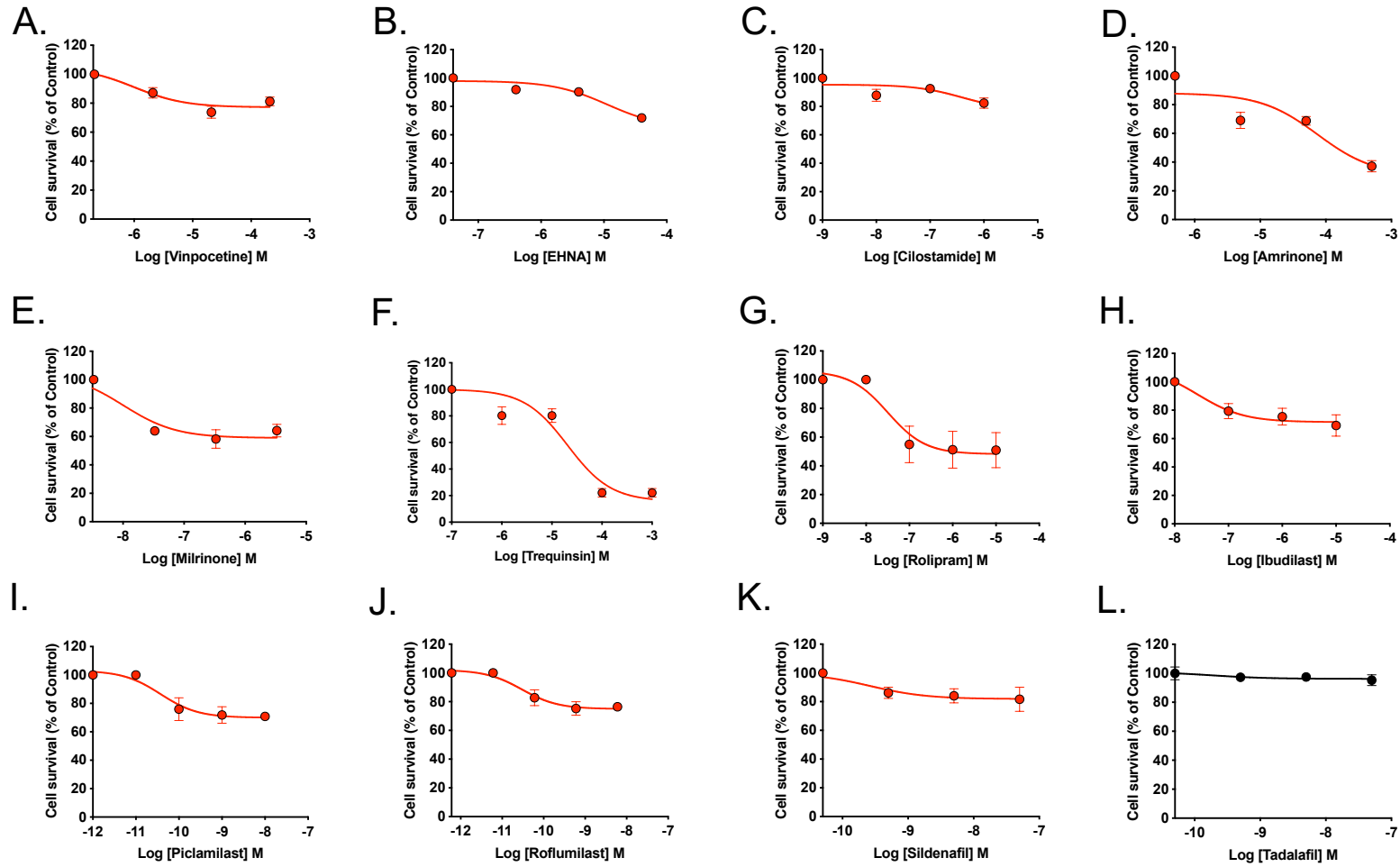


Figure 4.7 Effect of a panel of established PDE inhibitors, forskolin, and cisplatin on modulating U87 cell growth. Cell survival was determined in U87 cells following 72 hours incubation with each PDE inhibitor. Cisplatin was used as cytotoxic reference compound exhibiting anti-proliferative action. Data are expressed as percentage of cell proliferation relative to vehicle (complete medium containing 1% DMSO) from 6-9 data sets. Data are expressed as mean \pm SEM. Compounds that suppress cell growth are red colour coded, whereas those pro-proliferative are displayed in blue. Compounds that show no effect are shown as black curves.



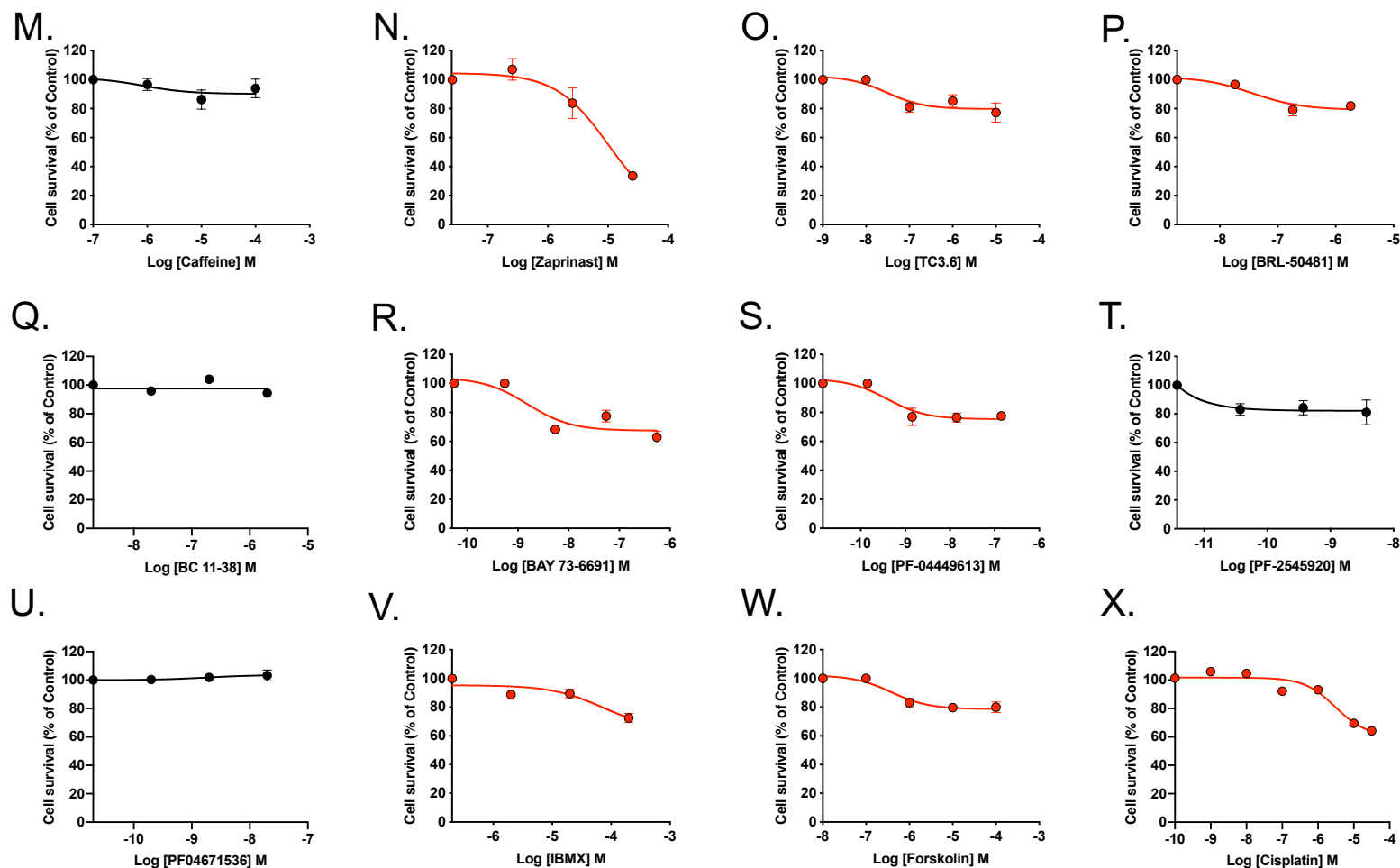
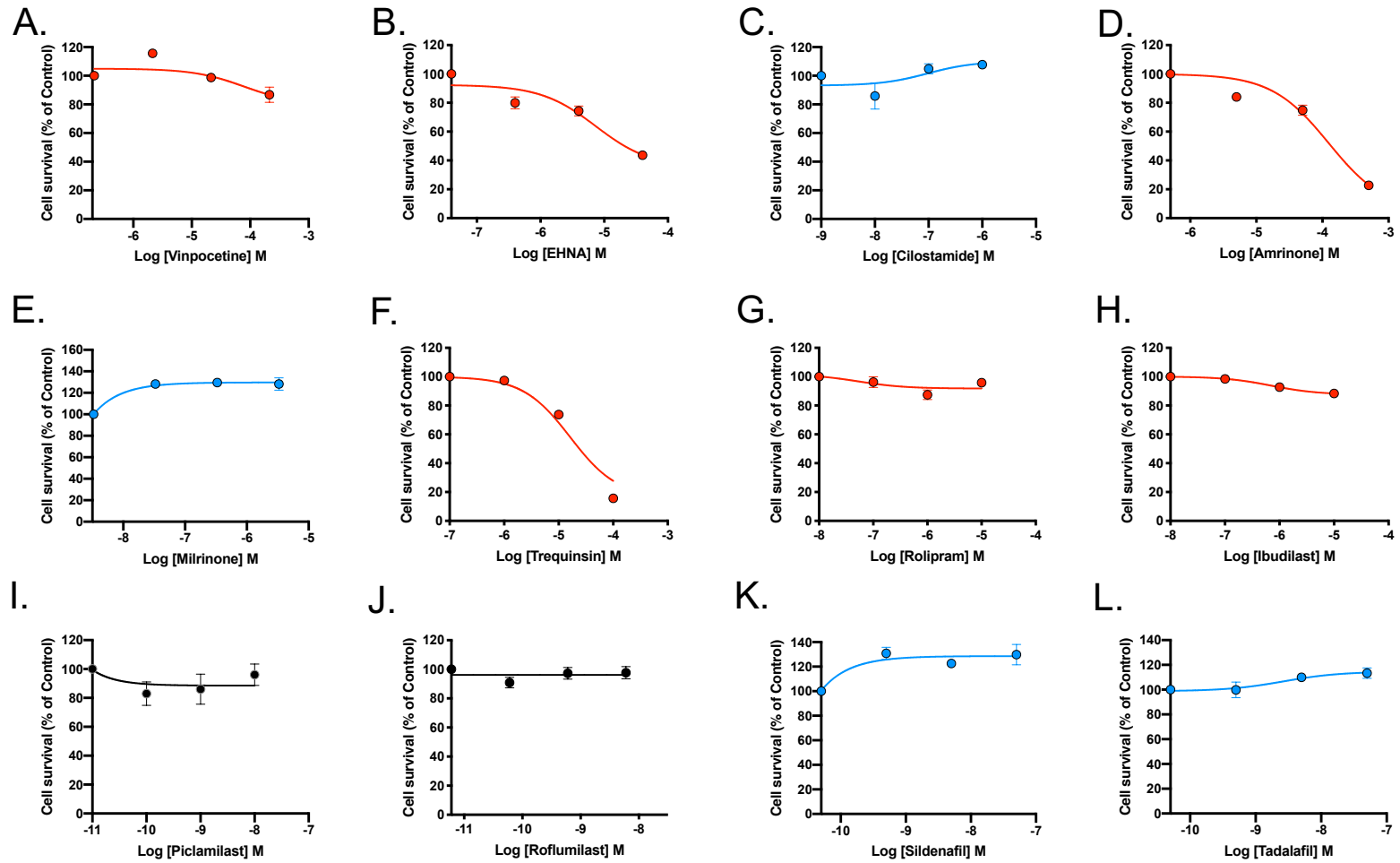


Figure 4.8 Effect of a panel of established PDE inhibitors, forskolin, and cisplatin on modulating T98 cell growth. Cell survival was determined in U87 cells following 72 hours incubation with each PDE inhibitor. Cisplatin was used as cytotoxic reference compound exhibiting anti-proliferative action. Data are expressed as percentage of cell proliferation relative to vehicle (complete medium containing 1% DMSO) from 6-9 data sets. Data are expressed as mean \pm SEM. Compounds that suppress cell growth are red colour coded, whereas those pro-proliferative are displayed in blue. Compounds that show no effect are shown as black curves.



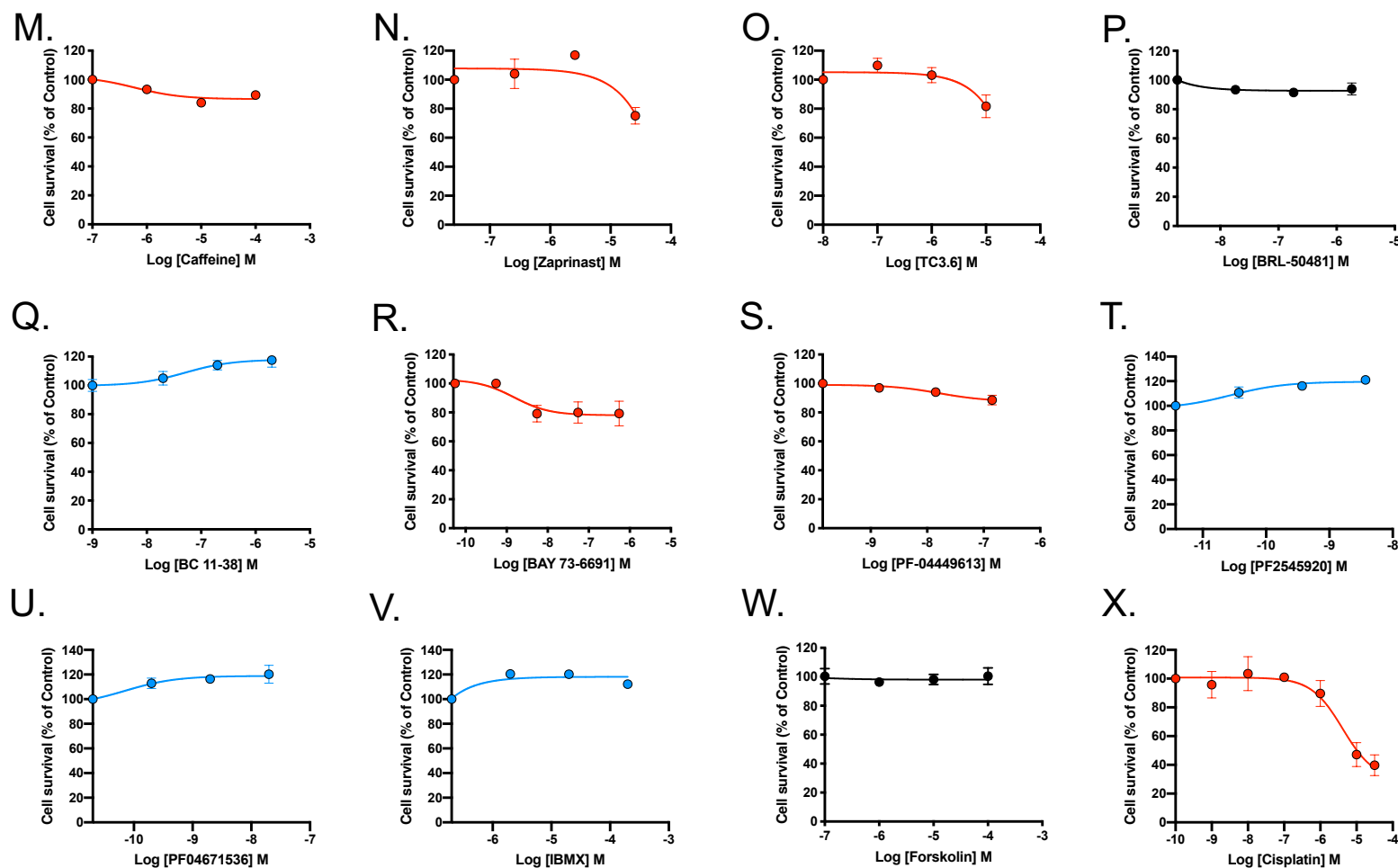


Figure 4.9 Effect of a panel of established PDE inhibitors, forskolin, and cisplatin on modulating HEK293S cell growth. Cell survival was determined in HEK293S cells following 72 hours incubation with each PDE inhibitor. Cisplatin was used as cytotoxic reference compound exhibiting anti-proliferative action. Data are expressed as percentage of cell proliferation relative to vehicle (complete medium containing 1% DMSO) from 6-9 data sets. Data are expressed as mean \pm SEM. Compounds that suppress cell growth are red colour coded, whereas those pro-proliferative are displayed in blue. Compounds that show no effect are shown as black curves.

Table 4.5

Summary of the pharmacological effects of each PDE inhibitor on cAMP production and cell proliferation

| Compound | Target | U87 | | T98 | | HEK293S | |
|-------------|-------------------|------|--------------------|------|--------------------|---------|--------------------|
| | | cAMP | Prolife- ration | cAMP | Prolife- ration | cAMP | Prolife- ration |
| Vinpocetine | 1 | N.R. | ↓↓ | ↓ | ↓ | ↑ | ↓ |
| EHNA | 2 | ↑ | ↓ | N.R. | ↓ | N.R. | ↓ |
| Cilostamide | 3 | N.R. | ↓ | N.R. | ↓ | N.R. | ↑ |
| Amrinone | 3 | ↑↑↑ | ↓↓↓ | ↑↑↑ | ↓↓↓ | ↑↑↑ | ↓↓↓ |
| Milrinone | 3 | N.R. | ↓↓ | N.R. | ↓↓ | ↑ | ↑ |
| Trequinsin | 2,3,7 | ↑↑↑ | ↓↓↓ | ↑↑ | ↓↓↓ | ↑↑↑ | ↓↓↓ |
| Rolipram | 4 | ↑ | ↓ | ↑ | ↓↓↓ | ↑ | ↑ |
| Ibudilast | 4 | ↑ | ↓↓ | ↑↑ | ↓↓ | ↑ | ↓ |
| Piclamilast | 4 | ↑ | ↓↓ | ↑ | ↓↓ | ↑ | N.R. |
| Roflumilast | 4 | ↑ | ↓ | ↑ | ↓ | ↑ | N.R. |
| Sildenafil | 5 | ↓ | ↓ | ↑ | ↓ | ↑ | ↑ |
| Tadalafil | 5 | ↑ | ↓ | N.R. | ↓↓ | N.R. | ↑ |
| Caffeine | 1,4,5 | ↑ | ↓↓ | N.R. | ↓↓ | N.R. | ↓ |
| Zaprinast | 5,6,9,11 | N.R. | N.R. | N.R. | ↓↓↓ | N.R. | ↓ |
| TC3.6 | 7 | N.R. | N.R. | N.R. | ↓ | ↑ | ↓ |
| BRL-50481 | 7 | ↑ | ↓ | N.R. | ↓ | ↑ | N.R. |
| BC 11-38 | 8 | N.R. | ↓ | - | N.R. | N.R. | ↑ |
| BAY-736691 | 9 | ↑ | ↓↓ | N.R. | ↓↓ | ↑ | ↓ |
| PF-0449613 | 9 | ↑ | ↓↓ | N.R. | ↓ | ↓ | ↓ |
| PF 2545920 | 10A | ↓ | N.R. | N.R. | ↓ | ↑ | ↑ |
| PF 04671536 | 11 | N.R. | ↑ | - | N.R. | ↑ | ↑ |
| IBMX | Non- selective | ↑ | N.R. | ↑ | ↓↓ | ↑ | N.R. |

N.R. No response

↑ = increase 10-30%, ↑↑ = increase 31-50%, ↑↑↑ = increase >50%, ↓: suppress 10-30%, ↓↓: suppress 31-50%, ↓↓↓: suppress >50%

4.3 Elevation of cAMP by targeting PDEs positively correlated with cell growth suppression

Subsequently, Pearson's correlation coefficient was calculated to determine if there was a correlation between these two pathways (Figure 4.10). Indeed, there was a strong association between cAMP production and cell growth inhibition in all human cells tested, with Pearson's correlation (r) of 0.87 in U87 cells (95% confidence interval = 0.58 – 0.96), 0.96 in T98 cells (95% confidence interval = 0.81 – 0.99), and 0.88 in HEK293S cells (95% confidence interval = 0.39 - 0.98). Nevertheless, most of the compounds were found to be more efficacious in glioblastoma cells lines: U87 and T98 cells in comparison to HEK293S cells. As displayed in Figure 4.10C, the slope of correlation was steeper in HEK293S cells compared to any other cell line (Figure

4.10C). The small range in changes of cAMP within the cells drives a more potent anti-proliferative effect. This demonstrates that HEK293S cells possess a mechanism to control cAMP levels compared to U87 or T98 cells, which is very likely generated by the presence of various PDEs. Based on the cAMP accumulation assay, forskolin showed lower potency in HEK293S cell (Figure 4.3). Taken together, all results corroborated that HEK293S cells have a particular mechanism to keep maintaining lower cAMP by expressing more PDEs, as displayed in Figure 4.2.

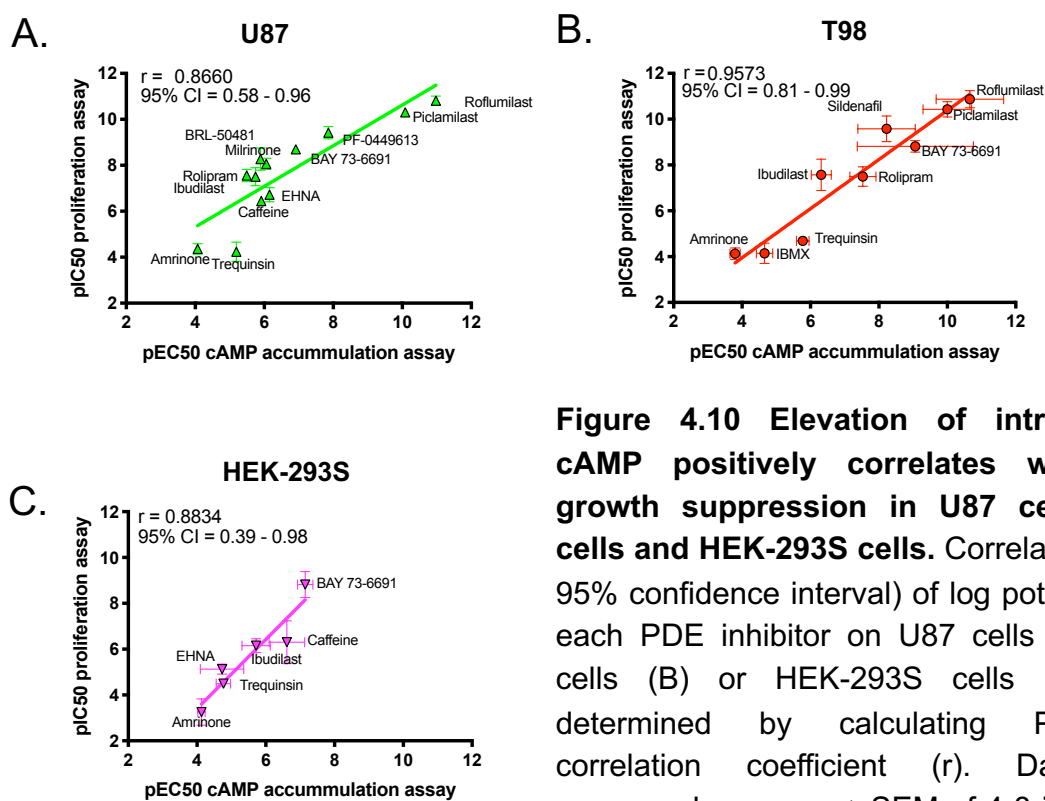


Figure 4.10 Elevation of intracellular cAMP positively correlates with cell growth suppression in U87 cells, T98 cells and HEK-293S cells. Correlation (with 95% confidence interval) of log potencies of each PDE inhibitor on U87 cells (A), T98 cells (B) or HEK-293S cells (C) was determined by calculating Pearson's correlation coefficient (r). Data are expressed as mean \pm SEM of 4-8 individual repeats.

Similar to chapter 3, selection criteria were applied to quantify how efficacious the compounds were at inhibiting cell proliferation. The top and bottom thresholds were again set to 350 and 200, respectively. Interestingly, cisplatin exhibited much less potent anti-proliferative effects in T98 cells compared to U87 or HEK293S cells (Figure 4.11). Although the data is not as robust as that obtained in rat C6 glioma cells, there are more compounds that reach the threshold in human glioblastoma cell lines. The efficacy of PDE inhibitors were generally less profound in HEK293S cells, with only EHNA, amrinone and trequinsin reaching the selection criteria threshold. This suggests that the majority of compounds display selectivity towards glioblastoma cell lines.

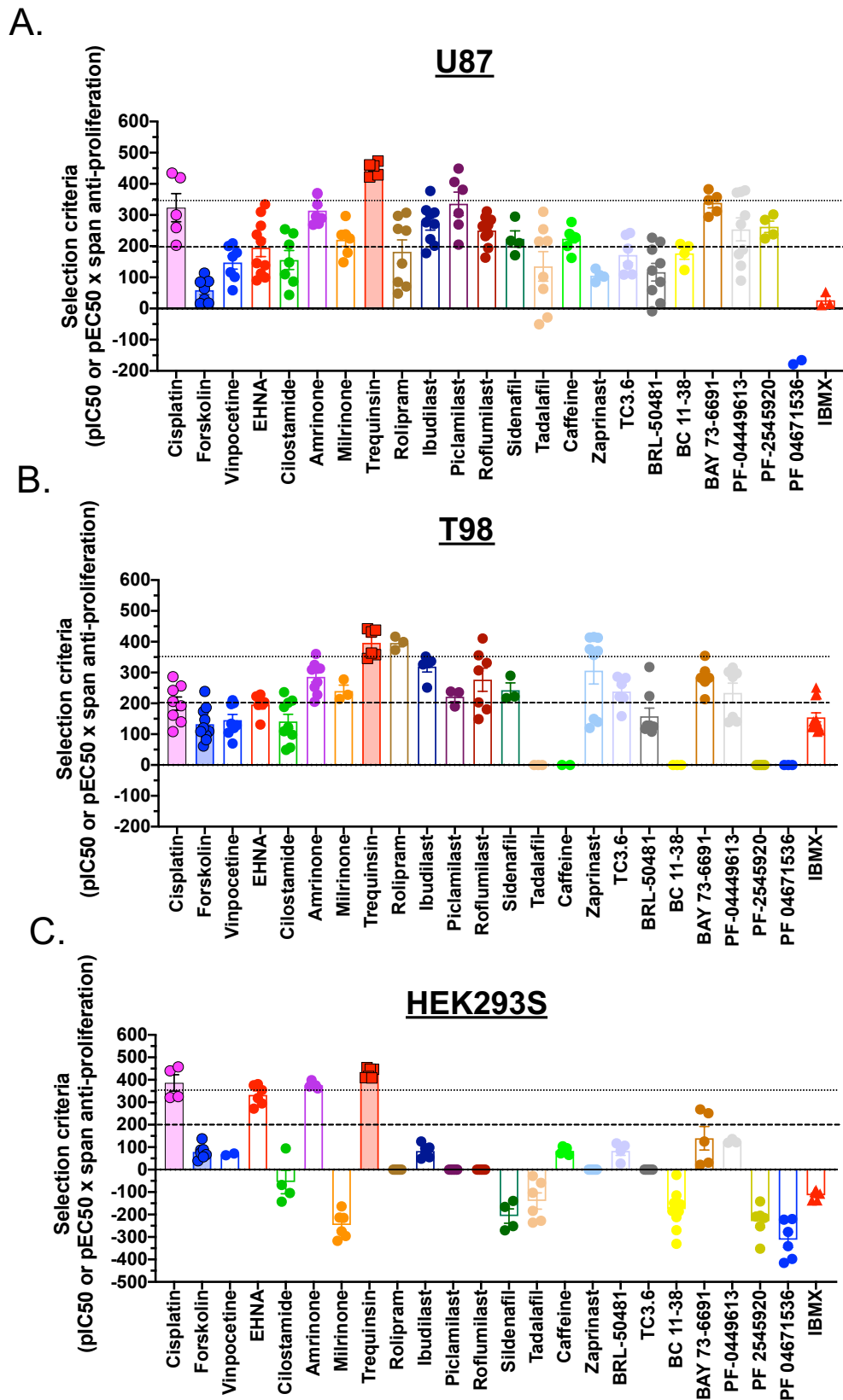


Figure 4.11 Selection criteria of PDE inhibitor in U87, T98, and HEK293S cells. Compound selection criteria was calculated based on potency and efficacy in proliferation assay. The dashed lines represent threshold value of 200 (less stringent criteria) and the dotted lines a higher criteria value of 350. Individual data point was

obtained from Figures 4.7 – 4.9. Data are expressed as mean \pm SEM of 3-8 individual repeats.

4.4 The combinatorial effect of PDE2, PDE3, and PDE7 inhibitors mimicks the effect of trequinsin

As shown above, trequinsin scored the highest in selection criteria for both GBM model cell lines. With regards to the combinatorial effect of individual PDE2 (EHNA), PDE3 (amrinone), and PDE7 (BRL-50481) inhibitor in rat glioma cells (Chapter 3), in this chapter the study was extended to investigate whether this has potential to be translated to human glioblastoma cell lines. To do this, the similar approach described in chapter 3 was adopted for probing mechanism of action of trequinsin, by using PDE2, PDE3, and PDE7 inhibitor.

All cell lines were stimulated with PDE inhibitors alone, in pairs, and as PDE inhibitor cocktail. Whilst no individual compound was as efficacious as trequinsin in these cell lines, both potency and E_{max} was improved when PDE inhibitors were combined in pairs compared to their individual effects (Figure 4.12, Table 4.6). Whilst PDE inhibitor cocktails appeared to be less potent than trequinsin in U87 cells, the combinatorial effect was similar to that of trequinsin in T98 and HEK293S cells.

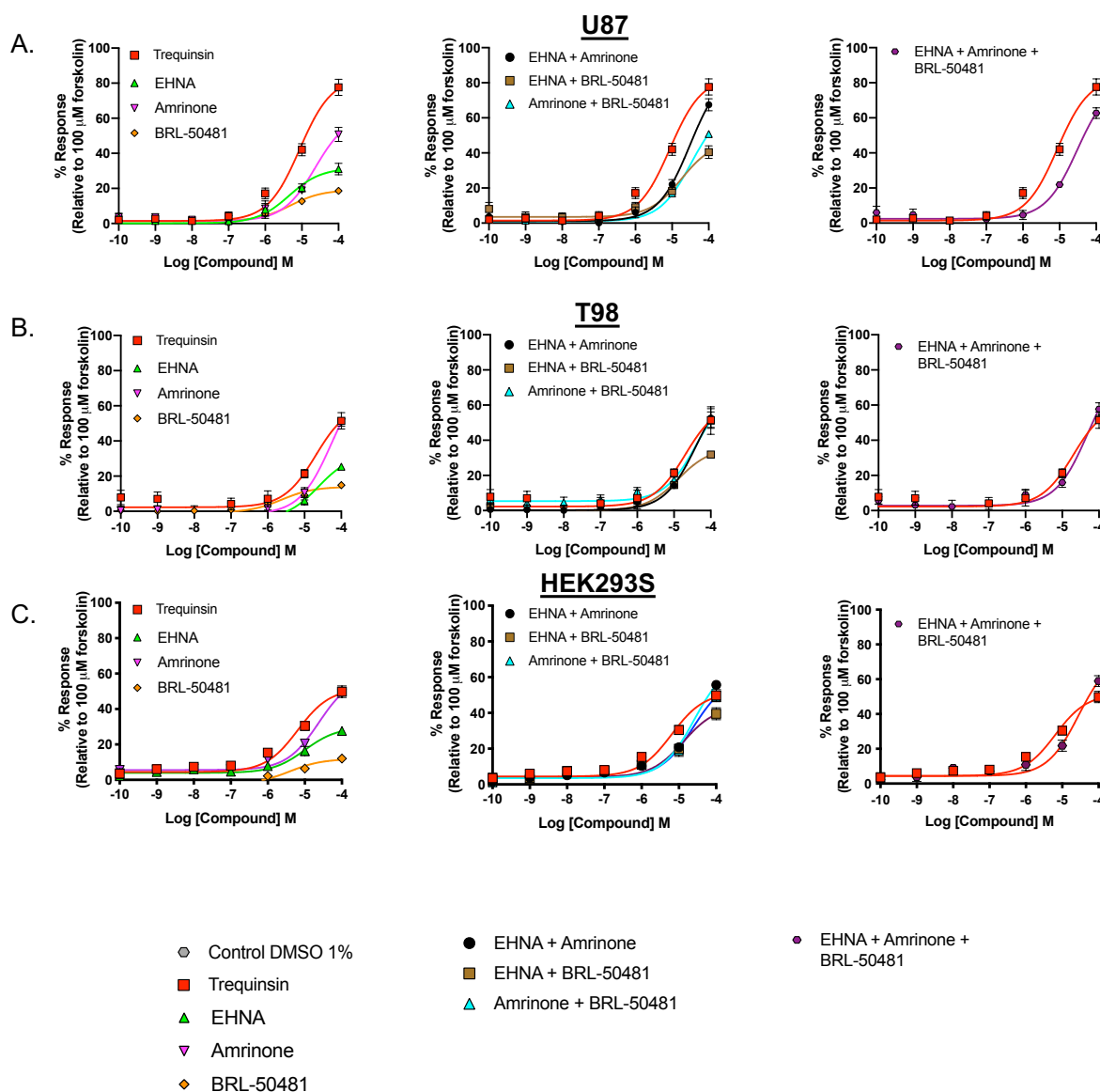


Figure 4.12. The combinatorial effect of PDE2, PDE3, and PDE7 inhibitor was similar to that of trequinsin in modulating cAMP production. cAMP accumulation was determined in C6 cells following 30-minute stimulation with EHNA (PDE2 inhibitor), amrinone (PDE3 inhibitor), or BRL-50481 (PDE7 inhibitor) alone (left panel), in pairs (middle), or in combination (right panel). The effects were observed across human glioblastoma U87 (A), T98 (B), and HEK293S (C) cells. Data are expressed relative to 100 μM forskolin and are the mean \pm SEM of 6-9 data sets. The effect of trequinsin alone is displayed on each graph for comparison.

While PDE2, PDE3, and PDE7 inhibitors were combined either in pairs or as cocktails, there was a marginal effect observed in cell growth on U87 cells (Figure 4.13A, Table 4.7). However, with the exception of 100 μM trequinsin, the curve between the PDE inhibitor cocktail and trequinsin overlapped. As mentioned in the previous chapter, the observed effect of 100 μM trequinsin was most likely generated

by its activity towards caspase-3/-7 (chapter 3). When the PDE inhibitors were combined in pairs and added to T98 cells, the anti-proliferative effect was enhanced compared to the individual compounds as indicated by potency (pIC_{50}) or span values (Figure 4.13B, Table 4.7). Equivalent suppression by the PDE inhibitor cocktail (combined three inhibitors) to that of trequinsin was observed in T98 cells. The improvement generated by the combination of these PDEs is clearer when the selection criteria was applied (Table 4.7). Using this approach, it is evident that T98 cells appeared to be less resistant to the PDE inhibitor cocktail than U87 cells. Meanwhile in HEK293S cells, combination of PDE2, PDE3, and PDE7 inhibitors exhibited a greater reduction in comparison to individual compounds but did not exceed the activity of trequinsin alone. It is most likely that the trequinsin-mediated antiproliferative effect in HEK293S cells results from caspase-3/-7 activation, as described in chapter 3. Taken together, these data suggest that trequinsin activity can be mimicked by combining PDE2, PDE3, and PDE 7 inhibition and may only be applicable to less resistant glioblastoma phenotype, such as T98 cells.

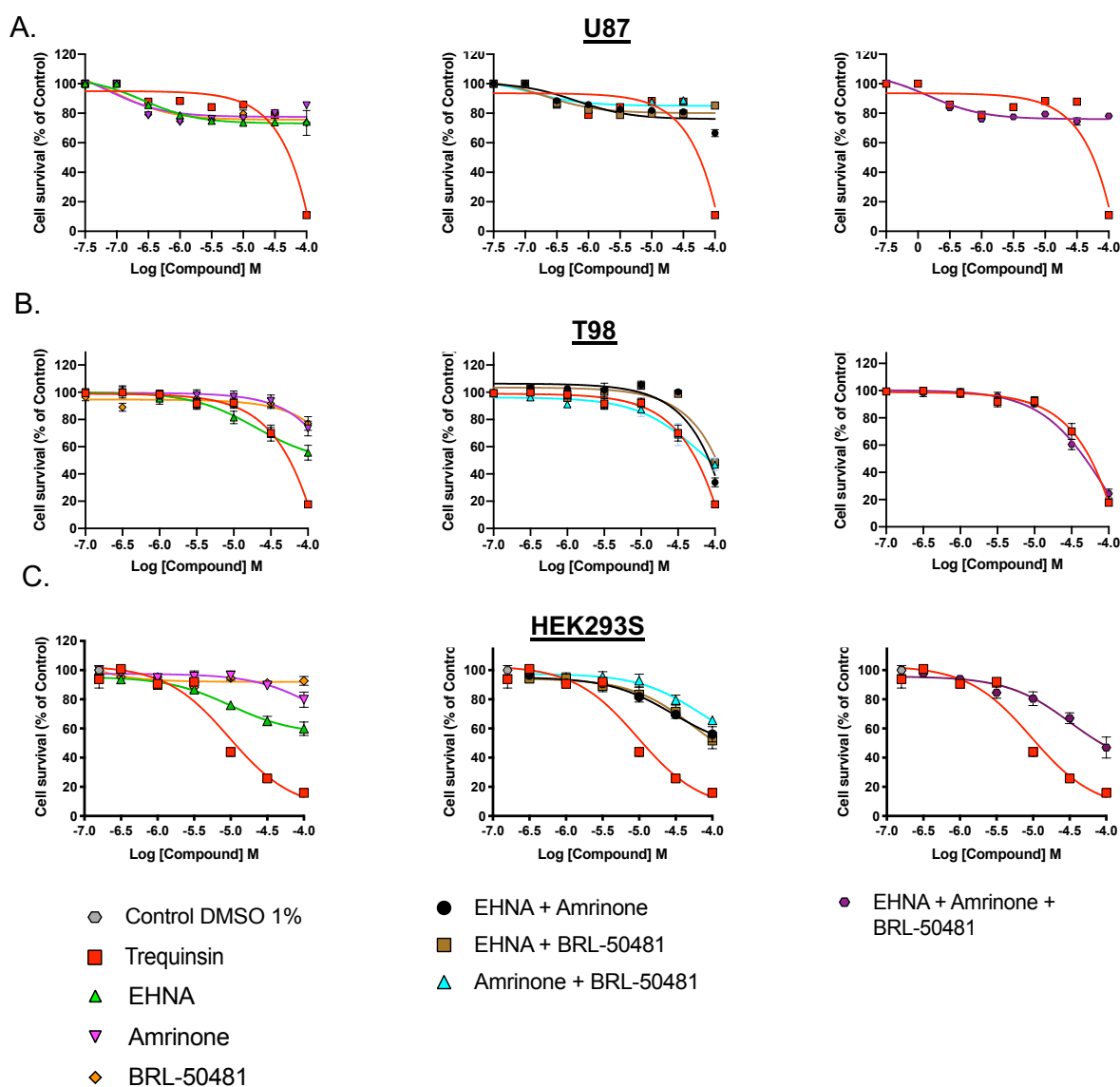


Figure 4.13 Anti-proliferative effect of trequinsin can be mimicked by combining individual PDE2, PDE3, and PDE7 inhibitor. Cell survival was determined in these cells following 72 hours incubation with EHNA, amrinone or BRL-50481 alone, in pairs, or in combination. Data are expressed as percentage of cell proliferation relative to vehicle. The curve of trequinsin alone is displayed on each graph for comparison. All data are the mean \pm SEM of 6–9 data.

Table 4.6

Combinatorial effect of individual PDE2, PDE3, and PDE7 inhibitor in glioblastoma cell lines U87 and T98 cells in comparison to HEK293S cells

| Compound | cAMP accumulation assay | | | Proliferation Assay | | | Selection criteria |
|--|--------------------------------|-----------------------|---|--------------------------------|-----------------------|---|--------------------|
| | pEC ₅₀ ^a | Span ^b (%) | n | pIC ₅₀ ^c | Span ^d (%) | n | |
| U87 | | | | | | | |
| Trequinsin [§] | 5.06 ± 0.09 | 81.8 ± 4.3 | 6 | 4.46 ± 0.05 | 89.0 ± 0.3 | 9 | 396.50 ± 4.79 |
| EHNA | 5.35 ± 0.20 | 31.5 ± 3.2 | 6 | 6.58 ± 0.07 | 31.5 ± 1.1 | 9 | 207.18 ± 7.86 |
| Amrinone | 4.64 ± 0.14 | 60.5 ± 5.4 | 6 | 7.12 ± 0.22 | 34.9 ± 6.8 | 9 | 248.87 ± 48.68 |
| BRL-50481 | 5.31 ± 0.22 | 17.7 ± 2.0 | 6 | 6.99 ± 0.30 | 35.1 ± 8.4 | 9 | 245.51 ± 59.70 |
| EHNA + amrinone | 4.51 ± 0.11 | 86.7 ± 6.5 | 6 | 6.19 ± 0.16 | 24.9 ± 2.2 | 9 | 153.99 ± 14.13 |
| EHNA + BRL-50481 | 4.74 ± 0.19 | 43.5 ± 5.4 | 6 | 6.71 ± 0.13 | 23.9 ± 1.9 | 9 | 160.38 ± 13.39 |
| Amrinone + BRL-50481 | 4.48 ± 0.16 | 66.4 ± 7.4 | 6 | 6.93 ± 0.18 | 18.9 ± 2.4 | 9 | 131.35 ± 17.22 |
| EHNA + amrinone + BRL-50481 | 4.52 ± 0.14 | 78.6 ± 7.8 | 6 | 6.84 ± 0.14 | 31.9 ± 3.2 | 9 | 218.76 ± 22.59 |
| T98 | | | | | | | |
| Trequinsin [§] | 4.69 ± 0.20 | 58.9 ± 7.6 | 6 | 4.41 ± 0.06 | 81.8 ± 3.4 | 9 | 360.32 ± 15.92 |
| EHNA | 4.63 ± 0.23 | 36.9 ± 5.7 | 6 | 4.65 ± 0.10 | 55.2 ± 5.9 | 9 | 257.03 ± 28.33 |
| Amrinone | 4.56 ± 0.08 | 56.7 ± 4.6 | 6 | 4.41 ± 0.09 | 43.7 ± 1.1 | 6 | 192.85 ± 6.31 |
| BRL-50481 [§] | 5.62 ± 0.46 | 14.7 ± 3.1 | 6 | 4.58 ± 0.18 | 24.9 ± 4.6 | 6 | 113.81 ± 21.41 |
| EHNA + amrinone [§] | 4.63 ± 0.09 | 56.8 ± 6.7 | 6 | 4.08 ± 0.03 | 68.1 ± 2.6 | 6 | 277.60 ± 10.87 |
| EHNA + BRL-50481 [§] | 4.89 ± 0.17 | 35.7 ± 3.7 | 6 | 3.88 ± 0.05 | 53.4 ± 3.1 | 6 | 206.85 ± 12.19 |
| Amrinone + BRL-50481 | 4.38 ± 0.29 | 64.7 ± 14.5 | 6 | 4.69 ± 0.18 | 68.5 ± 11.8 | 6 | 321.40 ± 56.96 |
| EHNA + amrinone + BRL-50481 [§] | 4.70 ± 0.12 | 57.4 ± 6.8 | 3 | 4.40 ± 0.07 | 74.9 ± 4.7 | 9 | 330.17 ± 21.25 |
| HEK293S | | | | | | | |
| Trequinsin [§] | 5.19 ± 0.14 | 47.2 ± 3.7 | 6 | 5.10 ± 0.05 | 81.4 ± 2.0 | 5 | 415.29 ± 11.15 |
| EHNA | 5.00 ± 0.16 | 25.9 ± 2.4 | 6 | 5.00 ± 0.17 | 39.3 ± 3.6 | 9 | 196.76 ± 19.02 |
| Amrinone | 4.81 ± 0.08 | 50.9 ± 2.6 | 6 | N/A | N/A | 6 | N/A |
| BRL-50481 | 5.20 ± 0.26 | 13.7 ± 1.8 | 5 | N/A | N/A | 8 | N/A |
| EHNA + amrinone | 4.58 ± 0.14 | 65.6 ± 6.0 | 6 | 4.54 ± 0.19 | 50.2 ± 6.7 | 6 | 228.01 ± 31.77 |
| EHNA + BRL-50481 [§] | 4.88 ± 0.18 | 39.9 ± 4.5 | 6 | 4.77 ± 0.10 | 50.3 ± 4.6 | 6 | 239.63 ± 22.43 |
| Amrinone + BRL-50481 | 4.61 ± 0.20 | 55.9 ± 7.4 | 6 | 4.14 ± 0.33 | 55.4 ± 19.1 | 6 | 229.49 ± 81.53 |
| EHNA + amrinone + BRL-50481 [§] | 4.55 ± 0.16 | 69.9 ± 7.6 | 6 | 4.94 ± 0.10 | 52.5 ± 6.3 | 9 | 259.69 ± 31.71 |

§ The curve was fit by constraining top value to 100 and bottom minimum value observed from proliferation assay

^a The negative logarithm of the agonist concentration required to produce a half-maximal response.

^b the range between basal and E_{max} on cAMP accumulation assay

^c The negative logarithm of the inhibitor concentration required to inhibit a half-maximal response

^d The range between survival in vehicle control and inhibitory maximal in cell proliferation assay

N/A – not applicable; compounds did not have any effect on cAMP production or cell growth inhibition.

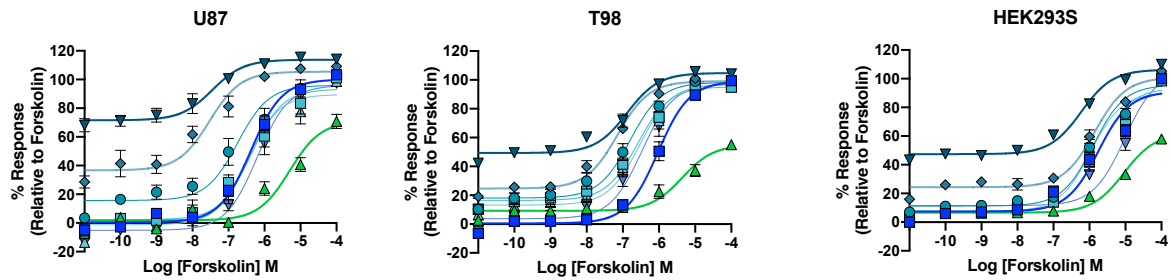
* selection criteria were calculated based on pIC_{50} and span on proliferation assay from Figure 4.13

4.5 Concomitant targeting AC and PDEs only affects short-term cAMP production, but is insufficient to modulate cell proliferation in human glioblastoma cells

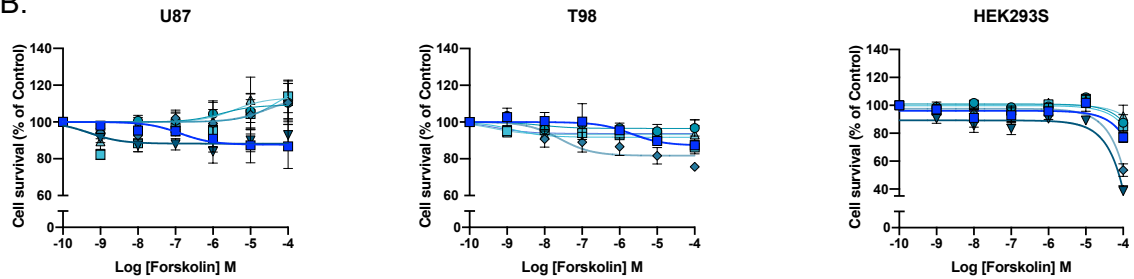
Although forskolin alone significantly suppressed rat glioma cell lines (described in chapter 3), it only reduced cell growth by ~15% on human glioblastoma cells. Forskolin acts through AC activation that subsequently increases the production of cAMP. Trequinsin has been shown to inhibit multiple PDEs, including PDE2, PDE3, and PDE7, leading to improved activity modulating both cAMP production and cell growth. Therefore, this study was performed to investigate if increasing cAMP levels by concomitant targeting of both AC and PDEs will improve anti-proliferative effects compared to individual treatments. To do this, glioblastoma cells were co-treated with forskolin and trequinsin.

Upon 30-minute stimulation with forskolin, cAMP accumulation was differentially increased in a dose-dependent manner by trequinsin (Figure 4.14A). Interestingly, the baseline levels were also dose-dependently increased in all cell lines with U87 cells displaying the most sensitivity towards forskolin and trequinsin combinations. The most prominent effect was shown in U87 cells, followed by T98 and HEK293S cells, respectively. Interestingly, there was no potentiation of cell growth suppression when forskolin was co-treated with trequinsin in any of the cell lines tested (Figure 4.14B). In U87 cells, the relative cell number tended to increase compared to forskolin alone suggesting that the co-treatment was pro-proliferative. In T98 cells, only the combination of forskolin and 10 μ M trequinsin enhanced anti-proliferation which was not observed at lower concentrations of trequinsin. There was no significant effect of trequinsin co-treatment at any concentration on forskolin-mediated anti-proliferation in HEK293S cells. Titration of forskolin with 100 μ M trequinsin in all tested cell lines completely abolished cell growth (Figure 4.14C). Given that trequinsin at 100 μ M also activates caspase-3/-7, the effect observed in these combinations indicate a cAMP-independent mechanism that causes apoptosis.

A.



B.



C.

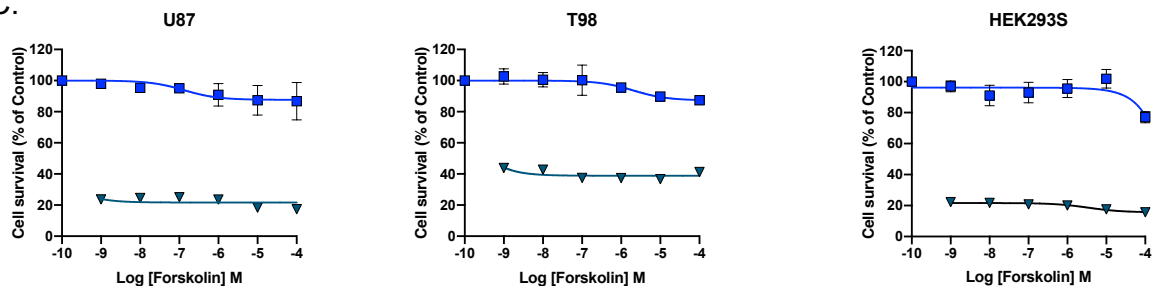


Figure 4.14 Co-treatment of forskolin and trequinsin mediated elevation of cAMP levels but showed marginal effect in cell proliferation across human glioblastoma cell lines. (A) dose-dependent effect of trequinsin upon cAMP accumulation following 30-minute stimulation with forskolin or trequinsin alone (\blacktriangle) in U87, T98, and HEK293S cells. Response are normalised to 100 μ M forskolin. Each data point is expressed as mean \pm SEM of 4-6 data. (B) Cell survival of U87, T98, and HEK293S cells after being exposed to forskolin and combination of forskolin trequinsin (1nM – 10 μ M), and (C) with trequinsin 100 μ M. Combination of forskolin and trequinsin 100 μ M diminished cell growth in all test cell lines.

The minimal effect of co-treatment in all tested cells, indicates that the concomitant targeting of AC and multiple PDE inhibition by trequinsin is insufficient to translate into observable pharmacological effects. Since the expression of PDEs at mRNA levels in human cells: U87, T98, and HEK293S cells are higher (Figure 4.3) compared to C6 rat glioma cells (Figure 3.4), it is possible that these cell lines may restore cAMP levels to the resting state after intracellular cAMP was increased by

forskolin and trequinsin. Thus, in longer exposure, elevation in cAMP will be tuned down by the activity of many PDEs. This also suggests cells may have other mechanisms to fine-tune any modulation occurred within the intracellular compartment, possibly through cAMP efflux transporter.

4.6 The pharmacological effect of cAMP efflux transporter in glioblastoma: MRP4

Having confirmed that glioblastoma cells were less responsive to the combination of forskolin and PDE inhibitor treatment, a different pathway that may contribute to cAMP regulation was investigated. Concentration of cAMP is also maintained by its transport into the extracellular compartment by the ABC efflux transporter, MRP4. ABC efflux transporters are highly expressed in human glioblastoma and have been reported to contribute to chemoresistance (Declèves *et al.*, 2002; Rama *et al.*, 2014; Tivnan *et al.*, 2015; Hill *et al.*, 2016)

In the previous chapter it was validated that PU23 effectively blocks MRP4 to transfer cAMP out of cells and retain cAMP within intracellular compartment. Therefore, this study would be focused on the effect of MRP4 inhibition on cell proliferation. In U87 cells, whilst treatment with forskolin resulted in cell growth suppression of only approximately 15%, cotreatment with PU23 enhanced suppression in cell growth in a dose-dependent manner (Figure 4.15). In T98 cells, the potentiation of the forskolin-mediated anti-proliferative effect was only observed upon cotreatment with 10 μ M PU23. The findings in both cells further suggest that cAMP is anti-proliferative in glioblastoma cell lines. Although the role of PDEs may be less pronounced in human glioblastoma U87 and T98 cells compared to rat C6 cells, all these data suggest that cAMP mediates an anti-proliferative effect.

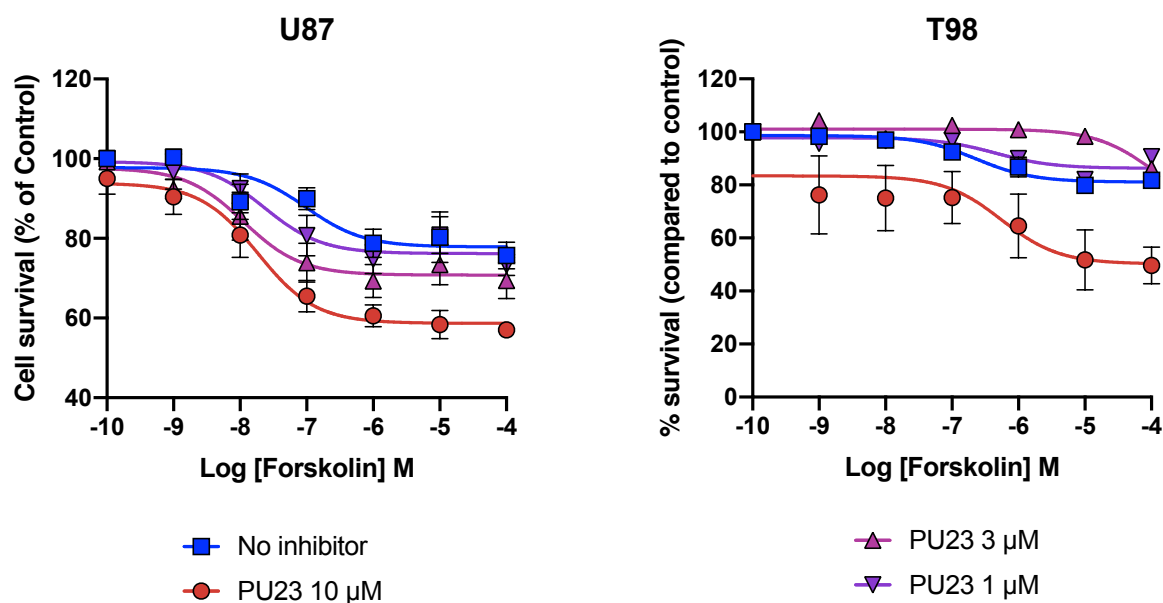


Figure 4.15 PU23, an MRP4 inhibitor, potentiates anti-proliferative effect of forskolin on human glioblastoma U87 and T98 cells. Cell survival was determined upon 72-hour treatment with forskolin in the absence and presence of increasing concentrations of PU23, an MRP4 inhibitor. Data are expressed as percentage cell survival relative to vehicle. All data are the mean \pm SEM of 3-6 individual data.

4.7 Modulation of calcium signalling through SOCE mechanism exhibited negative effect on glioma/glioblastoma cell proliferation

Although targeting cAMP signalling can suppress cell growth, it appears that targeting PDEs and cAMP signalling may not optimally control abnormalities in glioblastoma cell growth. Hence, another secondary messenger may also be involved.

Calcium is a universal intracellular messenger that controls the vast majority of proteins and contributes to physiological changes at the tissue and cellular level, including fertilisation, cell death, cell differentiation and proliferation, B cell activation, mast cell degranulation and insulin secretion (Hoth and Penner, 1992; Berridge, Lipp and Bootman, 2000; Feske, 2007; Rorsman, Braun and Zhang, 2012; Rahman and Rahman, 2017). In collaboration with Dr. Rahman (Department of Pharmacology, University of Cambridge), the functional significance of calcium signalling in cell growth was examined. Specifically, the transient receptor potential cation channels (TRPC) channel was targeted using small molecule inhibitors; Pyr6, teriflunomide, brequinar sodium, and vidoflunimus. All the compounds tested in this study were already approved by FDA for various indications with the main mechanism to inhibit dihydroorotate dehydrogenase (DHODH) as well as inhibiting SOCE activity (Rahman and Rahman, 2017).

In this experiment, repurposed compounds were validated on glioma and glioblastoma cells: C6, U87, and T98 cells utilising cell proliferation assay (Figure 4.16, Table 4.8). Although cisplatin dose-dependently suppressed C6 cells, it appeared to be less profound in T98 cells (Figure 4.16A and C). On the contrary, anti-proliferative effect of cisplatin on U87 cells was negligible (Figure 4.16E). This observation was in agreement with previous studies highlighting the resistance of human glioblastoma U87 cells.

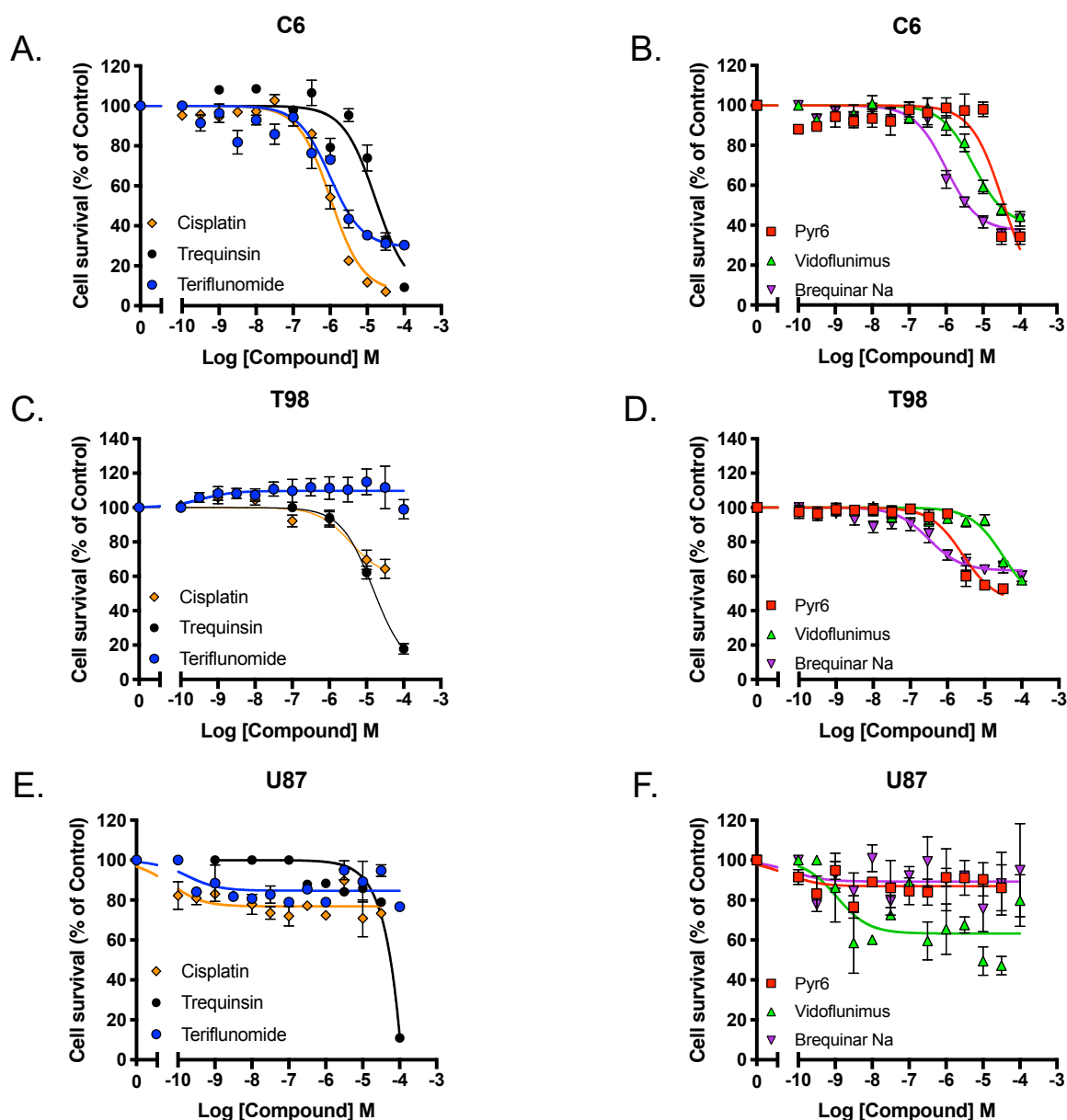


Figure 4.16 Some compounds that inhibit SOCE displayed anti-proliferative action in glioma and glioblastoma cell lines. Cell survival was determined after 72 h treatment by selected compounds in C6 (A,B), T98 (C,D), and U87 (E,F) cells normalisation to vehicle control. Data are expressed as the mean \pm SEM of 3-10 data.

All tested compounds exhibited anti-proliferative effects on both C6 and T98 cells (Figure 4.16 A-D), except teriflunomide on T98 cells. These compounds were more apparent in C6 cells, with the rank order of potency: brequinar Na > teriflunamide > vidoflunimus > Pyr6 (Table 4.8). With the exception of teriflunamide, the rank order of potency of SOCE inhibitor in T98 cells was also the same. Similar to what was observed in cisplatin-treated cells, teriflunomide exhibited minimal anti-proliferative effects in U87 cells (Figure 4.16.E). Despite variable repeats, only vidoflunimus was able to reduce U87 cell growth (Figure 4.16.F). Again, U87 cells were resistance to these treatments.

Table 4.7

The summary of pharmacological parameters of SOCE inhibitors in modulating cell growth

| Compound | C6 | | | T98 | | | U87 | | |
|---------------|-------------------|-----------------|---|-------------------|-----------------|----|-------------------|-------------------------------|----------------|
| | pIC ₅₀ | Span | n | pIC ₅₀ | Span | n | pIC ₅₀ | Span | n |
| Cisplatin | 5.91 ± 0.06 | 93.00 ± 0.58 | 6 | 5.81 ± 0.32 | 41.47 ± 5.85 | 10 | 4.82 ± 1.87 | 26.62 ± 0.61 | 4 |
| Trequinsin | 4.78 ± 0.07*** | 90.76 ± 0.99 | 8 | 4.99 ± 0.06 | 82.20 ± 3.04*** | 9 | N/A | 87.52 ± 0.28*** ^{\$} | 9 |
| Teriflunamide | 6.09 ± 0.14 | 69.88 ± 1.35*** | 6 | N/D | N/D | 8 | 9.78 ± 0.43*** | 13.17 ± 3.04** | 4 |
| Pyr6 | 4.50 ± 0.06*** | 65.74 ± 3.77*** | 6 | 5.59 ± 0.12 | 47.21 ± 1.98 | 6 | N/D | N/D | 3 |
| Vidoflunimus | 5.27 ± 0.41*** | 61.16 ± 1.41*** | 6 | 4.49 ± 0.13*** | 42.22 ± 2.24 | 8 | 9.17 ± 0.51*** | 46.31 ± 16.24** | 2 [#] |
| Brequinar Na | 6.01 ± 0.05 | 62.84 ± 1.67*** | 6 | 6.50 ± 0.13* | 39.82 ± 3.11 | 6 | N/D | N/D | 2 [#] |

When necessary, the curve was constrained to 100 for top plateau and inhibition maximum from each treatment

N/D, not determined

N/A, not applicable

Statistical significance was determined by comparing the value of n data sets to that of forskolin using a one-way ANOVA and Dunnett's *post-hoc* analysis. (**, p<0.01; ***, p<0.001).

^{\$} the parameter was calculated based in top and bottom value for the selected experiment

[#] cannot be investigated further due to Covid-19 pandemic

4.8 Discussion

4.8.1 Human glioblastoma cell lines are more aggressive model compared to rat C6 glioma cells

Although C6 cells are considered to be a gold standard to study glioma, it is necessary to include the human glioblastoma model to see if PDE effects are translatable into human cells. Therefore, the study was extended using U87 and T98 cells. Despite the heterogeneity of human glioblastoma cell lines, Cheng and colleagues reported that cyclic nucleotide signalling and PDE isoenzymes are well preserved in cultured cells providing a robust model to dissect PDE roles in human-derived cell lines (Cheng and Grande, 2007).

In clinical findings, the only pathway that consistently appears in various cancer cells including glioblastoma and urothelial carcinoma, breast cancer, lung adenocarcinoma, stomach and oesophageal carcinoma (Daniel, Filiz and Mantamadiotis, 2016) is cAMP signalling. While glioma cells were reported to have cAMP suppressed, no information is available on non-cancerous cells such as HEK293S cells. Since HEK293S cells expressed many more PDEs compared to U87 and T98 cells, it is possible that any modulation of cAMP levels will trigger PDE sequestration and tune down the second messenger. Considering that HEK293S cells are considered as “normal” cell lines, it is possible if the cAMP pathway controls other signalling events that may not directly correlate to cell growth. It is also worth noting that kidney epithelial cells may have different machinery where the elevation of cAMP by particular PDEs may promote cell proliferation.

Although in human cell lines, each PDE inhibitor's span was not as high as that in C6 cells, almost all PDE inhibitors differentially suppressed human glioblastoma cell growth (Figure 4.7-4.8). The Pearson correlation calculation also showed that, regardless of a broad distribution of each data, a number of compounds were considered effective in U87 and T98 cells.

4.8.2 Differential responses towards PDE inhibitors: U87 vs T98 cells

Both human glioblastoma U87 and T98 cells have been widely used as glioblastoma models. Although many reports highlighted that both cells can be used as model for GBM, these cells may respond to chemotherapeutic agents differently due to biological varieties (Lee, 2016).

The most significant feature observed between both glioblastoma models was the expression of PDE5A (Figure 4.3). PDE5A, a cGMP specific PDE, was highly

expressed in T98 cells compared to U87 and HEK293S cells. Despite this, there was a slight increase in cAMP upon stimulation with PDE5 inhibitors, sildenafil and tadalafil, on both T98 and U87 cells. Treatment of these compounds also positively correlated with PDE5 inhibitor-mediated anti-proliferative effect. Since many other PDEs were also expressed on human glioblastoma cell lines, elevation on cGMP by PDE5 inhibition may promote activation of dual substrate PDEs by sequestering the signalling towards the cAMP pathway. However, this effect was not observed with zaprinast treatment, another PDE5, PDE6, and PDE9 inhibitors classified as cGMP specific PDEs. This inconsistency may occur because of the non-selective action of zaprinast, being an agonist towards GPR35 that is coupled with $G\alpha_i$ and $G\alpha_{13}$ (Divorty *et al.*, 2015). While PDE5A was also present on HEK293S cells, the treatments with sildenafil and tadalafil enhanced HEK293S cell growth. The effect is likely due to PDEs general expression on HEK293S cells were more abundant than the glioblastoma models. Since HEK293S cells' origin was also different, this cell line may have different machinery by having PDEs to be coupled to different signalosomes. Indeed, this notion needs to be investigated further.

This study found that cells that were sensitive towards forskolin appeared to be more responsive towards PDE treatments. In this particular case, despite forskolin increasing total cAMP levels, no effect was observed in HEK293S cell growth. This observation agrees with selection criteria, where most PDE inhibitors were deemed to not have an effect on HEK293S cells. Again, this indicates that probably PDEs may not directly control cell growth in cell originating from the kidney. Lack of PDE effect on non-cancerous HEK293S cells also demonstrates the selectivity of PDE inhibitor mediated-antiproliferative effect towards cancer cells.

Further experiments targeting AC and PDEs concomitantly displayed distinct responses between U87 and T98 cells. It appears that in this study T98 cells are more sensitive compared to U87 cells. It has been reported that overexpression of PDE2A, PDE5A, and PDE10A dictate the sensitivity towards cAMP-elevating agents (Daniel, Filiz and Mantamadiotis, 2016). Although expression of PDE2 seems to be similar between both cells, in agreement with this finding, PDE5A and PDE10A were highly expressed in T98 cells than U87 cell lines.

The ability of cells to translate their sensitivity towards cAMP to cell growth suppression has been reported to be associated to BIM expression, that was predominantly influenced by PDE expressions (Daniel, Filiz and Mantamadiotis, 2016). Upregulation of BIM negatively correlates with MAPK signalling that directly suppress

cell proliferation (Ciechomska *et al.*, 2020). In addition, the dominance of RAF isoform is postulated to dictate the sensitivity of GBM cells towards cAMP elevating agents. Daniel and colleagues reported that in more sensitive cells, such as T98 cells, C-RAF is more dominant and plays a role in inhibiting MAPK signalling and upregulating expression of BIM (Daniel, Filiz and Mantamadiotis, 2016). In these sensitive cells, cAMP not only activates PKA but also further increases BIM expression. On the other hand, B-RAF dominance was found in more resistant cells. B-RAF existence will increase MAPK signalling and therefore suppress BIM expression.

4.8.3 Elevation of cAMP by PDE inhibitor cocktail and concomitant targeting at AC and PDEs cannot optimally induce anti-proliferation in U87 cells

As in the rat glioma model, the trequinsin effect can be mimicked by the combination of individual PDE2, PDE3, and PDE7 inhibitors in human cells. The effects were more apparent in short-term stimulation than in extended stimulation periods in a cell proliferation assay. Surprisingly, U87 cells were more prone to produce cAMP upon short-term stimulation by the compounds. The effects were indicated by the span (range between top and bottom responses in cAMP accumulation). Whilst there was no individual inhibitor that better than trequinsin, either potency and/or E_{max} of combination in pair was also improved. As expected, the PDE inhibitor cocktail curve was overlapped with trequinsin, suggesting that the combinatorial effect has a similar action with trequinsin in modulating total cAMP concentration.

The resistance of U87 cells to cAMP-elevating agents is demonstrated by the fact that even at the highest concentration of trequinsin, it was only able to suppress cell growth by ~80% but only reduced 20% on lower concentrations (Figure 4.13). Except for response at 100 μ M, the PDE inhibitor cocktail showed a similar effect to trequinsin on U87 cells. Although the study cannot provide further evidence on the toxic effect of trequinsin, the findings in rat glioma cells suggest that trequinsin 100 μ M exerts its effect through activation of caspase-3/-7.

Indeed, the equipotency of the PDE inhibitor cocktail was more evident in T98 cells. The similar pattern was also observed in concomitant targeting of AC and PDEs, short-term stimulation giving rise to cAMP concentration cannot be directly translated into cell proliferation. Whilst there was clear potentiation by trequinsin in forskolin-mediated cAMP production in all cells, the degree of antiproliferative effect was not as clear as that of rat glioma cells. In some reports, cAMP-elevating agents: forskolin, IBMX, and forskolin IBMX has a negative effect on cell growth on T98 cells, but the

effect was insignificant in more resistant cells such as U113 and U87 cells (Formolo *et al.*, 2011). Therefore, differential responses from both cell lines strongly depend on each cell line's sensitivity. Due to the effect of Covid-19, the experiment cannot be performed to investigate whether anti-proliferation observed in human glioblastoma cell lines is due to cAMP/PKA pathways.

Although anti-proliferative effects were insignificant in more resistant cell lines, the elevation of cAMP may also affect aggressiveness, invasive and migration ability, and induce cells into cell senescence. Xing *et al.* reported that activation on cAMP pathway through PKA/CREB/PGC1 α induces metabolic reprogramming called the anti-Warburg effect (Xing *et al.*, 2017). This indicates that elevating cAMP levels may not be only limited to control cell proliferation, but also to modulate other cellular responses such as metabolic functions or other second messengers. The cAMP-elevating agents induce U87 cell differentiation from glioblastoma phenotypes onto normal astrocytes that are more prone to cytotoxic agents. Besides, treatment of PDE inhibitor with xanthine-based backbones reduced the aggressiveness of glioblastoma cells by modulating calcium levels and Rho-associated protein kinase (ROCK), which may be independent of cell proliferation (Kang *et al.*, 2010; Ying Chen *et al.*, 2014).

Since elevating cAMP by targeting AC and/or PDEs may not optimally affecting cell proliferation, targeting other proteins such as MRPs and those involved in second messenger signalling might be worth investigating further.

4.8.4 Inhibiting MRP4 efflux transporter improves forskolin- and trequinsin-mediated antiproliferative effect

As mentioned in chapter 3, MRP4, an ABC-cassette efflux transporter, plays an essential role in maintaining the intracellular concentration of cAMP. MRP4 inhibition potentiated the effects of forskolin and trequinsin on glioblastoma cell growth (Figure 4.15), which was not significantly observed in the previous sections.

Although this study did not specify the MRP4 efflux transporter's expression level on both U87 and T98 cell lines, other studies have highlighted MRP4 upregulation in human glioblastoma taken from patients (Rama *et al.*, 2014). Another report also showed that both U87 and T98 cells express a series of MRP transmembrane proteins responsible for chemotherapeutics resistance (Mohri, Nitta and Yamashita, 2000). Together with MRP4 as a cAMP efflux pump, both glioblastoma cell model and from clinical specimens, have been reported to express MRP1, MRP3, MRP5 and P-glycoproteins (Pgp) that also extrude cytotoxic drug from the cells (Mohri, Nitta and

Yamashita, 2000; Calatuzzolo *et al.*, 2005; Decleves *et al.*, 2008; Tivnan *et al.*, 2015). In agreement with this, the degree of anti-proliferative effect of cisplatin on glioblastoma cell lines in this study was lower than that of rat glioma and HEK293S cells. This effect implies the presence of efflux pump may reduce not only cAMP but also chemotherapeutics. Thereby these therapeutic agents have never reached effective exposure to modulate cell growth signalling. Taken together, the action of MRP4 and other transmembrane transporter contributes to the resistant phenotypes and sensitivity of glioblastoma cell models.

Given the impacts of Covid-19, investigation on the effect of MRP4 blockage on cAMP production and on PDE inhibitor cocktail-mediated responses cannot be included. It would be of interest to dissect the role of MRP4 and presumably other MRP proteins in regulating cAMP levels and cell growth.

4.8.5 Inhibiting SOCE as another approach to inhibiting human glioblastoma cell growth: is it a feasible target?

Abnormalities in calcium signalling have been reported to be involved in various pathological conditions. A previous study from Rahman and colleagues found a series of compounds were characterised to inhibit mainly SOCE, but not IP₃R and voltage-gated calcium entry (Rahman and Rahman, 2017). Two classes of compounds were identified to be able to inhibit SOCE, including PDE inhibitors (trequinsin, roflumilast, BAY 73-6691) and DHODH inhibitors (vidoflunimus, brequinar sodium, Pyr6, and teriflunomide). The mechanism of action of SOCE was further investigated to determine the particular protein target these compounds work on inhibition of TRPC-mediated calcium entry and formation STIM1-Orai1 complexes. Whilst no specific action from almost all the compounds, only trequinsin and roflumilast inhibited TRPC, but not the STIM-Orai1 clustering formation. In contrast, vidoflunimus was found to be specific inhibiting STIM1-Orai puncta formation (Rahman, 2020).

PDE inhibitors, roflumilast and trequinsin, were found to be able to inhibit SOCE and TRPC-channel besides their activity in elevating cAMP levels (Rahman, 2020; Safitri *et al.*, 2020). However, none of these compounds affected STIM1-Orai1 complex formation (Rahman, 2020). Although the idea of crosstalk between calcium and cAMP signalling has been initiated, but the interconnected point between these pathways has not been completely elucidated. To date, the mechanism of interaction between both second messengers is postulated through cAMP induced SOCE formation (Willoughby *et al.*, 2012) and SOcAMPS mechanism (Lefkimmiatis *et al.*, 2009; Maiellaro *et al.*,

2012) . The latter has been reported to be independent from calcium influx changes but requires calcium depletion in the ER leading to STIM1 clustering at the plasma membrane (Lefkimmiatis *et al.*, 2009; M. Hofer, 2012; Spirli *et al.*, 2012; Ahuja *et al.*, 2014). Since this particular part was not explored in the previous nor current studies, it would be interesting to unravel the crosstalk between cAMP and calcium signalling and how PDE inhibitors affect this regulation.

The second classes, DHODH inhibitors, displayed differential responses in glioma/glioblastoma cell proliferation. As the most potent inhibitor for human DHODH (Sainas *et al.*, 2017), brequinar sodium was effective in suppressing cell proliferation in C6 and T98 cells, but not U87 cells. Only did vidoflunimus exert anti-proliferative effect in a dose-dependent manner on more resistant model, U87 cells. In addition, vidoflunimus as a SOCE inhibitor also disrupted NFAT translocation to the nucleus (Rahman, 2020). Considering that NFAT is highly expressed in glioma cell (Urso *et al.*, 2019), it is assumed that the NFAT transcription factor plays a more critical role in U87 cells than other glioblastoma models. Taken together, SOCE inhibition by DHODH inhibitors appeared to contribute to anti-proliferative actions. However, further validation is necessary to see if these compounds act through different mechanisms.

4.9 Summary

Using human glioblastoma cells that were reported to be more aggressive and more resistant to any treatment, we validated our finding that were previously validated in rat derived cells. We found that small compounds that are classified as PDE inhibitors were found to be active in human glioblastoma T98 and U87 cells, although the activity was not as prominent as in rat C6 cells. There was a strong correlation between cAMP production and cell growth suppression, suggesting that targeting cAMP signalling may become a feasible target to control cell growth. Applying the selection criteria, more PDE inhibitors were revealed as promising compounds for future studies compared to C6 cells.

Similar to the previous study, trequinsin showed remarkable pharmacological activity in modulating cAMP levels which led to suppressing cell growth. Using three different cell lines, we proved that trequinsin inhibits multiple PDEs which include PDE2, PDE3, and PDE7. Although in HEK293S cells, the trequinsin effect was generated through a cAMP-independent mechanism via caspase-3/-7 activation. Unfortunately, concomitant targeting of both AC and PDEs, by combining forskolin and trequinsin only affected short-term cAMP production but failed to suppress cell growth.

However, the combination of forskolin and PU23, an MRP4 inhibitor, led to greater suppression compared to forskolin alone. Therefore, it is possible that overexpression of a cAMP efflux transporter in glioblastoma may attenuate any antiproliferative effect of PDE inhibition.

Not only was this study performed to investigate cAMP signalling, but it revealed a potential role of SOCE/calcium pathways in modulating cell proliferation. Here, compounds that were previously characterised to inhibit DHODH and modulate SOCE, were examined using the cell proliferation assay. Although only vidoflunimus was found to be effective in the more aggressive U87 cell lines, almost all compounds, except teriflunomide, reduced cell growth after 72h treatment, in both C6 and T98 cells.

CHAPTER 5

IDENTIFYING DUAL-ACTION LIGANDS AGONISING A_{2A}R AND INHIBITING PDE10A

5.1 Introduction

In the previous chapters, impaired cAMP signalling was shown to have an impact on cell growth and therefore targeting PDEs may offer therapeutic benefits to suppress tumour progression in glioma and glioblastoma models. Amongst the 24 types of PDE isoenzymes, PDE10A is often thought to play a significant role in maintaining various physiological functions within the brain, including controlling behavioural and motor functions (Fujishige, Kotera and Omori, 1999). Due to the abundance of PDE10A expression in the striatum, this particular enzyme has been shown to be involved in various neurological diseases such as psychosis, Huntington's disease, and schizophrenia (Siuciak *et al.*, 2006; Grauer *et al.*, 2009; Niccolini *et al.*, 2015). Recently, PDE10A also has been reported to be involved in caloric intake and therefore is proposed to be a potential target to type 2 diabetes mellitus treatment (Nawrocki *et al.*, 2014). Furthermore, PDE10A has been shown to contribute to tumourigenesis in numerous types of cancers including colorectum, breast, brain, and lung (Lindsey *et al.*, 2016; Zhu *et al.*, 2017), although the mechanism of action is not well understood to date.

PDE10A is a dual-substrate PDE that degrades both cAMP and cGMP (Soderling, Bayuga and Beavo, 1999). Although PDE10A has been shown to bind to both cyclic nucleotides, kinetic studies suggest that cGMP hydrolysis by PDE10A may be regulated by cAMP (Soderling, Bayuga and Beavo, 1999). Interestingly, compared to other cGMP-hydrolysing PDE families including PDE2, PDE5, and PDE6; PDE10A has a higher affinity towards cAMP (Soderling, Bayuga and Beavo, 1999), making this enzyme to be known as a cAMP-inhibited dual-substrate PDE (Kenji Omori and Kotera, 2007). Given its unique property to modulate intracellular levels of cAMP, this study focused on concomitant targeting of PDE10A and other proteins that mediate cAMP synthesis at the receptor levels and their concomitant effect to modulate cell proliferation. To do this, the study was extended to include A_{2A}R which is postulated to be a target that will increase intracellular cAMP levels upon activation (Sattin and Rall, 1970; Londos and Wolff, 1977; Calker, Müller and Hamprecht, 1979).

A_{2A}R is a subtype of the adenosine receptors (other subtypes include A₁R, A_{2B}R, and A₃R) which is predominantly coupled to G_s and therefore activation of this receptor stimulates AC leading to cAMP production. Due to its localisation in the brain, A_{2A}R plays an important role in modulating the release of all known neurotransmitters and neuromodulators, including neuropeptides and neurotropic factors (Sebastiao and Ribeiro, 2009). The A_{2A}R has been reported to be linked to CNS disorders such as epilepsy, hypoxia, ischemia, Parkinson's, Alzheimer's, and Huntington's Diseases (Dale and Frenguelli, 2009; Fredholm, 2010; Knight *et al.*, 2016b). In addition, A_{2A}R can also be found in adipose tissues, cardiac tissues, and inflammatory cells (Sachdeva and Gupta, 2013). A_{2A}R has been shown to be overexpressed in many cancer cells such as colorectal, non-small lung cancer (NSCLC). Therefore, it may play a role in tumour progression (Inoue *et al.*, 2017).

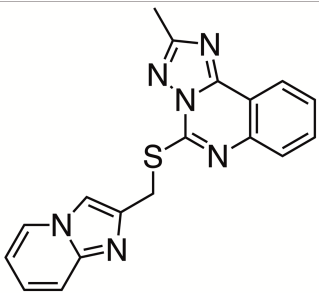
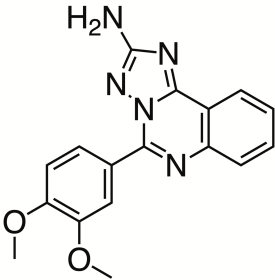
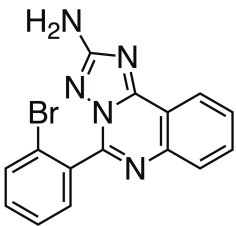
Whilst the previous chapter validated the approach of using ligand combinations to modulate cAMP levels through numerous proteins, in this chapter the study was conducted using a different approach, utilising a single ligand that synergistically modulates multiple targets. Here, structure-based virtual screening was performed by Dr. Kalash (University of Cambridge) to identify compounds that may simultaneously inhibit PDE10A and activate A_{2A}R. Top hits were selected based on the optimum values of computing Matthews correlation coefficient (Kalash *et al.*, 2017). In particular, six compounds with triazoloquinazoline backbones, which have been found initially to inhibit PDE10A (Kehler *et al.*, 2011), were shown to bind to the orthosteric sites of the A_{2A}R. These compounds were further reported to display differential extent of selectivity across all adenosine receptors in yeast and mammalian surrogate overexpression systems (Winfield, 2017). The structure of the compounds as well as their pharmacological parameters (pIC₅₀) at PDE10A, determined previously through *in vitro* experiments (Winfield, 2017), are summarised in the table 5.1.

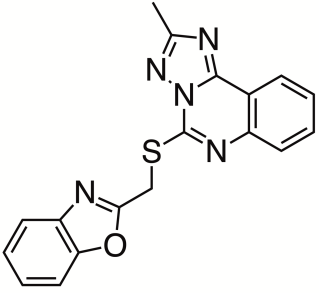
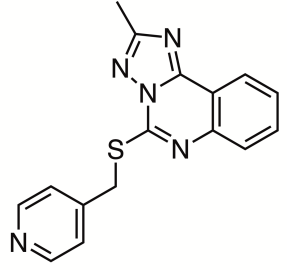
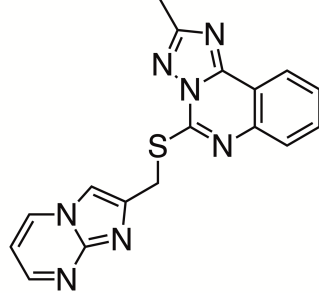
While the use of overexpression system provides benefits for dissecting the molecular mechanism, using more physiologically relevant cells or tissues confers distinct advantages for translating the effect across physiologically relevant settings. The data presented in this chapter is part of a wider study to evaluate triazoloquinazoline-based compounds as dual-target ligands for the A_{2A}R and PDE10A. Where appropriate, I will summarise the studies conducted by my co-authors (Dr. Kalash and Dr. Winfield) to enable full understanding of the story, while focussing, in depth, on my contributions to the project. Data related to the use of yeast as a screen platform and heterologous overexpression are cited as appropriate. Summary of

characterisation of triazoloquinazoline-based compounds at the A_{2A}R prior to my contributions are displayed in Table 5.2-5.4 (details are available in Appendix 1). Dr. Kalash performed the *in silico* docking and target identifications aspects of the project, Dr. Winfield characterised triazoloquinazolines, compound **1-6** for adenosine receptor subtype activity (using yeast assays and CHO-K1 cell lines) while I determined the affinity constants for the triazoloquinazolines compounds at the A_{2A}R and characterised their activity on lung cancer cell lines. This study has now been published (Kalash *et al.*, 2021) for which I am a joint-first author. Finally, in this chapter I describe how I have extended the investigation of the triazoloquinazolines into glioma and glioblastoma models that differentially express A_{2A}R and PDE10A.

Table 5.1

The reference of triazoloquinazolines used in this study

| Structure | Compound reference | | PDE10A pIC ₅₀ ^a |
|---|--------------------|---------------|--|
| | Kehler, 2011 | Our reference | |
|  | 46 | Compound 1 | 9.87 ± 0.10 |
|  | 5c | Compound 2 | 6.71 ± 0.03 |
|  | 5a | Compound 3 | 7.01 ± 0.07 |

| Structure | Compound reference | | PDE10A |
|--|--------------------|---------------|--------------------------------|
| | Kehler, 2011 | Our reference | pIC ₅₀ ^a |
|  | 44 | Compound 4 | 8.47 ± 0.04 |
|  | 40 | Compound 5 | 7.49 ± 0.10 |
|  | 45 | Compound 6 | 8.62 ± 0.12 |

^a The potency of selected compound to inhibit 50% of PDE10A activity. The experiment was performed by Dr. Winfield (Winfield, 2017).

Table 5.2

Potency (pEC₅₀) and E_{max} values for NECA, CGS 21680 and trizaoloquinazoline stimulation of adenosine A₁, A_{2A} and A_{2B} receptors in yeast expressing GPA1/Gα_{i1/2} or GPA1/Gα_s and CHO-K1-A₃R cells.

| | A₁R - GPA1/Gα_{i1/2} | | A_{2A}R - GPA1/Gα_s | | A_{2B}R - GPA1/Gα_s | | CHO-K1-A₃R | |
|------------|--|------------------------------------|--|------------------------------------|--|------------------------------------|-------------------------------------|-----------------------------|
| | pEC₅₀^a | E_{max}^b | pEC₅₀^a | E_{max}^b | pEC₅₀^a | E_{max}^b | pEC₅₀^a | Range^c |
| NECA | 5.87 ± 0.1 | 100.40 ± 3.2 | 6.27 ± 0.2 | 91.14 ± 4.8 | 4.15 ± 0.1 | 99.76 ± 13.2 | 9.50 ± 0.2 | -44.19 ± 2.7 |
| CGS21680 | ND | ND | 4.80 ± 0.2 | 107.2 ± 12.2 | ND | ND | 7.58 ± 0.2 ^{***} | -52.87 ± 2.4 [*] |
| Compound 1 | NR | NR | 5.29 ± 0.2 | 69.01 ± 1.9 | NR | NR | NR | NR |
| Compound 2 | NR | NR | 5.91 ± 0.2 | 54.33 ± 5.1 ^{***} | NR | NR | NR | NR |
| Compound 3 | NR | NR | 5.79 ± 0.2 | 60.16 ± 5.5 ^{**} | NR | NR | NR | NR |
| Compound 4 | 5.44 ± 0.3 | 60.88 ± 9.0 ^{**} | 6.14 ± 0.5 | 38.78 ± 5.3 ^{***} | 4.79 ± 0.2 [*] | 17.62 ± 2.5 ^{***} | 9.43 ± 0.1 | -17.04 ± 0.9 ^{***} |
| Compound 5 | 4.95 ± 0.6 | 22.7 ± 8.1 ^{***} | 8.33 ± 0.9 ^{**} | 9.96 ± 4.0 ^{***} | 4.64 ± 0.3 | 8.66 ± 2.2 ^{***} | NR | NR |
| Compound 6 | NR | NR | NR | NR | NR | NR | NR | NR |

Data ± SEM of 4-6 individual replicates

^a Negative logarithm of agonist concentration producing half-maximal response

^b Maximal response observed upon agonist stimulation, as a percentage of that observed upon stimulation with 100 μM NECA

^c Range of response, as a percentage of that observed upon stimulation with 100 μM forskolin

ND – Not determined – full dose-response curve not feasible

NR – No response

Statistical difference between each agonist and NECA was calculated using a one-way ANOVA with Dunnett's post-test (*, p < 0.05, **, p < 0.01, ***, p < 0.001)

Data was taken from the previous study performed by Dr. Winfield and Sabrina Carvalho (University of Cambridge)

Table 5.3.

Potency (pEC₅₀) and range of responses for cAMP production upon CGS 21680 and triazoloquinazoline stimulated cAMP accumulation in CHO-K1-A_{2A}R and CHO-K1 cells.

| | CHO-K1-A _{2A} R | | | CHO-K1 | | | CHO-K1-A _{2A} R vs CHO-K1 | |
|------------|--------------------------------|--------------------|---|--------------------------------|--------------------|---|------------------------------------|----------------------|
| | pEC ₅₀ ^a | Range ^b | n | pEC ₅₀ ^a | Range ^b | n | Δ pEC ₅₀ ^c | Δ Range ^d |
| CGS21680 | 8.78 ± 0.2 | 86.33 ± 7.2 | 9 | ND | ND | 4 | - | - |
| Compound 1 | 7.32 ± 0.2 | 61.14 ± 5.2*** | 8 | 6.49 ± 0.3 | 20.19 ± 2.7 | 4 | 0.83 ± 0.5 | 40.95 ± 7.8 |
| Compound 2 | 6.29 ± 0.5** | 30.50 ± 8.1 | 6 | 4.85 ± 0.2 | 39.46 ± 3.9 | 4 | 1.44 ± 0.6 | -8.96 ± 10.6 |
| Compound 3 | 7.26 ± 0.3** | 28.95 ± 6.3 | 6 | 5.90 ± 0.3 | 18.32 ± 2.3 | 4 | 1.21 ± 0.5 | 10.63 ± 8.7 |
| Compound 4 | 7.55 ± 0.2 | 37.71 ± 2.9** | 5 | 6.62 ± 0.2 | 18.75 ± 1.7 | 4 | 0.93 ± 0.6 | 18.96 ± 3.6 |
| Compound 5 | 7.70 ± 0.4** | 27.42 ± 4.4 | 6 | 6.30 ± 0.2 | 19.49 ± 1.7 | 4 | 1.28 ± 2.4 | 7.93 ± 6.1 |
| Compound 6 | 6.52 ± 0.4 | 33.87 ± 5.3 | 6 | 6.35 ± 0.3 | 31.42 ± 4.6 | 4 | 0.17 ± 0.8 | 2.45 ± 9.9 |

Data ± SEM of n individual replicates

^a Negative logarithm of agonist concentration producing half-maximal response

^b Percentage range of response observed upon agonist stimulation, relative to that obtained with CGS21680 stimulation in each cell type.

^c Change in pEC₅₀ between CHO-K1 and CHO-K1-A_{2A}R cells (Δ pEC₅₀ = pEC₅₀(CHO-K1-A_{2A}R) - pEC₅₀(CHO-K1))

^d Change in range between CHO-K1 and CHO-K1-A_{2A}R cells (Δ Range = Range (CHO-K1-A_{2A}R) - Range (CHO-K1))

ND – Not determined, full dose-response curve not feasible

Statistical difference, between CHO-K1-A_{2A}R cells and CHO-K1 cells, was calculated using pair-wise t-tests, for each agonist (*, p < 0.05, **, p < 0.01, ***, p < 0.001)

Data was taken from the previous study performed by Dr. Winfield (University of Cambridge)

Table 5.4

The summary of triazoloquinazolines-based compound according to previous characterisation on yeast and heterologous overexpression system

| Compound | Summary of previous characterisation |
|-----------------|--|
| Compound 1 | PDE10 inhibitor, selective A _{2A} R agonist |
| Compound 2 | PDE10 inhibitor, selective A _{2A} R agonist |
| Compound 3 | PDE10A inhibitor, selective A _{2A} R agonist |
| Compound 4 | PDE10A inhibitor, non-selective AR agonist |
| Compound 5 | PDE10 inhibitor, A _{2A} R and A _{2B} R agonist |
| Compound 6 | PDE10 inhibitor, no effect on AR |

5.2 Triazoloquinazolines displayed differential binding affinities at A_{2A}R

The initial findings from the computational study by Kalash suggested that triazoloquinazolines (compound 1-6) bound to A_{2A}R with the involvement of His₂₅₂ and Val₈₄ residues leading to conformational changes (Kalash *et al.*, 2017). Here, the finding from the *in-silico* study were to be confirmed in the overexpression heterologous mammalian systems to specifically characterise their binding at the A_{2A}R.

To do so, the ligand binding studies were conducted to determine the binding properties of triazoloquinazoline at the A_{2A}R. Traditionally, competitive radioligand binding assays are performed (Kenakin, 1988; Bylund and Toews, 1993). In this study, however, radioligands were substituted with fluorescent ligands, and any effects on the ligand binding properties were evaluated using Nano-BRET technology (Stoddart *et al.*, 2015). Aside from its practicality and cost efficiency, Nano-BRET assays offer several advantages including utilising the robust and sensitive methods, a lower chance to cause steric hindrance, and allowing the ligand-receptor interaction to be tracked in real-time in live cells (Xu, Piston and Johnson, 1999; Stoddart *et al.*, 2015; Dale *et al.*, 2019). Therefore, BRET-based ligand binding assays have potential for profiling applications.

CA200645 was selected to be the probe in this ligand binding assay. The compound is a xanthine amine congener (XAC)-based fluorescent antagonist and shows differential affinity towards adenosine receptor families CA200645 has been routinely used to characterise ligand properties towards A₁R and A₃R (Stoddart *et al.*, 2012; Barkan *et al.*, 2019; Soave *et al.*, 2020), and the results have shown that this compound displays high binding affinity towards A₁R and A₃R subtypes. Despite

having lower affinities towards the remaining adenosine receptors, CA200645 can still be used to determine binding properties at A_{2A}R and A_{2B}R.

Before establishing the binding affinity of triazoloquinazoline-based compounds, the affinity constant, K_D (dissociation constant of CA200645) was calculated in HEK293T cells transiently transfected with human A_{2A}R N-terminally tagged with Nluc. Firstly, the saturation assays were performed to determine the K_D parameter, during which a series of concentrations of CA200645 were applied to the cells. The BRET signal reached steady state 10 minutes after the addition of CA200645 (Figure 5.1A), and hence the 10-minute time point was used to generate a saturation curve (Figure 5.1C). In addition, cells were also co-treated with both CA200645 at a range of concentrations and a selective A_{2A}R antagonist ZM241385 at 10 μM was used to determine the non-specific binding at A_{2A}R (Figure 5.1B). From the saturation curve (Figure 5.1C), the K_D was calculated to be about 200 nM, yet an apparent equilibrium state was not achieved. Therefore, there is a possibility that the K_D reported here may be overestimated. Many reports have highlighted that kinetic studies offer a better accuracy in obtaining the true K_D value (Sullivan *et al.*, 2006; Hulme and Trevethick, 2010). To further the true K_D parameter, kinetic studies were next performed to act as a comparison to the constant determined by the saturation binding assays.

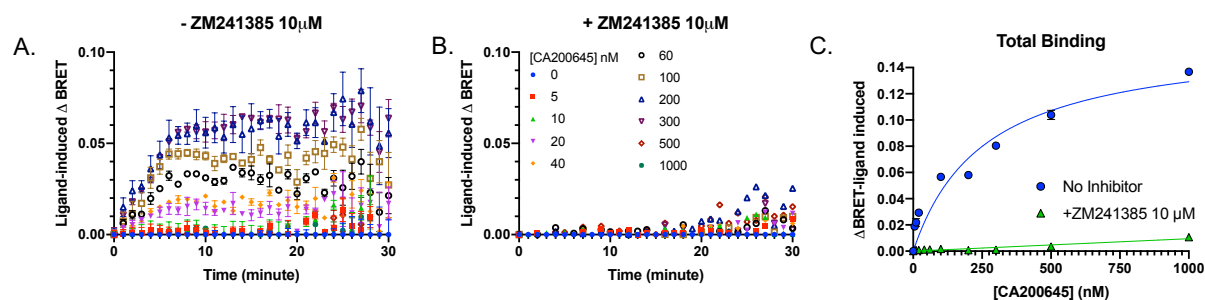


Figure 5.1 Representative traces of BRET signal in ligand binding saturation assay of CA200645 in the absence or presence of ZM241385. HEK-293T cells transiently transfected with Nluc-A_{2A}R were stimulated with increasing concentrations of fluorescent A_{2A}R ligand CA200645 for 30 minutes in the absence (A) or presence of selective A_{2A}R antagonist ZM241385 (B). Data were background subtracted to the vehicle and are expressed as ligand-induced ΔBRET. The ΔBRET signal at t=10 minute was taken to generate saturation curve shown in (C). The representative saturation curves were fitted using one-site binding in GraphPad Prism 8.4.

Similar to the saturation binding assays, CA200645 was applied to HEK293T cells transiently transfected with Nluc-A_{2A}R until reaching plateau. Subsequently,

CGS21680, a selective agonist of A_{2A}R, was injected to displace binding of CA200645 from Nluc-A_{2A}R (Figure 5.2A). In spite of the unusual association binding curve, steady state was reached after 5 minutes. Surprisingly, following the fitting of the data set to the association-dissociation binding kinetic model, a K_D of 65 nM was obtained (Figure 5.2B). This value calculated using a kinetic binding approach was approximately 3-fold lower than that obtained with the use of saturation binding to reach equilibrium. Therefore, the K_D obtained from the kinetic binding assay was used for the competition assays to determine binding properties of triazoloquinazolines.

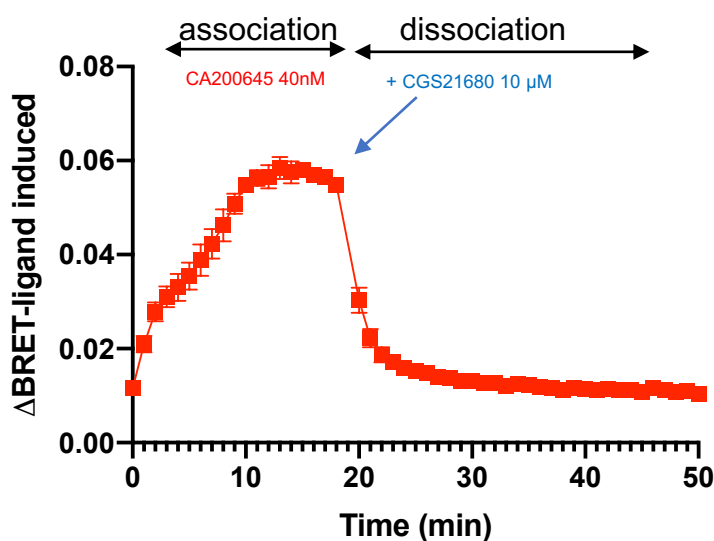


Figure 5.2 Determination of dissociation constant of CA200645 using BRET-based kinetic binding studies. Kinetic binding curve of CA200645 expressed HEK293T cells transiently expressing Nluc-A_{2A}R. After 19 minutes of association with 40 nM CA200645, CGS21680 was injected to give a final concentration of 10 μM in order to displace the fluorescent probe. The curve was fit into “association then dissociation” regression built in Prism 8.4.3 by constraining maximal specific binding (B_{max}) to 0.1 and non-specific binding (NS) to 0.01.

Characterisation of the binding properties of selected triazoloquinazolines-based compounds was then performed by applying CA200645 together with a series of concentration of test compounds in the HEK293T cells transiently expressing Nluc A_{2A}R. Taken into the account the background noise that may affect the signal, a concentration above the calculated K_D (300nM) was chosen to ensure that the number of occupied receptors is sufficient to give window of observation from displacement.

To confirm if this approach was suitable for evaluating the binding properties of the test compounds, the following reference compounds were included: CGS21680, NECA, and isoprenaline. As noted, CGS21680 is an A_{2A}R selective agonist, whereas

NECA is a non-selective adenosine receptor agonist (Jarvis *et al.*, 1989; Monopoli *et al.*, 1994). Isoprenaline, which is a beta-adrenoceptor agonist, was also included as a negative control to show that the compounds selectively bind A_{2A}R. The representative traces of BRET signal are displayed in Figure 5.3 which were recorded over 20 minutes after co-treatment with CA200645 and the reference compounds. As displayed in Figure 5.3A and B, there was a dose-dependent decrease in BRET signal, suggesting CA200645 was displaced by CGS21680 and NECA, respectively. While these two compounds were shown to bind to the A_{2A}R, isoprenaline failed to compete with the binding of fluorescent probe (Figure 5.3C). Using this assay, the affinity constants (pK_i) obtained in this study was 6.39 ± 0.04 for CGS21680 and 6.36 ± 0.09 for NECA (Figure 5.3D, Table 5.5). However, these values were slightly lower than those previously reported values range CGS21680: 6.7 – 8.1 and NECA: 6.9 – 8.7, respectively (Table 5.5).

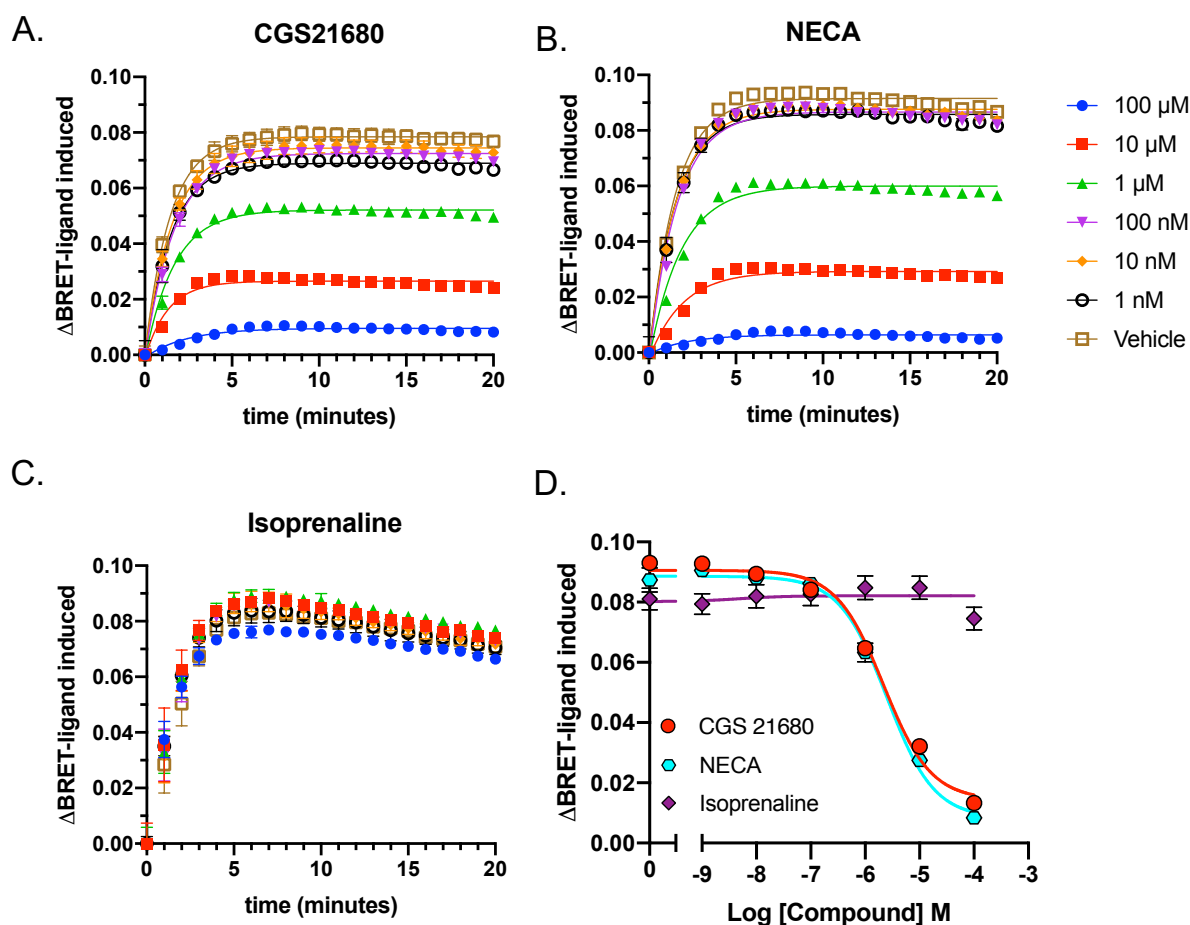


Figure 5.3 BRET signal traces from competition binding assays of reference compounds at A_{2A}R. Representative ligand induced Δ BRET traces in competition

binding method to determine binding properties of CGS21680 (A), isoprenaline (B), and NECA (C). After 5 minutes curve seems to be reached plateau in for almost all reference compounds. Ten-minute time point was taken to generate competition curve (D).

Having validated the ligand binding approach to determine the pK_i values of the reference compounds, the binding affinities of triazoloquinazolines were determined. As shown in Figure 5.4A, all triazoloquinazolines were able to displace the binding of CA200645 at A_{2A}R in a dose-dependent manner. The association constants were determined by fitting the data set to “one-site K_i” equation where K_D and the concentration of hot ligand were set to be at 65 nM and 300 nM, respectively. The summary of pK_i from each test compound is displayed in bar charts (Figure 5.4B) and Table 5.5. The rank order of affinities for the triazoloquinazoline compounds at the A_{2A}R was as follows: compound 4 > compound 2 > compound 6 > compound 1 = compound 3 > compound 5 (note: under condition tested, compound 5 was unable to fully displace CA200645, with the maximum inhibition up to 37% compared to CGS21680) (Figure 5.4). Interestingly, compound 6 also bound to the A_{2A}R from this assay. Given the fact that previous validation compound 6 did not display any effect in a yeast assay (Table 5.2, Appendix 1), therefore it is probable that compound 6 may act as an antagonist to the A_{2A}R. However, further validation is necessary to confirm this hypothesis.

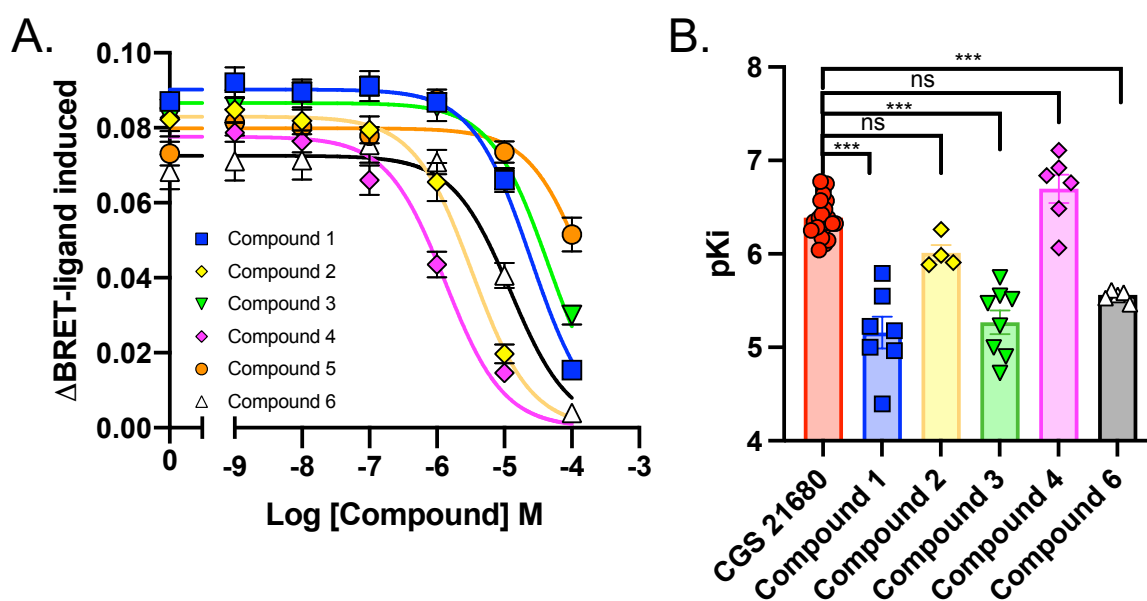


Figure 5.4. Triazoloquinazolines were confirmed to bind at the A_{2A}R. (A) Displacement curve of CA200645 (300nM) by triazoloquinazolines. The curves were generated by fitting the data to the “one-site K_i” equation where K_D and concentration

of hot ligand were set to 65 nM and 300 nM, respectively. Data points are the mean \pm SEM from 3-27 repeats performed in duplicate. (B) The summary of binding affinities (pK_i) of tested ligands. pK_i values were calculated from inhibition of CA200645 binding at equilibrium to Nluc-A_{2A}R-expressed HEK293T cells. # Cmpd 5 did not fully displace binding of CA200645 under condition tested. Statistical significance (***, p<0.001) compared to CGS21680 was determined by one-way ANOVA with *Dunnett's post-test*

Table 5.5

Binding affinities of triazoloquinazolines at the human A_{2A}R using fluorescent probes CA200645

| Compound | pK _i ^a | pK _i ref ^b | n |
|--------------|------------------------------|----------------------------------|----|
| CGS21680 | 6.39 \pm 0.04 | 6.7 – 8.1 | 27 |
| NECA | 6.36 \pm 0.09 | 6.9 – 8.7 | 6 |
| Isoprenaline | N/R | N/A | 4 |
| Compound 1 | 5.26 \pm 0.17*** | N/A | 7 |
| Compound 2 | 6.01 \pm 0.09 | N/A | 4 |
| Compound 3 | 5.27 \pm 0.13*** | N/A | 8 |
| Compound 4 | 6.70 \pm 0.15 | N/A | 6 |
| Compound 5 | N/A | N/A | 3 |
| Compound 6 | 5.55 \pm 0.03*** | N/A | 5 |

^apK_i values were calculated from the inhibition of equilibrium fluorescent probe CA200645 binding to HEK293T cells expressing Nluc-A_{2A}R.

^bpK_i reference values were accessed from

<https://www.guidetopharmacology.org/GRAC/LigandListForward?type=Synthetic-organic&database=all#C>

N/A – not available

N/R – no results

Statistical significance (***, p<0.001) compared to CGS21680 was determined by one-way ANOVA with *Dunnett's post-hoc* analysis.

To conclude, based on previous characterisation using yeast and heterologous overexpression system, it is confirmed that all compounds inhibit PDE10. While compound 1-3 are found to be selective A_{2A}R agonist, compound 4 elicited activity on all adenosine receptor subtypes and compound 5 also stimulated A_{2B}R-mediated responses. According to ligand binding data, it suggests that compound 6 may act as an antagonist to the A_{2A}R.

5.3 Non-small lung cancer cell lines as the appropriate model to validate multi-target ligand against A_{2A}R/PDE10A

To validate that triazoloquinazoline compounds have synergistic mechanisms to activate A_{2A}R and inhibit PDE10A simultaneously, NSCLC cell lines were used as they show differential cumulative expression of A_{2A}R and PDE10A (Figure 5.5). These cells can be further categorised as LUSC (lung squamous cell carcinoma) and LUAD (lung

adenocarcinoma). In this study, four types of cells were used: LK2 and H520 cells (LUSC), as well as H1792 and H1563 cells (LUAD). Despite the differences between these cell lines in molecular machinery, their endogenous expression of adenosine receptors and PDE10A warranted their use in the subsequent pharmacological characterisation studies.

In order to evaluate the expression levels of adenosine receptor subtypes and PDE10A in these four cell lines, rt-PCR was performed. As shown in Figure 5.5A, the aforementioned cell lines expressed, to different extent, the 4 adenosine receptors subtypes and PDE10A. While all cell lines expressed almost all adenosine receptors, there was no detectable band for A_{2A}R and A₃R in LK2 cells and very low levels of A₃R expression in H1563 cells (Figure 5.5B). The expression of PDE10A amongst these cells were also diverse with LK2 expressing the lowest, followed by H1792 cells, and H1563 cells. However, PDE10A was not detected in H520 cell lines. Interestingly, these systems had cumulative expression of both targets A_{2A}R and PDE10A, with the cumulative expression as follows: LK2 < H520 < H1792 < H1563 (Figure 5.5B). These results indicated that using these cells lines that endogenously express proteins of interests may serve as useful cell systems for validation of compounds at physiologically relevant settings.

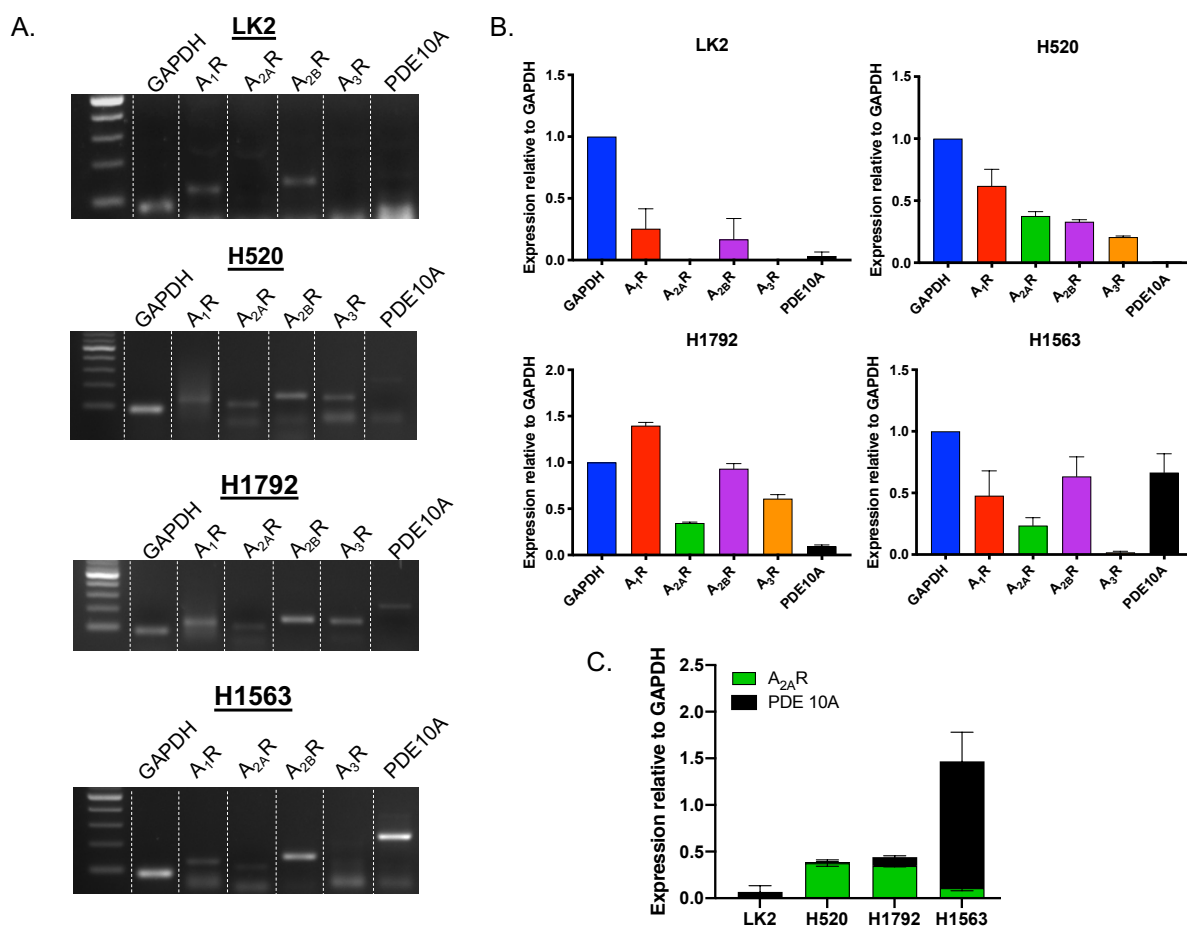


Figure 5.5 Non-small lung carcinoma (NSCLC) cell lines differentially expressed different levels of adenosine receptors and PDE10A. (A) Representative gel picture of amplified adenosine receptors and PDE10A genes. (B) Semi-quantitative expression profile of adenosine receptors and PDE10A in mRNA levels. Expression of each gene of interest was normalised relative to GAPDH and was determined in LK2, H520, H1792, and H1563 cell lines. (C) Comparison of cumulative A_{2A}R plus PDE10A expression amongst NSCLC cells. Data are expressed as the mean \pm SEM from 4-6 individual repeats.

5.4 Synergistic activities of dual mechanism of PDE10A inhibition and A_{2A}R agonism on ligand-mediated cAMP accumulation leading to cell growth suppression in human lung cancer cell lines

5.4.1 Triazoloquinazolines promoted cAMP production in human NSCLC cells

Having determined the individual expressions of adenosine receptor subtypes and PDE10A in the designated NSCLC cell lines, compound **1-6** were further validated in these physiologically relevant cell lines. In this experiment, CGS21680 was also included, which acted as the reference compound to compare cAMP responses with the test compounds. Since the expression of A_{2A}R varied amongst the four cell lines, different extents of cAMP accumulation were observed upon stimulation with CGS21680 (Figure 5.6A). Here, the LK2 cells showed the weakest cAMP accumulation

potency (pEC₅₀ 4.84 ± 0.38) and efficacy relative to forskolin (pEC₅₀ 6.85 ± 1.62) responses upon CGS21680 stimulation (Table 5.6). The potencies were increased in H1563 (pEC₅₀ 5.34 ± 0.21), H520 (pEC₅₀ 5.46 ± 0.11), and H1792 (pEC₅₀ 5.52 ± 0.17) cell lines, which results aligned well with the previously determined A_{2A}R expression profile (Figure 5.2, Table 5.6).

Compound **1** displayed the negligible activity in LK2 cells, which was improved when applied to H520 and H1792 cells, with the pEC₅₀ of 5.49 ± 0.24 and 6.09 ± 0.22, respectively. The most potent activity of compound **1** was observed in H1563 cells (pEC₅₀ 6.44 ± 0.11) which express the highest levels of cumulative A_{2A}R and PDE10A expression (Figure 5.5B). In general, compound **1** activity was enhanced in the cells that expressed higher cumulative expression levels of A_{2A}R and PDE10A (Figure 5.5C). As for compound **5**, its efficacy exerted a similar pattern to compound **1**, which was in agreement with the previous characterisation in yeast and overexpression mammalian systems (Winfield, 2017). Interestingly, compound **2** (Figure 5.6C) showed consistent effects regardless of cell types suggesting the effect was most likely due to action independent of A_{2A}R and/or PDE10A. Furthermore, compound **3** elevated similar cAMP responses in both LK2 and H1563 cells with potency values in the micromolar range (Figure 5.6D, Table 5.6). There was also an increase of efficacy upon stimulation with compound **3** in H520 (E_{max} 22.36 ± 1.53) and H1792 (E_{max} 24.17 ± 1.83) cells compared to other cell lines. As expected, the results demonstrated here were consistent with the previous study highlighting the action of compound **3** towards A_{2A}R, which were both H520 and H1792 cells expressed to the similar extent on A_{2A}R expression (Figure 5.5).

Due to additional action towards A_{2B}R, compound **4** promoted a higher cAMP production in cells that showed higher level of A_{2B}R. This is verified by its increased activity in H1792 cells (pEC₅₀ of 7.47 ± 0.31) that expressed more A_{2B}R than LK2 cells (4.74 ± 0.61) (Figure 5.6E). Although compound **6** showed affinity at the A_{2A}R in the previous ligand binding experiment, there was only a slight increase of cAMP accumulation upon stimulation with compound **6** in NSCLC cell lines (Figure 5.6G, details in Table 5.6). It is possible that cAMP elevation by compound **6** was generated by rolipram (a PDE4 inhibitor) which was present in the stimulation buffer. Corroborated with the previous study using the yeast system expressing A_{2A}R, here compound **6** also did not show any pharmacological action. These indicate that compound **6** may act as an antagonist at the A_{2A}R, as described in Table 5.4 and Appendix 1.

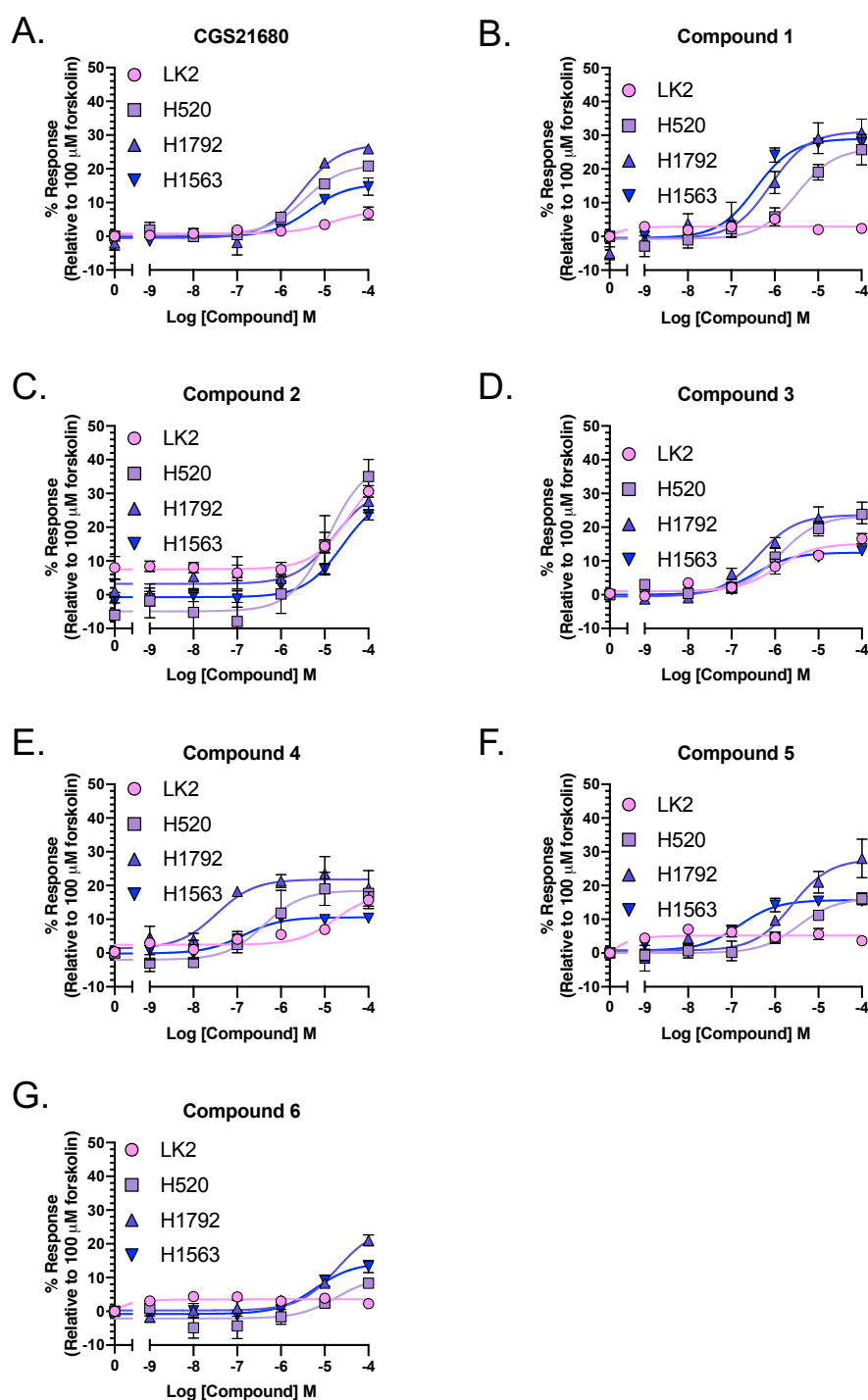


Figure 5.6 Multitarget ligand mediated cAMP accumulation on NSCLC cell lines. Accumulation of cAMP was determined following 30 minutes stimulation with compound 1-6 (B to G) in LK2, H520, H1792, and H1563 cells in the presence of rolipram. CGS21680 (A) is a selective A_{2A}R compound and is used as a reference compound for cAMP accumulation assay. Data are expressed relative to the maximal response produced by 100 μM forskolin. Values are expressed as mean ± SEM of 4-8 individual data sets.

5.4.2 Triazoloquinazolines mediated anti-proliferative effects on human NSCLC cell lines

Having established that triazoloquinazolines were able to modulate cAMP levels to different extents in NSCLC cell lines, cell proliferation assays were performed to investigate if these compounds influence cell growth. Here, forskolin, a pan-AC activator, was used as a reference compound to determine the effect of cAMP activation on cell growth. Upon treating the four cell lines with forskolin for 72 h, forskolin suppressed cell growth by approximately 25% (Figure 5.7A). Next, these cell lines were treated with CGS21680. Interestingly, cell growth on selected cells was unaffected by selective agonism of A_{2A}R induced by CGS21680 (Figure 5.7B). This suggests that short-lived CGS21680-mediated cAMP accumulation did not lead to anti-proliferation, which may be explained by receptor desensitisation, as similar effect was also observed in glioma cells (chapter 3) where stimulation at receptor levels were inadequate to alter cell proliferation.

These four cell lines were treated with compound **1-6** for 72h in order to compare their effect on cell proliferation with the reference compound, forskolin. Here, change to higher potencies and larger suppressions of compound **1** and **5** was observed on NSCLC cell lines (Figure 5.7C and G, Table 5.6). These observations aligned with the previous results in the cAMP accumulation assay (chapter 5.3.1), whereby potent cAMP responses induced by compound **1** and **5** were presumably mediated through the synergistic agonism of A_{2A}R and inhibition of PDE10A. As expected, the activity of compound **2** across lung carcinoma cell lines remained constant, suggesting the anti-proliferative or cytotoxic effects were independent of the dual targets (Figure 5.7D). Furthermore, compound **3**, previously established as a selective A_{2A}R receptor agonist (Table 5.4), induced a similar extent of anti-proliferative effects on all cell lines (Figure 5.7E). As for compound **4**, its effect aligned with its ability to elevate cAMP levels in the presence of A_{2AB}R, with greater suppression on cell growth observed in cells expressing higher A_{2B}R (H1792 cells) (Figure 5.7F). Finally, although there were slight increases in cell proliferation at high concentration, compound **6** did not significantly affect cell growth on any human lung cancer cell lines (Figure 5.7G). To determine the extent to which the compounds inhibit cell growth, again, a proliferation factor, which was similar to the selection criteria in chapter 3 and 4, was applied by multiplying potency (pIC₅₀) and span from individual anti-proliferation curves (from Figure 5.7).

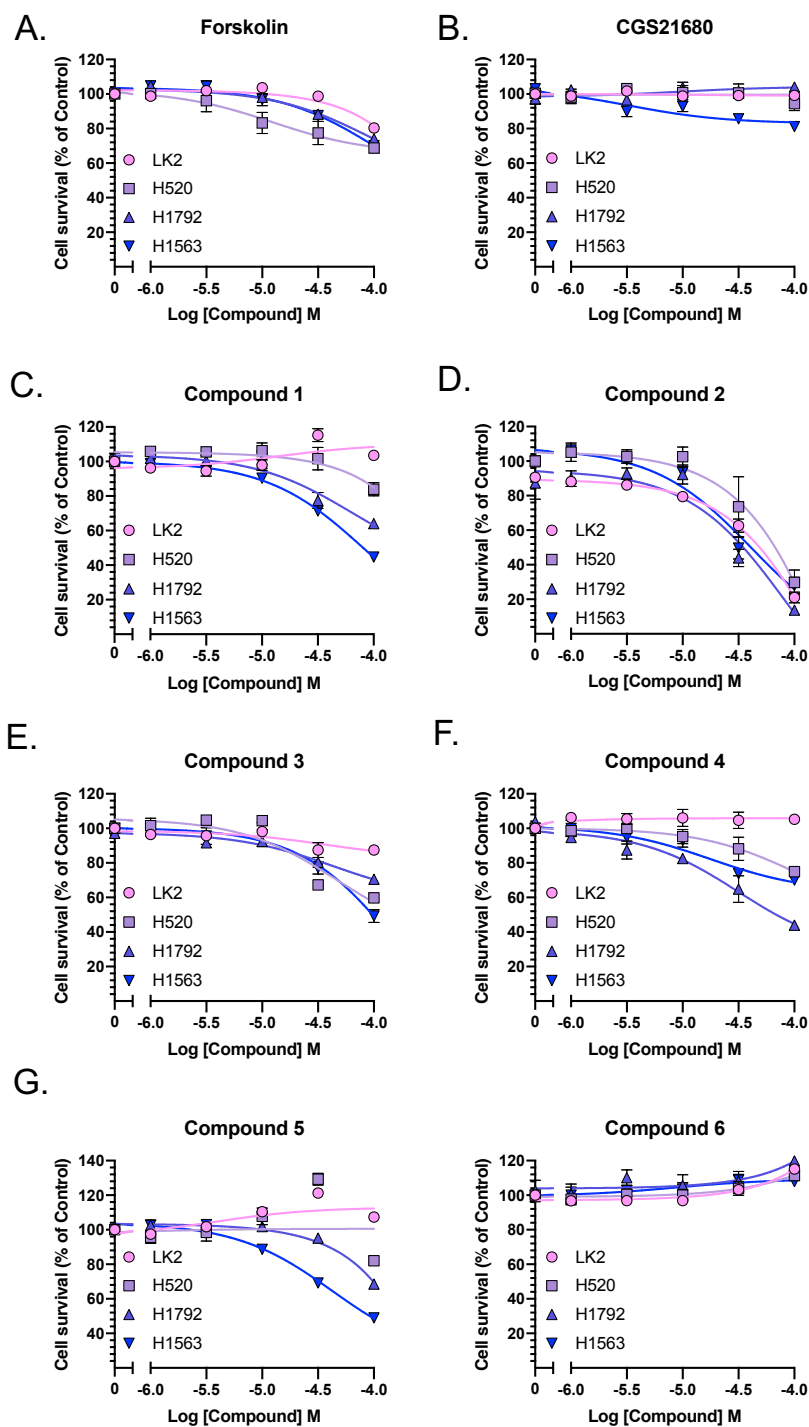


Figure 5.7 Differential anti-proliferative effect in NSCLC cell lines after triazoloquinazolines treatment. Dose-response curves of forskolin (A), CGS21680 (B), compound 1 to 6 (C-H) on LK2, H520, H1792, and H1563 cells. Cell survival was determined upon 72h treatment. Data are expressed as percentage survival relative to vehicle alone and are the mean \pm SEM of 4-9 individual data.

5.5 Multi-target ligands simultaneously displayed better efficacy across human lung cancer cell lines corresponding to cumulative expression of A_{2A}R and PDE10A

To determine if the modulation of cAMP concentration had any association with anti-proliferative effect, Pearson's correlation coefficient was calculated by correlating the potency of each compound in both cAMP accumulation and cell proliferation pathways. As displayed in Figure 5.8A, strong correlation was observed between potency of compound in elevating cAMP levels and potency in inhibiting cell growth ($r = 0.801$ with 95% confidence interval of 0.85 – 0.91). Since potency was not the only measurement to determine how good the compounds were in inhibiting cell growth, the magnitude of anti-proliferative effect was also taken into account. Therefore, proliferation factors were calculated based on pIC_{50} and I_{max} from individual dose-response curves (Figure 5.8B). As expected, this approach confirmed that only compound **1** and **5** exhibited progressive improvement parallel to the cumulative expression of A_{2A}R and PDE10A (Figure 5.2). Whilst compound **3** and **4** also elicited improved efficacies, compound **2** remained the same irrespective of cell types. Taken together, it was corroborated that compound **1** and **5** work through dual actions: agonism at A_{2A}R and inhibition of PDE10A, whereas compound **3** appeared to be a non-selective adenosine receptor agonist with some action towards PDE10A, and compound **4** was more pronounced when A_{2B}R was present in the cells. It was only compound **2** that modulated both cAMP and inhibit cell growth independent of A_{2A}R-PDE10A expression suggesting the probability of an off-target mechanism leading to toxic effects.

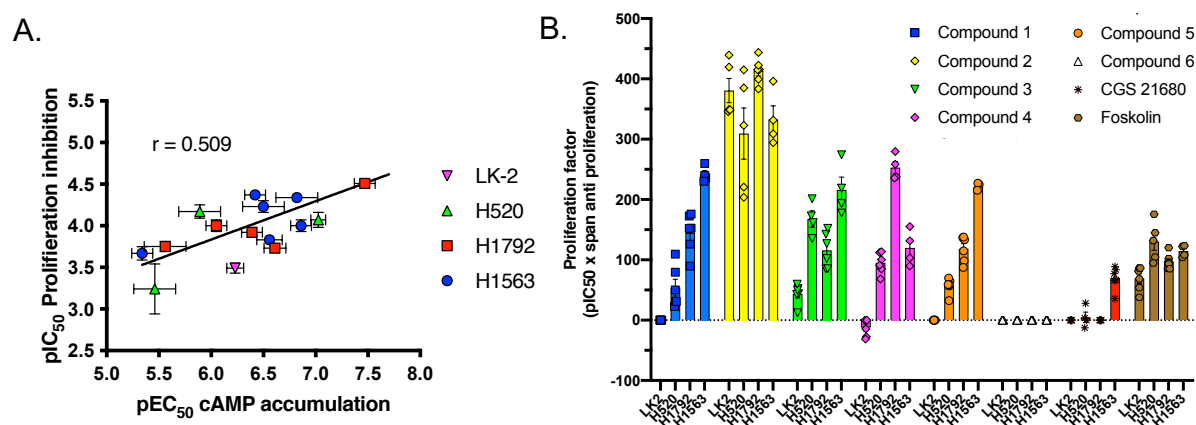


Figure 5.8 Multi-target ligands simultaneously displayed better efficacies across cell lines corresponding to the cumulative expression of A_{2A}R and PDE10A. A. Correlation plot of log potencies of each ligand in all NSCLC cell lines. Correlation plot (with 95% confidence interval) was determined by calculating Pearson's correlation coefficient (r). Data are expressed as mean \pm SEM of 4-8 individual repeats. B. Proliferation factor of each ligand across NSCLC cell lines. Proliferation factor was calculated based on potency and efficacy of each ligand in proliferation assay.

Table 5.6

Summary of pharmacological activities of triazoloquinazolines across human NSCLC cells

| Compound | cAMP | | | Cell proliferation | | | n |
|--------------|-------------------|---------------|---|--------------------|---------------|----------------------|---|
| | pEC ₅₀ | Span (%) | n | pIC ₅₀ | Span (%) | Proliferation Factor | |
| LK2 | | | | | | | |
| Forskolin | 6.23 ± 0.08 | 89.0 ± 4.7 | 6 | 3.47 ± 0.19 | 19.7 ± 4.8 | 69.12 ± 19.84 | 6 |
| CGS21680 | 4.84 ± 0.38 | 6.9 ± 1.6*** | 8 | N/A | N/A | N/A | 4 |
| Compound 1 | N/A | N/A | 4 | N/A | N/A | N/A | 6 |
| Compound 2 | 4.42 ± 0.28 | 31.8 ± 6.6*** | 5 | 4.81 ± 0.15 | 78.9 ± 6.9*** | 380.57 ± 45.22*** | 5 |
| Compound 3 | 5.96 ± 0.21 | 14.1 ± 1.4*** | 4 | N/A | 43.5 ± 16.5 | 43.51 ± 16.52 | 6 |
| Compound 4 | 5.08 ± 0.32 | 15.6 ± 2.4*** | 6 | N/A | -4.1 ± 4.9 | -12.19 ± 14.48* | 9 |
| Compound 5 | N/A | N/A | 6 | N/A | N/A | N/A | 6 |
| Compound 6 | N/A | N/A | 7 | N/A | N/A | N/A | 6 |
| H520 | | | | | | | |
| Forskolin | 7.02 ± 0.07 | 99.3 ± 3.2 | 8 | 4.13 ± 0.43 | 31.2 ± 4.6 | 130.38 ± 32.48 | 5 |
| CGS21680 | 5.46 ± 0.11*** | 20.3 ± 1.1*** | 6 | N/A | 1.9 ± 4.3** | 4.72 ± 17.13 | 4 |
| Compound 1 | 5.49 ± 0.24*** | 26.9 ± 3.1*** | 6 | N/A | 16.0 ± 9.4 | 53.96 ± 33.97 | 6 |
| Compound 2 | 4.91 ± 0.31*** | 44.8 ± 8.6*** | 6 | 4.34 ± 0.37 | 70.2 ± 16.1 | 309.40 ± 95.00* | 5 |
| Compound 3 | 5.87 ± 0.15*** | 22.4 ± 1.5*** | 6 | 4.16 ± 0.07 | 40.2 ± 5.9 | 167.77 ± 27.33 | 4 |
| Compound 4 | 6.39 ± 0.17 | 20.5 ± 2.1*** | 4 | 3.78 ± 0.28 | 25.0 ± 3.6 | 95.05 ± 17.22 | 6 |
| Compound 5 | 5.45 ± 0.22*** | 16.3 ± 1.5*** | 3 | N/A | 17.9 ± 2.3 | 57.00 ± 12.99 | 6 |
| Compound 6 | 4.74 ± 0.65*** | 12.4 ± 4.5*** | 4 | N/A | N/A | N/A | 6 |
| H1792 | | | | | | | |

| Compound | cAMP | | | Cell proliferation | | | n |
|--------------|-------------------|---------------|---|--------------------|---------------|----------------------|---|
| | pEC ₅₀ | Span (%) | n | pIC ₅₀ | Span (%) | Proliferation Factor | |
| Forskolin | 6.98 ± 0.11 | 84.8 ± 4.7 | 8 | 3.73 ± 0.10 | 25.9 ± 2.6 | 96.97 ± 11.75 | 7 |
| CGS21680 | 5.52 ± 0.17*** | 27.8 ± 2.2*** | 8 | N/A | N/A | N/A | 4 |
| Compound 1 | 6.09 ± 0.22*** | 31.8 ± 3.3*** | 7 | 4.00 ± 0.23 | 35.9 ± 6.7 | 144.86 ± 32.40 | 6 |
| Compound 2 | 4.78 ± 0.36*** | 28.4 ± 6.4*** | 6 | 4.79 ± 0.18*** | 86.2 ± 1.4*** | 413.37 ± 20.56*** | 6 |
| Compound 3 | 6.39 ± 0.17 | 24.2 ± 1.8*** | 5 | 3.92 ± 0.08 | 29.4 ± 6.9 | 115.63 ± 29.13 | 6 |
| Compound 4 | 7.47 ± 0.31 | 20.5 ± 2.6*** | 6 | 4.51 ± 0.23* | 56.0 ± 1.7** | 252.83 ± 20.64*** | 4 |
| Compound 5 | 5.61 ± 0.27*** | 27.1 ± 3.4*** | 5 | 3.74 ± 0.11 | 31.5 ± 4.9 | 118.17 ± 21.47 | 6 |
| Compound 6 | 4.72 ± 0.16*** | 24.7 ± 2.5*** | 6 | N/A | N/A | N/A | 6 |
| H1563 | | | | | | | |
| Forskolin | 6.54 ± 0.08 | 99.4 ± 3.3 | 6 | 3.83 ± 0.06 | 29.9 ± 2.1 | 114.44 ± 9.70 | 4 |
| CGS21680 | 5.34 ± 0.21* | 15.6 ± 1.6*** | 7 | 3.66 ± 0.22* | 18.9 ± 4.3 | 69.77 ± 18.94** | 6 |
| Compound 1 | 6.44 ± 0.11 | 29.4 ± 1.3*** | 7 | 4.37 ± 0.06 | 55.3 ± 2.9 | 241.55 ± 12.73*** | 4 |
| Compound 2 | 4.60 ± 0.22 | 30.5 ± 4.6*** | 6 | 4.62 ± 0.10 | 71.9 ± 9.5 | 332.70 ± 44.98 | 4 |
| Compound 3 | 6.46 ± 0.17*** | 12.5 ± 0.9*** | 6 | 4.24 ± 0.22 | 50.7 ± 42.4 | 207.52 ± 22.83 | 4 |
| Compound 4 | 6.86 ± 0.20 | 10.7 ± 0.9*** | 5 | 3.98 ± 0.21 | 29.9 ± 5.8 | 119.88 ± 29.21 | 4 |
| Compound 5 | 6.82 ± 0.20 | 14.9 ± 1.0*** | 7 | 4.34 ± 0.02 | 51.0 ± 1.0 | 221.22 ± 5.65* | 4 |
| Compound 6 | 5.22 ± 0.18** | 15.1 ± 1.5*** | 8 | N/A | N/A | N/A | 4 |

N/A – not applicable

Negative values in represented mean selected compound promoted cell growth

Statistical significance was calculated using one way ANOVA compared to forskolin followed by Dunnet's post-hoc analysis (*p<0.05, **, p<0.01, ***, p<0.001)

The study on NSCLC cell lines as the relevant model to validate the dual-target mechanism has proved the ability of triazoloquinazolines in elevating the concentration of cAMP, which leads to anti-proliferative effects. As expected, triazoloquinazolines actions on cell growth were aligned with their ability to modulate cAMP levels with both actions dependent on cumulative expressions of $A_{2A}R$ and PDE10A.

5.6 Targeting $A_{2A}R/PDE10A$ elevated cAMP levels but did not optimally suppressed glioma/glioblastoma model

5.6.1 Expression profile of $A_{2A}R$ and PDE10A in glioma/glioblastoma cell models

As mentioned previously, targeting particular PDEs or another second messenger such as those proteins that are involved in SOCE mechanism (chapter 4) have resulted in anti-proliferation to some extent in glioma and glioblastoma cells. Since the synergism of targeting $A_{2A}R$ and PDE10A sufficiently suppressing NSCLC cell lines, the study was extended to identify whether targeting PDE10A and $A_{2A}R$ from multi-target ligand will have similar effects in inhibiting brain-derived cancer cells. To do this, C6 cells were used as glioma model that is derived from rat origins, U87 and T98 cells as human glioblastoma model, and HEK293S cells as non-cancerous human normal cells.

Firstly, the expression profile of all subtypes of adenosine receptors and PDE10A at the mRNA level was determined by rt-PCR. Displayed in Figure 5.9A, all cell lines expressed most of the adenosine receptor subtypes with differential expression of PDE10A. The rat C6 glioma cells displayed similar levels of expression of adenosine receptors and PDE10A (with expression of A_1R the highest). U87 and T98 cells also expressed A_1R , $A_{2A}R$, and $A_{2B}R$, with the latter receptor showing the highest expression among the ARs. A_3R expression was very low in T98 cells and undetectable in U87 cells. Regarding the PDE10A expression, U87 cells showed a higher intensity band than that of T98 cells. Similar to U87 cell line, there was no detectable band for A_3R whilst other genes of interests were present in HEK293S cells. To conclude, the cumulative expression of both targets ($A_{2A}R$ and PDE10A) appeared to be similar between rat C6 and human T98 cells, whereas U87 cells was similar to that of HEK293S cells expressing higher concordance targets (Figure 5.9C).

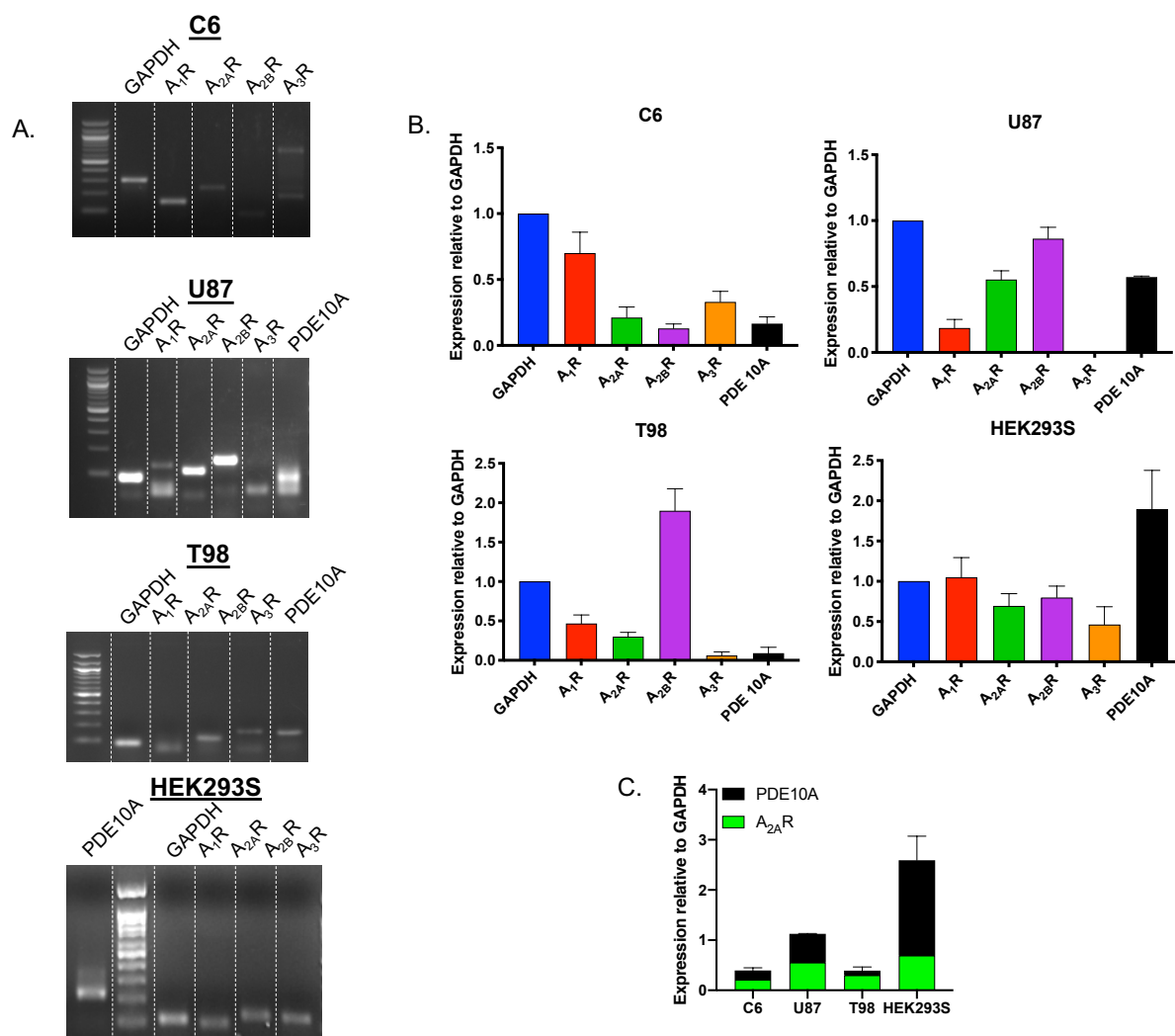


Figure 5.9 Glioma and glioblastoma cell lines differentially expressed all subtypes of adenosine receptors and PDE10A. (A) Representative of gels and expression profiles of gene of interests from glioma and glioblastoma cell lines: C6, U87, T98, and HEK293S cells. (B) Expression profile of adenosine receptors (ARs) and PDE10A from glioma/glioblastoma cell lines including HEK293S cells as comparison. (C) Comparison of cumulative $A_{2A}R$ plus PDE10A expression amongst glioma, glioblastoma and HEK293 cell lines. Relative expression was calculated based on GAPDH band and are expressed as the mean \pm SEM from 3-6 individual repeats.

5.6.2 Triazoloquinazolines mediated cAMP accumulation in glioma and glioblastoma cells

Having confirmed the expression levels of the genes of interests in the previous section, the functional assays were applied to determine compounds activity in modulating total cAMP accumulation in C6, U87, and T98 glioma/glioblastoma cell lines, as well as HEK293S cells as a control. To do this, cells were stimulated for 30 minutes with the selected compounds in buffer containing rolipram (PDE4 inhibitor) to avoid extensive cAMP degradation during the process.

CGS21680 was tested to confirm $A_{2A}R$ activation in promoting cAMP synthesis. As depicted in Figure 5.10A, there was a dose-dependent increase upon stimulation with CGS21680 in all cell lines, with the largest effect was observed in U87 cells, which expressed the highest $A_{2A}R$ levels (Figure 5.10B) amongst all cell lines, followed by HEK293S cells. The efficacies of CGS21680 appeared to be similar in C6 and T98 cells.

The similar approach was applied by applying triazoloquinazolines to all cell lines. However, the effect of compounds on cAMP production were minimal in U87 cells regardless of the abundant expression of both targets. Interestingly, the basal responses were lower in U87 cells compared to remaining cells suggesting intrinsic activity of the compounds in U87 cells, with the exception of compound **4** (Figure 5.10).

The efficacies of compound **1** and **4** were the most profound in T98 cells, followed by C6 cells (Figure 5.10B and E). While compound **1** was equipotent in C6 and HEK293S cells, compound **4** was only active in C6 glioma and human glioblastoma T98 cells. Interestingly, no difference in cAMP accumulation in all cells was observed when they were stimulated by compound **2** or compound **3** (Figure 5.10 C and D). Compound **5**, that was previously shown to be a dual ligand at $A_{2A}R/PDE10A$ was more potent in T98 and HEK293S cells, while it showed less potent responses in C6 and U87 cells (Figure 5.10F). Whilst compound **6** did not elicit any activities in yeast and CHO-K1 cell systems (Data were displayed in Table 5.2-5.3, summarised in Table 5.4), there was a dose-dependent increase in cAMP accumulation in the rat and human glioblastoma models. Since rolipram was added in the stimulation buffer, it is possible that the effect was generated from the activity of PDE4 inhibition.

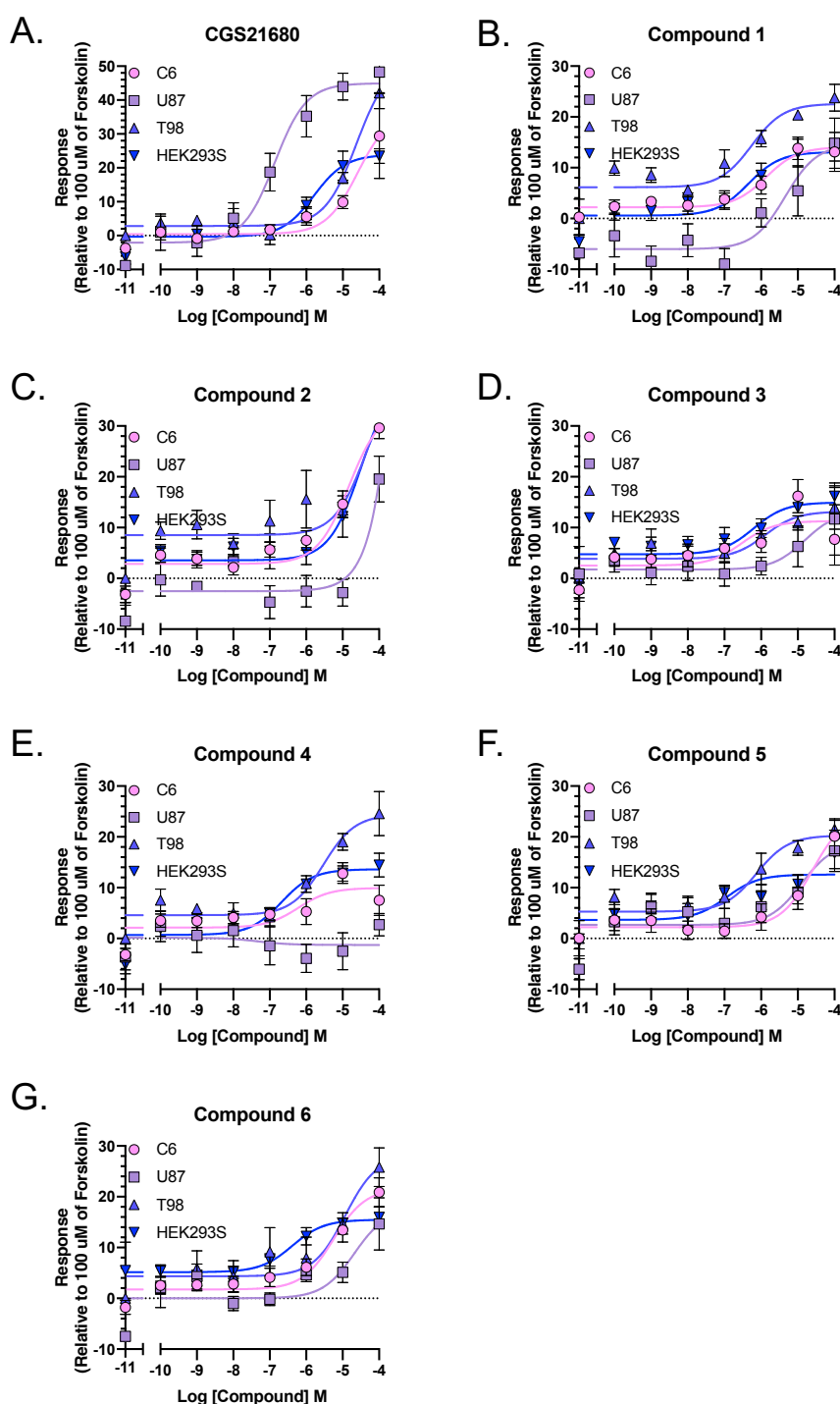


Figure 5.10 Different effects of multi-target ligands on cAMP accumulation in glioma and glioblastoma cell lines. CGS21680 (A) is a selective $A_{2A}R$ compound and used as a reference compound for cAMP accumulation assay. The accumulation of cAMP was determined following 30 minutes stimulation with compound 1-6 (B to G) in C6, U87, T98, and HEK293S cells in the presence of rolipram. Data are expressed relative to the maximal response produced by 100 μ M forskolin. Values are expressed as mean \pm SEM of 4-8 individual data sets.

5.6.3 Multi-target ligands suppressed cell proliferation on C6 cells but elicited differential responses across human glioblastoma cells

After confirming the efficacies of triazoloquinazolines in stimulating cAMP production, the investigation was further performed to determine whether modulation at cAMP levels can be translated to cell proliferation. In this study, both rat and human glioma/glioblastoma cells were selected and further exposed to the test compounds for 72 hours before adding CCK-8 reagent.

Overall, C6 cells were more reactive upon treatment with the triazoloquinazolines class of compounds compared to human glioblastoma cells or HEK293S cells. Forskolin, a pan AC activator, stimulates cAMP synthesis independent of any receptors, thus it can be used as a reference compound to show the association between cAMP and cell proliferation. Here, forskolin decreased C6 cell growth (Figure 5.11A). Whereas human glioblastoma cells were more resistant towards forskolin (indicated by only ~20% suppression), forskolin did not sufficiently show an anti-proliferative effect on HEK293S cells (Figure 5.11A).

Interestingly, selective activation of $A_{2A}R$ by CGS21680 appeared to be pro-proliferative in human glioblastoma cells (Figure 5.11B). Although CGS21680 was able to increase cAMP accumulation on these cell lines (Figure 5.11A), stimulation at $A_{2A}R$ alone was insufficient to inhibit cell growth. Similar observations were also found when glioma cells were treated with a beta-adrenergic agonist (Chapter 3). It is possible that the signalling through GPCRs was desensitised throughout the treatment period and therefore no anti-proliferative effects were observed.

Compound **1** and **3** dose-dependently suppressed C6 and T98 cell growth. However, no effect was detected on U87 and HEK293S cells (Figure 5.11C and E). It is possible that the elevation of cAMP mediated by $A_{2A}R$ agonism and inhibition of PDE10A were more noticeable on C6 and T98 cells because these cells expressed fewer PDE families compared to U87 or HEK293S cells (chapter 3 and 4). It is also worth noting that PDE10A is a dual substrate PDE, therefore any elevation in cAMP concentration will eventually affect cGMP signalling and activate various alternative signalling cascades leading to distinctive physiological/cellular responses beyond proliferation. Thus, cells with complex machinery such as U87 and HEK293S cells were more likely to be resistant to triazoloquinazolines.

In previous studies in lung cancer cells, compound **2** was suggested to have non-specific effects independent of $A_{2A}R$ agonism/PDE10A inhibition. Although U87 cell line is considered more resistant, compound **2** dose-dependently suppressed cell

proliferation. These results indicate, again, that compound **2** may have off-target toxic effects leading to cell growth suppression.

While the human glioblastoma models (U87 and T98 cells) did not respond to compound **3**, this compound reduced cell proliferation in HEK293S cells (Figure 5.11E). These effects were expected since HEK293S cells expressed the highest levels of adenosine receptors and PDE10A at the mRNA level (Figure 5.9B). With the exception of U87 cells, compound **4** induced anti-proliferative effects in all cells (Figure 5.11F). As noted earlier, the compound **4** effect was more pronounced in cells expressing $A_{2B}R$, thereby the cell growth suppression occurred was most likely due to the non-selective action towards $A_{2B}R$.

While the efficacy of compound **5** was greater in human lung cancer cell lines expressing higher levels of $A_{2A}R$ and PDE10A, in this experiment the anti-proliferative effect of compound **5** can only be seen in C6 and T98 cells, and the anti-proliferative effect induced by compound **5** was comparable to that of compound **1** (Figure 5.11G). Despite the differences in the origins of human and rat cells, the similar effects of compound **5** on the rat C6 and human T98 cells lines were likely due to the similar cumulative expression of $A_{2A}R/PDE10A$ (Figure 5.12B). In this study compound **6** was able to inhibit cell proliferation on C6 cells but no other cell types. Although compound **6** may be an antagonist at the $A_{2A}R$, the anti-proliferative effects that were displayed in Figure 5.11H were most likely due to PDE10A inhibition only (Table 5.1). Likewise, comparing with selective PDE10 inhibitor that was used in the previous chapters, inhibition at PDE10A alone was not able to exhibit substantial cell growth suppression.

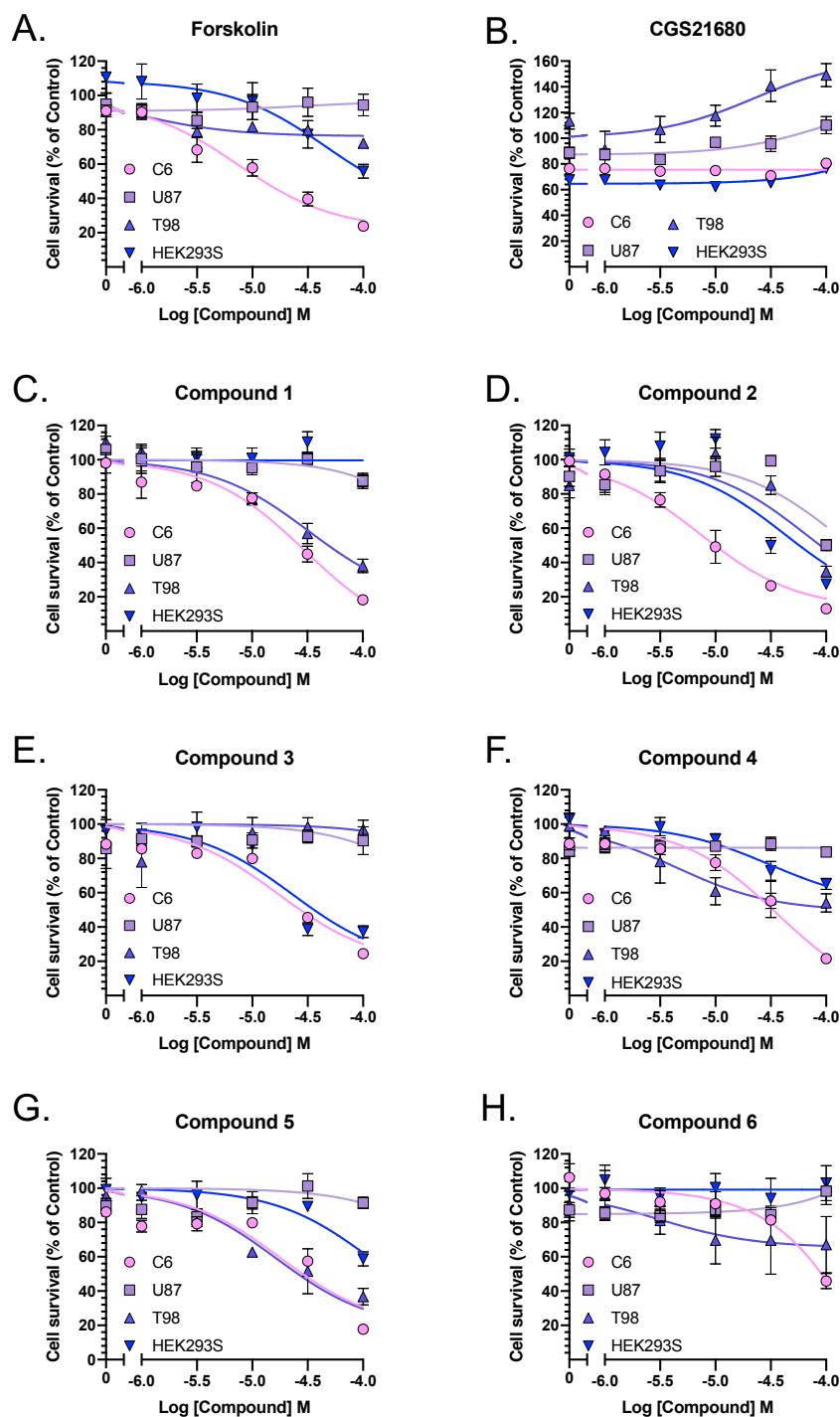


Figure 5.11 Multi-target ligands did not show any particular pattern in inhibiting cell proliferation across cell lines tested. Dose-response curves of glioma/glioblastoma cell growth upon 72h treatment with forskolin (A), CGS21680 (B), triazoloquinazolines compound 1-6 (C-H) on glioma/glioblastoma cell lines after 72 h treatment. Each data point is displayed as mean \pm SEM from 3-8 individual data.

5.7 Elevation of cAMP levels by triazoloquinazolines failed to be translated into cell proliferation in glioma and glioblastoma cells

Similar to the approach in lung cancer cell lines, Pearson's correlation was calculated to determine the efficacies of compounds in glioma/glioblastoma cell models. There was a weak association between cAMP and cell proliferation pathways in C6 and T98 cells ($r = 0.42$, 95% confidence interval -0.14 – 0.78 , Figure 5.12A), but not with U87 and HEK293S cells. It is interesting to note that even though cAMP augmentation within the intracellular compartment by inhibiting PDEs has a strong correlation with cell growth (chapter 3 and 4), concomitant targeting of PDE10A/A_{2A}R only showed weak correlation in glioma/glioblastoma cell model: C6 and T98 cells. Both U87 and HEK293S cells, on the other hand, expressed more abundant PDE isoenzymes (Chapter 4). This suggests both cell lines have more control to maintain cAMP levels and to prevent this dynamic to alter further signalling cascades. Proliferation factors on glioblastoma models were also shown in Figure 5.12B. With the exception of CGS21680, a broad range of proliferation factor values were observed in all compounds tested. Overall, U87 cells had very low proliferation factors compared to the other cell lines, except in the presence of compound **2**. While some compounds differentially suppressed cell growth in all cell lines, there was no specific pattern indicating improvement in efficacy regardless of the cumulative expression of A_{2A}R/PDE10A, unlike the observation in lung cancer cell lines. The pharmacological effects of triazoloquinazoline compounds on both cAMP and proliferation pathways in the glioblastoma models were summarised in terms of pharmacological parameters, potencies and spans, as well as proliferation factors (Table 5.4).

Since multiple downstream signalling cascades are involved between cAMP pathways as initial signalling events and cell growth as a final biological response, it is worth noting that elevation of cAMP by triazoloquinazolines may influence particular signalling in glioblastoma model, but the effect may be inadequate to modulate cell proliferation.

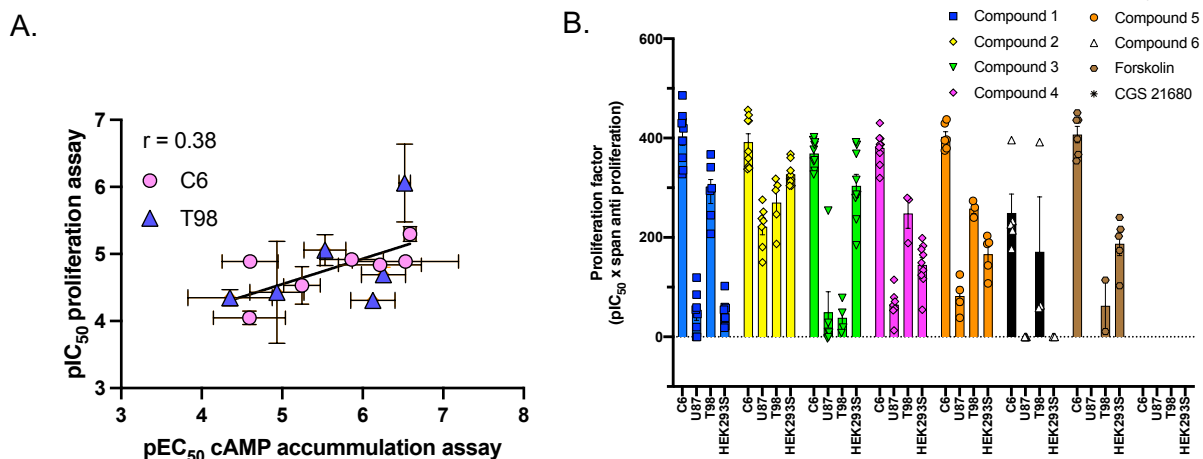


Figure 5.12 There is no correlation between the elevation of cAMP level and cell growth upon stimulation with triazoloquinazolines on rat and human glioblastoma cells. (A). Pearson's correlation plot of triazoloquinazolines across glioma/glioblastoma cell lines. There was association between both cAMP and cell growth pathways in C6 and T98 cells. (B) Proliferation factor of triazoloquinazolines, forskolin, and CGS21680 across glioma and glioblastoma cell lines as well as HEK293S cell.

Table 5.7

Summary of pharmacological activities of triazoloquinazolines across glioma and glioblastoma cells

| Compound | cAMP | | | Cell proliferation | | | n |
|------------|-------------------|----------------|----|--------------------|---------------|----------------------|---|
| | pEC ₅₀ | Span (%) | n | pIC ₅₀ | Span (%) | Proliferation Factor | |
| C6 | | | | | | | |
| Forskolin | 6.59 ± 0.07 | 97.3 ± 2.9 | 16 | 5.30 ± 0.11 | 76.6 ± 1.7 | 407.11 ± 16.42 | 4 |
| CGS21680 | 4.59 ± 0.45* | 36.2 ± 10.6*** | 7 | N/A | N/A | N/A | 5 |
| Compound 1 | 5.86 ± 0.39 | 11.9 ± 2.2*** | 10 | 4.92 ± 0.09 | 81.7 ± 2.5 | 403.13 ± 17.68 | 9 |
| Compound 2 | 4.83 ± 0.16*** | 30.6 ± 3.0*** | 9 | 5.31 ± 0.10 | 73.6 ± 2.0 | 391.80 ± 16.81 | 9 |
| Compound 3 | 6.53 ± 0.66* | 8.8 ± 2.4*** | 10 | 4.89 ± 0.03 | 75.5 ± 1.9 | 368.95 ± 9.19 | 9 |
| Compound 4 | 6.22 ± 0.52 | 7.8 ± 1.7*** | 10 | 4.84 ± 0.10* | 78.5 ± 1.4 | 380.15 ± 10.72 | 9 |
| Compound 5 | 4.60 ± 0.35*** | 22.4 ± 5.2*** | 8 | 4.89 ± 0.07 | 82.2 ± 1.9 | 402.24 ± 10.52 | 6 |
| Compound 6 | 5.25 ± 0.23** | 19.8 ± 2.3*** | 8 | 4.52 ± 0.28*** | 54.1 ± 4.4*** | 249.28 ± 37.92*** | 6 |
| U87 | | | | | | | |
| Forskolin | 6.93 ± 0.08 | 96.6 ± 3.3 | 16 | N/A | N/A | N/A | 6 |
| CGS21680 | 6.87 ± 0.21 | 47.0 ± 4.2*** | 9 | N/A | N/A | N/A | 4 |
| Compound 1 | 5.34 ± 0.40* | 20.7 ± 4.0*** | 6 | N/A | N/A | N/A | 8 |
| Compound 2 | 4.46 ± 0.19*** | 21.9 ± 2.2*** | 4 | 4.46 ± 0.23 | 49.8 ± 3.2 | 221.53 ± 16.27 | 7 |
| Compound 3 | 4.81 ± 0.75 | 11.5 ± 6.3*** | 8 | N/A | 11.5 ± 9.3 | 49.46 ± 41.17 | 7 |
| Compound 4 | N/A | N/A | 6 | N/A | N/A | N/A | 7 |
| Compound 5 | 4.90 ± 0.49 | 16.2 ± 4.9*** | 5 | 4.83 ± 0.54 | 8.6 ± 3.3 | 82.04 ± 18.40 | 8 |
| Compound 6 | 4.68 ± 0.48 | 10.3 ± 2.7*** | 4 | N/A | N/A | N/A | 7 |
| T98 | | | | | | | |
| Forskolin | 6.52 ± 0.07 | 99.0 ± 2.9 | 6 | 6.06 ± 0.58 | 18.2 ± 6.6 | 137.38 ± 30.64 | 3 |
| CGS21680 | 4.62 ± 0.15** | 48.6 ± 4.8*** | 8 | N/A | N/A | N/A | 3 |

| Compound | cAMP | | | Cell proliferation | | | n |
|----------------|-------------------|----------------|----|--------------------|---------------|----------------------|---|
| | pEC ₅₀ | Span (%) | n | pIC ₅₀ | Span (%) | Proliferation Factor | |
| Compound 1 | 6.26 ± 0.27 | 16.4 ± 2.0*** | 4 | 4.69 ± 0.11* | 61.9 ± 3.9*** | 292.30 ± 24.16* | 6 |
| Compound 2 | 4.35 ± 0.52* | 32.5 ± 13.6*** | 8 | 4.35 ± 0.12** | 61.7 ± 4.4*** | 270.27 ± 24.09* | 5 |
| Compound 3 | 5.89 ± 0.51 | 9.3 ± 2.3*** | 4 | N/A | 3.1 ± 5.4 | 38.28 ± 15.90 | 6 |
| Compound 4 | 5.53 ± 0.26 | 19.8 ± 2.5*** | 6 | 5.06 ± 0.23 | 48.8 ± 4.2* | 248.17 ± 29.80 | 3 |
| Compound 5 | 6.13 ± 0.27 | 15.0 ± 1.9*** | 4 | 4.31 ± 0.08** | 59.9 ± 1.5** | 258.06 ± 9.75 | 3 |
| Compound 6 | 4.93 ± 0.34 | 23.8 ± 4.9*** | 5 | 4.43 ± 0.76* | 32.9 ± 16.4 | 171.04 ± 110.43 | 3 |
| HEK293S | | | | | | | |
| Forskolin | 6.29 ± 0.06 | 99.9 ± 2.5 | 8 | 4.17 ± 0.45 | 44.2 ± 4.0 | 187.22 ± 23.66 | 5 |
| CGS21680 | 5.79 ± 0.24 | 24.3 ± 2.7*** | 8 | N/A | N/A | N/A | 5 |
| Compound 1 | 6.35 ± 0.33 | 12.5 ± 1.8*** | 10 | N/A | N/A | N/A | 9 |
| Compound 2 | 4.50 ± 0.27** | 36.5 ± 6.9*** | 13 | 4.51 ± 0.03 | 72.5 ± 1.5 | 327.13 ± 7.68*** | 9 |
| Compound 3 | 6.20 ± 0.41 | 10.2 ± 1.9*** | 8 | 4.79 ± 0.12** | 62.7 ± 3.4 | 303.70 ± 23.27*** | 9 |
| Compound 4 | 6.68 ± 0.31 | 12.9 ± 1.6*** | 12 | 4.11 ± 0.10 | 34.8 ± 3.2 | 144.67 ± 14.55 | 9 |
| Compound 5 | 6.94 ± 0.51 | 8.9 ± 1.9*** | 7 | 4.02 ± 0.04 | 41.3 ± 4.2 | 166.17 ± 17.73 | 6 |
| Compound 6 | 6.39 ± 0.61 | 10.3 ± 2.7*** | 8 | N/A | N/A | N/A | 6 |

Statistical significance was calculated using one way ANOVA compared to forskolin followed by Dunnet's post-hoc analysis (*p<0.05, **, p<0.01, ***, p<0.001)

5.8 Discussion

5.8.1 Validation using functional assays proving triazoloquinazolines as dual-target ligands working on A_{2A}R and PDE10A

In the collaborative study with Dr. Kalash, using a computer-aided design of multi-target ligand identified a series of compounds that elevate cAMP levels. The study was accomplished by docking triazoloquinazolines, which are known as PDE10A inhibitors (Kehler *et al.*, 2011), into the orthosteric site of the active form of A_{2A}R crystal (Lebon *et al.*, 2011). This work was then further validated using MD simulations to identify Val₈₄ as the conformational descriptor for activation of A_{2A}R (Lebon *et al.*, 2011, 2015; Carpenter and Lebon, 2017). Although it was found that triazoloquinazolines showed binding through computational studies on the orthosteric site of A_{2A}R, this needed validation through functional assay.

To validate that a series of triazoloquinazolines binds to A_{2A}R, it was necessary to assess ligand-binding. As an alternative to using the classical radioactive ligand binding approach, the Nano-BRET ligand binding assay offers many advantages due to its practicalities and allowing real-time detection of interactions in living cells without compromising the membrane integrity (Kenakin, 1988; Briddon *et al.*, 2004). Since CA200645 has been shown to be membrane impermeable and thus label only surface receptors, this compound was used as a probe. Although CA200645 exhibits a higher affinity against A₁R and A₃R, this probe also binds to some extent to A_{2A}R and A_{2B}R. Given the fact of limitation of CA200645 and until this study was performed, a very limited number of probes were available to serve as a suitable tool for detecting ligand - A_{2A}R interactions using BRET or imaging. It was not until Comeo reported the new fluorescent ligand that has better affinity to leverage binding profiling at the A_{2A}R (Comeo *et al.*, 2020). The preferences of CA200645 towards A₁R and A₃R then may explain lower pK_i values for the reference compounds in this study. The calculated pK_i for both NECA and CSG21680 were low compared to previously published values. Aside from different the protocols used to obtain pK_i, the discrepancy of K_D and pK_i may also come from the influence of endogenous expression of A₁R and/or A₃R, which are expressed in kidney-derived cells (Figure 5.9), and presumably are also expressed in HEK293T cells.

In agreement with Kehler (Kehler *et al.*, 2011), a series of triazoloquinazolines were revalidated to be PDE10A inhibitors through PDE *in vitro* assay (Table 5.1, appendix 1). Furthermore, all triazoloquinazolines were shown to bind to the A_{2A}R *in vitro* (Figure 5.4). Based upon previous characterisation on the yeast and CHO-K1

cells, compound **5** activity was considered effective when both A_{2A}R and PDE10A were expressed. Of all triazoloquinazolines, surprisingly, compound **5** exerted the weakest binding property. Based on previous study using yeast and heterologous expression system, stimulation by compound **5** elicited pharmacological responses through A_{2B}R (Table 5.2 and Table 5.3). In addition, compound **5** also showed better activity on human lung cancer cell lines (Figure 5.10), where both A_{2A}R and PDE10A were expressed. This phenomenon may be explained by the functional group in compound **5**. The pyridine moiety in compound **5** is considerably more polar than in the other triazoloquinazolines (Table 5.1). Therefore, this functional group may affect the permeability of compound **5**. Even though compound **5** has a considerably low binding affinity at the A_{2A}R (Figure 5.4), this compound may more easily cross the plasma membrane, further enhancing its action towards PDE10A.

Taken together, it was evident that compound **1-6** are all PDE10 inhibitors and synergistically bind to the orthosteric site of the A_{2A}R. Although previous computational studies also highlighted the role of Val₈₄ as a conformational descriptor for A_{2A}R activation and the His₂₅₂ residue that contributed to triazoloquinazolines activity towards A_{2A}R, indeed, these notions require further validation using mutagenesis studies.

5.8.2 Differential effects of triazoloquinazolines in various cancer models

In the previous chapters, concomitant targeting of two essential proteins involved in regulating cAMP concentration in the intracellular compartment has been explored. As mentioned, the elevation of cAMP is beneficial in circumventing tumour progression in the glioma model. Using ligand combinations is a common approach to target multiple effectors to produce similar biological effects providing some advantages, including the use of lower concentration, which leads to less toxicity and better tolerability (Lehár *et al.*, 2009). In this chapter, an alternative approach was applied to discover compounds that simultaneously act as a PDE10A inhibitor and A_{2A}R agonist. It was hypothesised that concomitant targeting will potentiate cAMP signalling cascades by enhancing its production and inhibiting its degradation through PDE10A.

Triazoloquinazolines have been proven to inhibit PDE10A activity (Table 5.1, appendix 1). Although PDE10A was firstly postulated to be involved in neurological functions mainly such as motoric and cognitive functions, PDE10A has grown to be a potential cancer target. The inhibition of PDE10A has been reported to be beneficial in the colorectal, oral, lung, and prostate cancer (De Alexandre *et al.*, 2015; Lee *et al.*,

2015, 2016; Titulaer, Irani and Lassmann, 2019). As a dual-substrate enzyme, PDE10A is commonly known as a cAMP-inhibited cGMP PDE and it is believed that an increase in cAMP concentration would potentiate cGMP-mediated signalling pathways (Fujishige, Kotera and Omori, 1999). Although it is evident from this study that there is a strong association between elevation on cAMP and cell growth suppression in NSCLC cells, other reports highlighted opposing mechanisms. Instead of influencing cAMP levels, PDE10A has been reported to mediate cell growth suppression by increasing cGMP in human cancer cell lines (HT29, SW480, and HCT116) which further phosphorylate PKG and β -catenin (Mehta and Patel, 2019; Zagórska, 2020). However, the work presented in this chapter demonstrated triazoloquinazoline-mediated cAMP accumulation, yet it did not investigate changes in cGMP concentration. It would be of interest to investigate the cGMP signalling cascade by triazoloquinazolines in future studies.

As modulation of cAMP by triazoloquinazolines lead to diverse effects on cell proliferation, it is also worth noting there is a gap between upstream cAMP levels and the cell growth axis. From the previous studies, triazoloquinazolines were found be biased towards ERK1/2 signalling in an A_{2A}R-dependent manner (Winfield, 2017). As a member of the MAPK family that mainly control cell proliferation and programmed cell death, it is assumed that the effect of triazoloquinazoline may involve ERK1/2 activation. Activation of ERK1/2 can result in phosphorylation of transcription factor leading to cell growth or activation of cyclin families that further induce growth arrest (Mebratu and Tesfaigzi, 2009; Thérèse Keravis and Lugnier, 2012a). However, since cascades connecting cAMP and cell proliferation have not been fully elucidated, it is necessary to identify the key target genes/proteins between upstream and downstream signalling, which may also depend on spatiotemporal of the intracellular responses.

The importance of A_{2A}R signalling has been an intriguing topic in cancer. The underlying mechanism of A_{2A}R in cancer has not been fully elucidated as the role of A_{2A}R has been mainly studied in immune cells and more complex organisation involving tumour microenvironment (TME). In a model involving TME and immune cells, A_{2A}R acts as an immune checkpoint. Therefore, the blockade of A_{2A}R functions as an immunosuppressive axis through immune cells, such as T cells, NK cells, NKT cells, and dendritic cells (Ohta *et al.*, 2006, 2012; Kalhan *et al.*, 2012; Steingold and Hatfield, 2020). However, only a few reports showcased the A_{2A}R signalling cascade in cancer cells (Inoue *et al.*, 2017) and are not without contradicting results. Activation

on A_{2A}R has been shown to decrease cell survival by inducing apoptosis in PC12 cell lines (Trincavelli *et al.*, 2003). On the contrary, antagonistic action induced apoptotic programmed cell death in H1975, PC9, and A540 lung cancer cells (Kuzumaki *et al.*, 2012; Beavis *et al.*, 2013; Mediavilla-Varela *et al.*, 2013). Since then, studies have suggested that A_{2A}R inhibition is more beneficial to affect immune cells but not on tumour expressing A_{2A}R (Beavis *et al.*, 2013).

Different cellular machinery may underlie diverse effects in triazoloquinazoline-mediated anti-proliferative effects among cancer models. For instance, the expression level of A_{2A}R is different depending on cell types, which contribute to its G protein coupling preferences, receptor oligomerisation, and desensitisation (Cieslak *et al.*, 2008; Fredholm, 2014, Carpenter and Lebon 2017). This has been implicated in affecting the agonist binding affinity, which gives distinct signalling profiles (Snyder and Rajagopal, 2020). The recent finding also highlighted that A_{2A}R was found to have different isoforms in different tissues (Marti-Solano *et al.*, 2020). Taken together, it is possible that A_{2A}R couples to different signalosomes exhibiting diverse signalling. The effect may not be limited to cell proliferation in this case but may activate different signalling pathways, which requires further investigation.

Similar to A_{2A}R, each PDE can have different splice variants and the expression patterns can vary in tissues, in particular, subcellular localisation (Beavo, 1995; Fujishige *et al.*, 1999). Different splice variants of PDE10A dictated different kinases and associated proteins (O'Connell *et al.*, 1996; Degerman, Belfrage and Manganiello, 1997). These associations appeared to be cell-dependent (O'Connell *et al.*, 1996). In mouse striatum, for instance, PDE10A was tethered to more complex signalosomes involving PKA, AKAP150, and PSD95 that altogether influenced the signalling of NMDA receptors (Russwurm, Koesling and Russwurm, 2015). Different cell types may also influence which receptor population and PDE10A would be colocalised (Hennenberg *et al.*, 2016). Although the impact of PDE10A signalosomes in cancer are not fully elucidated, PDE10A from different cell types or origins may form a particular macromolecular complex that controls specific cellular functions.

Despite the fact that triazoloquinazolines were more effective in human lung cancer cells than glioblastoma models, application of triazoloquinazolines may be useful as an alternative approach to cancer therapy. It would be interesting if triazoloquinazolines can be deployed into a translational tangent. Again, further investigation is required to circumvent any adverse indiscriminate toxic effects on normal cells or possible off-target actions from these compounds.

5.9 Summary

From this study and previous characterisation, it was confirmed that all triazoloquinazolines elicited concomitant inhibition of PDE10A and stimulation of A_{2A}R. All compounds were also shown to differentially bind to the A_{2A}R based on the BRET-based ligand binding experiments.

Triazoloquinazolines inhibited lung cancer cell growth and these effects had strong correlation with the elevated total cAMP levels. While it was confirmed that compound 1 and 5 selectively targeted A_{2A}R/PDE10A, compound 2 may have off-target effects leading to potential toxicity. Not only did compound 3 inhibit PDE10A but also non-selectively targeted ARs, whilst compound 4 was more efficacious in the presence of A_{2B}R. Regardless of the cumulative expression of both targets, compound 6 did not have any effect on the human lung cancer cells.

Interestingly, in spite of the apparent anti-proliferative effect of these triazoloquinazoline-based compounds on the lung cancer cells, a similar effect was not observed in the glioblastoma models, even though there was a slight increase in cAMP accumulation. Glioblastoma cell lines may have better mechanism to lowering cAMP concentration by overexpressing cAMP efflux transporters. It is possible that this compound-induced differential effect in the lung cancers vs glioma/glioblastoma were due to differences in cell-type dependent molecular machinery. Almost all compounds were less effective on human glioblastoma cells suggesting there is another mechanism or interacting partners that are significantly different from those of human lung cancer cell lines. While the individual components in the downstream signalling cascades between these two pathways (cAMP and cell proliferation) is not fully elucidated within this study, cells from different origins may have different distributions of isoenzymes, mutation, or couple to different protein targets that contributed to different responses. Therefore, although there was no significant effect through A_{2A}R and PDE10A targeting, the elevation of cAMP may affect other signalling cascades that are not covered in this study.

To conclude, increasing cAMP by a synergistic mechanism between agonism at A_{2A}R and inhibition of PDE10A appeared to show potential benefits in preventing cell growth in human lung cancer cells. Although there was a short-term increased in total cAMP levels, the same mechanisms failed to promote significant anti-proliferative effects in more resistant glioblastoma cell model such as U87 cell line. For the future

studies, computational techniques may be applied to improve the physicochemical properties of triazoloquinazolines.

CHAPTER 6

RECEPTOR ACTIVITY MODIFYING PROTEIN (RAMP) MODULATION OF PROTEASE-ACTIVATED RECEPTOR 4 (PAR4) AND CALCITONIN-LIKE RECEPTOR (CLR) SIGNALLING

6.1 Introduction

RAMPs are single transmembrane proteins that were first found to associate with calcitonin receptor-like receptor (CLR) (McLatchie *et al.*, 1998). Although firstly identified as chaperones for CLR, since then RAMPs have been shown to allosterically modulate CLR pharmacology. In addition, they also provide direct ligand contact points leading to alteration of ligand binding, G protein-coupling, and receptor internalisation (Simms *et al.*, 2009; Woolley *et al.*, 2017; Garelja *et al.*, 2018). Interestingly, RAMPs have also been reported to interact with a broader range of receptors, not only limited to class B GPCRs but also class A and C (Poyner *et al.*, 2002; Hay *et al.*, 2016; Barbash *et al.*, 2017; Mackie *et al.*, 2019). Recent studies have shown that these accessory proteins interact with chemokine receptors leading to control important physiological responses (Mackie *et al.*, 2019).

Protease-activated receptor 4 (PAR4), together with other PAR isotypes (PAR1-3), are class A GPCRs distributed in various tissues such as adipose, breast, and lung⁸. Although PAR4 is expressed by many tissues, this receptor is enriched in blood and endothelial cells, showing a pivotal role in platelet activation (Coughlin, 1999). Like other PAR family members, PAR4 is known to be activated by endogenous serine protease thrombin with a putative cleavage site at R47/G48 revealing tethered ligand GYPGQV (details in Chapter 1). Peptide agonists for PAR4 are currently limited, although the low potency synthetic peptide AYPGKF-NH₂ has been widely used as an agonist to activate PAR4 without proteolysis (Faruqi *et al.*, 2000; Hollenberg and Saifeddine, 2001). Interest in targeting PAR4 has been increasing over other PARs due to less bleeding liability (Ramachandran *et al.*, 2017)

Single nucleotide polymorphism (SNP) *rs773902* was identified in the coding sequence of PAR4 gene *F2RL3* leading to amino acid substitution at residue 120 from alanine to threonine. Interestingly, clinical findings on the PAR4 polymorphism at

⁸ <https://www.proteinatlas.org/ENSG00000127533-F2RL3>

residue 120 has been shown to account for the differential degrees of platelet aggregation by thrombin, PAR4 agonist peptide (PAR4-AP), or antagonists. These variants will be referred as PAR4-A120 and PAR4-T120. PAR4-T120 isoform appears to show hyper-reactivity to thrombin-mediated responses compared to the A120 form (Tourdot *et al.*, 2015). Taking blood samples from a population with homozygous genotypes, platelet expressing Thr120/Thr120 needs less thrombin to promote platelet aggregation compared to Ala120/Ala120 variants. This Thr120/Thr120 is believed to occur in race-dependent responses which is more commonly found in black ancestry than in Caucasian people. Another study conducted within the Japanese population found that there were less people with Thr120/Thr120 variant (Morikawa *et al.*, 2018). Whilst the residue substitution has led to different responsivity towards thrombin, PAR4-agonist peptide, or antagonist, there is no evident that this variant alters the number of receptors expressed on platelets (Li *et al.*, 2020)

Biased signalling is now widely accepted as an approach to modify receptor signalling and has shown therapeutic benefits (Foley, 2018). However, little is known about biased signalling of PAR4, thereby this particular field remains to be explored (Zhao, Metcalf and Bunnett, 2014). The distinct signalling events may affect various signalling events, including receptor phosphorylation by GRKs, pleiotropy to activate numerous G proteins, and act as “barcodes” to recruit β -arrestin leading to different functional responses (Zhao, Metcalf and Bunnett, 2014).

Although many studies highlight that PAR4 forms heterodimers with P2Y₁₂R, little is known about RAMP modulation on PAR4 signalling. RAMPs have been shown to be expressed in platelets but, to date, there were no known canonical RAMP-interacting GPCRs partner also expressed (Rowley *et al.*, 2011). Therefore, it is hypothesised that PARs may interact with RAMP. To understand and confirm this hypothesis, the study focused on dissecting the PAR4 signalling profile using a heterologous overexpression system. Understanding this mechanism would give some insight into providing a potential target for drug development.

Firstly, this chapter presents data that dissects the functional impact of the PAR4 polymorphism and determines if RAMPs act as accessory proteins to PAR4 so modulating its signalling profile. Unfortunately, due to the impact of the COVID-19 pandemic, and subsequent restricted access to the laboratory most of the results in this chapter can only be considered preliminary.

Secondly, this chapter also displays the role of RAMP in CLR pharmacology in various cell lines. The RAMPs and CLR forms new receptors that activate specific

signalling by different peptide ligands: CGRP, adrenomedullin (AM), and AM2. As part of collaborative work with Dr. Clark (University of Cambridge), the results presented in this chapter will focus on the impact of CLR-RAMP interaction on the canonical cAMP pathway and its impact on cell growth. The study was performed using various human cell lines, including human glioblastoma, human umbilical vein endothelial cells (HUVECs), and human cardiomyocytes (hCMs). The investigation of CLR-RAMP interaction on primary human cardiovascular cells on upstream signalling cascades have been extensively studied and are available as a pre-print (currently under review at *Communication Biology*) to which I am a co-author (Clark *et al.*, 2021) .

6.2 PAR4 is coupled to $G\alpha_q$ to promote intracellular calcium release

To understand the clinical impact of the polymorphism of PAR4, both PAR4-A120 and PAR4-T120 variants were used. To compare and investigate whether protease and agonist peptide may contribute to biased signalling, α -thrombin as the endogenous ligand for PAR4 and AYPGKF-NH₂, as agonist/activating peptide were included as pharmacological tools to dissect the signalling profile of PAR4.

It has been widely known that PAR4 couples to $G\alpha_q$ and $G\alpha_{12/13}$ after being activated. Since dissociation of $G\alpha_q$ subunit will lead to activation of phospholipase C (PLC), which promotes intracellular calcium mobilisation from the endoplasmic reticulum (ER) to cytoplasm, it is possible to observe calcium release. To do this, HEK293T cells transiently expressing either PAR4-A120 or PAR4-T120 were labelled using calcium indicator, Fluo-4 AM. To quantify the intracellular calcium release level from ER to cytoplasm, the change of fluorescence intensity was monitored for approximately 2.5 minutes. Representative images captured for this experiment are displayed in Figure 6.2A and B. By taking the peak of each treatment Figure 6.1B, the dose-response curve can be generated, as shown in Figure 6.1C.

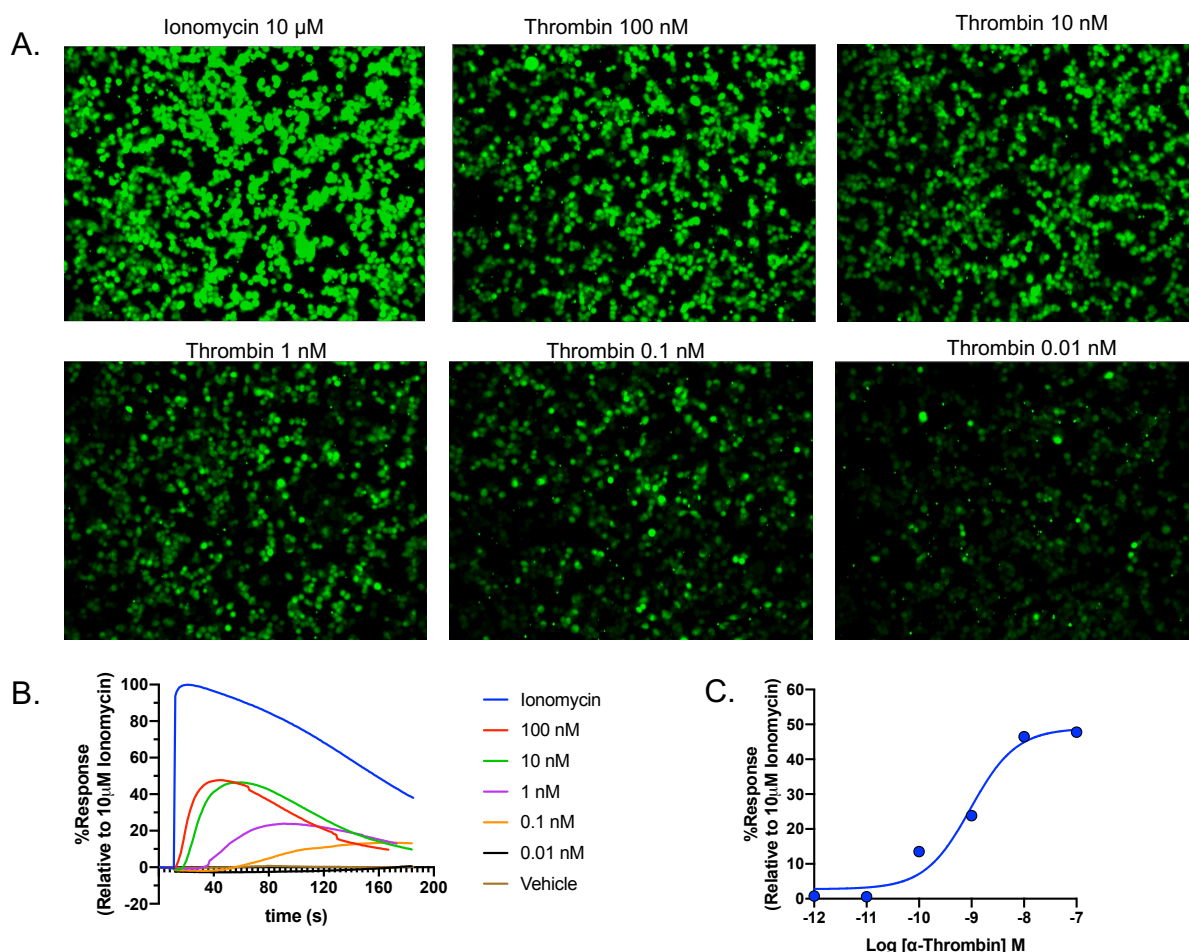


Figure 6.1 Representative figures of intracellular calcium release on HEK293T cells expressing PAR4-A120 upon stimulation with thrombin. ((A) The sequence of the image captured at the peak of calcium release after PAR4-A120 expressed HEK293T cell were treated by the ligands. (B) The traces of intracellular calcium mobilisation in response to various concentrations of thrombin after normalisation to 10 μM ionomycin. (C) Dose-response curve of thrombin at PAR4 was generated by taking peak intensity from the traces displayed in Figure B and was fit into three parameter non-linear regression built-in Prism 8.4.

In this study, both endogenous ligand and agonist peptide were tested against both PAR4 variants. Thrombin dose-dependently promoted intracellular calcium mobilisation on both PAR4 variants. Interestingly, the E_{max} of thrombin in PAR4-T120 expressing cells was slightly higher (Figure 6.2A and Table 6.1) even though it was less potent than its counterpart. AYPGKF-NH₂, on the other hand, was far less potent, and the dose-response curve did not reach a plateau. This is in agreement with what has been published in many studies (Faruqi *et al.*, 2000; Ma, Hollenberg and Wallace, 2001; Thibeault *et al.*, 2020). However, whilst we saw a discrepancy in thrombin-mediated calcium release, there was no difference in all pharmacological parameters upon stimulation with PAR4-AP (Figure 6.3B and Table 6.1).

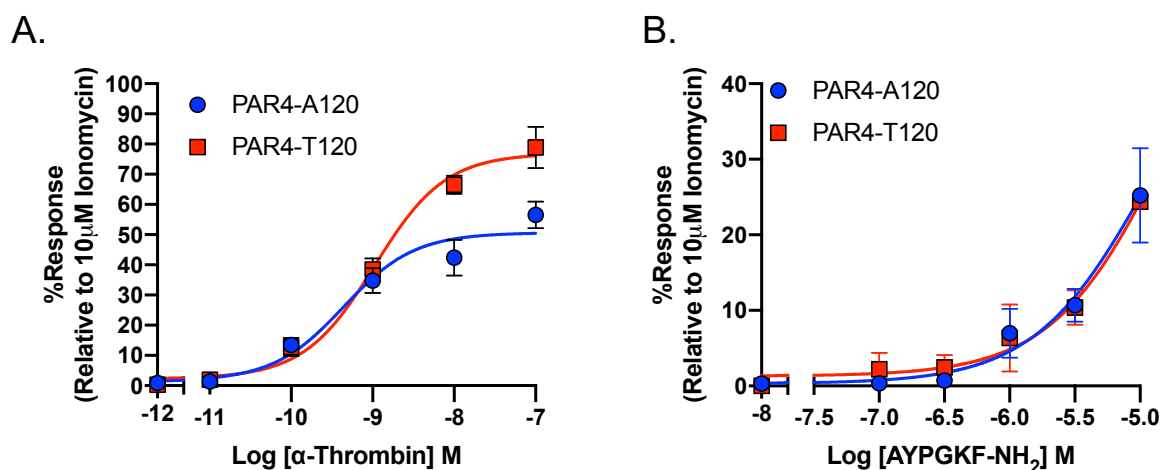


Figure 6.2 Both thrombin and PAR4-agonist peptide promote intracellular calcium release. Dose-response curve of thrombin (A) and AYPGKF-NH₂ (PAR4-agonist peptide) (B) in stimulating calcium mobilisation on HEK293T cells transiently expressing both PAR4 variants. PAR4-T120 variant appeared to be more responsive towards thrombin, but no difference was found in AYPGKF-NH₂ treated cells. Each data point is presented as the mean \pm SEM of 2 – 15 individual data.

Table 6.1

Pharmacological parameters of thrombin and PAR4-agonist peptide on PAR4-A120 and PAR4-T120 variants

| Receptor | Ligand | $i[Ca^{2+}]$ | | <i>n</i> |
|-----------|------------------------|-------------------|----------------------|----------|
| | | pEC ₅₀ | E _{max} (%) | |
| PAR4-A120 | Thrombin | 9.30 \pm 0.09 | 52.89 \pm 3.34 | 4 |
| PAR4-T120 | | 8.90 \pm 0.32 | 81.45 \pm 4.80 | 5 |
| PAR4-A120 | AYPGKF-NH ₂ | 4.89 \pm 0.41 | 33.07 \pm 6.09 | 5 |
| PAR4-T120 | | 5.34 \pm 0.32 | 43.74 \pm 15.47 | 3 |

Calcium data was displayed after normalisation to that of 10 μ M ionomycin. Data are represented as mean \pm SEM of 3-5 individual data. Data were determined as statistically different compared to receptor only using one-way ANOVA followed by Dunnett's *post-hoc* analysis.

6.3 PAR4 recruits β -arrestin

Upon PAR4 activation, like many other GPCRs, it will couple to various regulatory proteins, which mainly engage to G proteins. Beside, recruitment of β -arrestin has been reported to occur following PAR4 activation (Lin *et al.*, 2019; Vanderboor *et al.*, 2020) or after dimerization of PAR4 and P2Y12R (Li *et al.*, 2011; Khan *et al.*, 2014; Smith *et al.*, 2016). As mentioned before, when necessary, both thrombin and agonist peptide of PAR4 were included in this study. However, using the BRET-based β -arrestin recruitment assay, it was not possible to detect a BRET signal upon stimulation with thrombin. It is also possible that endogenous expression of thrombin-activated

PAR1 and PAR2, which are known to express in HEK293 cells (Atwood *et al.*, 2011) may affect detection of β -arrestin recruitment to PAR4 in response to thrombin. Regardless of this fact, the recruitment of β -arrestins was still detected when cells were stimulated with AYPGKF-NH₂. The BRET signal was vehicle subtracted and plotted as net BRET ratio (Figure 6.3A, using β -arrestin1 recruitment to PAR4-A120 variant as an example). There was a dose-dependent increase in the max ligand-induced change in BRET. Taking 13 minutes time point, the dose-response curve can be generated with the EC₅₀ of 6.08 \pm 0.59 (Figure 6.3B).

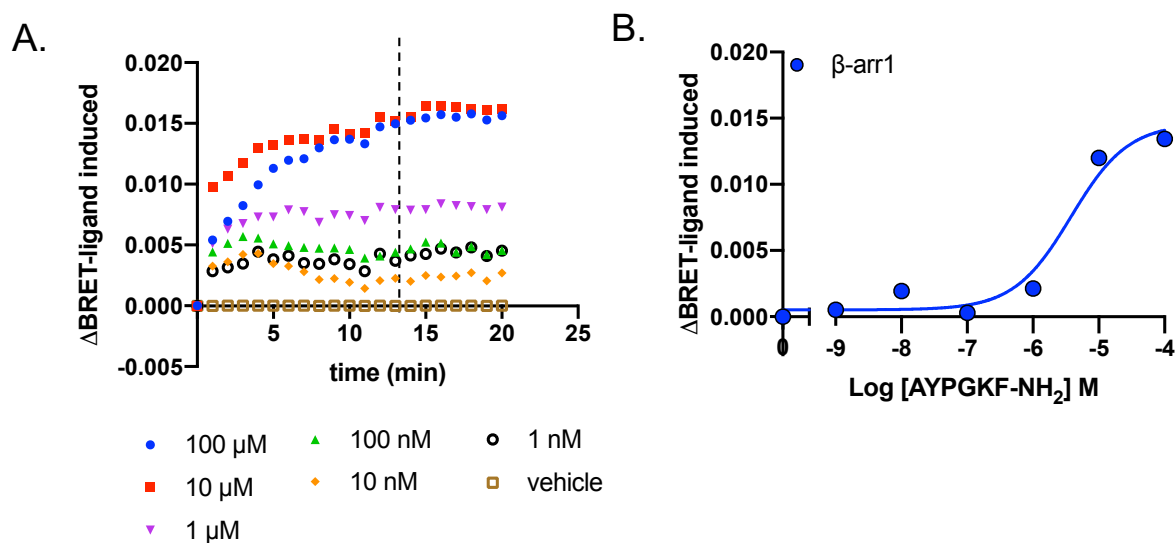


Figure 6.3 The representative of BRET signal on β -arrestin recruitment assay. (A) Kinetics of BRET signal recorded from HEK293T cells transiently expressing PAR4 in response to various concentrations of PAR4-AP. (B) The dose-response curve was generated by taking the max ligand-induced BRET signal from A. The graph was taken from an experiment conducted on PAR4-A120 using the β -arrestin1 sensor.

Using the same approach, further investigation was conducted to assess the signalling of PAR4 polymorphism in recruiting β -arrestins. Surprisingly, PAR4-A120 showed a distinct β -arrestin recruitment profile compared to PAR4-T120 (Figure 6.4, Table 6.2). Despite different concentration intervals between experiments, it is clear that PAR4 variants elicited different β -arrestin recruitment response profiles. PAR4-T120 variant recruited β -arrestin1/2 more potently, but lower in E_{max}, in response to PAR4-AP compared to PAR4-A120 variants (Figure 6.5A and B). This polymorphism in PAR4 therefore appears to dictate a distinct signalling profile, especially in recruiting β -arrestins.

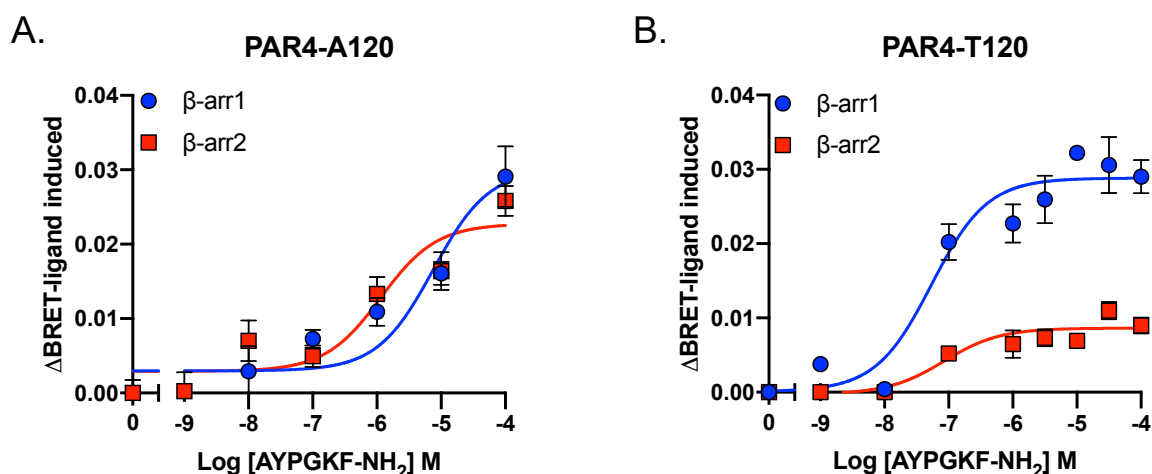


Figure 6.4 PAR4 both variants differentially recruited β -arrestin upon stimulation with AYPGKF-NH₂. HEK293T cells were cotransfected with PAR4-A120 or T120 and β -arrestin1/2 at ratio of 1:1. Recruitment of β -arrestin was measured after subtracting with vehicle control and is expressed as Δ BRET-ligand induced. Concentration-response curves for β -arrestin1/2 recruitment after 13 minutes stimulation with PAR4-AP on PAR4-A120 (A) and PAR4-T120 (B) variants. Data are expressed as the mean \pm SEM from 3-5 individual data. HL Jia-Qi performed the experiment of BRET-based β -arrestin assay using PAR4-T120 variant.

Table 6.2

The potency (pEC_{50}) and E_{max} value of PAR-agonist peptide on both PAR4 variants in recruiting β -arrestins

| PAR4 variants | Ligand | β -arr1 | | | β -arr2 | | |
|---------------|------------------------|-----------------|------------------|---|-----------------|------------------|----|
| | | pEC_{50} | E_{max} (%) | n | pEC_{50} | E_{max} (%) | n |
| A120 | AYPGKF-NH ₂ | 6.08 \pm 0.59 | 27.13 \pm 4.43 | 9 | 6.20 \pm 0.33 | 26.69 \pm 2.99 | 15 |
| T120 | | 7.37 \pm 0.15 | 27.86 \pm 1.94 | 3 | 6.86 \pm 0.45 | 9.12 \pm 0.75 | 3 |

Calcium data was displayed after normalisation to that of 10 μ M ionomycin. Data are represented as mean \pm SEM of 3-15 individual data. Data were determined as statistically different compared to receptor only using one-way ANOVA followed by Dunnett's *post-hoc* analysis.

6.4 RAMPs are promoted to plasma membrane in the presence of PAR4-A120 and PAR4-T120

Having investigated the signalling profile of both PAR4 variants, the study was expanded to investigate if RAMPs could interact with PAR4 and alter their signalling. To determine the interaction between RAMPs and PAR4, it was necessary to investigate whether the presence of PAR4 promote cell surface expression of RAMPs. RAMPs are poorly trafficked to the plasma membrane in mammalian cells. Forming heterodimers between RAMPs and a GPCR enhanced RAMP translocation to the cell surface (McLatchie *et al.*, 1998). A couple of methods have been developed to investigate association of RAMP and GPCRs, which include co-immunoprecipitation

(Bouschet, Martin and Henley, 2005), suspension bead array (SBA) (Lorenzen *et al.*, 2019b), and BRET based assay (H eroux *et al.*, 2007a; Harikumar *et al.*, 2009; Lenhart *et al.*, 2013). Bailey and colleague firstly developed a FACS method to observe RAMP-GPCR interaction (Bailey *et al.*, 2019) and recently, Mackie also observed RAMP-GPCR interaction using FACS confirming functional localisation of RAMP with a series of GPCRs that were previously determined by BRET (Mackie *et al.*, 2019).

In this study, the FACS method was applied to determine the effect of co-expression of PAR4 to RAMP cell surface expression. To do this, COS-7 cells, a fibroblast-like cell line derived from African monkey kidney tissue, were used as they do not endogenously express RAMPs (Bouschet, Martin and Henley, 2005). Thus COS-7 cells serve as a suitable system to investigate RAMP-receptor interactions. COS-7 cells were co-transfected with PAR4 and N-terminal FLAG-tagged RAMPs, at a ratio of 1:1 for 48 hours. Since the antibody used (anti-FLAG antibody conjugated with APC, details in chapter 2) in the FACS experiment was non-cell permeable, only RAMPs expressed at the plasma membrane would be detected. Therefore, APC intensity in the presence of PAR4 variants could be compared to control levels to indicate whether PAR4 co-expression promoted RAMP cell surface expression.

In the absence of receptor, there was a marginal cell-surface expression of RAMP1 and RAMP2 (Figure 6.5). The surface expression of RAMP1 and RAMP2 were significantly increased when co-expressed with PAR4-A120 or PAR4-T120. Interestingly, in the absence of the receptor, the plasma membrane expression of RAMP3 was considerably higher, suggesting it can traffic to the cell surface without interacting partners. Despite this observation, co-expression with PAR4-T120, but not PAR4-A120, further enhanced RAMP3 localisation to the plasma membrane.

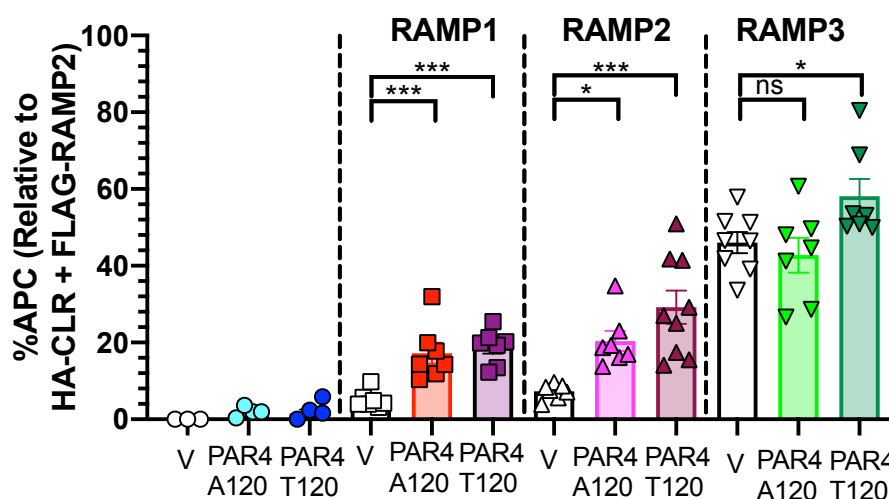


Figure 6.5 The presence of PAR4 influence RAMPs cell surface expression. COS-7 cells were co-transfected with FLAG-RAMP1/2/3 and PAR4-A120/PAR4T120 at a ratio of 1:1. Control vehicle cells was transfected with pcDNA3.1-zeo with the same amount of DNA and served as control. Cell surface expression of FLAG-RAMPs was determined by FACS. The expression was normalised to that of control (0%) and HA-CLR+FLAG-RAMP2 (as 100%). Data are expressed as the mean \pm SEM of 3-9 individual data. Data were determined as statistically different (*, $p < 0.05$; **, $p < 0.01$; ***, $p < 0.001$) compared to vector using one-way ANOVA followed by Dunnett's *post-hoc* analysis.

6.5 RAMPs alter thrombin-mediated intracellular calcium mobilisation

Having demonstrated a difference in the pharmacological action of both PAR4 variants and identified interactions with RAMPs, the study was extended to investigate if RAMPs affect PAR4 signalling.

While the PAR4-A120 variant was less responsive compared to PAR4-T120 upon stimulation with thrombin (Figure 6.6A), the co-expression with RAMP1 increased the E_{max} of calcium release (from 52.89 ± 3.34 % to 68.23 ± 6.74 %, Figure 6.6B). RAMP2 and RAMP3 also enhanced calcium mobilisation equal to that of PAR4-A120 in the presence of RAMP1 (70.47 ± 3.69 % and 72.44 ± 4.87 %, respectively, Figure 6.6C and D). Interestingly, whilst RAMP increased E_{max} in PAR4-A120, the interaction resulted in E_{max} reduction on the PAR4-T120 variant (Table 6.3). RAMP1 appeared to equalise the signalling, whereas RAMP2/3 reversed the effects of both variants. No changes were observed in pEC_{50} values in all groups (Figure 6.6, Table 6.3).

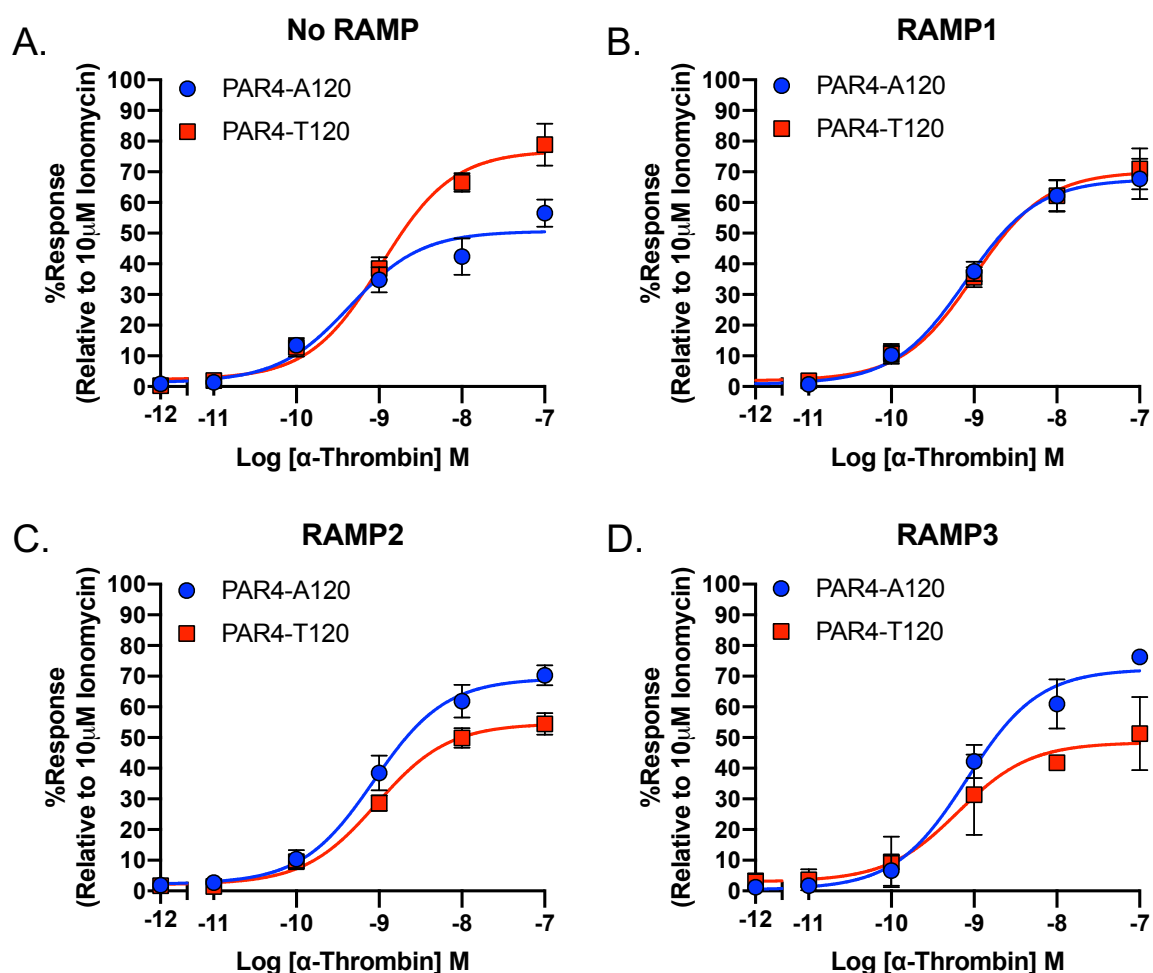


Figure 6.6 The presence of RAMPs modulate intracellular calcium mobilisation at PAR4 upon stimulation with thrombin. HEK293T cells were transiently transfected with PAR4, RAMP1/2/3 or pcDNA3.1-zeo with the ratio of 1:1. The dose-response curve of thrombin on both PAR4-A120 and PAR4-T120 variants in the absence of RAMP (A) and the presence of RAMP1 (B), RAMP2 (C), or RAMP3 (D) were determined after normalisation to 10 μ M ionomycin. Each data point is the mean \pm SEM from n of 2 – 5 individual repeats

Using the much less potent PAR4-AP (AYPGKF-NH₂), there were no changes observed to calcium responses in the presence of RAMPs (Figure 6.7A-D). The values of each group's span and potency (Table 6.2) showed that these parameters remained the same regardless of RAMP co-expression. Due to the impact of Covid-19, it was not possible to perform further experiments to obtain more repeats on this particular section.

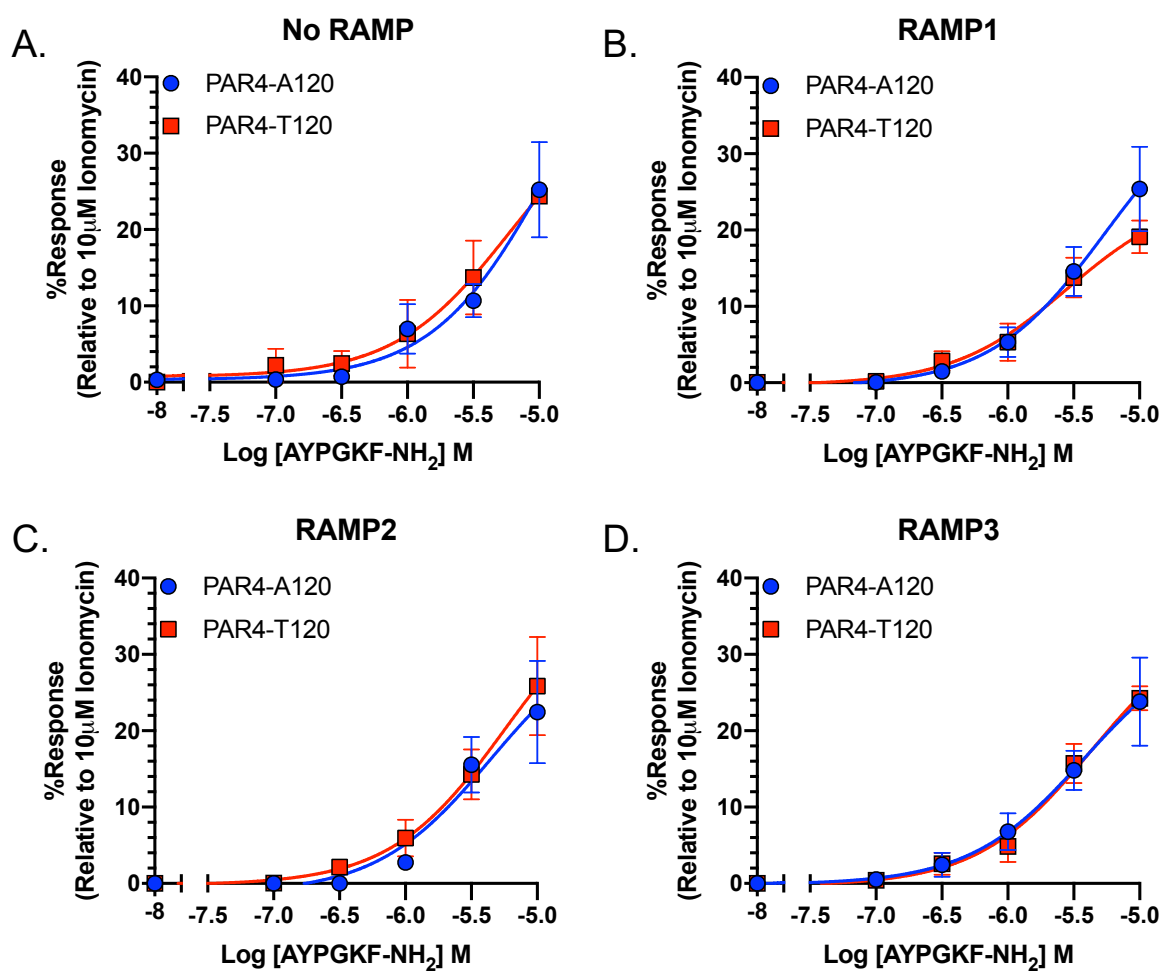


Figure 6.7 PAR4 agonist peptide-mediated calcium release remain unaffected in RAMPs co-expressed with PAR4 in HEK293T cells. (A) The dose-response curves of AYPGKF-NH₂ on both PAR4-A120 and PAR4-T120 variants that were transiently transfected in HEK293T cells in the absence of RAMP (A) and co-expressed with RAMP1 (B), RAMP2 (C), and RAMP3 (D). Each data point is the mean \pm SEM from 2 – 4 individual repeats.

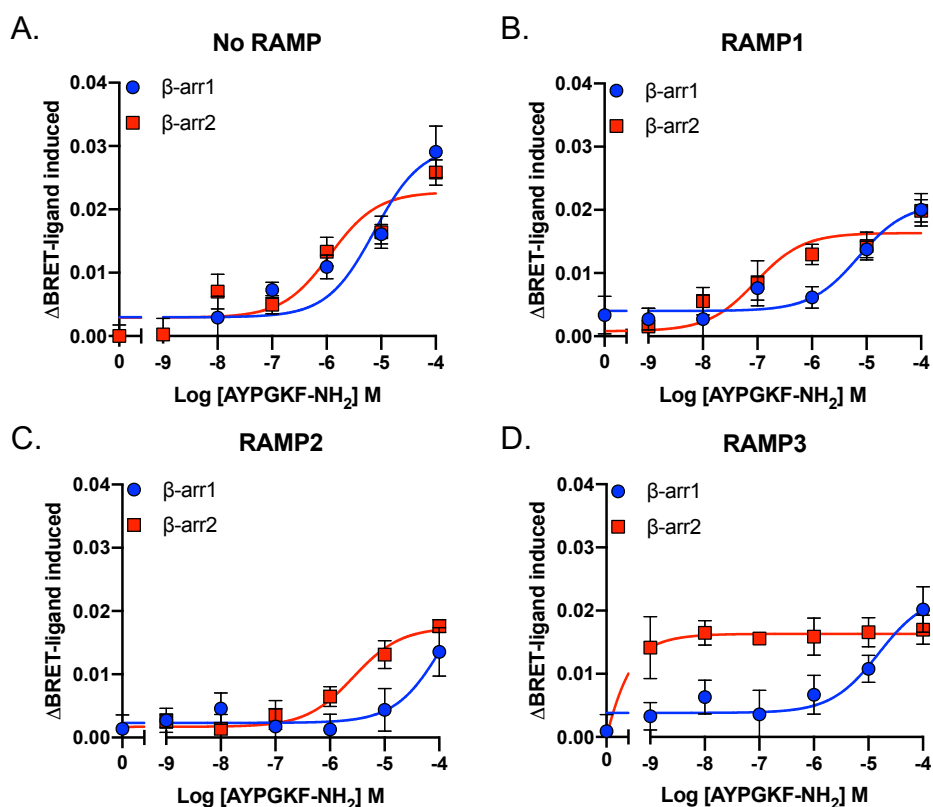
6.6 RAMP alters β -arrestin recruitment to PAR4

Next, the effect of RAMPs on recruitment of β -arrestin was investigated. As mentioned in the previous section, both variants of PAR4 were able to couple to β -arrestin1/2 upon stimulation with AYPGKF-NH₂ in a dose-dependent manner (Figure 6.4). As displayed in Figure 6.8A-D, there was no difference observed in β -arrestin1 recruitment by PAR4-AP. Interestingly, ligand-mediated β -arrestin2 recruitment was slightly potentiated in the presence of RAMP1 and RAMP3, but not RAMP2. While the potencies of AYPGKF-NH₂ were increased, the E_{max} for both PAR4s was reduced in the presence of RAMPs (Figure 6.8, Table 6.3). It was only with RAMP3 that AYPGKF-NH₂ became significantly more potent compared to PAR4-A120 alone (Table 6.3,

pEC₅₀ from 6.20 ± 0.33 to 10.81 ± 1.72). The presence of RAMP3 appears to induce PAR4-AP to be more potent. Due to limited access during COVID-19, the effect observed on PAR4:RAMP3 interaction to modulate β-arrestin recruitment was considered preliminary only. It is necessary to obtain more repeats to validate the observed effects.

The presence of RAMPs also altered β-arrestin recruitment on the PAR4-T120 variant. There was a reduction in PAR4-AP potencies in recruiting β-arrestin1, which was associated with a reduction in the E_{max} parameter in the presence of RAMP (Table 6.1). In contrast, recruitment of β-arrestin2 upon stimulation with AYPGKF-NH₂ was potentiated in cells expressing both RAMP and PAR4-T120. The E_{max} values for β-arrestin2 recruitment were significantly increased compared to receptor alone (from 9.12 ± 0.75 to 18.84 ± 2.96 (RAMP1), 20.51 ± 1.33 (RAMP2), 23.41 ± 0.58 (RAMP3)).

PAR4-A120



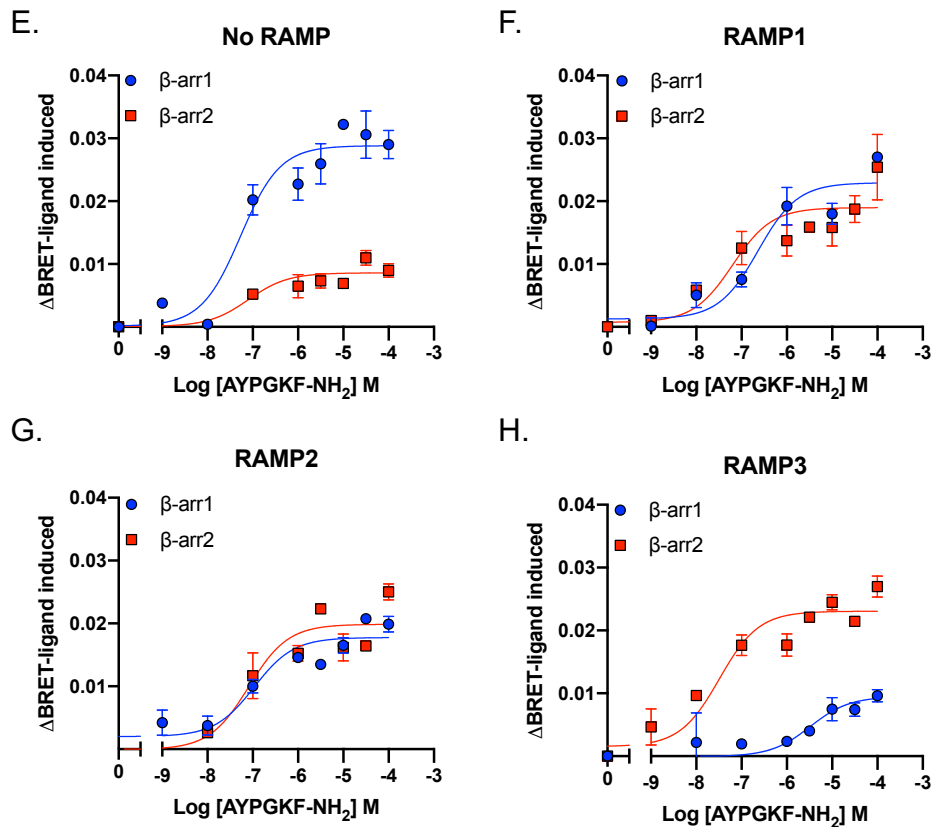
PAR4-T120

Figure 6.8 RAMPs differentially modulate β -arrestin recruitment on both PAR4 polymorphisms upon stimulation with PAR4-agonist peptide. AYPGKF-NH₂ promote β -arrestins recruitment in HEK293T cells transiently expressing PAR4-A120 in the absence of RAMP (A), RAMP1 (B), RAMP2 (C), or RAMP3 (D). The same peptide also recruits β -arrestin either in the absence of RAMP (E) or in the presence of RAMPs (F-H) on HEK293T cells transiently expressing PAR4-T120 variant. Each data point is the mean \pm SEM from 3 – 15 individual repeats. HL Jia-Qi performed BRET-based β -arrestin recruitment using the PAR4-T120 variant.

Table 6.3

Pharmacological parameters of PAR4-agonist peptide on PAR4-A120 and PAR4-T120 variants in the absence and presence of RAMPs

| Receptor | Ligand | $i[Ca^{2+}]$ | | | β -arr1 | | | β -arr2 | | |
|-----------|-----------------|-------------------|----------------------|---|-------------------|----------------------|---|-------------------|----------------------|----|
| | | pEC ₅₀ | E _{max} (%) | n | pEC ₅₀ | E _{max} (%) | N | pEC ₅₀ | E _{max} (%) | n |
| PAR4-A120 | AYPGKF- | 4.89 ± 0.41 | 33.07 ± 6.09 | 5 | 6.08 ± 0.59 | 27.13 ± 4.43 | 9 | 6.20 ± 0.33 | 26.69 ± 2.99 | 15 |
| +RAMP1 | NH ₂ | 5.21 ± 0.27 | 27.67 ± 4.79 | 4 | 5.99 ± 0.64 | 19.19 ± 2.60 | 9 | 6.94 ± 0.21 | 17.47 ± 1.65 | 11 |
| +RAMP2 | | 5.31 ± 0.22 | 26.17 ± 2.23 | 3 | 6.20 ± 0.76 | 21.05 ± 6.89 | 9 | 5.59 ± 0.22 | 18.09 ± 1.30 | 8 |
| +RAMP3 | | 5.36 ± 0.30 | 32.84 ± 9.82 | 4 | 7.54 ± 0.63 | 17.23 ± 3.56 | 9 | 10.81 ± 1.72*** | 18.38 ± 0.90 | 3 |
| PAR4-T120 | AYPGKF- | 5.34 ± 0.32 | 43.74 ± 15.47 | 3 | 7.37 ± 0.15 | 27.86 ± 1.94 | 3 | 6.86 ± 0.45 | 9.12 ± 0.75 | 3 |
| +RAMP1 | NH ₂ | 5.53 ± 0.26 | 28.65 ± 6.55 | 3 | 6.63 ± 0.17 | 23.17 ± 0.75 | 3 | 7.18 ± 0.08 | 18.84 ± 2.96** | 3 |
| +RAMP2 | | 5.29 ± 0.19 | 27.00 ± 6.14 | 3 | 7.01 ± 0.25 | 18.16 ± 0.89*** | 5 | 6.98 ± 0.32 | 20.51 ± 1.33** | 3 |
| +RAMP3 | | 5.51 ± 0.41 | 31.49 ± 3.99 | 3 | 5.31 ± 0.17*** | 9.54 ± 0.98*** | 4 | 7.43 ± 0.16 | 23.41 ± 0.58*** | 4 |

Calcium data was displayed after normalisation to that of 10µM ionomycin, whereas for β arr1/2 data was corrected after subtracting with vehicle control. E_{max} in β arr1/2 is displayed in mBU unit. Data are represented as mean ± SEM of 3-15 individual data. Data were determined as statistically different (*, p< 0.05; **, p<0.01; ***, p<0.001) compared to receptor only using one-way ANOVA followed by Dunnett's *post-hoc* analysis.

6.7 Quantification of signalling bias at PAR4 in the presence of RAMPs

Having confirmed RAMPs altered the signalling profile of PAR4, the study was then followed by quantification of signalling bias. Here, biased agonism is calculated through two methods including relative activity (RA_i) of PAR4 in the presence of each RAMP and calculating bias factor (β). The later was used to allow comparison between pathways, which in this case, the β value was expressed relative to calcium – since calcium responses remained unaffected by RAMPs. By calculating the bias factor (β), it is possible to compare signalling between two pathways and receptor complexes (Smith, Lefkowitz and Rajagopal, 2018). To determine bias, the following formula was used:

$$RA_{i,ref}^{pathA} = \frac{E_{max,+RAMP} \times EC_{50,PAR4}}{EC_{50,+RAMP} \times E_{max,PAR4}} \quad (3)$$

$$\beta = \log_{10} \left(\frac{RA_{i,ref}^{pathA}}{RA_{i,ref}^{pathB}} \right) \quad (4)$$

RA_i – relative activity of PAR4 in the presence of RAMP relative to PAR4 in Ca^{2+} mobilisation assay as a reference

E_{max} – % response maximum

EC_{50} – concentration of PAR4-agonist peptide that gives 50% of the maximal response

β – bias vector

From the study presented in this chapter, it is only possible to calculate signalling bias using PAR4-AP as the ligand, but not with thrombin. As mentioned previously, thrombin-induced β -arrestin recruitment was undetectable. In PAR4A-120, not only did RAMP2 regulate receptor towards β -arrestin1 but also include β -arrestin2. Whereas RAMP1 drove the biased away from β -arrestin2 (Figure 6.9A). However, due to limited data for this particular section, it is not possible to show the biased of PAR4-A120 variants by RAMP3.

Interestingly, PAR4-T120 displayed different behaviour. Whilst there was an indication that PAR4-AP showed β -arrestin bias over the calcium pathway, RAMP3 biased signalling towards β -arrestin2 and away from β -arrestin1 (Figure 6.9B). RAMPs, therefore, appear to govern functional selectivity on PAR4 signalling. The polymorphism of these receptors also dictated the signalling consequences of PAR4 and RAMP interaction.

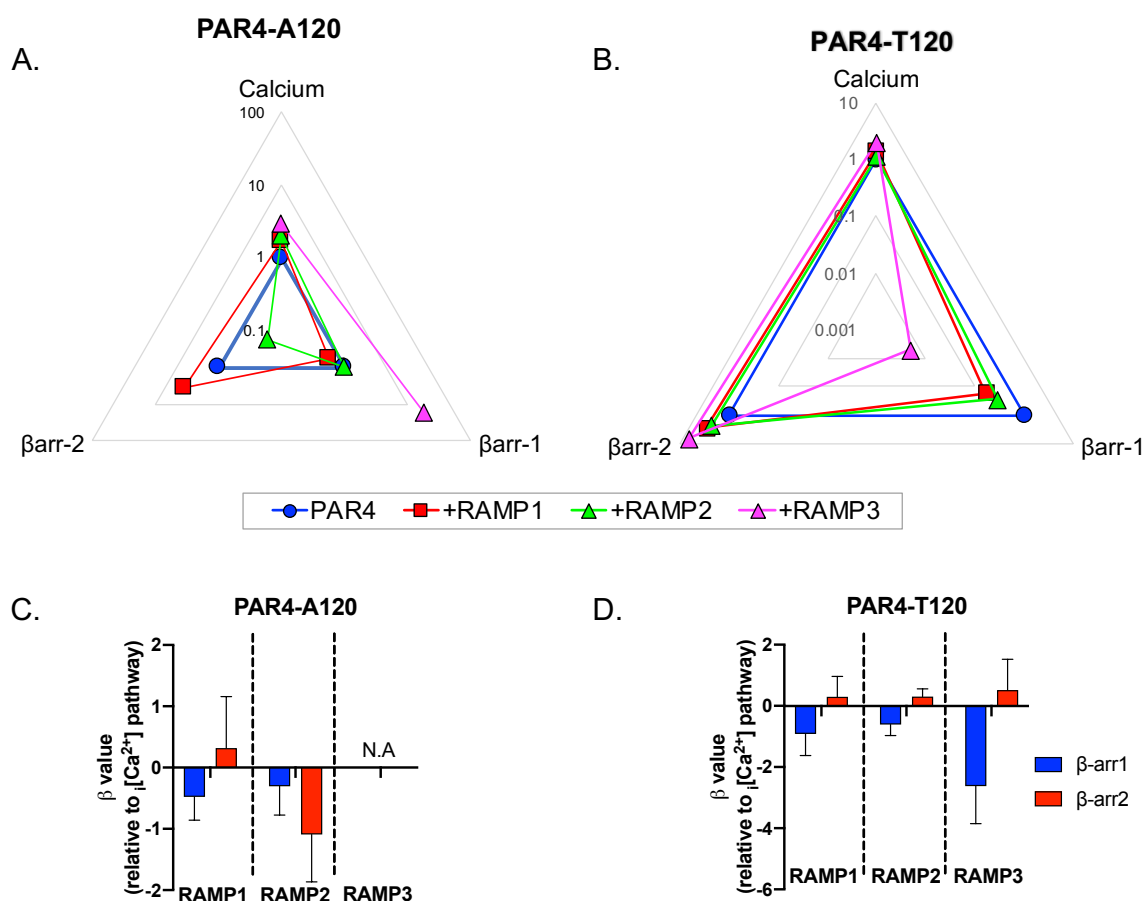


Figure 6.9 Quantification of biased signalling at PAR4 both variants by the presence of RAMPs. The radar plot of PAR4 variants in releasing intracellular calcium and recruiting arrestin1/2 on PAR4-A120 (A) and PAR4-T120 (B) variants. Biased plot was then recalculated relative to intracellular calcium mobilisation for both PAR4 variants (C,D). N.A: not applicable. Bias of RAMP3 in PAR-A120 mediated responses cannot be calculated using the current data.

6.8 Stimulation by CGRP-based peptide agonists elevated cAMP concentration and promoted glioblastoma U87 cell growth

The role of RAMPs for functional CLR signalling has been well documented (McLatchie *et al.*, 1998; Christopoulos *et al.*, 1999; Husmann *et al.*, 2003; Garelja *et al.*, 2020; Hendrikse *et al.*, 2020; Pioszak and Hay, 2020), although the mechanism is not fully elucidated. It is an absolute necessity for CLR to oligomerise with RAMP to traffic to the plasma membrane and to interact with their cognate ligand: CGRP, AM, and AM2 (intermedin). Targeting CGRP-R has been proved to be beneficial in treating migraine (Bhakta *et al.*, 2021). Ubrogepant has been proven to be an affective CGRP antagonist (ubrogepant) to relieve migraine, whereas monoclonal antibodies against CGRP (eptinezumab, fremanezumab, galcanezumab) and CGRP-R (erenumab) have also been used in clinical settings. Ostrovskaya and colleagues reported that CLR was also expressed in glioblastoma and investigated its functional effect on CLR and

RAMPs (Ostrovskaya *et al.*, 2019). This study found that stimulation with CGRP, AM, and AM2 dose-dependently increased cAMP production with the rank order of potency CGRP > AM > AM2 (Figure 6.10, Table 6.4). Unlike the findings in the previous chapters where elevated cAMP levels induced anti-proliferative effects; CGRP-based peptide agonists also increased cAMP production; however, it did not lead to cell growth suppression. Instead, activation by CGRP, AM, or AM2 promoted cell proliferation to different extents (Figure 6.10, Table 6.4). In comparison, forskolin elevated cAMP concentration and suppressed cell proliferation. These results suggest that CLR has different pharmacological actions that drive different cellular responses. This finding led to the hypothesis that whether the stimulation of CLR would be applicable to degenerative disease models or cellular protection that require repairment in cell growth. CGRP, AM and AM2 are known as vasodilatory peptides with pleiotropic effects (Nuki *et al.*, 1993; Cui *et al.*, 2021). Given the fact that AM and RAMPs (especially RAMP2/3) are highly expressed in the heart^{9,10} (Tippins, 1986; Ishiyama *et al.*, 1993), the study was then followed by investigating the role of RAMP in cardiovascular system. Thus, HUVECs and hCMs were used to investigate this objective particularly in corresponding to cell growth.

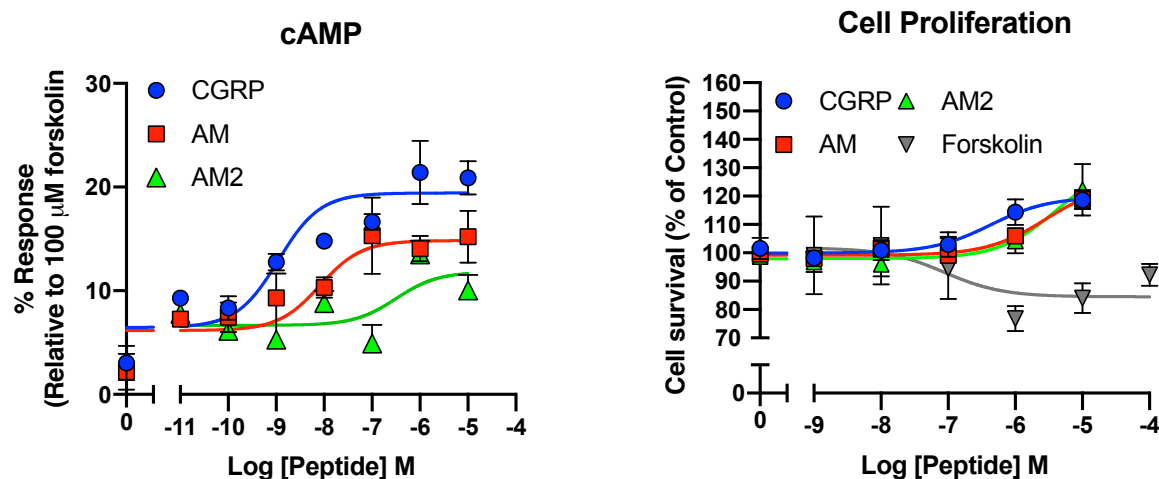


Figure 6.10 Elevation on cAMP concentration by peptide ligands induced cell proliferation on U87 cells. Accumulation of cAMP was determined upon 30-minute stimulation by the selected agonist. The response was normalised to that of forskolin 100 μ M. Cell survival was calculated as the percentage response relative to vehicle control, determined upon 72h treatment. Each data point is expressed as mean \pm SEM from 3-6 individual data.

⁹ <https://www.proteinatlas.org/ENSG00000131477-RAMP2/tissue>

¹⁰ <https://www.proteinatlas.org/ENSG00000122679-RAMP3/tissue>

Table 6.4

The value of potency (pEC_{50}) and maximum responses (E_{max}) of agonist peptide on cAMP production and cell growth in U87 cells

| Ligand | cAMP | | | Cell Proliferation | | |
|-----------|--------------|-----------------|---|--------------------|-----------------|---|
| | pEC_{50}^a | E_{max}^b (%) | n | pEC_{50}^a | E_{max}^b (%) | n |
| Forskolin | 7.39 ± 0.09 | 98.62 ± 2.66 | 4 | 7.06 ± 1.14 | 84.50 ± 5.98 | 5 |
| CGRP | 8.95 ± 0.29 | 19.43 ± 1.10*** | 3 | 6.37 ± 0.44 | 119.73 ± 3.99 | 6 |
| AM | 8.09 ± 0.36 | 14.84 ± 1.08*** | 4 | 5.55 ± 0.32 | 124.36 ± 5.54* | 6 |
| AM2 | 6.49 ± 0.95 | 11.82 ± 2.18*** | 3 | 5.38 ± 0.69 | 132.32 ± 18.79* | 6 |

^a The negative logarithm of the agonist concentration required to produce a half-maximal response.

^b The maximal response to the agonist expressed as a percentage of the system maximal as defined for corresponding.

Data are expressed as the mean ± SEM of 3-6 individual data. Data were determined as statistically different (*, $p < 0.05$; **, $p < 0.01$; ***, $p < 0.001$) compared to forskolin using one-way ANOVA followed by Dunnett's *post-hoc* analysis.

6.9 RAMP regulate cellular signalling and cell growth of HUVECs and hCMs

Stimulation of hetero oligomers of CLR and RAMPs has been shown to promote cell proliferation of U87 cells. The study was then extended to explore the effect of stimulation of CLR and RAMP in human cardiovascular systems. To do this, HUVECs and hCMs were utilised.

In the study performed by Dr. Clark, HUVECs and hCMs expressed CLR and different types of RAMP (Clark *et al.*, 2021). Whilst HUVECs expressed RAMP2, RAMP1 amplicon was detected in hCMs (Appendix 4). The difference in RAMP expression appeared to contribute to a distinct signalling profile involving cAMP synthesis, calcium release, ERK1/2 activation, and NO release.

Since HUVECs expressed RAMP2 and CLR, allowing both proteins to form the AM1-R (adenomedullin receptor). As expected, AM was the most potent ligand in the canonical cAMP pathway (Appendix 4). However, for ERK1/2 activation, CGRP was the most potent ligand to activate ERK1/2, aligning with the effects observed on cell growth (Figure 6.11, Table 6.5). In hCMs that expressed RAMP1 and CLR, the cognate peptide for this receptor (CGRP-R) showed the highest activity in promoting cAMP production (Appendix 4) but not in ERK1/2 activation. Again, the most active ligand, AM, in activating ERK1/2 elicited a similar activity in cell proliferation (Figure 6.11, Table 6.5). Investigation of other signalling events has been reported in more detail (Clark *et al.*, 2021). Taken together, it is apparent that RAMPs regulate the pharmacological action of CLR in endogenous systems.

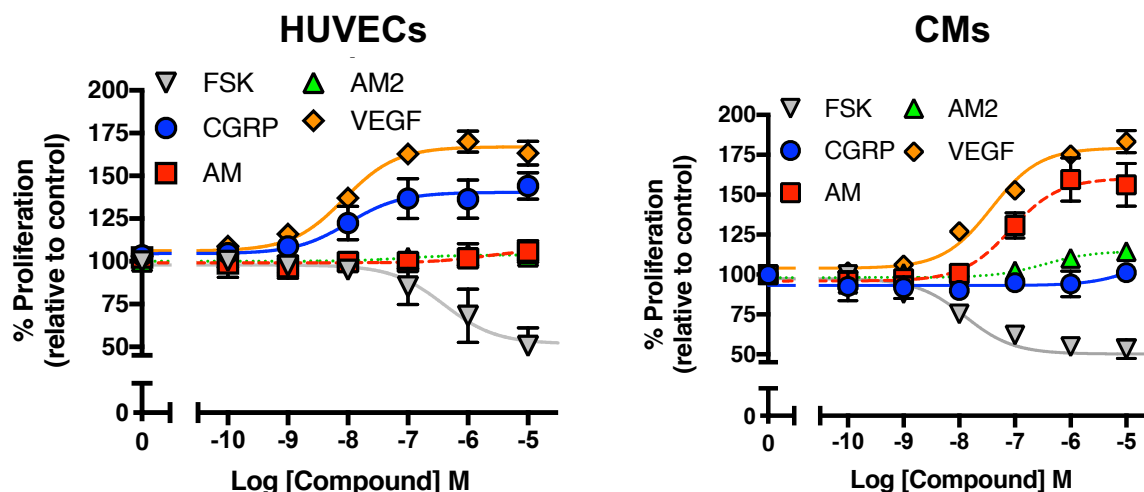


Figure 6.11 Stimulation by CGRP family peptides induced cell proliferation to different extents on HUVECs and hCMs. The effects were observed in both cells appeared to be related to predominant RAMP expressed in corresponding cells (Appendix 2). Percent proliferation was defined relative to control vehicle upon 72h treatment. Each data point is expressed as mean \pm SEM from 3-8 individual data.

Table 6.5

The value of potency (pEC_{50}) and maximum responses (E_{max}) of agonist peptides on cell growth in HUVECs and hCMs

| Ligand | HUVECs | | hCMs | |
|--------|-------------------------|----------------------------|-------------------------|----------------------------|
| | pEC_{50} ^a | E_{max} ^b (%) | pEC_{50} ^a | E_{max} ^b (%) |
| CGRP | $8.00 \pm 0.19^*$ | 140.39 ± 2.13 | 5.32 ± 0.80 | 108.80 ± 24.2 |
| AM | 5.73 ± 0.68 | 106.90 ± 3.47 | $7.08 \pm 0.23^*$ | 160.32 ± 6.82 |
| AM2 | 7.06 ± 0.90 | 103.74 ± 1.43 | 6.48 ± 0.58 | 114.68 ± 3.58 |

^a The negative logarithm of the agonist concentration required to produce a half-maximal response.

^b The maximal response to the agonist expressed as a percentage of the system maximal as defined for corresponding assays.

Data are expressed as the mean \pm SEM of 3-8 individual data. Data were determined as statistically different (*, $p < 0.05$; **, $p < 0.01$; ***, $p < 0.001$) compared to AM for HUVECs and CGRP for hCMs using one-way ANOVA followed by Dunnett's *post-hoc* analysis.

6.10 Discussion

6.10.1 The novel interaction of PAR4 with RAMPs changes β -arrestin1/2 recruitment

Polymorphisms and variants of GPCRs have recently been found to dictate distinct signalling profiles. This may also explain why drugs targeting particular GPCRs fail in clinical trials due to differential expression of isoforms in tissue and cells (Marti-Solano *et al.*, 2020; Snyder and Rajagopal, 2020). In the case of PAR4, there are two

polymorphisms reported which influence platelet aggregation; that influences residue 120 in the second transmembrane domain to be alanine (A120) or threonine (T120); and the less common form of Phe296Val (Edelstein *et al.*, 2014). Dimorphism at residue 120 has been reported to be associated with responsiveness towards thrombin, where the T120 variant appears to be hyper-responsive compared to its counterpart leading to a higher risk of CV events. In agreement with this study, the PAR4-T120 variant induced intracellular calcium mobilisation with higher magnitude upon stimulation with thrombin, but not with PAR4-AP (Figure 6.2). It is worth noting that using HEK293T cells may not be an ideal surrogate system to dissect PAR4 pharmacology in modulating calcium release. As Atwood investigated, HEK293 cells endogenously express PAR1 and PAR2 (Atwood *et al.*, 2011). It is widely known that PAR1 and PAR4 can be activated by thrombin (Xu *et al.*, 1998; Adam *et al.*, 2003) with different kinetics. Since Fluo4-AM acts as a general calcium sensor, the signal observed may need further investigation to validate if the signals come from cumulative activation from PAR1 and PAR4 receptor populations. Considering there was no manipulation of expression of other PARs, it was assumed that calcium release (Figure 6.2) might reflect the activity of PAR4.

It has been reported that different ways to activate PAR4 lead to distinct receptor signalling (Zhao, Metcalf and Bunnett, 2014), however, it was not possible to detect thrombin-mediated β -arrestin recruitment from this study. As an endogenous ligand for both PAR1 and PAR4, thrombin failed to generate BRET signals in our β -arrestin recruitment assay. Ayoub *et al.* demonstrated that thrombin very rapidly promoted β -arrestin recruitment to PAR1 in COS-7 cells, with the signal rapidly returning to baseline (Ayoub *et al.*, 2007). Given the higher expression of endogenous PAR1 in HEK293T and higher thrombin affinity towards PAR1, it is very likely that the PAR1 population sequestered β -arrestin recruitment over PAR4. Again, this notion requires further validation.

Upon PAR4 activation, like other GPCRs, G proteins or non-canonical β -arrestin-mediated signalling pathways are engaged. Here, selective PAR4 stimulation recruited β -arrestin1/2. Indeed, further investigation of G protein activation will be of great interest to dissect PAR4 pharmacology, this can be achieved through utilisation of NanoBit or BRET-based G protein dissociation assay. It has been reported that activating PAR4 signalling, either by selective activation/inhibition of G protein coupling or β -arrestin signalling, showed a potential strategy to develop therapeutic agents to reduce platelet aggregation without bleeding liability. Previously, the signalling bias of

PAR4 was studied by synthesising ligands that were selectively activating certain cascades (Bar-Shavit *et al.*, 2016; Thibeault *et al.*, 2019). The preliminary results presented in this chapter demonstrate that signalling bias can also be achieved by interaction with RAMPs. The advantages of signalling bias have been shown for various receptors to promote desired responses or circumvent potential adverse reactions, these have been demonstrated in μ -opioid receptors (Kliwer *et al.*, 2020), GIPR ((Harris, 2019) restricted access), apelin receptor (Gargalovic *et al.*, 2021), and ghrelin receptor (Nagi and Habib, 2021).

Until now, PAR4 was only known to form dimers with the P2Y₁₂ receptor with this interaction leading to different signalling events compared to individual receptors (Smith *et al.*, 2017). Notably, this study confers PAR4 as a new interacting partner of RAMP. Through analysis by FACS, it enables the detection of RAMP and receptor interaction in a more functional setting (Bailey *et al.*, 2019). Whilst this approach offers more advantages over other available methods, including suspension bead array (SBA) or BRET-based method (Lorenzen *et al.*, 2019b; Mackie *et al.*, 2019), observation using FACS may not be sufficient to rule out the possibility of endogenous GPCR in influencing RAMPs trafficking. Based on FACS analysis, there were significant increases in RAMP1 and RAMP2 cell surface expression when they were co-expressed with both PAR4 variants (Figure 6.5). However, it was observed that RAMP3 was also expressed in vehicle control that did not contain any receptor. This data suggests that either RAMP3 can traffic to the plasma membrane without interacting partner or there are effects from endogenous GPCRs that promote RAMP3 expression to the plasma membrane. RAMP3, in particular, contains a type I PDZ-motif (DTLL) in its C-terminal, which has been reported to be responsible to maintain its cell surface expression ((Harris, 2019), restricted access). This also contributes to the interaction with PDZ domain-containing proteins such as Na⁺/H⁺ exchange regulatory factor (NHERF), N-ethylmaleimide-sensitive factor (NSF), which modulate GPCR signalling (Reczek, Berryman and Bretscher, 1997; Bomberger, Parameswaran, *et al.*, 2005; Bomberger, Spielman, *et al.*, 2005; Serafin *et al.*, 2020)

Based upon this study, AYPGKF-NH₂ recruited β -arrestin after PAR4 activation, and this is in agreement with other reports highlighting the ability of PAR-AP to stimulate β -arrestin-mediated signalling (Ramachandran *et al.*, 2017; Thibeault *et al.*, 2020; Vanderboor *et al.*, 2020). The classical mechanism after receptor activation is that receptors couple to β -arrestin, undergo internalisation, thereby terminating receptor signalling and mediating receptor desensitisation (Pierce, Premont and

Lefkowitz, 2002; Shenoy and Lefkowitz, 2005; Hanyaloglu and Von Zastrow, 2008). Aside from platelet aggregation, signal transduction mediated by β -arrestins has been shown in other studies to induce membrane blebbing that would be a potential target for preventing cellular migration, which is a common feature in cancer (Vanderboor *et al.*, 2020). Since this study is limited to observing initial signalling events that involve canonical G protein-mediated signalling and non-canonical pathways through β -arrestin, it would be of interest to investigate further if this dynamic will impact receptor internalisation, receptor trafficking and further downstream PAR4 signalling.

6.10.2 RAMP regulate CLR pharmacology: the study on cell growth

As the first receptor reported to interact with RAMPs, CLR-RAMP heteromers have been extensively studied (McLatchie *et al.*, 1998; Christopoulos *et al.*, 1999; Husmann *et al.*, 2003; Garelja *et al.*, 2020; Hendrikse *et al.*, 2020; Pioszak and Hay, 2020). Whilst CLR pairs with RAMP1/2/3 forming new receptors that differentially bind to CGRP, AM, and AM2; development of drug discovery has shown that targeting CGRP is beneficial in various physiological functions. This includes its cardioprotective effect, pivotal role in migraine pathogenesis, bone formation and may be of value in cancer treatment (Kiriya *et al.*, 1997; Schönauer, Els-Heindl and Beck-Sickinger, 2017; Booe *et al.*, 2018; Ostrovskaya *et al.*, 2019; Xu *et al.*, 2020; Bhakta *et al.*, 2021).

As mentioned in the previous chapter, elevating intracellular cAMP through various targets suppressed suppression of glioma and human lung cancer cell lines. However, this was not sufficient in human glioblastoma U87 cells. Therefore, in this chapter, the study was performed to explore the possibility of other GPCRs in the GBM cell model. Although CLR is pleiotropically coupled to different G proteins (including $G_{q/11/14}$ and $G_{i/o}$), it is widely known that this receptor predominantly recruited G_s , therefore, increasing cAMP production within cells (Wootten *et al.*, 2018; Garelja *et al.*, 2020). Since CLR is predominantly coupled to G_s , it is not surprising that all peptides dose-dependently increase cAMP accumulation in U87 cells. The order of potency appears to be CGRP>AM>AM2, suggesting that U87 cells express functional CLR and RAMPs, with RAMP1 is most likely higher than other RAMP subtypes. Surprisingly, elevation of cAMP levels induced by these peptides did not suppress cell growth as expected from the previous chapters. Instead, the treatments promoted cell proliferation, with the order of potency was aligned with that of in cAMP pathway. Another study using CGRP-related peptides showed that elevation of cAMP differentially activates the ERK1/2 pathway, which correlates to cell growth control on

human cardiovascular cells (Clark *et al.*, 2021). In comparison, elevation on cAMP levels induced by forskolin suppressed U87 cell growth. These contradictory results suggest that CLR-RAMP interaction may have specific mechanisms or different downstream targets that result in different outcomes. Some of the GPCRs from different tissues have been reported to have different ability to coupling to different regulatory proteins. These phenomena have been reviewed in more details (Snyder and Rajagopal, 2020). This possibility can be taken into account to demonstrate that CGRP, AM, and AM2 may activate particular cascades that result in distinct responses which presumably cell-type or tissue-dependent.

In both HUVECs and hCMs, the most potent compounds in canonical cAMP pathway did not exhibit the same activity in cell growth (Appendix 2). These peptides, in fact, elicited differential actions on ERK1/2 activation in both primary cell lines, which was aligned with that of cell proliferation. Given that these peptides have not been validated for ERK1/2 phosphorylation U87 cells, it would be of interest to investigate this particular aspect for the future experiments.

The study was expanded to use other systems where cell proliferation is measured to determine the different CLR-RAMP effects on cell growth. The extensive study from Dr. Clark has shown that interaction between RAMPs and CLR dictates different signalling profiles and, proved that signalling bias is naturally occurring in more physiologically relevant cells (Clark *et al.*, 2021). HUVECs are reported to express RAMP2, whereas hCMs predominantly express RAMP1; CLR was present in both primary cells (Appendix 2). Notably, whilst AM was the most potent ligand in promoting cAMP production in HUVECs, this ligand did not exhibit similar activities in mediating G_q -mediated calcium mobilisation nor ERK1/2 phosphorylation. Interestingly, a similar pattern was observed between calcium release and NO production and ERK1/2 stimulation- cell growth axis. In comparison, CGRP was the most potent peptide in elevating cAMP levels and calcium release in hCMs, but in the case of ERK1/2 phosphorylation, the most remarkable effect was shown by AM. While all ligands: CGRP, AM, and AM2 were able to promote total cAMP production to different extends, their activation on ERK1/2 is believed to be independent of this canonical pathway in both cells. Rather, it is mediated through G_i/o activation for CGRP and AM2, and activation of $G_{q/11/14}$ and EPAC for AM (Clark *et al.*, 2021). These unique findings govern the multifaceted signalling on CLR pharmacology which is driven by RAMPs. Taken together, RAMPs appear to serve as a key or cellular barcode that specifically activates particular signalling cascades.

HUVECs and hCMs, as previously mentioned, expressed different types of RAMPs: RAMP2 and RAMP1, respectively. Close analysis of the cAMP responses in U87 cells would suggest a potential biphasic fit for CGRP and AM but not AM2 (as shown below, Figure 6.12, Table 6.5). This may suggest that U87 cells express, at least RAMP1 and RAMP2. CLR-RAMPs complexes can bind to all CGRP, AM, and AM2 with differential affinities; thus, it suggests that cAMP production in U87 cells may be driven by more than a single receptor population, presumably from CGRP-R and AM1-R. Although this requires further investigation, the observation obtained from HUVECs and hCMs may explain biphasic responses observed in cAMP accumulation on U87 cells.

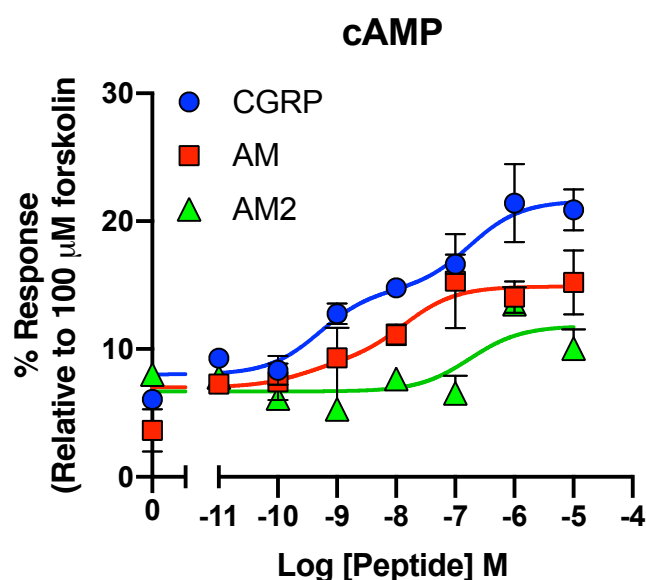


Figure 6.12. CGRP and AM, but not AM2, mediate biphasic responses on cAMP production in U87 cells. Accumulation of cAMP was determined upon 30-minute stimulation by the selected agonist. The response was normalised to that of forskolin 100 μ M. The biphasic curve fitting was generated using Prism 9.0 by constraining LogEC_{50-n1} to be <-7 and LogEC_{50-n2} set to <-5 .

Table 6.6

The value of potency and E_{max} of CGRP and AM after stimulation in U87 cells in cAMP accumulation assay

| Ligand | pEC_{50} (1) | pEC_{50} (2) | E_{max} (%) | n |
|--------|-----------------------|-----------------------|----------------------|---|
| CGRP | 9.29 ± 0.79 | 6.75 ± 0.75 | 21.59 ± 1.43 | 3 |
| AM | 9.52 ± 3.57 | 7.85 ± 1.30 | 14.89 ± 1.07 | 4 |

6.11 Summary

Signalling bias has been long known to affect GPCR pharmacology. This chapter provides preliminary evidence of RAMPs as an interacting partner of PAR4. Indeed, RAMPs were demonstrated to interact with both A120 and T120 variants of PAR4. The interaction of RAMPs and PAR4 changed cell surface expression of the RAMP, which was characterised by FACS. Interestingly, this interaction can be translated to a distinct signalling profiles, depending on which RAMP is expressed with PAR4. These preliminary results demonstrate that RAMPs serve as a cellular barcode that selectively activates particular signalling events. Due to restrictions during Covid-19, further experiments could not be performed. It would be of interest to dissect the impact of RAMP-PAR4 interactions on other upstream signalling events and physiological consequences in more relevant models.

As the second part of this chapter, cAMP elevation by stimulating CLR-RAMP heteromers differentially stimulated cell growth, which is different from that observed in the previous chapters. In both glioblastoma and human primary cardiovascular cells, selective stimulation using CGRP, AM, and AM2 differentially activated canonical cAMP pathways to promote cell growth. Although this finding may not be directly translatable for cancer therapy, these experiments highlight the possibility of targeting RAMP-CLR to provide cellular protection such as cardioprotective actions or promoting tissue regeneration for the model that requires repairing in cell growth such as in degenerative diseases.

Together, the preliminary results focusing on RAMP-PAR4 interaction may become a potential target to manipulate cellular responses and provide therapeutic benefit with minimal adverse reactions in cardiovascular events. Further studies on RAMP-CLR complexes in this study also demonstrated a role of RAMPs in dictating specific signalling profiles, leading to different cellular responses, such as cell growth. This may shed light on how to manipulate receptor signalling and minimise adverse reactions in particular pathological conditions.

CHAPTER 7

GENERAL DISCUSSION AND FUTURE DIRECTIONS

7.1 Discussion

7.1.1 Targeting cAMP pathway and its therapeutic benefits in cancer

Glioblastoma and lung cancer carcinoma are considered as fatal types of tumours and are a leading cause of death, respectively¹¹ (Schwartzbaum *et al.*, 2006; Delgado-López and Corrales-García, 2016). Due to the nature of their resistance, their heterogeneity and plasticity, it has been challenging to find compounds that can inhibit tumour progression. Of all abnormalities that have been reported, alteration in cAMP signalling has been found in numerous cancers including GBM and lung cancers (Daniel, Filiz and Mantamadiotis, 2016).

As previously mentioned in the introduction, cAMP has been reported to have divergent effects on cell growth. Depending on cell types, cAMP may elicit pro-proliferative or anti-proliferative actions. This has been demonstrated in several types of cells such as neuronal derived cells (dorsal root ganglion, spinal motor, dopaminergic neurons, cerebral granule and cholinergic neurons); endocrines (pancreatic β -cells), gastrointestinal cells, hepatocytes, and myeloid (Lerner and Epstein, 2006). On the contrary, we and others have observed negative effects of cAMP on cell proliferation in glioblastoma and primary cardiomyocytes (Ding *et al.*, 2005; Kang *et al.*, 2014). Not only were the effects shown by aforementioned cells but also was observed in other mesenchymal and epithelial cells including fibroblasts, ovarian granulosa cells, and thyroid cells (Zwain and Amato, 2001; Huston *et al.*, 2006; Sawa *et al.*, 2017). Due to the limited number of cells included in this study, elevation of intracellular cAMP levels may promote cell growth in other cell types.

In this thesis, we have performed an in-depth analysis to characterise the actions of this second messenger in modulating cancer cell growth. This study provides some insights on how cAMP is generated and retained within intracellular compartments lead to cell growth suppression in cancer cells. Moreover, our study was accomplished using multiple models of cancer: glioma and glioblastoma cell lines from two different species - rat (C6 cells) and human glioblastoma (U87 and T98 cells), and subsequently expanded to use human lung cancer cell lines. The study was also

¹¹ <https://www.cancerresearchuk.org/health-professional/cancer-statistics/statistics-by-cancer-type/lung-cancer#heading-One>

extended, to include human primary HUVECs and hCMs (Chapter 6) to determine the effects of different GPCR agonists on cell proliferation.

Across all cells that have been tested, it was revealed that elevation of cAMP levels by forskolin displayed negative effects on cell growth. Interestingly, cells that responded to forskolin stimulation in cell growth, were also found to be suppressed by a number of PDE inhibitors, as demonstrated in Chapter 3 and 4. Following short-term stimulation (30 minutes), all compounds including forskolin, PDE inhibitors (particularly those that worked on cAMP and a few compounds that inhibited dual-substrate PDEs) as well as β_2 -AR agonist, A_{2A} R agonist and CGRP-based peptides promoted the production of cAMP. However, only those that activate directly on AC and inhibit PDE were able to exhibit greater suppression on cell growth. The negative effect of cAMP was corroborated by blocking the MRP4 transporter - an efflux pump for cyclic nucleotides, to retain cAMP within the intracellular compartment. The treatment with MRP4 inhibitor further enhanced the anti-proliferative actions of cAMP-elevating agents (forskolin and PDE inhibitors). Interestingly, in the case of stimulation at the A_{2A} R alone and CLR-RAMP complexes, long-term exposure did not exhibit anti-proliferative effects (with the exception of H1563 cells). Instead, activation at these receptors was deemed to be pro-proliferative. Interestingly, dual-target ligands displayed antiproliferative actions through their dual activities as agonist at the A_{2A} R and inhibitors of PDE10A (Chapter 6). These findings, in fact, open up further questions on whether the elevation of cAMP levels by different stimuli induce different cellular outcomes. The following sections will discuss the difference of these findings, discuss the limitation within the study, and recommend future research within the field.

7.1.1.1 Different signalling profile between GPCR ligand-mediated and AC-/PDE-mediated cAMP responses

Enzymes and GPCRs have different regulatory mechanisms. The concentration of a substrate mainly controls enzymes (AC and PDE), whereas agonist-occupied GPCRs typically undergo desensitisation or internalisation, although not all receptors encounter these processes. As demonstrated within this study, the elevation of cAMP levels by forskolin displayed anti-proliferative effects across all cell lines tested: rat and human glioblastoma (except U87 cells), human lung cancer cells, including primary cardiovascular cells HUVECs and hCMs. Stimulation at the GPCR level, or modulating the activity of Gas or Gai, promoted cAMP production, yet the cell growth suppression was considerably less profound compared to that of forskolin. This notion has been

clearly demonstrated through the effects of forskolin (direct activation of AC) and GPCR ligands (indirect activation), as shown in Chapter 3 using isoproterenol, PTx, and CTx; in Chapter 5, both NSCLC and GBM models were stimulated by the A_{2A}R agonist: CGS21680; and Chapter 6 through stimulation of CLR-RAMP complexes by CGRP, AM, and AM2.

Although the dose-dependent increase was observed in cAMP production, the potency and/or I_{max} of these ligands was weaker than that of forskolin in cell growth assay, with some of them being pro-proliferative (CGS21680 and CGR- related peptides). In agreement with other studies, prolonged exposure of β₂-AR agonist-induced receptor desensitisation or internalisation, mediated by GRKs and β-arrestins (Hausdorff, Caron and Lefkowitz, 1990; Shi *et al.*, 2017). Some reports noted that A_{2A}R was desensitised over more prolonged stimulation by CGS21680 in various cells (Ramkumar *et al.*, 1991; Chern *et al.*, 1993; Mundell, Benovic and Kelly, 1997; Mundell and Kelly, 1998), nevertheless, this mechanism remains poorly characterised. Notably, no palmitoylation identified at the C-terminal of A_{2A}R, which is thought to be phosphorylation sites for GRKs or β-arrestin binding (Klaasse *et al.*, 2008). In the case of CLR-RAMP complexes, it has been suggested that CLR is coupled to β-arrestin and undergoes internalisation (Hilairet *et al.*, 2001).

Although internalisation has been widely documented to terminate cellular signalling, more evidence has implicated the ability of GPCRs to maintain signal transduction from intracellular compartments (Calebiro *et al.*, 2009; Ferrandon *et al.*, 2009). The complex of CLR-RAMPs and β-arrestin was found to transduce their own signalling to modulate cell growth despite being localised to endosomes (Kuwasako *et al.*, 2000; Guidolin, 2010). In comparison, some GPCRs such as A_{2A}R and GIPR-RAMP heteromers have been shown to sustain their signal from the plasma membrane without undergoing internalisation (Carvalho *et al.*, 2020; Harris *et al.*, 2021). Indeed, the distinct regulation of GPCRs is appealing to investigate further. It will be interesting to determine how sustain and how strong a signal is required to be able to activate growth signalling cascade.

7.1.1.2 Short-term vs prolonged exposure of cAMP and factors that may influence cell growth

Although there is a discrepancy between cAMP production (30 minutes) and the cell proliferation assay (72h) utilised in this study, prolonged treatment was chosen to enhance the response that may not be detected for the short-term stimulation. Cell

growth can be determined after 24h, but longer exposure permits a better window for observation in terms of cell growth (see Chapter 2 optimisation of cell growth assay). In agreement with this, Vitali and colleagues also reported that either stimulatory or inhibitory effects on cell growth started 24h post-exposure, with the maximum effect at 72h (Vitali *et al.*, 2014). The more prolonged exposure may influence the expression of many proteins and most likely cause resistance. However, the latter requires a much more extended period of about 6-12 months, depending on cell types, to develop cell lines resistant to particular drugs.

Among all PDEs characterised within this study, only those that mainly regulate cAMP could suppress cell growth, but a similar effect was not observed for cGMP-specific PDE inhibitors. Instead of directly influencing cell growth, cGMP may act as an allosteric modulator that influences cAMP concentration through PDEs. Later, it was revealed that GC activators enhanced forskolin-mediated anti-proliferative effects indicating that dynamics in cGMP levels may control cAMP-mediated responses, possibly through dual-substrate PDEs. This finding opens up further questions: i) why did only PDEs that hydrolyse cAMP showed anti-proliferative effects but not others? ii) how does the change in cAMP concentration by different stimuli result in displaying different effects on cell growth? The following sections provide several viewpoints to explain the differential responses regarding the previous questions.

A. Spatiotemporal control by PDEs and association with other proteins within specific subcellular domain

It has been suggested that PDEs are distributed in specific compartments within the cells. This microcellular domain is responsible for sculpting local pools of cAMP and dictating the activation of particular regulatory proteins to promote specific cellular responses. Of all PDEs, PDE4 is one of the most extensively studied to form macromolecule complexes that control the cAMP fine-tuning mechanism. In a report by Hoshi *et al.*, the assembly of a signalosome containing PKA, PDE4, and AKAP79 has disseminated different signals from two distinct receptors: bradykinin and muscarinic receptor onto two different effector systems (Hoshi, Langeberg and Scott, 2005). Another signal complex comprising mAkap, PKA, PDE4D3, EPAC, and MEKK/MEK/ERK5 controlled cAMP concentrations in the intracellular microdomain. The association of these proteins, in turn, dictate PKA, PDE4D3 enzymatic actions, and EPAC activity, providing the negative feedback loop to maintain physiological cAMP levels (Dodge-Kafka *et al.*, 2005). Other mechanisms to control cAMP

concentration have also been reported by other studies highlighting the important role of PKA to activate PDE3, PDE4 and inhibit AC (AC5 and AC6) so maintaining cAMP homeostasis (Murthy, Zhou and Makhlouf, 2002; Khannpnavar *et al.*, 2020). In addition, PDE10A has been shown to be tethered to a macromolecule complex involving PKA, AKAP150, and PSD95 that altogether influenced the signalling of N-methyl-D-aspartate (NMDA) receptors (Russwurm, Koesling and Russwurm, 2015).

The study presented in this thesis focused on producing total cellular cAMP and has not interrogated subcellular signalling. Given that PDEs control the spatiotemporal regulation of cAMP signalling in activating specific proteins, it would be of interest to investigate the role of prospective PDEs to identify the mechanism of PDE inhibitors in interfering with this signalling.

B. Multiple proteins activated by cAMP are cell type-dependent

In brain tumours, activation of PKA by cAMP induces the activation of the downstream transcription factor CREB to upregulate p27 and p21, both of which are cyclin-dependent kinase (CDK) inhibitors (T Keravis and Lugnier, 2012). Both p27 and p21 are known to mediate cell cycle arrest, therefore, inhibiting cell growth. In comparison, in lung cancer, PKA activation by cAMP-induced protein phosphatase 2A (PP2A) has been reported to recruit PDE4 to generate a macromolecular complex. The association of these proteins are reported to inhibit tumour suppressor genes such as ataxia telangiectasia mutated (ATM) gene encoding a serine-protein kinase that targets p53, breast cancer type 1 susceptibility protein (BRCA1), checkpoint kinase 2 (CHK2), H2A histone family member X (H2AX), and nibrin (NBS1); and NF- κ B, as well as pro-apoptotic proteins BCL2-interacting mediator of cell death (BIM) and BCL2 associated agonist of cell death (BAD) (H. Zhang *et al.*, 2020).

Aside from the differential proteins activated to control cell growth, the distribution of PKA isoforms has also been suggested to contribute to cell growth control. The expression ratio of RI and RII of the PKA subunits may determine the net effect between the pro- and anti-proliferative actions (Sapio *et al.*, 2014). Furthermore, the activation of PKA-RII β , but not RI α isoform, appears to associate with cell growth suppression. Not only are they distributed into different domain within the cellular architecture, but also the patterns are different from each cell type (Cheadle *et al.*, 2008; Ilouz *et al.*, 2017). Taken this into account, the types and distribution of PKA may be different between cell types and can be determined to better understand the effects of cAMP/PKA signalling.

Although many studies showed that the anti-proliferative actions could be driven by PKA or EPAC or both, in this study, the anti-proliferative effects of forskolin and PDE inhibitor in glioma cells were predominantly driven by PKA. In Chapter 3, we also showed that inhibition of EPAC enhanced the anti-proliferative effects of forskolin and PDE inhibitor. These suggest that there is a crosstalk between EPAC and PKA thereby driving the signalling through PKA leading to cell growth suppression. Interestingly, in A172 cells, another model of glioblastoma, the elevation of cAMP activated PKA and EPAC1/Rap1 signalling that together induces growth arrest and apoptosis (H. Zhang *et al.*, 2020). Despite PKA and EPAC being cAMP effectors, each of these proteins can transduce its own signal. The activation of both proteins can be synergistic and antagonistic action in modulating cell growth.

C. Crosstalk with MAPK signalling

Amongst all regulatory pathways, the MAPK signalling cascade is widely known as a critical key player controlling cell growth, cell migration, proliferation, differentiation and apoptosis. The MAPK pathway is commonly known to be activated through stimulation of RTKs. Interestingly, evidence has emerged that suggests this cascade can be modulated through EPAC and PKA (Cheng *et al.*, 2008; Borland, Smith and Yarwood, 2009). Within the MAPK cascade, p38 and JNK are known to be activated in relation to stress responses, whereas ERK1/2 is primarily involved in cell growth following Ras-Raf activation (Yue and López, 2020). Interestingly, activation of these proteins can promote both cell growth and cell death.

As part of the collaborative studies presented in this thesis, stimulation at the GPCR levels differentially modulates the ERK1/2 activation. Activation of CLR-RAMP complexes by CGRP-based peptides displayed activation of ERK1/2 and the pattern was aligned with the pro-proliferative effects following prolonged agonist exposure (Clark *et al.*, 2021). In comparison, both CGS21680 and the triazoloquinazoline-based compounds were found to stimulate ERK1/2 phosphorylation upon short-term stimulation (Winfield, 2017), but both treatments displayed different final responses in cell growth. Stimulation at Gai-coupled A₁R by a series of newly synthesised agonists was also found to activate ERK1/2, even though its activation reduced cAMP concentration (Winfield, 2017). Given that ERK1/2 may trigger both anti- and pro-proliferation, it requires further characterisation to understand better how this cascade works.

Many reviews marked the dual action of ERK1/2 phosphorylation, but the exact mechanism remains unsolved. It is suggested that the balance between intensity and duration between pro-and anti-apoptotic signals transmitted by ERK1/2 will determine the net effect of cell proliferation and growth inhibition (Zha *et al.*, 1996). A recent review by Yue highlighted that ERK1/2 and proteins involved in MAPK cascade display bimodal actions with ultrasensitive responses (Yue and López, 2020). These properties mean that any changes in the upstream levels may produce extensive responses in the MAPK pathway and ERK1/2 signalling works like a “switch”. The changes need to exceed a certain threshold to activate apoptotic responses. This notion has been demonstrated in *Xenopus* oocytes, where the low and transient changes activated pro-proliferative actions, whereas intense and sustained signal-induced apoptotic responses (Yue and López, 2020). It is also known that MAPK signalling requires a feedback loop to work, therefore once activated, the signal will be transmitted continuously until all cells showed synchronised responses.

Furthermore, it has been suggested that not only the activation of ERK1/2 but also the translocation of ERK1/2 to the nucleus stipulates the pathway to be activated (Mebratu and Tesfaigzi, 2009). It has also been suggested that sustainability and the strength of the signal influences ERK1/2 phosphorylation to influence cell proliferation. There is currently limited understanding of how strong and how long the signal is transmitted by stimulating cells with forskolin and different GPCR ligands to finally influence cell growth. This particular aspect would be of interest to be investigated further. The real-time ERK kinase translocation reporters (KTRs) biosensor can be used as an alternative method to visualise ERK1/2 signalling by treating cells with different ligands (Yang *et al.*, 2018).

7.1.1.3 Physicochemical properties of tested compounds

From what we have found from this study, it suggests that cAMP prevents cell growth across various cell lines tested except the resistant types of U87 cells. Aside from the different machinery that influences cellular responses, the stability of each compound used needs to be taken into account. For instance, isoprenaline was an agonist that eliciting a very potent activity in cAMP production compared to forskolin in glioma cells (Chapter 3). Due to the instability of isoprenaline in the aqueous solution, it is most likely that isoprenaline may be degraded during the proliferation assay. Thereby the ability of isoprenaline to suppress cell growth was less potent compared to forskolin. It may also occur that β 2-ARs undergoes desensitisation followed by receptor recycling

after prolonged exposure. Thus, we can still observe, to some extent, the anti-proliferation on glioma cells upon isoprenaline treatment, even though it was less potent than forskolin. However, some compounds may be degraded either because of their physicochemical properties or by cellular metabolic activity, leading to weaker actions or even elicited no effect on cell growth. Whilst some of the compound may still be active, little is known if the compounds tested here may generate inactive substances. Since there is limited information on the stability properties of each compound used within this study, it will be necessary to perform pharmacokinetics studies.

7.1.1.4 Resistance cells were not responsive towards forskolin and PDE inhibitor

Between the two cell lines of glioblastoma, U87 cells were found to be very resistant towards forskolin and PDE inhibitors. The possible explanation may come from the abundance of PDEs expressed within this cell line, as depicted in Chapter 4. Despite the fact that U87 cells are more sensitive for producing cAMP in short-term stimulation, this may trigger the activation of other PDEs to keep suppressing cAMP to the baseline level. Therefore, the anti-proliferative effect is negligible for prolonged exposure. Not only did U87 cells show resistance towards forskolin and PDE inhibitors, but also cisplatin – a reference cytotoxic drug.

A few essential proteins have been reported to contribute to the resistant nature of U87 cells. One of them is Raf kinase – a family of three serine/threonine-specific protein kinases in MAPK signalling. Raf has been reported to modulate the balance between pro-apoptotic and anti-apoptotic proteins (Häfner *et al.*, 1994; Vossler *et al.*, 1997). Interestingly, the subtype Raf dominance is positively affected by PDE expression (Daniel, Filiz and Mantamadiotis, 2016). It has been reported that cells expressing the C-Raf isoform inhibit MAPK signalling through the cAMP/PKA pathway. The activation of PKA increases an anti-apoptotic protein BIM. Whereas in a more resistant type of cell, B-RAF is more dominant, so conferring the opposite effect in MAPK signalling and BIM expression (Daniel, Filiz and Mantamadiotis, 2016).

It has been reported that U87 cells express MRP4, an efflux transporter that we and others have shown to be responsible for exporting cAMP into extracellular regions. Several proteins were also upregulated in U87 cells, such as ectonucleotide pyrophosphatase/ phosphodiesterase 1 (ENPP1) and CD73, encoded by the NT5E gene (Bageritz and Goidts, 2014; Wang and Matosevic, 2019). Both proteins are membrane-bound enzymes that mediate the conversion of extracellular cAMP into

AMP, ADP, ATP, and adenosine, which cells can subsequently use to modulate cell growth. Since multiple mechanisms possibly contribute to the resistance nature of U87 cells, to disseminate the role of these proteins, application of selective inhibitors can be performed, such as dabrafenib, vemurafenib, or encorafenib (B-RAF inhibitor); ENPP1C (ENPP1C inhibitor), CP5244, AB680, and PB-12379 (CD73 inhibitor).

Besides the upregulation of the proteins mentioned earlier, glioblastoma cells have also been shown to have metabolic reprogramming for rapid proliferation by utilising aerobic glycolysis – namely the Warburg effect, rather than oxidative phosphorylation that is generally found in normal cells. Interestingly, a study by Xing showed that treating resistant glioblastoma cells by forskolin or PDE inhibitor reversing glioblastoma phenotypes to astrocytes through the cAMP/PGC1 α pathway (Xing *et al.*, 2017). Therefore, it has been suggested that reinstating normal oxidative phosphorylation may be beneficial to inhibit cancer cell growth and impair the metastatic ability (Schulz *et al.*, 2006). For future studies, it is worth treating U87 cells with cisplatin after exposing cells to forskolin or PDE inhibitor to U87 cells to confirm the benefit of reversing the Warburg effect.

7.1.1.5 Drug combination vs multi-target ligands

Another aspect that can be highlighted is the advantage of drug combination to optimise therapeutic outcomes. Classically, drugs have been designed to target a single biological entity with high selectivity to evade unwanted off-target effects. However, drug design has faced remarkable challenges with the undesirable actions as the major drawback. This includes the possible toxicities of a single agent by non-selective actions. The drug combination strategy has been applied to numerous diseases, including AIDS, atherosclerosis, cancer, antibiotic regimens and neurodegenerative disorders, all of which involve complex pathogenesis (Mokhtari *et al.*, 2017; Ramsay *et al.*, 2018; Tyers and Wright, 2019). The combination of A_{2A}R agonists with particular PDE inhibitors has shown to be able to prevent uncontrollable cell growth in B-cell malignancies (Rickles *et al.*, 2010). Based upon prospective approaches through PDE inhibition, the work presented in this thesis further explored two approaches to optimise enhancement in cAMP signalling: multiple targeting by drug combinations and developing multi-target ligands.

Combination treatment is one of the most common strategies to improve drug efficacies. These have been demonstrated in detail in Chapters 3 and 4. Concomitant targeting of direct activation at AC and multiple PDE inhibition showed significant

advantages over the individual compounds. The improvement on efficacy by drug combinations may tackle the issues raised due to the compound toxicity, such as that of trequinsin. Taken together, targeting multiple proteins may be attained by using lower doses without compromising efficacy and with a better safety profile.

The development of multi-target ligands was applied in Chapter 5. An approach, named the "multi-target lead discovery" can be considered a promising tool for identifying novel combinatorial effects of drugs (Overington, Al-Lazikani and Hopkins, 2006). As previously mentioned, targeting receptors alone might be insufficient to be translated into cell growth. Similar to the stimulation on $A_{2A}R$ by CGS21680, an individual treatment by a PDE10 inhibitor caused a marginal effect on cell growth suppression. This study showed that the efficacy in inhibiting cell growth was enhanced by a multi-target ligand (Chapter 5). Despite showing notable anti-proliferative actions, triazoloquinazoline-based compounds exhibited low binding affinity at the $A_{2A}R$, displaying pK_i values in the micromolar range. This is not surprising because the vast majority of issues (>80%) in developing multi-target ligands arise from this particular aspect. Regardless of low affinities, these findings can be used as a starting point to improve binding affinities and develop better chemical entities for the future studies.

Based on the therapeutic benefits of drug combination within this study, a couple of strategies may be prospective to inhibit cancer cell growth. Since cAMP has been shown to have a negative effect on cell proliferation, particularly in cancer models that were utilised in this study, it may be necessary to consider the following combination to enhance the intracellular concentration of cAMP. Aside from pairing with AC activator or $A_{2A}R$ agonist, the PDE inhibitor can be combined with other agents that increase cAMP action. These may include a combination with a $G\alpha_i$ -coupled GPCR antagonist, an MRP4 inhibitor, a PKA activator, and a GC activator. The latter is proposed given our findings in Chapter 3. The disturbance in cAMP and cGMP balance may sequester signalling to go through PKA, therefore, enhancing the antiproliferative effect mediated by cAMP/PKA.

To conclude, either utilising drug combinations or developing multi-target ligands may be a practical strategy to design better drugs. However, the integrated rational characterisation at the chemical and biological aspects needs to be carried out carefully to develop effective small molecule candidates.

7.1.1.6 Potential use of cAMP elevating agent and further consideration for targeting cAMP pathway

We have proven that elevating cAMP levels by targeting AC and/or multiple PDEs elicited beneficial effects to prevent tumour progression. Although it is considered to be prospective, many tissues express AC and PDEs to maintain cellular functions. Therefore, the systemic use of forskolin or PDE inhibitor may become a limiting factor. Given this constraint, some strategies should be developed to ensure localised forskolin and PDE inhibitors without exerting an adverse effect on healthy cells. Otherwise, another aspect that needs to be validated is the ability of compounds to cross the blood-brain barrier (BBB). Despite not being covered within this study, numerous models of the human BBB have been established and can be used for future studies, such as human immortalised endothelial hCMEC/D3 cell line, cord blood-derived endothelial progenitor cells, or recent model utilising human pluripotent stem cells (hPSCs).

It is also worth noted that cAMP may promote cell growth depending on cell type. The application of cAMP elevating agent such as forskolin and PDE inhibitor, therefore, needs to be used deliberately to maximise the anti-proliferative effects by targeting cAMP pathways.

7.1.2 Modulatory action of RAMPs in dictating PAR4 and CLR pharmacology

The role of RAMPs in modulating GPCRs has been well appreciated, although, in the very beginning, it is first thought to be as a chaperone for CLR (McLatchie *et al.*, 1998). Recent findings have shown that more receptors form an association with RAMPs, leading to distinctive signalling profiles. Serafin and colleagues culminated in an advancement discovery of 44 receptors as interacting partners of RAMPs, compared to 11 previously reported receptors (Serafin *et al.*, 2020).

Aside from the receptors mentioned in the recent review by Serafin (Serafin *et al.*, 2020), the study in this thesis has suggested that both PAR4 variants (PAR4-A120 and PAR4-T120) can interact with RAMPs, leading to differential recruitment of β -arrestins. Compared to other PAR families, different proteases induced signalling bias of PAR1 and PAR2, yet little is known about PAR4. Pharmacological substances such as peptides/peptidomimetics, blocking antibodies, small molecules, pepducins, parmodulins, or designer receptors exclusively activated by designer drugs (DREADDs) have been developed to modulate PAR family activities (Heuberger and Schuepbach, 2019), but it has not been validated in PAR4. Although it is considered

preliminary, the finding within this study opens up avenues of investigation on how the interactions with RAMPs change PAR4 pharmacology and its physiological consequences. Since PAR4 plays an essential role in blood clot formation and inflammatory processes (Faruqi *et al.*, 2000; Heuberger and Schuepbach, 2019), signalling biased can be postulated to optimise therapeutic outcomes and reducing adverse reaction such as severe bleeding that was imposed by PAR1 antagonist or predominantly driven by Ca²⁺-mediated signalling upon PAR4 stimulation.

Further exploration on RAMP-CLR in native systems: glioblastoma model and primary human cardiovascular cells, corroborates that signalling bias driven by RAMPs may occur in physiological settings to provoke differential effects. Although there was a significant pattern observed between both systems, there was a clear connection between endogenous peptides used for the studies. Together with the study by Clark *et al.*, it is apparent that each ligand promotes distinct signalling signatures and was aligned with what was observed in heterologous systems (Weston *et al.*, 2016; Woolley *et al.*, 2017; Clark *et al.*, 2021)

CGRP is known to be a potent vasodilator and is currently being used as a target for migraine therapy and has been suggested to be involved in cancer-related pain (Y. Zhang *et al.*, 2020). AM and AM2 also display vasorelaxation effects and the expression of both peptides are upregulated by the hypoxia-inducible factor (HIF). AM, in particular, has been suggested to promote expression of anti-apoptotic factors and contributes to the tumour resistance to hypoxia, thereby promoting cell growth (Oehler *et al.*, 2001). In spite of the indication that CLR and RAMPs are expressed in GBM cell lines, the role of CLR-RAMP complexes in cancer is not fully characterised. A number of studies highlighted that CGRP can both directly and indirectly influence cancer development by upregulating CLR and RAMP expression (Hoppener *et al.*, 1987; Ostrovskaya *et al.*, 2019; Y. Zhang *et al.*, 2020). Kiriyama reported that activation of CGRP promoted secretion of IL-6 that has main function to induce nerve growth factor production in astrocytes as the response to cytokines and neuropeptides in glial cells (Kiriyama *et al.*, 1997). Arguably, the expression of CLR and another family receptor, CTR, and their activation might not be correlated with the outcomes in patient-derived GBM cells (Ostrovskaya *et al.*, 2019).

Since the cells used for this study were native with endogenous expression of receptor of interests, there is also a possibility that another receptor - CTR, may interfere with the CGRP-mediated responses in glioblastoma. From the preliminary study, we found that U87 cells expressed CTR at mRNA levels (data not shown). While

CGRP shows a higher affinity to CLR-RAMP1 complexes, it also binds to CTR-RAMP1 heterodimers showing a similar affinity to amylin (AMY). The binding of CGRP on different subsets of receptors has been reported to undergo a distinct receptor internalisation pattern (Gingell *et al.*, 2020). However, there is not yet any evidence if the differences may have physiological consequences. Aside from what was reported by Clark and colleagues using cardiovascular cells, there is little other evidence to emphasise RAMPs modulatory effect on CLR in native physiological cells (Clark *et al.*, 2021). Given that the preliminary indications from this study, further characterisation is required to address the involvement of CLR-RAMP association in pathological circumstances.

7.2 Future Directions

Targeting multiple PDEs to promote anti-proliferative effects was explored in-depth within this study. Some PDE inhibitors have been shown to have potential in preventing cancer cell growth. To better understand these PDEs' mechanism in sculpting cAMP gradient in cellular microdomain, the investigation could be conducted using cAMP reporters, either PKA-based or EPAC-based sensor or modifying PDE of interest with fluorescence protein to aid cellular visualisation. Furthermore, co-immunoprecipitation studies may provide further insight into whether PDEs are tethered with other proteins and how this interaction regulates the spatiotemporal of cAMP within the cells. It is also worth noting that quantification on ERK1/2 phosphorylation throughout the proliferation period is required to connect a gap between upstream cAMP production and cell growth. As a translational tangent, the prospective compounds can be further characterised in vivo, such as applying it using the xenograft brain tumour model. For a series of considered prospective compounds for future studies, an appropriate BBB model and pharmacokinetic studies can be performed.

PAR4 was discovered as a novel interacting partner of RAMPs from this study. However, this work only explored the upstream canonical Ca^{2+} mobilisation, but it remains unknown if the effect was mediated by $G\alpha_q$ or from $G\beta\gamma$ dimers. The use of specific inhibitors could help to disseminate the involvement of G protein-mediated responses. Since this study is only preliminary, numerous aspects can be explored, including the pleiotropic coupling of PAR4 to other G proteins, receptor downstream signalling, and the mechanism of RAMP-PAR4 association. The presence of FRET-based sensor, bioluminescence resonance energy transfer- (BRET) or enhanced bystander BRET- (ebBRET) based protocol, and functional complementation assay,

allow exploration to reveal PAR4 pharmacology in interacting with other regulatory proteins or G proteins (Zhao *et al.*, 2014). Further elucidation on β -arrestin signalling and its consequences in receptor internalisation would also be of interest for future studies.

The modulation of RAMPs on CLR pharmacology has been widely studied in heterologous expression systems. Based upon current data, it can be further explored if targeting these complexes may suppress cancer cell growth. The availability of antagonists or an antibody targeting CLR-RAMP heteromers may give aid to explore this hypothesis. Besides, pro-proliferative actions by CGRP and related peptides on cardiovascular cells can be seen as targets to regenerate endothelial functions. Therefore, it would be an attractive approach for treating ischemic heart disease or other pathological settings that require vascularisations such as tissue engineering.

BIBLIOGRAPHY

- Adam, F. *et al.* (2003) 'Thrombin-induced platelet PAR4 activation: Role of glycoprotein ibandadp', *Journal of Thrombosis and Haemostasis*. J Thromb Haemost, 1(4), pp. 798–804. doi: 10.1046/j.1538-7836.2003.00138.x.
- Ahlstrom, M. *et al.* (2005) 'Dexamethasone down-regulates cAMP-phosphodiesterase in human osteosarcoma cells', *Biochem Pharmacol.* 2005/01/04, 69(2), pp. 267–275. doi: 10.1016/j.bcp.2004.09.012.
- Ahuja, M. *et al.* (2014) 'cAMP and Ca²⁺ signaling in secretory epithelia: Crosstalk and synergism', *Cell Calcium*. doi: 10.1016/j.ceca.2014.01.006.
- De Alexandre, R. B. *et al.* (2015) 'Phosphodiesterase sequence variants may predispose to prostate cancer', *Endocrine-Related Cancer*. BioScientifica Ltd., 22(4), pp. 519–530. doi: 10.1530/ERC-15-0134.
- Allard, B. *et al.* (2016) 'Immunosuppressive activities of adenosine in cancer', *Current Opinion in Pharmacology*. Elsevier Ltd, pp. 7–16. doi: 10.1016/j.coph.2016.04.001.
- Almahariq, M. *et al.* (2013) 'A novel EPAC-specific inhibitor suppresses pancreatic cancer cell migration and invasion', *Molecular Pharmacology*. American Society for Pharmacology and Experimental Therapeutics, 83(1), pp. 122–128. doi: 10.1124/mol.112.080689.
- Ambudkar, I. S. (2016) 'Calcium signalling in salivary gland physiology and dysfunction', *Journal of Physiology*. Blackwell Publishing Ltd, pp. 2813–2824. doi: 10.1113/JP271143.
- Andric, S. A., Kostic, T. S. and Stojilkovic, S. S. (2006) 'Contribution of multidrug resistance protein MRP5 in control of cyclic guanosine 5'-monophosphate intracellular signaling in anterior pituitary cells', *Endocrinology*. 2006/04/15, 147(7), pp. 3435–3445. doi: 10.1210/en.2006-0091.
- Antonoli, L. *et al.* (2021) 'Adenosine signaling in the tumor microenvironment', in *Advances in Experimental Medicine and Biology*. Springer, pp. 145–167. doi: 10.1007/978-3-030-47189-7_9.
- Arey, B. J. (2014) 'An Historical Introduction to Biased Signaling', in *Biased Signaling in Physiology, Pharmacology and Therapeutics*. Elsevier Inc., pp. 1–39. doi: 10.1016/B978-0-12-411460-9.00001-X.
- Attwood, T. K. and Findlay, J. B. C. (1994) 'Fingerprinting G-protein-coupled

- receptors', *Protein Engineering, Design and Selection*. Oxford Academic, 7(2), pp. 195–203. doi: 10.1093/protein/7.2.195.
- Atwood, B. K. *et al.* (2011) 'Expression of G protein-coupled receptors and related proteins in HEK293, AtT20, BV2, and N18 cell lines as revealed by microarray analysis', *BMC Genomics*. BioMed Central Ltd, 12(1), p. 14. doi: 10.1186/1471-2164-12-14.
- Auer, R. N., Maestro, R. F. D. and Anderson, R. (1981) 'A Simple and Reproducible Experimental in Vivo Glioma Model', *Canadian Journal of Neurological Sciences / Journal Canadien des Sciences Neurologiques*. doi: 10.1017/S0317167100043468.
- Aydin, Y. and Coin, I. (2021) 'Biochemical Insights into Structure and Function of Arrestins', *The FEBS Journal*, p. febs.15811. doi: 10.1111/febs.15811.
- Ayoub, M. A. *et al.* (2007) 'Real-time analysis of agonist-induced activation of protease-activated receptor 1/Gai1 protein complex measured by bioluminescence resonance energy transfer in living cells', *Molecular Pharmacology*, 71(5), pp. 1329–1340. doi: 10.1124/mol.106.030304.
- Ayoub, M. A., Al-Senaidy, A. and Pin, J. P. (2012) 'Receptor-G protein interaction studied by bioluminescence resonance energy transfer: Lessons from protease-activated receptor 1', *Frontiers in Endocrinology*. Front Endocrinol (Lausanne), 3(JUN). doi: 10.3389/fendo.2012.00082.
- Baehr, W., Devlin, M. J. and Applebury, M. L. (1979) *Isolation and Characterization of cGMP Phosphodiesterase from Bovine Rod Outer Segments**, *Journal of Biological Chemistry*. doi: 10.1016/S0021-9258(19)86536-5.
- Bageritz, J. and Goidts, V. (2014) 'Functional characterization of ENPP1 reveals a link between cell cycle progression and stem-like phenotype in glioblastoma', *Molecular and Cellular Oncology*. Taylor and Francis Ltd., 1(3). doi: 10.4161/23723548.2014.964028.
- Bailey, S. *et al.* (2019) 'Interactions between RAMP2 and CRF receptors: The effect of receptor subtypes, splice variants and cell context', *Biochimica et Biophysica Acta - Biomembranes*. Elsevier B.V., 1861(5), pp. 997–1003. doi: 10.1016/j.bbamem.2019.02.008.
- Bar-Shavit, R. *et al.* (2016) 'Protease-activated receptors (PARs) in cancer: Novel biased signaling and targets for therapy', *Methods in Cell Biology*. Academic Press Inc., 132, pp. 341–358. doi: 10.1016/bs.mcb.2015.11.006.
- Baraldi, P. G. *et al.* (1998) 'Design, synthesis, and biological evaluation of a second

- generation of pyrazolo[4,3-e]-1,2,4-triazolo[1,5-c]pyrimidines as potent and selective A(2A) adenosine receptor antagonists', *Journal of Medicinal Chemistry*. *J Med Chem*, 41(12), pp. 2126–2133. doi: 10.1021/jm9708689.
- Barbash, S. *et al.* (2017) 'GPCRs globally coevolved with receptor activity-modifying proteins, RAMPs', *Proceedings of the National Academy of Sciences of the United States of America*. National Academy of Sciences, 114(45), pp. 12015–12020. doi: 10.1073/pnas.1713074114.
- Barber, R. D. *et al.* (2005) 'GAPDH as a housekeeping gene: Analysis of GAPDH mRNA expression in a panel of 72 human tissues', *Physiological Genomics*. doi: 10.1152/physiolgenomics.00025.2005.
- Barkan, K. *et al.* (2019) 'Pharmacological Characterisation of Novel Adenosine Receptor A_{2A} Antagonists', *bioRxiv*, p. 693796. doi: 10.1101/693796.
- Beavis, P. A. *et al.* (2013) 'Blockade of A_{2A} receptors potently suppresses the metastasis of CD73+ tumors', *Proceedings of the National Academy of Sciences of the United States of America*. doi: 10.1073/pnas.1308209110.
- Beavo, J. A. (1995) 'Cyclic nucleotide phosphodiesterases: functional implications of multiple isoforms', *Physiol Rev*, 75(4), pp. 725–748. Available at: <https://www.ncbi.nlm.nih.gov/pubmed/7480160>.
- Beebe, S. J. *et al.* (1990) 'Molecular cloning of a tissue-specific protein kinase (Cy) from human testis—representing a third isoform for the catalytic subunit of cAMP-dependent protein kinase', *Molecular Endocrinology*. *Mol Endocrinol*, 4(3), pp. 465–475. doi: 10.1210/mend-4-3-465.
- Benda, P. *et al.* (1968) 'Differentiated rat glial cell strain in tissue culture', *Science*. doi: 10.1126/science.161.3839.370.
- Bender, A. T. and Beavo, J. A. (2006) 'Cyclic nucleotide phosphodiesterases: Molecular regulation to clinical use', *Pharmacological Reviews*, pp. 488–520. doi: 10.1124/pr.58.3.5.
- Berridge, M. J. (2012) 'Calcium signalling remodelling and disease', *Biochemical Society Transactions*. *Biochem Soc Trans*, pp. 297–309. doi: 10.1042/BST20110766.
- Berridge, M. J. (2016) 'The inositol trisphosphate/calcium signaling pathway in health and disease', *Physiological Reviews*. American Physiological Society, 96(4), pp. 1261–1296. doi: 10.1152/physrev.00006.2016.
- Berridge, M. J., Lipp, P. and Bootman, M. D. (2000) 'The versatility and universality of

Bibliography

- calcium signalling', *Nature Reviews Molecular Cell Biology*. doi: 10.1038/35036035.
- Bhakta, M. *et al.* (2021) 'Migraine therapeutics differentially modulate the CGRP pathway', *Cephalalgia*. SAGE Publications Ltd. doi: 10.1177/0333102420983282.
- Biel, M. (2013) 'Cyclic Nucleotide-Regulated Cation Channels', in *Encyclopedia of Biological Chemistry: Second Edition*. Elsevier Inc., pp. 586–588. doi: 10.1016/B978-0-12-378630-2.00455-2.
- Birnbaumer, L. *et al.* (1990) 'Molecular basis of regulation of ionic channels by G proteins', *Recent Progress in Hormone Research*. Recent Prog Horm Res, 45(1), pp. 121–206. doi: 10.1016/b978-0-12-571145-6.50008-x.
- Blättermann, S. *et al.* (2012) 'A biased ligand for OXE-R uncouples G α and G $\beta\gamma$ signaling within a heterotrimer', *Nature Chemical Biology*. Nature Publishing Group, 8(7), pp. 631–638. doi: 10.1038/nchembio.962.
- Bloise, E. *et al.* (2016) 'ATP-binding cassette transporters in reproduction: a new frontier'. doi: 10.1093/humupd/dmv049.
- Bohn, L. M. *et al.* (1999) 'Enhanced morphine analgesia in mice lacking β -arrestin 2', *Science*. Science, 286(5449), pp. 2495–2498. doi: 10.1126/science.286.5449.2495.
- Bohn, L. M., Lefkowitz, R. J. and Caron, M. G. (2002) 'Differential mechanisms of morphine antinociceptive tolerance revealed in β arrestin-2 knock-out mice', *Journal of Neuroscience*. Society for Neuroscience, 22(23), pp. 10494–10500. doi: 10.1523/jneurosci.22-23-10494.2002.
- Bolger, G. B., Conti, M. and Houslay, M. D. (2019) 'Cellular Functions of PDE4 Enzymes', in *Cyclic Nucleotide Phosphodiesterases in Health and Disease*. CRC Press, pp. 99–129. doi: 10.1201/9781420020847-6.
- Bomberger, J. M., Parameswaran, N., *et al.* (2005) 'Novel function for Receptor Activity-modifying Proteins (RAMPs) in post-endocytic receptor trafficking', *Journal of Biological Chemistry*. Elsevier, 280(10), pp. 9297–9307. doi: 10.1074/jbc.M413786200.
- Bomberger, J. M., Spielman, W. S., *et al.* (2005) 'Receptor activity-modifying protein (RAMP) isoform-specific regulation of adrenomedullin receptor trafficking by NHERF-1', *Journal of Biological Chemistry*. Elsevier, 280(25), pp. 23926–23935. doi: 10.1074/jbc.M501751200.
- Booe, J. M. *et al.* (2018) 'Probing the mechanism of receptor activity-modifying protein

- modulation of GPCR ligand selectivity through rational design of potent adrenomedullin and calcitonin gene-related peptide antagonists', *Molecular Pharmacology*. American Society for Pharmacology and Experimental Therapy, 93(4), pp. 355–367. doi: 10.1124/mol.117.110916.
- Borea, P. A. *et al.* (2018) 'Pharmacology of adenosine receptors: The state of the art', *Physiological Reviews*. American Physiological Society, pp. 1591–1625. doi: 10.1152/physrev.00049.2017.
- Borland, G., Smith, B. O. and Yarwood, S. J. (2009) 'EPAC proteins transduce diverse cellular actions of cAMP', *British Journal of Pharmacology*. Wiley-Blackwell, pp. 70–86. doi: 10.1111/j.1476-5381.2008.00087.x.
- Borst, P. and Oude Elferink, R. (2002) 'Mammalian ABC transporters in health and disease', *Annual Review of Biochemistry*. Annu Rev Biochem, pp. 537–592. doi: 10.1146/annurev.biochem.71.102301.093055.
- Bos, J. L. (2003) 'Epac: a new cAMP target and new avenues in cAMP research', *Nature Reviews Molecular Cell Biology*, 4(9), pp. 733–738. doi: 10.1038/nrm1197.
- Boullaran, C. and Gales, C. (2015) 'Cardiac cAMP: Production, hydrolysis, modulation and detection', *Frontiers in Pharmacology*. Frontiers Media S.A., p. 203. doi: 10.3389/fphar.2015.00203.
- Boullaran, C. and Kehrl, J. H. (2014) 'Implications of non-canonical G-protein signaling for the immune system', *Cellular Signalling*. Elsevier Inc., pp. 1269–1282. doi: 10.1016/j.cellsig.2014.02.010.
- Bouschet, T., Martin, S. and Henley, J. M. (2005) 'Receptor-activity-modifying proteins are required for forward trafficking of the calcium-sensing receptor to the plasma membrane', *Journal of Cell Science*, 118, pp. 4709–4720. doi: 10.1242/jcs.02598.
- Bradley, J. *et al.* (2001) 'Nomenclature for ion channel subunits [4]', *Science*. Science, pp. 2095–2096. doi: 10.1126/science.294.5549.2095.
- Brand, T. (2018) 'The Popeye Domain Containing Genes and Their Function as cAMP Effector Proteins in Striated Muscle', *Journal of Cardiovascular Development and Disease*. MDPI AG, 5(1), p. 18. doi: 10.3390/jcdd5010018.
- Brand, T. and Schindler, R. (2017) 'New kids on the block: The Popeye domain containing (POPDC) protein family acting as a novel class of cAMP effector proteins in striated muscle', *Cellular Signalling*. Elsevier Inc., pp. 156–165. doi: 10.1016/j.cellsig.2017.09.015.

- Brandt, D. R. and Ross, E. M. (1985) 'GTPase activity of the stimulatory GTP-binding regulatory of adenylate cyclase, G(s). Accumulation and turnover of enzyme-nucleotide intermediates', *Journal of Biological Chemistry*. Elsevier, 260(1), pp. 266–272. doi: 10.1016/s0021-9258(18)89726-5.
- Briddon, S. J. *et al.* (2004) 'Quantitative analysis of the formation and diffusion of A 1-adenosine receptor-antagonist complexes in single living cells', *Proceedings of the National Academy of Sciences of the United States of America*. National Academy of Sciences, 101(13), pp. 4673–4678. doi: 10.1073/pnas.0400420101.
- Brooks, M. D. *et al.* (2014) 'PDE7B Is a Novel, Prognostically Significant Mediator of Glioblastoma Growth Whose Expression Is Regulated by Endothelial Cells', *PLoS One*. Public Library of Science, 9(9), p. e107397. doi: 10.1371/journal.pone.0107397.
- Bubis, J., Saraswat, L. D. and Taylor, S. S. (1988) 'Tyrosine-371 contributes to the positive cooperativity between the two cAMP binding sites in the regulatory subunit of cAMP-dependent protein kinase I', *Biochemistry*. American Chemical Society, 27(5), pp. 1570–1576. doi: 10.1021/bi00405a026.
- Burns, D. L. (1988) 'Subunit structure and enzymic activity of pertussis toxin', *Microbiological Sciences*, pp. 285–287. Available at: <https://europepmc.org/article/med/2908558> (Accessed: 27 March 2021).
- Burns, K. L. *et al.* (1998) 'Molecular genetic correlates of p16, cdk4, and pRb immunohistochemistry in glioblastomas', *J Neuropathol Exp Neurol*. 1998/05/26, 57(2), pp. 122–130. Available at: <https://www.ncbi.nlm.nih.gov/pubmed/9600204>.
- Bylund, D. B. and Toews, M. L. (1993) 'Radioligand binding methods practical guide and tips', *American Journal of Physiology - Lung Cellular and Molecular Physiology*. doi: 10.1152/ajplung.1993.265.5.l421.
- Calatuzzolo, C. *et al.* (2005) 'Expression of drug resistance proteins Pgp, MRP1, MRP3, MRP5 AND GST- π in human glioma', *Journal of Neuro-Oncology*. doi: 10.1007/s11060-004-6152-7.
- Calebiro, D. *et al.* (2009) 'Persistent cAMP-signals triggered by internalized G-protein-coupled receptors', *PLoS Biology*. Public Library of Science, 7(8). doi: 10.1371/journal.pbio.1000172.
- Calker, D. van, Müller, M. and Hamprecht, B. (1979) 'ADENOSINE REGULATES VIA TWO DIFFERENT TYPES OF RECEPTORS, THE ACCUMULATION OF

- CYCLIC AMP IN CULTURED BRAIN CELLS', *Journal of Neurochemistry*, 33(5), pp. 999–1005. doi: 10.1111/j.1471-4159.1979.tb05236.x.
- Campbell, A. P. and Smrcka, A. V. (2018) 'Targeting G protein-coupled receptor signalling by blocking G proteins', *Nature Reviews Drug Discovery*. Nature Publishing Group, pp. 789–803. doi: 10.1038/nrd.2018.135.
- Cao, T. T. *et al.* (1999) 'A kinase-regulated PDZ-domain interaction controls endocytic sorting of the β 2-adrenergic receptor', *Nature*. Nature Publishing Group, 401(6750), pp. 286–290. doi: 10.1038/45816.
- Card, G. L. *et al.* (2004) 'Structural basis for the activity of drugs that inhibit phosphodiesterases', *Structure*, 12(12), pp. 2233–2247. doi: 10.1016/j.str.2004.10.004.
- Carozzo, A. *et al.* (2019) 'Identification of MRP4/ABCC4 as a target for reducing the proliferation of pancreatic ductal adenocarcinoma cells by modulating the cAMP efflux', *Molecular Pharmacology*. American Society for Pharmacology and Experimental Therapy, 96(1), pp. 13–25. doi: 10.1124/mol.118.115444.
- Carpenter, B. and Lebon, G. (2017) 'Human Adenosine A2A Receptor: Molecular Mechanism of Ligand Binding and Activation', *Front Pharmacol.* 2018/01/10. Warwick Integrative Synthetic Biology Centre, School of Life Sciences, University of Warwick, Coventry, United Kingdom. Institut de Genomique Fonctionnelle, Neuroscience Department, UMR CNRS 5203, INSERM U1191, Universite de Montpellier, Montpellier, Fran, 8, p. 898. doi: 10.3389/fphar.2017.00898.
- Carvalho, S. *et al.* (2020) 'The Adenosine A2A Receptor DoesNot Appear To Undergo Agonist-InducedInternalisation', in *Selected Abstracts From Pharmacology 2020*. British Pharmacological Society, pp. 438–439.
- Cegla, J. *et al.* (2017) 'RAMP2 influences glucagon receptor pharmacology via trafficking and signaling', *Endocrinology*. Endocrine Society, 158(8), pp. 2680–2693. doi: 10.1210/en.2016-1755.
- Cesarini, V. *et al.* (2017) 'Type 5 phosphodiesterase regulates glioblastoma multiforme aggressiveness and clinical outcome', *Oncotarget*. 2017/01/19, 8(8), pp. 13223–13239. doi: 10.18632/oncotarget.14656.
- Cheadle, C. *et al.* (2008) 'Regulatory subunits of PKA define an axis of cellular proliferation/differentiation in ovarian cancer cells', *BMC Medical Genomics*. Springer Science and Business Media LLC, 1(1), pp. 1–14. doi: 10.1186/1755-8794-1-43.

- Chen, H. *et al.* (2013) 'Identification and characterization of small molecules as potent and specific EPAC2 antagonists', *Journal of Medicinal Chemistry*. *J Med Chem*, 56(3), pp. 952–962. doi: 10.1021/jm3014162.
- Chen, R. W. *et al.* (2007) 'Broad spectrum neuroprotection profile of phosphodiesterase inhibitors as related to modulation of cell-cycle elements and caspase-3 activation', *Neuroscience Letters*, 418(2), pp. 165–169. doi: 10.1016/j.neulet.2007.03.033.
- Chen, Yao *et al.* (2014) 'A PKA activity sensor for quantitative analysis of endogenous GPCR signaling via 2-photon FRET-FLIM imaging', *Frontiers in Pharmacology*. Frontiers Media S.A., 5, p. 56. doi: 10.3389/fphar.2014.00056.
- Chen, Ying *et al.* (2014) 'Caffeine inhibits migration in glioma cells through the ROCK-FAK pathway', *Cellular Physiology and Biochemistry*. doi: 10.1159/000362966.
- Cheng, J. and Grande, J. P. (2007) 'Cyclic nucleotide phosphodiesterase (PDE) inhibitors: Novel therapeutic agents for progressive renal disease', *Experimental Biology and Medicine*. doi: 10.3181/00379727-207-2320038.
- Cheng, X. *et al.* (2008) 'Epac and PKA: A tale of two intracellular cAMP receptors', *Acta Biochimica et Biophysica Sinica*. *Acta Biochim Biophys Sin (Shanghai)*, pp. 651–662. doi: 10.1111/j.1745-7270.2008.00438.x.
- Chern, Y. *et al.* (1993) 'Multiple mechanisms for desensitization of A2a adenosine receptor-mediated cAMP elevation in rat pheochromocytoma PC12 cells.', *Molecular Pharmacology*, 44(5).
- Christopoulos, A. *et al.* (2003) 'Novel receptor partners and function of receptor activity-modifying proteins', *Journal of Biological Chemistry*. *JBC Papers in Press*, 278(5), pp. 3293–3297. doi: 10.1074/jbc.C200629200.
- Christopoulos, G. *et al.* (1999) 'Multiple amylin receptors arise from receptor activity-modifying protein interaction with the calcitonin receptor gene product', *Molecular Pharmacology*. American Society for Pharmacology and Experimental Therapy, 56(1), pp. 235–242. doi: 10.1124/mol.56.1.235.
- Ciechomska, I. A. *et al.* (2020) 'EGFR/FOXO3a/BIM signaling pathway determines chemosensitivity of BMP4-differentiated glioma stem cells to temozolomide', *Experimental and Molecular Medicine*. doi: 10.1038/s12276-020-0479-9.
- Clapham, D. E. (2007) 'Calcium Signaling', *Cell*, 131(6), pp. 1047–1058. doi: 10.1016/j.cell.2007.11.028.
- Clark, A. J. *et al.* (2021) 'CGRP-receptor family reveals endogenous GPCR agonist bias and its significance in primary human cardiovascular cells', *bioRxiv*.

- bioRxiv, p. 2020.12.21.423730. doi: 10.1101/2020.12.21.423730.
- Comeo, E. *et al.* (2020) 'Subtype-Selective Fluorescent Ligands as Pharmacological Research Tools for the Human Adenosine A2A Receptor', *Journal of Medicinal Chemistry*. American Chemical Society, 63(5), pp. 2656–2672. doi: 10.1021/acs.jmedchem.9b01856.
- Conti, M. *et al.* (1991) 'Hormonal regulation of cyclic nucleotide phosphodiesterases', *Endocr Rev*, 12(3), pp. 218–234. doi: 10.1210/edrv-12-3-218.
- Conti, M. *et al.* (1995) 'Recent progress in understanding the hormonal regulation of phosphodiesterases', *Endocr Rev*, 16(3), pp. 370–389. doi: 10.1210/edrv-16-3-370.
- Conti, M and Beavo, J. (2007) 'Biochemistry and physiology of cyclic nucleotide phosphodiesterases: essential components in cyclic nucleotide signaling', *Annu Rev Biochem*, 76, pp. 481–511. doi: 10.1146/annurev.biochem.76.060305.150444.
- Conti, Marco and Beavo, J. (2007) 'Biochemistry and Physiology of Cyclic Nucleotide Phosphodiesterases: Essential Components in Cyclic Nucleotide Signaling'. doi: 10.1146/annurev.biochem.76.060305.150444.
- Conti, M., Mika, D. and Richter, W. (2014) 'Cyclic AMP compartments and signaling specificity: role of cyclic nucleotide phosphodiesterases', *J Gen Physiol*. 2014/01/01, 143(1), pp. 29–38. doi: 10.1085/jgp.201311083.
- Coughlin, S. R. (1999) 'How the protease thrombin talks to cells', *Proceedings of the National Academy of Sciences of the United States of America*. National Academy of Sciences, 96(20), pp. 11023–11027. doi: 10.1073/pnas.96.20.11023.
- Courilleau, D. *et al.* (2013) 'The (R)-enantiomer of CE3F4 is a preferential inhibitor of human exchange protein directly activated by cyclic AMP isoform 1 (Epac1)', *Biochemical and Biophysical Research Communications*. Academic Press Inc., 440(3), pp. 443–448. doi: 10.1016/j.bbrc.2013.09.107.
- Coussens, L. M. and Werb, Z. (2002) 'Inflammation and cancer', *Nature*. NIH Public Access, pp. 860–867. doi: 10.1038/nature01322.
- Cui, N. *et al.* (2021) 'Adrenomedullin-RAMP2 and -RAMP3 Systems Regulate Cardiac Homeostasis during Cardiovascular Stress', *Endocrinology*. The Endocrine Society, 162(3). doi: 10.1210/endocr/bqab001.
- Cullen, K. A. *et al.* (2004) 'Activation of cAMP-guanine exchange factor confers PKA-independent protection from hepatocyte apoptosis', *Am J Physiol Gastrointest*

- Liver Physiol.* 2004/03/27, 287(2), pp. G334-43. doi: 10.1152/ajpgi.00517.2003.
- Cunningham, M. R. *et al.* (2012) 'Novel role for proteinase-activated receptor 2 (PAR2) in membrane trafficking of proteinase-activated receptor 4 (PAR4)', *Journal of Biological Chemistry*. doi: 10.1074/jbc.M111.315911.
- Dale, N. C. *et al.* (2019) 'NanoBRET: The bright future of proximity-based assays', *Frontiers in Bioengineering and Biotechnology*. Frontiers Media S.A., p. 56. doi: 10.3389/fbioe.2019.00056.
- Dale, N. and Frenguelli, B. G. (2009) 'Release of adenosine and ATP during ischemia and epilepsy', *Curr Neuropharmacol*, 7(3), pp. 160–179. doi: 10.2174/157015909789152146.
- Dalton, G. D. and Dewey, W. L. (2006) 'Protein kinase inhibitor peptide (PKI): A family of endogenous neuropeptides that modulate neuronal cAMP-dependent protein kinase function', *Neuropeptides*. *Neuropeptides*, pp. 23–34. doi: 10.1016/j.npep.2005.10.002.
- Daniel, P. M., Filiz, G. and Mantamadiotis, T. (2016) 'Sensitivity of GBM cells to cAMP agonist-mediated apoptosis correlates with CD44 expression and agonist resistance with MAPK signaling', *Cell Death & Disease*, 7. doi: ARTN e249410.1038/cddis.2016.393.
- Davidson, A. L. *et al.* (2008) 'Structure, Function, and Evolution of Bacterial ATP-Binding Cassette Systems', *MICROBIOLOGY AND MOLECULAR BIOLOGY REVIEWS*, 72(2), pp. 317–364. doi: 10.1128/MMBR.00031-07.
- Deb, A., Frank, S. and Testa, C. M. (2017) 'New symptomatic therapies for Huntington disease', in *Handbook of Clinical Neurology*. Elsevier B.V., pp. 199–207. doi: 10.1016/B978-0-12-801893-4.00017-1.
- Decleves, X. *et al.* (2008) 'ABC transporters and the accumulation of imatinib and its active metabolite CGP74588 in rat C6 glioma cells', *Pharmacol Res.* 2008/03/14, 57(3), pp. 214–222. doi: 10.1016/j.phrs.2008.01.006.
- Declèves, X. *et al.* (2002) 'Molecular and functional MDR1-PGP and MRPS expression in human glioblastoma multiforme cell lines', *International Journal of Cancer*. doi: 10.1002/ijc.10135.
- DeFea, K. A. *et al.* (2000) 'The proliferative and antiapoptotic effects of substance P are facilitated by formation of a β -arrestin-dependent scaffolding complex', *Proceedings of the National Academy of Sciences of the United States of America*. National Academy of Sciences, 97(20), pp. 11086–11091. doi: 10.1073/pnas.190276697.

- Degerman, E. *et al.* (2011) 'From PDE3B to the regulation of energy homeostasis', *Current Opinion in Pharmacology*. Elsevier Ltd, pp. 676–682. doi: 10.1016/j.coph.2011.09.015.
- Degerman, E., Belfrage, P. and Manganiello, V. C. (1997) 'Structure, localization, and regulation of cGMP-inhibited phosphodiesterase (PDE3)', *J Biol Chem*, 272(11), pp. 6823–6826. Available at: <http://www.ncbi.nlm.nih.gov/pubmed/9102399>.
- Delgado-López, P. D. and Corrales-García, E. M. (2016) 'Survival in glioblastoma: a review on the impact of treatment modalities', *Clinical and Translational Oncology*. Springer-Verlag Italia s.r.l., pp. 1062–1071. doi: 10.1007/s12094-016-1497-x.
- DeNinno, M. P. (2012) 'Future directions in phosphodiesterase drug discovery', *Bioorg Med Chem Lett*, 22(22), pp. 6794–6800. doi: 10.1016/j.bmcl.2012.09.028.
- Depry, C., Allen, M. D. and Zhang, J. (2011) 'Visualization of PKA activity in plasma membrane microdomains', *Molecular BioSystems*. Mol Biosyst, 7(1), pp. 52–58. doi: 10.1039/c0mb00079e.
- Ding, B. *et al.* (2005) 'Functional role of phosphodiesterase 3 in cardiomyocyte apoptosis - Implication in heart failure', *Circulation*, 111(19), pp. 2469–2476. doi: 10.1161/01.Cir.0000165128.39715.87.
- Divorcy, N. *et al.* (2015) 'G protein-coupled receptor 35: An emerging target in inflammatory and cardiovascular disease', *Frontiers in Pharmacology*. doi: 10.3389/fphar.2015.00041.
- Dixon, A. K. *et al.* (1996) 'Tissue distribution of adenosine receptor mRNAs in the rat', *British Journal of Pharmacology*. doi: 10.1111/j.1476-5381.1996.tb15561.x.
- Dodge-Kafka, K. L. *et al.* (2005) 'The protein kinase A anchoring protein mAKAP coordinates two integrated cAMP effector pathways', *Nature*. Nature Publishing Group, 437(7058), pp. 574–578. doi: 10.1038/nature03966.
- Dousa, T. P. (1999) 'Cyclic-3',5'-nucleotide phosphodiesterase isozymes in cell biology and pathophysiology of the kidney', *Kidney International*. Blackwell Publishing Inc., 55(1), pp. 29–62. doi: 10.1046/j.1523-1755.1999.00233.x.
- Downes, G. B. and Gautam, N. (1999) 'The G protein subunit gene families', *Genomics*. Academic Press Inc., 62(3), pp. 544–552. doi: 10.1006/geno.1999.5992.
- Dunn, Gavin P., Old, L. J. and Schreiber, R. D. (2004) 'The Immunobiology of Cancer Immunosurveillance and Immunoediting', *Immunity*. Cell Press, 21(2), pp. 137–148. doi: 10.1016/J.IMMUNI.2004.07.017.

- Dunn, Gavin P, Old, L. J. and Schreiber, R. D. (2004) 'THE THREE ES OF CANCER IMMUNOEDITING', *Annu. Rev. Immunol.*, 22, pp. 329–60. doi: 10.1146/annurev.immunol.22.012703.104803.
- Dupré, D. J., Rola-Pleszczynski, M. and Stankova, J. (2012) 'Rescue of internalization-defective platelet-activating factor receptor function by EBP50/NHERF1', *Journal of Cell Communication and Signaling*. Kluwer Academic Publishers, 6(4), pp. 205–216. doi: 10.1007/s12079-012-0175-1.
- Edelstein, L. C. *et al.* (2014) 'Common variants in the human platelet PAR4 thrombin receptor alter platelet function and differ by race', *Blood*. American Society of Hematology, 124(23), pp. 3450–3458. doi: 10.1182/blood-2014-04-572479.
- Edvinsson, L. *et al.* (2018) 'CGRP as the target of new migraine therapies - Successful translation from bench to clinic', *Nature Reviews Neurology*. Nature Publishing Group, pp. 338–350. doi: 10.1038/s41582-018-0003-1.
- Ehrlich, M. E. *et al.* (2001) 'ST14A cells have properties of a medium-size spiny neuron', *Experimental Neurology*, 167(2), pp. 215–226. doi: DOI 10.1006/exnr.2000.7551.
- Eitinger, T. *et al.* (2011) 'Canonical and ECF-type ATP-binding cassette importers in prokaryotes: Diversity in modular organization and cellular functions', *FEMS Microbiology Reviews*. Oxford Academic, pp. 3–67. doi: 10.1111/j.1574-6976.2010.00230.x.
- El-Tayeb, A. *et al.* (2011) 'Development of polar adenosine A_{2A} receptor agonists for inflammatory bowel disease: Synergism with A_{2B} antagonists', *ACS Medicinal Chemistry Letters*. American Chemical Society, 2(12), pp. 890–895. doi: 10.1021/ml200189u.
- Ellinghaus, Peter; Wilmen, Andreas; Hendrix, Martin; Tersteegen, A. (2006) 'Inhibition der PDE2A'. Canada.
- Engh, R. A. *et al.* (1996) 'Crystal structures of catalytic subunit of cAMP-dependent protein kinase in complex with isoquinolinesulfonyl protein kinase inhibitors H7, H8, and H89', *Journal of Biological Chemistry*. J Biol Chem, 271(42), pp. 26157–26164. doi: 10.1074/jbc.271.42.26157.
- Farmer, R. *et al.* (2020) 'Phosphodiesterases PDE2A and PDE10A both change mRNA expression in the human brain with age, but only PDE2A changes in a region-specific manner with psychiatric disease', *Cellular Signalling*. Elsevier Inc., 70. doi: 10.1016/j.cellsig.2020.109592.
- Faruqi, T. R. *et al.* (2000) 'Structure-function analysis of protease-activated receptor 4

- thetered Ligand peptides. Determinants of specificity and utility in assays of receptor function', *Journal of Biological Chemistry*. J Biol Chem, 275(26), pp. 19728–19734. doi: 10.1074/jbc.M909960199.
- Favot, L. *et al.* (2003) 'VEGF-induced HUVEC migration and proliferation are decreased by PDE2 and PDE4 inhibitors', *Thromb Haemost.* 2003/07/31, 90(2), pp. 334–343. doi: 10.1160/TH03-02-0084.
- Feng, Z. *et al.* (2020) 'A Putative Efflux Transporter of the ABC Family, YbhFSR, in Escherichia coli Functions in Tetracycline Efflux and Na⁺(Li⁺)/H⁺ Transport', *Frontiers in Microbiology*. Frontiers Media S.A., 11, p. 556. doi: 10.3389/fmicb.2020.00556.
- Ferrandon, S. *et al.* (2009) 'Sustained cyclic AMP production by parathyroid hormone receptor endocytosis', *Nature Chemical Biology*. Nature Publishing Group, 5(10), pp. 734–742. doi: 10.1038/nchembio.206.
- Ferre, S. *et al.* (1991) 'Stimulation of high-affinity adenosine A2 receptors decreases the affinity of dopamine D2 receptors in rat striatal membranes', *Proceedings of the National Academy of Sciences of the United States of America*. National Academy of Sciences, 88(16), pp. 7238–7241. doi: 10.1073/pnas.88.16.7238.
- Feske, S. (2007) 'Calcium signalling in lymphocyte activation and disease', *Nature Reviews Immunology*. doi: 10.1038/nri2152.
- Flynn, G. E., Johnson, J. P. and Zagotta, W. N. (2001) 'Cyclic nucleotide-gated channels: Shedding light on the opening of a channel pore', *Nature Reviews Neuroscience*. Nat Rev Neurosci, pp. 643–651. doi: 10.1038/35090015.
- Foley, J. F. (2018) 'New connections: Taking advantage of bias', *Science Signaling*. doi: 10.1126/scisignal.aav9344.
- Fong, L. *et al.* (2020) 'Adenosine 2A receptor blockade as an immunotherapy for treatment-refractory renal cell cancer', *Cancer Discovery*. American Association for Cancer Research Inc., 10(1), pp. 40–53. doi: 10.1158/2159-8290.CD-19-0980.
- Formolo, C. A. *et al.* (2011) 'Secretome signature of invasive glioblastoma multiforme', *Journal of Proteome Research*. doi: 10.1021/pr200210w.
- Francis, S. H. *et al.* (2010) 'cGMP-dependent protein kinases and cGMP phosphodiesterases in nitric oxide and cGMP action', *Pharmacol Rev.* 2010/08/19, 62(3), pp. 525–563. doi: 10.1124/pr.110.002907.
- Francis, S. H., Blount, M. A. and Corbin, J. D. (2011) 'Mammalian cyclic nucleotide phosphodiesterases: molecular mechanisms and physiological functions',

- Physiol Rev*, 91(2), pp. 651–690. doi: 10.1152/physrev.00030.2010.
- Fredholm, B. B. (2010) 'Adenosine receptors as drug targets', *Experimental Cell Research*, 316(8), pp. 1284–1288. doi: 10.1016/j.yexcr.2010.02.004.
- Fredriksson, R. *et al.* (2003) 'The G-protein-coupled receptors in the human genome form five main families. Phylogenetic analysis, paralogon groups, and fingerprints', *Molecular Pharmacology*. American Society for Pharmacology and Experimental Therapeutics, 63(6), pp. 1256–1272. doi: 10.1124/mol.63.6.1256.
- French, S. L. and Hamilton, J. R. (2016) 'Protease-activated receptor 4: from structure to function and back again', *British Journal of Pharmacology*. doi: 10.1111/bph.13455.
- Friebe, D. *et al.* (2014) 'Purinergic signaling on leukocytes infiltrating the LPS-injured lung', *PLoS ONE*. Public Library of Science, 9(4). doi: 10.1371/journal.pone.0095382.
- Froese, A. *et al.* (2012) 'Popeye domain containing proteins are essential for stress-mediated modulation of cardiac pacemaking in mice', *Journal of Clinical Investigation*. American Society for Clinical Investigation, 122(3), pp. 1119–1130. doi: 10.1172/JCI59410.
- Fujishige, K. *et al.* (1999) 'Cloning and characterization of a novel human phosphodiesterase that hydrolyzes both cAMP and cGMP (PDE10A)', *J Biol Chem*. 1999/06/22, 274(26), pp. 18438–18445. doi: 10.1074/jbc.274.26.18438.
- Fujishige, K., Kotera, J. and Omori, K. (1999) 'Striatum- and testis-specific phosphodiesterase PDE10A', *European Journal of Biochemistry*. John Wiley & Sons, Ltd, 266(3), pp. 1118–1127. doi: 10.1046/j.1432-1327.1999.00963.x.
- Furman, M. A. and Shulman, K. (1977) 'Cyclic AMP and adenylyl cyclase in brain tumors', *J Neurosurg*. 1977/04/01, 46(4), pp. 477–483. doi: 10.3171/jns.1977.46.4.0477.
- Galvan, M. and Schudt, C. (1990) 'Actions of the phosphodiesterase inhibitor zardaverine on guinea-pig ventricular muscle', *Naunyn-Schmiedeberg's Archives of Pharmacology*. Springer-Verlag, 342(2), pp. 221–227. doi: 10.1007/BF00166968.
- Gamanuma, M. *et al.* (2003) 'Comparison of enzymatic characterization and gene organization of cyclic nucleotide phosphodiesterase 8 family in humans', *Cellular Signalling*. Elsevier Inc., 15(6), pp. 565–574. doi: 10.1016/S0898-6568(02)00146-8.
- Garelja, M. L. *et al.* (2018) 'Receptor Activity Modifying Proteins Have Limited Effects

- on the Class B G Protein-Coupled Receptor Calcitonin Receptor-Like Receptor Stalk', *Biochemistry*. American Chemical Society, 57(8), pp. 1410–1422. doi: 10.1021/acs.biochem.7b01180.
- Garelja, M. L. *et al.* (2020) 'Molecular Mechanisms of Class B GPCR Activation: Insights from Adrenomedullin Receptors', *ACS Pharmacology & Translational Science*. American Chemical Society, 3(2), pp. 246–262. doi: 10.1021/acspsci.9b00083.
- Gargalovic, P. *et al.* (2021) 'In Vitro and In Vivo Evaluation of a Small-Molecule APJ (Apelin Receptor) Agonist, BMS-986224, as a Potential Treatment for Heart Failure.', *Circulation. Heart failure*, p. CIRCHEARTFAILURE120007351. doi: 10.1161/CIRCHEARTFAILURE.120.007351.
- Gether, U. and Kobilka, B. K. (1998) 'G protein-coupled receptors', *Journal of Biological Chemistry*. *J Biol Chem*, pp. 17979–17982. doi: 10.1074/jbc.273.29.17979.
- Ghai, G. *et al.* (1987) *Pharmacological Characterization of CGS 1 5943A: A Novel Nonxanthine Adenosine Antagonist*.
- Giakoumettis, D., Kritis, A. and Foroglou, N. (2018) 'C6 cell line: The gold standard in glioma research', *Hippokratia*.
- Gingell, J. J. *et al.* (2020) 'Distinct Patterns of Internalization of Different Calcitonin Gene-Related Peptide Receptors', *ACS Pharmacology and Translational Science*. American Chemical Society, 3(2), pp. 296–304. doi: 10.1021/acspsci.9b00089.
- Giorgi, M. *et al.* (2002) 'Differential expression and localization of calmodulin-dependent phosphodiesterase genes during ontogenesis of chick dorsal root ganglion', *J Neurochem*. 2002/04/16, 80(6), pp. 970–979. doi: 10.1046/j.0022-3042.2002.00786.x.
- Glover, D. M. (1991) *DNA Cloning: A Practical Approach. Vol. 1*. IRL Press. Available at: <https://books.google.co.uk/books?id=aZMAzQEACAAJ>.
- Gluzman, Y. (1981) 'SV40-transformed simian cells support the replication of early SV40 mutants', *Cell*. Elsevier, 23(1), pp. 175–182. doi: 10.1016/0092-8674(81)90282-8.
- Goricanec, D. *et al.* (2016) 'Conformational dynamics of a G-protein α subunit is tightly regulated by nucleotide binding', *Proceedings of the National Academy of Sciences of the United States of America*. National Academy of Sciences, 113(26), pp. E3629–E3638. doi: 10.1073/pnas.1604125113.

- Grauer, S. M. *et al.* (2009) 'Phosphodiesterase 10A inhibitor activity in preclinical models of the positive, cognitive, and negative symptoms of schizophrenia', *Journal of Pharmacology and Experimental Therapeutics*. doi: 10.1124/jpet.109.155994.
- Greten, F. R. and Grivennikov, S. I. (2019) 'Inflammation and Cancer: Triggers, Mechanisms, and Consequences', *Immunity*. Cell Press, pp. 27–41. doi: 10.1016/j.immuni.2019.06.025.
- Grivennikov, S. I., Greten, F. R. and Karin, M. (2010) 'Immunity, Inflammation, and Cancer', *Cell*. Cell, pp. 883–899. doi: 10.1016/j.cell.2010.01.025.
- Grobben, B., De Deyn, P. P. and Slegers, H. (2002) 'Rat C6 glioma as experimental model system for the study of glioblastoma growth and invasion', *Cell and Tissue Research*, 310(3), pp. 257–270. doi: 10.1007/s00441-002-0651-7.
- Guidolin (2010) 'Involvement of vascular endothelial growth factor signaling in CLR/RAMP1 and CLR/RAMP2-mediated pro-angiogenic effect of intermedin on human vascular endothelial cells', *International Journal of Molecular Medicine*. Spandidos Publications, 26(2). doi: 10.3892/ijmm_00000464.
- Gupta, R. C., Singh-Gupta, V. and Sabbah, H. N. (2019) 'MULTIDRUG RESISTANCE PROTEIN 5 (MRP5), A CGMP EFFLUX TRANSPORTER IS UPREGULATED IN LEFT VENTRICULAR MYOCARDIUM OF DOGS WITH CHRONIC HEART FAILURE', *Journal of the American College of Cardiology*. Elsevier BV, 73(9), p. 755. doi: 10.1016/s0735-1097(19)31363-4.
- Gurevich, E. V. *et al.* (2012) 'G protein-coupled receptor kinases: More than just kinases and not only for GPCRs', *Pharmacology and Therapeutics*. Elsevier Inc., pp. 40–69. doi: 10.1016/j.pharmthera.2011.08.001.
- Gurevich, V. V. and Gurevich, E. V. (2017) 'Molecular mechanisms of GPCR signaling: A structural perspective', *International Journal of Molecular Sciences*. MDPI AG. doi: 10.3390/ijms18122519.
- Gurevich, V. V. and Gurevich, E. V. (2019) 'GPCR signaling regulation: The role of GRKs and arrestins', *Frontiers in Pharmacology*. Frontiers Media S.A., 10(FEB), p. 125. doi: 10.3389/fphar.2019.00125.
- Gurevich, V. V. and Gurevich, E. V. (2020) 'Biased GPCR signaling: Possible mechanisms and inherent limitations', *Pharmacology and Therapeutics*. Elsevier Inc. doi: 10.1016/j.pharmthera.2020.107540.
- Gurney, M. E. *et al.* (2011) 'Small molecule allosteric modulators of phosphodiesterase 4', *Handbook of Experimental Pharmacology*, 204, pp. 167–192. doi:

10.1007/978-3-642-17969-3_7.

- ter Haar, E. *et al.* (2010) 'Crystal structure of the ectodomain complex of the CGRP receptor, a class-B GPCR, reveals the site of drug antagonism', *Structure*. Structure, 18(9), pp. 1083–1093. doi: 10.1016/j.str.2010.05.014.
- Häfner, S. *et al.* (1994) 'Mechanism of inhibition of Raf-1 by protein kinase A.', *Molecular and Cellular Biology*. American Society for Microbiology, 14(10), pp. 6696–6703. doi: 10.1128/mcb.14.10.6696.
- Hall, R. A. *et al.* (1998) 'A C-terminal motif found in the β 2-adrenergic receptor, P2Y1 receptor and cystic fibrosis transmembrane conductance regulator determines binding to the Na⁺/H⁺ exchanger regulatory factor family of PDZ proteins', *Proceedings of the National Academy of Sciences of the United States of America*. National Academy of Sciences, 95(15), pp. 8496–8501. doi: 10.1073/pnas.95.15.8496.
- Han, C. C. *et al.* (2016) 'Regulatory effects of GRK2 on GPCRs and non-GPCRs and possible use as a drug target (Review)', *International Journal of Molecular Medicine*. Spandidos Publications, pp. 987–994. doi: 10.3892/ijmm.2016.2720.
- Han, P. *et al.* (2014) 'BVES inhibition triggers epithelial-mesenchymal transition in human hepatocellular carcinoma', *Digestive Diseases and Sciences*. Springer New York LLC, 59(5), pp. 992–1000. doi: 10.1007/s10620-013-2992-3.
- Hanahan, D. and Weinberg, R. A. (2011) 'Hallmarks of Cancer: The Next Generation', *Cell*. Elsevier, 144(5), pp. 646–674. doi: 10.1016/J.CELL.2011.02.013.
- Hanyaloglu, A. C. and Von Zastrow, M. (2008) 'Regulation of GPCRs by endocytic membrane trafficking and its potential implications', *Annual Review of Pharmacology and Toxicology*, pp. 537–568. doi: 10.1146/annurev.pharmtox.48.113006.094830.
- Harikumar, K. G. *et al.* (2009) 'Molecular basis of association of receptor activity-modifying protein 3 with the family B G protein-coupled secretin receptor', *Biochemistry*. Biochemistry, 48(49), pp. 11773–11785. doi: 10.1021/bi901326k.
- Härndahl, L. *et al.* (2002) 'Important role of phosphodiesterase 3B for the stimulatory action of cAMP on pancreatic β -cell exocytosis and release of insulin', *Journal of Biological Chemistry*. Elsevier, 277(40), pp. 37446–37455. doi: 10.1074/jbc.M205401200.
- Harris, M. *et al.* (2018) 'Emerging patents in the therapeutic areas of glioma and glioblastoma', *Expert Opin Ther Pat*. 2018/06/29, 28(7), pp. 573–590. doi: 10.1080/13543776.2018.1494155.

- Harris, M. (2019) *Receptor activity-modifying protein and small molecule modulation of the gastric inhibitory polypeptide receptor*. University of Cambridge.
- Harris, M. *et al.* (2021) 'RAMPs regulate signalling bias and internalisation of the GIPR', *bioRxiv*. Cold Spring Harbor Laboratory, p. 2021.04.08.436756. doi: 10.1101/2021.04.08.436756.
- HartMG, G. R. (2016) 'Cochrane Library Cochrane Database of Systematic Reviews Temozolomide for high grade glioma (Review)'. doi: 10.1002/14651858.CD007415.pub2.
- Haslam, R. J., Davidson, M. M. L. and Desjardins, J. V. (1978) 'Inhibition of adenylate cyclase by adenosine analogues in preparations of broken and intact human platelets. Evidence for the unidirectional control of platelet function by cyclic AMP', *Biochemical Journal*. *Biochem J*, 176(1), pp. 83–95. doi: 10.1042/bj1760083.
- Hausdorff, W. P., Caron, M. G. and Lefkowitz, R. J. (1990) 'Turning off the signal: desensitization of beta-adrenergic receptor function', *FASEB J*. 1990/08/01, 4(11), pp. 2881–2889. Available at: <https://www.ncbi.nlm.nih.gov/pubmed/2165947>.
- Hauser, A. S. *et al.* (2017) 'Trends in GPCR drug discovery: New agents, targets and indications', *Nature Reviews Drug Discovery*. Nature Publishing Group, 16(12), pp. 829–842. doi: 10.1038/nrd.2017.178.
- Hay, D. L. *et al.* (2016) 'Receptor activity-modifying proteins; multifunctional G protein-coupled receptor accessory proteins', *Biochem Soc Trans*, 44(2), pp. 568–573. doi: 10.1042/BST20150237.
- Hayashi, M. *et al.* (2002) 'Genomic organization, chromosomal localization, and alternative splicing of the human phosphodiesterase 8B gene', *Biochemical and Biophysical Research Communications*. *Biochem Biophys Res Commun*, 297(5), pp. 1253–1258. doi: 10.1016/S0006-291X(02)02371-9.
- Healy, J. A. *et al.* (2016) 'GNA13 loss in germinal center B cells leads to impaired apoptosis and promotes lymphoma in vivo', *Blood*. American Society of Hematology, 127(22), pp. 2723–2731. doi: 10.1182/blood-2015-07-659938.
- Hein, P. and Bünemann, M. (2009) 'Coupling mode of receptors and G proteins', *Naunyn-Schmiedeberg's Archives of Pharmacology*. *Naunyn Schmiedebergs Arch Pharmacol*, pp. 435–443. doi: 10.1007/s00210-008-0383-7.
- Hejtmancik, J. F. and Comstock, J. P. (1976) 'Isolation and Purification of Hen Oviduct Protein Synthesis Initiation Factors A2A and A2B', *Biochemistry*. *Biochemistry*,

15(17), pp. 3804–3812. doi: 10.1021/bi00662a024.

Hendrikse, E. R. *et al.* (2020) 'Identification of Small-Molecule Positive Modulators of Calcitonin-like Receptor-Based Receptors', *ACS Pharmacology and Translational Science*. American Chemical Society, 3(2), pp. 305–320. doi: 10.1021/acspsci.9b00108.

Hennenberg, M. *et al.* (2016) 'Inhibition of Adrenergic and Non-Adrenergic Smooth Muscle Contraction in the Human Prostate by the Phosphodiesterase 10-Selective Inhibitor TC-E 5005', *The Prostate*. John Wiley and Sons Inc., 76(15), pp. 1364–1374. doi: 10.1002/pros.23208.

Héroux, M. *et al.* (2007a) 'Functional calcitonin gene-related peptide receptors are formed by the asymmetric assembly of a calcitonin receptor-like receptor homooligomer and a monomer of receptor activity-modifying protein-1', *Journal of Biological Chemistry*. J Biol Chem, 282(43), pp. 31610–31620. doi: 10.1074/jbc.M701790200.

Héroux, M. *et al.* (2007b) 'Functional calcitonin gene-related peptide receptors are formed by the asymmetric assembly of a calcitonin receptor-like receptor homooligomer and a monomer of receptor activity-modifying protein-1', *Journal of Biological Chemistry*. J Biol Chem, 282(43), pp. 31610–31620. doi: 10.1074/jbc.M701790200.

Herradón, E. *et al.* (2017) 'Characterization of cardiovascular alterations induced by different chronic cisplatin treatments', *Frontiers in Pharmacology*, 8(MAY). doi: 10.3389/fphar.2017.00196.

Heuberger, D. M. and Schuepbach, R. A. (2019) 'Protease-activated receptors (PARs): Mechanisms of action and potential therapeutic modulators in PAR-driven inflammatory diseases', *Thrombosis Journal*. BioMed Central Ltd. doi: 10.1186/s12959-019-0194-8.

Higashijima, T., Ferguson, K. M. and Sternweis, P. C. (1987) 'Effects of Mg²⁺ and the $\beta\gamma$ -subunit complex on the interactions of guanine nucleotides with G proteins', *Journal of Biological Chemistry*. Elsevier, 262(2), pp. 762–766. doi: 10.1016/s0021-9258(19)75851-7.

Higgins, J. B. and Casey, P. J. (1994) 'In vitro processing of recombinant G protein gamma subunits. Requirements for assembly of an active beta gamma complex.', *The Journal of biological chemistry*. United States, 269(12), pp. 9067–9073.

Hilairret, S. *et al.* (2001) 'Agonist-promoted Internalization of a Ternary Complex

- between Calcitonin Receptor-like Receptor, Receptor Activity-modifying Protein 1 (RAMP1), and β -Arrestin', *Journal of Biological Chemistry*. J Biol Chem, 276(45), pp. 42182–42190. doi: 10.1074/jbc.M107323200.
- Hill, R. *et al.* (2016) 'Drug Repurposing to Circumvent Chemotherapy Resistance in Brain Tumours', in. doi: 10.1007/978-3-319-46505-0_6.
- Hirsh, L. *et al.* (2004) 'Phosphodiesterase inhibitors as anti-cancer drugs', *Biochem Pharmacol.* 2004/08/18, 68(6), pp. 981–988. doi: 10.1016/j.bcp.2004.05.026.
- Hofmann, F. *et al.* (1975) 'Comparison of adenosine 3':5' monophosphate dependent protein kinases from rabbit skeletal and bovine heart muscle', *Journal of Biological Chemistry*. J Biol Chem, 250(19), pp. 7795–7801. doi: 10.1016/s0021-9258(19)40885-5.
- Hohenegger, M. *et al.* (1998) 'Gsq-selective G protein antagonists', *Proceedings of the National Academy of Sciences of the United States of America*. National Academy of Sciences, 95(1), pp. 346–351. doi: 10.1073/pnas.95.1.346.
- Hollenberg, M. D. and Saifeddine, M. (2001) 'Proteinase-activated receptor 4 (PAR4): Activation and inhibition of rat platelet aggregation by PAR4-derived peptides', *Canadian Journal of Physiology and Pharmacology*. National Research Council of Canada, 79(5), pp. 439–442. doi: 10.1139/y01-013.
- Hoppener, J. W. M. *et al.* (1987) 'Expression of the second calcitonin/calcitonin gene-related peptide gene in ewing sarcoma cell lines', *Journal of Clinical Endocrinology and Metabolism*. J Clin Endocrinol Metab, 64(4), pp. 809–817. doi: 10.1210/jcem-64-4-809.
- Hoshi, N., Langeberg, L. K. and Scott, J. D. (2005) 'Distinct enzyme combinations in AKAP signalling complexes permit functional diversity', *Nature Cell Biology*. Nat Cell Biol, 7(11), pp. 1066–1073. doi: 10.1038/ncb1315.
- Hoth, M. and Penner, R. (1992) 'Depletion of intracellular calcium stores activates a calcium current in mast cells', *Nature*. doi: 10.1038/355353a0.
- Hsia, J. A. *et al.* (1984) 'Requirement for both cholera toxin and pertussis toxin to obtain maximal activation of adenylate cyclase in cultured cells', *Biochemical and Biophysical Research Communications*. Academic Press, 119(3), pp. 1068–1074. doi: 10.1016/0006-291X(84)90883-0.
- Huai, Q., Wang, H., *et al.* (2004) 'Crystal structure of phosphodiesterase 9 shows orientation variation of inhibitor 3-isobutyl-1-methylxanthine binding', *Proceedings of the National Academy of Sciences of the United States of America*, 101(26), pp. 9624–9629. doi: 10.1073/pnas.0401120101.

- Huai, Q., Liu, Y., *et al.* (2004) 'Crystal Structures of Phosphodiesterases 4 and 5 in Complex with Inhibitor 3-Isobutyl-1-methylxanthine Suggest a Conformation Determinant of Inhibitor Selectivity', *Journal of Biological Chemistry*, 279(13), pp. 13095–13101. doi: 10.1074/jbc.M311556200.
- Huai, Q., Colicelli, J. and Ke, H. (2003) 'The Crystal Structure of AMP-Bound PDE4 Suggests a Mechanism for Phosphodiesterase Catalysis', *Biochemistry*, 42(45), pp. 13220–13226. doi: 10.1021/bi034653e.
- Hulme, E. C. and Trevethick, M. A. (2010) 'Ligand binding assays at equilibrium: Validation and interpretation', *British Journal of Pharmacology*. doi: 10.1111/j.1476-5381.2009.00604.x.
- Hung, S. H. *et al.* (2006) 'New insights from the structure-function analysis of the catalytic region of human platelet phosphodiesterase 3A: A role for the unique 44-amino acid insert', *Journal of Biological Chemistry*. Elsevier, 281(39), pp. 29236–29244. doi: 10.1074/jbc.M606558200.
- Husmann, K. *et al.* (2003) 'Three receptor-activity-modifying proteins define calcitonin gene-related peptide or adrenomedullin selectivity of the mouse calcitonin-like receptor in COS-7 cells', *Biochemical Pharmacology*. Elsevier Inc., 66(11), pp. 2107–2115. doi: 10.1016/j.bcp.2003.07.009.
- Huston, E. *et al.* (2006) 'cAMP phosphodiesterase-4A1 (PDE4A1) has provided the paradigm for the intracellular targeting of phosphodiesterases, a process that underpins compartmentalized cAMP signalling', *Biochem Soc Trans*, 34(Pt 4), pp. 504–509. doi: 10.1042/BST0340504.
- Iffland, A. *et al.* (2005) 'Structural determinants for inhibitor specificity and selectivity in PDE2A using the wheat germ in vitro translation system', *Biochemistry*. *Biochemistry*, 44(23), pp. 8312–8325. doi: 10.1021/bi047313h.
- Ikeda, S. R. (1996) 'Voltage-dependent modulation of N-type calcium channels by G-protein $\beta\gamma$ subunits', *Nature*. Macmillan Magazines Ltd, 380(6571), pp. 255–258. doi: 10.1038/380255a0.
- Illiano, M. *et al.* (2018) 'Forskolin improves sensitivity to doxorubicin of triple negative breast cancer cells via Protein Kinase A-mediated ERK1/2 inhibition', *Biochemical Pharmacology*, 152, pp. 104–113. doi: 10.1016/j.bcp.2018.03.023.
- Ilouz, R. *et al.* (2017) 'Isoform-specific subcellular localization and function of protein kinase a identified by mosaic imaging of mouse brain', *eLife*. eLife Sciences Publications Ltd, 6. doi: 10.7554/eLife.17681.
- Indrischek, H. *et al.* (2017) 'Uncovering missing pieces: Duplication and deletion

- history of arrestins in deuterostomes', *BMC Evolutionary Biology*. BioMed Central Ltd., p. 163. doi: 10.1186/s12862-017-1001-4.
- Inoue, Y. *et al.* (2017) 'Prognostic impact of CD73 and A2A adenosine receptor expression in non-small-cell lung cancer', *Oncotarget*. 2017/01/07. Department of Tumor Pathology, Hamamatsu University School of Medicine, Hamamatsu, Shizuoka, Japan. Second Division, Department of Internal Medicine, Hamamatsu University School of Medicine, Hamamatsu, Shizuoka, Japan. First Department of Surgery, Hamamatsu, 8(5), pp. 8738–8751. doi: 10.18632/oncotarget.14434.
- Insel, P. A. *et al.* (2012) 'Cyclic AMP is both a pro-apoptotic and anti-apoptotic second messenger', *Acta Physiologica*, 204(2), pp. 277–287. doi: 10.1111/j.1748-1716.2011.02273.x.
- Ishiyama, Y. *et al.* (1993) 'Hemodynamic effects of a novel hypotensive peptide, human adrenomedullin, in rats', *European Journal of Pharmacology*. Eur J Pharmacol, 241(2–3), pp. 271–273. doi: 10.1016/0014-2999(93)90214-3.
- Jacobson, K. A. *et al.* (1997) 'Pharmacological characterization of novel A3 adenosine receptor- selective antagonists', *Neuropharmacology*. Elsevier Ltd, pp. 1157–1165. doi: 10.1016/S0028-3908(97)00104-4.
- Jacobson, K. A. and Gao, Z. G. (2006) 'Adenosine receptors as therapeutic targets', *Nature Reviews Drug Discovery*. doi: 10.1038/nrd1983.
- Jahani-As, A. *et al.* (2016) 'Control of glioblastoma tumorigenesis by feed-forward cytokine signaling', *Nature Neuroscience*. doi: 10.1038/nn.4295.
- Jarvis, M. F. *et al.* (1989) '[3H]CGS 21680, a selective A2 adenosine receptor agonist directly labels A2 receptors in rat brain', *Journal of Pharmacology and Experimental Therapeutics*. J Pharmacol Exp Ther, 251(3), pp. 888–893. Available at: <https://pubmed.ncbi.nlm.nih.gov/2600819/> (Accessed: 3 March 2021).
- Jeon, Y. H. *et al.* (2005) 'Phosphodiesterase: Overview of protein structures, potential therapeutic applications and recent progress in drug development', *Cellular and Molecular Life Sciences*. Cell Mol Life Sci, pp. 1198–1220. doi: 10.1007/s00018-005-4533-5.
- Jeon, Y H *et al.* (2005) 'Review Phosphodiesterase: overview of protein structures, potential therapeutic applications and recent progress in drug development'. doi: 10.1007/s00018-005-4533-5.
- Jin, S. L. C., Swinnen, J. V. and Conti, M. (1992) 'Characterization of the structure of

- a low $K(m)$, rolipram-sensitive cAMP phosphodiesterase. Mapping of the catalytic domain', *Journal of Biological Chemistry*. Elsevier, 267(26), pp. 18929–18939. doi: 10.1016/s0021-9258(19)37050-4.
- Jones, D. T. and Reed, R. R. (1989) 'Golf: An olfactory neuron specific-G protein involved in odorant signal transduction', *Science*. American Association for the Advancement of Science, 244(4906), pp. 790–795. doi: 10.1126/science.2499043.
- Kahn, M. L. *et al.* (1998) 'A dual thrombin receptor system for platelet activation', *Nature* 1998 394:6694. Nature Publishing Group, 394(6694), pp. 690–694. doi: 10.1038/29325.
- Kalash, L. *et al.* (2017) 'Computer-aided design of multi-target ligands at A1R, A2AR and PDE10A, key proteins in neurodegenerative diseases', *Journal of Cheminformatics*. Springer International Publishing, 9(1), pp. 1–19. doi: 10.1186/s13321-017-0249-4.
- Kalash, L. *et al.* (2021) 'Structure-based identification of dual ligands at the A2AR and PDE10A with anti-proliferative effects in lung cancer cell-lines.', *Journal of cheminformatics*, 13(1), p. 17. doi: 10.1186/s13321-021-00492-5.
- Kalhan, A. *et al.* (2012) 'Adenosine A 2A and A 2B receptor expression in neuroendocrine tumours: Potential targets for therapy', *Purinergic Signalling*. Purinergic Signal, 8(2), pp. 265–274. doi: 10.1007/s11302-011-9280-5.
- Kamato, D. *et al.* (2015) 'Structure, Function, Pharmacology, and Therapeutic Potential of the G Protein, $G\alpha/q,11$ ', *Frontiers in Cardiovascular Medicine*. Frontiers Media S.A. doi: 10.3389/fcvm.2015.00014.
- Kang, S. S. *et al.* (2010) 'Caffeine-mediated inhibition of calcium release channel inositol 1,4,5-trisphosphate receptor subtype 3 blocks glioblastoma invasion and extends survival', *Cancer Research*. doi: 10.1158/0008-5472.CAN-09-2886.
- Kang, T. W. *et al.* (2014) 'Growth arrest and forced differentiation of human primary glioblastoma multiforme by a novel small molecule', *Scientific Reports*, 4. doi: ARTN 554610.1038/srep05546.
- Kang, X. *et al.* (2015) 'Expression profile analysis of zinc transporters (ZIP4, ZIP9, ZIP11, ZnT9) in gliomas and their correlation with IDH1 mutation status', *Asian Pacific Journal of Cancer Prevention*. doi: 10.7314/APJCP.2015.16.8.3355.
- Karge, W. H., Schaefer, E. J. and Ordovas, J. M. (1998) 'Quantification of mRNA by polymerase chain reaction (PCR) using an internal standard and a

- nonradioactive detection method.', *Methods in molecular biology (Clifton, N.J.)*. doi: 10.1385/1-59259-582-0:43.
- Kase, H. *et al.* (1987) 'K-252 compounds, novel and potent inhibitors of protein kinase C and cyclic nucleotide-dependent protein kinases', *Biochemical and Biophysical Research Communications*. *Biochem Biophys Res Commun*, 142(2), pp. 436–440. doi: 10.1016/0006-291X(87)90293-2.
- Kawasaki, H. *et al.* (1998) 'A family of cAMP-binding proteins that directly activate Rap1', *Science*. American Association for the Advancement of Science, 282(5397), pp. 2275–2279. doi: 10.1126/science.282.5397.2275.
- Ke, H. (2004) 'Implications of PDE4 structure on inhibitor selectivity across PDE families', *International Journal of Impotence Research*, 16(SUPPL. 1). doi: 10.1038/sj.ijir.3901211.
- Kehler, J. *et al.* (2011) 'Triazoloquinazolines as a novel class of phosphodiesterase 10A (PDE10A) inhibitors', *Bioorg Med Chem Lett*, 21(12), pp. 3738–3742. doi: 10.1016/j.bmcl.2011.04.067.
- Kenakin, K. T. (1988) 'Pharmacologic Analysis of Drug Receptor Interaction', *Therapeutic Drug Monitoring*. doi: 10.1097/00007691-198803000-00029.
- Keravis, T and Lugnier, C. (2012) 'Cyclic nucleotide phosphodiesterase (PDE) isozymes as targets of the intracellular signalling network: benefits of PDE inhibitors in various diseases and perspectives for future therapeutic developments', *Br J Pharmacol*, 165(5), pp. 1288–1305. doi: 10.1111/j.1476-5381.2011.01729.x.
- Keravis, Thérèse and Lugnier, C. (2012a) 'Cyclic nucleotide phosphodiesterase (PDE) isozymes as targets of the intracellular signalling network: benefits of PDE inhibitors in various diseases and perspectives for future therapeutic developments', *Br J Pharmacol*. Blackwell Publishing Ltd, 165(5), pp. 1288–1305. doi: 10.1111/j.1476-5381.2011.01729.x.
- Keravis, Thérèse and Lugnier, C. (2012b) 'Cyclic nucleotide phosphodiesterase (PDE) isozymes as targets of the intracellular signalling network: Benefits of PDE inhibitors in various diseases and perspectives for future therapeutic developments', *British Journal of Pharmacology*, pp. 1288–1305. doi: 10.1111/j.1476-5381.2011.01729.x.
- Khan, A. *et al.* (2014) 'The physical association of the P2Y₁₂ receptor with PAR4 regulates arrestin-mediated akt activation', *Molecular Pharmacology*. American Society for Pharmacology and Experimental Therapy, 86(1), pp. 1–11. doi:

10.1124/mol.114.091595.

Khannpnavar, B. *et al.* (2020) 'Structure and function of adenylyl cyclases, key enzymes in cellular signaling', *Current Opinion in Structural Biology*. Elsevier Ltd, pp. 34–41. doi: 10.1016/j.sbi.2020.03.003.

Khoury, H. *et al.* (2018) 'Octadecyloxyethyl Adefovir Exhibits Potent in vitro and in vivo Cytotoxic Activity and Has Synergistic Effects with Ara-C in Acute Myeloid Leukemia', *Chemotherapy*. S. Karger AG, 63(4), pp. 225–237. doi: 10.1159/000491705.

Kim, M. *et al.* (2010) 'Frequent silencing of popeye domain-containing genes, BVES and POPDC3, is associated with promoter hypermethylation in gastric cancer', *Carcinogenesis*. Carcinogenesis, 31(9), pp. 1685–1693. doi: 10.1093/carcin/bgq144.

Kiriyama, Y. *et al.* (1997) 'Protein kinase A-dependent IL-6 production induced by calcitonin in human glioblastoma A172 cells', *Journal of Neuroimmunology*. J Neuroimmunol, 76(1–2), pp. 139–144. doi: 10.1016/S0165-5728(97)00044-1.

Klaasse, E. C. *et al.* (2008) 'Internalization and desensitization of adenosine receptors', *Purinergic Signalling*. Springer, pp. 21–37. doi: 10.1007/s11302-007-9086-7.

Klein, K. R., Matson, B. C. and Caron, K. M. (2016) 'The expanding repertoire of receptor activity modifying protein (RAMP) function', *Critical Reviews in Biochemistry and Molecular Biology*. Taylor and Francis Ltd, pp. 66–71. doi: 10.3109/10409238.2015.1128875.

Kliwer, A. *et al.* (2020) 'Morphine-induced respiratory depression is independent of β -arrestin2 signalling', *British Journal of Pharmacology*. John Wiley and Sons Inc., 177(13), pp. 2923–2931. doi: 10.1111/bph.15004.

Klotz, K. N. and Kachler, S. (2016) 'Inhibitors of membranous adenylyl cyclases with affinity for adenosine receptors', *Naunyn-Schmiedeberg's Archives of Pharmacology*. Springer Verlag, 389(3), pp. 349–352. doi: 10.1007/s00210-015-1197-z.

Knight, A. *et al.* (2016a) 'Discovery of Novel Adenosine Receptor Agonists That Exhibit Subtype Selectivity', *J Med Chem*. Systems Biology Doctoral Training Centre, University of Warwick, Coventry CV4 7AL, U.K. Department of Chemistry and Biochemistry, University of Bern, 3012 Bern, Switzerland. Division of Biomedical Cell Biology, Warwick Medical School, University of Warw, 59(3), pp. 947–964. doi: 10.1021/acs.jmedchem.5b01402.

Knight, A. *et al.* (2016b) 'Discovery of Novel Adenosine Receptor Agonists That Exhibit

Bibliography

- Subtype Selectivity', *J Med Chem*, 59(3), pp. 947–964. doi: 10.1021/acs.jmedchem.5b01402.
- Knight, W. and Yan, C. (2013) 'Therapeutic potential of PDE modulation in treating heart disease', *Future Med Chem*, 5(14), pp. 1607–1620. doi: 10.4155/fmc.13.127.
- Kochel, T. J. *et al.* (2017) 'Multiple drug resistance-associated protein (MRP4) exports prostaglandin E2 (PGE2) and contributes to metastasis in basal/ triple negative breast cancer', *Oncotarget*. Impact Journals LLC, 8(4), pp. 6540–6554. doi: 10.18632/oncotarget.14145.
- Komatsu, N. *et al.* (2011) 'Development of an optimized backbone of FRET biosensors for kinases and GTPases', *Molecular Biology of the Cell*. Mol Biol Cell, 22(23), pp. 4647–4656. doi: 10.1091/mbc.E11-01-0072.
- Komolov, K. E. and Benovic, J. L. (2018) 'G protein-coupled receptor kinases: Past, present and future', *Cellular Signalling*. Elsevier Inc., pp. 17–24. doi: 10.1016/j.cellsig.2017.07.004.
- Kooistra, A. J. *et al.* (2021) 'GPCRdb in 2021: Integrating GPCR sequence, structure and function', *Nucleic Acids Research*. Oxford University Press, 49(D1), pp. D335–D343. doi: 10.1093/nar/gkaa1080.
- Kostic, M. M. *et al.* (1997) 'Altered expression of PDE1 and PDE4 cyclic nucleotide phosphodiesterase isoforms in 7-oxo-prostacyclin-preconditioned rat heart', *J Mol Cell Cardiol*. 1998/02/28, 29(11), pp. 3135–3146. doi: 10.1006/jmcc.1997.0544.
- Krähling, A. M. *et al.* (2013) 'CRIS—A Novel cAMP-Binding Protein Controlling Spermiogenesis and the Development of Flagellar Bending', *PLoS Genetics*. Edited by G. S. McKnight. Public Library of Science, 9(12), p. e1003960. doi: 10.1371/journal.pgen.1003960.
- Kruh, G. D. and Belinsky, M. G. (2003) 'The MRP family of drug efflux pumps', *Oncogene*. Nature Publishing Group, pp. 7537–7552. doi: 10.1038/sj.onc.1206953.
- Kühn, H. and Dreyer, W. J. (1972) 'Light dependent phosphorylation of rhodopsin by ATP', *FEBS Letters*. John Wiley & Sons, Ltd, 20(1), pp. 1–6. doi: 10.1016/0014-5793(72)80002-4.
- Kull, B., Svenningsson, P. and Fredholm, B. B. (2000) 'Adenosine A(2A) receptors are colocalized with and activate G(olf) in rat striatum', *Molecular Pharmacology*. American Society for Pharmacology and Experimental Therapy, 58(4), pp. 771–

777. doi: 10.1124/mol.58.4.771.

- Kuo, J. F. and Greengard, P. (1969) 'Cyclic nucleotide-dependent protein kinases. IV. Widespread occurrence of adenosine 3',5'-monophosphate-dependent protein kinase in various tissues and phyla of the animal kingdom.', *Proceedings of the National Academy of Sciences of the United States of America*. Proc Natl Acad Sci U S A, 64(4), pp. 1349–1355. doi: 10.1073/pnas.64.4.1349.
- Kuwasako, K. *et al.* (2000) 'Visualization of the calcitonin receptor-like receptor and its receptor activity-modifying proteins during internalization and recycling', *Journal of Biological Chemistry*. J Biol Chem, 275(38), pp. 29602–29609. doi: 10.1074/jbc.M004534200.
- Kuzumaki, N. *et al.* (2012) 'Multiple Analyses of G-Protein Coupled Receptor (GPCR) Expression in the Development of Gefitinib-Resistance in Transforming Non-Small-Cell Lung Cancer', *PLoS ONE*. doi: 10.1371/journal.pone.0044368.
- Ladilov, Y. and Appukuttan, A. (2014) 'Role of soluble adenylyl cyclase in cell death and growth', *Biochim Biophys Acta*. 2014/07/11, 1842(12 Pt B), pp. 2646–2655. doi: 10.1016/j.bbadis.2014.06.034.
- Lauffer, B. E. L. *et al.* (2009) 'Engineered protein connectivity to actin mimics PDZ-dependent recycling of G protein-coupled receptors but not its regulation by Hrs', *Journal of Biological Chemistry*. J Biol Chem, 284(4), pp. 2448–2458. doi: 10.1074/jbc.M806370200.
- De Lean, A., Stadel, J. M. and Lefkowitz, R. J. (1980) 'A ternary complex model explains the agonist-specific binding properties of the adenylate cyclase-coupled β -adrenergic receptor', *Journal of Biological Chemistry*. Elsevier, 255(15), pp. 7108–7117. doi: 10.1016/s0021-9258(20)79672-9.
- Lebon, G. *et al.* (2011) 'Agonist-bound adenosine A2A receptor structures reveal common features of GPCR activation', *Nature*. 2011/05/20. MRC Laboratory of Molecular Biology, Hills Road, Cambridge CB2 0QH, UK., 474(7352), pp. 521–525. doi: 10.1038/nature10136.
- Lebon, G. *et al.* (2015) 'Molecular Determinants of CGS21680 Binding to the Human Adenosine A2A Receptor', *Mol Pharmacol*. 2015/03/13. Institut de Genomique Fonctionnelle, Centre National de la Recherche Scientifique, Unite Mixte de Recherche 5203, Institut National de la Sante et de la Recherche Medicale U1191, Universite de Montpellier, Montpellier, France (G.L.); and Medical Research C, 87(6), pp. 907–915. doi: 10.1124/mol.114.097360.
- Lee, E. S. *et al.* (2009) 'Estrogen and tamoxifen reverse manganese-induced

- glutamate transporter impairment in astrocytes', *J Neurochem.* 2009/05/21, 110(2), pp. 530–544. doi: 10.1111/j.1471-4159.2009.06105.x.
- Lee, K. *et al.* (2015) 'Validation of phosphodiesterase 10A as a cancer target', *Cancer Research*, 75. doi: 10.1158/1538-7445.Am2015-4360.
- Lee, K. *et al.* (2016) 'beta-catenin nuclear translocation in colorectal cancer cells is suppressed by PDE10A inhibition, cGMP elevation, and activation of PKG', *Oncotarget*. 2015/12/30, 7(5), pp. 5353–5365. doi: 10.18632/oncotarget.6705.
- Lee, M. E. *et al.* (2002) 'Crystal structure of phosphodiesterase 4D and inhibitor complex', *FEBS Letters*, 530(1–3), pp. 53–58. doi: 10.1016/S0014-5793(02)03396-3.
- Lee, S. Y. (2016) 'Temozolomide resistance in glioblastoma multiforme', *Genes Dis.* 2016/05/11, 3(3), pp. 198–210. doi: 10.1016/j.gendis.2016.04.007.
- Lee, Y. Y. *et al.* (2019) 'The phosphodiesterase 10 inhibitor papaverine exerts anti-inflammatory and neuroprotective effects via the PKA signaling pathway in neuroinflammation and Parkinson's disease mouse models', *Journal of Neuroinflammation*. BioMed Central Ltd., 16(1). doi: 10.1186/s12974-019-1649-3.
- Lefkimmiatis, K. *et al.* (2009) 'Store-operated cyclic AMP signalling mediated by STIM1', *Nature Cell Biology*. Nat Cell Biol, 11(4), pp. 433–442. doi: 10.1038/ncb1850.
- Lehár, J. *et al.* (2009) 'Synergistic drug combinations tend to improve therapeutically relevant selectivity', *Nature Biotechnology*. doi: 10.1038/nbt.1549.
- Lehmann, D. M., Seneviratne, A. M. P. B. and Smrcka, A. V (2008) 'Small Molecule Disruption of G Protein $\beta\gamma$ Subunit Signaling Inhibits Neutrophil Chemotaxis and Inflammation', *Molecular pharmacology*, 73(2), pp. 410–418. doi: 10.1124/mol.107.041780.
- Lenhart, P. M. *et al.* (2013) 'G-protein-coupled receptor 30 interacts with receptor activity-modifying protein 3 and confers sex-dependent cardioprotection', *Journal of Molecular Endocrinology*. J Mol Endocrinol, 51(1), pp. 191–202. doi: 10.1530/JME-13-0021.
- Leone, R. D. *et al.* (2018) 'Inhibition of the adenosine A2a receptor modulates expression of T cell coinhibitory receptors and improves effector function for enhanced checkpoint blockade and ACT in murine cancer models', *Cancer Immunology, Immunotherapy*. Springer Science and Business Media Deutschland GmbH, 67(8), pp. 1271–1284. doi: 10.1007/s00262-018-2186-0.

- De Lera Ruiz, M., Lim, Y. H. and Zheng, J. (2014) 'Adenosine A2A receptor as a drug discovery target', *Journal of Medicinal Chemistry*. American Chemical Society, 57(9), pp. 3623–3650. doi: 10.1021/jm4011669.
- Lerner, A. and Epstein, P. M. (2006) 'Cyclic nucleotide phosphodiesterases as targets for treatment of haematological malignancies', *Biochem J*. 2005/12/13, 393(Pt 1), pp. 21–41. doi: 10.1042/BJ20051368.
- Levy, J. H., Ramsay, J. and Bailey, J. M. (1990) 'Pharmacokinetics and pharmacodynamics of phosphodiesterase-III inhibitors', *Journal of Cardiothoracic Anesthesia*. W.B. Saunders, 4(6 SUPPL. 5), pp. 7–11. doi: 10.1016/0888-6296(90)90226-6.
- Li, D. *et al.* (2011) 'Arrestin-2 differentially regulates PAR4 and ADP receptor signaling in platelets', *Journal of Biological Chemistry*. J Biol Chem, 286(5), pp. 3805–3814. doi: 10.1074/jbc.M110.118018.
- Li, J. *et al.* (2007) 'Cyclic adenosine 5'-monophosphate-stimulated neurotensin secretion is mediated through Rap1 downstream of both Epac and protein kinase A signaling pathways', *Molecular Endocrinology*. Mol Endocrinol, 21(1), pp. 159–171. doi: 10.1210/me.2006-0340.
- Li, S. *et al.* (2020) 'Determination of PAR4 numbers on the surface of human platelets: no effect of the single nucleotide polymorphism rs773902', *Platelets*. Taylor and Francis Ltd. doi: 10.1080/09537104.2020.1810654.
- Li, X. *et al.* (2016) 'PI3K/Akt/mTOR signaling pathway and targeted therapy for glioblastoma', *Oncotarget*. 2016/03/12, 7(22), pp. 33440–33450. doi: 10.18632/oncotarget.7961.
- Li, Y. *et al.* (2016) 'Protein kinase A-independent Ras protein activation cooperates with Rap1 protein to mediate activation of the extracellular signal-regulated kinases (ERK) by cAMP', *Journal of Biological Chemistry*. American Society for Biochemistry and Molecular Biology Inc., 291(41), pp. 21584–21595. doi: 10.1074/jbc.M116.730978.
- Liang, Y. L. *et al.* (2018) 'Cryo-EM structure of the active, G s -protein complexed, human CGRP receptor', *Nature*. Nature Publishing Group, 561(7724), pp. 492–497. doi: 10.1038/s41586-018-0535-y.
- Limbird, L. E., Gill, D. M. and Lefkowitz, R. J. (1980) 'Agonist-promoted coupling of the β -adrenergic receptor with the guanine nucleotide regulatory protein of the adenylate cyclase system', *Proceedings of the National Academy of Sciences of the United States of America*. Proc Natl Acad Sci U S A, 77(2 II), pp. 775–

779. doi: 10.1073/pnas.77.2.775.
- Lin, Y. *et al.* (2013) 'ZIP4 is a novel molecular marker for glioma', *Neuro-Oncology*. doi: 10.1093/neuonc/not042.
- Lin, Y. C. *et al.* (2019) 'Selective Inhibition of PAR4 (Protease-Activated Receptor 4)-Mediated Platelet Activation by a Synthetic Nonanticoagulant Heparin Analog', *Arteriosclerosis, thrombosis, and vascular biology*. NLM (Medline), 39(4), pp. 694–703. doi: 10.1161/ATVBAHA.118.311758.
- Lindsey, A. S. *et al.* (2016) 'Abstract 4736: PDE10A overexpression in cancer cells and tumors as compared to normal cells and tissues', in. doi: 10.1158/1538-7445.am2016-4736.
- Lodish, H. *et al.* (2016) *Molecular Cell Biology*. 8th edn. Macmillan.
- Lohse, M. J., Nuber, S. and Hoffmann, C. (2012) 'Fluorescence/bioluminescence resonance energy transfer techniques to study g-protein-coupled receptor activation and signaling', *Pharmacological Reviews*. *Pharmacol Rev*, pp. 299–336. doi: 10.1124/pr.110.004309.
- Lombardi, M. Y. and Assem, M. (2017) 'Glioblastoma Genomics: A Very Complicated Story', in *Glioblastoma*. Codon Publications, pp. 3–25. doi: 10.15586/codon.glioblastoma.2017.ch1.
- Londos, C. and Wolff, J. (1977) 'Two distinct adenosine-sensitive sites on adenylate cyclase.', *Proceedings of the National Academy of Sciences of the United States of America*. *Proc Natl Acad Sci U S A*, 74(12), pp. 5482–5486. doi: 10.1073/pnas.74.12.5482.
- Lorenzen, E. *et al.* (2019a) 'Multiplexed analysis of the secretin-like GPCR-RAMP interactome', *Science Advances*. American Association for the Advancement of Science, 5(9), p. eaaw2778. doi: 10.1126/sciadv.aaw2778.
- Lorenzen, E. *et al.* (2019b) 'Multiplexed analysis of the secretin-like GPCR-RAMP interactome', *Science Advances*. American Association for the Advancement of Science, 5(9). doi: 10.1126/sciadv.aaw2778.
- Lugnier, C. (2006) 'Cyclic nucleotide phosphodiesterase (PDE) superfamily: A new target for the development of specific therapeutic agents', *Pharmacology and Therapeutics*. *Pharmacol Ther*, pp. 366–398. doi: 10.1016/j.pharmthera.2005.07.003.
- Lundby, A. *et al.* (2013) *In Vivo Phosphoproteomics Analysis Reveals the Cardiac Targets of β -Adrenergic Receptor Signaling*. Available at: www.SCIENCESIGNALING.org.

- Luo, D. *et al.* (2012) 'Reduced Popdc3 expression correlates with high risk and poor survival in patients with gastric cancer', *World Journal of Gastroenterology*. Baishideng Publishing Group Inc, 18(19), pp. 2423–2429. doi: 10.3748/wjg.v18.i19.2423.
- Lüscher, C. and Slesinger, P. A. (2010) 'Emerging roles for G protein-gated inwardly rectifying potassium (GIRK) channels in health and disease', *Nature Reviews Neuroscience*. Nature Publishing Group, pp. 301–315. doi: 10.1038/nrn2834.
- Luttrell, L. M. *et al.* (2001) 'Activation and targeting of extracellular signal-regulated kinases by β -arrestin scaffolds', *Proceedings of the National Academy of Sciences of the United States of America*. National Academy of Sciences, 98(5), pp. 2449–2454. doi: 10.1073/pnas.041604898.
- Lynch, M. J. *et al.* (2005) 'RNA silencing identifies PDE4D5 as the functionally relevant cAMP phosphodiesterase interacting with β arrestin to control the protein kinase A/AKAP79-mediated switching of the β 2-adrenergic receptor to activation of ERK in HEK293B2 cells', *Journal of Biological Chemistry*, 280(39), pp. 33178–33189. doi: 10.1074/jbc.M414316200.
- M. Hofer, A. (2012) 'Interactions Between Calcium and cAMP Signaling', *Current Medicinal Chemistry*. doi: 10.2174/092986712804143286.
- Ma, L. *et al.* (2018) 'A Highly Sensitive A-Kinase Activity Reporter for Imaging Neuromodulatory Events in Awake Mice', *Neuron*. Cell Press, 99(4), pp. 665–679.e5. doi: 10.1016/j.neuron.2018.07.020.
- Ma, L., Hollenberg, M. D. and Wallace, J. L. (2001) 'Thrombin-induced platelet endostatin release is blocked by a proteinase activated receptor-4 (PAR4) antagonist', *British Journal of Pharmacology*. John Wiley and Sons Inc., 134(4), pp. 701–704. doi: 10.1038/sj.bjp.0704312.
- Mackie, D. I. *et al.* (2019) 'RAMP3 determines rapid recycling of atypical chemokine receptor-3 for guided angiogenesis', *Proceedings of the National Academy of Sciences of the United States of America*, 116(48), pp. 24093–24099. doi: 10.1073/pnas.1905561116.
- Maiello, I. *et al.* (2012) 'Termination and activation of store-operated cyclic AMP production', *Journal of Cellular and Molecular Medicine*, 16(11), pp. 2715–2725. doi: 10.1111/j.1582-4934.2012.01592.x.
- Mamelak, A. N. and Jacoby, D. B. (2007) 'Targeted delivery of antitumoral therapy to glioma and other malignancies with synthetic chlorotoxin (TM-601)', *Expert Opin Drug Deliv*. 2007/03/06, 4(2), pp. 175–186. doi: 10.1517/17425247.4.2.175.

Bibliography

- Mangmool, S. and Kurose, H. (2011) 'Gi/o protein-dependent and -independent actions of pertussis toxin (ptx)', *Toxins*. Multidisciplinary Digital Publishing Institute (MDPI), 3(7), pp. 884–899. doi: 10.3390/toxins3070884.
- Manning, G. *et al.* (2002) 'The protein kinase complement of the human genome', *Science*. American Association for the Advancement of Science, pp. 1912–1934. doi: 10.1126/science.1075762.
- Mao, H. *et al.* (2012) 'Deregulated signaling pathways in glioblastoma multiforme: molecular mechanisms and therapeutic targets', *Cancer Invest.* 2012/01/13, 30(1), pp. 48–56. doi: 10.3109/07357907.2011.630050.
- Marti-Solano, M. *et al.* (2020) 'Combinatorial expression of GPCR isoforms affects signalling and drug responses', *Nature*. Nature Research, 587(7835), pp. 650–656. doi: 10.1038/s41586-020-2888-2.
- Masetto, F. *et al.* (2020) 'MRP5 nitration by NO-releasing gemcitabine encapsulated in liposomes confers sensitivity in chemoresistant pancreatic adenocarcinoma cells', *Biochimica et Biophysica Acta - Molecular Cell Research*. Elsevier B.V., 1867(12), p. 118824. doi: 10.1016/j.bbamcr.2020.118824.
- Matthews, J. M. and Sunde, M. (2012) 'Dimers, oligomers, everywhere', *Advances in Experimental Medicine and Biology*. Springer New York LLC, pp. 1–18. doi: 10.1007/978-1-4614-3229-6_1.
- McCahill, A. *et al.* (2005) 'In resting COS1 cells a dominant negative approach shows that specific, anchored PDE4 cAMP phosphodiesterase isoforms gate the activation, by basal', *Elsevier*. Available at: <https://www.sciencedirect.com/science/article/pii/S0898656805000835> (Accessed: 19 March 2021).
- McCudden, C. R. *et al.* (2005) 'G-protein signaling: Back to the future', *Cellular and Molecular Life Sciences*. Cell Mol Life Sci, pp. 551–577. doi: 10.1007/s00018-004-4462-3.
- McCurdy, R. D., McGrath, J. J. and Mackay-Sim, A. (2008) 'Validation of the comparative quantification method of real-time PCR analysis and a cautionary tale of housekeeping gene selection', *Gene Therapy and Molecular Biology*.
- McDonald, P. H. (2000) 'beta -Arrestin 2: A Receptor-Regulated MAPK Scaffold for the Activation of JNK3', *Science*. American Association for the Advancement of Science (AAAS), 290(5496), pp. 1574–1577. doi: 10.1126/science.290.5496.1574.
- McLatchie, L. M. *et al.* (1998) 'RAMPS regulate the transport and ligand specificity of

- the calcitonin- receptor-like receptor', *Nature*. *Nature*, 393(6683), pp. 333–339. doi: 10.1038/30666.
- Mebratu, Y. and Tesfaigzi, Y. (2009) 'How ERK1/2 activation controls cell proliferation and cell death is subcellular localization the answer?', *Cell Cycle*. Taylor and Francis Inc., pp. 1168–1175. doi: 10.4161/cc.8.8.8147.
- Mediavilla-Varela, M. *et al.* (2013) 'Antagonism of adenosine A2A receptor expressed by lung adenocarcinoma tumor cells and cancer associated fibroblasts inhibits their growth', *Cancer Biol Ther*. 2013/08/07. Department of Immunology; H. Lee Moffitt Cancer Center; Tampa, FL USA. Anatomic Pathology Department; H. Lee Moffitt Cancer Center; Tampa, FL USA. Translational Research Core; Clinical Pharmacology Lab; H. Lee Moffitt Cancer Center; Tampa, FL USA. *Departm*, 14(9), pp. 860–868. doi: 10.4161/cbt.25643.
- Meester, B. J. *et al.* (1998) 'Pharmacological analysis of the activity of the adenosine uptake inhibitor, dipyridamole, on the sinoatrial and atrioventricular nodes of the guinea-pig', *British Journal of Pharmacology*. *Br J Pharmacol*, 124(4), pp. 729–741. doi: 10.1038/sj.bjp.0701892.
- Mehta, A. and Patel, B. M. (2019) 'Therapeutic opportunities in colon cancer: Focus on phosphodiesterase inhibitors', *Life Sciences*. doi: 10.1016/j.lfs.2019.05.043.
- Melani, A. *et al.* (2014) 'Low doses of the selective adenosine A2A receptor agonist CGS21680 are protective in a rat model of transient cerebral ischemia', *Brain Research*. *Brain Res*, 1551, pp. 59–72. doi: 10.1016/j.brainres.2014.01.014.
- Meloche, S. and Pouysse´gur, J. P. (2007) 'The ERK1/2 mitogen-activated protein kinase pathway as a master regulator of the G1-to S-phase transition', *Oncogene*, 26, pp. 3227–3239. doi: 10.1038/sj.onc.1210414.
- Menniti, F. S., Faraci, W. S. and Schmidt, C. J. (2006) 'Phosphodiesterases in the CNS: targets for drug development', *Nat Rev Drug Discov*, 5(8), pp. 660–670. doi: 10.1038/nrd2058.
- Merighi, S. *et al.* (2002) 'Adenosine receptors as mediators of both cell proliferation and cell death of cultured human melanoma cells', *Journal of Investigative Dermatology*. *J Invest Dermatol*, 119(4), pp. 923–933. doi: 10.1046/j.1523-1747.2002.00111.x.
- Meyer, M. R. *et al.* (2000) 'A cGMP-signaling pathway in a subset of olfactory sensory neurons', *Proceedings of the National Academy of Sciences of the United States of America*. *National Academy of Sciences*, 97(19), pp. 10595–10600. doi: 10.1073/pnas.97.19.10595.

- Milligan, G. and Kostenis, E. (2006) 'Heterotrimeric G-proteins: A short history', *British Journal of Pharmacology*. Br J Pharmacol. doi: 10.1038/sj.bjp.0706405.
- Mohri, M., Nitta, H. and Yamashita, J. (2000) 'Expression of multidrug resistance-associated protein (MRP) in human gliomas', *Journal of Neuro-Oncology*. doi: 10.1023/A:1026528926482.
- Mokhtari, R. B. *et al.* (2017) 'Combination therapy in combating cancer', *Oncotarget*. Impact Journals LLC, pp. 38022–38043. doi: 10.18632/oncotarget.16723.
- Monopoli, A. *et al.* (1994) *Pharmacology of the new selective A2a adenosine receptor agonist 2-hexynyl-5'-N-ethylcarboxamidoadenosine* - PubMed. Available at: <https://pubmed.ncbi.nlm.nih.gov/7848347/> (Accessed: 3 March 2021).
- Moon, E. Y. *et al.* (2012) 'Phosphodiesterase inhibitors control A172 human glioblastoma cell death through cAMP-mediated activation of protein kinase A and Epac1/Rap1 pathways', *Life Sciences*, 90(9–10), pp. 373–380. doi: 10.1016/j.lfs.2011.12.010.
- Moorthy, B. S., Gao, Y. and Anand, G. S. (2011) 'Phosphodiesterases catalyze hydrolysis of cAMP-bound to regulatory subunit of protein kinase A and mediate signal termination', *Mol Cell Proteomics*, 10(2), p. M110 002295. doi: 10.1074/mcp.M110.002295.
- Morgan, A. J., Murray, K. J. and Challiss, R. A. (1993) 'Comparison of the effect of isobutylmethylxanthine and phosphodiesterase-selective inhibitors on cAMP levels in SH-SY5Y neuroblastoma cells', *Biochem Pharmacol.* 1993/06/22, 45(12), pp. 2373–2380. doi: 10.1016/0006-2952(93)90216-j.
- Morikawa, Y. *et al.* (2018) 'Protease-activated receptor-4 (PAR4) variant influences on platelet reactivity induced by PAR4-activating peptide through altered Ca²⁺ mobilization and ERK phosphorylation in healthy Japanese subjects', *Thrombosis Research*. Elsevier Ltd, 162, pp. 44–52. doi: 10.1016/j.thromres.2017.12.014.
- Moschonas, I. C. *et al.* (2017) 'Molecular requirements involving the human platelet protease-activated receptor-4 mechanism of activation by peptide analogues of its tethered-ligand', *Platelets*. Taylor and Francis Ltd, 28(8), pp. 812–821. doi: 10.1080/09537104.2017.1282607.
- Moussatova, A. *et al.* (2008) 'ATP-binding cassette transporters in Escherichia coli', *Biochimica et Biophysica Acta - Biomembranes*. Elsevier, pp. 1757–1771. doi: 10.1016/j.bbamem.2008.06.009.
- Mundell, S. J., Benovic, J. L. and Kelly, E. (1997) 'A dominant negative mutant of the

Bibliography

- G protein-coupled receptor kinase 2 selectively attenuates adenosine A₂ receptor desensitization', *Molecular Pharmacology*. American Society for Pharmacology and Experimental Therapy, 51(6), pp. 991–998. doi: 10.1124/mol.51.6.991.
- Mundell, S. J. and Kelly, E. (1998) 'Evidence for co-expression and desensitization of A_{2a} and A_{2b} adenosine receptors in NG108-15 cells', *Biochemical Pharmacology*. *Biochem Pharmacol*, 55(5), pp. 595–603. doi: 10.1016/S0006-2952(97)00466-8.
- Murray, A. J. (2008) 'Pharmacological PKA inhibition: All may not be what it seems', *Science Signaling*. doi: 10.1126/scisignal.122re4.
- Murthy, K. S., Zhou, H. and Makhlof, G. M. (2002) 'PKA-dependent activation of PDE3A and PDE4 and inhibition of adenylyl cyclase V/VI in smooth muscle', *American Journal of Physiology - Cell Physiology*. American Physiological Society, 282(3 51-3). doi: 10.1152/ajpcell.00373.2001.
- Nagano, N. *et al.* (1993) 'Invasion of experimental rat brain tumor: early morphological changes following microinjection of C6 glioma cells', *Acta Neuropathologica*. doi: 10.1007/BF00334878.
- Nagi, K. and Habib, A. M. (2021) 'Biased signaling: A viable strategy to drug ghrelin receptors for the treatment of obesity.', *Cellular signalling*, p. 109976. doi: 10.1016/j.cellsig.2021.109976.
- Natarajan, K. and Berk, B. C. (2006) 'Crosstalk coregulation mechanisms of G protein-coupled receptors and receptor tyrosine kinases.', *Methods in molecular biology (Clifton, N.J.)*. Humana Press, pp. 51–77. doi: 10.1385/1-59745-048-0:51.
- Naviglio, S. *et al.* (2010) 'Leptin potentiates antiproliferative action of cAMP elevation via protein kinase A down-regulation in breast cancer cells', *Journal of Cellular Physiology*, 225(3), pp. 801–809. doi: 10.1002/jcp.22288.
- Nawrocki, A. R. *et al.* (2014) 'Genetic deletion and pharmacological inhibition of phosphodiesterase 10A protects mice from diet-induced obesity and insulin resistance', *Diabetes*. doi: 10.2337/db13-0247.
- Newton, A. C., Bootman, M. D. and Scott, J. (2016) 'Second messengers', *Cold Spring Harbor Perspectives in Biology*. Cold Spring Harbor Laboratory Press, 8(8). doi: 10.1101/cshperspect.a005926.
- Niccolini, F. *et al.* (2015) 'Altered PDE10A expression detectable early before symptomatic onset in Huntington's disease', *Brain*. doi: 10.1093/brain/awv214.
- Nichols, J. M. *et al.* (2015) "Store-operated" cAMP signaling contributes to Ca²⁺-

- activated Cl⁻ secretion in T84 colonic cells', *American Journal of Physiology - Gastrointestinal and Liver Physiology*. American Physiological Society, 309(8), pp. G670–G679. doi: 10.1152/ajpgi.00214.2015.
- Nikolova, S. *et al.* (2010) 'Phosphodiesterase 6 subunits are expressed and altered in idiopathic pulmonary fibrosis', *Respiratory Research*. doi: 10.1186/1465-9921-11-146.
- Noguera, M. A. *et al.* (2001) 'Role of cyclic nucleotide phosphodiesterase isoenzymes in contractile responses of denuded rat aorta related to various Ca²⁺ sources', *Naunyn-Schmiedeberg's Archives of Pharmacology*. Naunyn Schmiedebergs Arch Pharmacol, 363(6), pp. 612–619. doi: 10.1007/s002100100397.
- Nozal, V. *et al.* (2021) 'Improved Controlled Release and Brain Penetration of the Small Molecule S14 Using PLGA Nanoparticles †'. doi: 10.3390/ijms22063206.
- Nuki, C. *et al.* (1993) 'Vasodilator effect of adrenomedullin and calcitonin gene-related peptide receptors in rat mesenteric vascular beds', *Biochemical and Biophysical Research Communications*. Biochem Biophys Res Commun, 196(1), pp. 245–251. doi: 10.1006/bbrc.1993.2241.
- Nürnberg, B., Gudermann, T. and Schultz, G. (1995) 'Receptors and G proteins as primary components of transmembrane signal transduction - Part 2. G proteins: structure and function', *Journal of Molecular Medicine*. Springer-Verlag, pp. 123–132. doi: 10.1007/BF00198240.
- O'Connell, J. C. *et al.* (1996) 'The SH3 domain of Src tyrosyl protein kinase interacts with the N-terminal splice region of the PDE4A cAMP-specific phosphodiesterase RPDE-6 (RNPDE4A5)', *Biochemical Journal*. doi: 10.1042/bj3180255.
- Oehler, M. K. *et al.* (2001) 'Adrenomedullin inhibits hypoxic cell death by upregulation of Bcl-2 in endometrial cancer cells: A possible promotion mechanism for tumour growth', *Oncogene*. Oncogene, 20(23), pp. 2937–2945. doi: 10.1038/sj.onc.1204422.
- Oestreich, E. A. *et al.* (2007) 'Epac-mediated activation of phospholipase C ϵ plays a critical role in β -adrenergic receptor-dependent enhancement of Ca²⁺ mobilization in cardiac myocytes', *Journal of Biological Chemistry*. J Biol Chem, 282(8), pp. 5488–5495. doi: 10.1074/jbc.M608495200.
- Offermanns, S. and Simon, M. I. (1995) 'G α 15 and G α 16 couple a wide variety of receptors to phospholipase C', *Journal of Biological Chemistry*. American Society for Biochemistry and Molecular Biology Inc., 270(25), pp. 15175–15180.

doi: 10.1074/jbc.270.25.15175.

- Ohta, A. *et al.* (2006) 'A2A adenosine receptor protects tumors from antitumor T cells', *Proceedings of the National Academy of Sciences of the United States of America*. doi: 10.1073/pnas.0605251103.
- Ohta, Akio *et al.* (2012) 'The development and immunosuppressive functions of CD4+ CD25+ FoxP3+ regulatory T cells are under influence of the adenosine-A2A adenosine receptor pathway', *Frontiers in Immunology*. *Front Immunol*, 3(JUL). doi: 10.3389/fimmu.2012.00190.
- Okashah, N. *et al.* (2020) 'Agonist-induced formation of unproductive receptor-G12 complexes', *Proceedings of the National Academy of Sciences of the United States of America*. National Academy of Sciences, 117(35), pp. 21723–21730. doi: 10.1073/pnas.2003787117.
- Omar, B. *et al.* (2009) 'Regulation of AMP-activated protein kinase by cAMP in adipocytes: Roles for phosphodiesterases, protein kinase B, protein kinase A, Epac and lipolysis', *Cellular Signalling*. Pergamon, 21(5), pp. 760–766. doi: 10.1016/j.cellsig.2009.01.015.
- Omori, K and Kotera, J. (2007a) 'Overview of PDEs and their regulation', *Circ Res*. 2007/02/20, 100(3), pp. 309–327. doi: 10.1161/01.RES.0000256354.95791.f1.
- Omori, Kenji and Kotera, J. (2007) 'Overview of PDEs and their regulation', *Circulation Research*. 2007/02/20, 100(3), pp. 309–327. doi: 10.1161/01.RES.0000256354.95791.f1.
- Omori, K and Kotera, J. (2007b) 'Overview of PDEs and their regulation', *Circulation Research*, 100(3), pp. 309–327. doi: 10.1161/01.RES.0000256354.95791.f1.
- Ostrovskaya, A. *et al.* (2016) 'Calcitonin', in *The Curated Reference Collection in Neuroscience and Biobehavioral Psychology*. Elsevier Science Ltd., pp. 220–230. doi: 10.1016/B978-0-12-809324-5.03223-5.
- Ostrovskaya, A. *et al.* (2019) 'Expression and activity of the calcitonin receptor family in a sample of primary human high-grade gliomas', *BMC Cancer*. BioMed Central Ltd., 19(1). doi: 10.1186/s12885-019-5369-y.
- Overington, J. P., Al-Lazikani, B. and Hopkins, A. L. (2006) 'Opinion - How many drug targets are there?', *Nature Reviews Drug Discovery*, 5(12), pp. 993–996. doi: 10.1038/nrd2199.
- Paccauds, J.-P. *et al.* (1993) *THE JOURNAL OF BIOLOGICAL CHEMISTRY* Clathrin-coated Pit-mediated Receptor Internalization ROLE OF INTERNALIZATION SIGNALS AND RECEPTOR MOBILITY*, *The Journal of Biological Chemistry*.

- doi: 10.1016/S0021-9258(19)49446-5.
- Pawson, T. and Scott, J. D. (1997) 'Signaling through scaffold, anchoring, and adaptor proteins', *Science*. *Science*, 278(5346), pp. 2075–2080. doi: 10.1126/science.278.5346.2075.
- Pei, H. and Linden, J. (2016) 'Adenosine influences myeloid cells to inhibit aeroallergen sensitization', *American Journal of Physiology - Lung Cellular and Molecular Physiology*. American Physiological Society, 310(10), pp. L985–L992. doi: 10.1152/ajplung.00330.2015.
- Peitzsch, R. M. and McLaughlin, S. (1993) 'Binding of Acylated Peptides and Fatty Acids to Phospholipid Vesicles: Pertinence to Myristoylated Proteins', *Biochemistry*. *Biochemistry*, 32(39), pp. 10436–10443. doi: 10.1021/bi00090a020.
- Peng, Q. *et al.* (2021) 'Functional evidence for biased inhibition of G protein signaling by YM-254890 in human coronary artery endothelial cells', *European Journal of Pharmacology*. Elsevier B.V., 891, p. 173706. doi: 10.1016/j.ejphar.2020.173706.
- Pereira, L. *et al.* (2007) 'The cAMP binding protein Epac modulates Ca²⁺ sparks by a Ca²⁺/calmodulin kinase signalling pathway in rat cardiac myocytes', *Journal of Physiology*. *J Physiol*, 583(2), pp. 685–694. doi: 10.1113/jphysiol.2007.133066.
- Perry, M., biology, G. H.-C. opinion in chemical and 1998, undefined (no date) 'Chemotherapeutic potential of phosphodiesterase inhibitors', *Elsevier*. Available at: <https://www.sciencedirect.com/science/article/pii/S1367593198801233> (Accessed: 19 March 2021).
- Pham, N. *et al.* (2000) 'The guanine nucleotide exchange factor CNrasGEF activates Ras in response to cAMP and cGMP', *Current Biology*. Current Biology Ltd, 10(9), pp. 555–558. doi: 10.1016/S0960-9822(00)00473-5.
- Pierce, K. L., Premont, R. T. and Lefkowitz, R. J. (2002) 'Seven-transmembrane receptors', *Nature Reviews Molecular Cell Biology*, pp. 639–650. doi: 10.1038/nrm908.
- Pioszak, A. A. and Hay, D. L. (2020) 'RAMPs as allosteric modulators of the calcitonin and calcitonin-like class B G protein-coupled receptors', in *Advances in Pharmacology*. Academic Press Inc., pp. 115–141. doi: 10.1016/bs.apha.2020.01.001.
- Pitcher, J. A. *et al.* (1999) 'Feedback inhibition of G protein-coupled receptor kinase 2

- (GRK2) activity by extracellular signal-regulated kinases', *Journal of Biological Chemistry*. *J Biol Chem*, 274(49), pp. 34531–34534. doi: 10.1074/jbc.274.49.34531.
- Pitcher, J. A., Freedman, N. J. and Lefkowitz, R. J. (1998) *G PROTEIN-COUPLED RECEPTOR KINASES*. Available at: www.annualreviews.org (Accessed: 3 April 2021).
- Podda, M. V. (2013) 'Article in Pflügers Archiv', *European Journal of Physiology*. doi: 10.1007/s00424-013-1373-2.
- Poyner, D. R. *et al.* (2002) 'International Union of Pharmacology. XXXII. The mammalian calcitonin gene-related peptides, adrenomedullin, amylin, and calcitonin receptors', *Pharmacological Reviews*. American Society for Pharmacology and Experimental Therapy, pp. 233–246. doi: 10.1124/pr.54.2.233.
- Preti, D. *et al.* (2015) 'History and Perspectives of A2A Adenosine Receptor Antagonists as Potential Therapeutic Agents', *Medicinal Research Reviews*. John Wiley and Sons Inc., 35(4), pp. 790–848. doi: 10.1002/med.21344.
- Prévost, G. P. *et al.* (2006) 'Anticancer activity of BIM-46174, a new inhibitor of the heterotrimeric Gα/Gβγ protein complex', *Cancer Research*. American Association for Cancer Research, 66(18), pp. 9227–9234. doi: 10.1158/0008-5472.CAN-05-4205.
- Public Health England (2014) *Incidence and outcomes for cerebral Glioblastoma in England*. Available at: [http://www.ncin.org.uk/view?rid=2662#:~:text=Around 55%25 of malignant \(ie,IV\) brain tumours are GBMs.&text=GBM has an extremely poor,median survival ~ 6 months](http://www.ncin.org.uk/view?rid=2662#:~:text=Around 55%25 of malignant (ie,IV) brain tumours are GBMs.&text=GBM has an extremely poor,median survival ~ 6 months)) (Accessed: 15 October 2020).
- Putney, J. W. (2009) 'SOC: Now also store-operated cyclase', *Nature Cell Biology*, 11(4), pp. 381–382. doi: 10.1038/ncb0409-381.
- Quinn, S. N. *et al.* (2017) 'Adenylyl cyclase 3/adenylyl cyclase-associated protein 1 (CAP1) complex mediates the anti-migratory effect of forskolin in pancreatic cancer cells', *Molecular Carcinogenesis*. John Wiley and Sons Inc., 56(4), pp. 1344–1360. doi: 10.1002/mc.22598.
- Rahman, S. (2020) *Drug repurposing against the store-operated calcium entry (SOCE) pathway and subsequent exploration of SOCE in oligodendrocyte progenitor cells*. University of Cambridge.
- Rahman, S. and Rahman, T. (2017) 'Unveiling some FDA-Approved drugs as inhibitors of the store-operated Ca²⁺ entry pathway', *Scientific Reports*. doi:

- 10.1038/s41598-017-13343-x.
- Rall, T. W. and Sutherland, E. W. (1958) *FORMATION OF A CYCLIC ADENINE RIBONUCLEOTIDE BY TISSUE PARTICLES**, *Journal of Biological Chemistry*. doi: 10.1016/S0021-9258(19)77422-5.
- Rama, A. R. *et al.* (2014) 'ABC transporters as differentiation markers in glioblastoma cells', *Molecular Biology Reports*. doi: 10.1007/s11033-014-3423-z.
- Ramachandran, R. *et al.* (2017) 'Targeting a proteinase-activated receptor 4 (PAR4) carboxyl terminal motif to regulate platelet function', *Molecular Pharmacology*. American Society for Pharmacology and Experimental Therapy, 91(4), pp. 287–295. doi: 10.1124/mol.116.106526.
- Ramkumar, V. *et al.* (1991) 'Distinct pathways of desensitization of A1- and A2-adenosine receptors in DDT1 MF-2 cells', *Molecular Pharmacology*. NIH Public Access, 40(5), pp. 639–647. Available at: [/pmc/articles/PMC5602552/](#) (Accessed: 4 April 2021).
- Ramsay, R. R. *et al.* (2018) 'A perspective on multi-target drug discovery and design for complex diseases', *Clinical and Translational Medicine*. Wiley, 7(1). doi: 10.1186/s40169-017-0181-2.
- Rang, H. P. (2006) 'The receptor concept: Pharmacology's big idea', *British Journal of Pharmacology*. Wiley-Blackwell, p. S9. doi: 10.1038/sj.bjp.0706457.
- Rappaport, J. A. and Waldman, S. A. (2018) 'The guanylate cyclase C-cGMP signaling axis opposes intestinal epithelial injury and neoplasia', *Frontiers in Oncology*. Frontiers Media S.A., p. 299. doi: 10.3389/fonc.2018.00299.
- Rarick, H. M., Artemyev, N. O and Hamm, H. E. (no date) *A Site on Rod G Protein α Subunit That Mediates Effector Activation*, [science.sciencemag.org](#). Available at: <http://science.sciencemag.org/> (Accessed: 23 March 2021).
- Rasmussen, H. (1970) 'Cell communication, calcium ion, and cyclic adenosine monophosphate', *Science*. American Association for the Advancement of Science, 170(3956), pp. 404–412. doi: 10.1126/science.170.3956.404.
- Reczek, D., Berryman, M. and Bretscher, A. (1997) 'Identification of EPB50: A PDZ-containing phosphoprotein that associates with members of the ezrin-radixin-moesin family', *Journal of Cell Biology*. J Cell Biol, 139(1), pp. 169–179. doi: 10.1083/jcb.139.1.169.
- Rekers, N. H., Sminia, P. and Peters, G. J. (2011) 'Towards Tailored therapy of glioblastoma multiforme', *Journal of Chemotherapy*. doi: 10.1179/joc.2011.23.4.187.

- Rickles, R. J. *et al.* (2010) 'Adenosine A2A receptor agonists and PDE inhibitors: a synergistic multitarget mechanism discovered through systematic combination screening in B-cell malignancies', *Blood*, 116(4), pp. 593–602. doi: 10.1182/blood-2009-11-252668.
- Ringheim, G. E. and Taylor, S. S. (1990) 'Effects of cAMP-binding site mutations on intradomain cross-communication in the regulatory subunit of cAMP-dependent protein kinase I', *J Biol Chem.* 1990/11/15, 265(32), pp. 19472–19478. Available at: <https://www.ncbi.nlm.nih.gov/pubmed/2174038>.
- Rizzuto, R. *et al.* (2003) 'Calcium and apoptosis: Facts and hypotheses', *Oncogene*. Nature Publishing Group, pp. 8619–8627. doi: 10.1038/sj.onc.1207105.
- Romero, G. G. (2014) 'The Role of the Cell Background in Biased Signaling', in *Biased Signaling in Physiology, Pharmacology and Therapeutics*. Elsevier Inc., pp. 41–79. doi: 10.1016/B978-0-12-411460-9.00002-1.
- de Rooij, J. *et al.* (1998) 'Epac is a Rap1 guanine-nucleotide-exchange factor directly activated by cyclic AMP', *Nature*, 396(6710), pp. 474–477.
- De Rooij, J. *et al.* (2000) 'Mechanism of regulation of the Epac family of cAMP-dependent RapGEFs', *Journal of Biological Chemistry*. J Biol Chem, 275(27), pp. 20829–20836. doi: 10.1074/jbc.M001113200.
- Rorsman, P., Braun, M. and Zhang, Q. (2012) 'Regulation of calcium in pancreatic α - and β -cells in health and disease', *Cell Calcium*. doi: 10.1016/j.ceca.2011.11.006.
- Rosenbaum, D. M., Rasmussen, S. G. F. and Kobilka, B. K. (2009) 'The structure and function of G-protein-coupled receptors', *Nature*. NIH Public Access, pp. 356–363. doi: 10.1038/nature08144.
- Rowley, J. W. *et al.* (2011) 'Genome-wide RNA-seq analysis of human and mouse platelet transcriptomes', *Blood*. American Society of Hematology, 118(14), pp. e101–e111. doi: 10.1182/blood-2011-03-339705.
- Ruggiero, A. *et al.* (2017) 'Hypersensitivity to carboplatin in children with malignancy', *Frontiers in Pharmacology*. doi: 10.3389/fphar.2017.00201.
- Russwurm, C., Koesling, D. and Russwurm, M. (2015) 'Phosphodiesterase 10A is tethered to a synaptic signaling complex in striatum', *Journal of Biological Chemistry*. American Society for Biochemistry and Molecular Biology Inc., 290(19), pp. 11936–11947. doi: 10.1074/jbc.M114.595769.
- Sachdeva, S. and Gupta, M. (2013) 'Adenosine and its receptors as therapeutic targets: An overview', *Saudi Pharm J*, 21(3), pp. 245–253. doi:

Bibliography

- 10.1016/j.jsps.2012.05.011.
- Safitri, D. *et al.* (2020) 'Elevated intracellular cAMP concentration mediates growth suppression in glioma cells', *Biochemical Pharmacology*, 174. doi: 10.1016/j.bcp.2020.113823.
- Sanada, K. and Tsai, L. H. (2005) 'G protein $\beta\gamma$ subunits and AGS3 control spindle orientation and asymmetric cell fate of cerebral cortical progenitors', *Cell*. Elsevier B.V., 122(1), pp. 119–131. doi: 10.1016/j.cell.2005.05.009.
- Sapio, L. *et al.* (2014) 'Targeting protein kinase a in cancer therapy: An update', *EXCLI Journal*. Leibniz Research Centre for Working Environment and Human Factors, pp. 843–855. doi: 10.17877/DE290R-6736.
- Sassi, Y. *et al.* (2008) 'Multidrug resistance-associated protein 4 regulates cAMP-dependent signaling pathways and controls human and rat SMC proliferation', *Journal of Clinical Investigation*. The American Society for Clinical Investigation, 118(8), pp. 2747–2757. doi: 10.1172/JCI35067.
- Sassone-Corsi, P. (2012) 'The Cyclic AMP pathway', *Cold Spring Harbor Perspectives in Biology*. Cold Spring Harbor Laboratory Press, 4(12). doi: 10.1101/cshperspect.a011148.
- Sattin, A. and Rall, T. W. (1970) 'The effect of adenosine and adenine nucleotides on the cyclic adenosine 3', 5'-phosphate content of guinea pig cerebral cortex slices.', *Molecular Pharmacology*, 6(1), pp. 13–23.
- Savai, R. *et al.* (2010a) 'Targeting cancer with phosphodiesterase inhibitors', *Expert Opin Investig Drugs*. 2009/12/17, 19(1), pp. 117–131. doi: 10.1517/13543780903485642.
- Savai, R. *et al.* (2010b) 'Targeting cancer with phosphodiesterase inhibitors', *Expert Opin Investig Drugs*. 2009/12/17, 19(1), pp. 117–131. doi: 10.1517/13543780903485642.
- Sawa, A. *et al.* (2017) 'Effects of sorafenib and an adenylyl cyclase activator on in vitro growth of well-differentiated thyroid cancer cells', *Endocr J*. doi: 10.1507/endocrj.EJ16-0525.
- Scapin, G. *et al.* (2004) 'Crystal structure of human phosphodiesterase 3B: Atomic basis for substrate and inhibitor specificity', *Biochemistry*, 43(20), pp. 6091–6100. doi: 10.1021/bi049868i.
- Schindelin, J. *et al.* (2012) 'Fiji: an open-source platform for biological-image analysis', *Nature Methods* 2012 9:7. Nature Publishing Group, 9(7), pp. 676–682. doi: 10.1038/nmeth.2019.

- Schmidt, C. J. *et al.* (1992) 'Specificity of G protein β and γ subunit interactions', *Journal of Biological Chemistry*. *J Biol Chem*, 267(20), pp. 13807–13810. doi: 10.1074/jbc.270.7.2946.
- Schmidt, C. J. *et al.* (2008) 'Preclinical characterization of selective phosphodiesterase 10A inhibitors: A new therapeutic approach to the treatment of schizophrenia', *Journal of Pharmacology and Experimental Therapeutics*. *J Pharmacol Exp Ther*, 325(2), pp. 681–690. doi: 10.1124/jpet.107.132910.
- Schmitz, A. L. *et al.* (2014) 'A cell-permeable inhibitor to trap G α_q proteins in the empty pocket conformation', *Chemistry and Biology*. Elsevier Ltd, 21(7), pp. 890–902. doi: 10.1016/j.chembiol.2014.06.003.
- Schönauer, R., Els-Heindl, S. and Beck-Sickinger, A. G. (2017) 'Adrenomedullin – new perspectives of a potent peptide hormone', *Journal of Peptide Science*. John Wiley and Sons Ltd, pp. 472–485. doi: 10.1002/psc.2953.
- Schulz, T. J. *et al.* (2006) 'Induction of oxidative metabolism by mitochondrial frataxin inhibits cancer growth: Otto Warburg revisited', *Journal of Biological Chemistry*. *J Biol Chem*, 281(2), pp. 977–981. doi: 10.1074/jbc.M511064200.
- Schwartzbaum, J. A. *et al.* (2006) 'Epidemiology and molecular pathology of glioma', *Nat Clin Pract Neurol*. 2006/08/26, 2(9), pp. 494–503; quiz 1 p following 516. doi: 10.1038/ncpneuro0289.
- Scicchitano, P. *et al.* (2012) 'HCN Channels and Heart Rate', *Molecules*. Molecular Diversity Preservation International, 17(4), pp. 4225–4235. doi: 10.3390/molecules17044225.
- Sebastiani, G. *et al.* (2018) 'G-protein-coupled receptors (GPCRs) in the treatment of diabetes: Current view and future perspectives', *Best Practice and Research: Clinical Endocrinology and Metabolism*. Bailliere Tindall Ltd, pp. 201–213. doi: 10.1016/j.beem.2018.02.005.
- Sebastiao, A. M. and Ribeiro, J. A. (2009) 'Adenosine receptors and the central nervous system', *Handb Exp Pharmacol*, (193), pp. 471–534. doi: 10.1007/978-3-540-89615-9_16.
- Sellers, Z. M. *et al.* (2012) 'MRP4 and CFTR in the regulation of cAMP and β -adrenergic contraction in cardiac myocytes', *European Journal of Pharmacology*. *Eur J Pharmacol*, 681(1–3), pp. 80–87. doi: 10.1016/j.ejphar.2012.02.018.
- Sengupta, R. *et al.* (2011) 'Treating brain tumors with PDE4 inhibitors', *Trends in Pharmacological Sciences*, 32(6), pp. 337–344. doi:

- 10.1016/j.tips.2011.02.015.
- Serafin, D. S. *et al.* (2020) 'Dawn of a New RAMPAGE', *Trends in Pharmacological Sciences*. Elsevier Ltd, pp. 249–265. doi: 10.1016/j.tips.2020.01.009.
- Sexton, P. M. *et al.* (2009) 'Modulating receptor function through RAMPs: can they represent drug targets in themselves?', *Drug Discovery Today*. Drug Discov Today, pp. 413–419. doi: 10.1016/j.drudis.2008.12.009.
- Shah, B. H. and Catt, K. J. (2004) 'GPCR-mediated transactivation of RTKs in the CNS: Mechanisms and consequences', *Trends in Neurosciences*. Elsevier Ltd, pp. 48–53. doi: 10.1016/j.tins.2003.11.003.
- Shapiro, M. J. *et al.* (2000) 'Protease-activated receptors 1 and 4 are shut off with distinct kinetics after activation by thrombin', *Journal of Biological Chemistry*. J Biol Chem, 275(33), pp. 25216–25221. doi: 10.1074/jbc.M004589200.
- Shchepinova, M. M. *et al.* (2020) 'Chemical biology of noncanonical G protein–coupled receptor signaling: Toward advanced therapeutics', *Current Opinion in Chemical Biology*. Elsevier Ltd, pp. 98–110. doi: 10.1016/j.cbpa.2020.04.012.
- Shenoy, S. K. and Lefkowitz, R. J. (2005) 'Seven-transmembrane receptor signaling through beta-arrestin', *Sci STKE*. 2005/11/04, 2005(308), p. cm10. doi: 10.1126/stke.2005/308/cm10.
- Shi, Q. *et al.* (2017) 'Heterologous desensitization of cardiac β -adrenergic signal via hormone-induced β AR/arrestin/PDE4 complexes', *Cardiovascular Research*. Oxford University Press, 113(6), pp. 656–670. doi: 10.1093/cvr/cvx036.
- Silver, P. J. (1989) 'Biochemical aspects of inhibition of cardiovascular low (Km) cyclic adenosine monophosphate phosphodiesterase', *The American Journal of Cardiology*. Am J Cardiol, 63(2). doi: 10.1016/0002-9149(89)90384-6.
- Simms, J. *et al.* (2009) 'Structure-function analysis of RAMP1 by alanine mutagenesis', *Biochemistry*. Biochemistry, 48(1), pp. 198–205. doi: 10.1021/bi801869n.
- Simon, M. I., Strathmann, M. P. and Gautam, N. (1991) 'Diversity of G proteins in signal transduction', *Science*. Science, 252(5007), pp. 802–808. doi: 10.1126/science.1902986.
- Singh, S. and Tandon, J. S. (1982) 'Coleonol and forskolin from *Coleus forskohlii*', *Planta Medica*. Planta Med, 45(1), pp. 62–63. doi: 10.1055/s-2007-971249.
- Siuciak, J. A. *et al.* (2006) 'Inhibition of the striatum-enriched phosphodiesterase PDE10A: A novel approach to the treatment of psychosis', *Neuropharmacology*. doi: 10.1016/j.neuropharm.2006.04.013.
- Smith, J. S. *et al.* (2021) 'Noncanonical scaffolding of G α i and β -arrestin by G protein–

- coupled receptors', *Science*. American Association for the Advancement of Science (AAAS), p. eaay1833. doi: 10.1126/science.aay1833.
- Smith, J. S., Lefkowitz, R. J. and Rajagopal, S. (2018) 'Biased signalling: From simple switches to allosteric microprocessors', *Nature Reviews Drug Discovery*. doi: 10.1038/nrd.2017.229.
- Smith, T. H. *et al.* (2016) 'Protease-activated Receptor-4 Signaling and Trafficking Is Regulated by the Clathrin Adaptor Protein Complex-2 Independent of β -Arrestins', *Journal of Biological Chemistry*. American Society for Biochemistry and Molecular Biology Inc., 291(35), pp. 18453–18464. doi: 10.1074/jbc.M116.729285.
- Smith, T. H. *et al.* (2017) 'Protease-activated receptor-4 and purinergic receptor P2Y12 dimerize, co-internalize, and activate Akt signaling via endosomal recruitment of -arrestin', *Journal of Biological Chemistry*. American Society for Biochemistry and Molecular Biology Inc., 292(33), pp. 13867–13878. doi: 10.1074/jbc.M117.782359.
- Snyder, J. C. and Rajagopal, S. (2020) 'Isoforms of GPCR proteins combine for diverse signalling', *Nature*. NLM (Medline), pp. 553–554. doi: 10.1038/d41586-020-03001-0.
- Soave, M. *et al.* (2020) 'NanoBiT Complementation to Monitor Agonist-Induced Adenosine A1 Receptor Internalization', *SLAS Discovery*. doi: 10.1177/2472555219880475.
- Soderling, S. H., Bayuga, S. J. and Beavo, J. A. (1999) 'Isolation and characterization of a dual-substrate phosphodiesterase gene family: PDE10A', *Proceedings of the National Academy of Sciences of the United States of America*, 96(12), pp. 7071–7076. doi: 10.1073/pnas.96.12.7071.
- Soderling, S. H. and Beavo, J. A. (2000) 'Regulation of cAMP and cGMP signaling: new phosphodiesterases and new functions', *Curr Opin Cell Biol*. 2000/03/14, 12(2), pp. 174–179. Available at: <https://www.ncbi.nlm.nih.gov/pubmed/10712916>.
- Somekawa, S. *et al.* (2005) 'Enhanced functional gap junction neofunction by protein kinase A-dependent and Epac-dependent signals downstream of cAMP in cardiac myocytes', *Circulation Research*. Circ Res, 97(7), pp. 655–662. doi: 10.1161/01.RES.0000183880.49270.f9.
- Song, X. *et al.* (2009) 'How does arrestin assemble MAPKs into a signaling complex?', *Journal of Biological Chemistry*. J Biol Chem, 284(1), pp. 685–695. doi:

- 10.1074/jbc.M806124200.
- Spirli, C. *et al.* (2012) 'Altered store operated calcium entry increases cyclic 3',5'-adenosine monophosphate production and extracellular signal-regulated kinases 1 and 2 phosphorylation in polycystin-2-defective cholangiocytes', *Hepatology*. doi: 10.1002/hep.24723.
- Steingold, J. M. and Hatfield, S. M. (2020) 'Targeting Hypoxia-A2A Adenosinergic Immunosuppression of Antitumor T Cells During Cancer Immunotherapy', *Frontiers in Immunology*. Frontiers Media S.A. doi: 10.3389/fimmu.2020.570041.
- Stessin, A. M. *et al.* (2006) 'Soluble adenylyl cyclase mediates nerve growth factor-induced activation of Rap1', *Journal of Biological Chemistry*. J Biol Chem, 281(25), pp. 17253–17258. doi: 10.1074/jbc.M603500200.
- Stoddart, L. A. *et al.* (2012) 'Fragment screening at adenosine-A3 receptors in living cells using a fluorescence-based binding assay', *Chemistry and Biology*. doi: 10.1016/j.chembiol.2012.07.014.
- Stoddart, L. A. *et al.* (2015) 'Application of BRET to monitor ligand binding to GPCRs', *Nature Methods*. Nature Publishing Group, 12(7), pp. 661–663. doi: 10.1038/nmeth.3398.
- Stoffel, R. H., Pitcher, J. A. and Lefkowitz, R. J. (1997) 'Targeting G protein-coupled receptor kinases to their receptor substrates', *Journal of Membrane Biology*. J Membr Biol, pp. 1–8. doi: 10.1007/s002329900210.
- Stupp, R. *et al.* (2017) 'Effect of tumor-treating fields plus maintenance temozolomide vs maintenance temozolomide alone on survival in patients with glioblastoma a randomized clinical trial', *JAMA - Journal of the American Medical Association*. American Medical Association, 318(23), pp. 2306–2316. doi: 10.1001/jama.2017.18718.
- Sullivan, S. K. *et al.* (2006) 'Kinetics of nonpeptide antagonist binding to the human gonadotropin-releasing hormone receptor: Implications for structure-activity relationships and insurmountable antagonism', *Biochemical Pharmacology*, 72(7). doi: 10.1016/j.bcp.2006.07.011.
- Sun, N. and Kim, K.-M. (2021) 'Mechanistic diversity involved in the desensitization of G protein-coupled receptors', *Archives of Pharmacal Research*. Springer, 1, p. 3. doi: 10.1007/s12272-021-01320-y.
- Sunahara, R. K., Dessauer, C. W. and Gilman, A. G. (1996) 'Complexity and diversity of mammalian adenylyl cyclases', *Annual Review of Pharmacology and*

Bibliography

- Toxicology*. Annual Reviews Inc., pp. 461–480. doi: 10.1146/annurev.pa.36.040196.002333.
- Sung, B. J. *et al.* (2003) 'Structure of the catalytic domain of human phosphodiesterase 5 with bound drug molecules', *Nature*, 425(6953), pp. 98–102. doi: 10.1038/nature01914.
- Surapisitchat, J. *et al.* (2007) 'Differential regulation of endothelial cell permeability by cGMP via phosphodiesterases 2 and 3', *Circ Res*. 2007/08/21, 101(8), pp. 811–818. doi: 10.1161/CIRCRESAHA.107.154229.
- Sutherland, E. and Rall, T. W. (1958) *FRACTIONATION AND CHARACTERIZATION OF A CYCLIC ADENINE RIBONUCLEOTIDE FORMED BY TISSUE PARTICLES**. doi: 10.1016/S0021-9258(19)77423-7.
- Sutherland, E. W. (1972) 'Studies on the mechanism of hormone action', *Science*. 1972/08/04, 177(4047), pp. 401–408. Available at: <https://www.ncbi.nlm.nih.gov/pubmed/4339614>.
- Suzuki, N. *et al.* (2003) 'G α 12 activates Rho GTPase through tyrosine-phosphorylated leukemia-associated RhoGEF', *Proceedings of the National Academy of Sciences of the United States of America*. National Academy of Sciences, 100(2), pp. 733–738. doi: 10.1073/pnas.0234057100.
- Swan, A. H. *et al.* (2019) 'The Popeye domain containing gene family encoding a family of cAMP-effector proteins with important functions in striated muscle and beyond', *Journal of Muscle Research and Cell Motility*. Springer International Publishing, 40(2), pp. 169–183. doi: 10.1007/s10974-019-09523-z.
- Szczyпка, M. (2020) 'Role of phosphodiesterase 7 (PDE7) in T cell activity. effects of selective pde7 inhibitors and dual pde4/7 inhibitors on T cell functions', *International Journal of Molecular Sciences*. MDPI AG, pp. 1–15. doi: 10.3390/ijms21176118.
- Takimoto, E. (2012) 'Cyclic GMP-dependent signaling in cardiac myocytes', *Circulation Journal*. Circ J, pp. 1819–1825. doi: 10.1253/circj.CJ-12-0664.
- Tan, C. M. *et al.* (2001) 'Tyrosine kinase-mediated serine phosphorylation of adenylyl cyclase', *Biochemistry*. Biochemistry, 40(6), pp. 1702–1709. doi: 10.1021/bi0015818.
- Taniguchi, Y., Tonai-Kachi, H. and Shinjo, K. (2006) 'Zaprinast, a well-known cyclic guanosine monophosphate-specific phosphodiesterase inhibitor, is an agonist for GPR35', *FEBS Lett*. 2006/08/29, 580(21), pp. 5003–5008. doi: 10.1016/j.febslet.2006.08.015.

- Tate, R. J., Arshavsky, V. Y. and Pyne, N. J. (2002) 'The identification of the inhibitory γ -subunits of the type 6 retinal cyclic guanosine monophosphate phosphodiesterase in non-retinal tissues: Differential processing of mRNA transcripts', *Genomics*. Academic Press Inc., 79(4), pp. 582–586. doi: 10.1006/geno.2002.6740.
- Taussig, R. (2013) 'Adenylyl Cyclases', in *Encyclopedia of Biological Chemistry: Second Edition*. Elsevier Inc., pp. 42–46. doi: 10.1016/B978-0-12-378630-2.00401-1.
- Teichmann, L. *et al.* (2017) 'From substrate specificity to promiscuity: hybrid ABC transporters for osmoprotectants', *Molecular Microbiology*. Blackwell Publishing Ltd, 104(5), pp. 761–780. doi: 10.1111/mmi.13660.
- Thibeault, P. E. *et al.* (2019) 'Molecular Basis for G-protein-Coupled Receptor (GPCR) Activation and Biased Signalling at the Platelet Thrombin Receptor Proteinase Activated', *bioRxiv*, pp. 1–67.
- Thibeault, P. E. *et al.* (2020) 'Molecular basis for activation and biased signaling at the thrombin-activated GPCR proteinase activated receptor-4 (PAR4)', *Journal of Biological Chemistry*. American Society for Biochemistry and Molecular Biology Inc., 295(8), pp. 2520–2540. doi: 10.1074/jbc.RA119.011461.
- Tian, X. *et al.* (2011) 'Phosphodiesterase 10A upregulation contributes to pulmonary vascular remodeling', *PLoS ONE*. doi: 10.1371/journal.pone.0018136.
- Tibbo, A. J. *et al.* (2020) 'Phosphodiesterase type 4 anchoring regulates cAMP signaling to Popeye domain-containing proteins', *bioRxiv*. bioRxiv, p. 2020.09.10.290825. doi: 10.1101/2020.09.10.290825.
- Tippins, J. R. (1986) 'CGRP: A novel neuropeptide from the calcitonin gene is the most potent vasodilator known', *Journal of Hypertension*. J Hypertens Suppl. Available at: <https://pubmed.ncbi.nlm.nih.gov/3553470/> (Accessed: 21 March 2021).
- Titulaer, M. J., Irani, S. R. and Lassmann, H. (2019) 'PDE10A antibodies in autoimmune encephalitis: A possible marker of cancer immunotherapy?', *Neurology*. NLM (Medline), pp. 327–328. doi: 10.1212/WNL.0000000000007965.
- Tivnan, A. *et al.* (2015) 'Inhibition of multidrug resistance protein 1 (MRP1) improves chemotherapy drug response in primary and recurrent glioblastoma multiforme', *Frontiers in Neuroscience*. doi: 10.3389/fnins.2015.00218.
- Torphy, T. J. (1998) 'Phosphodiesterase isozymes: molecular targets for novel

- antiasthma agents', *Am J Respir Crit Care Med*. 1998/02/26, 157(2), pp. 351–370. doi: 10.1164/ajrccm.157.2.9708012.
- Torphy, T. J. and Undem, B. J. (1991) 'Phosphodiesterase inhibitors: new opportunities for the treatment of asthma', *Thorax*, 46(7), pp. 512–523. Available at: <https://www.ncbi.nlm.nih.gov/pubmed/1877039>.
- Toth, A. B., Shum, A. K. and Prakriya, M. (2016) 'Regulation of neurogenesis by calcium signaling', *Cell Calcium*. Churchill Livingstone, pp. 124–134. doi: 10.1016/j.ceca.2016.02.011.
- Touhara, K. *et al.* (1994) 'Binding of G protein beta gamma-subunits to pleckstrin homology domains.', *Elsevier*. Available at: <https://www.sciencedirect.com/science/article/pii/S0021925817340486> (Accessed: 18 March 2021).
- Tourdot, B. *et al.* (2015) 'Pharmacogenocis of PAR4: PAR4 Polymorphism Determines Platelet Response in the Presence of Dual Anti-Platelet Therapy', *Blood*. doi: 10.1182/blood.v126.23.3446.3446.
- Trincavelli, M. L. *et al.* (2003) 'A2A adenosine receptor ligands and proinflammatory cytokines induce PC 12 cell death through apoptosis', *Biochemical Pharmacology*. doi: 10.1016/j.bcp.2003.07.006.
- Tsalkova, T. *et al.* (2012) 'Isoform-specific antagonists of exchange proteins directly activated by cAMP', *Proceedings of the National Academy of Sciences of the United States of America*. Proc Natl Acad Sci U S A, 109(45), pp. 18613–18618. doi: 10.1073/pnas.1210209109.
- Tucker, S. J. and Zorn, A. J. (2021) 'The Role of POPDC1 in the Progression of the Malignant Phenotype', *British Journal of Pharmacology*. Wiley. doi: 10.1111/bph.15403.
- Tyers, M. and Wright, G. D. (2019) 'Drug combinations: a strategy to extend the life of antibiotics in the 21st century', *Nature Reviews Microbiology*. Nature Publishing Group, pp. 141–155. doi: 10.1038/s41579-018-0141-x.
- Udawela, M. *et al.* (2006) 'Distinct receptor activity-modifying protein domains differentially modulate interaction with calcitonin receptors', *Molecular Pharmacology*. Mol Pharmacol, 69(6), pp. 1984–1989. doi: 10.1124/mol.105.021915.
- Uhler, M. D., Chrivia, J. C. and McKnight, G. S. (1986) 'Evidence for a second isoform of the catalytic subunit of cAMP-dependent protein kinase', *Journal of Biological Chemistry*. J Biol Chem, 261(33), pp. 15360–15363. doi: 10.1016/s0021-

- 9258(18)66717-1.
- Urso, K. *et al.* (2019) 'NFATc3 controls tumour growth by regulating proliferation and migration of human astrogloma cells', *Scientific Reports*. doi: 10.1038/s41598-019-45731-w.
- Vadiveloo, P. K. *et al.* (1997) 'G1 phase arrest of human smooth muscle cells by heparin, IL-4 and cAMP is linked to repression of cyclin D1 and cdk2', *Atherosclerosis*. 1997/08/01, 133(1), pp. 61–69. doi: 10.1016/s0021-9150(97)00116-0.
- Vanderboor, C. M. G. *et al.* (2020) 'Proteinase-activated receptor 4 activation triggers cell membrane blebbing through RhoA and β -arrestin', *Molecular Pharmacology*. American Society for Pharmacology and Experimental Therapy, 97(6), pp. 365–376. doi: 10.1124/MOL.119.118232.
- Vasta, V., Shimizu-Albergine, M. and Beavo, J. A. (2006) 'Modulation of Leydig cell function by cyclic nucleotide phosphodiesterase 8A', *Proceedings of the National Academy of Sciences of the United States of America*. Proc Natl Acad Sci U S A, 103(52), pp. 19925–19930. doi: 10.1073/pnas.0609483103.
- Vinay, D. S. *et al.* (2015) 'Immune evasion in cancer: Mechanistic basis and therapeutic strategies', *Seminars in Cancer Biology*. Academic Press, 35, pp. S185–S198. doi: 10.1016/J.SEMCANCER.2015.03.004.
- Vitali, E. *et al.* (2014) 'Cyclic adenosine 3'-5'-monophosphate (cAMP) exerts proliferative and anti-proliferative effects in pituitary cells of different types by activating both cAMP-dependent protein kinase A (PKA) and exchange proteins directly activated by cAMP (Epac)', *Molecular and Cellular Endocrinology*. Mol Cell Endocrinol, 383(1–2), pp. 193–202. doi: 10.1016/j.mce.2013.12.006.
- Vossler, M. R. *et al.* (1997) 'cAMP activates MAP kinase and Elk-1 through a B-Raf- and Rap1-dependent pathway', *Cell*. Elsevier B.V., 89(1), pp. 73–82. doi: 10.1016/S0092-8674(00)80184-1.
- Wan, K. F. *et al.* (2001) 'The Inhibitory of gamma Subunit of the Type 6 Retinal Cyclic Guanosine Monophosphate Phosphodiesterase Is a Novel Intermediate Regulating p42/p44 Mitogen-activated Protein Kinase Signaling in Human Embryonic Kidney 293 Cells *', *Journal of Biological Chemistry*. Elsevier, 276(41), pp. 37802–37808. doi: 10.1074/jbc.M105087200.
- Wang, H. *et al.* (2005) 'Multiple elements jointly determine inhibitor selectivity of cyclic nucleotide phosphodiesterases 4 and 7', *Journal of Biological Chemistry*, 280(35), pp. 30949–30955. doi: 10.1074/jbc.M504398200.

Bibliography

- Wang, H. *et al.* (2007) 'Structural insight into substrate specificity of phosphodiesterase 10', *Proceedings of the National Academy of Sciences of the United States of America*. Proc Natl Acad Sci U S A, 104(14), pp. 5782–5787. doi: 10.1073/pnas.0700279104.
- Wang, H. *et al.* (2008) 'Kinetic and structural studies of phosphodiesterase-8A and implication on the inhibitor selectivity', *Biochemistry*. American Chemical Society, 47(48), pp. 12760–12768. doi: 10.1021/bi801487x.
- Wang, J. and Matosevic, S. (2019) 'NT5E/CD73 as Correlative Factor of Patient Survival and Natural Killer Cell Infiltration in Glioblastoma', *Journal of Clinical Medicine*. MDPI AG, 8(10), p. 1526. doi: 10.3390/jcm8101526.
- Wang, J. Q. *et al.* (2021) 'Multidrug resistance proteins (MRPs): Structure, function and the overcoming of cancer multidrug resistance', *Drug Resistance Updates*. Churchill Livingstone, 54, p. 100743. doi: 10.1016/j.drug.2021.100743.
- Wang, P. *et al.* (2001) 'Human phosphodiesterase 8A splice variants: Cloning, gene organization, and tissue distribution', *Gene*. Gene, 280(1–2), pp. 183–194. doi: 10.1016/S0378-1119(01)00783-1.
- Wedegaertner, P. B., Wilson, P. T. and Bourne, H. R. (1995) 'Lipid modifications of trimeric G proteins', *Journal of Biological Chemistry*. J Biol Chem, pp. 503–506. doi: 10.1074/jbc.270.2.503.
- Werry, T. D., Sexton, P. M. and Christopoulos, A. (2005) "Ins and outs" of seven-transmembrane receptor signalling to ERK', *Trends in Endocrinology and Metabolism*. Trends Endocrinol Metab, pp. 26–33. doi: 10.1016/j.tem.2004.11.008.
- Weston, C. *et al.* (2016) 'Receptor activity-modifying protein-directed G protein signaling specificity for the calcitonin gene-related peptide family of receptors', *J Biol Chem*, 291(49), p. 25763. doi: 10.1074/jbc.A116.751362.
- Wetzker, R. and Böhmer, F. D. (2003) 'Transactivation joins multiple tracks to the ERK/MAPK cascade', *Nature Reviews Molecular Cell Biology*. Nat Rev Mol Cell Biol, pp. 651–657. doi: 10.1038/nrm1173.
- Whitaker, M. (2006) 'Calcium at fertilization and in early development', *Physiological Reviews*. Europe PMC Funders, pp. 25–88. doi: 10.1152/physrev.00023.2005.
- Williams, C. S. *et al.* (2011) 'BVES regulates EMT in human corneal and colon cancer cells and is silenced via promoter methylation in human colorectal carcinoma', *Journal of Clinical Investigation*. J Clin Invest, 121(10), pp. 4056–4069. doi: 10.1172/JCI44228.

- Williams, M. *et al.* (1987) 'Biochemical characterization of the triazoloquinazoline, CGS 15943, a novel, non-xanthine adenosine antagonist.', *Journal of Pharmacology and Experimental Therapeutics*, 241(2).
- Willoughby, D. *et al.* (2012) 'Direct binding between Orai1 and AC8 mediates dynamic interplay between Ca²⁺ and cAMP signaling', *Science Signaling*. doi: 10.1126/scisignal.2002299.
- Wilson, L. S. *et al.* (2011) 'A phosphodiesterase 3B-based signaling complex integrates exchange protein activated by cAMP 1 and phosphatidylinositol 3-kinase signals in human arterial endothelial cells', *Journal of Biological Chemistry*. *J Biol Chem*, 286(18), pp. 16285–16296. doi: 10.1074/jbc.M110.217026.
- Winfield, I. (2017) *Quantifying biased agonism of adenosine and calcitonin-like receptorse.* University of Warwick. Available at: <http://wrap.warwick.ac.uk/100406/>.
- Wisler, J. W. *et al.* (2007) 'A unique mechanism of β -blocker action: Carvedilol stimulates β -arrestin signaling', *Proceedings of the National Academy of Sciences of the United States of America*. National Academy of Sciences, 104(42), pp. 16657–16662. doi: 10.1073/pnas.0707936104.
- Wong, W. and Scott, J. D. (2004) 'AKAP signalling complexes: Focal points in space and time', *Nature Reviews Molecular Cell Biology*. *Nat Rev Mol Cell Biol*, pp. 959–970. doi: 10.1038/nrm1527.
- Woolley, M. J. *et al.* (2017) 'Receptor activity-modifying protein dependent and independent activation mechanisms in the coupling of calcitonin gene-related peptide and adrenomedullin receptors to Gs', *Biochemical Pharmacology*. Elsevier Inc., 142, pp. 96–110. doi: 10.1016/j.bcp.2017.07.005.
- Wootten, D. *et al.* (2013) 'Receptor activity modifying proteins (RAMPs) interact with the VPAC 2 receptor and CRF1 receptors and modulate their function', *British Journal of Pharmacology*. *Br J Pharmacol*, 168(4), pp. 822–834. doi: 10.1111/j.1476-5381.2012.02202.x.
- Wootten, D *et al.* (2013) 'Receptor activity modifying proteins (RAMPs) interact with the VPAC2 receptor and CRF1 receptors and modulate their function.', *British journal of pharmacology*. England, 168(4), pp. 822–834. doi: 10.1111/j.1476-5381.2012.02202.x.
- Wootten, D. *et al.* (2018) 'Mechanisms of signalling and biased agonism in G protein-coupled receptors', *Nature Reviews Molecular Cell Biology*. Nature Publishing

- Group, 19(10), pp. 638–653. doi: 10.1038/s41580-018-0049-3.
- Wu, C. C. *et al.* (2000) 'YD-3, a novel inhibitor of protease-induced platelet activation.', *British journal of pharmacology*. John Wiley and Sons Inc., 130(6), pp. 1289–96. doi: 10.1038/sj.bjp.0703437.
- Wu, Y. L., Pei, G. and Fan, G. H. (1998) 'Inhibition of phospholipase C blocks opioid receptor-mediated activation of Gi proteins', *NeuroReport*. Lippincott Williams and Wilkins, 9(1), pp. 99–103. doi: 10.1097/00001756-199801050-00020.
- Wynands, J. E. (1994) 'The role of amrinone in treating heart failure during and after coronary artery surgery supported by cardiopulmonary bypass', in *Journal of Cardiac Surgery*. Blackwell Publishing Inc., pp. 453–458. doi: 10.1111/jocs.1994.9.3s.453.
- Xing, F. *et al.* (2017) 'The Anti-Warburg Effect Elicited by the cAMP-PGC1 α Pathway Drives Differentiation of Glioblastoma Cells into Astrocytes', *Cell Reports*. doi: 10.1016/j.celrep.2016.12.037.
- Xu, J. *et al.* (2020) 'The Effects of Calcitonin Gene-Related Peptide on Bone Homeostasis and Regeneration', *Current Osteoporosis Reports*. Springer, pp. 621–632. doi: 10.1007/s11914-020-00624-0.
- Xu, R. X. *et al.* (2000) 'Atomic structure of PDE4: Insights into phosphodiesterase mechanism and specificity', *Science*, 288(5472), pp. 1822–1825. doi: 10.1126/science.288.5472.1822.
- Xu, W. F. *et al.* (1998) 'Cloning and characterization of human protease-activated receptor 4', *Proceedings of the National Academy of Sciences of the United States of America*. Proc Natl Acad Sci U S A, 95(12), pp. 6642–6646. doi: 10.1073/pnas.95.12.6642.
- Xu, Y., Piston, D. W. and Johnson, C. H. (1999) 'A bioluminescence resonance energy transfer (BRET) system: Application to interacting circadian clock proteins', *Proceedings of the National Academy of Sciences of the United States of America*. National Academy of Sciences, 96(1), pp. 151–156. doi: 10.1073/pnas.96.1.151.
- Yan, W. *et al.* (2001) 'Bitter taste transduced by PLC- β 2-dependent rise in IP3 and α -gustducin-dependent fall in cyclic nucleotides', *American Journal of Physiology - Cell Physiology*. American Physiological Society, 280(4 49-4). doi: 10.1152/ajpcell.2001.280.4.c742.
- Yang, D. *et al.* (2021) 'G protein-coupled receptors: structure- and function-based drug discovery', *Signal Transduction and Targeted Therapy*. Springer Nature, pp. 1–

27. doi: 10.1038/s41392-020-00435-w.
- Yang, J. M. *et al.* (2018) 'Integrating chemical and mechanical signals through dynamic coupling between cellular protrusions and pulsed ERK activation', *Nature Communications*. Nature Publishing Group, 9(1), pp. 1–13. doi: 10.1038/s41467-018-07150-9.
- Yang, R. *et al.* (2020) 'Conversion of ATP to adenosine by CD39 and CD73 in multiple myeloma can be successfully targeted together with adenosine receptor A2A blockade', *Journal for ImmunoTherapy of Cancer*. BMJ Publishing Group, 8(1). doi: 10.1136/jitc-2020-000610.
- Yang, X. L. *et al.* (2003) 'Pleckstrin homology domain of G protein-coupled receptor kinase-2 blinds to PKC and affects the activity of PKC kinase', *World Journal of Gastroenterology*. Baishideng Publishing Group Co, 9(4), pp. 800–803. doi: 10.3748/wjg.v9.i4.800.
- Yang, Y. M. *et al.* (2020) 'G α 12/13 signaling in metabolic diseases', *Experimental and Molecular Medicine*. Springer Nature, pp. 896–910. doi: 10.1038/s12276-020-0454-5.
- Yatani, A. and Brown, A. M. (1989) 'Rapid β -adrenergic modulation of cardiac calcium channel currents by a fast G protein pathway', *Science*. American Association for the Advancement of Science, 245(4913), pp. 71–74. doi: 10.1126/science.2544999.
- Yoshikawa, M. *et al.* (2016) 'Design and synthesis of potent and selective pyridazin-4(1H)-one-based PDE10A inhibitors interacting with Tyr683 in the PDE10A selectivity pocket', *Bioorganic and Medicinal Chemistry*. Elsevier Ltd, 24(16), pp. 3447–3455. doi: 10.1016/j.bmc.2016.05.049.
- Yuasa, K. *et al.* (2001) 'Identification of rat cyclic nucleotide phosphodiesterase 11A (PDE11A)', *European Journal of Biochemistry*. John Wiley & Sons, Ltd, 268(16), pp. 4440–4448. doi: 10.1046/j.1432-1327.2001.02366.x.
- Yue, J. and López, J. M. (2020) 'Understanding MAPK signaling pathways in apoptosis', *International Journal of Molecular Sciences*. MDPI AG. doi: 10.3390/ijms21072346.
- Zaccolo, M. and Movsesian, M. A. (2007) 'cAMP and cGMP signaling cross-talk: role of phosphodiesterases and implications for cardiac pathophysiology', *Circ Res*. 2007/06/09, 100(11), pp. 1569–1578. doi: 10.1161/CIRCRESAHA.106.144501.
- Zagórska, A. (2020) 'Phosphodiesterase 10 (PDE10) inhibitors: an updated patent review (2014-present)', *Expert Opinion on Therapeutic Patents*. doi:

10.1080/13543776.2020.1709444.

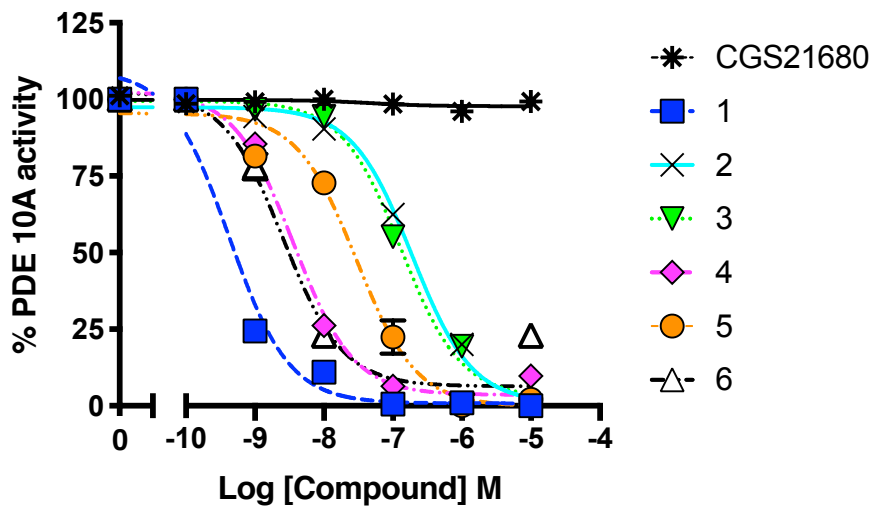
- Zha, J. *et al.* (1996) 'Serine phosphorylation of death agonist BAD in response to survival factor results in binding to 14-3-3 not BCL-X(L)', *Cell*. Cell Press, 87(4), pp. 619–628. doi: 10.1016/S0092-8674(00)81382-3.
- Zhan, X. *et al.* (2016) 'Peptide mini-scaffold facilitates JNK3 activation in cells', *Scientific Reports*. Nature Publishing Group, 6(1), pp. 1–9. doi: 10.1038/srep21025.
- Zhang, H. *et al.* (2020) 'Complex roles of cAMP–PKA–CREB signaling in cancer', *Experimental Hematology and Oncology*. BioMed Central Ltd. doi: 10.1186/s40164-020-00191-1.
- Zhang, J. F. *et al.* (2021) 'An ultrasensitive biosensor for high-resolution kinase activity imaging in awake mice', *Nature Chemical Biology*. Nature Research, 17(1), pp. 39–46. doi: 10.1038/s41589-020-00660-y.
- Zhang, K. Y. J. *et al.* (2004) 'cA glutamine switch mechanism for nucleotide selectivity by phosphodiesterases', *Molecular Cell*, 15(2), pp. 279–286. doi: 10.1016/j.molcel.2004.07.005.
- Zhang, Y. *et al.* (2020) 'Calcitonin gene-related peptide: A promising bridge between cancer development and cancer-associated pain in oral squamous cell carcinoma (Review)', *Oncology Letters*. Spandidos Publications. doi: 10.3892/ol.2020.12116.
- Zhang, Z. *et al.* (2015) 'Domain organization and conformational plasticity of the G protein effector, PDE6', *Journal of Biological Chemistry*. doi: 10.1074/jbc.M115.647636.
- Zhao, P. *et al.* (2014) 'Biased signaling of protease-activated receptors'. doi: 10.3389/fendo.2014.00067.
- Zhao, P., Metcalf, M. and Bunnett, N. W. (2014) 'Biased signaling of protease-activated receptors', *Front Endocrinol (Lausanne)*. 2014/05/27, 5, p. 67. doi: 10.3389/fendo.2014.00067.
- Zhu, B. *et al.* (2017) 'Phosphodiesterase 10A is overexpressed in lung tumor cells and inhibitors selectively suppress growth by blocking β -catenin and MAPK signaling', *Oncotarget*. 2017/10/21. Drug Discovery Research Center, Mitchell Cancer Institute, University of South Alabama, Mobile, Alabama, USA. Department of Biochemistry and Molecular Biology, The University of Alabama at Birmingham, Birmingham, Alabama, USA. Department of Chemistry, Uni, 8(41), pp. 69264–69280. doi: 10.18632/oncotarget.20566.

Bibliography

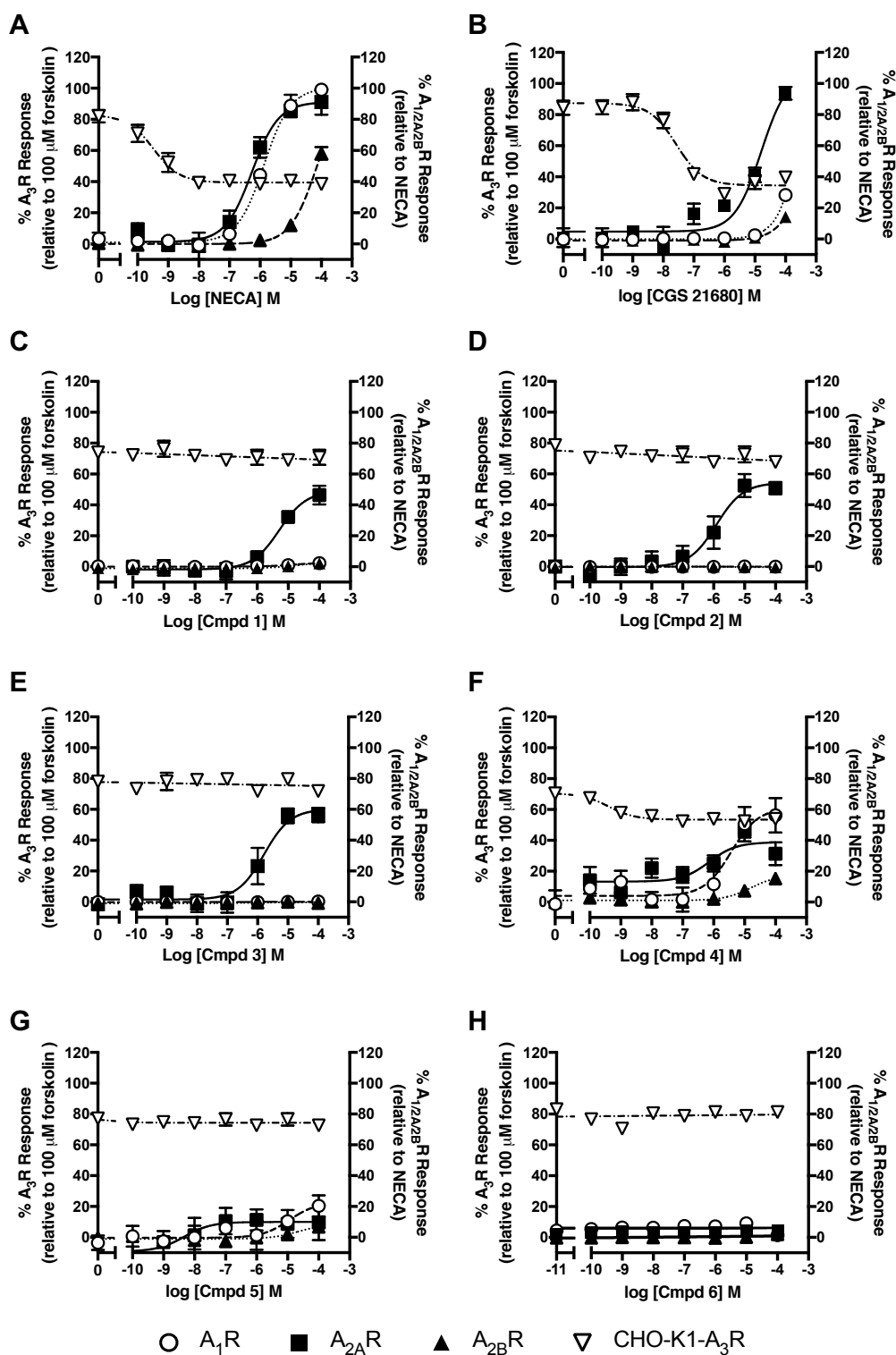
- Zoraghi, R., Corbin, J. D. and Francis, S. H. (2006) 'Phosphodiesterase-5 Gln817 is critical for cGMP, vardenafil, or sildenafil affinity: Its orientation impacts cGMP but not cAMP affinity', *Journal of Biological Chemistry*. Elsevier, 281(9), pp. 5553–5558. doi: 10.1074/jbc.M510372200.
- Zwain, I. H. and Amato, P. (2001) 'cAMP-induced apoptosis in granulosa cells is associated with up-regulation of P53 and bax and down-regulation of clusterin', *Endocrine Research*, 27(1–2), pp. 233–249. doi: Doi 10.1081/Erc-100107184.

Appendix 1

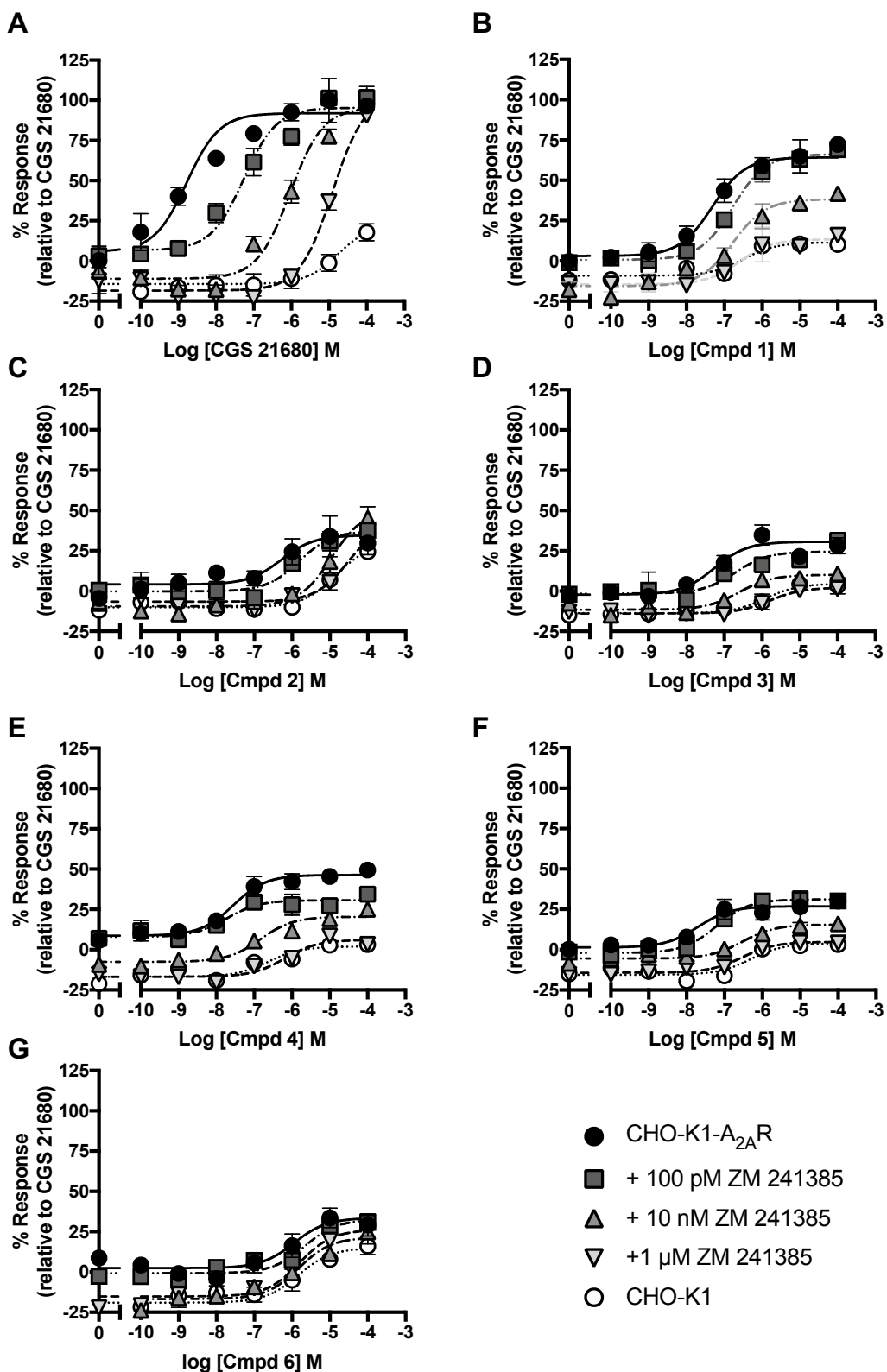
Additional Figures



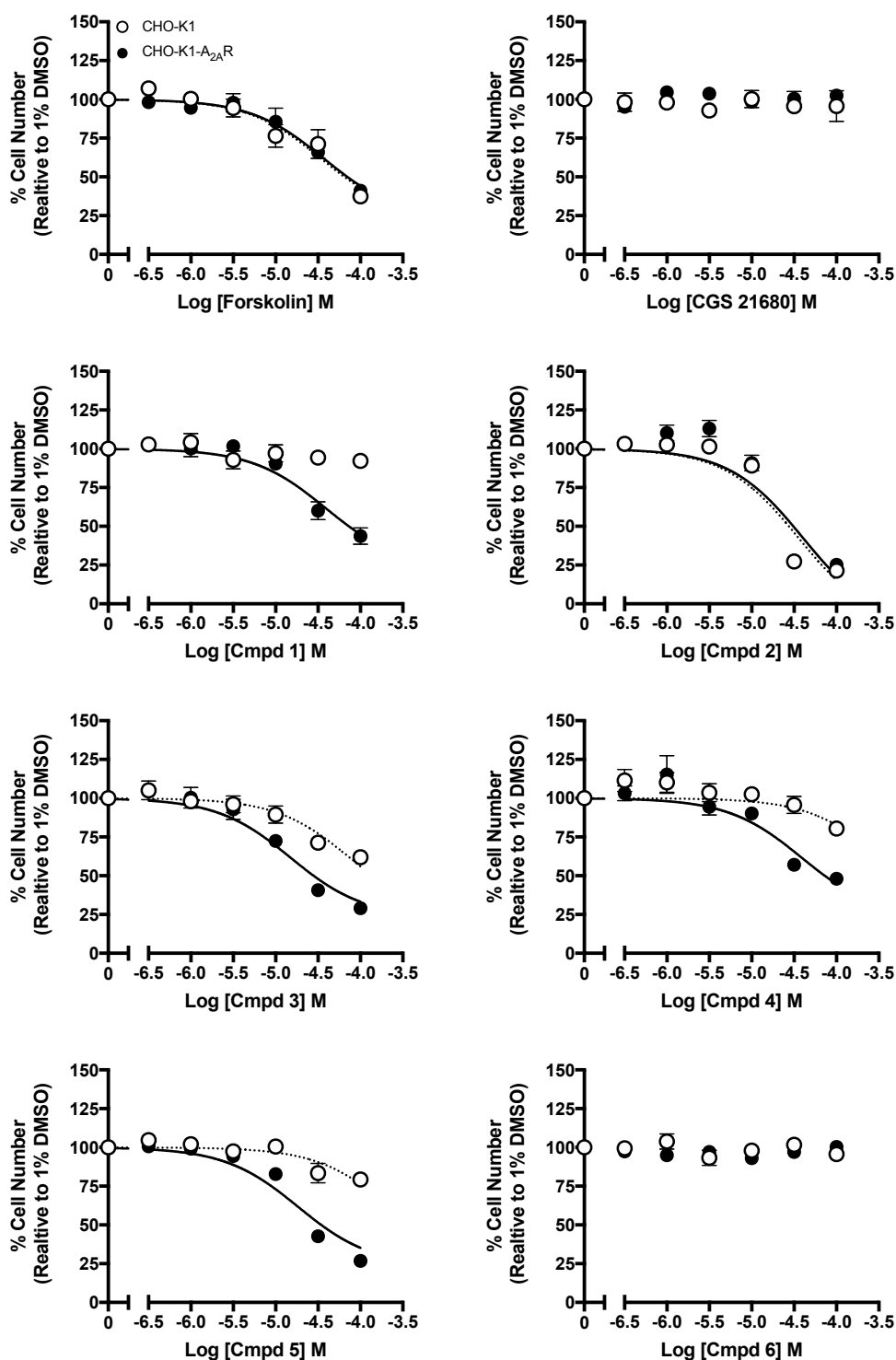
Appendix Figure 1. Triazoloquinazolines differentially inhibit PDE10A activity *in vitro*. Concentration-response curves were displayed for compound 1-6 and CGS21680 at PDE10A. Data are expressed as the mean \pm SEM of 6 individual data. This data was generated from previous study conducted by Dr. Winfield (University of Cambridge).



Appendix Figure 2. Triazoloquinazolines promote differential activations across all adenosine receptor subtypes. The selectivity characterisation to all adenosine receptors using yeast systems and CHO-K1 expressing A₃R. To characterise selectivity of triazoloquinazolines, yeast systems were used as appropriate: A₁R and GPA1/Gα_{i1/2}, A_{2A}R and GPA1/Gα_s, or the A_{2B}R (with GPA1/Gα_s expressed in yeast strains). The efficacy of the compounds (1–6) was measured against A₃R in CHO-K1-A₃R cells. Each data point represents the mean of responses from 6 repeats after normalisation with either NECA (for A₁R, A_{2A}R, and A_{2B}R) or forskolin 100 μM (for A₃R). This data was generated from previous study conducted by Sabrina Carvalho (Department of Pharmacology, University of Cambridge).



Appendix Figure 3. Triazoloquinazoline-based compounds promote the production of cAMP in CHO-K1 stably expressing A_{2A}R. Accumulation of cAMP was determined following 30 minutes stimulation with CGS21680 (A), compound 1-6 (B-G) in the presence of rolipram. Data are expressed relative to the maximal response produced by CGS21680 100 μM. Values are expressed as mean ± SEM of 4 – 9 individual repeats. This data was generated from previous study conducted by Dr. Winfield (University of Cambridge).



Appendix Figure 4. Anti-proliferative actions of forskolin and triazoloquinazolines (compound 1-5) was potentiated in CHO-K1 cells stably expressing A_{2A}R. Percentage of cell number was determined upon 72h treatment. Data are expressed as relative cell number to the vehicle alone and are the mean \pm SEM from 4 – 6 individual data. This data was generated from previous study conducted by Dr. Winfield (University of Cambridge).

Appendix 2

Publication: Safitri, D. *et al.* 2020

This appendix contains:

Safitri, D., Harris, M., Potter, H., Yan Yeung, H., Winfield, I., Kopanitsa, L., Svensson, F., Rahman, T., Harper, M.T., Bailey, D., Ladds, G. (2020). Elevated intracellular cAMP concentration mediates growth suppression in glioma cells. *Biochemical Pharmacology*, 174. <https://doi.org/10.1016/j.bcp.2020.113823>



Contents lists available at ScienceDirect

Biochemical Pharmacology

journal homepage: www.elsevier.com/locate/biochempharm

Elevated intracellular cAMP concentration mediates growth suppression in glioma cells

Dewi Safitri^{a,b}, Matthew Harris^a, Harriet Potter^a, Ho Yan Yeung^a, Ian Winfield^a, Liliya Kopanitsa^c, Fredrik Svensson^c, Taufiq Rahman^a, Matthew T Harper^a, David Bailey^c, Graham Ladds^{a,*}^a Department of Pharmacology, University of Cambridge, Tennis Court Road, Cambridge CB2 1PD, United Kingdom^b Pharmacology and Clinical Pharmacy Research Group, School of Pharmacy, Bandung Institute of Technology, Bandung 40132, Indonesia^c IOTA Pharmaceuticals Ltd, Cambridge University Biomedical Innovation Hub, Clifford Allbutt Building, Hills Road, Cambridge CB2 0AH, United Kingdom

ARTICLE INFO

Keywords:
cAMP
Phosphodiesterase inhibitors
Proliferation
Glioma
Caspase
Cell cycle

ABSTRACT

Suppressed levels of intracellular cAMP have been associated with malignancy. Thus, elevating cAMP through activation of adenylyl cyclase (AC) or by inhibition of phosphodiesterase (PDE) may be therapeutically beneficial. Here, we demonstrate that elevated cAMP levels suppress growth in C6 cells (a model of glioma) through treatment with forskolin, an AC activator, or a range of small molecule PDE inhibitors with differing selectivity profiles. Forskolin suppressed cell growth in a PKA-dependent manner by inducing a G₂/M phase cell cycle arrest. In contrast, trequinsin (a non-selective PDE_{2/3/7} inhibitor), not only inhibited cell growth via PKA, but also stimulated (independent of PKA) caspase-3/-7 and induced an aneuploidy phenotype. Interestingly, a cocktail of individual PDE 2,3,7 inhibitors suppressed cell growth in a manner analogous to forskolin but not trequinsin. Finally, we demonstrate that concomitant targeting of both AC and PDEs synergistically elevated intracellular cAMP levels thereby potentiating their antiproliferative actions.

1. Introduction

Glioma is a general term for brain tumours that originate from glial cells in the central nervous system and which may progressively lead to death if not treated early [1,2], with glioblastoma, the most common type of glioma, showing particularly poor survival [3]. The development of novel therapeutic approaches targeting glioma and glioblastoma are urgently required.

Defects in a number of signalling pathways have been reported in glioma pathogenesis, including the phosphatidylinositol-3 kinases/phosphatase and tensin/protein kinase B/mammalian target of rapamycin (PI3K/PTEN/Akt/mTOR) cascade; the retinoblastoma pathway (pRB); the Ras/mitogen-activated protein kinase (RAS/MAPK) pathway; signal transducer and activator of transcription 3 (STAT3); zinc transporter 4 (ZIP4); as well as the adenylyl cyclase (AC) system [4].

Importantly, lower cAMP levels are observed in brain tumour tissue (25.8 pmol/mg protein) compared to normal healthy tissue (98.8 pmol/mg protein) [5]. Indeed forskolin, an AC activator that elevates cAMP levels, has shown promising results in ameliorating cancer development [6]. While high levels of intracellular cAMP may kill cancer cells, the exact molecular mechanisms have not been clearly elucidated. Direct

elevation of cAMP using the cAMP analogues 8-bromo-cAMP, 8-chloro-cAMP, monobutyl cAMP and dibutyl cAMP, however, cannot be recommended due to the toxicity of these compounds [7]. Thus, there is a need to develop safe and effective compounds that can increase cAMP levels by pharmacological intervention.

Depending on the cell type where the malfunctions are observed, cAMP may play a role in either promoting or suppressing cell proliferation. This incongruity can be explained by two theories on the cAMP signalling cascade. The first theory proposes that elevation of intracellular cAMP is beneficial for suppressing cell proliferation in most mesenchymal and epithelial cell lines, such as glioblastoma [8], thyroid cells [9], ovarian granulosa cells [10], fibroblasts [11], and primary cardiomyocytes [12]. In contrast, the second theory proposes that cAMP promotes cell survival, which has been observed in myeloid cells, pancreatic β -cells, hepatocytes, gastric and intestinal cells, spinal motor, superior cervical ganglion sympathetic, dorsal root ganglion, dopaminergic neurons, cerebral granule and septal cholinergic neurons [13]. These two divergent roles of cAMP may be crucial in both physiological maintenance and pathological conditions, but whether these signalling cascades are interconnected remains unclear.

It has been well established that after synthesis by AC activation, cAMP diffuses within cells and is hydrolyzed to 5'AMP by

* Corresponding author.

E-mail address: grl30@cam.ac.uk (G. Ladds).<https://doi.org/10.1016/j.bcp.2020.113823>

Received 23 September 2019; Accepted 22 January 2020

Available online 25 January 2020

0006-2952/ © 2020 Elsevier Inc. All rights reserved.

phosphodiesterases (PDEs). PDEs are a subfamily of ectonucleotidases consisting of 11 isoforms (PDE1–11) in mammals and are encoded by 21 different genes [14], which are distributed in many types of tissue [15]. Each isoenzyme possesses different affinities for cAMP and/or cGMP, kinetic characteristics, allosteric regulation by cAMP/cGMP and, phosphorylation control by various protein kinases, that result in their distinctive response to a stimulus [16,17]. To date, there are 3 classes of PDEs subdivided according to their substrate specificities: cAMP-specific PDEs (PDE4, PDE7 and PDE8), cGMP-specific PDEs (PDE5, PDE6 and PDE9), and dual-substrate PDEs (PDE1, PDE2, PDE3, PDE10 and PDE11) [18]. Through metabolizing both cAMP and cGMP, PDEs generate intracellular gradients and microdomains of these second messengers to regulate their spatio-temporal signalling [19]. PDEs prevent non-specific activation, enabling both specificity and selectivity towards intracellular targets [20].

Overexpression of some PDEs, such as PDE1, PDE4, PDE5, and PDE7, has been reported to alter patterns of cAMP in the brain [21–24]. Some evidence shows that particular PDE inhibitors, such as rolipram, a selective PDE4 inhibitor, prevents leukaemia proliferation through an elevation of cAMP and an induction of apoptosis. This suggests that using specific PDE inhibitors is a viable approach for cancer therapy [25]. Given that PDE inhibitors may offer therapeutic efficacy against cancer, we investigated the role of each PDE upon cAMP accumulation and cell proliferation in a glioma cell model using a range of pharmacological inhibitors. Our data indicates that tumour cell regression is linearly correlated with elevation of cAMP. Among all PDE inhibitors tested, trequinsin (a non-selective PDE2/3/7 inhibitor [26]) was found to be the most potent at inhibiting cell proliferation. More importantly, by using small molecule compounds we highlight that simultaneous elevation of cAMP through activation of AC and inhibition of multiple PDEs (specifically PDE2, PDE3 and PDE7) had synergistic anti-proliferative effects on the glioma cells, predominantly by altering cell cycle progression and inducing activation of caspase-3/7, providing a novel treatment strategy for glioma.

2. Materials and methods

2.1. Cell lines

C6 glioma cells (a gift from Prof. Colin Taylor, University of Cambridge) were cultured in Gibco® Minimum Essential Medium (Thermo Fisher Scientific, UK) supplemented with 10% foetal bovine serum (FBS, Sigma, UK), 2 mM L-glutamine (Sigma, UK), and 1% antibiotic/antimycotic (Sigma, UK). ST14A cells (rat-derived striatal cells (Tissue and Cell Biotechnologies, Italy) were grown in Gibco® DMEM/F12 1:1 (1X) – Glutamax TM (Thermo Fisher Scientific, UK), supplemented with 10% FBS and 1% antibiotic/antimycotic. C6 cells were maintained at 37 °C in humidified 95% air and 5% CO₂. ST14A cells were grown at 33 °C in humidified 95% air and 5% CO₂ because propagation of ST14A cells at 37 °C has been shown to induce differentiation into glial cells [27]. Where appropriate cells were treated with pertussis toxin (PTX, Thermo Fisher, UK) at a range concentration of 2 pg/ml to 200 ng/ml or cholera toxin (CTX, Sigma, UK), at a concentration of 3.5 pg/ml to 350 ng/ml. PTX uncouples receptor-mediated G_α-dependent inhibition of cAMP production, meanwhile CTX inhibits GTPase activity of G_αs and causes permanent activation [28,29].

2.2. Compounds

Forskolin (Sigma, UK) was diluted to a stock of 100 mM in DMSO (Sigma, UK). Cholera toxin (CTX) was diluted in water to a stock of 35 µg/ml, whereas pertussis toxin (PTX) was diluted at a stock of 100 µg/ml. Isoprenaline hydrochloride (Sigma, UK) was dissolved in water to a stock of 10 mM. Trequinsin, PF-2545920, vinpocetine, sildenafil, rolipram, cilostamide, caffeine, SQ22536, EHNA, amrinone,

zaprinast, TC3.6, ibudilast, milrinone, BAY 73-6691, BRL-50481, pliclamilast, IBMX, roflumilast, tadalafil, PF-04449613 (all purchased from Sigma, UK), BC 11-38, and PF 04671536 (both obtained from Tocris, UK) were dissolved in DMSO to stock concentrations of either 100 mM or 10 mM. Guanylyl cyclase activators BAY 41-8543 and YC-1 were purchased from Tocris and diluted to a stock of 100 mM in DMSO. Exchange protein directly regulated by cAMP (Epac) inhibitors ESI-09, HJC0350, and CE3F4 (all purchased from Sigma, UK) were diluted to 10 mM stocks in DMSO. Protein kinase A (PKA) and protein kinase G (PKG) inhibitors, KT5720 and KT5823, respectively (all obtained from Cambridge Insight Biotechnology, UK) were diluted to stocks of 100 mM and 1 mM, respectively. MRP4 (multidrug resistant protein 4) inhibitor, PU23 (Tocris, UK), was dissolved in DMSO to a stock of 50 mM.

2.3. Reverse transcription PCR

RNA was extracted from C6 and ST14A cells using RNAqueous®-4PCR Total RNA Isolation Kit (Life Technologies, UK) according to manufacturer's instructions. In order to remove any contamination of genomic DNA, all RNA samples were treated with DNase I included in the kit. The purity of RNA samples was quantified using a NanoDrop™ Lite spectrophotometer (Thermo Scientific, UK) and only samples that had a minimum yield of 100 ng/µL and A_{260/280} > 1.9 were used in the experiments. Complementary DNA was synthesized using a QuantiTect reverse transcription kit (Qiagen, UK). The oligonucleotides (Sigma, UK) used for PCR were designed specifically for rat, including *GAPDH*: forward 5'-TCCCTCAAGATTGTCAGCAA-3', reverse 5'-AGATCCACAACGGATACATT-3' (309 bp); *PDE1A*: forward 5'-CGCCTGAAA GGAATACTAAGA-3', reverse 5'-TAGAAGCCAACCCAGTCCCGGA-3' (211 bp); *PDE1B*: forward 5'-CTGTCACCCCGCAGTCTCCG-3', reverse 5'-GAAGGTGGAGGCCAGCCAGTC-3' (309/306 bp); *PDE1C* forward 5'-CGCGGGCTGAGGAAATATAAG-3', reverse 5'-GAAGGTGGAGGCCA GCCAGTC-3' (237 bp); *PDE2A*: forward 5'-CCAAATCAGGGACCTCATA TTCC-3', reverse 5'-GGTGTCCCAAGTTCACCAT-3' (86 bp); *PDE3A*: forward 5'-CACAAAGCCAGAGTGAACC-3', reverse 5'-TGGAGGCAAC TTCTTCTCAG-3' (123 bp); *PDE3B*: forward 5'-GTCTGTGCCITGTATT CTCC-3', reverse 5'-AACTGCATTTCCACCTCCAGA-3' (103 bp); *PDE4A*: forward 5'-CGACAAGCACACAGCCTCT-3', reverse 5'-CTCCCAATGG ATGAACAAT-3' (73 bp); *PDE4B*: forward 5'-CAGTCTATGACCCAGAT AAGTGG-3', reverse 5'-GTCTGCACAAGTGTACCATGTTGGG-3' (787 bp); *PDE4C*: forward 5'-ATGGCCAGATCACTGGGGTCCGG-3', reverse 5'-GCTGAGTTCTGGAAGATGTCGAG-3' (582 bp); *PDE4D*: forward 5'-CCCTCTTGACTGTTATCATGCACACC-3', reverse 5'-GATCC TACATCATGTATTGCACTGGC-3' (262 bp); *PDE5A*: forward 5'-CCCTG GCCTATTAACAACGG-3', reverse 5'-ACGTGGTCCAGGCTCATA-3' (192 bp); *PDE7A*: forward 5'-GAAGAGGTTCCACCCGTA-3', reverse 5'-CTGATGTTCTGGCGGAGA-3' (85 bp); *PDE7B*: forward 5'-GGTCC TTGCTCATTGCG-3', 5'-GGAACCTATTCTGTCTGTTGATG-3' (99 bp); *PDE8A*: forward 5'-TGCCAGCAATAAGGTTGAGA-3', reverse 5'-CGAA TGTTCCCTCCTGTCTTT-3' (97 bp); *PDE8B*: forward 5'-CTCGGTCCCTC CTCTTCC-3', 5'-AACTTCCCGTGTCTATTGA-3' (147 bp); *PDE9A*: forward 5'-GTGGGTGGACTGTTTACTGGA-3', reverse 5'-TCGCTTTGGT CACTTTGTCTC-3' (107 bp); *PDE10A*: forward 5'-GACTTGATTGGCAT CCTTGAA-3', reverse 5'-CCTGGTATTGCTACGGAAG-3' (115 bp); and *PDE11A*: forward 5'-CCCAGGGGATAAATAAGGTTTC-3', reverse 5'-TGCCACAGAATGGAAGATACA-3' (87 bp).

All PCR products were run on a 2% agarose gel. The gel was visualised in the presence of ethidium bromide and imaged using a G Box iChem gel documentation system. Density of each band was analysed with GeneTools analysis software (Syngene, UK). Correct band size was compared to that of previous works.

2.4. cAMP accumulation assay

Cells were grown to confluency in complete MEM growth medium.

Cells were then trypsinised for 1 min, re-suspended in stimulation buffer (PBS with 0.1% BSA) and plated onto 384-well optiplates (Perkin Elmer, UK) at a density of 2000 cells/well. To determine the efficacy of individual PDE inhibitors, cells were co-stimulated, immediately after seeding, with three different concentrations of compounds (which spanned 100-fold either side of the individual IC_{50} value in vitro) and pEC_{20} values of forskolin (1.6 μ M for C6 cells and 50 nM for ST14A cells) for 30 min. Stimulating cells with the pEC_{20} of forskolin, enables a larger range to observe any effect of the PDE inhibitors on cAMP production. To generate full dose response curves, compounds were added to cells in the range of 0.1 pM – 100 μ M for 30 min. Detection of cAMP was assessed using LANCE cAMP detection kit (Perkin Elmer, UK) and end-point measurement was performed using a Mithras LB940 microplate reader (Berthold Technologies, Germany). The lysed cells were excited at 340 nm wavelength with fluorescence from homogeneous time-resolved FRET detected at 665 nm.

To determine the effects of G proteins on cAMP production, C6 cells were grown in complete MEM medium in the presence of either PTX or CTX for 16 h (as a pre-treatment). Subsequently, cells were dissociated using trypsin for 1 min after which, complete medium was added to inactivate trypsin. Cells were washed, resuspended in PBS containing 0.1% BSA, and plated onto 384-well optiplates at a density of 8000 cells/well. Total accumulation of cAMP was determined using the same protocol as described above. Data were either normalised to the maximal level of cAMP accumulation from cells in response to 100 μ M forskolin stimulation or were interpolated to the cAMP standard curve and expressed as the concentration cAMP per 10^6 cells. Where stated, cAMP levels are quoted as pmoles per mg of protein mass, determined using Bradford protein assay (Biorad, UK) following the manufacturer's instruction.

2.5. Determination of intracellular and extracellular cAMP levels

C6 cells were trypsinised and resuspended in PBS containing 0.1% BSA. 150,000 cells were then treated with various concentrations of PU23 (10 μ M, 3.16 μ M, and 1 μ M, diluted in PBS containing 0.1% BSA) for 30 min. After treatment, cells were washed with PBS containing 0.1% BSA and stimulated with the pEC_{50} concentration of forskolin (3.16 μ M), trequinsin (4.7 μ M) or the PDE inhibitor cocktail (26 μ M) for 1 or 2 h, in the presence or absence of each concentration of PU23. After stimulation, cells were centrifuged at $1677 \times g$ for 4 min to separate supernatant and cell pellet. LANCE cAMP detection kit (Perkin Elmer, UK) was used to determine extracellular cAMP levels (supernatant) and intracellular cAMP levels (cell pellet). The concentration of cAMP was determined by interpolating the HTR-FRET values to the cAMP standard curve. cAMP levels are expressed as the concentration per 10^6 cells.

2.6. cGMP accumulation assay

Confluent C6 cells were trypsinised and resuspended in PBS containing 0.1% BSA. Cells were plated onto a 384-well plate at a density of 500,000 cells/well and immediately stimulated with compounds for 30 min. After stimulation, 5 μ l of d2-cGMP analogue and 5 μ l mAb-criptate were added to each well and incubated for 1 h at room temperature as per the manufacturer's instruction (Cisbio, France). The d2-cGMP fluorophore was excited at a wavelength of 337 nm and emission was detected at 665 nm and 620 nm. Fluorescence was measured using a Mithras LB940 microplate reader (Berthold Technologies, Germany). Delta $F\%$ values were calculated using the 665 nm/620 nm ratio and all data were interpolated to a standard curve which covered an average cGMP range of 0.5–50 nM.

2.7. Cell proliferation assay

C6 cells were seeded at a density of 2500 cells/well in a clear flat

bottom 96-well plate (Corning). After 24 h, cells were exposed to test compounds or vehicle, in complete MEM growth medium, and were incubated for 72 h. To further investigate whether downstream pathways of cAMP influenced cell proliferation, cells were cotreated with selective inhibitors that target cAMP/cGMP sensors including PKA, PKG, and Epac. Cells were seeded as previously described and treated with either forskolin, trequinsin, or PDE inhibitor cocktail in the presence of the following inhibitors: KT5720 to inhibit PKA, KT5823 to inhibit PKG, ESI-09 as non-selective Epac inhibitor, CE3F4 as a selective Epac1 inhibitor, and HJC0350 as a selective Epac2 inhibitor. In order to investigate the effect of blockade of cAMP export on cell proliferation, cells were treated with forskolin, trequinsin or PDE inhibitor cocktail in the presence, or absence, of various concentrations of PU23 (10 μ M, 3.16 μ M, and 1 μ M). After 72 h incubation, 5 μ l of Cell Counting Kit – 8 (CCK-8, Sigma, UK) was added to each well and the cells were incubated for an additional 2–3 h at 37 °C in the dark. The absorbance of each well was measured using a Mithras LB940 microplate reader (Berthold Technologies, Germany) with an excitation of 450 nm. The amount of formazan formed is directly proportional to the number of viable cells. Cell proliferation was calculated as a percentage of number of cells treated with vehicle alone.

2.8. Caspase assay

C6 cells were seeded into clear bottom black 96-well plates (Corning) and treated with forskolin (1–100 μ M), trequinsin (1–100 μ M) or staurosporine (1 μ M, a pan caspase activator) in complete MEM media. 1% DMSO was used as vehicle control. Cells were exposed to test compounds for 72 h, plates were treated with 2 μ M of the CellEvent™ Caspase-3/7 green detection reagent (Life Technologies, UK) for 60 min at 37 °C in the dark. Caspase activity was detected by cleavage of the tetrapeptide substrate DEVD, which is conjugated to a nucleic acid binding dye. Intracellular caspase-3/7 activities were imaged using a BD Pathway 855. To normalise the number of cells with caspase activated, cells were also labelled with Hoechst 33342 (Cambridge Bioscience, UK). Activated caspase-3/7 cleaves substrate and produce green fluorescence which was visualised using FITC/Alexa Fluor™ 488 filter setting. The total number of cells stained with Hoechst 33342 was measured using Hoechst filter (350/461 nm).

2.9. Cell cycle analysis

Cell cycle analysis using flow cytometry provides information on the distribution of cells in interphase stages of the cell cycle (G_0/G_1 , S, and G_2/M). C6 cells were seeded in to 24-well plates and cultured for 24 h. Cells were exposed to selected treatments including forskolin, trequinsin, and a combination of individual PDE2,3,7 inhibitor, for 72 h. Subsequently, cells were harvested and resuspended in PBS containing 0.1% Triton X-100, 10 μ g/ml RNase A, and 5 μ g/ml propidium iodide (PI) before incubation at 37 °C for 15 min. Samples were analysed using a BD Accuri C6 flow cytometer and cell cycle analysis was performed using BD C6 software.

2.10. Statistical analysis

To quantify gene expression through RT-PCR, the densitometry results of each gene of interest were normalised to GAPDH signal. For cAMP accumulation and cell proliferation assays, data were fitted to obtain concentration–response curves using the three-parameter logistic equation using GraphPad Prism 8 (GraphPad Software, San Diego) to obtain values of E_{max}/I_{max} , pEC_{50}/pIC_{50} , baseline, and span. Statistical differences were analysed using one-way ANOVA followed by Dunnett's post-hoc (for comparisons amongst more than two groups) or independent Student's *t*-test (for comparison between two groups). To determine the correlation of cAMP levels and cell proliferation of each PDE inhibitor in both C6 and ST14A cells, Pearson's correlation

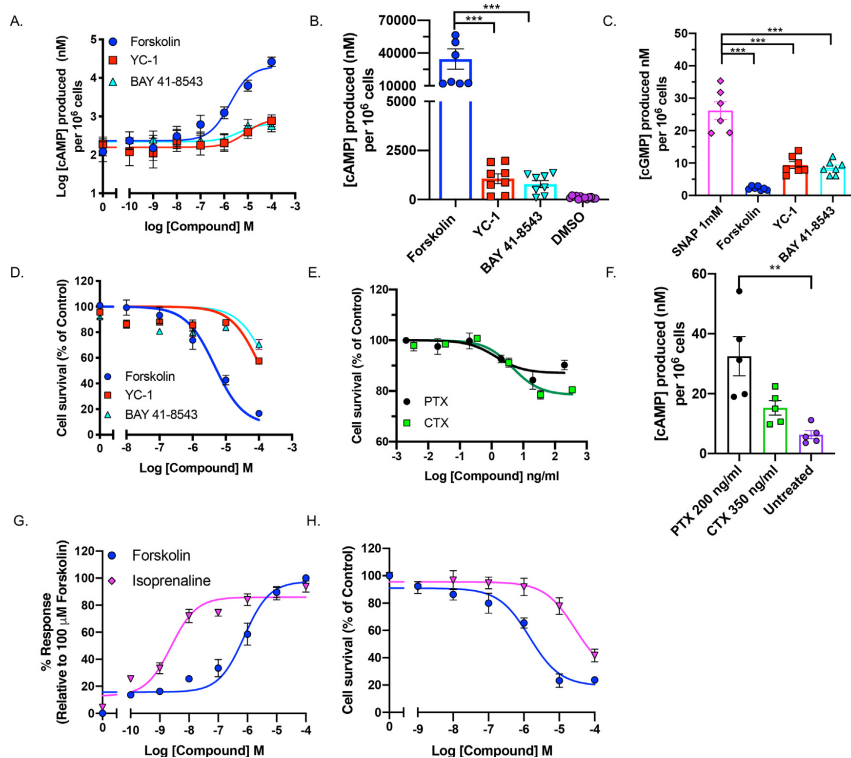


Fig. 1. Elevation of cAMP, but not cGMP, mediates cell growth suppression. **A.** cAMP levels following 30 min treatment with adenylyl cyclase activator (forskolin) or guanylyl cyclase activators (YC-1 and BAY 41-8543). **B-C.** Comparison of accumulation of cAMP and cGMP in C6 cells in response to forskolin (100 μ M), BAY 41-8543 (100 μ M), YC-1 (100 μ M), or SNAP (100 μ M). **D.** Survival of C6 cells following 72 h treatment with forskolin, BAY 41-8543 or YC-1. **E.** cAMP levels after 16 h pre-treatment with PTX or CTX in comparison to untreated cells. **F.** cAMP levels in C6 cells following 30 min stimulation with forskolin or the non-selective beta-adrenergic agonist, isoprenaline. Data are expressed relative to 100 μ M forskolin. **G.** cAMP levels in C6 cells following 30 min stimulation with forskolin or the non-selective beta-adrenergic agonist, isoprenaline. Data are expressed as percentage survival relative to vehicle alone and are the mean \pm SEM of 6–9 individual experiments. **H.** Cell survival of C6 cells following 72 h treatment with forskolin or isoprenaline. Data are expressed as percentage survival relative to vehicle alone and are the mean \pm SEM of 6–9 individual experiments. Statistical significance was determined using a one-way analysis of variance followed by Dunnett's *post hoc* test (*, $p < 0.05$; ***, $p < 0.001$).

coefficient (r) was calculated with 95% confidence interval. To compare the ability of compounds to suppress C6 cell proliferation a selection criterion was applied, whereby the term for affinity (pIC_{50}) was multiplied by the term for efficacy (span). Error for this composite measure was propagated by applying the following equation.

$$\text{Pooled SEM} = \sqrt{\left(\frac{SEM_A}{\bar{x}_A}\right)^2 + \left(\frac{SEM_B}{\bar{x}_B}\right)^2} \times \bar{x}_{AB}$$

where SEM_A and SEM_B are the standard errors of the mean of measurement A and B with mean of \bar{x}_A and \bar{x}_B , \bar{x}_{AB} is the composite mean.

3. Results

3.1. Elevation of cAMP levels reduces cell proliferation in a glioma cell line

We first sought to determine if changes in cAMP concentration modulated glioma cell growth. When C6 cells, a rat-derived model for glioma, were exposed to the pan-AC activator, forskolin, we observed a dose-dependent increase in cAMP levels, up to $34,566 \pm 9,346$ nM per 10^6 cells which equates to 484.23 ± 134.11 pmol cAMP/mg protein (lysed cells) (Fig. 1A, B), and reduced cell proliferation (Fig. 1D).

Given the fact that there is crosstalk between the cAMP and cGMP pathways [30], we also evaluated the role of the cGMP pathway on cell proliferation by treating cells with the small molecule guanylyl cyclase activators, BAY 41-8543 and YC-1. Both compounds elevated cGMP levels (Fig. 1C), however, cGMP production was $\sim 1000\times$ lower than cAMP production in C6 cells, even in response to treatment with the nitric oxide (NO) donor, S-Nitroso-N-acetyl-DL-penicillamine (SNAP) (0.37 ± 0.04 pmol cGMP/mg protein). Surprisingly, both BAY 41-8543 and YC-1 also dose-dependently increased cAMP levels (Fig. 1A) but only $\sim 20\%$ relative to that of forskolin (Fig. 1A). BAY 41-8543 and YC-1 also had a minimal effect on cell proliferation compared to forskolin, with a reduction in cell survival only observed at 100 μ M (Fig. 1D). These anti-proliferative effects may occur due to a modulatory effect between cAMP and cGMP. Accumulation of cGMP levels may lead to allosteric regulation of dual-substrate PDEs leading to potentiation of cAMP and suppression of cell growth. These results suggest that that elevation cAMP pathway plays a more important role in reducing cell proliferation.

Heterotrimeric G proteins are the primary effectors of G protein-coupled receptors (GPCRs) with G_{α_s} activating AC and $G_{\alpha_{i/o}}$ inhibiting AC [29]. Pertussis toxin (PTX) and cholera toxin (CTX) were utilised to determine whether G protein-mediated cAMP production inhibits C6

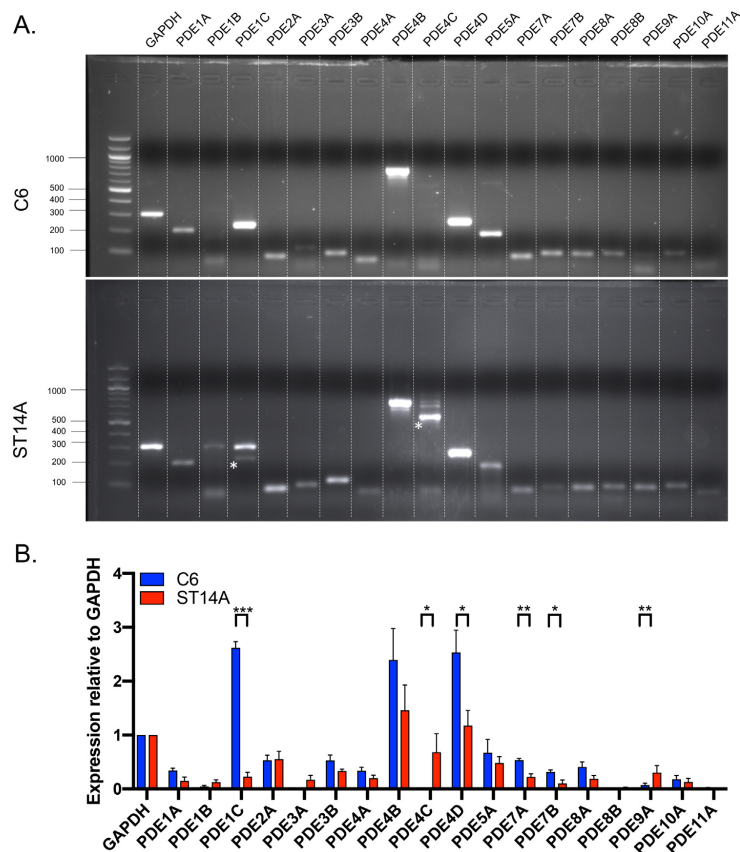


Fig. 2. Expression profile of PDE isoenzymes in C6 and ST14A cells. **A.** Representative gel documentation showing amplified PDEs genes from C6 and ST14A cell line. (*) on the gel showed correct band size. **B.** Semi-quantitative mRNA levels in C6 cells and ST14A cells. Expression of each gene of interest was normalised relative to GAPDH. Data are expressed as the mean \pm SEM from 5 to 7 individual repeats. Data were determined as statistically different (*, $p < 0.05$; **, $p < 0.01$; ***, $p < 0.001$) compared to individual isoenzyme between both cell lines using Student's *t*-test analysis.

cell growth. Treatment with CTX or PTX induced only a small elevation in cAMP levels and only suppressed C6 cell growth by 20% in a dose-dependent manner (Fig. 1D). Furthermore, despite potent stimulation of cAMP accumulation upon treatment with the non-selective β -adrenoceptor agonist, isoprenaline, suppression of cell growth was significantly poorer than treatment with forskolin. This implies that GPCR-mediated cAMP accumulation is insufficient to maximally suppress C6 cell growth and is likely a result of transient effector activation, receptor desensitisation or spatially localised signalling. Together, these results suggest that increasing cAMP concentration, through direct pharmacological activation of AC, plays a pivotal role in inhibiting cell growth with a minimal involvement of cGMP.

3.2. Specific inhibition of PDEs indicates reliance on PDE expression levels

Given that intracellular concentrations of cAMP are modulated both by its production and degradation, we next sought to investigate the expression of PDEs in a glioma cell line. Reverse transcription PCR (rt-PCR) was performed to determine the expression of each PDE isoenzyme in C6 cells, compared to ST14A cells, a rodent model for

healthy neurons. As shown in Fig. 2, the overall expression level of PDEs was higher in C6 cells compared to ST14A cells. With the exception of PDE1C, there was little overall difference in the profiles of PDEs expressed between C6 cells and ST14A cells. PDE1C, PDE4D, PDE7A, and PDE7B were the only PDEs to display significant elevation in C6 cells.

The rt-PCR expression profiles showed a wide number of PDEs to be expressed in glioma cells. However, this was only semi-quantitative, thereby, not providing a clear indication as to which PDEs might be the most important. Thus, we next investigated the role of PDEs in regulating cAMP levels and cell proliferation in C6 cells by applying small molecule selective PDE inhibitors as tools to modify their action. The small compounds were blindly screened and subsequently decoded after data analysis (see methods). Both cell lines were stimulated with the pEC₂₀ concentration of forskolin to increase the range for detecting an elevation of cAMP in the presence of selected PDE inhibitor. pEC₅₀ values for cAMP production and pIC₅₀ values for cell growth inhibition for each compound are quoted in Table 1 and their pharmacological actions are summarised in Table 2.

Plotting the potencies of each PDE inhibitor revealed a significant

Table 1
Potency values for cAMP production (pEC₅₀) and for cell growth inhibition (pIC₅₀) of each PDE inhibitor in C6 glioma cells and ST14A cells.

| Compounds | Target PDE(X) ^a | C6 | | | | ST14A | | | |
|---------------|----------------------------|-----------------------------|-----------------------------|-----------------------------|-----------------------------|-----------------------------|------------------------------|-----------------------------|-----------------------------|
| | | pEC ₅₀ | Span (cAMP) | pIC ₅₀ | Span (proliferation) | pEC ₅₀ | Span (cAMP) | pIC ₅₀ | Span (proliferation) |
| Vinopetine | 1 | 15.10 ± 0.08 ^{***} | 27.86 ± 1.05 ^{***} | 5.83 ± 0.13 [*] | 45.33 ± 3.12 ^{***} | 4.16 ± 0.04 ^{***} | 13.15 ± 2.22 ^{***} | N/A | N/A |
| EHNA | 2 | 15.06 ± 0.07 ^{***} | 24.26 ± 1.78 ^{***} | 5.04 ± 0.25 | 36.34 ± 3.31 ^{***} | N/A | N/A | 6.57 ± 0.08 ^{***} | 20.86 ± 1.20 ^{***} |
| Clostramide | 3 | 17.19 ± 0.09 ^{***} | 15.20 ± 1.45 ^{***} | N/A | N/A | N/A | N/A | 8.39 ± 0.15 ^{***} | 10.56 ± 1.90 ^{***} |
| Amrinone | 3 | 13.68 ± 0.08 ^{***} | 108.9 ± 4.82 ^{***} | 4.11 ± 0.04 ^{***} | 86.44 ± 2.26 ^{***} | 3.84 ± 0.02 ^{***} | 89.70 ± 1.12 ^{**} | 3.91 ± 0.11 ^{***} | 54.37 ± 6.17 ^{***} |
| Milrinone | 3 | N/A | N/A | 8.06 ± 0.13 ^{***} | 34.49 ± 4.66 ^{***} | 7.05 ± 0.18 ^{***} | 27.45 ± 2.35 | N/A | N/A |
| Trequinsin | 2,3,7 | 15.65 ± 0.08 ^{***} | 50.57 ± 2.02 ^{***} | 4.87 ± 0.07 [*] | 96.93 ± 0.94 ^{***} | 6.21 ± 0.06 ^{***} | 80.31 ± 1.85 | 4.62 ± 0.04 ^{***} | 75.82 ± 0.79 ^{***} |
| Rolipram | 4 | 16.96 ± 0.04 ^{***} | 60.46 ± 3.74 ^{***} | 6.78 ± 0.20 ^{***} | 23.44 ± 2.94 ^{***} | 7.41 ± 0.04 ^{***} | 59.26 ± 4.11 ^{***} | 7.23 ± 0.05 | 15.57 ± 1.28 ^{***} |
| Ibudilast | 4 | 16.03 ± 0.11 ^{***} | 64.21 ± 3.46 ^{***} | N/A | 31.76 ± 1.30 | 6.15 ± 0.12 ^{***} | 48.64 ± 2.18 ^{***} | N/A | N/A |
| Picamilast | 4 | 18.73 ± 0.04 ^{***} | 41.32 ± 2.87 ^{***} | 7.05 ± 0.17 ^{***} | N/A | 9.02 ± 0.14 ^{***} | 35.24 ± 1.96 ^{***} | N/A | N/A |
| Roflumilast | 4 | 10.47 ± 0.03 ^{***} | 54.58 ± 3.12 | 10.57 ± 0.22 ^{***} | 14.72 ± 1.66 ^{***} | 10.48 ± 0.08 ^{***} | 28.77 ± 0.78 ^{***} | 10.92 ± 0.09 ^{***} | 47.19 ± 1.63 ^{***} |
| Sildenafil | 5 | N/A | N/A | 8.56 ± 0.16 ^{***} | -6.77 ± 3.54 ^{***} | 8.79 ± 0.20 ^{***} | -4.57 ± 0.93 ^{***} | 9.67 ± 0.11 ^{***} | 12.71 ± 2.02 ^{***} |
| Tadalafil | 5 | N/A | N/A | N/A | N/A | 7.88 ± 0.04 ^{***} | -23.15 ± 1.38 | 8.81 ± 0.43 ^{***} | -2.69 ± 1.55 |
| Caffeine | 1,4,5 | N/A | N/A | N/A | N/A | N/A | N/A | 6.65 ± 0.06 ^{***} | a9.02 ± 1.08 ^{***} |
| Zaprinas | 5,6,9,11 | 5.61 ± 0.11 ^{***} | 14.27 ± 1.12 ^{***} | 6.03 ± 0.30 ^{***} | 49.70 ± 4.60 ^{***} | N/A | N/A | 5.86 ± 0.09 ^{***} | 46.71 ± 1.45 ^{***} |
| TC3.6 | 7 | N/A | N/A | 7.53 ± 0.26 ^{***} | 15.31 ± 2.47 ^{***} | N/A | N/A | 5.69 ± 0.05 ^{***} | 21.22 ± 1.49 ^{***} |
| BRL-50481 | 7 | a6.41 ± 0.09 ^{***} | 31.3 ± 1.67 ^{***} | 6.70 ± 0.15 ^{***} | 33.07 ± 2.74 ^{***} | N/A | N/A | 7.73 ± 0.24 ^{***} | a4.52 ± 1.68 ^{***} |
| BC 11-38 | 8 | N/A | N/A | N/A | N/A | N/A | N/A | N/A | N/A |
| BAY-736691 | 9 | N/A | N/A | N/A | N/A | N/A | N/A | N/A | N/A |
| PF-0449613 | 9 | N/A | N/A | N/A | N/A | 7.55 ± 0.12 ^{***} | -23.48 ± 1.75 ^{***} | 8.05 ± 0.08 ^{***} | a6.37 ± 0.72 ^{***} |
| PF 2.545.920 | 10A | N/A | N/A | 9.46 ± 0.06 ^{***} | -8.97 ± 3.05 ^{***} | N/A | N/A | 10.78 ± 0.11 ^{***} | 11.94 ± 4.13 ^{***} |
| PF 04.671.536 | 11 | N/A | N/A | N/A | N/A | N/A | N/A | N/A | N/A |
| IBMX | Non-selective | a4.30 ± 0.06 ^{***} | 42.79 ± 1.53 ^{***} | 6.12 ± 0.06 ^{***} | 54.17 ± 3.20 ^{***} | 4.56 ± 0.06 ^{***} | 57.53 ± 3.52 | 4.20 ± 0.09 | 47.95 ± 2.70 |
| Forskolin | AC activator | a5.43 ± 0.08 ^{***} | 64.97 ± 3.51 ^{***} | 5.12 ± 0.06 ^{***} | 84.70 ± 1.44 ^{***} | 6.43 ± 0.12 | 74.06 ± 3.07 | 6.44 ± 0.02 | 45.11 ± 1.22 |
| Cisplatin | DNA crosslinker | N/A | N/A | 6.02 ± 0.09 ^{***} | 96.85 ± 2.57 | N/A | N/A | 5.92 ± 0.09 ^{***} | 86.50 ± 2.30 ^{***} |

N/A – not applicable; compounds did not have any effect on cAMP production or cell growth inhibition. ^{***} unless mentioned, targets refer to particular PDE isoform. Data are presented as the mean ± SEM of 6–9 individual repeat. Data were determined as statistically different (*, p < 0.05; ***, p < 0.001) compared to forskolin using one-way ANOVA followed by Dunnett's post-hoc analysis. #, showing negative responses, either suppressing cAMP accumulation or being proliferative.

Table 2
Summary of the pharmacological effects of each PDE inhibitor on cAMP production and cell proliferation.

| Compound | Target | C6 | | ST14A | |
|---------------|---------------|------------|---------------|-------|---------------|
| | | cAMP | Proliferation | cAMP | Proliferation |
| Vinpocetine | 1 | ↑ | ↓↓ | ↑ | – |
| EHNA | 2 | ↑ | ↓↓ | – | ↓ |
| Cilostamide | 3 | ↑↑ | – | – | ↓ |
| Amrinone | 3 | ↑↑↑ | ↓↓↓ | ↑↑↑ | ↓↓↓ |
| Milrinone | 3 | – | ↓↓ | ↑ | – |
| Trequinsin | 2,3,7 | ↑↑↑ | ↓↓↓ | ↑↑↑ | ↓↓↓ |
| Rolipram | 4 | ↑↑↑ | ↓ | ↑↑↑ | ↓ |
| Ibudilast | 4 | ↑↑↑ | ↓ | ↑↑ | – |
| Piclamilast | 4 | ↑↑ | – | ↑↑ | – |
| Roflumilast | 4 | ↑↑↑ | ↓ | ↑ | ↓ |
| Sildenafil | 5 | – | ↑ | ↓ | ↓ |
| Tadalafil | 5 | – | ↑ | ↓ | ↑ |
| Caffeine | 1,4,5 | Bell-shape | – | – | ↓ |
| Zaprinast | 5,6,9,11 | ↑ | ↓↓ | – | ↓↓ |
| TC3.6 | 7 | – | ↓ | – | ↓ |
| BRL-50481 | 7 | ↑↑ | ↓↓ | – | ↓ |
| BC 11-38 | 8 | – | – | – | – |
| BAY-736691 | 9 | – | – | – | – |
| PF-0449613 | 9 | – | – | ↓ | ↓ |
| PF 2,545,920 | 10A | – | ↑ | – | ↓ |
| PF 04,671,536 | 11 | – | – | – | – |
| IBMX | Non-selective | ↑↑ | ↓↓↓ | ↑ | ↓↓ |

↑ = increase 10–30%, ↑↑ = increase 31–50%, ↑↑↑ = increase > 50%, ↓ = suppress 10–30%, ↓↓ = suppress 31–50%, ↓↓↓ = suppress > 50%.

($p < 0.001$) positive correlation between elevation of cAMP levels and inhibition of cell growth (Fig. 3A and 3B) for both C6 cells ($r = 0.83$ (95% confidence interval 0.46–0.95)) and ST14A cells ($r = 0.97$ (95% confidence interval (0.73–0.99)). To provide a convenient and rapid method for comparing each PDE inhibitor for effects on cell growth, the terms for efficacy and affinity (potency and span values) were multiplied for both C6 and ST14A cells (arbitrary units – Fig. 3C and D). An ideal compound would be one that shows high potency for inhibition of growth and a large range. An arbitrary threshold of 200 was set to determine compounds that might be worth further investigation. Cisplatin, a widely used non-selective anti-proliferative agent, was used as a reference to validate our method (with pIC_{50} of 6.02 and 5.92 in C6 and ST14A cells, respectively, Table 1). In both C6 and ST14A cells, cisplatin showed the highest selection criteria value (582.1 in C6 cells and 511.1 in ST14A cells), thus proving that this calculation may help to determine how effective the compounds are at inhibiting cell proliferation. From our initial screen only 9 compounds were deemed to have passed the threshold: vinpocetine (PDE1 inhibitor), amrinone, milrinone (both PDE3 inhibitors), ibudilast (PDE4 inhibitor), trequinsin, IBMX and zaprinast (multiple PDE isoform inhibitors), BRL50481 (PDE7 inhibitor), and forskolin. The selectivity of the inhibitors that were successful in the screen correlated well with PDE expression levels in C6 cells (Fig. 2A and B). The compounds that showed the highest values (> 350) were forskolin, trequinsin, amrinone, and IBMX. Apart from amrinone, these compounds target multiple components in the cAMP synthesis/degradation pathway, thus explaining their greater affinity/efficacy. IBMX and zaprinast were not used in future studies due to selectivity issues. IBMX is an adenosine receptor antagonist [31], whilst zaprinast is a GPR35 agonist [32]. Finally, it is worth noting that all compounds displayed lower affinity/efficacy values in ST14A cells (Fig. 3D) and this is consistent with the reduced PDE expression compared to C6 cells (Fig. 2B).

3.3. Cocktail of individual PDE2, PDE3, and PDE7 inhibitors exhibited a similar effect to that of trequinsin, both upon elevating cAMP levels and suppressing cell growth

Of all the compounds tested, trequinsin was the most potent at increasing cAMP levels and suppressing cell growth. Trequinsin is known to potently inhibit PDE3, but is suggested to also block the cAMP binding site of PDE2 and PDE7 [26]. This, however, has not been thoroughly investigated. Therefore, we probed the mechanism by which trequinsin exerts its antiproliferative effects by combining selective inhibitors against PDE2, PDE3, and PDE7 – by using EHNA, amrinone, and BRL-50481, respectively. None of the selective PDE inhibitors were more potent at stimulating cAMP accumulation or inhibiting cell proliferation in C6 cells, as individual treatments, than trequinsin (Fig. 4A and D). Although amrinone displayed a similar E_{max} to that of trequinsin for cAMP accumulation, the I_{max} for cell growth inhibition was ~50% relative to trequinsin (Fig. 4A and D, Table 3). Subsequently, we investigated the combinatorial effect of individual PDE2, 3, and 7 inhibitors. The combination of EHNA and amrinone (PDE2 and PDE3 inhibitors), as well as EHNA and BRL-50481 (PDE2 and PDE7 inhibitors), enhanced the potency of effect compared to when these drugs were used individually (Fig. 4B and E, Table 3). However, the combination of BRL-50481 with amrinone (PDE3 and PDE7 inhibitors) was comparable to that of amrinone alone. Interestingly, when all three selective inhibitors were combined, the potency and efficacy were similar to that of trequinsin (Fig. 4C and F, Table 3). Overall, this suggests that simultaneous inhibition of PDE2, PDE3, and PDE7 can mimic the antiproliferative effect of trequinsin.

3.4. Targeting both AC and PDEs enhances the anti-proliferative effect

Our data suggests that elevation of cAMP levels through either, activation of AC, or inhibition of PDEs, positively correlates with reduced cell proliferation. Thus, we hypothesised that dual activation of AC and inhibition of PDEs would induce larger suppression in cell growth beyond that of a single target treatment. To test this, we determined the combinatorial effect of forskolin and trequinsin on cAMP accumulation and cell proliferation (Fig. 5).

There was a similar pattern of effects observed upon forskolin and trequinsin co-treatment on both cAMP accumulation and cell proliferation assays. The combination of forskolin and trequinsin significantly enhanced cAMP accumulation and reduced C6 cell growth in a dose-dependent manner compared to forskolin alone (Fig. 5A–C). The potency of the forskolin-mediated anti-proliferative effect was enhanced approximately 10-fold in the presence of 10 μ M trequinsin (pIC_{50} of forskolin is 5.75, that of forskolin in combination with 10 μ M trequinsin is 6.87). These data demonstrate synergistic elevation of cAMP by targeting AC and PDEs resulting in greater suppression of C6 cell growth. Indeed, the effect of the combination of 1 μ M forskolin and 0.1 μ M trequinsin was approximately equal to that of cisplatin (pIC_{50} of 6.09, Table 1).

3.5. Blockade of cAMP export enhances the anti-proliferative effect of forskolin, trequinsin, and the PDE inhibitor cocktail

C6 cells are known to express MRP4 [33] a transporter known to export intracellular cAMP. Having confirmed that inhibiting PDEs, or activating AC, elevates total cAMP levels and suppresses proliferation of C6 cells, we aimed to investigate if these effects could be enhanced by preventing cellular export of cAMP.

Pre-treatment with PU23, a small molecule inhibitor of MRP4, resulted in a dose-dependent reduction in extracellular cAMP levels post stimulation with forskolin, trequinsin or the PDE inhibitor cocktail (Fig. 6A, C and D). There was also a substantial elevation in intracellular concentrations of cAMP in the presence of PU23 after 2 h stimulation with forskolin (Fig. 6B). This suggests that in the absence of

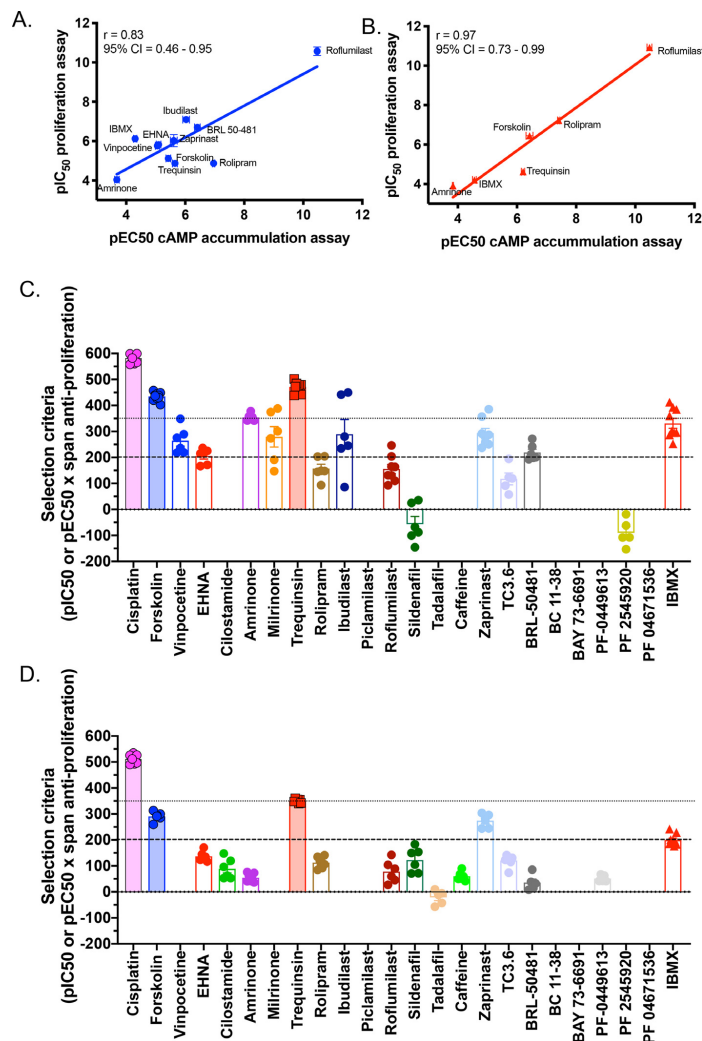


Fig. 3. Elevation of intracellular cAMP is positively correlated with cell growth suppression. A, B. Correlation (with 95% confidence interval) of log potencies of each PDE inhibitor in C6 (A) and ST14A cells (B) was determined by calculating Pearson's correlation coefficient (r). C, D. Compound selection criteria from C6 (C) and ST14A cells (D) was calculated based on potency and efficacy in proliferation assay. The dashed lines represent threshold value of 200 (less stringent criteria) and the dotted lines a higher criteria value of 350. Individual data point was obtained from supplemental information (Figs. 1–4).

PDE inhibitor, blockade of cAMP export maintains high intracellular cAMP levels. Indeed, the combination of PU23 with forskolin, trequinsin, or the PDE inhibitor cocktail enhanced the anti-proliferative effect of each compound (Fig. 6E–G). Taken together, these data suggest that suppression of C6 cell proliferation can be enhanced by blockade of cAMP export.

3.6. The anti-proliferative effect of forskolin is mediated through a PKA-dependent mechanism

Having confirmed the effect of cAMP on C6 cell growth, we next

wanted to investigate the involvement of downstream effectors of cAMP, such as PKA and Epac type I and II, as well as the cGMP effector, PKG, and GC activation on proliferation of C6 cells (Fig. 7A). To do this, we utilised a range of small molecule inhibitors: KT5720 (PKA), ESI-09 (non-selective Epac), CE3F4 (Epac1), HJC0350 (Epac2), and KT5823 (PKG), and the GC activator (BAY 41-8543). Co-treatment of 10 μ M KT5720 significantly attenuated the anti-proliferative effects of forskolin ($p < 0.01$), trequinsin ($p < 0.001$) and the PDE inhibitor cocktail ($p < 0.05$) on C6 cells (Fig. 7B–D). None of the selective or non-selective Epac inhibitors had any effect on trequinsin-mediated cell growth suppression, although there was an elevation of forskolin-

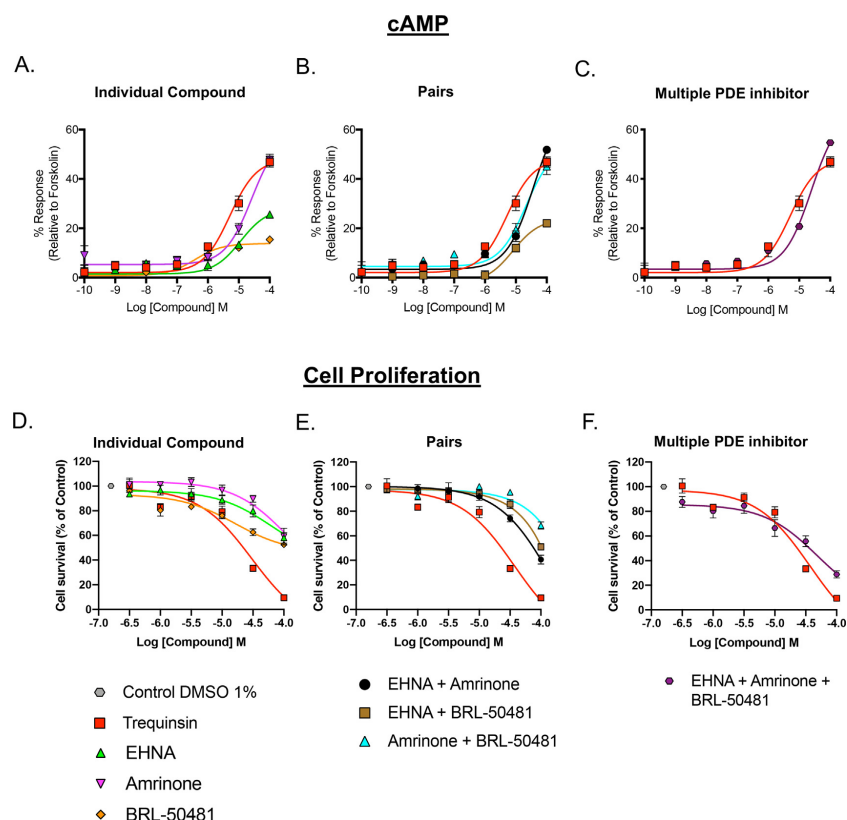


Fig. 4. The effect of selective PDE inhibitors, as individual, dual, or multiple treatments, on intracellular cAMP levels and cell proliferation in C6 glioma cells. A–C. cAMP accumulation was determined in C6 cells following 30 min stimulation with EHNA, Amrinone or BRL-50481 alone (A), in pairs (B), or combined (C). Data are expressed relative to 100 μ M forskolin. D–F. Cell survival was determined in C6 cells following 72 h incubation with EHNA, Amrinone or BRL-50481 alone (D), in pairs (E), or combined (F). Data are expressed as percentage of cell survival relative to vehicle from 6 to 9 data sets. The effect of trequinsin alone is displayed on each graph for comparison. All data are the mean \pm SEM of 6–9 individual repeats.

Table 3
C6- proliferation assay-combinatorial effect of PDE2, 3, 7 inhibitors.

| Compound | cAMP accumulation assay | | Proliferation Assay | | Selection criteria* |
|-----------------------------|-------------------------|------------------|---------------------|-------------------|---------------------|
| | pEC ₅₀ | Span | pIC ₅₀ | Span | |
| Trequinsin | 5.33 \pm 0.11 | 46.31 \pm 1.98 | 4.52 \pm 0.11 | 91.21 \pm 8.26 | 411.94 \pm 38.52 |
| EHNA | 4.91 \pm 0.10 | 26.19 \pm 0.89 | 4.20 \pm 0.21 | 57.21 \pm 10.48 | 240.44 \pm 45.57 |
| Amrinone | 4.58 \pm 0.04 | 53.88 \pm 1.63 | 3.94 \pm 0.15 | 87.79 \pm 13.62 | 346.01 \pm 55.26 |
| BRL-50481 | 6.20 \pm 0.34 | 13.86 \pm 0.74 | 4.79 \pm 0.17 | 47.02 \pm 4.45 | 225.39 \pm 22.73 |
| EHNA + amrinone | 4.58 \pm 0.03 | 62.51 \pm 2.17 | 4.19 \pm 0.17 | 85.97 \pm 12.32 | 361.56 \pm 53.66 |
| EHNA + BRL-50481 | 5.05 \pm 0.20 | 27.21 \pm 1.40 | 4.07 \pm 0.13 | 77.77 \pm 9.73 | 316.34 \pm 40.85 |
| Amrinone + BRL-50481 | 4.65 \pm 0.07 | 49.65 \pm 2.95 | 3.77 \pm 0.17 | 66.75 \pm 11.94 | 248.98 \pm 45.30 |
| EHNA + amrinone + BRL-50481 | 4.58 \pm 0.07 | 64.97 \pm 1.82 | 4.52 \pm 0.14 | 84.64 \pm 8.69 | 382.12 \pm 41.10 |

Data are expressed as mean \pm SEM from 7 to 10 individual data.

*Compound selection criteria was calculated based on potency and efficacy in proliferation assay (data obtained from Fig. 4).

mediated cell growth suppression with CE3F4 ($p < 0.01$) (Fig. 7B). Interestingly, cotreatment with KT5823 significantly enhanced the anti-proliferative effects of forskolin and trequinsin ($p < 0.001$), whilst BAY 41-8543 treatment also increased forskolin-mediated suppression of cell proliferation ($p < 0.01$). This indicates an involvement of cGMP

signalling pathways in cell proliferation. It is possible that accumulation of cGMP, in the presence of the PKG inhibitor or GC activator, potentiates cAMP/PKA signalling pathways through the sequestration of non-selective PDEs, thereby reducing cell growth. There was, however, no significant effect of BAY 41-8543 treatment on the anti-

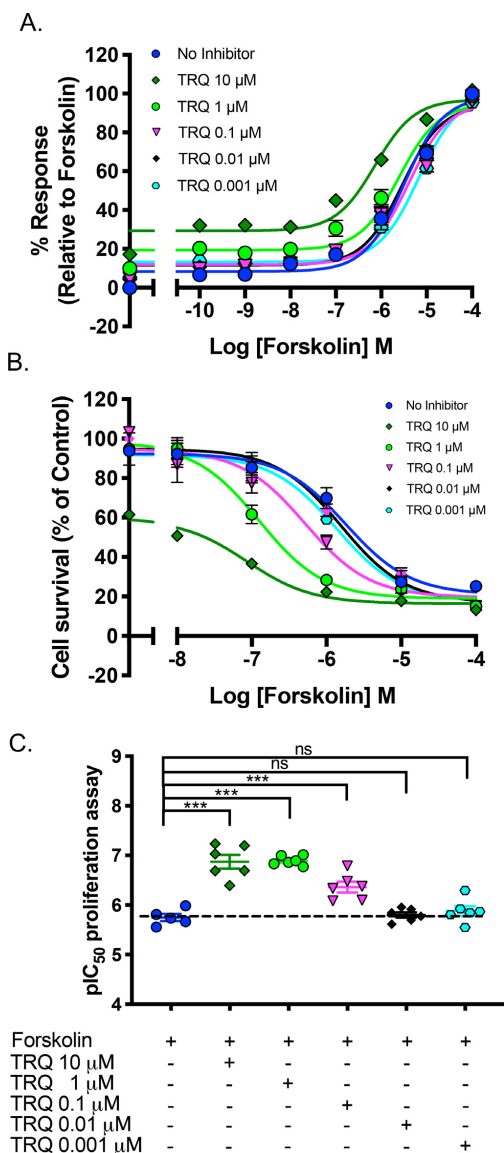


Fig. 5. Forskolin and trequinsin act synergistically to increase cAMP accumulation and suppress cell growth. **A.** Concentration-dependent effect of trequinsin upon cAMP accumulation in C6 cells following 30 min stimulation with forskolin. Data are expressed relative to 100 μ M forskolin in the absence of trequinsin. **B.** Concentration-dependent inhibitory effect of trequinsin on C6 cell growth following 72-hour incubation with forskolin. Data are expressed as percentage cell survival relative to vehicle. **C.** pIC_{50} values for individual cell survival curves for each treatment condition. All data are the mean \pm SEM of 6–9 individual repeats. Data were determined as statistically different (ns, not significant; ***, $p < 0.001$) compared to forskolin using one-way ANOVA followed by Dunnett's *post-hoc* analysis. TRQ – trequinsin.

proliferative effects of trequinsin or the PDE inhibitor cocktail. This may suggest that the actions observed for KT5823 are not purely due to inhibition of PKG. These data highlight the importance of the homeostasis between cAMP and cGMP, as well as that the anti-proliferative effects of forskolin, trequinsin and the PDE inhibitor cocktail are largely mediated through a cAMP/PKA-dependent pathway.

3.7. Trequinsin, but not forskolin or the PDE inhibitor cocktail, has cAMP-independent actions leading to apoptosis

In order to delineate the mechanism by which cAMP promotes cell death or inhibits cell growth, we investigated if the anti-proliferative effects on C6 cells were related to apoptosis. Early apoptotic events can be detected through the protease activity of caspase-3 and caspase-7 that will eventually degrade proteins pivotal for cell survival. In this study, we quantified cells positive for caspase-3 and -7 activity in C6 cells using fluorescence microscopy after treatment with CellEvent™ Caspase-3/-7 green detection kit. Cells were co-stained with Hoechst 33,342 and propidium iodide to label all nuclei and dead cells.

Staurosporine is a known pan caspase activator. Quantitative analysis revealed that staurosporine-treated cells were entirely positive for active caspase-3/-7 (Fig. 8A). Consistent with these results, activated caspase-3/-7 resulted in cell death which was confirmed by propidium iodide staining (Fig. 8A). Among all other treatments, only 100 μ M trequinsin exhibited comparable effects on cell death and caspase activity to that of staurosporine. Treatment with forskolin or the PDE 2,3,7 inhibitor cocktail resulted in $< 10\%$ caspase activity and cell death (Fig. 7A). This suggests that 100 μ M trequinsin may have toxic, non-cAMP-dependent effects, on C6 cells.

3.8. Elevated intracellular cAMP induces growth arrest at the G_2/M phase of the cell cycle

Having demonstrated that elevation of cAMP inhibits cell proliferation, without inducing extensive apoptotic events on cells treated with forskolin, PDE inhibitor cocktail, or a low concentration of trequinsin, we postulated that this effect arose due to cell growth arrest. Thus, we investigated the individual stages of the cell cycle of C6 cells post-treatment with forskolin, trequinsin or the PDE2,3,7 inhibitor cocktail by using propidium iodide staining and flow cytometry. Cell cycle analysis showed that forskolin, trequinsin, and the PDE2,3,7 inhibitor cocktail altered the cell phase (Fig. 8B–E). While there was no significant difference between complete media and DMSO, forskolin or PDE inhibitor cocktail treated cells arrested predominantly in G_2/M phase. This indicates that both forskolin and the PDE2,3,7 inhibitor cocktail alter C6 cell cycle by a similar mechanism. In contrast, of the proportion of cells that survived treatment with 100 μ M trequinsin, approximately 70% were aneuploid, with the remaining alive cells arrested in G_2/M phase. Interestingly, when lower concentrations of trequinsin ($< 100 \mu$ M) were considered, the cell phase profile more closely matched that of 10 μ M PDE2,3,7 inhibitor cocktail (Fig. 8B). This data suggests that 100 μ M trequinsin induces a toxic effect on the C6 cells that is most likely independent of its action upon the cAMP pathway.

4. Discussion

cAMP is a ubiquitous second messenger, which together with cGMP, controls a myriad of physiological responses [34] including reparative processes. Interestingly, cAMP signalling has been reported to have different effects on cell proliferation; either causing or arresting proliferation, depending on the cell type investigated [9,13,35]. These divergent effects of cAMP on the proliferative response are believed to be controlled by several factors including stimulus, the nature of the intracellular cAMP effectors within the cells, the strength of signal, and subcellular compartmentalisation [36]. In brain tumours, suppression

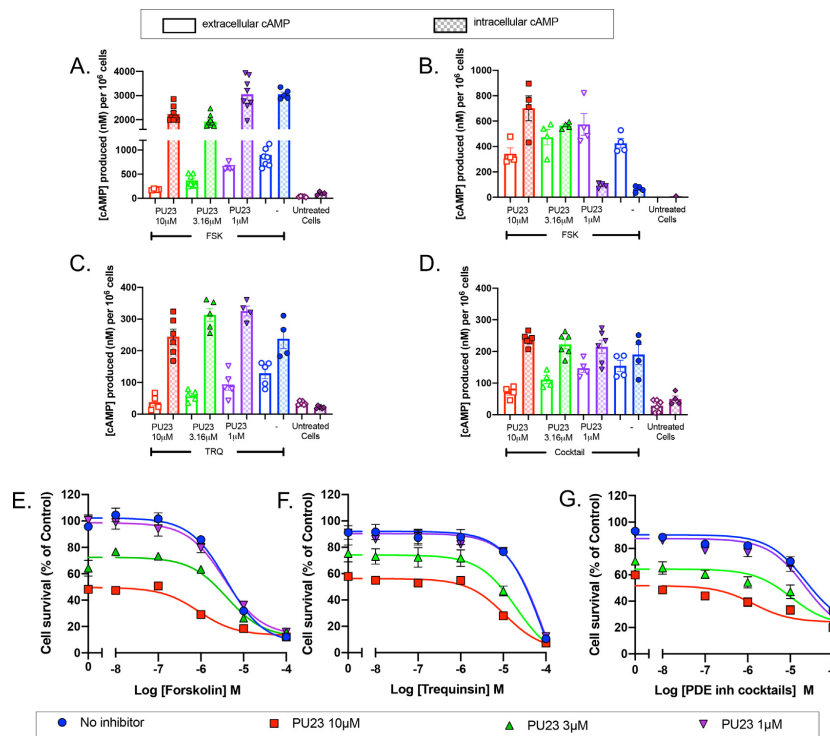


Fig. 6. Elevation of intracellular cAMP by inhibiting its efflux is correlated with cell growth suppression in C6 cells. A–D. Extracellular and intracellular cAMP levels from C6 cells following stimulation with; forskolin for 1 h (A) and 2 h (B); trequinsin for 2 h (C); or PDE inhibitor cocktail for 2 h (D), in the presence and absence of a range of concentrations of the MRP4 inhibitor, PU23. E–G. Survival of C6 cells following 72-hour treatment with forskolin (E), trequinsin (F), or PDE inhibitor cocktail (G) in the absence and presence of increasing concentrations of PU23. Data are expressed as percentage cell survival relative to vehicle. All data are the mean \pm SEM of 4–8 individual repeats. FSK – forskolin, TRQ – trequinsin.

of cAMP is associated with gliomagenesis compared to non-tumour controls [37,38]. As cAMP levels are suppressed 4-fold in brain tumours compared to those in normal tissue [5], we hypothesised that augmenting production of cAMP may restore intracellular signalling and have beneficial antiproliferative effects.

Although PDEs have long been targets for pharmacological modulation, there have been no studies characterising PDE isoenzyme expression in glioma cells or the effect of PDE modulation. In the present study, we demonstrate that direct pharmacological activation of AC and inhibition of PDEs results in greater suppression of glioma cell proliferation than G protein-mediated AC activation. Although activation of G_s-coupled β -ARs by isoprenaline, or modulation of G protein activity by PTX or CTX treatment increased cAMP production, neither substantially suppressed glioma cell growth. This is possibly due to only transient activation of cAMP effectors, receptor desensitisation, spatially localised cAMP accumulation, or, the instability of isoprenaline in aqueous solution. Prolonged stimulation with GPCR agonists not only induces desensitisation through receptor internalisation, but may also alter transcription levels resulting in receptor downregulation [39]. It is worth noting that addition of antioxidant such as ascorbic acid or EDTA may be useful to minimise the degradation of isoprenaline during the treatment.

Evaluation of PDE mRNA expression level in C6 cells revealed that almost all PDE isoenzymes are expressed. Interestingly, inhibitors of cAMP-specific or cGMP-specific PDEs showed minimal effects on cell

growth, except for ibudilast (a cAMP-specific PDE4 inhibitor). Inhibition of PDE1, PDE2, PDE3, PDE4, and PDE7 resulted in greater modulation of cAMP levels and cell growth. These PDEs, with the exception of PDE4 and PDE7, hydrolyse both cAMP and cGMP. Dual substrate PDEs provide a point for crosstalk between cGMP and cAMP signalling pathways and have unique mechanisms of regulation [40,41].

The most potent anti-proliferative effects were observed in trequinsin-treated cells. Trequinsin is commonly known as an ultrapotent PDE3 inhibitor, although it has also been shown to have activity against PDE2 and PDE7 [26]. There have, however, been no studies into inhibition of PDE2 and PDE7 by trequinsin. A combination of inhibitors of PDE2, PDE3, and PDE7, the PDE inhibitor cocktail, had a similar magnitude of effect to that of trequinsin, whilst inhibition of single or dual PDEs failed to mimic the effect. In order to enhance anti-proliferative activity further, the selectivity of individual compounds towards each PDE needs to be improved.

Through the use of several pharmacological tools we attributed forskolin and trequinsin, and the PDE inhibitor cocktail mediated inhibition of cell growth to enhanced activation of PKA. Considering the greater affinity of cAMP for PKA than Epac1/2 (5–24.6 nM versus 4 μ M/1.2 μ M, respectively) [42–44], it is possible that elevated cAMP, upon treatment with forskolin or PDE inhibitors will preferentially activate PKA over Epac1/2. Taken together, there is a possibility that stimulation of AC by forskolin or by PDE inhibitors will trigger massive

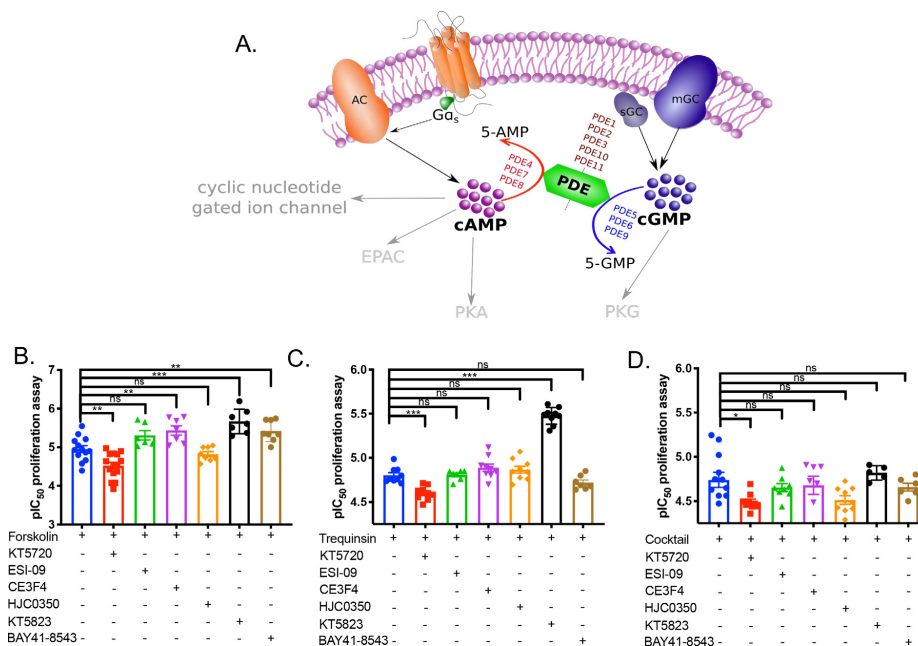


Fig. 7. The effect of downstream effectors of cAMP and cGMP on forskolin and trequinsin-mediated cell growth suppression of C6 cells. **A.** Schematic diagram illustrating cAMP and cGMP synthesis, degradation and downstream effectors. **B-D.** Cell survival was determined in C6 cells following 72 h incubation with forskolin (B), trequinsin (C), or a combination of PDE2,3,7 inhibitors (D) in the presence either KT5720 (10 μ M), ESI-09 (10 μ M), CE3F4 (10 μ M), HJC0350 (10 μ M), BAY41-8543 (10 μ M). Data are represented as individual plC_{50} values for anti-proliferation curves for each treatment condition. Data were determined as statistically different (ns, not significant; *, $p < 0.05$; **, $p < 0.01$; ***, $p < 0.001$) compared to in the absence of compounds using one-way ANOVA followed by Dunnett's *post-hoc* analysis. KT5720 – PKA inhibitor, ESI-09 – non-selective Epac1/2 inhibitor, CE3F4 – Epac1 inhibitor, HJC0350 – Epac2 inhibitor, KT5823 PKG inhibitor, BAY41-8543 – GC activator.

production of cAMP and consequently the PKA pathway will be predominantly activated with minor involvement of Epac1/2. The inhibitory action of cAMP on cell growth has also been reported to involve a complex mechanism between PKA, MAPK/ERK, and cyclin-dependent kinase 2 [45,46].

Somewhat unexpectedly, this study demonstrated that PKG inhibition increased the anti-proliferative effects of forskolin- and trequinsin-treated cells, whilst GC activation also potentiated forskolin-mediated cell growth suppression. This is most likely due to cross talk between the cGMP and cAMP pathways via dual substrate PDEs. For instance, while cGMP binding to PDE2 allosterically enhances hydrolysis of cAMP, cGMP competitively inhibits PDE3 to reduce the rate of cAMP breakdown [17]. This control is, however, dependent on the concentration of cGMP, with allosteric regulation of PDE2 requiring higher (1–5 μ M) [47] cGMP levels than the affinity of cGMP for the catalytic site of PDE3 (180 nM) [17]. We have shown that C6 cells have a weaker propensity to elevate cGMP levels than cAMP. Thus, a modest increase in cGMP may compete with cAMP to occupy catalytic sites resulting in a decrease in the hydrolysis rate of cAMP by dual substrate PDE isoforms, thus activating the cAMP/PKA pathway triggering enhanced cell growth suppression.

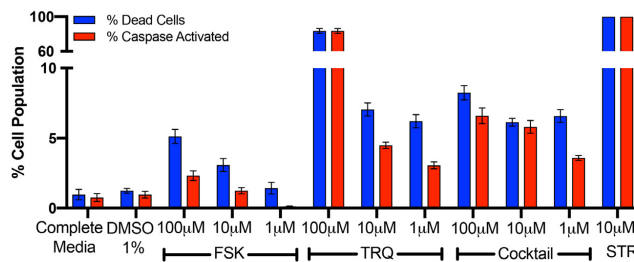
Surprisingly, there was no effect of PKG inhibition or GC activation on the anti-proliferative effects of the PDE inhibitor cocktail. Whilst this may suggest that the actions observed for KT5823 are not purely due to inhibition of PKG, the functional effect of the PDE inhibitor cocktail may be affected by compartmentalisation and local activation of PKA. A small increase in cGMP may elevate cAMP levels only in distinct

subcellular regions in the presence of the PDE inhibitor cocktail to activate PKA through anchoring proteins (AKAP) to different intracellular microstructures [47]. Although further investigation is required, these phenomena can be taken into account in explaining the differential responses observed upon PDE inhibitor cocktail treatment.

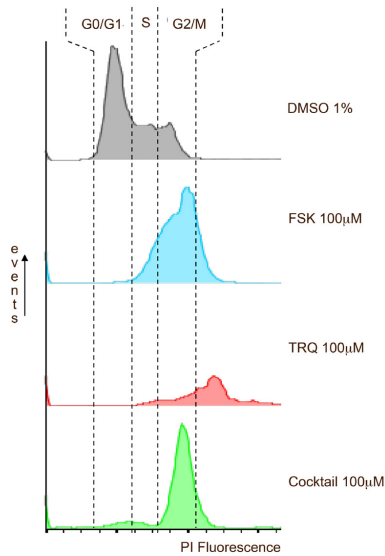
Although trequinsin has a comparable potency to that of forskolin for elevating intracellular cAMP levels and suppressing cell proliferation, at high concentrations (100 μ M) trequinsin induced substantial cell death of C6 cells and ST14A cells. This implies that at such high concentrations trequinsin binds to other non-PDE proteins that results in direct activation of caspase-3/7 to trigger cell death. Adequate activation of PKA will activate p53 and induce apoptosis [48] although we observed only < 10% cell death. Nonetheless, the remaining cells were aneuploidy with at least 4 N. It is likely that cells underwent faulty cell division and were not able to exit the mitotic state due to rapid and massive elevation of cAMP by 100 μ M trequinsin. There are no studies on the mechanism by which trequinsin causes aneuploidy and apoptosis, however, there are several reports that in other types of cancer where cAMP levels are elevated by PDE inhibition, activation of PKA resulted in activation of protein phosphatase 2A (PP2A) and Bim/BAD expression [13] that eventually cleaves caspases to mediate apoptosis.

Despite this, the study demonstrates that multitarget enhancement of cAMP signalling elevates anti-proliferative effects in a glioma cell model. Increasing cAMP levels through activation of AC (forskolin) and multiple PDE inhibition (by trequinsin) demonstrated synergistic cell growth suppression. Similarly, whilst it has been suggested that cyclic nucleotide efflux pumps may not contribute to controlling cAMP

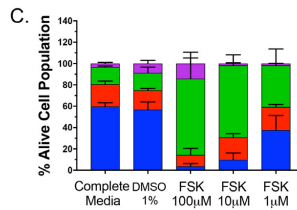
A.



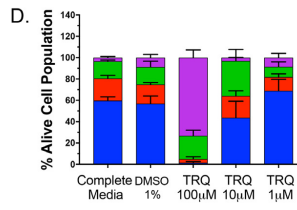
B.



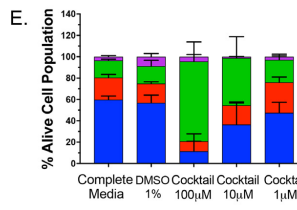
C.



D.



E.



aneuploidy G2/M S G0/G1

Fig. 8. Population of dead cells and activity of caspase-3/7 in C6 cells after 72 h treatment and cell cycle analysis by flow cytometry after PI staining. **A.** Percentage of dead cells determined by staining with propidium iodide and the percentage of cells with activated caspase-3/7, visualised by CellEvent caspase-3/7. All values are normalised to total cell number in each well. Staurosporine 1 μ M was used as a control for apoptotic cell death and cause 100% dead cells. **B.** Representative histograms of cell cycle distribution of C6 cells with selected treatment. **C–E.** Representative histograms of cells following treatment with forskolin (C), trequinsin (D), or PDE2,3,7 inhibitor cocktail (E) for 72 h. The percentage of cell distribution for each treatment including G₁, S, G₂/M, and dead cell population ($n = 4–8$ individual data). All data are the mean \pm SEM of 5 individual repeats. Data were determined as statistically different (*, $p < 0.05$; **, $p < 0.01$; ***, $p < 0.001$) compared to 1% DMSO using a one-way ANOVA followed by Dunnett's *post hoc* analysis. * $p < 0.05$, ** $p < 0.005$, *** $p < 0.001$. FSK – forskolin, TRQ – trequinsin, STR – staurosporine.

signalling [49], our study shows that inhibiting export of cAMP significantly enhances forskolin and multiple PDE inhibition mediated cell growth suppression. Thus, the dose of each compound could be reduced to potentially prevent any toxic side effects from trequinsin. Alternatively, combining individual selective inhibitors against PDE2,3,7 together showed similar efficacy to that of trequinsin but without significant toxicity in glioma cells. The inhibitor cocktail shows a higher number of cells with active caspase-3/7 activity compared to forskolin, possibly due to the availability of PDEs, which have been shown to be caspase substrates [13]. Both forskolin and the inhibitor cocktail trapped cells in G₂/M phase, which may lead to the loss of essential cellular components that are required for replication. Whilst this study has demonstrated that targeting the cyclic nucleotide pathway can suppress C6 cell growth, it should be noted that PDEs play an important role in many systems throughout the body, including the cardiovascular system, and thus targeting PDEs may cause off-target effects.

In conclusion, we have used a chemical biology approach to demonstrate that cAMP inhibits growth of glioma cells. Anti-proliferative effects of forskolin are mediated by elevating cAMP levels leading to activation of PKA and arrest of cells in the G₂/M phase of the cell cycle. In comparison, multiple inhibition of PDEs by trequinsin not only inhibits cell growth via the cAMP/PKA cascade, but also triggers cell death through caspase-3/-7 activation. Concomitant targeting of both AC and PDEs synergistically elevates intracellular cAMP levels within glioma cells. Due to possible side effects of trequinsin, a cocktail of individual PDE2, PDE3, and PDE7 inhibitors can be used as an alternative to trequinsin to obtain similar functional effects without any toxicity. This study offers insight to identify new therapeutic approaches which have potential beneficial effects against glioma/glioblastoma.

Author contributions

DS, MH, LK, FS, DB, GL conceived and designed the research; DS, HP, HYY, IW performed the experiments; DS, MTH, TR, and GL analyzed data; DS, MH, HYY and GL wrote manuscript, DB, LK, TR, MTH revised and edited the manuscript.

CRedit authorship contribution statement

Dewi Safitri: Conceptualization, Methodology, Validation, Formal analysis, Investigation, Writing - original draft, Visualization. **Matthew Harris:** Conceptualization, Methodology, Formal analysis, Writing - review & editing. **Harriet Potter:** Investigation, Formal analysis. **Ho Yan Yeung:** Investigation, Writing - review & editing. **Ian Winfield:** Investigation, Writing - review & editing. **Liliya Kopanitsa:** Conceptualization, Resources, Writing - review & editing. **Fredrik Svensson:** Conceptualization, Resources. **Taufiq Rahman:** Formal analysis, Writing - review & editing. **Matthew T Harper:** Formal analysis, Writing - review & editing. **David Bailey:** Conceptualization, Resources, Writing - review & editing. **Graham Ladds:** Conceptualization, Methodology, Formal analysis, Resources, Writing - review & editing, Supervision.

Acknowledgements

Authors acknowledge the support of Endowment Fund for education from Ministry of Finance Republic of Indonesia (DS), a BBSRC Flexible Talent Mobility Account scheme award (GL and LK), BBSRC Doctoral Training Partnership BB/JO1454/1 (MH), Rosetrees Trust (to HYY and GL), and the Brain Tumour Charity (UK) grant GN-000429 (LK, FS, DB). HYY is also supported by the Cambridge Trust International Scholarship. We thank Sampurna Chakrabarty for support throughout preparation of this article. Finally, we would like to thank Colin Taylor for the C6 cell line.

Declarations

DB and LK are current employees of *IOTA Pharmaceuticals Ltd*; FS is a former employee.

References

- A.N. Mamelak, D.B. Jacoby, Targeted delivery of antitumoral therapy to glioma and other malignancies with synthetic chlorotoxin (TM-601), *Expert Opin. Drug Deliv.* 4 (2) (2007) 175–186.
- M. Harris, F. Svensson, L. Kopanitsa, G. Ladds, D. Bailey, Emerging patents in the therapeutic areas of glioma and glioblastoma, *Expert Opin. Ther. Pat.* 28 (7) (2018) 573–590.
- Judith A Schwartzbaum, James L Fisher, Kenneth D Aldape, Margaret Wrensch, Epidemiology and molecular pathology of glioma, *Nat. Rev. Neurol.* 2 (9) (2006) 494–503 quiz 1 p following 516.
- H. Mao, D.G. Lebrun, J. Yang, V.F. Zhu, M. Li, Deregulated signaling pathways in glioblastoma multiforme: molecular mechanisms and therapeutic targets, *Cancer Invest.* 30 (1) (2012) 48–56.
- M.A. Furman, K. Shulman, Cyclic AMP and adenylyl cyclase in brain tumors, *J. Neurosurg.* 46 (4) (1977) 477–483.
- M. Illiano, L. Sapio, A. Salzillo, L. Capasso, I. Caiafa, E. Chiosi, A. Spina, S. Naviglio, Forskolin improves sensitivity to doxorubicin of triple negative breast cancer cells via Protein Kinase A-mediated ERK1/2 inhibition, *Biochem. Pharmacol.* 152 (2018) 104–113.
- L. Hirsh, A. Dantes, B.S. Suh, Y. Yoshida, K. Hosokawa, K. Tajima, F. Kotsuji, O. Merimsky, A. Amsterdam, Phosphodiesterase inhibitors as anti-cancer drugs, *Biochem. Pharmacol.* 68 (6) (2004) 981–988.
- T.W. Kang, S.W. Choi, S.R. Yang, T.H. Shin, H.S. Kim, K.R. Yu, I.S. Hong, S. Ro, J.M. Cho, K.S. Kang, Growth arrest and forced differentiation of human primary glioblastoma multiforme by a novel small molecule, *Sci. Rep.-UK* 4 (2014).
- A. Sawa, T. Chiba, J. Ishii, H. Yamamoto, H. Hara, H. Kamma, Effects of sorafenib and an adenylyl cyclase activator on in vitro growth of well-differentiated thyroid cancer cells, *Endocr. J.* (2017).
- I.H. Zwain, P. Amato, cAMP-induced apoptosis in granulosa cells is associated with up-regulation of P53 and bax and down-regulation of clusterin, *Endocr. Res.* 27 (1–2) (2001) 233–249.
- E. Huston, T.M. Houslay, G.S. Baillie, M.D. Houslay, cAMP phosphodiesterase-4A1 (PDE4A1) has provided the paradigm for the intracellular targeting of phosphodiesterases, a process that underpins compartmentalized cAMP signalling, *Biochem. Soc. Trans.* 34 (Pt 4) (2006) 504–509.
- B. Ding, J.L. Abe, H. Wei, Q.H. Huang, R.A. Walsh, C.A. Molina, A. Zhao, J. Sadoshima, B.C. Blaxall, B.C. Berk, C. Yan, Functional role of phosphodiesterase 3 in cardiomyocyte apoptosis – Implication in heart failure, *Circulation* 111 (19) (2005) 2469–2476.
- A. Lerner, P.M. Epstein, Cyclic nucleotide phosphodiesterases as targets for treatment of haematological malignancies, *Biochem. J.* 393 (Pt 1) (2006) 21–41.
- J.A. Beavo, Cyclic nucleotide phosphodiesterases: functional implications of multiple isoforms, *Physiol. Rev.* 75 (4) (1995) 725–748.
- S.H. Soderling, J.A. Beavo, Regulation of cAMP and cGMP signaling: new phosphodiesterases and new functions, *Curr. Opin. Cell Biol.* 12 (2) (2000) 174–179.
- F.S. Menniti, W.S. Faraci, C.J. Schmidt, Phosphodiesterases in the CNS: targets for drug development, *Nat. Rev. Drug Discov.* 5 (8) (2006) 660–670.
- K. Omori, J. Kotera, Overview of PDEs and their regulation, *Circ. Res.* 100 (3) (2007) 309–327.
- S.H. Francis, M.A. Blount, J.D. Corbin, Mammalian cyclic nucleotide phosphodiesterases: molecular mechanisms and physiological functions, *Physiol. Rev.* 91 (2) (2011) 651–690.
- M. Conti, D. Mika, W. Richter, Cyclic AMP compartments and signaling specificity: role of cyclic nucleotide phosphodiesterases, *J. Gen. Physiol.* 143 (1) (2014) 29–38.
- Y. Ladilov, A. Appukuttan, Role of soluble adenylyl cyclase in cell death and growth, *Biochim. Biophys. Acta* 1842 (12 Pt B) (2014) 2646–2655.
- R. Sengupta, T. Sun, N.M. Warrington, J.B. Rubin, Treating brain tumors with PDE4 inhibitors, *Trends Pharmacol. Sci.* 32 (6) (2011) 337–344.
- V. Cesarini, M. Martini, L.R. Vitiani, G.L. Gravina, S. Di Agostino, G. Graziani, Q.G. D'Alessandris, R. Pallini, L.M. Larocca, P. Rossi, E.A. Jannini, S. Dolci, Type 5 phosphodiesterase regulates glioblastoma multiforme aggressiveness and clinical outcome, *Oncotarget* 8 (8) (2017) 13223–13239.
- R. Savai, S.S. Pullamsetti, G.A. Banat, N. Weissmann, H.A. Ghofrani, F. Grimminger, R.T. Schermuly, Targeting cancer with phosphodiesterase inhibitors, *Expert Opin. Invest. Drug* 19 (1) (2010) 117–131.
- M.D. Brooks, E. Jackson, N.M. Warrington, J. Luo, J.T. Forsy, S. Taylor, D.D. Mao, J.R. Leonard, A.H. Kim, D. Piwnica-Worms, R.D. Mitra, J.B. Rubin, PDE7B is a novel, prognostically significant mediator of glioblastoma growth whose expression is regulated by endothelial cells, *PLoS ONE* 9 (9) (2014) e107397.
- R.W. Chen, A.J. Williams, Z.L. Liao, C.P. Yao, F.C. Tortella, J.R. Dave, Broad spectrum neuroprotection profile of phosphodiesterase inhibitors as related to modulation of cell-cycle elements and caspase-3 activation, *Neurosci. Lett.* 418 (2) (2007) 165–169.
- R.J. Rickles, L.T. Pierce, T.P. Giordano, W.F. Tam, D.W. McMillin, J. Delmore, J.P. Laubach, A.A. Borisy, P.G. Richardson, M.S. Lee, Adenosine A2A receptor agonists and PDE inhibitors: a synergistic multitarget mechanism discovered through systematic combination screening in B-cell malignancies, *Blood* 116 (4) (2010) 593–602.
- M.E. Ehrlich, L. Conti, M. Toselli, L. Taglietti, E. Fiorillo, V. Taglietti, S. Ivkovic, B. Guinea, A. Tranberg, S. Sipione, D. Rigamonti, E. Cattaneo, ST14A cells have properties of a medium-size spiny neuron, *Exp. Neurol.* 167 (2) (2001) 215–226.
- A.G. Gilman, Regulation of adenylyl cyclase by G proteins, *Adv. Second Messenger Phosphoprotein Res.* 24 (1990) 51–57.
- J.D. Hildebrandt, Role of subunit diversity in signaling by heterotrimeric G proteins, *Biochem. Pharmacol.* 54 (3) (1997) 325–339.
- M. Zaccolo, M.A. Movsesian, cAMP and cGMP signaling cross-talk: role of phosphodiesterases and implications for cardiac pathophysiology, *Circ. Res.* 100 (11) (2007) 1569–1578.
- A.J. Morgan, K.J. Murray, R.A. Challiss, Comparison of the effect of isobutylmethylxanthine and phosphodiesterase-selective inhibitors on cAMP levels in SH-SY5Y neuroblastoma cells, *Biochem. Pharmacol.* 45 (12) (1993) 2373–2380.
- Y. Taniguchi, H. Tonal-Kachi, K. Shinjo, Zaprinast, a well-known cyclic guanosine monophosphate-specific phosphodiesterase inhibitor, is an agonist for GPR35, *FEBS Lett.* 580 (21) (2006) 5003–5008.
- X. Decleves, S. Bihorel, M. Debray, S. Yousif, G. Camenisch, J.M. Scherrmann, ABC transporters and the accumulation of imatinib and its active metabolite CGP74588 in rat C6 glioma cells, *Pharmacol. Res.* 57 (3) (2008) 214–222.
- E.W. Sutherland, Studies on the mechanism of hormone action, *Science* 177 (4047) (1972) 401–408.
- K.A. Cullen, J. McCool, M.S. Anwer, C.R.L. Webster, Activation of cAMP-guanine exchange factor confers PKA-independent protection from hepatocyte apoptosis, *Am. J. Physiol.-Gastr. L* 287 (2) (2004) G334–G343.
- P.A. Insel, L. Zhang, F. Murray, H. Yokouchi, A.C. Zamboni, Cyclic AMP is both a pro-apoptotic and anti-apoptotic second messenger, *Acta Physiol.* 204 (2) (2012) 277–287.
- N.M. Warrington, S.M. Gianino, E. Jackson, P. Goldhoff, J.R. Garbow, D. Piwnica-Worms, D.H. Gutmann, J.B. Rubin, Cyclic AMP suppression is sufficient to induce gliomagenesis in a mouse model of neurofibromatosis-1, *Cancer Res.* 70 (14) (2010) 5717–5727.
- P.M. Daniel, G. Filiz, T. Mantamadiotis, Sensitivity of GBM cells to cAMP agonist-mediated apoptosis correlates with CD44 expression and agonist resistance with MAPK signaling, *Cell Death Dis.* 7 (2016).
- W.P. Hausdorff, M.G. Caron, R.J. Lefkowitz, Turning off the signal: desensitization of beta-adrenergic receptor function, *FASEB J.* 4 (11) (1990) 2881–2889.
- J. Surapitschat, K.I. Jeon, C. Yan, J.A. Beavo, Differential regulation of endothelial cell permeability by cGMP via phosphodiesterases 2 and 3, *Circ. Res.* 101 (8) (2007) 811–818.
- S.H. Francis, J.L. Busch, J.D. Corbin, D. Sibley, cGMP-dependent protein kinases

- and cGMP phosphodiesterases in nitric oxide and cGMP action, *Pharmacol. Rev.* 62 (3) (2010) 525–563.
- [42] J. de Rooij, F.J.T. Zwartkruis, M.H.G. Verheijen, R.H. Cool, S.M.B. Nijman, A. Wittinghofer, J.L. Bos, Epac is a Rap1 guanine-nucleotide-exchange factor directly activated by cyclic AMP, *Nature* 396 (6710) (1998) 474–477.
- [43] J. Bubis, L.D. Saraswat, S.S. Taylor, Tyrosine-371 contributes to the positive cooperativity between the two cAMP binding sites in the regulatory subunit of cAMP-dependent protein kinase I, *Biochemistry* 27 (5) (1988) 1570–1576.
- [44] G.E. Ringheim, S.S. Taylor, Effects of cAMP-binding site mutations on intradomain cross-communication in the regulatory subunit of cAMP-dependent protein kinase I, *J. Biol. Chem.* 265 (32) (1990) 19472–19478.
- [45] L. Favot, T. Keravis, V. Holl, A. Le Bec, C. Lugnier, VEGF-induced HUVEC migration and proliferation are decreased by PDE2 and PDE4 inhibitors, *Thromb. Haemost.* 90 (2) (2003) 334–343.
- [46] P.K. Vadiveloo, E.L. Filonzi, H.R. Stanton, J.A. Hamilton, G1 phase arrest of human smooth muscle cells by heparin, IL-4 and cAMP is linked to repression of cyclin D1 and cdk2, *Atherosclerosis* 133 (1) (1997) 61–69.
- [47] T. Keravis, C. Lugnier, Cyclic nucleotide phosphodiesterase (PDE) isozymes as targets of the intracellular signalling network: benefits of PDE inhibitors in various diseases and perspectives for future therapeutic developments, *Br. J. Pharmacol.* 165 (5) (2012) 1288–1305.
- [48] T. Fujita, Y. Ishikawa, Apoptosis in heart failure. -The role of the beta-adrenergic receptor-mediated signaling pathway and p53-mediated signaling pathway in the apoptosis of cardiomyocytes, *Circ. J.* 75 (8) (2011) 1811–1818.
- [49] M. Adachi, G. Reid, J.D. Schuetz, Therapeutic and biological importance of getting nucleotides out of cells: a case for the ABC transporters, MRP4 and 5, *Adv. Drug Deliv. Rev.* 54 (10) (2002) 1333–1342.

Appendix 3

Publication: Kalash, L. *et al.* 2021

This appendix contains:

Kalash, L., Winfield, I., Safitri, D., Bermudez, M., Carvalho, S., Glen, R., Ladds, G., Bender, A. (2021). Structure-based identification of dual ligands at the A2AR and PDE10A with anti-proliferative effects in lung cancer cell-lines. *Journal of Cheminformatics*, 13(1), 17. <https://doi.org/10.1186/s13321-021-00492-5>

RESEARCH ARTICLE

Open Access



Structure-based identification of dual ligands at the A_{2A}R and PDE10A with anti-proliferative effects in lung cancer cell-lines

Leen Kalash^{1,6†}, Ian Winfield^{1,2†}, Dewi Safitri^{2,3†}, Marcel Bermudez^{1,4}, Sabrina Carvalho², Robert Glen^{1,5}, Graham Ladds² and Andreas Bender^{1*}

Abstract

Enhanced/prolonged cAMP signalling has been suggested as a suppressor of cancer proliferation. Interestingly, two key modulators that elevate cAMP, the A_{2A} receptor (A_{2A}R) and phosphodiesterase 10A (PDE10A), are differentially co-expressed in various types of non-small lung cancer (NSCLC) cell-lines. Thus, finding dual-target compounds, which are simultaneously agonists at the A_{2A}R whilst also inhibiting PDE10A, could be a novel anti-proliferative approach. Using ligand- and structure-based modelling combined with MD simulations (which identified Val₈₄ displacement as a novel conformational descriptor of A_{2A}R activation), a series of known PDE10A inhibitors were shown to dock to the orthosteric site of the A_{2A}R. Subsequent in-vitro analysis confirmed that these compounds bind to the A_{2A}R and exhibit dual-activity at both the A_{2A}R and PDE10A. Furthermore, many of the compounds exhibited promising anti-proliferative effects upon NSCLC cell-lines, which directly correlated with the expression of both PDE10A and the A_{2A}R. Thus, we propose a structure-based methodology, which has been validated in in-vitro binding and functional assays, and demonstrated a promising therapeutic value.

Keywords: Docking, MD simulations, Structure-based design, Virtual screening, A_{2A}R, PDE10A, Anti-proliferative, Dual target, Triazoloquinazolines, NSCLC, Lung cancer

Introduction

Cyclic adenosine monophosphate (cAMP) is a second messenger that has a major role in transduction and cell signaling in several pathways and biological systems [1]. cAMP elevation may be achieved *via* the activation of the adenylate cyclases by Gs proteins, and the inhibition of cAMP-degrading phosphodiesterases [2], and has been shown to inhibit proliferation of several cancer cell types

such as breast cancer, colon cancer, lung cancer, glioblastoma etc [3–6].

Two key modulators of intracellular cAMP are the adenosine A_{2A} receptor (A_{2A}R) and the phosphodiesterase 10A (PDE10A), which are often co-expressed in different amounts across NSCLC cell-lines. The A_{2A}R is expressed in the two histologically distinct types of NSCLC cell-lines, lung adenocarcinoma and squamous carcinoma cell-lines [7, 8]. Likewise, PDE10A is overexpressed in lung adenocarcinoma, and its inhibition was found to suppress growth [9], demonstrating a correlation between the levels of overexpression and survival [10]. This makes these systems interesting avenues of investigation for relating the amount of co-expression of these two protein targets and their ability to elevate cAMP as well as induce anti-proliferation in these cell-lines.

*Correspondence: grl30@cam.ac.uk; ab454@cam.ac.uk

[†]Leen Kalash, Ian Winfield and Dewi Safitri contributed equally to the work

¹ Centre for Molecular Informatics, Department of Chemistry, University of Cambridge, Lensfield Road, CB21EW Cambridge, UK

² Department of Pharmacology, University of Cambridge, Tennis Court Road, CB2 1PD Cambridge, UK

Full list of author information is available at the end of the article



© The Author(s) 2021. This article is licensed under a Creative Commons Attribution 4.0 International License, which permits use, sharing, adaptation, distribution and reproduction in any medium or format, as long as you give appropriate credit to the original author(s) and the source, provide a link to the Creative Commons licence, and indicate if changes were made. The images or other third party material in this article are included in the article's Creative Commons licence, unless indicated otherwise in a credit line to the material. If material is not included in the article's Creative Commons licence and your intended use is not permitted by statutory regulation or exceeds the permitted use, you will need to obtain permission directly from the copyright holder. To view a copy of this licence, visit <http://creativecommons.org/licenses/by/4.0/>. The Creative Commons Public Domain Dedication waiver (<http://creativecommons.org/publicdomain/zero/1.0/>) applies to the data made available in this article, unless otherwise stated in a credit line to the data.

We hypothesized that a novel approach would be to discover compounds, which act simultaneously as agonists of the $A_{2A}R$ that are also inhibitors of PDE10A. cAMP elevation could be achieved through the $A_{2A}R$ -Gas-adenylate cyclase axis, while further promoted by the inhibition of its breakdown *via* PDE10A [7, 8]. A multi-target approach is a departure from standard drug discovery practice, where one target is often the driving force in compound optimization. A multi-target compound could, through synergistic effects, be more effective in elevating cAMP. Indeed, dual PDE inhibition and $A_{2A}R$ activation *via* compound combinations exhibited synergy (according to isobologram analysis) in cAMP elevation, and was observed to inhibit proliferation in other cancer cell types such as multiple myeloma and diffuse large B-cell lymphoma [11]. The use of multitarget ligands have also demonstrated beneficial effects on Alzheimer's and Parkinson's disease [12, 13]. Therefore, combining this approach in single dual-targeted compounds at the $A_{2A}R$ and PDE10A could be explored as a novel anti-proliferative strategy for adenocarcinoma and squamous carcinoma cell-lines.

For the purpose of designing PDE10A inhibitors and $A_{2A}R$ agonists, many virtual screening protocols have been reported in the literature, implementing either ligand- or structure-based approaches. Examples of ligand-based protocols include *in silico* target prediction, pharmacophore-based and fragment-based approaches and comparative molecular field analysis (CoMFA) [14–19]. Docking, as a structure-based approach, has also been employed for the design of either PDE10A inhibitors or $A_{2A}R$ agonists [20]. In addition, molecular dynamics has been used extensively to investigate the conformational dynamics at the A_{2A} adenosine receptor or PDE10A [20–27]. However, none of the reported protocols rationalizes or correctly predicts the functional activity of ligands against the targets of interest, in particular the $A_{2A}R$, which is addressed in this work.

Here, a novel structure-based methodology for identifying ligands that activate the $A_{2A}R$ while simultaneously inhibiting the PDE10A is devised. Given that PDE10A is an enzyme, compounds that target the active site would most likely confer inhibition. However, binding to the orthosteric site of the $A_{2A}R$ may not guarantee the desired functional activity. For this reason, the structure-based computational approach was focused on the more challenging goal, which involved identifying whether known PDE10A inhibitors are $A_{2A}R$ agonists.

The focus of this approach was on the key interacting residues, which are reported in the literature to discriminate between agonist and antagonist activity of $A_{2A}R$ ligands [28–31]. It is postulated that the motion of the residue Val₈₄ in Transmembrane Helix 3, upon $A_{2A}R$

ligand binding, might discriminate between agonist and antagonist activity, which has not previously been studied by any MD approaches [19–24, 32]. Hence, the motion of this residue has been investigated as a conformational descriptor for the characterization of receptor activation by $A_{2A}R$ ligands.

Subsequently, the selected compounds were evaluated pharmacologically *in vitro* using both binding and functional assays. We then extended our studies to evaluate the compounds for their abilities to modulate cell proliferation in lung squamous cell carcinoma and lung adenocarcinoma cell-lines. Their anti-proliferative effects were correlated with the co-expression of the $A_{2A}R$ and PDE10A and (increased) cellular levels of cAMP.

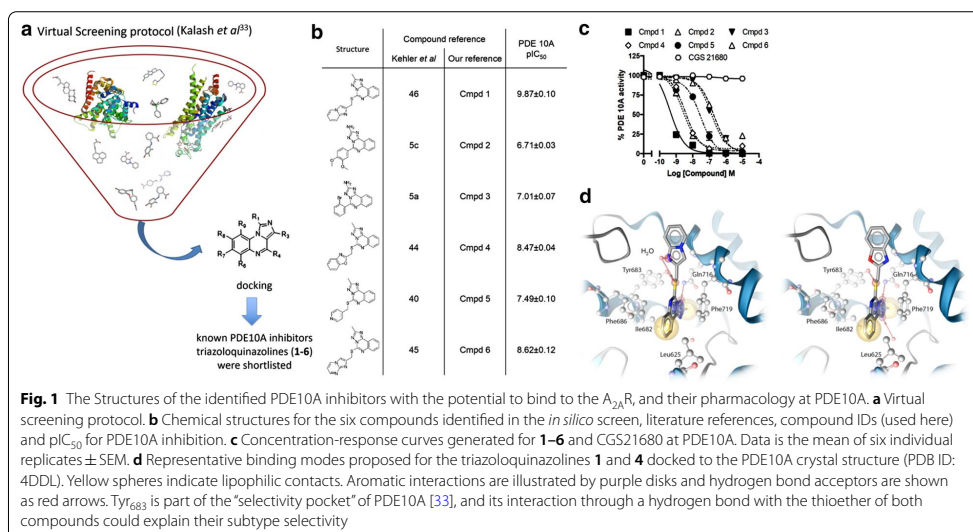
Results

Method for selecting triazoloquinazolines as candidates for dual ligand activity at $A_{2A}R$ and PDE10A

Triazoloquinazolines were identified by Kalash et al. as a compound series that showed the highest frequency of prediction as binders at the $A_{2A}R$ and PDE10A by ligand- and structure-based approaches (Fig. 1a) [33]. For the purpose of finding dual-target ligands that elevate cAMP, the focus was on ligands that could simultaneously activate the $A_{2A}R$ (agonists) and inhibit PDE10A.

From the ZINC database, six purchasable triazoloquinazolines (1–6) were shortlisted (compound 1–6 Fig. 1a, see methods for details) [34], which were (Fig. 1b, c) previously shown to display inhibition of PDE10A (with a rank order of potency of $1 > 6 = 4 > 5 > 3 = 2$) [34]. Importantly, for future reference, no significant activity of the $A_{2A}R$ selective agonist CGS21680 at PDE10A was detected. Using a crystal structure of PDE10A (PDB ID: 4DDL) and ligand/protein docking, binding poses were found that appeared consistent (i.e. docking in approximately the same position) for all six compounds (Fig. 1d—illustration of predicted binding modes of representative triazoloquinazolines 1 and 4). Importantly, this analysis highlighted that the interaction of Tyr683, a residue belonging to a 'selectivity pocket' of PDE10A, through a hydrogen bond with the thioether of the compounds could explain their PDE10A subtype selectivity.

Following the initial shortlisting (based on PDE10A activity), compounds 1–6 were docked into the orthosteric site of the $A_{2A}R$ protein crystal structure (PDB ID: 2YDO). In this structure a relatively large displacement of the Val₈₄ residue was observed (when referenced to its average distance to Leu₂₄₉, a residue that is comparatively static in position relative to the structure as a whole (Additional file 1: Table S1). The relative motion of this amino acid residue is essential for $A_{2A}R$ activation, in order to avoid the steric clash that might otherwise result between the agonist and the receptor.



The selection of the structure to be used as the docking model for the A_{2A}R was based on the Val₃₄-Leu₂₄₉ inter-residue distances found for the active/inactive forms of the A_{2A}R protein crystal structures reported in the protein data bank (PDB). Based on this criterion, the A_{2A}R crystal structure (PDB ID: 2YDO) was selected since it exhibited the largest inter-residue distance. It was hypothesized that this would allow ligand exploration of a conformational space most likely to be occupied by A_{2A}R agonists when docked into the orthosteric site. Indeed, this enabled enrichment of A_{2A}R agonists over A_{2A}R antagonists and A_{2A}R inactives (refer to methods for details). This is in agreement with a previous study by Rodríguez et al. [26], where the A_{2A}R crystal structure (PDB ID: 2YDO) displayed the highest enrichment factor value (EF1%) for docked agonists over the other active crystal structures of the A_{2A}R. The 2YDO crystal structure enriched agonists 63.5-fold better than random and 2.9-fold better than antagonists (63.5% versus 21.9%) [26]. However, their docking approach failed to find any A_{2A}R agonists (which used three active structures: PDB IDs: 2YDO, 2YDV, and 3QAK). The authors rationalized this as resulting from bias of the chosen chemical libraries towards A_{2A}R antagonists over agonists.

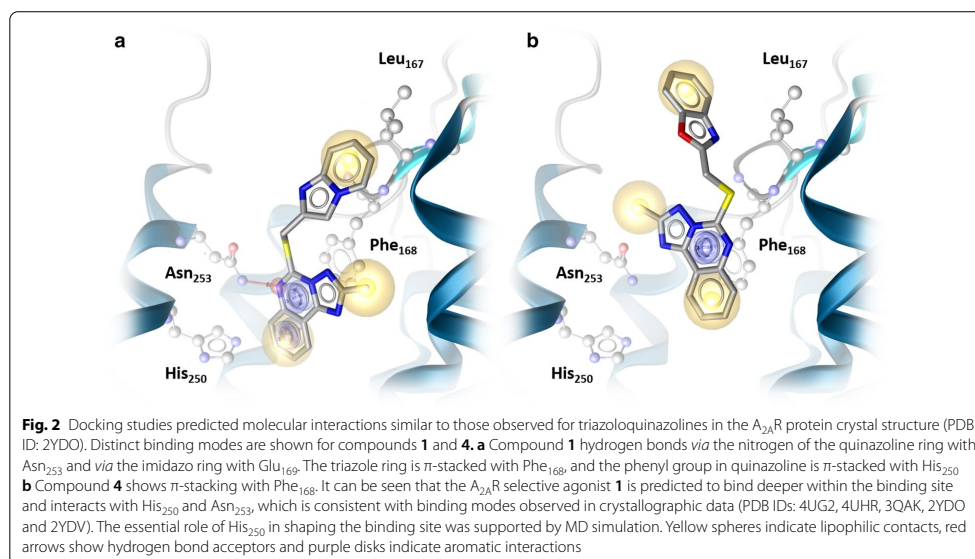
The evaluation of the six triazoloquinazolines 1–6 (Fig. 1a), as promising candidates for A_{2A}R agonism, was based on their docking scores. Compounds were selected based on their scores below the score threshold value of -7.33, which was determined as the optimum selection

criteria for agonists based on computing the Matthews correlation coefficient (see Methods for more details).

Compounds 1–6 were screened against PAINS (PAN Assay Interference Compounds) with regard to the recent analysis of the use of this approach by Tropsha using FAFDrug3 [35], and none of the compounds exhibited any potential PAINS liability.

Analysis of the molecular docking studies of the representative triazoloquinazolines 1–4 shortlisted for experimental validation

Docking studies predicted consistent molecular interactions for the triazoloquinazolines, similar to those of the co-crystallized ligand bound to the A_{2A}R protein crystal structure (PDB ID: 2YDO). Representative and distinct binding modes are illustrated in Fig. 2. Compounds 1–3, were predicted to be selective A_{2A}R ligands, which was attributed to interactions with His₂₅₀ [36, 37]. This residue is located in the core region of the receptor and part of a sub-pocket formed by Leu₈₅, Met₁₇₇, Trp₂₄₆ and Leu₂₄₉. Despite the fact that it is conserved among the A₁R and the A_{2A}R subtypes (as suggested by a recent study [38], due to the high conservation of amino acid residues in the adenosine receptor subtypes), subtype selectivity might not be attributed to the receptor-specific amino acid residues, but rather to conformational differences. Also, given that mutation experiments have failed so far to highlight any receptor-specific amino acid residues responsible for subtype selectivity, this would



add weight to the suggested hypothesis [37, 39]. Hence, the selectivity of $A_{2A}R$ agonists could be attributed to the conformational preferences of the His_{250} amino acid residue that contributes to shaping the orthosteric site to favor their selectivity [38]. Indeed, the interaction with this residue is only observed for the selective $A_{2A}R$ co-crystallized agonists, CGS21680 (PDB ID: 4UHR) and UK432097 (PDB ID: 3QAK) but not for the non-selective co-crystallized agonists NECA (PDB ID: 2YDV) and adenosine (PDB ID: 2YDO). These results appear to confirm that interactions with His_{250} serve to improve binding to the lipophilic sub-pocket which suggests this is a driver for $A_{2A}R$ sub-type selectivity. In terms of functional activity however, the occurrence of this interaction cannot discriminate between agonists and antagonists [37, 39].

Compound **1** hydrogen bonds *via* the nitrogen of the quinazoline ring with Asn_{253} , and *via* the imidazo ring with Glu_{169} . The triazole ring is π -stacked with Phe_{168} , and the phenyl group in quinazoline is π -stacked with His_{250} (Fig. 2). Compound **4** shows π -stacking with Phe_{168} . The selective $A_{2A}R$ agonist, compound **1** is predicted to bind deeper within the receptor core and to directly interact with His_{250} and Asn_{253} , which is consistent with the experimentally observed interactions between the co-crystallized ligands and the active $A_{2A}R$ crystal structures (PDB IDs: 4UG2, 4UHR, 3QAK, 2YDO and 2YDV). The compounds were not predicted

to display all the interactions exhibited by the agonist co-crystallized ligands [28–30], in particular the Thr_{88} and Ser_{277} interactions, which are also characteristic of the ZM241385 antagonist [27]. Hence, these interaction types are not characteristic of agonist activity. However, it has been reported in the literature that mutating these residues has a stronger influence on agonist activity than upon the antagonist activity of the $A_{2A}R$ ligands, but not on the binding to the $A_{2A}R$ [37–39]. As for the co-crystallized $A_{2A}R$ antagonists (PDB ID: 5IU4 3UZA, 5K2A, 4EY, 3EML, 5NM2, 5JTB, 5UVI, and 5UIG), these only show interactions with Phe_{168} , Asn_{253} , and Glu_{169} residues. Therefore, the type of predicted interaction is not indicative of receptor activation by the triazoloquinazolines. However, the docking model used enriched $A_{2A}R$ agonists (exhibited higher docking score distribution) over $A_{2A}R$ antagonists and $A_{2A}R$ inactives (compounds that do not bind to the $A_{2A}R$). This suggested an investigation (using molecular dynamics) into whether the His_{250} movement would differ between selective versus non-selective $A_{2A}R$ agonist binding (discussed in the supporting information) and also to investigate whether the motion of Val_{84} would vary upon agonist and antagonist binding. This could allow discrimination between these different classes of compounds.

Analysis of MD Simulations reveals that a shift in Val₈₄ is one requirement for receptor activation by A_{2A}R ligands
The analysis of the active and inactive forms of the available A_{2A}R crystal structures is in accordance with reports in the literature, which mention that Val₈₄ in TM3 has to move by approximately 2 Å upon agonist binding to avoid a steric clash between the ligand and the receptor [29–31]. This gave rise to the hypothesis that the motion of this residue might discriminate between agonist and antagonist binding (Fig. 3a).

MD simulations (100 ns) were performed for the co-crystallized structures (PDB IDs: 5IU4 and 2YDO), which exhibited the largest differences observed in the distance between the α-carbons of Val₈₄ in TM3, and Leu₂₄₉, a relatively fixed residue in TM6 (12.96 Å and 14.53 Å, see methods for details). The same MD analysis was carried out for the apo structure of the A_{2A}R (PDB ID: 5IU4), the docked triazoloquinazolines **1**, **4** and **5** with the highest predicted affinities, compound **6** (with lowest predicted affinity), CHEMBL3799351 (a potent antagonist), and CGS21680 (the selective and potent A_{2A}R agonist). All these compounds were docked into the orthosteric site of the inactive form of the A_{2A}R protein crystal structure (PDB ID: 5IU4), Additional file 1: Figure S4. For the first 50 ns the structures were considered to be relaxing to an annealed state. For the subsequent 50 ns the agonist bound structures showed an increase of the Ca distances between Val₈₄ and Leu₂₄₉, with an increased distance

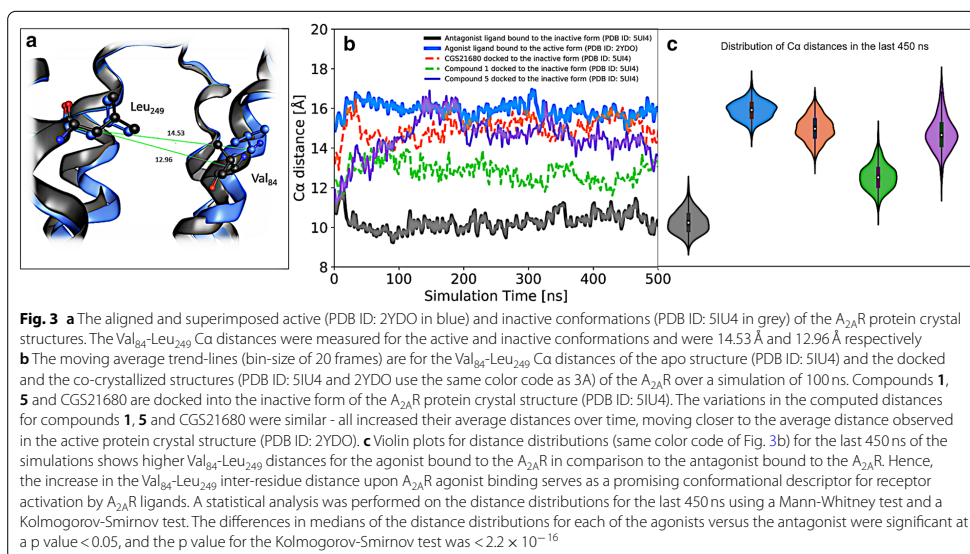
equivalent to the active protein crystal structure (PDB ID: 2YDO). Compound **6**, the apo structure, and the antagonist bound structures did not exhibit this increase in Ca distances and instead showed a slight decrease in the Ca distances for the antagonist bound structures in comparison to the apo structure and compound **6**.

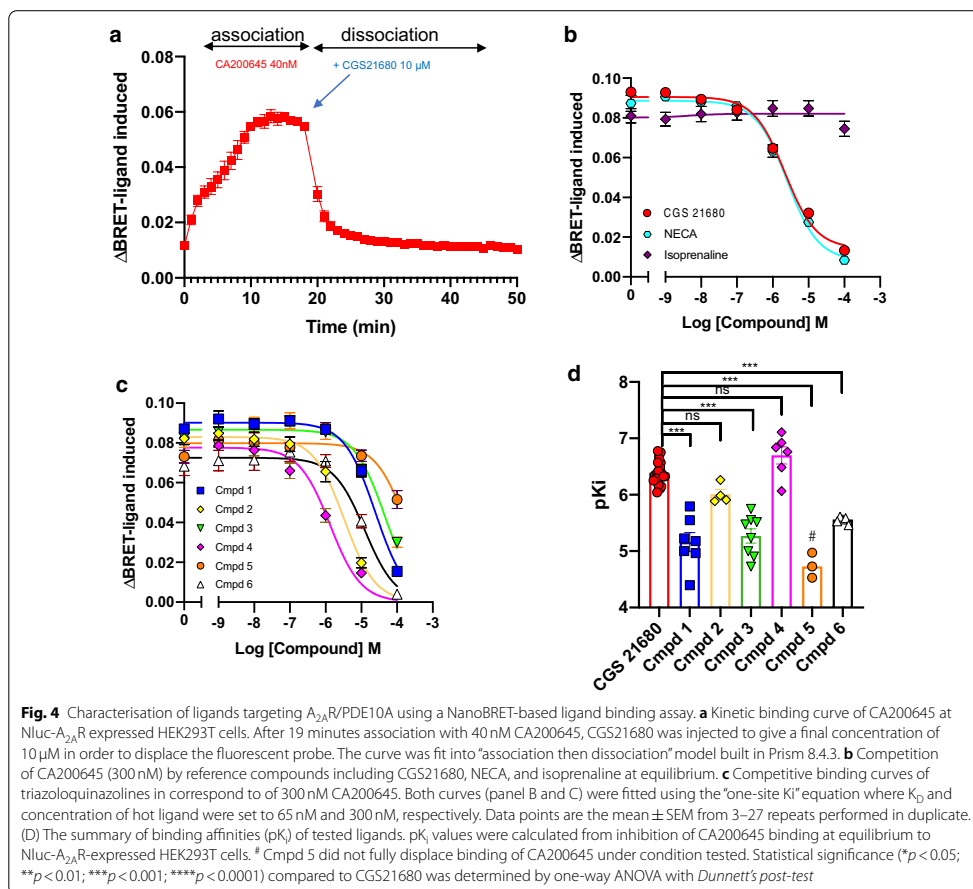
To gain further insights from the change in the Ca distances between Val₈₄ and Leu₂₄₉ for the agonist bound structures (which are the systems of interest in this study), longer simulations of 500 ns were carried for compounds **1**, **5**, and CGS21680, in addition to the active and inactive cocrystal structures (PDB IDs: 2YDO and 5IU4). The simulations were run in duplicate.

The same trends were observed in the longer simulations. Over the first 50 ns the structures were annealing, and for the rest of the simulation (the last 450 ns) compounds **1**, **5** and CGS21680 increased their Ca distances between Val₈₄ and approaching the distance observed for the active protein crystal structure (PDB ID: 2YDO), as shown in Fig. 3b, c. Hence, the increase in the distance between Val₈₄ and Leu₂₄₉ residues observed upon A_{2A}R agonist binding appears to serve as a useful conformational descriptor for receptor activation by A_{2A}R ligands.

Characterisation of triazoloquinazolines affinity constant at adenosine A_{2A}R

We sought to validate the docking studies by quantifying the affinity of each compound at the A_{2A}R using a





NanoBRET binding assay. In this experiment, we used N-terminally tagged $A_{2A}R$ with Nanoluciferase (Nluc) that will emit bioluminescence in close proximity with the fluorescent probe, CA200645, in the presence of Nluc substrate. Firstly, we determine the affinity constant of CA200645 in our expression system. CA200645 has been extensively used to characterise ligand binding properties at adenosine receptor subtypes [40–42]. Using HEK293 cells we determined the dissociation constant (K_D) of CA200645 at the Nluc- $A_{2A}R$ to be 65 nM (Fig. 4a). We next extended our studies to use a classical competition binding assay ([43, 44]) where non-fluorescent ligands compete for binding at the Nluc- $A_{2A}R$ with CA200645. Using this approach, we determined the pKi for NECA as

6.36 ± 0.09 and CGS21680 as 6.39 ± 0.04 while isoprenaline (a non-selective agonist of β -adrenoceptors) failed to displace CA200645 (Fig. 4b). We next determined the rank order of affinities for the six triazoloquinazolines at the $A_{2A}R$ to be: **cmpd 4 > cmpd 2 > cmpd 6 > cmpd 1 = cmpd 3 > cmpd 5** (note: under condition tested, cmpd 5 was unable to fully displace CA200645) (Fig. 4c, d).

Identifying AR subtype selectivity of triazoloquinazolines
Identification of AR subtype selectivity of triazoloquinazolines was performed using previously characterised yeast strains expressing human A_1R , $A_{2A}R$ or $A_{2B}R$ [45]. The A_3R cannot be functionally expressed in yeast

(See figure on next page.)

Fig. 5 Dose-response curves for NECA, CGS21680 and compounds **1–6** in either the A_1R and $GPA1/G\alpha_{1/2}$, $A_{2A}R$ and $GPA1/G\alpha_s$, or the $A_{2B}R$ (with $GPA1/G\alpha_s$ expressed in yeast strains). The efficacy of the compounds (**1–6**) was measured against A_3R in CHO-K1- A_3R cells. Reporter gene activity in yeast was determined using β -galactosidase assays, after 16-hours stimulation with either: NECA (**a**), CGS21680 (**b**) compound **1** (**c**), compound **2** (**d**), compound **3** (**e**), compound **4** (**f**), compound **5** (**g**), compound **6** (**h**), whereas cAMP inhibition was determined when in CHO-K1- A_3R cells which were co-stimulated with each of the compounds **1–6** and 1 μ M Forskolin. In general, the triazoloquinazolines **1–5** exhibited agonistic activity against the adenosine receptor sub-types, with compounds **1–3** being selective $A_{2A}R$ agonists. The data is represented as either percentage of the response obtained upon stimulating each receptor (A_1R , $A_{2A}R$, or $A_{2B}R$) with NECA stimulation, or as a percentage response relative to 100 μ M Forskolin stimulation in the A_3R \pm SEM of 4–6 individual replicates

(Knight et al., 2016), therefore we utilised CHO-K1 cells stably expressing A_3R (CHO-K1- A_3R). Testing the compounds in these systems identified compounds **1**, **2**, **3**, **4**, **5** to be $A_{2A}R$ agonists, whilst compounds **1**, **2**, **3** are $A_{2A}R$ -selective (Fig. 5, Additional file 1: Table S2). It is interesting to note that compound **6** was able to bind to the $A_{2A}R$ but given that in the yeast based assay it failed to elicit a functional response, we suggest it maybe an $A_{2A}R$ antagonist.

To further verify the efficacy of compounds against the $A_{2A}R$, we assayed their ability to stimulate cAMP production using CHO-K1 cells stably expressing human $A_{2A}R$ (CHO-K1- $A_{2A}R$). All compounds tested were observed to be partial agonists, relative to CGS21680, with a rank order of potency of $CGS21680 > 5 = 4 > 1 = 3 > 6 > 2$ (Fig. 6; Table 1). Antagonism with ZM241385 displayed non-classical antagonism, which is presumed to be due to the dual effects upon endogenous PDE10A (Additional file 1: Figure S5). For compound **6**, treatment with ZM241385 solely reduced E_{max} and basal levels, with no effect on the response range (Fig. 6; Table 1). ZM241385 has been suggested to be an inverse agonist at the $A_{2A}R$ potentially explaining these effects [30]. Importantly, all compounds were able to stimulate cAMP production in the absence of the $A_{2A}R$, or in the presence of 1 μ M ZM241385, presumably from inhibition of PDE10A. Thus, we observe a significant increase in efficacy of compounds **1–5** via the additional action upon the $A_{2A}R$ (Fig. 6; Table 1), which could be attributed to an additive action in elevating intracellular cAMP levels.

Dual PDE 10A inhibition and $A_{2A}R$ agonism is anti-proliferative in CHO-K1- $A_{2A}R$ cells

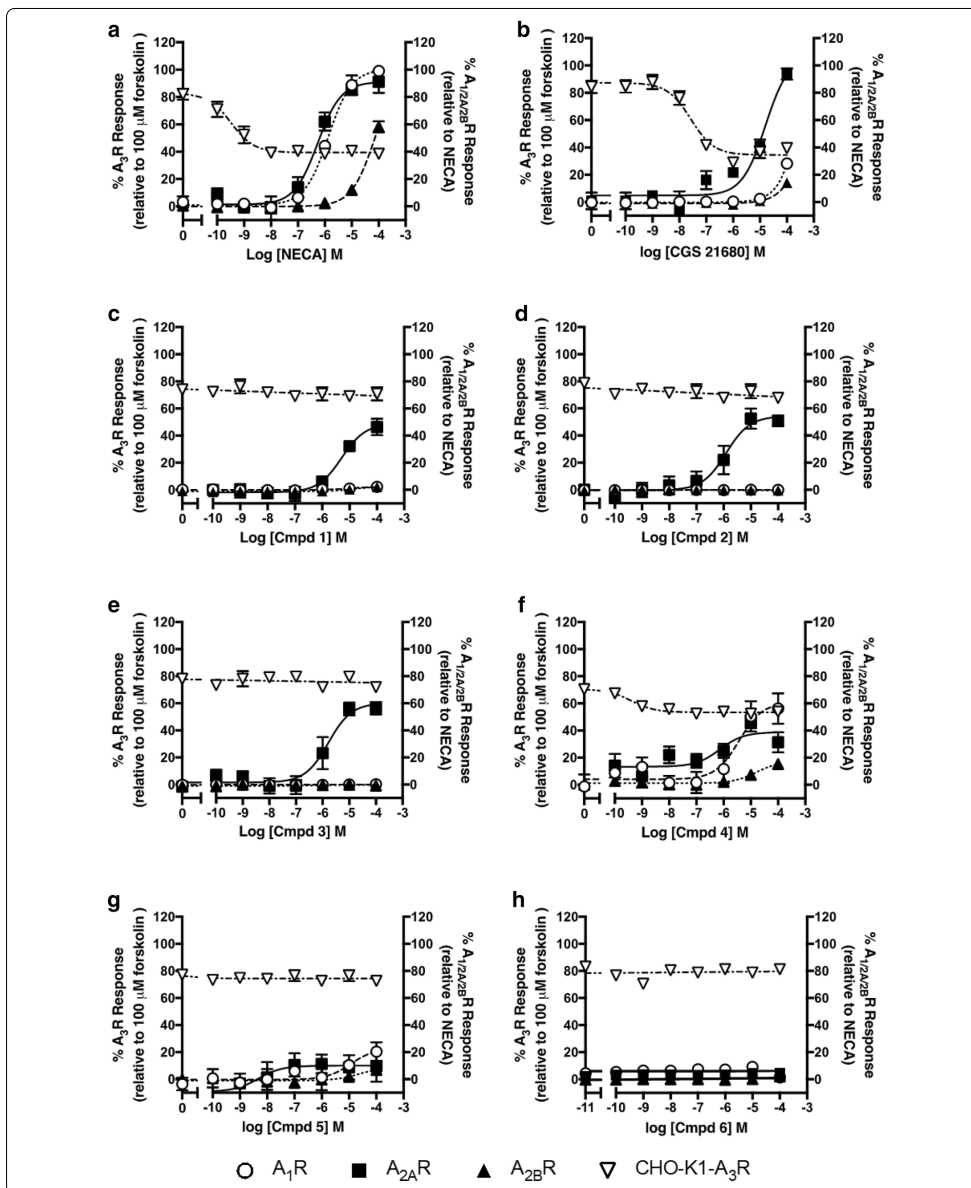
Both CHO-K1 and CHO-K1- $A_{2A}R$ cells displayed concentration-dependent inhibition of cell proliferation when stimulated with forskolin (Additional file 1: Figure S6, Table S3), confirming the anti-proliferative effects of cAMP. However, sole activation of the $A_{2A}R$, via CGS21680 stimulation, had no anti-proliferative effects upon either cell type (Additional file 1: Figure S6, Table S3). In contrast stimulation with compound **1** displayed $A_{2A}R$ -dependent inhibition of cell growth. Compounds **3–5** show anti-proliferative effects in CHO-K1

cells, which increased in terms of both potency and efficacy when the $A_{2A}R$ was expressed (Additional file 1: Figure S6, Table S3). Compound **2** appeared to be anti-proliferative regardless of the cell type tested whereas Compound **6** displayed little anti-proliferative action implying that that sole inhibition of PDE 10A has little effect upon the proliferation of CHO-K1 cells (Additional file 1: Figure S6, Table S3).

Dual PDE 10A inhibition and $A_{2A}R$ agonism is anti-proliferative in Lung carcinoma cells

Having established that the compounds **1–5** appear to have dual activity in CHO-K1 cells where the $A_{2A}R$ was over expressed we then extended our studies to a series of lung carcinoma cells: two lung squamous cell carcinomas (LUSC): LK-2 and H520, and two lung adenocarcinoma cells (LUAC): H1563 and H1792, which express differing levels of the four adenosine receptor subtypes and PDE10A (Fig. 7a). Using these cell lines, we investigated the effects of compounds of our dual-target compounds upon cAMP production and proliferation (Fig. 7). Note, compound **2** was not analysed for cAMP production in this study due to apparent off-target toxic effects upon CHO-K1 cell proliferation—a feature also noted in all four lung carcinoma cell lines.

LK-2 cells express the A_1R , $A_{2B}R$ and very low levels of PDE10A, but lacked expression of the $A_{2A}R$ (Fig. 7a). In these cells compound **3** and to a lesser extent compound **4** were able to stimulate cAMP production (Fig. 7a, Additional file 1: Table S4). However, only forskolin and compound **3** (Fig. 7a, Additional file 1: Table S5) displayed any anti-proliferative actions. Thus, in the absence of significant PDE10A or $A_{2A}R$ expression, compound **1** and **5** displayed little activity. Compound **4** is an agonist for the $A_{2B}R$ so presumably this explains its ability to stimulate cAMP production. The action of compound **3** was somewhat of a surprise and may suggest it has additional activities beyond $A_{2A}R$ and PDE10A. By means of a comparison, H520 cells express all four ARs, but no PDE 10A. In these cells, we were able to observe stimulation of cAMP accumulation when exposed to all compounds except for compound **6**, which displayed low potency and efficacy (Fig. 7,



(See figure on next page.)

Fig. 6 CGS21680 and compounds **1–6** elevated cAMP in $A_{2A}R$ stably expressed in CHO-K1 cells, which were antagonized by ZM241385. $A_{2A}R$ stably expressed in CHO-K1 cells (CHO-K1- $A_{2A}R$) were stimulated for 30 minutes with: CGS21680 (**a**), compound **1** (**b**), compound **2** (**c**), compound **3** (**d**), compound **4** (**e**), compound **5** (**f**), or compound **6** (**g**), after which the cAMP levels were determined. Subsequently compounds were antagonized with either 100 pM, 10 nM or 1 μ M ZM241385, which decreased the cAMP levels to the same level of CHO-K1 cells (no $A_{2A}R$ stably expressed). Data represented are relative to the response of CGS21680, \pm SEM of 4–9 individual replicates

Additional file 1: Table S4). The increase in activity of the compounds was also apparent for proliferation assays, where compounds **1**, **3–5** all displayed anti-proliferative activity with higher affinity and efficacy than that observed in the LK-2 cells (Fig. 7, Additional file 1: Table S5). This data highlights the potential of the compounds to prevent proliferation when the $A_{2A}R$ is expressed. Likewise, in H1792 cells we observe the expression of all four ARs and an increase in PDE10A expression, relative to H520 cells (Fig. 7). Again, we observed the ability of all compounds to elevate cAMP levels, whilst compounds **1**, **3**, **4** and **5** act in an anti-proliferative manner (Fig. 7, Additional file 1: Tables S4, S5). The same was also apparent for H1563 cells, which in contrast to H1792 cells express much higher levels of PDE10A (Fig. 7, Additional file 1: Tables S4, S5). By comparing the observed potencies for proliferation and cAMP assays, across all cell types, for all anti-proliferative compounds, a strong correlation was observed (Fig. 7B, $r = 0.80$, 95% CI: 0.85–0.91). This suggests that through improving efficacy in terms of cAMP production, an increased efficacy can also be achieved in terms of proliferation inhibition.

Finally, to provide convenient means by which to compare the anti-proliferative activities of the compounds tested in this study, we multiplied the potency term (affinity) for the compounds by their efficacy (span of antiproliferation)—generating a ‘proliferation factor’ term as described previously [46]. Using this analysis, we can observe that compounds **1**, **3**, **4** and **5**, all display improved efficacy when both PDE10A and $A_{2A}R$ are present in the cells (Fig. 7). In contrast, compound **6** displays no anti-proliferative activity in any cell type tested whilst CGS21680 is only anti-proliferative in H1563 cells (Fig. 7, Additional file 1: Table S5), suggesting these are more sensitive to proliferation inhibition. In contrast, forskolin displays near equal activity in all cell types tested. As described earlier, compound **3** displayed activity in all four NSCLC cell lines suggesting it may display off target effects. Significantly, it is worth highlighting that compound **4** displayed higher efficacy when the $A_{2B}R$ was most abundantly expressed in cells. This directly correlates with it being non-selective at the different AR subtypes and suggests it may be a pan-AR/PDE10A compound.

Conclusions

In this work, a novel structure-based approach has been successful in identifying triazoloquinazolines as the first dual ligands that activate the $A_{2A}R$ and inhibit PDE10A simultaneously. Docking of the triazoloquinazolines **1–6**, which are known PDE10A inhibitors, was performed on the orthosteric site of the $A_{2A}R$ (PDB ID: 2YDO). It is demonstrated experimentally using a BRET-based ligand-binding assay that these ligands indeed bind to the $A_{2A}R$. The rank order of affinity for the six triazoloquinazolines at the $A_{2A}R$ was found to be: cmpd **4** > cmpd **2** > cmpd **6** > cmpd **1** = cmpd **3** > cmpd **5**.

Functional analysis in yeast-screening assay and in mammalian cells demonstrated that compounds **1–5** were $A_{2A}R$ agonists and revealed that compounds **1–3** are selective for the $A_{2A}R$. It is suggested that the observed $A_{2A}R$ sub-type selectivity for **1–3** is attributed to their predicted interactions with the His₂₅₀ residue, which is an interaction present only in the selective co-crystallized $A_{2A}R$ agonists, such as CGS21680 and UK432097. It was further demonstrated by MD simulation analysis that this residue undergoes conformational changes only when selective $A_{2A}R$ agonists are bound and not when non-selective agonists bind to $A_{2A}R$. This could contribute to shaping the orthosteric site to favor selectivity of $A_{2A}R$ agonists. Moreover, MD analysis highlighted the motion of Val₈₄ in TM3 as an essential requirement for $A_{2A}R$ activation.

Compounds **1** and **3–5** exhibited promising concentration-dependent anti-proliferative effects in lung squamous cell carcinoma cells and lung adenocarcinoma cells, which correlated with co-expression of $A_{2A}R$ and PDE10A and increased cellular levels of cAMP. Compound **1** (as a selective $A_{2A}R$ agonist and a PDE10A inhibitor) exhibited increased potency for both cAMP accumulation and anti-proliferative actions, which increased in tandem with the combined target expression ($A_{2A}R$ and PDE10A) across the NSCLC cell lines, from LK-2-H520-H1792-H1563. Hence, the structure-based approach proposed in this work has been successfully validated using binding and functional assays, and it provides a template for generating $A_{2A}R$ agonists as part of a dual-target design objective.

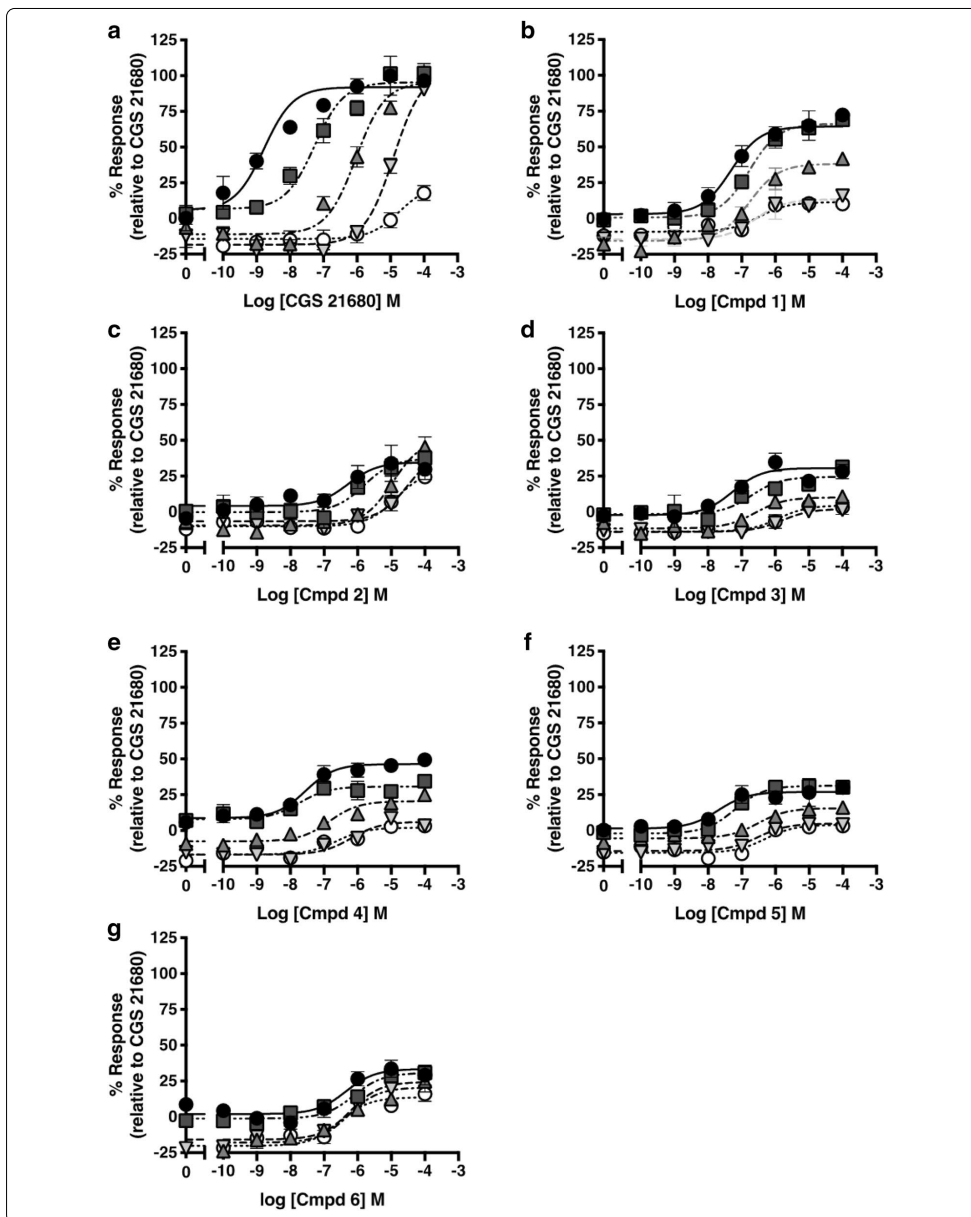


Table 1 Potency (pEC₅₀) and range of responses for cAMP production upon CGS21680 and triazoloquinazoline stimulated cAMP accumulation in CHO-K1-A_{2A}R and CHO-K1 cells

| | CHO-K1-A _{2A} R | | | CHO-K1 | | | CHO-K1-A _{2A} R vs. CHO-K1 | |
|----------|--------------------------------|--------------------|---|--------------------------------|--------------------|---|-------------------------------------|----------------------|
| | pEC ₅₀ ^a | Range ^b | n | pEC ₅₀ ^a | Range ^b | n | Δ pEC ₅₀ ^c | Δ Range ^d |
| CGS21680 | 8.78 ± 0.2 | 86.33 ± 7.2 | 9 | ND | ND | 4 | – | – |
| Cmpd 1 | 7.32 ± 0.2 | 61.14 ± 5.2*** | 8 | 6.49 ± 0.3 | 20.19 ± 2.7 | 4 | 0.83 ± 0.5 | 40.95 ± 7.80 |
| Cmpd 2 | 6.29 ± 0.5** | 30.50 ± 8.1 | 6 | 4.85 ± 0.2 | 39.46 ± 3.9 | 4 | 1.44 ± 0.6 | – 8.96 ± 10.6 |
| Cmpd 3 | 7.26 ± 0.3** | 28.95 ± 6.3 | 6 | 5.90 ± 0.3 | 18.32 ± 2.3 | 4 | 1.21 ± 0.5 | 10.63 ± 8.70 |
| Cmpd 4 | 7.55 ± 0.2 | 37.71 ± 2.9** | 5 | 6.62 ± 0.2 | 18.75 ± 1.7 | 4 | 0.93 ± 0.6 | 18.96 ± 3.60 |
| Cmpd 5 | 7.70 ± 0.4** | 27.42 ± 4.4 | 6 | 6.30 ± 0.2 | 19.49 ± 1.7 | 4 | 1.28 ± 2.4 | 7.93 ± 6.1 |
| Cmpd 6 | 6.52 ± 0.4 | 33.87 ± 5.3 | 6 | 6.35 ± 0.3 | 31.42 ± 4.6 | 4 | 0.17 ± 0.8 | 2.45 ± 9.9 |

Data ± SEM of *n* individual replicates. ^aNegative logarithm of agonist concentration producing half-maximal response. ^bPercentage range of response observed upon agonist stimulation, relative to that obtained with CGS21680 stimulation in each cell type. ^cChange in pEC₅₀ between CHO-K1 and CHO-K1-A_{2A}R cells (Δ pEC₅₀ = pEC₅₀(CHO-K1-A_{2A}R) - pEC₅₀(CHO-K1)). ^dChange in range between CHO-K1 and CHO-K1-A_{2A}R cells (Δ Range = Range (CHO-K1-A_{2A}R) - Range (CHO-K1)). ND Not determined, full dose-response curve not feasible. Statistical difference, between CHO-K1-A_{2A}R cells and CHO-K1 cells, was calculated using pair-wise t-tests, for each agonist (**p* < 0.05, ***p* < 0.01, ****p* < 0.001)

Methods

Design approach for the discovery of dual ligands at the A_{2A}R and PDE10A

Triazoloquinazolines were shortlisted as candidates of dual ligands at the A_{2A}R and PDE10A since this chemical series were predicted to show activity based on ligand- and structure- based techniques [33]. The focus was on discovering compounds that elicited an elevation of cAMP by the activity of ligands having dual effects, simultaneously agonists at A_{2A}R and inhibitors of PDE10A.

From the ZINC database, eleven purchasable triazoloquinazolines that were experimentally determined as PDE10A inhibitors were identified using a search for the triazoloquinazoline substructure with the following criteria: Uniprot ID: Q9Y233 and IC₅₀ < 10 μM. Identified triazoloquinazolines had the following ZINC IDs: 3,154,141, 3,141,002, 6,206,233, 9,937,921, 9,939,949, 2,968,902, 14,728,559, 424,907, 13,229,753, 44,924,158, and 8,747,709. These were downloaded for subsequent docking into the orthosteric site of the A_{2A}R protein crystal structure.

Selection of the A_{2A}R protein crystal structure for shortlisting triazoloquinazoline candidates as A_{2A}R agonists

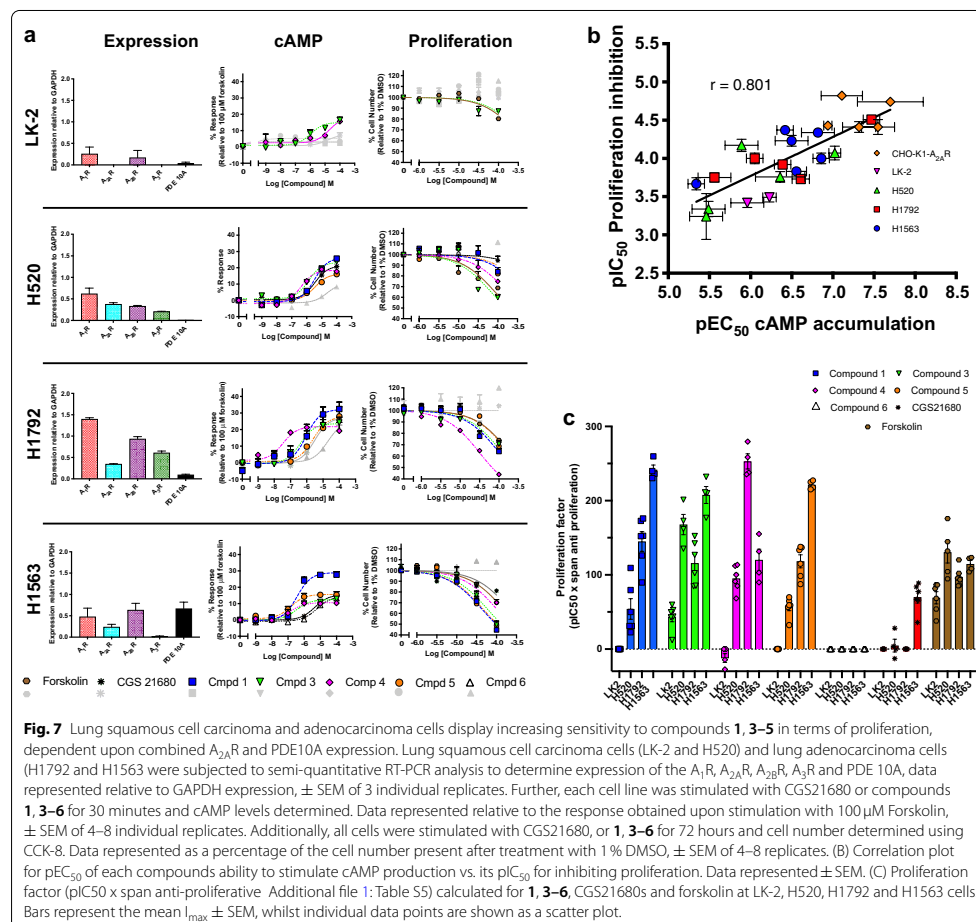
All the active forms of the A_{2A}R protein crystal structure with the following PDB IDs (4UG2, 4UHR, 3QAK, 2YDO, and 2YDV) and the inactive forms with the following PDB IDs (5IU4, 3UZA, 5K2A, 4E1Y, 3EML, 5NM2, 5JTB, 5UVI, and 5UIG) were downloaded into MOE [47]. It has been reported in the literature that Val₈₄ in TM3, which is located in the orthosteric site, has to shift its position upon agonist binding owing to a steric clash with the ligand, which may contribute to the 2 Å

shift observed in H3 [29–31]. To evaluate the change in the interaction upon agonist binding, the distance was calculated from a single amino acid residue to Val₈₄. This gave a frame of reference to compare structures. The ‘fixed’ amino acid residue selected was Leu₂₄₉ in TM6. This was achieved by aligning all the active and inactive forms of the A_{2A}R protein crystal structures (using the sequence editor > alignment > align/superimpose option). Then, the mean RMSD displacement from the mean of all the aligned structures was calculated for Leu₂₄₉, which turned out to be low (0.40 Å) confirming that it is reasonably static in its relative position.

For each PDB ID of the active and inactive forms of the A_{2A}R crystal structures, the distance between the α-carbons of Val₈₄ in TM3 and Leu₂₄₉ in TM6 was measured in MOE using the measure > distances option. Additional file 1: Table S1 lists all the Val₈₄-Leu₂₄₉ inter-residue distance values. The inter-residue distances of the active forms ranged from 14.30 to 14.53 Å, and for the inactive forms they ranged from 12.96 to 13.36 Å. The largest displacement of the Val₈₄ residue was measured for the active form in PDB ID: 2YDO, and the distance was equal to 14.53 Å. This can be compared to the inactive form of the A_{2A}R protein crystal structure (PDB ID: 5IU4), which had the minimum distance (12.96 Å). Given that Val₈₄ displayed the highest displacement from the Leu₂₄₉ residue in the protein crystal structure with the PDB ID: 2YDO, it was selected as the best candidate for shortlisting candidates of A_{2A}R agonists.

Ligand preparation

39 potent agonists and 38 potent antagonists of the A_{2A}R (Uniprot ID: P29274) with EC₅₀ and IC₅₀ values less than 1 μM and confidence scores equal to 9 were manually extracted from ChEMBL. 133 A_{2A}R inactives were



extracted from PubChem using SQL and the eleven purchasable triazoloquinazolines were selected from the ZINC database. The entire set of ligands were prepared for docking into the orthosteric site of the $A_{2A}R$ protein crystal structure, with LigPrep 2.5 [48], using the default settings and the Epik option, which introduces energy penalties associated with ionization and tautomerization [49].

Receptor preparation

Docking with Glide [50] was performed against the human $A_{2A}R$ protein crystal structure (PDB IDs: 2YDO and 5IU4). The protein structures were prepared using

the Protein Preparation Wizard of Maestro 9.3 [51], following the default protocol, which accounts for energy refinement, hydrogen addition, pKa assignment, side-chain rotational isomer refinement, and addition of missing residues and side-chains with Prime 3.1 [52]. Resolved water molecules were discarded, and the structure was centered using the co-crystallized ligand as the center of the receptor grid generated for each protein structure. The co-crystal structures of $A_{2A}R$ with Adenosine (PDB ID: 2YDO) and with ZM241385 (PDB ID: 5IU4) were selected as target structures.

Enrichment of agonists by the A_{2A}R docking model (PDB ID: 2YDO)

In an attempt to validate the A_{2A}R docking model, the set of prepared A_{2A}R agonists, antagonists and inactives were docked using Glide against the prepared protein structure.

The Glide docking parameters used were extra precision (XP) and flexible ligand sampling, which obtained the best separation for the medians of docking score distributions for agonists versus antagonists and agonists versus inactives of the A_{2A}R. This implies that this docking model enriches the agonists. Additional file 1: Figure S7 shows the separation of the medians for the A_{2A}R docking model: (A) – 11.24 (agonists) (B) – 7.88 (antagonists) and (C) – 6.74 (inactives). Statistical analysis was performed with R using a Mann-Whitney test on the agonist and antagonist docking score distributions, as well as agonist and inactive docking score distributions. The differences in medians were significant at a *p* value of less than 0.05 [33].

Cut-off generation for compound selection as candidates of A_{2A}R agonists from the docking model

The Matthews correlation coefficient (MCC), which takes into account true and false positives (agonists) and negatives (antagonists), was computed (using a Python script [33]) for the docking scores of the agonists and antagonists against the A_{2A}R docking model. A search was performed for a docking score threshold that gave the highest MCC in order to shortlist promising candidates of A_{2A}R agonists, which displayed docking scores that are lower than the score with the highest MCC, and this gave a threshold of -7.33 for the A_{2A}R docking model.

Docking

The eleven purchasable triazoloquinazolines, which were prepared with LigPrep, were docked against the A_{2A}R protein crystal structure (PDB ID: 2YDO). The Glide docking parameters used were extra precision (XP) and flexible ligand sampling. The parameters were deduced from docking experiments using known actives and inactives against the protein-docking model. The A_{2A}R protein is fairly rigid as assessed by thermal stability (B factor) in Glide [53]. Six triazoloquinazolines (1–6) displayed docking scores that are lower than -7.33, which was the docking score with the highest MCC for the known agonists and antagonists. Their chemical structures are depicted in Fig. 1. Additionally compounds 1, 4 and 5 (with the highest predicted affinities and the most potent agonists identified), compound 6 (which did not exhibit any agonist activity), CHEMBL3799351 (an antagonist with an IC₅₀ = 4.35 nM and confidence score equal to 9) and CGS21680 (the selective and potent A_{2A}R

agonist) and adenosine (a non-selective adenosine receptor agonist), were docked into the inactive form of the A_{2A}R protein crystal structure (PDB ID: 5IU4) for MD simulation and analysis. The six triazoloquinazolines (1–6) were then shortlisted for validation as A_{2A}R agonists in relevant biochemical assays.

MD simulations

Based on a structural analysis of the available A_{2A}R crystal structures, the distance between the α -carbons of Val₈₄ in TM3 and Leu₂₄₉ in TM6 was selected for investigation as a conformational descriptor for receptor activation. The two A_{2A}R co-crystallized structures (PDB IDs: 5IU4 and 2YDO), which exhibited the largest difference in α -carbon distances between Val₈₄ in TM3 and Leu₂₄₉ in TM6 (12.96 Å versus 14.53 Å respectively), were selected for molecular dynamics simulation. Subsequently, compounds 1, 4, 5, and 6 that were docked into the orthosteric site of the inactive form of the A_{2A}R protein crystal structure (PDB ID: 5IU4) were subjected to a 100 ns MD simulation protocol. Likewise, CHEMBL3799351, CGS21680 and adenosine were docked into the orthosteric site of the inactive form of the A_{2A}R protein crystal (PDB ID: 5IU4) to obtain simulations of control compounds. The apo structure (PDB ID: 5UI4) was also selected for the same analysis.

The starting structures were prepared using Maestro 9.3 following the default procedure for protein preparation. The protocol adds missing residues and sidechain information with Prime 3.1 [52], and uses the “Cap termini” option that adds the coordinates to the residue. Next, “Analyze network” in the interactive hydrogen bond optimizer was used to check on the assignments of hydrogen orientations in the hydrogen bonding network. They were subsequently optimized. All MD simulations described in this study were performed using Desmond 3.2, available in the Schrödinger software package Release 2016-3 with the default force field OPLS3 [54]. An orthorhombic box was used to build the model systems with periodic boundary conditions in an isothermal–isobaric ensemble with a constant number of particles (NPT ensemble). The system temperature was kept at 300 K, and the pressure was kept at atmospheric pressure. The definition of transmembrane regions was taken from the OPM database [55]. The receptor structures were embedded in a pre-equilibrated palmitoyl-oleoyl-phosphatidylcholine membrane (bilayer) and solvated with simple point charge water and 0.15 M NaCl. All other parameters were set to default values (refer to Additional file 1: Table S6 in supporting information). The 100 ns simulations were carried out with Desmond 3.2 *via* command line on the computer cluster CALCULON (University of Cambridge) by using 20 central processing units. For

each compound, the simulations were performed twice, and the trajectories obtained were analyzed with the software VMD. Then plots were obtained for the RMSD values of His₂₅₀ in TM6, and the α -carbons distances between Val₈₄ in TM3 and Leu₂₄₉ in TM6 for the simulated systems over 100 ns using the seaborn library [56]. The same protocol was repeated for the 500 ns simulations for compounds **1**, **5**, CGS21680, and the A_{2A}R protein crystal structures (PDB IDs: 2YDO and 5UI4) (each performed in duplicate).

Materials

Triazoloquinazolines **1–6** were supplied from Ambinter (Orléans, France), and CGS21680, NECA and ZM241385 from Tocris Biosciences (Abingdon, UK) (%purity \geq 95). All compounds were stored in 10 mM stock solutions in DMSO. Rolipram was purchased from Cayman chemicals (Michigan USA), and other laboratory reagents were from Sigma-Aldrich (Poole, UK), of analytical grade.

Mammalian cell culture

CHO-K1 (gifted by Dr. Ewan St. John Smith, University of Cambridge, UK) CHO-K1-A_{2A}R and CHO-K1-A_{3R} cells (gifted by Prof. Karl-Norbert Klotz, University of Wuerzburg, Germany), were routinely cultured in Hams F-12 nutrient mix, supplemented with 10% fetal bovine serum (FBS). H520, H1563, H1792 and LK-2 cells (gifted by Dr. Whalid Khaled, University of Cambridge, UK) were grown in RPMI media + 10% FBS. All media was further supplemented with 1X antibiotic, antimycotic solution (Sigma Aldrich, Poole, UK). Culturing of all cell types was done at 37°C in a humidified atmosphere containing 5% CO₂.

Generation of CHO-K1 cell line stably expressing the A_{2A}R

CHO-K1 cells stably expressing the A_{2A}R cells were generated *via* transfection with 500 ng pcDNA3.1-A_{2A}R (cDNA.org), per well of a 24-well plate, which was performed with FuGENE HD (Promega, Wisconsin, USA), at a 1:3 (w/v) DNA:FuGENE ratio. Prior to adding 800 μ g/ml G418 (Sigma Aldrich, Poole, UK), the cells were further cultured for 48 hours. Then every 48 hours, G418 containing media were replaced until foci of cells were attained, which were left to grow to 100% confluency. Afterwards, each well was tested for the ability of CGS21680 to elevate cAMP, performing further culturing with appropriately responding clones as described.

Phosphodiesterase 10A inhibition assays

A PDE10A assay kit (BPS Bioscience, San Diego, CA) was used to test the PDE10A inhibition of compounds **1–6** as described in the manufactures protocol. 400 pg of

purified PDE10A was used per reaction, and the plates were read using a TECAN infinite M200.

Yeast methods

Generation of yeast strains was done according to previously reported protocols, and they have been routinely grown as previously described [45]. Yeast cells expressing either the A_{1R}, A_{2A}R, or A_{2B}R were treated with either NECA, CGS21680 or compounds **1–6**, in order to measure the activity of each, as previously described [45].

Bioluminescence Resonance Energy transfer (BRET)-based ligand binding of triazoloquinazolines

HEK293T cells were seeded in 6-well plates at density of 10⁶ cells/well and grown overnight at 37°C in DMEM/F12 medium supplemented with 10% FBS and 1% antibiotic/antimycotic. Cells were then transfected with 1.5 μ g Nluc-A_{2A}R construct (a gift from Dr. Stephen Bridson, and Professor Steven Hill, University of Nottingham, UK) per well using PEI method. The ratio of DNA:PEI used for this transfection was 1:6 in 150 mM NaCl [57]. Cells were grown overnight, harvested and seeded at a density of 50,000 cells/well into PLL-coated white 96-well plates (Greiner, UK) in complete growth medium and cultured for a further 24 h. On the day of the assay, culture medium was discarded and replaced by 80 μ l BRET buffer which consist of PBS supplemented with 0.9 mM CaCl₂, 0.5 mM MgCl₂, and 1% BSA (w/v). The assay was started by adding 10 μ l of furimazine, the substrate of Nluc (Promega, UK) (diluted in BRET buffer) to a final concentration of 0.4 μ M and the plate was incubated in the dark at room temperature for 5 minutes.

For association-dissociation kinetic experiments, following furimazine incubation, 40 nM of CA200645 (purchased from Hello Bio, Bristol, UK) was added and the plate was immediately read. After 19 minutes stimulation, CGS21680 was injected to give a final concentration of 10 μ M. Whereas for competition association assays, after incubation with furimazine, CA200645 (300 nM) in the presence of unlabelled ligand (in a range of 10 pM to 100 μ M) were added simultaneously. BRET signal was recorded for either 50 minutes or 20 minutes, for kinetic experiments or competition assay as appropriate, on a Mithras LB940 plate reader allowing sequential integration of signal detected from fluorescent probe CA200645 and Nluc. The BRET ratio corresponds to the ratio of light emission from acceptor (red fluorescent probe, long pass filter >610 nm) over donor (Nluc 460 nm). Ligand-induced Δ BRET was used to construct the association-dissociation kinetic of the fluorescence probe and competition binding curve of unlabelled ligands.

To determine K_D value of CA200645, the signals from kinetic assay was fit into “association then dissociation” equation which was built in Prism 8.4. With the purpose of validating BRET-based competition assay, several reference compounds including CGS21680, NECA, and isoprenaline were also included. Binding affinities were calculated from competition assay by fitting data to non-linear regression using “one-site, fit K_i ” model built in Prism 8.4. The concentration and K_D values of ‘hot’ ligand were set to 300 nM and 65 nM, respectively.

cAMP accumulation assays

Prior to assay, harvesting of cells was performed with trypsin containing 0.05% EDTA, they were then washed with PBS, and subsequently resuspended in stimulation buffer (PBS Proliferation assays containing 0.1% BSA and 25 μ M rolipram). Seeding of cells was done at 2000 cells well^{-1} of a 384-well white optiplate, and then they were stimulated at room temperature with compounds 1–6 (ranging 100 pM–10 mM) for 30 minutes. The cells were subsequently lysed, and the measurement of cAMP levels was done using a LANCE cAMP detection kit (PerkinElmer), and the plates were read with a Mithras LB940 microplate reader.

Proliferation assays

To test the effect of compounds 1–6 upon proliferation, various cell types were seeded onto clear 96-well plates at proper densities for each; CHO-K1 (2000 cells well^{-1}), CHO-K1- $A_{2A}R$ (2000 cells well^{-1}), H520 (2500 cells well^{-1}), H1563 (2500 cells well^{-1}), H1792 (2500 cells well^{-1}), LK-2 (2500 cells well^{-1}). This was done in suitable media, and they were cultured for 24 hours. After the subsequent addition of compounds 1–6 (ranging 316 nM – 100 μ M), cells were allowed to grow further for 72 hours. Quantification of changes in cell number was done by adding 5 μ l CCK-8 reagent to each well, accompanied by incubation at 37 °C for 1–3 hours. The determination of OD_{450} was done using a Mithras LB940 micro-plate reader at 450 nm.

RT-PCR

Extraction of RNA from H520, H1792, H1563 and LK-2 cells was done using a RNAqueous[®]-4PCR Total RNA Isolation Kit (Life Technologies, Paisley, UK) as per the manufacturer’s instructions. Then, DNase I treatment was performed to remove the contamination by genomic DNA. Subsequently, the quantification of the degree of purity of RNA samples was performed using a NanoDrop[™] Lite spectrophotometer (Thermo Scientific, UK). The samples that were used in cDNA synthesis are those of yields > 100 ng/ μ l and $A_{260}/_{280}$ ratios > 1.9. The cDNA synthesis was done using a QuantiTect reverse transcription kit (Qiagen, Manchester, UK), for which a total of 1 μ g of freshly isolated RNA was consumed

per reaction. RT-PCR was subsequently implemented according to what has been previously reported [58]. The RT-PCR that has been done used gene specific primers to human: *GAPDH* (Sense 5'-TGACCACCAACTGC TTAGC-3'; Antisense 5'-GGCATGGACTGTGGTCAT GAG-3'), A_1R (Sense 5'-CCACAGACCTACTTCCAC ACC-3'; Antisense 5'-TACCGGAGAGGGATCTTG ACC-3'; Primerbank ID – 115305570C1), $A_{2A}R$ (Sense 5'-CGTCCGGTACAATGGCTT-3'; Antisense 5'-TTGTTCCAACCTAGCATGGGA-3'; Primerbank ID – 156142194C1), $A_{2B}R$ (Sense 5'-TGCACTGACTTC TACGGCTG-3'; Antisense 5'-GGTCCCGTGACCAA ACTT-3'; Primerbank ID – 22907046C1), A_3R (Sense 5'-GGCCAATGTTACTACATCACC-3'; Antisense 5'-CCAGGGCTAGAGAGACAATGAA-3'; Primerbank ID – 4501953A1) and *PDE10A* (Sense 5'-TGA TGACTT TTCTCTCGACGTTG-3'; Antisense 5'-AAGCCACCT ACACAGTGCTC-3'; Primerbank ID – 359465520C1). Then, gel electrophoresis (using 2% agarose gels) was performed to resolve PCR products. The imaging of gels was subsequently done using a G Box iChemi gel documentation system employing GeneTools analysis software (Syngene, Cambridge, UK) and densitometry.

Data analysis

Data analysis was performed using GraphPad Prism 8.2.1 (San Diego, CA). All data for β -galactosidase assays were normalized to the responses resulting from NECA stimulation, whereas the data for cAMP inhibition/accumulation assays were normalised to those obtained upon stimulation with 100 μ M Forskolin or CGS21680. As for proliferation assays, the normalization of all data was done relative to the responses obtained upon treating cells with 1% (v/v) DMSO. Subsequently, a three-parameter logistic equation was used for fitting each set of normalized data β -galactosidase or cAMP data, in order to calculate pEC_{50}/pIC_{50} and E_{max} values. Also, the fitting of the proliferation data was done using a three-parameter logistic equation constraining the basal value to 100 and the system maximum to the I_{Max} value obtained for compound 2, since it elicited the maximum inhibition of cellular proliferation in all cell types tested. A one-way ANOVA with Dunnett’s post-test, or Student’s t-test was used to assess the statistical significance for all assays, where $p < 0.05$ was considered to be significant.

Supplementary Information

The online version contains supplementary material available at <https://doi.org/10.1186/s13321-021-00492-5>.

Additional file 1. Discussion. Additional figures and tables

Authors' contributions

LK conceived the idea of the dual-target ligand design, designed the computational study, shortlisted the compounds for experimental validation, and wrote this manuscript. GL and IW designed while, IW, DS and SC performed, all in vitro experiments to validate the design approach. MB helped in running MD simulation analysis. DS, IW and GL analyzed in vitro data and wrote the pharmacology aspect of the manuscript. AB, RG, and GL supervised the project. All authors read and approved the final manuscript.

Funding

LK thanks the IDB Cambridge International Scholarship for support. This work was financially supported by an ERC grant to AB (No. 336159), and MRC Doctoral Training Partnership studentship to LW. (MR/J003964/1) and a Leverhulme Trust Grant to G.L. (RPG-2017-255). We would also like to thank the Endowment Fund for education from the Ministry of Finance of the Republic of Indonesia for supporting DS and the Posen fund (Murray Edwards College) awarded to SC. M.B. acknowledges funding from the German Research Foundation (grant number DFG-407626949) and the German Academic Exchange Service (DAAD). Finally, we thank the Dr Walid Khalid and members of the WTK laboratory (Pharmacology Cambridge) for the gift of the NSCLC cell lines.

Competing interests

The authors declare no competing interests.

Author details

¹ Centre for Molecular Informatics, Department of Chemistry, University of Cambridge, Lensfield Road, CB21EW Cambridge, UK. ² Department of Pharmacology, University of Cambridge, Tennis Court Road, CB2 1PD Cambridge, UK. ³ Pharmacology and Clinical Pharmacy Research Group, School of Pharmacy, Bandung Institute of Technology, 40132 Bandung, Indonesia. ⁴ Institute of Pharmacy, Freie Universität Berlin, Königin-Luise-Straße 2 und 4, 14195 Berlin, Germany. ⁵ Department of Metabolism Digestion and Reproduction, Faculty of Medicine, Imperial College London, SW7 2AZ London, UK. ⁶ Present Address: GlaxoSmithKline, Gunnels Wood Road, Hertfordshire SG1 2NY Stevenage, UK.

Received: 9 December 2020 Accepted: 1 February 2021

Published online: 03 March 2021

References

- Hellstrom M, Harvey AR (2014) Cyclic AMP and the regeneration of retinal ganglion cell axons. *Int J Biochem Cell Biol* 56:66–73. <https://doi.org/10.1016/j.jbiocel.2014.04.018>
- Errante FS, Leite AA, Caricati-Neto A, Bergantini LB (2017) RPM-R new antitumoral pharmacological strategies involving Ca2+/camp signaling pathways. *J Cancer Epidemiol Prev* 2:6
- Fajardo AM, Piazza GA, Tinsley HN (2014) The role of cyclic nucleotide signaling pathways in cancer: targets for prevention and treatment. *Cancers (Basel)* 6:436–458. <https://doi.org/10.3390/cancers6010436>
- Indolfi C, Avvedimento EV, Di Lorenzo E et al (1997) Activation of cAMP-PKA signaling in vivo inhibits smooth muscle cell proliferation induced by vascular injury. *Nat Med* 3:775–779. <https://doi.org/10.1038/nm0797-775>
- Toll L, Jimenez L, Waleh N et al (2011) [Beta]2-adrenergic receptor agonists inhibit the proliferation of 1321N1 astrocytoma cells. *J Pharmacol Exp Ther* 336:524–532. <https://doi.org/10.1124/jpet.110.173971>
- Rodríguez G, Ross JA, Nagy ZS, Kirken RA (2013) Forskolin-inducible cAMP pathway negatively regulates T-cell proliferation by uncoupling the interleukin-2 receptor complex. *J Biol Chem* 288:7137–7146. <https://doi.org/10.1074/jbc.M112.408765>
- Mediavilla-Varela M, Luddy K, Noyes D et al (2013) Antagonism of adenosine A2A receptor expressed by lung adenocarcinoma tumor cells and cancer associated fibroblasts inhibits their growth. *Cancer Biol Ther* 14:860–868. <https://doi.org/10.4161/cbt.25643>
- Inoue Y, Yoshimura K, Kurabe N et al (2017) Prognostic impact of CD73 and A2A adenosine receptor expression in non-small-cell lung cancer. *Oncotarget* 8:8738–8751. <https://doi.org/10.18632/oncotarget.14434>
- Zhu B, Lindsey A, Li N et al (2017) Phosphodiesterase 10A is overexpressed in lung tumor cells and inhibitors selectively suppress growth by blocking β -catenin and MAPK signaling. *Oncotarget* 8:69264–69280. <https://doi.org/10.18632/oncotarget.20566>
- Fusco JP, Pita G, Pajares MJ et al (2018) Genomic characterization of individuals presenting extreme phenotypes of high and low risk to develop tobacco-induced lung cancer. *Cancer Med*. <https://doi.org/10.1002/cam4.1500>
- Rickles RJ, Pierce LT, Giordano TP et al (2010) Adenosine A2A receptor agonists and PDE inhibitors: a synergistic multitarget mechanism discovered through systematic combination screening in B-cell malignancies. *Blood* 116:593–602. <https://doi.org/10.1182/blood-2009-11-252668>
- Jankowska A, Wesolowska A, Pawlowski M, Chłoń-Rzepa G (2019) Multifunctional ligands targeting phosphodiesterase as the future strategy for the symptomatic and disease-modifying treatment of Alzheimer's disease. *Curr Med Chem*. <https://doi.org/10.2174/0929867326666190620095623>
- Cheong SL, Federico S, Spalluto G et al (2019) The current status of pharmacotherapy for the treatment of Parkinson's disease: transition from single-target to multitarget therapy. *Drug Discov Today* 24:1769–1783
- Shipe WD, Sharik SS, Barrow JC et al (2015) Discovery and optimization of a series of pyrimidine-based phosphodiesterase 10A (PDE10A) inhibitors through fragment screening, structure-based design, and parallel synthesis. *J Med Chem* 58:7888–7894. <https://doi.org/10.1021/acs.jmedchem.5b00983>
- Rieger JM, Brown ML, Sullivan GW et al (2001) Design, synthesis, and evaluation of novel A2A adenosine receptor agonists. *J Med Chem* 44:531–539. <https://doi.org/10.1021/jm0003642>
- Chen JB, Liu EM, Chen TR et al (2011) Design and synthesis of novel dual-action compounds targeting the adenosine A2A receptor and adenosine transporter for neuroprotection. *ChemMedChem* 6:1390–1400. <https://doi.org/10.1002/cmdc.201100126>
- Halder AK, Amin SA, Jha T, Gayen S (2017) Insight into the structural requirements of pyrimidine-based phosphodiesterase 10A (PDE10A) inhibitors by multiple validated 3D QSAR approaches. *SAR QSAR Env Res* 28:253–273. <https://doi.org/10.1080/1062936x.2017.1302991>
- Yuan G, Gedeon NG, Jankins TC, Jones GB (2015) Novel approaches for targeting the adenosine A2A receptor. *Expert Opin Drug Discov* 10:63–80. <https://doi.org/10.1517/17460441.2015.971006>
- Pourbasheer E, Shokouhi Tabar S, Masand VH et al (2015) 3D-QSAR and docking studies on adenosine A2A receptor antagonists by the CoMFA method. *SAR QSAR Env Res* 26:461–477. <https://doi.org/10.1080/1062936x.2015.1049666>
- Hu E, Kunz RK, Rumpf S et al (2012) Use of structure based design to increase selectivity of pyridyl-cinnoline phosphodiesterase 10A (PDE10A) inhibitors against phosphodiesterase 3 (PDE3). *Bioorg Med Chem Lett* 22:6938–6942. <https://doi.org/10.1016/j.bmcl.2012.09.010>
- Deganutti G, Moro S (2017) Supporting the identification of novel fragment-based positive allosteric modulators using a supervised molecular dynamics approach: a retrospective analysis considering the human A2A adenosine receptor as a key example. *Molecules*. <https://doi.org/10.3390/molecules22050818>
- McGraw C, Yang L, Levental I et al (2019) Membrane cholesterol depletion reduces downstream signaling activity of the adenosine A2A receptor. *Biochim Biophys Acta Biomembr* 1861:760–767. <https://doi.org/10.1016/j.bbmem.2019.01.001>
- Yuan S, Hu Z, Filipek S, Vogel H (2015) W246(6.48) opens a gate for a continuous intrinsic water pathway during activation of the adenosine A2A receptor. *Angew Chem Int Ed Engl* 54:556–559. <https://doi.org/10.1002/anie.201409679>
- Guo D, Pan AC, Dror RO et al (2016) Molecular basis of ligand dissociation from the adenosine A2A receptor. *Mol Pharmacol* 89:485–491. <https://doi.org/10.1124/mol.115.102657>
- Mondal C, Halder AK, Adhikari N, Jha T (2014) Structural findings of cinnolines as anti-schizophrenic PDE10A inhibitors through comparative chemometric modeling. *Mol Divers* 18:655–671. <https://doi.org/10.1007/s11030-014-9523-9>
- Rodríguez D, Gao Z-G, Moss SM et al (2015) Molecular docking screening using agonist-bound GPCR structures: probing the A2A adenosine receptor. *J Chem Inf Model* 55:550–563. <https://doi.org/10.1021/ci500639g>
- Novikov GV, Sivozhelezov VS, Shaitan KV (2013) [Investigation of the conformational dynamics of the adenosine A2A receptor by means of molecular dynamics simulation]. *Biofizika* 58:618–634

28. Xu F, Wu H, Katritch V et al (2011) Structure of an agonist-bound human A2A adenosine receptor. *Science* 332:322–327. <https://doi.org/10.1126/science.1202793>
29. Lebon G, Edwards PC, Leslie AG, Tate CG (2015) Molecular determinants of CGS21680 binding to the human adenosine A2A receptor. *Mol Pharmacol* 87:907–915. <https://doi.org/10.1124/mol.114.097360>
30. Lebon G, Warne T, Edwards PC et al (2011) Agonist-bound adenosine A2A receptor structures reveal common features of GPCR activation. *Nature* 474:521–525. <https://doi.org/10.1038/nature10136>
31. Carpenter B, Lebon G (2017) Human adenosine A2A receptor: molecular mechanism of ligand binding and activation. *Front Pharmacol* 8:898. <https://doi.org/10.3389/fphar.2017.00898>
32. Ng HW, Laughton CA, Doughty SW (2013) Molecular dynamics simulations of the adenosine A2A receptor: structural stability, sampling, and convergence. *J Chem Inf Model* 53:1168–1178. <https://doi.org/10.1021/ci300610w>
33. Kalash L, Val C, Azuaje J et al (2017) Computer-aided design of multi-target ligands at A1R, A2AR and PDE10A, key proteins in neurodegenerative diseases. *J Cheminform* 9:1–19. <https://doi.org/10.1186/s13321-017-0249-4>
34. Kehrer J, Ritzen A, Langgard M et al (2011) Triazoloquinazolines as a novel class of phosphodiesterase 10A (PDE10A) inhibitors. *Bioorg Med Chem Lett* 21:3738–3742. <https://doi.org/10.1016/j.bmcl.2011.04.067>
35. Capuzzi SJ, Muratov EN, Tropsha A (2017) Phantom PAINS: problems with the utility of alerts for pan-assay interference compounds. *J Chem Inf Model* 57:417–427. <https://doi.org/10.1021/acs.jcim.6b00465>
36. Katritch V, Jaakola VP, Lane JR et al (2010) Structure-based discovery of novel chemotypes for adenosine A(2A) receptor antagonists. *J Med Chem* 53:1799–1809. <https://doi.org/10.1021/jm901647p>
37. Jaakola VP, Lane JR, Lin JY et al (2010) Ligand binding and subtype selectivity of the human A(2A) adenosine receptor: identification and characterization of essential amino acid residues. *J Biol Chem* 285:13032–13044. <https://doi.org/10.1074/jbc.M109.096974>
38. Glukhova A, Thal DM, Nguyen AT et al (2017) Structure of the adenosine A1 receptor reveals the basis for subtype selectivity. *Cell* 168:867–877 e13. <https://doi.org/10.1016/j.cell.2017.01.042>
39. Weston C, Poyner D, Patel V et al (2014) Investigating G protein signalling bias at the glucagon-like peptide-1 receptor in yeast. *Br J Pharmacol* 171:3651–3665. <https://doi.org/10.1111/bph.12716>
40. Stoddart LA, Vernall AJ, Denman JL et al (2012) Fragment screening at adenosine-A3 receptors in living cells using a fluorescence-based binding assay. *Chem Biol*. <https://doi.org/10.1016/j.chembiol.2012.07.014>
41. Soave M, Kellam B, Woolard J et al (2020) NanoBIT complementation to monitor agonist-induced adenosine A1 receptor internalization. *SLAS Discov*. <https://doi.org/10.1177/2472555219880475>
42. Barkan K, Lagarias P, Vrontaki E et al (2019) Pharmacological characterization of novel adenosine receptor A3R antagonists. *BioRxiv*. <https://doi.org/10.1101/693796>
43. Bylund DB, Toews ML (1993) Radioligand binding methods practical guide and tips. *Am J Physiol*. 265(5 Pt 1):L421–9
44. Kenakin KT (1988) Pharmacologic Analysis of drug receptor interaction. *Ther Drug Monit*. <https://doi.org/10.1097/00007691-198803000-00029>
45. Knight A, Hemmings JL, Winfield I et al (2016) Discovery of Novel Adenosine Receptor Agonists That Exhibit Subtype Selectivity. *J Med Chem* 59:947–964. <https://doi.org/10.1021/acs.jmedchem.5b01402>
46. Safitri D, Harris M, Potter H et al (2020) Elevated intracellular cAMP concentration mediates growth suppression in glioma cells. *Biochem Pharmacol*. <https://doi.org/10.1016/j.bcp.2020.113823>
47. Molecular Operating Environment (MOE) (2013) Chemical Computing Group Inc., Montreal, QC
48. Schrödinger Release 2016-4 (2016) LigPrep, Schrödinger, LLC, New York
49. Shelley JC, Cholleti A, Frye LL et al (2007) Epik: a software program for pK(a) prediction and protonation state generation for drug-like molecules. *J Comput Aided Mol Des* 21:681–691. <https://doi.org/10.1007/s10822-007-9133-z>
50. Halgren TA, Murphy RB, Friesner RA et al (2004) Glide: a new approach for rapid, accurate docking and scoring. 2. Enrichment factors in database screening. *J Med Chem* 47:1750–1759. <https://doi.org/10.1021/jm303644s>
51. Sastry GM, Adzhigirey M, Day T et al (2013) Protein and ligand preparation: parameters, protocols, and influence on virtual screening enrichments. *J Comput Aided Mol Des* 27:221–234. <https://doi.org/10.1007/s10822-013-9644-8>
52. Jacobson MP, Pincus DL, Rapp CS et al (2004) A hierarchical approach to all-atom protein loop prediction. *Proteins Struct Funct Genet*. <https://doi.org/10.1002/prot.10613>
53. Parthasarathy S, Murthy MRN (2000) Protein thermal stability: insights from atomic displacement parameters (B values). *Protein Eng Des Sel* 13:9–13. <https://doi.org/10.1093/protein/13.1.9>
54. Bowers KJ, Chow DE, Xu H, Dror RO, Eastwood MP, Gregersen BA, Klepeis JL, Kolossvary I, Moraes MA, Sacerdoti FD, Salmon JK, Shan Y, Shaw DE (2006) Scalable algorithms for molecular dynamics simulations on commodity clusters. In: SC'06: Proceedings of the 2006 ACM/IEEE Conference on Supercomputing, Tampa, FL, pp 43. <https://doi.org/10.1109/SC.2006.54>
55. Lomize MA, Pogozheva ID, Joo H et al (2012) OPM database and PPM web server: resources for positioning of proteins in membranes. *Nucleic Acids Res* 40:D370–D376. <https://doi.org/10.1093/nar/gkr703>
56. (2017) Seaborn: statistical data visualization. <http://seaborn.pydata.org>
57. Mackie DI, Nielsen NR, Harris M et al (2019) RAMP3 determines rapid recycling of atypical chemokine receptor-3 for guided angiogenesis. *Proc Natl Acad Sci U S A* 116:24093–24099. <https://doi.org/10.1073/pnas.1905561116>
58. Ladds G, Zervou S, Vatsis M et al (2009) Regulators of G protein signalling proteins in the human myocardium. *Eur J Pharmacol* 610:23–28. <https://doi.org/10.1016/j.ejphar.2009.03.042>

Publisher's note

Springer Nature remains neutral with regard to jurisdictional claims in published maps and institutional affiliations.

Ready to submit your research? Choose BMC and benefit from:

- fast, convenient online submission
- thorough peer review by experienced researchers in your field
- rapid publication on acceptance
- support for research data, including large and complex data types
- gold Open Access which fosters wider collaboration and increased citations
- maximum visibility for your research: over 100M website views per year

At BMC, research is always in progress.

Learn more biomedcentral.com/submissions



Appendix 4

Publication: Clark, A.J., *et al.* 2021

This appendix contains:

Clark, A. J., Mullooly, N., Safitri, D., Harris, M., de Vries, T., Van Brink, A. M., Poyner, D., Giani, D., Wigglesworth, M., Ladds, G. (2021). CGRP-receptor family reveals endogenous GPCR agonist bias and its significance in primary human cardiovascular cells. *BioRxiv*. [bioRxiv. https://doi.org/10.1101/2020.12.21.423730](https://doi.org/10.1101/2020.12.21.423730).

1 **Title:** CGRP-receptor family reveals endogenous GPCR agonist bias and its significance in
2 primary human cardiovascular cells

3
4 Ashley J. Clark¹, Niamh Mullooly², Dewi Safitri¹, Matthew Harris¹, Tessa de Vries⁴,
5 Antoinette Maassen Van Den Brink⁴, David R. Poyner³, Davide Giani², Mark Wigglesworth⁵,
6 Graham Ladds¹

7

8

9 Running title: RAMP-mediated agonist bias

10

11 ¹ Department of Pharmacology, University of Cambridge, Tennis Court Road, Cambridge,
12 CB2 1PD, UK.

13 ² Functional Genomics, Discovery Sciences, AstraZeneca, Cambridge CB2 0SL, United
14 Kingdom

15 ³ School of Life and Health Sciences, Aston University, Aston Triangle, Birmingham B4 7ET,
16 United Kingdom

17 ⁴ Department of Internal Medicine, Erasmus MC, Erasmus University Medical Centre,
18 Rotterdam, Rotterdam, Netherlands.

19 ⁵ Hit Discovery, Discovery Sciences, BioPharmaceuticals R&D, AstraZeneca, Alderley Park
20 SK10 4TG, UK

21

22 **Address for correspondence:**

23 Dr Graham Ladds, Department of Pharmacology, University of Cambridge, Tennis Court
24 Road, Cambridge, CB2 1PD Tel; +44 (0) 1223 334020. Email: grl30@cam.ac.uk.

25

26 **Author Contributions:**

27 DRP, AMD, MW and GL conceived and designed the research; AJC, TV and DS performed
28 the experiments; AJC, NM and DG designed the CRISPR-Cas9 experiments, AJC, GL, MH
29 and MW analysed data; AJC, MH and GL wrote manuscript, DRP, AMVDB, MW and DG
30 revised and edited the manuscript.

31

32 **Keywords**

33 G protein-coupled receptor, CGRP, adrenomedullin, adrenomedullin 2, receptor activity-
34 modifying protein, agonist bias, gene editing, physiological bias.

35

36 **Abstract**

37 Agonist bias at G protein-coupled receptors has attracted considerable interest, although its
38 relevance for physiologically-produced agonists is not always clear. Here, using primary
39 human cells and gene editing techniques, we demonstrate for the first time, endogenous
40 agonist bias with physiological consequences for the calcitonin-like receptor (CLR). We
41 reveal that by switching the accessory protein: receptor activity-modifying protein (RAMP)
42 associated with CLR we can re-route the physiological pathways activated by the stimulating
43 peptide agonists. These results have revealed a unique role in calcium-mediated nitric oxide
44 signalling for the little-understood peptide adrenomedullin 2 and distinct pro-proliferative
45 effects of calcitonin-gene related peptide (CGRP) and adrenomedullin in cardiovascular

1 cells. This work reveals that CLR-based agonist bias occurs naturally in human cells and
2 has a fundamental purpose for its existence. We anticipate this will be a starting point for
3 more studies into RAMP function in native environments and its importance in endogenous
4 GPCR signalling.

5

6 **Introduction**

7 G protein-coupled receptors (GPCRs) form the largest protein family in the human genome.
8 ~30% of marketed drugs target these receptors and therefore understanding their signalling
9 pathways is not simply an academic exercise. For many years it had been incorrectly
10 assumed that agonist-occupied GPCRs signalled through a single pathway to elicit their
11 response. However, there is now overwhelming evidence to suggest that many GPCRs exist
12 in multiple receptor conformations and can elicit numerous functional responses, both G
13 protein- and non-G protein-dependent. Furthermore, different agonists, acting at the same
14 receptor have the potential to activate different signalling pathways to varying extents; a
15 concept referred to as biased agonism or signalling bias^{1,2}. While the therapeutic promise
16 of biased agonists is obvious³: it allows design of ligands that actively engage with one
17 beneficial signalling outcome while reducing the contribution from those that mediate more
18 undesirable effects, it is not without controversy. For example, recent doubt has been cast
19 on validity of developing synthetic biased agonists against the μ -opioid receptor – a GPCR
20 that has been considered the trailblazer for therapeutic potential of biased agonism⁴. Thus,
21 further investigations into the role of agonist bias and its physiological importance,
22 particularly its relevance to endogenous agonists, are required to bridge the gap between
23 heterologous studies and in-vivo investigations.

24

25 While there are many well-studied GPCRs that exhibit signalling bias, including
26 adrenoceptors, and the aforementioned μ -opioid receptor, we have chosen to focus upon
27 the calcitonin-like receptor (CLR). Like many other GPCRs, CLR can couple to multiple G
28 proteins and β -arrestins. Importantly, when co-expressed with one of three receptor activity
29 modifying proteins, (RAMPs, see below), it can be activated by distinct endogenous
30 agonists; calcitonin-gene related polypeptide (CGRP), adrenomedullin (AM) and
31 adrenomedullin 2/intermedin (AM2). This makes it a good system to investigate the role of
32 bias for such endogenous ligands. CGRP, an abundant neuropeptide, is the most potent
33 microvascular vasodilator known. While it is thought to be cardioprotective, it has also been
34 implicated in diseases such as migraine⁵. AM is released by the vascular endothelium and
35 is also a potent vasodilator that can modulate vascular tone, it is involved in angiogenesis,
36 and is elevated in some cancers and heart failure⁶⁻⁸. AM2 is also a vasodilator and highly
37 expressed in the heart and vasculature^{9,10}. It can cause sympathetic activation, have
38 antidiuretic effects, and is upregulated in cardiac hypertrophy and myocardial infarction¹¹.

39

40 Molecularly, CLR and its close relative, the calcitonin receptor (CTR), are classical class B
41 GPCRs. CLR is pleiotropically coupled, predominately activating $G_{\alpha s}$ although there are
42 reports of couplings to both $G_{i/o}$ and $G_{q/11/14}$ ^{2,12} families. These G_{α} subunits promote
43 activation/inhibition of adenylyl cyclase and phospholipase C to generate intracellular
44 second messengers including cAMP and mobilise intracellular Ca^{2+} (Ca^{2+}_i) which then
45 activate their respective intracellular signalling cascades. Beyond the G_{α} subunits CLR has

2

1 been reported to couple to β -arrestins¹³⁻¹³ inducing internalisation, although it has been
2 suggested that this interaction can also lead to its own signalling events possible promoting
3 cell growth and proliferation¹⁴. Despite this high potential for agonist-induced pleiotropy,
4 CLR remains most closely associated with adenylyl cyclase activation and generation of
5 cAMP. It is unknown whether this is representative of CLR's true signalling pattern in the
6 endogenous setting.

7
8 Additional complexity is added to the pharmacology of the CLR since it has an absolute
9 requirement for the formation of a heterodimer with a RAMP^{15,16}. In overexpression studies,
10 each of the three RAMPs have been shown to differentially influence the affinity and agonist
11 bias of the CGRP family of peptides at the CLR^{17,18}. CLR in complex with RAMP1 generates
12 the CGRP receptor since CGRP has been demonstrated to be the most potent of the three
13 agonists at this receptor for generation of cAMP. Likewise, CLR-RAMP2 generates the
14 adrenomedullin 1 receptor (AM is the most potent at this receptor) and CLR-RAMP3
15 produces the AM2 receptor (here AM and AM2 are approximately equipotent). To date the
16 cognate receptor for AM2 and its physiological role remain unknown; no receptor shows
17 marked selectivity for it. While there is an abundance of evidence of GPCR signalling bias
18 in recombinant cell systems, and in this case CLR-mediated bias^{12,19}, documented
19 examples using natural agonists and endogenously expressed human receptors are
20 currently lacking. We wished to ascertain whether signalling bias at the CLR occurs in
21 primary cells and whether it plays a role in cellular function. We have chosen to focus our
22 research on RAMP1 and RAMP2 as the CGRP and AM1 receptors are the best described.

23
24 Using human endothelial cells which endogenously express the AM1 receptor (CLR-
25 RAMP2), we demonstrate for the first time that biased agonism is present and has a
26 fundamental role in the function of peptide hormones acting on primary human cells.
27 Moreover, through deletion of the endogenous RAMP2 and replacing it with RAMP1, we
28 highlight that not only is the RAMP essential for CLR function and CGRP peptide family
29 signalling in primary cell systems but that RAMPs direct the pattern of agonist bias observed.
30 Furthermore, we document previously unreported actions for the CGRP-based peptide
31 agonists; AM2, in particular, emerges as an agonist uniquely biased to elevate calcium-
32 mediated nitric oxide (NO) signalling while both CGRP and AM display distinct pro-
33 proliferative effects in cardiovascular cells. The work we describe here reveals that GPCR
34 agonist bias occurs naturally in human cells and plays fundamentally important physiological
35 roles.

36 37 **Results**

38 39 **Endothelial cells exclusively express functional CLR/RAMP2 (AM1 receptor)**

40 While there are many reports of biased agonism for GPCRs in recombinant systems (e.g.
41 ^{19,20}), few examples have been documented in primary human cells. Given the reported roles
42 of CGRP, AM and AM2 in the cardiovascular system we have focussed our studies upon
43 these peptides, and their receptors in primary human endothelial cells (both HUVECs and
44 human umbilical artery endothelial cells (HUAECs)). Both endothelial cell lines appear to
45 express the AM1 receptor since we could only detect transcripts for CLR and RAMP2 using

1 qRT-PCR (Figure 1 and Figure S1A). This was confirmed functionally, since when the
2 endothelial cells were stimulated with agonists and cAMP accumulation quantified, the rank
3 order of potency was AM>AM2>CGRP (Figure 1B, Figure S1B and Table S1). Furthermore,
4 application of the selective AM1 receptor antagonist AM22-52 which, at 100nM, abolished
5 agonist induced cAMP accumulation while 100nM olcegepant (a CGRP receptor selective
6 antagonist) had little effect (Figure S2A,B). An important factor in confirming receptor-
7 specific agonist bias is to ensure that competing receptors are not present in the system.
8 The closely related calcitonin receptor (CALCR/CTR) not only interacts with RAMPs²¹ but
9 has also been documented to bind CGRP²¹. Endothelial cells appear to not express the CTR
10 since we were unable to detect the presence of its transcript or obtain a significant functional
11 response upon application of two CTR agonists (calcitonin or amylin) (Figure S2C). Thus,
12 based upon these data, we suggested that endothelial cells specifically express the AM1
13 receptor alone (CLR-RAMP2) and are a useful primary cell line with which to study potential
14 endogenous agonist bias.

15

16 **Endogenous agonist bias at the CLR-RAMP2 receptor**

17 For studies of biased agonism, it is not simply the ability of different ligands to activate the
18 canonical second messenger pathway to varying extents that is important, but their ability
19 to differentially activate a multitude of downstream pathways. Having established that our
20 primary endothelial cells express only one of the receptor-RAMP complexes responsive to
21 our three peptides: CGRP, AM and AM2, we next sought to quantify the extent of
22 endogenous agonist-induced biased signalling through CLR-RAMP2 at other pathways.
23 Beyond coupling to G_{α_s} , in recombinant systems, it has been shown that the CLR can couple
24 to the G_{α_q} family of G proteins to mobilise Ca^{2+}_i ¹⁹. Consistent with these previous reports
25 we were able to observe concentration-dependent increases in Ca^{2+}_i in both HUVECs and
26 HUAECs upon application of AM and AM2 but little or none with CGRP (Figure 1C, Figure
27 S1C and Table S1). Importantly, all responses could be abolished with the co-treatment of
28 the $G_{\alpha_q/11/14}$ inhibitor YM-254890²² (Figure S2D) suggesting the response observed was
29 purely $G_{\alpha_q/11/14}$ -mediated and thereby confirming CLR-based pleiotropy in primary
30 endothelial cells. Interestingly, at the CLR-RAMP2 receptor in both endothelial cell lines,
31 AM2 produced the most potent response and not AM suggesting that a non-cognate agonist
32 can have a distinct and more potent effect than the cognate agonist at certain pathways
33 endogenously.

34 We subsequently turned our attention to the extracellular signal-regulated kinase
35 (ERK) pathway (assayed after 5 minutes stimulation) where we found that, again, the
36 'cognate' agonist (AM) was not the most potent. Perhaps surprisingly, CGRP (the agonist
37 reported to be the least potent at cAMP production at the AM1 receptor) was the most potent
38 at stimulating ERK_{1/2} phosphorylation (Figure 1D, Figure S1D and Table S1). Thus, despite
39 this being designated an AM1 receptor, it is CGRP and not AM that produces physiologically
40 relevant signalling via the ERK_{1/2} pathway.

41

42 **Physiological consequences of CGRP-based peptide agonist bias in primary 43 endothelial cells**

44 As we were exploring the AM1 receptor in its native environment, we sought to discover
45 whether the distinct patterns of agonist bias we have observed with CGRP, AM and AM2

1 were reflected further downstream as physiological bias. Here we considered two potential
2 physiological outcomes with important therapeutic potential – the generation of NO (a vital
3 modulator of vascular homeostasis) and cell proliferation. NO, generated through
4 endothelial nitric oxide synthase (eNOS) in endothelial cells²³ promotes
5 vasorelaxation/dilation in a cGMP dependent manner²⁴. In both HUVECs and HUAECs we
6 observed that all three agonists could evoke NO synthesis in the order of potencies
7 AM2>AM>CGRP (Figure 1E, Figure S1E and Table S1) although both AM and CGRP were
8 partial agonists for this pathway with the potencies closely resembling the trends observed
9 for Ca^{2+}_i mobilisation. Indeed, a direct correlation between Ca^{2+}_i mobilisation and NO
10 production in endothelial cells was confirmed through application of YM-254890 which
11 abolished all NO release (Figure S2E). Such observations are consistent with the role of
12 increases of Ca^{2+}_i concentrations leading to eNOS function²⁴ but to the best of our
13 knowledge have not been demonstrated previously for AM2.

14 Beyond NO production we also measured the long-term cell proliferation (72 hours)
15 response to the three peptides in both endothelial cell lines. Again, the different peptides
16 had varying effects on proliferation, with CGRP most potently promoting cell growth (Figure
17 1F, Figure S1F and Table S1). This is consistent with the data we describe for
18 phosphorylation of ERK_{1/2} suggesting proliferation is not mediated via a cAMP-dependent
19 pathway. This was further corroborated by the observation that application of the non-
20 selective adenylyl cyclase activator forskolin induced a concentration dependent inhibition
21 of cell proliferation. Together, this data suggests that CLR exerts important cellular effects
22 in a G_{α_s} -independent manner thus unveiling previously undocumented abilities for CGRP
23 to promote proliferation in human cells through the AM1 receptor.

24 To provide a means of comparison of the extent of agonist bias observed in the
25 endothelial cells (Figure 1G), and to remove potential confounding issue of system bias
26 (note, system bias may arise due to the differential expression of signalling components or
27 cofactors in the cellular background of choice) we fitted our data with operational model of
28 receptor agonism²⁷ for both endothelial cells (Figure 1H-J and Figure S1G-H and Table S1).
29 There was a strong similarity in the signalling profiles between the two endothelial cells
30 across the five different pathways (Figure 1H) with significant correlations in potency (Figure
31 S3C; $r = 0.73$ – 95% confidence interval 0.35 – 0.90; $p < 0.01$) and the transducer coefficient
32 (Figure 1I) (Figure S3C; τ/K_A ; $r = 0.94$ – 95% confidence interval 0.84 to 0.98; $p < 0.0001$)
33 suggesting primary endothelial cells share common AM1 receptor signalling properties.
34 Finally, this analysis reinforced the notion that AM2 is biased towards Ca^{2+}_i mobilisation and
35 NO production while CGRP favours pERK_{1/2} activation and cell proliferation.

36 37 **AM1 receptor-mediated cAMP accumulation and pERK_{1/2} activation exemplify agonist** 38 **bias**

39 The mechanism by which adenylyl cyclase is regulated involves competition between G_s
40 (activation) and members of the $G_{i/o}$ (inhibition) family of G proteins. Semi-quantitative RT-
41 PCR in both endothelial cell lines revealed the presence of the same G_{α} subunits (Figure
42 S3D-E) and both β -arrestin1 and 2 in both cell lines including members of $G_{i/o}$ family. We
43 and others have documented how the AM1 receptor (in agreement with other class B
44 GPCRs) can couple to the inhibitory G proteins^{21,28,29} although this is often observed in
45 overexpression systems and is cell type dependent. Application of pertussis toxin (PTX),

1 which ADP-ribosylates the inhibitory G proteins (with the exception of G_z), to the HUVECs
2 revealed a dose-dependent increase in cAMP accumulation (Figure 2A) and a suppression
3 of ERK_{1/2} phosphorylation upon application of CGRP and AM2 but not AM (Figure 2B). This
4 data, consistent with our previously reported work¹⁹ suggests that only the non-cognate
5 agonists (CGRP and AM2) are able to recruit G_{i/o} proteins to the CLR, and, particularly in
6 the case of CGRP, the purpose of this is to bias the response away from cAMP and towards
7 other pathways such as pERK_{1/2}. This is highly likely to contribute to the differences seen in
8 physiological outcomes such as proliferation, outlined above.

9 This did however pose the question as to how AM modulates the pERK_{1/2} response.
10 Inhibition of protein kinase A (PKA) had no significant effect (Figure 2C) however
11 antagonism of G_{q/11/14} signalling did reduce the potency of AM-mediated pERK_{1/2} activation
12 (Figure 2D). More strikingly, inhibition of the exchange proteins directly activated by cAMP
13 (EPAC)1/2 activation significantly attenuated both the potency and magnitude of the
14 maximal response (Figure 2E). Taken together, these data highlight the wide array of
15 different G protein couplings and their interlinking actions upon downstream signalling
16 events for the AM1 receptor. These couplings have not been engineered so are not
17 enhanced by overexpression artefacts and thereby represent pure endogenous agonist
18 bias.

19 **RAMP isoform is essential for CLR-mediated agonist bias.**

20 One of the advantages of using recombinant cell lines and/or model cell organisms is the
21 ability to switch the expressed GPCR or RAMP to observe effects on agonist bias. However,
22 these recombinant systems do not allow for observations of physiological bias. Thus, we
23 next sought to determine the effects of CGRP-based agonist bias in primary cells where the
24 endogenous RAMP had been switched using gene deletion followed by lentiviral
25 reintroduction. We chose the HUVEC cell line with which to perform the gene editing since
26 we have been able to grow HUVECs beyond passage P6 to P14 before loss of CGRP based
27 signalling responses are observed (Figure S4), and it is necessary to grow them past P6 to
28 develop the RAMP2 null cells. We used lentiviral CRISPR-Cas9 to knockout the RAMP2
29 gene from the HUVECs. We used a pooled sgRNA strategy using three sgRNAs in separate
30 lentivirus (Figure S5A) which were selected using a puromycin resistance cassette (Figure
31 S5B) to increase our efficiency of editing. We transduced HUVECs at a high multiplicity of
32 infection (MOI) of 10, ensuring that each cell was infected by several lentivirus to increase
33 the likelihood of achieving a deletion. Then sgRNA editing efficiency in the remaining cell
34 pool was assessed by PCR amplification of targeted region, Sanger sequencing and TIDE³⁰
35 analysis: all demonstrating an editing efficiency greater than 95%. This was then followed
36 by analysis by qRT-PCR for receptor and RAMP mRNA. The expression of CLR remained,
37 but RAMP2 was lost suggesting degradation through nonsense-mediated mRNA decay
38 (NMD) (Figure S5C). It is also important to note that the gene editing did not have any impact
39 upon the cells rate of proliferation (Figure S5E) and the G_α subunit/β-arrestin profile also
40 remained consistent with the wild type HUVECs (Figure S5D). Finally, convinced that the
41 cells were as near to wild type HUVECs as possible, except lacking RAMP2, we assessed
42 their signalling properties following stimulation with all three agonists. In all cases the
43 responses were abolished, although the extent of signalling for the positive controls
44

1 remained intact (Figure S5F-J). Thus, these data confirm, that loss of RAMP2 in HUVECs
2 abolishes CLR function.

3 We next introduced, using lentiviral overexpression and blasticidin selection, the
4 open reading frame of RAMP1 into our HUVEC Δ RAMP2 cell line so, in effect, switching the
5 expressed GPCR from the AM1 receptor to the CGRP receptor. mRNA levels were
6 quantified demonstrating successful introduction of a high level of RAMP1 expression
7 (Figure 3A). We next performed cAMP accumulation assays using CGRP, AM and AM2
8 confirming that a functional CLR receptor was formed in these modified HUVECs (Figure
9 3B and Table S2). Reassuringly, we now observed that CGRP was the most potent agonist
10 for the stimulation of cAMP – as expected for a cell line expressing the CGRP receptor
11 (CLR-RAMP1). Perhaps more interestingly, CGRP was also the most potent at mobilising
12 Ca^{2+}_i (Figure 3C and Table S2) and this was also the case in the associated NO production
13 (Figure 3E and Table S2). Comparison of the ERK $_{1/2}$ phosphorylation (Figure 3D and Table
14 S2) highlighted that AM was now the most potent agonist; a clear switch from wild type
15 HUVEC cells where CGRP was the most potent. This followed to proliferation where AM
16 was also the most potent ligand, although both AM2 and CGRP could also promote growth
17 (Figure 3F and Table S2) and was in contrast to the wild type HUVECs where neither could
18 cause proliferation. Thus switching the RAMP in the HUVEC cell line appears to have had
19 a dramatic effect on the agonist bias observed and the functional consequence (Figure 3G,H
20 and Table S2) – beyond just cAMP accumulation as would be expected. However, it should
21 be noted that as RAMP1 expression was high we should be cautious in our direct
22 comparisons between the wild type HUVECs and our RAMP1-HUVEC cell line.

23

24 **Endogenous agonist bias at the CLR-RAMP1 in primary human cardiac myocytes.**

25 In order to provide a comparison for RAMP1-HUVEC signalling with a primary cell line that
26 endogenously expressed the CGPR receptor we turned to primary human cardiomyocytes
27 (HCMs) since these cells only expressed CLR and RAMP1 (Figure 4A); analogous to
28 endothelial cells, HCMs also do not express a functional CTR (Figure 4A and Figure S6A).
29 To confirm that the mRNA expression translated to functional receptor expression we
30 performed cAMP accumulation assays for the CGRP family of peptides (Figure 4B and
31 Table S2). Here, CGRP was the most potent agonist followed by AM2 and AM, a pattern
32 consistent with the expression of the CGRP receptor²⁰ (also confirmed by application of
33 100nM olcegepant to inhibit cAMP accumulation for all three agonists (Figure S6B) while
34 100nM AM22-52 (Figure S6C) had little effect). Intriguingly, upon application of PTX to
35 HCMs we were unable to observe any significant change in the potency or maximal
36 signalling for any of the three peptide agonists (Figure S6D) although the transcript for $G_{\alpha_{12}}$
37 was lower than in the endothelial cells (Figure S5E) and this G_{α} subtype has previously
38 been suggested to be important for PTX-sensitive effects from CLR¹⁹. In contrast to the wild
39 type HUVECs but analogous to the RAMP1-HUVEC cells, not only was CGRP able to
40 stimulate $G_{q/11/14}$ -mediated- Ca^{2+}_i mobilisation in HCMs but it was the most potent agonist
41 (Figure 4C and Table S2). When quantifying ERK $_{1/2}$ phosphorylation we again observed that
42 the cognate ligand (CGRP) was not the most potent (Figure 4D and Table S2), but as in
43 HUVECs, it was the least potent ligand at cAMP accumulation that was the most potent for
44 ERK $_{1/2}$ phosphorylation. AM was the most potent at stimulating ERK $_{1/2}$ phosphorylation,
45 demonstrating that it can produce functionally relevant signalling responses at the CLR-

1 RAMP1. The order of potency for the three agonists for ERK_{1/2} phosphorylation was
2 replicated in the long-term cell proliferation assays (Figure 4F and Table S2) with AM
3 remaining the most potent. All three peptide agonists could also evoke G_{q/11/14}-mediated-NO
4 production (Figure 4E, Figure S6F,G and Table S2) although their responses were less
5 distinct from each other.

6 Analysis of the RAMP1-HUVEC signalling profile suggested a close overlap with the
7 properties of HCMs (Figure 5 and Table S2) for the five different signalling pathways as well
8 as an opposing signalling profile to HUVECs. We confirmed this using correlation plots
9 (Figure 5A-F) of both potency and the transducer coefficient $\text{Log}(\tau/K_A)$, obtained from
10 application of the operational model of receptor agonism²⁷ (values can be found in Table S2
11 and Table S3). Whilst a positive correlation was detected between RAMP1-HUVECs and
12 HCMs (potency; $r = 0.55$ – 95% confidence interval, 0.051 to 0.82; $p < 0.05$; transducer
13 coefficient; $r = 0.52$ – 95% confidence interval, 0.009 to 0.81; $p < 0.05$), a negative correlation
14 was observed between HUVECs and RAMP1-HUVECs (potency; $r = -0.54$ – 95%
15 confidence interval, -0.83 to -0.04; $p < 0.05$; transducer coefficient; $r = -0.58$ – 95%
16 confidence interval, -0.84 to -0.10; $p < 0.05$). We did not observe any correlations between
17 HUVECs and HCMs which, in part appears due to the HCMs having reduced capacity to
18 release NO. Finally, when we extended our analysis to determine the change in transducer
19 coefficient normalised to cAMP accumulation mediated by the non-cognate (for RAMP1-
20 CLR or RAMP2-CLR) agonist AM2 (Figure 5G and 5H) it becomes apparent how closely
21 aligned the signalling properties in RAMP1-HUVECs and HCMs are.

22 23 24 **Discussion**

25 We have shown for the first-time that the CGRP family of endogenous peptides demonstrate
26 biased agonism at the endogenous CLR in a physiological system; and that the RAMP
27 expressed dictates the intracellular response and ultimately the physiological outcome
28 (Figure 5). Many receptors have been shown to demonstrate agonist bias; but for the most
29 part this has been shown through synthetic ligands designed to target certain receptor
30 pathways². We have now shown that this is a process that can occur physiologically to direct
31 different outcomes. Through elucidating distinct patterns of signalling bias that each peptide-
32 receptor-RAMP produces, we have shown that bias is a naturally occurring phenomenon in
33 a range of human cardiovascular cells. Furthermore, while we have only begun to scratch
34 the surface of how important bias is physiologically, it is now clear it is an intrinsic part of
35 endogenous CLR function, and we anticipate this is the case for many more GPCRs that
36 exhibit signalling bias in over-expression studies. We have also demonstrated the
37 importance of studying GPCR second messenger signalling with the endogenous receptor
38 in its native environment, with the distinct signalling patterns of AM2 we have uncovered
39 providing a good example of this.

40 We have confirmed, as anticipated by the co-expression models, that endogenous
41 CLR is unable to function without RAMP expression through CRISPR-Cas9 KO of the
42 endogenous RAMP. This provides, to the best of our knowledge, the first example of
43 CRISPR-Cas9 interrogation of GPCR function in a primary cardiovascular cell. Furthermore,
44 we have shown that the expression of a different RAMP in the HUVECs can switch the

1 signalling bias of the CLR and associated peptide agonists, thus providing additional
2 evidence that RAMP targeting could become a powerful therapeutic tool²⁵.

3 We have compared the pharmacology of these receptors in terms of cAMP
4 accumulation to reports compiling multiple values from independent publications using the
5 human receptor in transfected systems²⁰. It was reassuring therefore to observe that CGRP,
6 AM, and AM2 displayed similar trends in cAMP potency at CLR-RAMP1/2 in the primary
7 cells to those seen in recombinant co-expression studies, as well as in the gene edited
8 RAMP1-HUVECs which reflected the cAMP data from transfected systems (Figure 5I). In
9 addition, we have performed a comprehensive analysis of the mechanisms used by RAMP2-
10 CLR complexes to stimulate ERK_{1/2} phosphorylation in endothelial cells (Figure 2). It is
11 apparent that each agonist uses unique mechanisms to activate ERK_{1/2}. For both CGRP
12 and AM2 it is mediated in a G_{i/o}-dependent manner, while AM uses a combination of G_{q/11/14}
13 signalling and EPAC activation. None of the agonists appear to mediate their ERK_{1/2}
14 stimulation through the so-called cognate pathway, cAMP accumulation. The data
15 presented is ERK_{1/2} phosphorylation after 5 minutes and it will be of interest to determine
16 the mechanisms and spatial locations that facilitating long term ERK_{1/2} phosphorylation.

17 What has become clear in this study is that each of the endogenous ligands have
18 very specific potencies at each pathway measured, whether it is at CLR-RAMP2 in
19 HUVECs/HUAECs or CLR-RAMP1 in HCMs or RAMP1-HUVEC cells. Each peptide
20 generates their own unique signalling profile (Figure 5J-L). In a concentration-dependent
21 manner, they individually recruit distinct G proteins in a manner regulated by the RAMP.
22 This leads to a specific pattern of second messenger production and therefore a 'signalling
23 barcode' for the cell to interpret and produce further physiologically necessary downstream
24 responses. Expression analysis reveals in our three primary cell lines that each only
25 expresses mRNA above the detection threshold for one RAMP and the CLR. Combined with
26 the cAMP signalling profile for each it appears that endothelial cells and HCM are an excellent
27 primary model cell types for the analysis of how the CLR-RAMP2 and CLR-RAMP1 signal
28 *in vivo*.

29 It is worth noting that the present method of classifying receptors for CGRP and AM
30 is based upon their potencies at cAMP production in addition to their affinities in binding
31 assays²⁶. This method arose due to the assumption that cAMP was the most physiologically
32 relevant pathway. Here, we have demonstrated that significantly different potencies are
33 observed for agonists and these lead to physiologically relevant outcomes. As such we need
34 to carefully consider how we classify CGRP-related receptors in the future, and more widely
35 all GPCRs that exhibit agonist bias.

36 We can also consider this work in the wider context of the organs and systems these
37 cells are found in as this sheds light on some of the pathways, and involvement of bias in
38 some of the established roles of CGRP family peptides in the cardiovascular system. It has long
39 been recognised that all three peptides show pleiotropic signalling, activating multiple G
40 proteins and signalling pathways³³ (and indeed this continues in current literature³⁴⁻³⁶), but
41 it has previously not been possible to fit this into any framework. We suggest our current
42 observations on RAMP-directed bias may assist with this.

43 AM has a multitude of important roles in vascular homeostasis⁶; one of which is
44 regulating endothelial barrier function³⁷. It is thought to cause barrier stabilisation and protect
45 against infection mediated junctional protein disappearance, all brought about initially

1 through cAMP production³⁸. This is supported by our work demonstrating AM produces a
2 potent cAMP response and is biased towards this pathway. It is also well documented that
3 AM is a potent vasodilator known to mediate some of its vasodilatory effects through NO
4 release from vascular endothelial cells^{25,39} which we have pharmacologically profiled here.

5 In contrast, the precise role of AM2, which is also found in endothelial cells, has been
6 unclear. We now provide evidence that AM2 is a potent stimulator of Ca²⁺_i mobilisation and
7 NO synthesis. It is possible therefore that this plays a vital role at least in umbilical
8 endothelial cell physiology, and indeed wider vascular physiology. Thus, the novel finding of
9 AM2's greater potency than AM at eliciting NO release via Ca²⁺_i mobilisation may have great
10 therapeutic potential.

11 Interestingly, in vascular endothelial cells CGPR inhibits adenylyl cyclase through G_{i/o}
12 and predominantly signals through pERK_{1/2}, and proliferation. The link between pERK_{1/2} and
13 cellular metabolism/proliferation is well established⁴⁰⁻⁴², as well as in endothelial cells
14 specifically⁴³⁻⁴⁵. We have shown that where an agonist has biased signalling towards ERK_{1/2}
15 phosphorylation, this is carried through to long term cellular proliferation. Importantly, this
16 shows overall that two non-cognate ligands, often not considered significant for receptor
17 function, do in fact have important signalling and physiological roles/capabilities. In addition,
18 we have demonstrated that endogenous pERK_{1/2} can come from a variety of sources
19 depending on the stimulating ligand. Together this shows that the CLR initiates a multitude
20 of intracellular pathways beyond simply G_s and cAMP/PKA in physiologically relevant cells.
21 Therefore, our data adds further evidence that AM for CLR-RAMP2 and CGPR for CLR-
22 RAMP1 should only be considered the cognate ligands in terms of G_s-mediated cAMP
23 signalling, and when looking at the physiology of RAMP2 in endothelial cells and the
24 vasculature as a whole, CGRP and AM2 should be considered alongside AM for their
25 different and potentially complementary roles.

26 On the heart, there are multiple reports that CGRP has a cAMP-mediated positive
27 inotropic and chronotropic effect^{5,46,47}, and our data showing its strong response in cAMP
28 accumulation assays on human myocytes (combined with its overall bias towards this
29 pathway) supports this. There are contrasting reports in the literature over AM's effect on
30 heart contractility^{7,48}; with some suggestions that it is a positive inotrope acting in the same
31 cAMP driven manner as β-adrenoceptor agonists⁴⁹, while others report it having negative
32 inotropic effects^{50,51}. Here we show that AM promotes a cAMP response through CLR-
33 RAMP1 in human cardiomyocytes, but it has weak potency. This may provide some
34 context/explanation for the contradictory literature reports. Furthermore, our report has
35 clearly revealed that cAMP is not AM's primary signalling pathway in HCMs and that it is
36 biased towards pERK_{1/2} and cell proliferation rather than cAMP and positive inotropy.
37 Nevertheless, evidence suggests that AM has an important role in the human heart. This
38 includes the observed elevation of AM in the failing heart⁵². Here, we have utilised
39 proliferating human ventricular myocytes *in vitro* and shown that AM (but not CGRP or AM2)
40 exhibits signalling bias specifically towards pERK_{1/2} and enhancing proliferation in these
41 cells. This work highlights AM as a novel peptide hormone that may promote cardiac
42 regeneration naturally *in vivo*, and provides a cellular mechanism for this. This may also
43 explain the elevation of AM in heart failure⁶ and the clinical trial data showing that AM
44 administration reduces infarct size²⁷. For AM2, its effect on contraction of the heart is

1 blocked by both inhibitors of PKA and PKC (i.e. $G_{q/11/14}$ -coupling), suggesting multiple
2 signalling pathways are activated by this peptide *in-vivo*⁵⁴.

3 It should be noted that not all studies reveal pleiotropic signalling for the CGRP family
4 of peptides, either involving direct measurements of G protein coupling in cell-free systems⁵⁵
5 or second messenger generation in cells¹². We suggest that there is cell membrane (e.g.
6 lipid composition) and cell line-specific factors (e.g. expression of G proteins) that influence
7 the observed bias.

8 In summary, we have gone beyond previous studies in recombinant systems to
9 observe agonist bias. While we have focused upon CLR-RAMP complexes, our ability to
10 switch the RAMP means we are, in effect, switching the expressed receptor and therefore
11 has general applicability to all GPCRs. Our data highlights how endogenous agonist bias
12 can have profound consequences for the cell and how important cell background is in
13 regulating this process. This work may even go as far as to suggest that to fully understand
14 bias at a GPCR, it has to be considered in its native environment. While our work takes an
15 important step closer to understanding how the CGRP family of peptides and receptors
16 function on a cellular level in the human cardiovascular system, it also highlights the
17 importance of endogenous agonist bias as a concept and emphasises its long-term
18 consequences for drug design.

19

20 **Materials and Methods**

21 *Cell Culture*

22 HUVECs and HUAECs (were both sourced from PromoCell, Germany) were cultured in
23 Endothelial Cell Growth Media (ECGM) (PromoCell). Human Cardiac Myocytes
24 (PromoCell,) were grown in Cardiac Myocyte Growth Media (CMGM) (PromoCell). All cell
25 lines were cultured in media containing 10% heat inactivated Fetal Bovine Serum (FBS)
26 (Sigma, USA). Cells were grown in 25cm² flasks or 75cm² flasks depending on cell density
27 required. They were passaged approximately every 4 days depending on confluency with a
28 final volume of 10ml produced from 1ml of the previous cell culture and 9ml of the growth
29 medium in 75cm² flasks, or 1ml using 4ml in 25cm² flasks, and used from passage 2-6 (with
30 the exception of HUVEC Δ RAMP2 and RAMP1-HUVEC). All cells grown with 1% antibiotic
31 antimycotic solution (100x Sigma, USA). The cells were maintained in an incubator (37 °C,
32 humidified 95% air, 5% CO₂) between passaging.

33

34 *Genome Engineering*

35 HUVECs with the RAMP2 gene knocked out were generated by CRISPR/Cas9 homology
36 directed repair as described previously⁵⁶. The sgRNA sequences were designed (5'-
37 CGCTCCGGGTGGAGCGCGCCGG-3'), (5'-TCCGGGTGGAGCGCGCCGGCGG-3'), and
38 (5'-CCC CGTCTCCCTAGGACCCGA-3') for Cas9 targeting to the human RAMP2 gene
39 (Sigma, US). All guides were delivered in the LV01 vector (U6-gRNA:ef1a-puro-2A-Cas9-
40 2A-tGFP) vector provided by (Sigma-Aldrich, US). Sequences were verified by Sanger
41 sequencing. The control cell line was established by transduction of LV01 vector not
42 containing sgRNA targeted to RAMP2 gene. HUVEC cells were seeded in 6 well plates at a
43 cell density of 160,000 cells/well and maintained at 37°C in 5% CO₂ with Complete
44 Endothelial Cell Growth Media containing 100µg/ml streptomycin (Sigma-Aldrich, US).

1 24hrs after seeding virus containing individual sgRNA/Cas9 constructs were pooled and
2 transduced into cells at a high MOI of 10, ensuring that each cell is infected by several
3 lentivirus and increasing the likelihood of achieving KO. Transduction was performed in
4 media containing 8µg/ml Polybrene (Sigma, USA). Cells were cultured for 24hrs then treated
5 with Puromycin (1µg/ml) (Thermo Fisher Scientific, UK) for 3 days to select for transduced
6 cells. Cells then cultured without puromycin and expanded before cells were collected for
7 genotyping by Sanger sequencing, qRT-PCR, and functional assays. All data shown were
8 from cells expanded from these colonies. RAMP1 expression achieved through transduction
9 of virus containing RAMP1 MISSION TRC3 Open Reading Frame (ORF) plasmid (pLX_304)
10 (Sigma, US) into RAMP2 KO-HUVECs. HUVEC cells were seeded in 6 well plates at a cell
11 density of 160,000 cells/well and maintained at 37°C in 5% CO₂ with Complete Endothelial
12 Cell Growth Media containing 100µg/ml streptomycin (Sigma, US). 24hrs after seeding,
13 virus containing the ORF construct was transduced into cells in media containing 8µg/ml
14 Polybrene. Cells were cultured for 24hrs then treated with blasticidin (5µg/ml) (Thermo
15 Fisher Scientific, UK) for 6 days to select for transduced cells. Cells were collected for
16 genotyping by qRT-PCR and expanded for functional assays. All 'HUVEC RAMP1' data
17 shown were from cells expanded from these colonies.

18

19 *Immunofluorescence*

20 HUVEC cells were seeded in Cell Carrier Ultra 96 well plate (Perkinelmer, Boston, MA, US)
21 at a cell density of 160,000 cells/well and maintained at 37°C in 5% CO₂ with Complete
22 Endothelial Cell Growth Media containing 100µg/ml streptomycin. Cells were washed twice
23 with PBS, fixed with 4% paraformaldehyde (PFA) in PBS (10 mins, RT) then washed three
24 times with PBS. The cells were permeabilized with 0.05% Tween 20 in PBS (60 mins, RT),
25 and then incubated with 10% goat serum in PBS (60mins, RT). The cells were then
26 incubated in primary antibody for cas9 protein (Cell signalling technology, MA, US) 7A9-
27 3A3, diluted 1/700 in PBS/0.05% Tween/3% BSA) at 4°C, overnight and protected from light.
28 The cells were washed three times with PBS and incubated with AlexaFluor 488 goat anti-
29 mouse (Invitrogen A11001, 1/500) (1hr, RT) protected from light. Cells were washed three
30 times with PBS, then nuclei were stained with Hoechst (Invitrogen) (1/2000 in PBS, 10mins,
31 RT). Cells were then washed three times with PBS w/o Mg²⁺ or Ca²⁺; and imaged at 20x
32 magnification (Cell Voyager 7000S, Yokogawa).

33

34 *Sequencing of genomic loci*

35 Genomic DNA was extracted from virally transduced HUVEC cells by: collecting
36 approximately 10,000 cells, washing in PBS (sigma-Aldrich, US) and then lysing with
37 DirectPCR Lysis Reagent (Viagen Biotech, US) containing Proteinase K (Qiagen, Germany)
38 at 0.4mg/ml. The lysate was incubated at 55°C for 4 hrs; 85°C, for 10mins; 12°C for 12hrs.
39 PCR reaction was then set up in (20µl) as follows: 2x Flash Phusion PCR Master Mix
40 (Thermo Fisher, US) (20µl), forward primer (5'- AATTCGGGGAGCGATCCTG -3')
41 (Eurogentec, Belgium) (1µl)(10µm), reverse primer (5'- GAGACCCTCCGAAAATAGGC -3')
42 (Eurogentec, Belgium) (1µl)(10µm), DNA (100ng/µl)(1µl), ddH₂O (7µl). The product was
43 amplified by PCR using the following program: 98°C, 1min; 35x (98°C, 10secs; 55°C,
44 10secs; 72°C, 15secs), 72°C, 1min; 4°C, hold. PCR clean-up was performed prior to
45 sequencing using the Illustra GFX PCR DNA and Gel-band Purification Kit (Illustra,

1 Germany) according to manufacturer's instructions. Editing of RAMP2 gene was confirmed
2 by Sanger sequencing (Eurofins) and TIDE analysis³⁰.

3
4 *Quantitative real-time reverse transcription polymerase chain reaction (qRT-PCR)*
5 HUVECs were cultured as above in Complete Endothelial Cell Growth medium and plated
6 in a 24 well plate at 100,000 cells/well. Media was then removed, and cells were washed in
7 PBS (Sigma, UK). RNA was extracted and genomic DNA eliminated using an RNA
8 extraction kit (QIAGEN, Germany) as per manufacturer's instructions. The yield and quality
9 of RNA was assessed by measuring absorbance at 260 and 280 nm (Nanodrop ND-1000
10 Spectrophotometer, NanoDrop technologies LLC, Wilmington DE USA). RNA was used
11 immediately for the preparation of cDNA using the Multiscribe reverse transcriptase. For the
12 preparation of cDNA 100ng of RNA was reverse transcribed using Taq-man reverse
13 transcription kit (Life Technology, MA, USA) according to manufacturer's instructions.
14 Reactions were performed on a thermal Cycler as following: 25°C, 10mins; 48°C, 30mins;
15 95°C, 5mins. cDNA was stored at -20°C.

16
17 For each independent sample, qPCR was performed using TaqMan Gene Expression
18 assays according to manufacturer's instructions (Life Technologies, MA, USA) for GAPDH
19 (Hs02786624_g1), CALCR (Hs01016882_m1), CALCRL (Hs00907738_m1), RAMP1
20 (Hs00195288_m1), RAMP2 (Hs01006937_g1), RAMP3 (Hs00389131_m1) and plated onto
21 fast microAmp plates containing 2µl cDNA, 1µl Taq-man probe, 10µl Taq-man fast universal
22 master mix (Applied Biosystems) and 10µl ddH₂O. PCR reactions were performed on ABI
23 7900 HT real time PCR system (Thermo Fisher Scientific, UK). The program involved the
24 following stages: 50°C, 2 mins; 95 °C, 10mins, the fluorescence detection over the course
25 of 40x (95°C, 15secs; 60°C, 1min). Data are expressed as relative expression of the gene
26 of interest to the reference gene GAPDH where: Relative expression = $2^{-((Cq \text{ of gene of interest}) - (Cq \text{ of GAPDH}))}$. For the genes where no mRNA was detected these samples
27 are omitted from graphs and labelled accordingly, as indicated in the figure legends.

28
29
30 *In vivo assays*

31 *Measurement of intracellular cAMP*

32 All primary cell lines were cultured as above. On the day of the experiment media was
33 removed and cells washed with PBS, before being dissociated with Trypsin-EDTA 0.05%
34 (Gibco, UK) and then resuspended in PBS/BSA (0.1%) (Sigma, UK). Cells were
35 immediately plated for use in cAMP assay as per manufacturer's instructions and as
36 described previously²¹, reagents used were provided by the LANCE® cAMP detection assay
37 kit (PerkinElmer, Boston, MA, USA), in 384 well optiplates (PerkinElmer (Boston, MA, USA))
38 at 2000 cells/well in 5µl aliquots. Human αCGRP, hAM and hAM2 (Bachem, Switzerland)
39 were diluted in PBS/BSA (0.1%) with 250µM IBMX (Sigma, UK), and used from 10pM to
40 10µM. Cells were incubated with compound for 30mins prior to adding detection buffer as
41 described previously^{28,57}. Plates were incubated for a further 60 mins (RT) and then read on
42 a plate reader (Mithras LB 940 microplate reader (Berthold technologies, Germany)). All
43 responses were normalised to 100µM forskolin (Tocris, UK). Antagonist studies were
44 performed in the same way through co-stimulation of the relevant concentration. Alongside

1 control treated cell. Experiments with PTX (Sigma, UK) required pretreatment (16hrs) prior
2 to assays

3

4 *Measurement of Phospho-ERK_{1/2} (Thr202/Tyr204)*

5 Primary cells were grown to in 6 well plates, on the day of the experiment media was
6 replaced with serum free media 4hrs prior to cell harvesting. Trypsin-EDTA was used to
7 dissociate the cells and they are spun down, counted and re-suspended HBSS/BSA (0.1%).
8 Ligands were also diluted in HBSS/BSA. Cells were then plated on 384 well plates in 8 μ l
9 aliquots at a density of 20,000 cells/well. Next, ligands were added (4 μ l) for 5min stimulation
10 at room temperature. Cells were then lysed as per to manufacturer's instructions with 4 μ l of
11 lysis buffer (Cisbio phospho-ERK_{1/2} cellular assay kit, Invitrogen, UK) for 30mins shaking
12 at room temperature. The 2 specific antibodies; were pre-mixed in a 1:1 ratio. 4 μ l of this was
13 added to each well and the plate incubated for a further 2hrs. Then fluorescence emissions
14 were read at 665nm and 620nm using a Mithras LB940 microplate reader. Antagonist
15 studies were performed in the same way through co-stimulation with PTX, Rp-8-Br-cAMPS,
16 YM-254890, or ESI-09 as appropriate alongside control treated cell.

17

18

19 *Measurement of Intracellular Calcium mobilisation*

20 All cell lines were plated at 20,000 cells/well on 96 well black clear-bottom plates (Costar,
21 UK) 24hrs before the experiment. Media was removed, and cells were washed with Hank's
22 Balance Salt Solution (HBSS) (Lonza, Switzerland) before cells were loaded with 10 μ M
23 Fluo-4/AM (Invitrogen, US) in the dark at room temperature for 30mins. Cells were then
24 washed twice with calcium-free HBSS, then were left in 100 μ l calcium-free HBSS for the
25 duration of the assay. In conditions where G $\alpha_{q/11/14}$ signalling is inhibited, cells were pre-
26 treated with 100nM YM-254890 (Alpha Laboratories, UK) (30mins)²². All assays were
27 performed using the BD Pathway 855 Bioimaging Systems (BD Biosciences, UK), which
28 dispenses ligands (20 μ l) and reads immediately for 2mins. Data was normalised to the
29 response seen with 10 μ M Ionomycin.

30

31 *Measurement of Cell Proliferation*

32 Both endothelial cell lines and HCMs were seeded at a density of 2500 cells/well in a clear
33 flat bottom 96-well plate (Corning, UK) and incubated at 37°C in 5% CO₂. After 24 hrs, cells
34 were exposed to test compounds or vehicle, in complete endothelial cell growth media
35 (HUVECs) or myocyte growth media (HCMs). Cells were incubated for a further 72hrs at
36 37°C in 5% CO₂. After 72 hrs incubation, 5 μ l of Cell Counting Kit – 8 (CCK-8, Sigma, UK)
37 was added to each well and cells were then incubated for another 2 hrs at 37°C in 5% CO₂
38 and in the dark. The absorbance of each well was measured using a Mithras LB940
39 microplate reader with an excitation of 450 nm. The absorbance is directly proportional to
40 the number of viable cells. Cell proliferation was calculated as a percentage of number of
41 cells treated with vehicle alone.

42

43 *Measurement of Nitric Oxide Production*

44 Endothelial cells and HCMs were cultured as above. 24 hours prior to assay cells were
45 plated on Costar 96 well black clear bottom plates at 40,000 cells/well. The assay was

1 performed according to manufacturer's protocol. Briefly; cells pre-incubated with NO dye
2 and assay buffer 1 (Fluorometric Nitric Oxide Assay Kit, Abcam, UK) for 30mins at 37°C in
3 5% CO₂. Any inhibitors requiring 30mins pre-treatment (YM/L-NAME/DMSO control) were
4 added at this point. Ligand stimulation occurred immediately after this for 15 mins at 37°C
5 C in 5% CO₂. Stain and ligand solution were removed, assay buffer II was added, and wells
6 were read immediately. The absorbance was measured using a Mithras LB940 microplate
7 reader with an excitation/emission of 540/590 nm. Endothelial cell responses were
8 normalised to 10µM acetylcholine⁵⁸. HCM responses were normalised to 10µM
9 isoproterenol^{59,60}.

10

11 **Statistical analysis**

12 Data analysis for cAMP accumulation, Ca²⁺_i mobilisation, NO accumulation, pERK_{1/2}
13 activation and cell proliferation assays were performed in GraphPad Prism 8.4 (GraphPad
14 Software, San Diego). Data were fitted to obtain concentration–response curves using either
15 the three-parameter logistic equation using to obtain values of E_{max} and pEC₅₀ or the
16 operational model of agonism²⁷. Statistical differences were analysed using one-way
17 ANOVA followed by Dunnett's *post-hoc* (for comparisons amongst more than two groups)
18 or unpaired Student's t test with Welch's correction (for comparison between two groups).
19 To account for the day-to-day variation experienced from the cultured cells, we used the
20 maximal level of cAMP accumulation from cells in response to 100µM forskolin stimulation
21 was used as a reference, 10µM ionomycin for Ca²⁺_i assays, 10µM phorbol 12-myristate 13-
22 acetate (PMA) for pERK_{1/2} activation, 10µM acetylcholine for NO production and 10µM
23 VEGF for cell proliferation. E_{max} values from these curves are reported as a percentage of
24 these controls, and all statistical analysis has been performed on these data. Where
25 appropriate the operational model for receptor agonism²⁷ was used to obtain efficacy (τ) and
26 equilibrium disassociation constant (K_A) values. In both cases, this normalization removes
27 the variation due to differences in days but retains the variance for control values. The
28 means of individual experiments were combined to generate the curves shown. Having
29 obtain values for τ and K_A these were then used to quantify signalling bias as the change in
30 Log(τ/K_A) as described previously^{18;24}. Error for this composite measure was propagated by
31 applying the following equation.

32

33

$$Pooled\ SEM = \sqrt{(SEM_A)^2 + (SEM_B)^2}$$

34

35 Where, SEM_A and SEM_B are the standard error of measurement A and B.

36 Correlations between pEC₅₀ values or transducer coefficients Log (τ/K_A) were assessed by
37 scatter plot and Pearson's correlation coefficient (*r*) was calculated with 95% confidence
38 interval.

39

40

41 **Acknowledgements**

42 This work was supported by the Biotechnology and Biological Sciences Research Council
43 [grant number BB/M000176/2] awarded to GL and DRP and the Endowment Fund for
44 education from Ministry of Finance Republic of Indonesia (DS). AJC is funded through an
45 AstraZeneca Scholarship.

1

2

3 **Declarations of interest**

4 MW, NM and DG are employees of, and shareholders in, AstraZeneca. The remaining
5 authors have no competing interests.

6

7

8

9

9 **References**

- 10 1 Smith, J. S., Lefkowitz, R. J. & Rajagopal, S. Biased signalling: from simple
11 switches to allosteric microprocessors. *Nat Rev Drug Discov* **17**, 243-260,
12 doi:10.1038/nrd.2017.229 (2018).
- 13 2 Wootten, D., Christopoulos, A., Marti-Solano, M., Babu, M. M. & Sexton, P. M.
14 Mechanisms of signalling and biased agonism in G protein-coupled receptors. *Nat*
15 *Rev Mol Cell Biol* **19**, 638-653, doi:10.1038/s41580-018-0049-3 (2018).
- 16 3 Davenport, A. P., Scully, C. C. G., de Graaf, C., Brown, A. J. H. & Maguire, J. J.
17 Advances in therapeutic peptides targeting G protein-coupled receptors. *Nat Rev*
18 *Drug Discov* **19**, 389-413, doi:10.1038/s41573-020-0062-z (2020).
- 19 4 Kliewer, A. et al. Morphine-induced respiratory depression is independent of beta-
20 arrestin2 signalling. *Br J Pharmacol* **177**, 2923-2931, doi:10.1111/bph.15004
21 (2020).
- 22 5 Russell, F. A., King, R., Smillie, S. J., Kodji, X. & Brain, S. D. Calcitonin gene-
23 related peptide: physiology and pathophysiology. *Physiol Rev* **94**, 1099-1142,
24 doi:10.1152/physrev.00034.2013 (2014).
- 25 6 Kato, J. & Kitamura, K. Bench-to-bedside pharmacology of adrenomedullin. *Eur J*
26 *Pharmacol* **764**, 140-148, doi:10.1016/j.ejphar.2015.06.061 (2015).
- 27 7 Tsuruda, T., Kato, J., Kuwasako, K. & Kitamura, K. Adrenomedullin: Continuing
28 to explore cardioprotection. *Peptides* **111**, 47-54,
29 doi:10.1016/j.peptides.2018.03.012 (2019).
- 30 8 Tanaka, M. et al. The endothelial adrenomedullin-RAMP2 system regulates
31 vascular integrity and suppresses tumour metastasis. *Cardiovasc Res* **111**, 398-
32 409, doi:10.1093/cvr/cvw166 (2016).
- 33 9 Morimoto, R. et al. Expression of adrenomedullin2/intermedin in human brain,
34 heart, and kidney. *Peptides* **28**, 1095-1103, doi:10.1016/j.peptides.2007.01.018
35 (2007).
- 36 10 Takei, Y. et al. Identification of novel adrenomedullin in mammals: a potent
37 cardiovascular and renal regulator. *FEBS Lett* **556**, 53-58, doi:10.1016/s0014-
38 5793(03)01368-1 (2004).
- 39 11 Zhang, S. Y., Xu, M. J. & Wang, X. Adrenomedullin 2/intermedin: a putative drug
40 candidate for treatment of cardiometabolic diseases. *Br J Pharmacol* **175**, 1230-
41 1240, doi:10.1111/bph.13814 (2018).
- 42 12 Garelja, M. L. et al. Molecular Mechanisms of Class B GPCR Activation: Insights
43 from Adrenomedullin Receptors. *ACS Pharmacol Transl Sci* **3**, 246-262,
44 doi:10.1021/acsptsci.9b00083 (2020).
- 45 13 Hilaiet, S. et al. Agonist-promoted internalization of a ternary complex between
46 calcitonin receptor-like receptor, receptor activity-modifying protein 1 (RAMP1),
47 and beta-arrestin. *J Biol Chem* **276**, 42182-42190, doi:10.1074/jbc.M107323200
48 (2001).
- 49 14 Kuwasako, K. et al. Visualization of the calcitonin receptor-like receptor and its
50 receptor activity-modifying proteins during internalization and recycling. *J Biol*
51 *Chem* **275**, 29602-29609, doi:10.1074/jbc.M004534200 (2000).

16

- 1 15 Heroux, M., Breton, B., Hogue, M. & Bouvier, M. Assembly and signaling of CRLR
2 and RAMP1 complexes assessed by BRET. *Biochemistry* **46**, 7022-7033,
3 doi:10.1021/bi0622470 (2007).
- 4 16 Hendrikse, E. R. et al. Identification of Small-Molecule Positive Modulators of
5 Calcitonin-like Receptor-Based Receptors. *ACS Pharmacol Transl Sci* **3**, 305-
6 320, doi:10.1021/acsptsci.9b00108 (2020).
- 7 17 Shenoy, S. K. et al. beta-arrestin-dependent, G protein-independent ERK1/2
8 activation by the beta2 adrenergic receptor. *J Biol Chem* **281**, 1261-1273,
9 doi:10.1074/jbc.M506576200 (2006).
- 10 18 McLatchie, L. M. et al. RAMPs regulate the transport and ligand specificity of the
11 calcitonin-receptor-like receptor. *Nature* **393**, 333-339, doi:10.1038/30666 (1998).
- 12 19 Klein, K. R., Matson, B. C. & Caron, K. M. The expanding repertoire of receptor
13 activity modifying protein (RAMP) function. *Crit Rev Biochem Mol Biol* **51**, 65-71,
14 doi:10.3109/10409238.2015.1128875 (2016).
- 15 20 Woolley, M. J. et al. Receptor activity-modifying protein dependent and
16 independent activation mechanisms in the coupling of calcitonin gene-related
17 peptide and adrenomedullin receptors to Gs. *Biochem Pharmacol* **142**, 96-110,
18 doi:10.1016/j.bcp.2017.07.005 (2017).
- 19 21 Weston, C. et al. Receptor Activity-modifying Protein-directed G Protein Signaling
20 Specificity for the Calcitonin Gene-related Peptide Family of Receptors. *J Biol*
21 *Chem* **291**, 21925-21944, doi:10.1074/jbc.M116.751362 (2016).
- 22 22 Hay, D. L., Garelja, M. L., Poyner, D. R. & Walker, C. S. Update on the
23 pharmacology of calcitonin/CGRP family of peptides: IUPHAR Review 25. *Br J*
24 *Pharmacol* **175**, 3-17, doi:10.1111/bph.14075 (2018).
- 25 23 Walker, C. S. et al. A second trigeminal CGRP receptor: function and expression
26 of the AMY1 receptor. *Ann Clin Transl Neurol* **2**, 595-608, doi:10.1002/acn3.197
27 (2015).
- 28 24 Takasaki, J. et al. A novel Galphaq/11-selective inhibitor. *J Biol Chem* **279**, 47438-
29 47445, doi:10.1074/jbc.M408846200 (2004).
- 30 25 Ueda, K. et al. Adrenomedullin causes coronary vasodilation in humans: effects
31 of inhibition of nitric oxide synthesis. *J Cardiovasc Pharmacol* **46**, 534-539,
32 doi:10.1097/01.fjc.0000179156.51985.db (2005).
- 33 26 Farah, C., Michel, L. Y. M. & Balligand, J. L. Nitric oxide signalling in
34 cardiovascular health and disease. *Nat Rev Cardiol* **15**, 292-316,
35 doi:10.1038/nrcardio.2017.224 (2018).
- 36 27 Black, J. W. & Leff, P. Operational models of pharmacological agonism. *Proc R*
37 *Soc Lond B Biol Sci* **220**, 141-162, doi:10.1098/rspb.1983.0093 (1983).
- 38 28 Weston, C. et al. Modulation of Glucagon Receptor Pharmacology by Receptor
39 Activity-modifying Protein-2 (RAMP2). *J Biol Chem* **290**, 23009-23022,
40 doi:10.1074/jbc.M114.624601 (2015).
- 41 29 Kuwasako, K., Kitamura, K., Nagata, S., Hikosaka, T. & Kato, J. Function of the
42 cytoplasmic tail of human calcitonin receptor-like receptor in complex with
43 receptor activity-modifying protein 2. *Biochem Biophys Res Commun* **392**, 380-
44 385, doi:10.1016/j.bbrc.2010.01.030 (2010).
- 45 30 Brinkman, E. K. et al. Easy quantification of template-directed CRISPR/Cas9
46 editing. *Nucleic Acids Res* **46**, e58, doi:10.1093/nar/gky164 (2018).
- 47 31 Sexton, P. M., Poyner, D. R., Simms, J., Christopoulos, A. & Hay, D. L. RAMPs
48 as drug targets. *Adv Exp Med Biol* **744**, 61-74, doi:10.1007/978-1-4614-2364-5_6
49 (2012).
- 50 32 Alexander, S. P. H. et al. THE CONCISE GUIDE TO PHARMACOLOGY 2019/20:
51 G protein-coupled receptors. *Br J Pharmacol* **176** Suppl 1, S21-S141,
52 doi:10.1111/bph.14748 (2019).

- 1 33 Walker, C. S. et al. Regulation of signal transduction by calcitonin gene-related
2 peptide receptors. *Trends Pharmacol Sci.* **31**:476-83, doi:
3 10.1016/j.tips.2010.06.006 (2010).
- 4 34 Ma, F. et al. Adrenomedullin Inhibits Osmotic Water Permeability in Rat Inner
5 Medullary Collecting Ducts. *Cells* **24**:E2533, doi: 10.3390/cells9122533 (2020).
- 6 35 Yarwood, R. E. et al. Endosomal signaling of the receptor for calcitonin gene-
7 related peptide mediates pain transmission *Proc Natl Acad Sci U S A.* **114**:12309-
8 12314, doi: 10.1073/pnas.1706656114 (2017).
- 9 36 Yoon, S. P. & Kim, J. Exogenous CGRP upregulates profibrogenic growth factors
10 through PKC/JNK signaling pathway in kidney proximal tubular cells *Cell Biol*
11 *Toxicol.* **34**:251-262, doi: 10.1007/s10565-017-9399-4 (2018).
- 12 37 Temmesfeld-Wollbrück, B., Hocke, A. C., Suttorp, N. & Hippenstiel, S.
13 Adrenomedullin and endothelial barrier function. *Thromb Haemost* **98**, 944-951,
14 doi:10.1160/th07-02-0128 (2007).
- 15 38 Hocke, A. C. et al. Perturbation of endothelial junction proteins by *Staphylococcus*
16 *aureus* alpha-toxin: inhibition of endothelial gap formation by adrenomedullin.
17 *Histochem Cell Biol* **126**, 305-316, doi:10.1007/s00418-006-0174-5 (2006).
- 18 39 De Matteo, R. & May, C. N. Direct coronary vasodilator action of adrenomedullin
19 is mediated by nitric oxide. *Br J Pharmacol* **140**, 1414-1420,
20 doi:10.1038/sj.bjp.0705572 (2003).
- 21 40 Chang, L. & Karin, M. Mammalian MAP kinase signalling cascades. *Nature* **410**,
22 37-40, doi:10.1038/35065000 (2001).
- 23 41 Pagès, G. et al. Mitogen-activated protein kinases p42mapk and p44mapk are
24 required for fibroblast proliferation. *Proc Natl Acad Sci U S A* **90**, 8319-8323,
25 doi:10.1073/pnas.90.18.8319 (1993).
- 26 42 Lefloch, R., Pouyssegur, J. & Lenormand, P. Total ERK1/2 activity regulates cell
27 proliferation. *Cell Cycle* **8**, 705-711, doi:10.4161/cc.8.5.7734 (2009).
- 28 43 Srinivasan, R. et al. Erk1 and Erk2 regulate endothelial cell proliferation and
29 migration during mouse embryonic angiogenesis. *PLoS One* **4**, e8283,
30 doi:10.1371/journal.pone.0008283 (2009).
- 31 44 Pintucci, G. et al. Lack of ERK activation and cell migration in FGF-2-deficient
32 endothelial cells. *FASEB J* **16**, 598-600, doi:10.1096/fj.01-0815fje (2002).
- 33 45 Mavria, G. et al. ERK-MAPK signaling opposes Rho-kinase to promote
34 endothelial cell survival and sprouting during angiogenesis. *Cancer Cell* **9**, 33-44,
35 doi:10.1016/j.ccr.2005.12.021 (2006).
- 36 46 Ando, K., Pegram, B. L. & Frohlich, E. D. Hemodynamic effects of calcitonin gene-
37 related peptide in spontaneously hypertensive rats. *Am J Physiol* **258**, R425-429,
38 doi:10.1152/ajpregu.1990.258.2.R425 (1990).
- 39 47 Gardiner, S. M. et al. Antagonistic effect of human alpha-calcitonin gene-related
40 peptide (8-37) on regional hemodynamic actions of rat islet amyloid polypeptide
41 in conscious Long-Evans rats. *Diabetes* **40**, 948-951, doi: 10.2337/diab.40.8.948
42 (1991).
- 43 48 Krzeminski, K. The Role of Adrenomedullin in Cardiovascular Response to
44 Exercise - A Review. *J Hum Kinet* **53**, 127-142, doi:10.1515/hukin-2016-0017
45 (2016).
- 46 49 Ihara, T., Ikeda, U., Tate, Y., Ishibashi, S. & Shimada, K. Positive inotropic effects
47 of adrenomedullin on rat papillary muscle. *Eur J Pharmacol* **390**, 167-172,
48 doi:10.1016/s0014-2999(00)00011-x (2000).
- 49 50 Perret, M. et al. The effect of adrenomedullin on the isolated heart. *Life Sci* **53**,
50 PL377-379, doi:10.1016/0024-3205(93)90213-m (1993).

- 1 51 Mukherjee, R. et al. Effects of adrenomedullin on human myocyte contractile
2 function and beta-adrenergic response. *J Cardiovasc Pharmacol Ther* **7**, 235-240,
3 doi:10.1177/107424840200700406 (2002).
- 4 52 Voors, A. A. et al. Adrenomedullin in heart failure: pathophysiology and
5 therapeutic application. *Eur J Heart Fail* **21**, 163-171, doi:10.1002/ejhf.1366
6 (2019).
- 7 53 Kataoka, Y. et al. The first clinical pilot study of intravenous adrenomedullin
8 administration in patients with acute myocardial infarction. *J Cardiovasc*
9 *Pharmacol* **56**, 413-419, doi:10.1097/FJC.0b013e3181f15b45 (2010).
- 10 54 Dong, F., Taylor, M. M., Samson, W. K. & Ren, J. Intermedin (adrenomedullin-2)
11 enhances cardiac contractile function via a protein kinase C- and protein kinase
12 A-dependent pathway in murine ventricular myocytes. *J Appl Physiol* **101**, 778-
13 784, doi:10.1152/jappphysiol.01631.2005 (2006).
- 14 55 Roehrkasse, A. M., Warner, M. L., Booe, J. M. & Pioszak, A. A. Biochemical
15 characterization of G protein coupling to calcitonin gene-related peptide and
16 adrenomedullin receptors using a native PAGE assay. *J Biol Chem* **295**: 9736-
17 9751, doi: 10.1074/jbc.RA120.013854 (2020).
- 18 56 Ran, F. A. et al. Genome engineering using the CRISPR-Cas9 system. *Nat Protoc*
19 **8**, 2281-2308, doi:10.1038/nprot.2013.143 (2013).
- 20 57 Knight, A. et al. Discovery of Novel Adenosine Receptor Agonists That Exhibit
21 Subtype Selectivity. *J Med Chem* **59**:947-964, doi:
22 10.1021/acs.jmedchem.5b01402 (2016).
- 23 58 Holton, M. et al. Endothelial nitric oxide synthase activity is inhibited by the plasma
24 membrane calcium ATPase in human endothelial cells. *Cardiovasc Res* **87**, 440-
25 448, doi:10.1093/cvr/cvq077 (2010).
- 26 59 Vaniotis, G. et al. Regulation of cardiac nitric oxide signaling by nuclear β -
27 adrenergic and endothelin receptors. *J Mol Cell Cardiol* **62**, 58-68,
28 doi:10.1016/j.yjmcc.2013.05.003 (2013).
- 29 60 Gauthier, C. et al. The negative inotropic effect of beta3-adrenoceptor stimulation
30 is mediated by activation of a nitric oxide synthase pathway in human ventricle. *J*
31 *Clin Invest* **102**, 1377-1384, doi:10.1172/JCI2191 (1998).

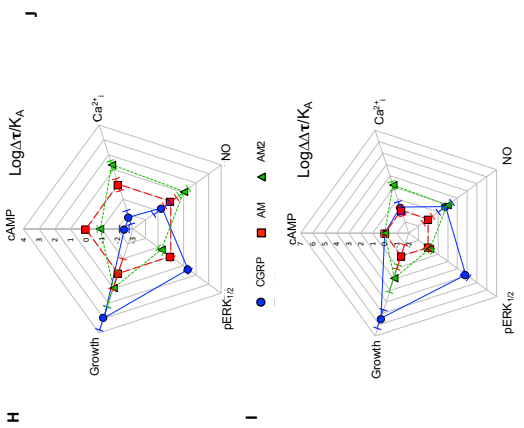
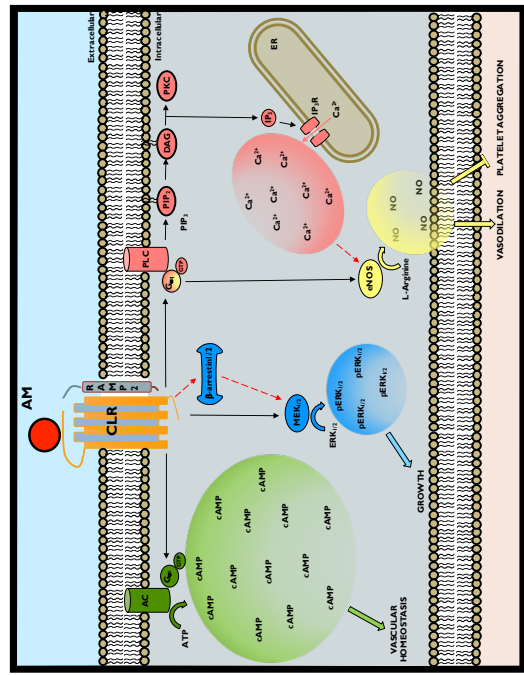
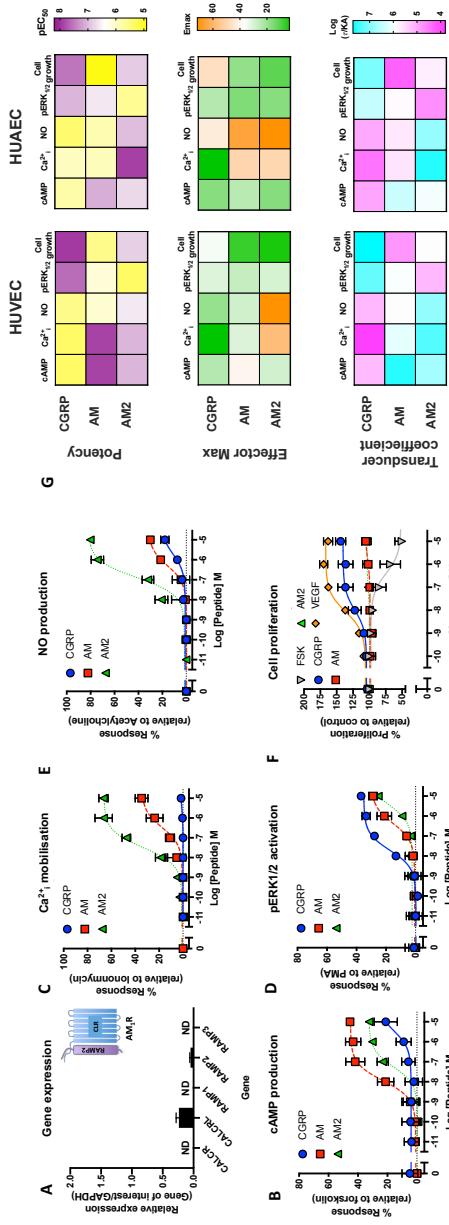


Figure 1. CGRP family peptide signalling bias in HUVECs. **A)** Expression of CALCR, CALCRL, RAMP1, RAMP2, and RAMP3 genes in HUVECs. Data represent mean \pm SEM of three independent experiments relative to GAPDH expression. ND = not detected in all three samples. **B-F)** Dose-response curves were constructed for HUVECs stimulated with CGRP, AM or AM2 and the cAMP levels quantified relative to forskolin (100 μ M) (**B**), mobilisation of Ca²⁺_i relative to ionomycin (10 μ M) (**C**), intracellular ERK_{1/2} phosphorylation relative to PMA (10 μ M) (**D**), total nitric oxide production relative to acetylcholine (10 μ M) (**E**), and extent of cell proliferation (after 72 hours) relative to vector treated control and VEGF (**F**). Data are analysed using a three-parameter non-linear regression curve or the operational model of receptor agonism²⁷. Data are analysed using a three-parameter non-linear regression curve. **G)** Heatmaps representing the signalling properties between HUVEC and HUAEC cells for potency, effector maximum and the transducer coefficient. **H-I)** Signalling bias plots were calculated as $\Delta\text{Log}(\tau/K_A)$ (**H**) or $\Delta\Delta\text{Log}(\tau/K_A)$ (**I**) for each agonist and for each signalling pathway. Determination of values requires normalisation to a reference agonist (AM) alone in **G**, while for **H** values were normalised to both a reference agonist (AM) and a reference pathway (cAMP). All data represent mean \pm SEM of at least 3-6 independent experiments. **J)** Representation of the signalling outcomes downstream of CLR-RAMP2 stimulated by adrenomedullin in a HUVEC. Including G proteins known to couple to CLR-RAMP2 and their signalling pathways as a result of AM mediated receptor activation. Solid arrows indicate known pathways. Dashed arrows represent possible pathways.

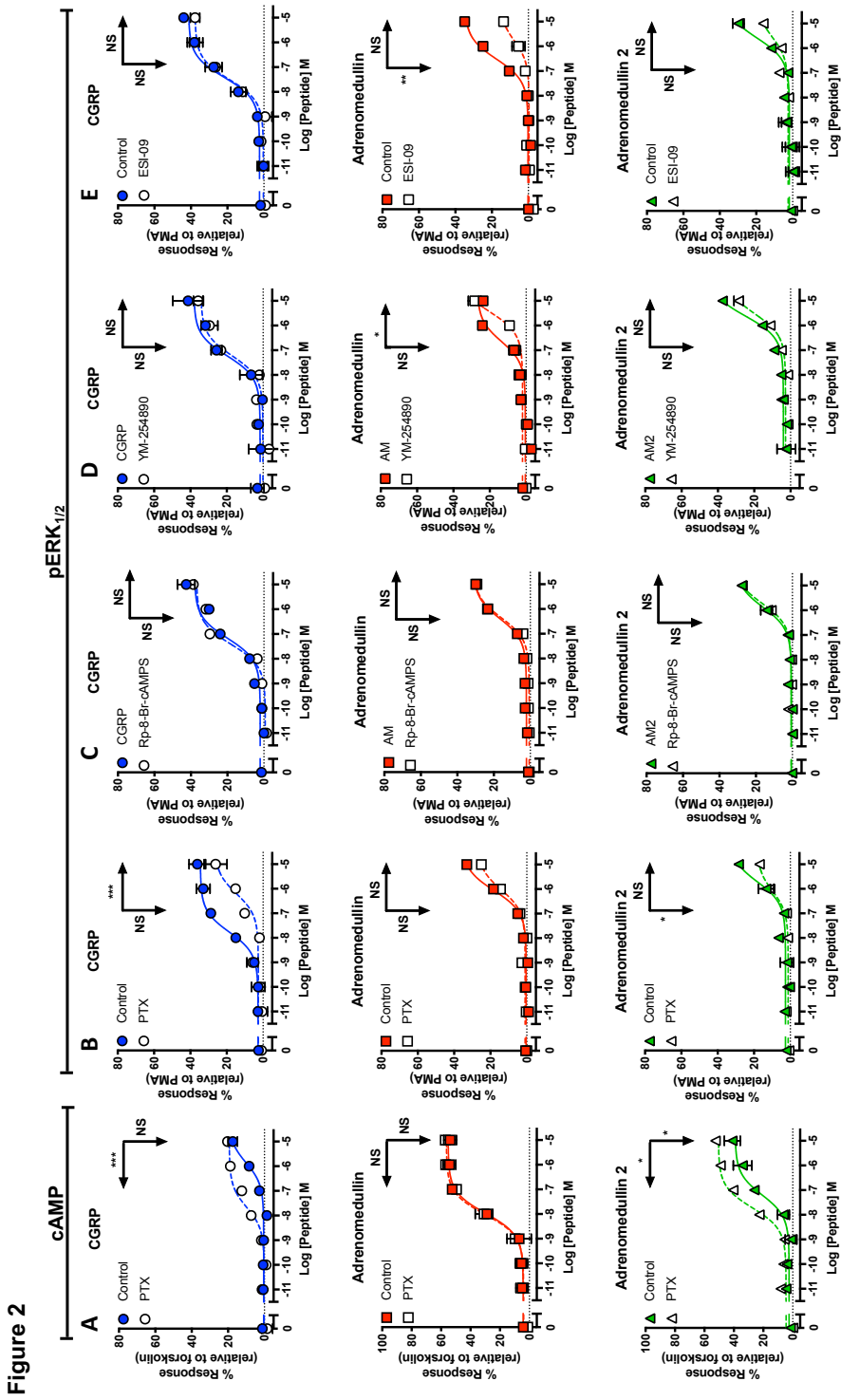


Figure 2. Non-cognate Gα couplings at the CLR-RAMP2 complex modulates cAMP accumulation and ERK_{1/2} phosphorylation. A) Characterisation of cAMP accumulation in response to stimulation by CGRP, AM and AM2 with and without PTX treatment relative to forskolin (100μM). **B-E)** Characterisation of ERK_{1/2} phosphorylation in response to stimulation by CGRP, AM and AM2 with and without PTX treatment relative to PMA (10μM) **(B)**, with/without YM-254890 relative to PMA (10μM) **(C)**, with/without Rp-8-Br-cAMPS (10 μM) **(D)**, and with/without ESI-09 **(E)**. Data are analysed using a three-parameter non-linear regression curve. All mean values ± SEM are calculated from 3-6 independent experiments. Statistical significance determined compared to control using an unpaired Student's t test with Welch's correction (*, p<0.05; **, p<0.01; ***, p<0.001; ****, p<0.0001). NS denotes no statistical significance observed. Rows show pEC₅₀, and vertical arrows show E_{max} statistical significance.

Figure 3

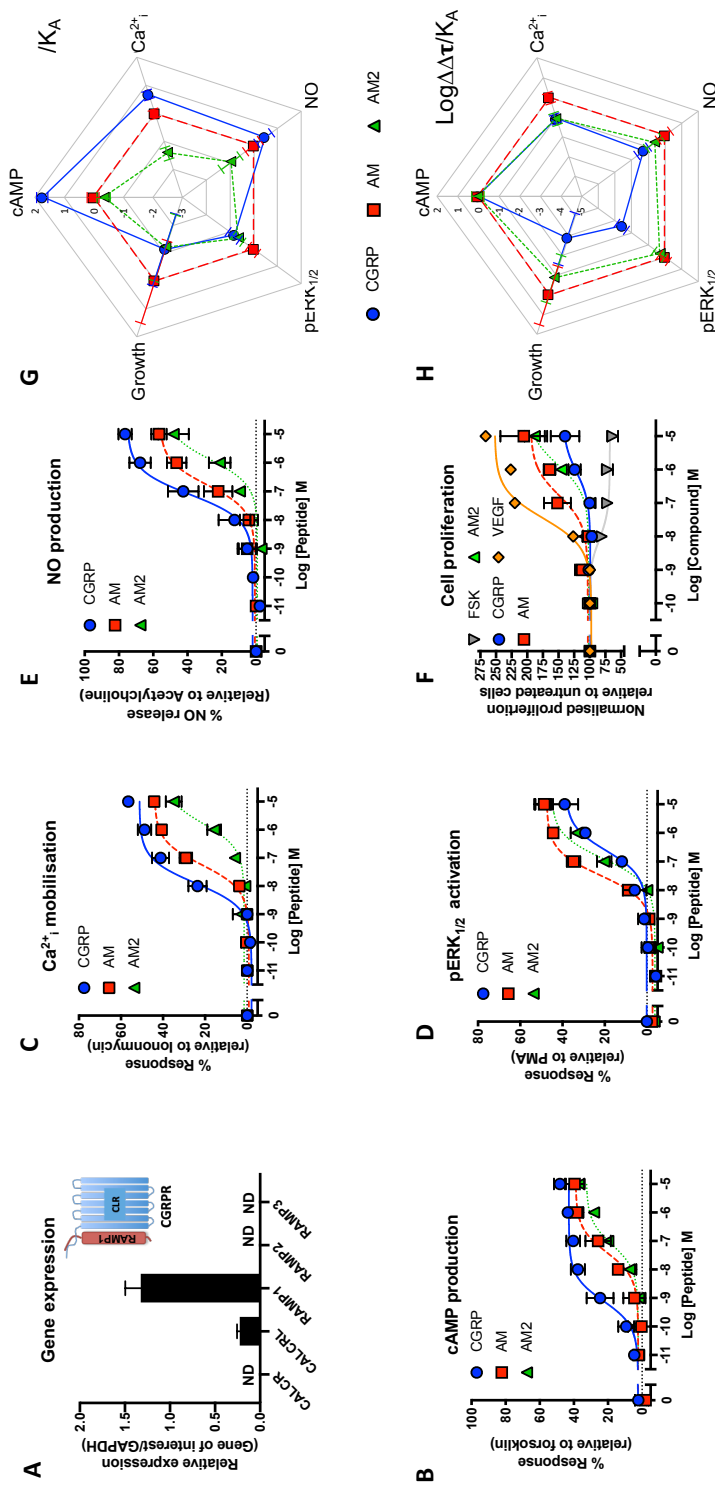


Figure 3. Switching RAMP expression in HUVECs produces unique signalling bias patterns for CGRP family of agonists. A) Expression of CALCR, CALCR, RAMP1, RAMP2, and RAMP3 genes in RAMP1 expressing HUVECs. Data represent mean + SEM of at least three independent experiments relative to GAPDH expression. ND = not detected in all three samples. **B-F)** Dose-response curves were constructed for RAMP1 expressing HUVECs stimulated with CGRP, AM or AM2 and the cAMP levels quantified relative to forskolin (100µM) (**B**), mobilisation of Ca²⁺_i relative to ionomycin (10µM) (**C**), intracellular ERK_{1/2} phosphorylation relative to PMA (10µM) (**D**), total

nitric oxide production relative to acetylcholine (10 μ M) (**E**), and extent of cell proliferation (after 72 hours) relative to vector treated control and VEGF (**F**) Data are analysed using a three-parameter non-linear regression curve or the operational model of receptor agonism²⁷. Data are analysed using a three-parameter non-linear regression curve. **G-H**) Signalling bias plots were calculated as $\Delta\text{Log}(\tau/K_A)$ (**G**) or $\Delta\Delta\text{Log}(\tau/K_A)$ (**H**) for each agonist and for each signalling pathway. Determination of values requires normalisation to a reference agonist (AM) alone in **G**, while for **H** values were normalised to both a reference agonist (AM) and a reference pathway (cAMP). All data represent mean \pm SEM of at least 3-6 independent experiments.

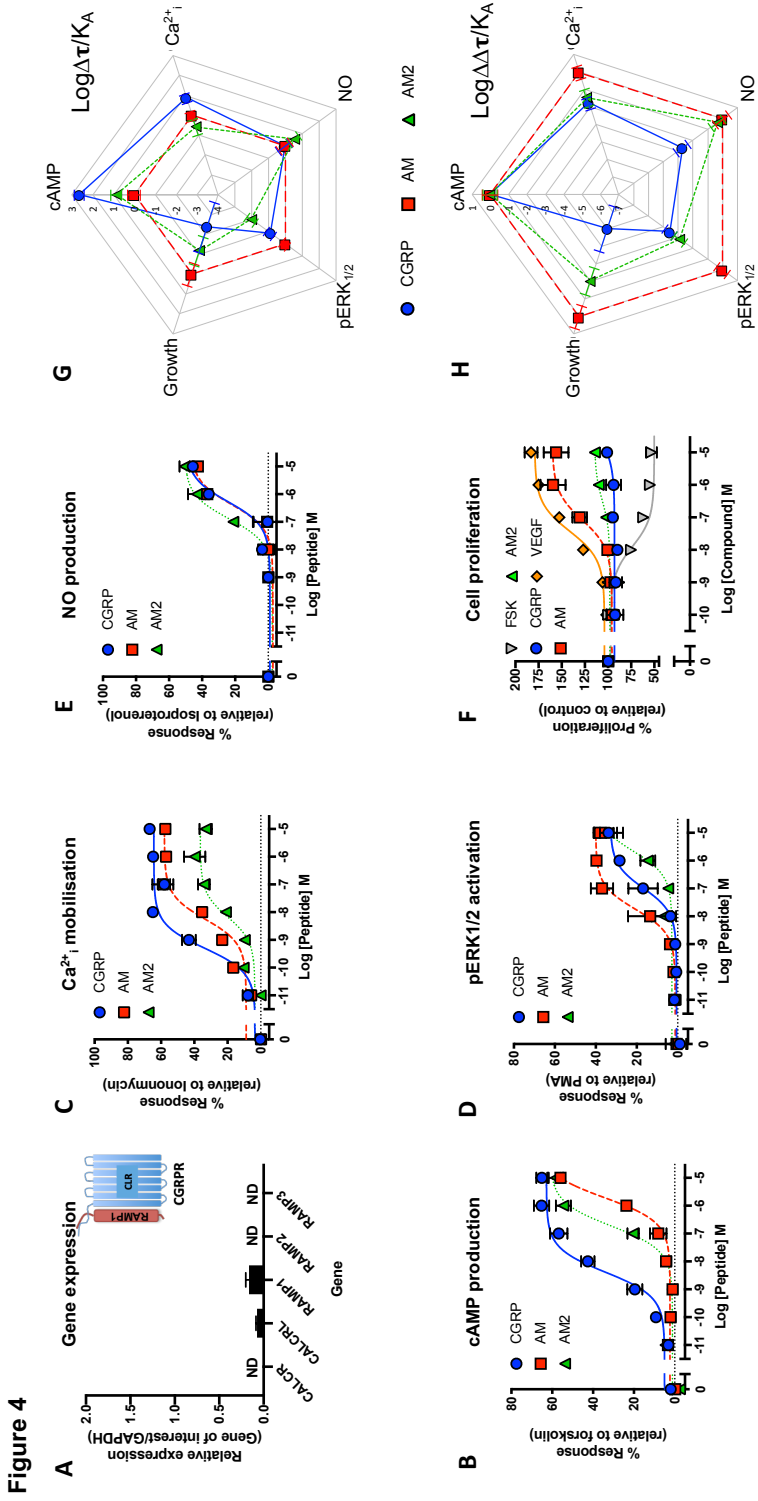


Figure 4. CGRP family peptide signalling bias in human cardiomyocytes. **A**) Expression of CALCR, CALCR_L, RAMP1, RAMP2, and RAMP3 genes in HCMs. Data represent mean ± SEM of three independent experiments relative to GAPDH expression. ND = not detected in all three samples. **B-F**) Dose-response curves were constructed for HCMs stimulated with CGRP, AM or AM2 and the cAMP levels quantified relative to forskolin (100μM) (**B**), mobilisation of Ca²⁺_i relative to ionomycin (10μM) (**C**), intracellular ERK_{1/2} phosphorylation relative to PMA (10μM) (**D**), total nitric oxide production relative to acetylcholine (10μM) (**E**) and extent of cell proliferation (after 72 hours) relative to vector treated control and VEGF (**F**) Data are analysed using a three-parameter non-linear regression curve or the operational

model of receptor agonism²⁷. Data are analysed using a three-parameter non-linear regression curve. **G-H** Signalling bias plots were calculated as $\Delta\text{Log}(\tau/K_A)$ (**G**) or $\Delta\Delta\text{Log}(\tau/K_A)$ (**H**) for each agonist and for each signalling pathway. Determination of values requires normalisation to a reference agonist (AM) alone in **G**, while for **H** values were normalised to both a reference agonist (AM) and a reference pathway (cAMP). All data represent mean \pm SEM of at least 3-6 independent experiments.

Figure 5

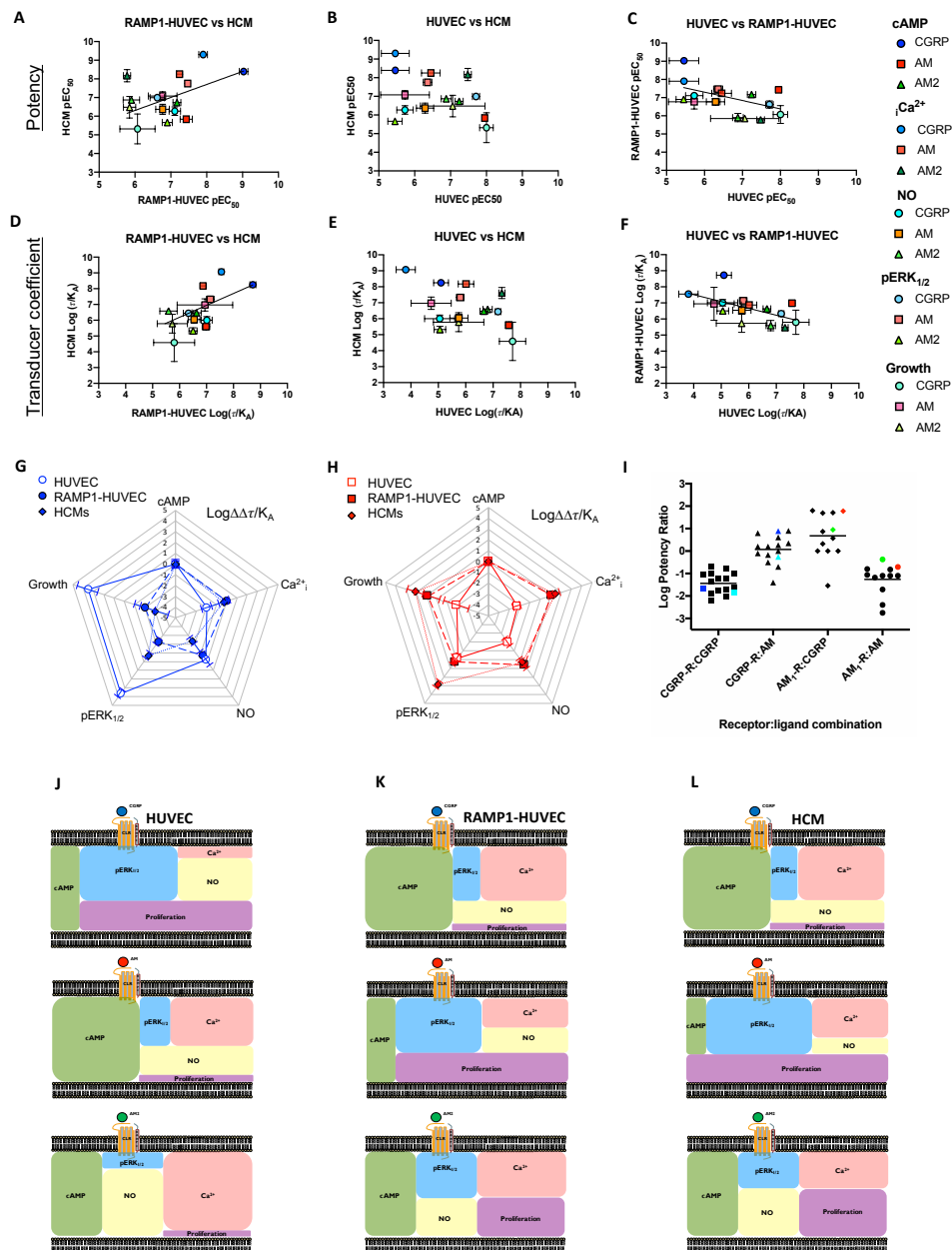


Figure 5. CGRP signalling bias in RAMP1 expressing HUVECs correlates with that in human cardiomyocytes. A-C) the correlation of Log agonist potencies \pm SEM for CGRP, AM and AM2 stimulated cAMP accumulation, mobilisation of Ca²⁺_i, NO production, intracellular ERK_{1/2} phosphorylation and cell proliferation in RAMP1 expressing HUVECs

and HCMs (**A**), HUVECs and HCMs (**B**) and HUVECs and RAMP1 expressing HUVECs (**C**) was analysed by a scatter plot and Pearson's correlation coefficients (r) were calculated. A significant positive correlation was observed for RAMP1 expressing HUVECs and HCMs. The presence of a line indicates a positive correlation. **D-F**) as for **A-C** except the transduction coefficient $\text{Log}(\tau/K_A)$ was calculated. A significant positive correlation was observed for RAMP1 expressing HUVECs and HCMs as indicated by the presence of a line. **G**) Signalling bias plots were calculated as $\Delta\Delta\text{Log}(\tau/K_A)$ for CGRP in the three cell lines, HUVECs, RAMP1 expressing HUVECs and HCMs for each pathway. Values have been normalised to a reference agonist (AM2) and the reference pathway (cAMP) for all three cell lines. **H**) as for **G** except the calculated values are for AM. **I**) Log potency ratios (as measured by the accumulation of cAMP) calculated as $\text{Log}(EC_{50}\text{AM2}/EC_{50}\text{agonist})$. Data are compiled from^{12,19}. HUVECs and HUAECs are shown in red and green respectively, HCMs in cyan and RAMP1-HUVECs in blue. **J-L**) Schematic representation of the signalling bias produced by CGPR (**J**), AM (**K**) and AM2 (**L**), and the intracellular 'signalling codes' they bring about based on the potencies recorded at individual pathways in HUVECs, RAMP1-HUVECs and HCMs.

